frontiers | Research Topics

Novel insights into sperm function and selection: From basic research to clinical application

Edited by
Kun Li, Tao Luo and Rossella Cannarella

Published in
Frontiers in Endocrinology

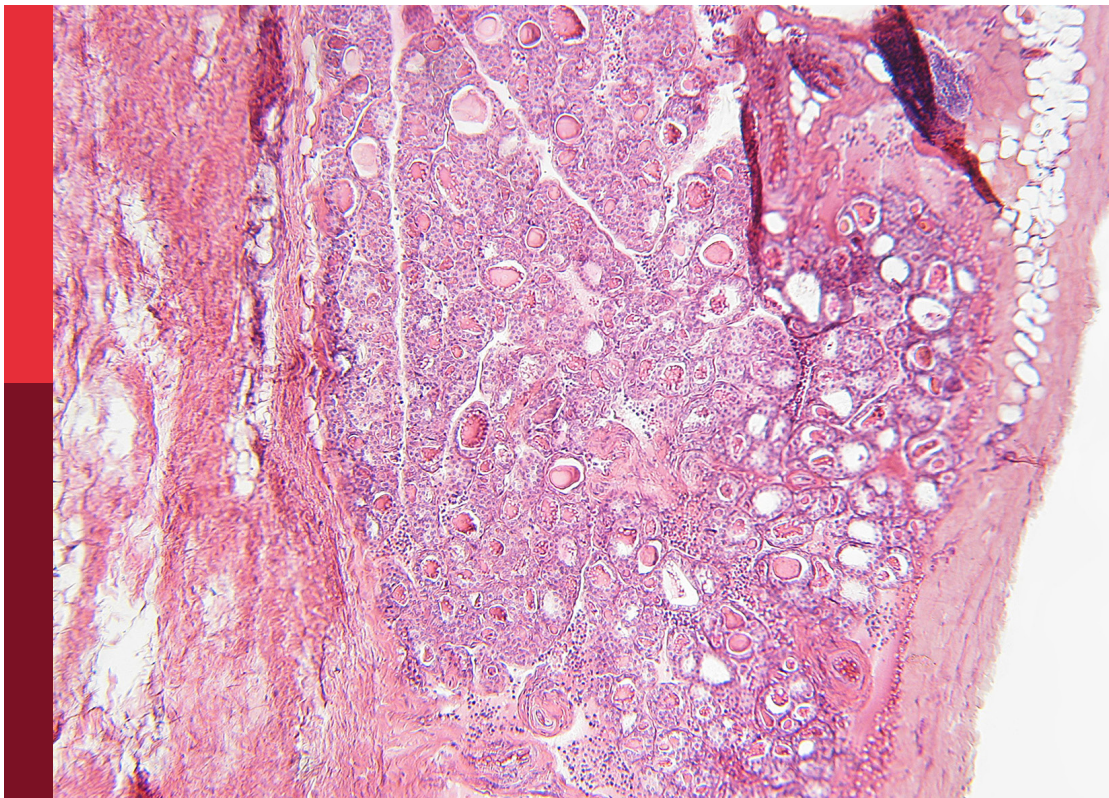

ISSN 1664-8714
ISBN 978-2-8325-3629-2
DOI 10.3389/978-2-8325-3629-2

About Frontiers

Frontiers is more than just an open access publisher of scholarly articles: it is a pioneering approach to the world of academia, radically improving the way scholarly research is managed. The grand vision of Frontiers is a world where all people have an equal opportunity to seek, share and generate knowledge. Frontiers provides immediate and permanent online open access to all its publications, but this alone is not enough to realize our grand goals.

Frontiers journal series

The Frontiers journal series is a multi-tier and interdisciplinary set of open-access, online journals, promising a paradigm shift from the current review, selection and dissemination processes in academic publishing. All Frontiers journals are driven by researchers for researchers; therefore, they constitute a service to the scholarly community. At the same time, the *Frontiers journal series* operates on a revolutionary invention, the tiered publishing system, initially addressing specific communities of scholars, and gradually climbing up to broader public understanding, thus serving the interests of the lay society, too.

Dedication to quality

Each Frontiers article is a landmark of the highest quality, thanks to genuinely collaborative interactions between authors and review editors, who include some of the world's best academicians. Research must be certified by peers before entering a stream of knowledge that may eventually reach the public - and shape society; therefore, Frontiers only applies the most rigorous and unbiased reviews. Frontiers revolutionizes research publishing by freely delivering the most outstanding research, evaluated with no bias from both the academic and social point of view. By applying the most advanced information technologies, Frontiers is catapulting scholarly publishing into a new generation.

What are Frontiers Research Topics?

Frontiers Research Topics are very popular trademarks of the *Frontiers journals series*: they are collections of at least ten articles, all centered on a particular subject. With their unique mix of varied contributions from Original Research to Review Articles, Frontiers Research Topics unify the most influential researchers, the latest key findings and historical advances in a hot research area.

Find out more on how to host your own Frontiers Research Topic or contribute to one as an author by contacting the Frontiers editorial office: frontiersin.org/about/contact

Novel insights into sperm function and selection: From basic research to clinical application

Topic editors

Kun Li — Hangzhou Medical College, China

Tao Luo — Nanchang University, China

Rossella Cannarella — University of Catania, Italy

Citation

Li, K., Luo, T., Cannarella, R., eds. (2023). *Novel insights into sperm function and selection: From basic research to clinical application*.

Lausanne: Frontiers Media SA. doi: 10.3389/978-2-8325-3629-2

Table of contents

05 Editorial: Novel insights into sperm function and selection: from basic research to clinical application
Kun Li, Tao Luo and Rossella Cannarella

08 The cryopreservation process induces alterations in proteins associated with bull sperm quality: The equilibration process could be a probable critical control point
Ramasamy Arunkumar, Arumugam Kumaresan, Manish Kumar Sinha, Kamaraj Elango, John Peter Ebenezer Samuel King, Pradeep Nag, Thirumalaisamy Karuthadurai, Rubina Kumari Baithalu, Tushar Kumar Mohanty, Rakesh Kumar and Tirtha Kumar Datta

21 Gene mutations associated with fertilization failure after *in vitro* fertilization/intracytoplasmic sperm injection
Yamei Xue, Xiaohong Cheng, Yuping Xiong and Kun Li

40 Identification of bi-allelic *KIF9* loss-of-function variants contributing to asthenospermia and male infertility in two Chinese families
Zhixiang Meng, Qingxia Meng, Tingting Gao, Hui Zhou, Jiajia Xue, Hong Li, Yibo Wu and Jinxing Lv

53 Deleterious variants in TAF7L cause human oligoasthenoteratozoospermia and its impairing histone to protamine exchange inducing reduced *in vitro* fertilization
Haowei Bai, Yanwei Sha, Yueqiu Tan, Peng Li, Yuxiang Zhang, Junwei Xu, Shuai Xu, Zhiyong Ji, Xiaobo Wang, Wei Chen, Jianxiong Zhang, Chencheng Yao, Zheng Li and Erlei Zhi

66 Homozygous mutation in *DNALI1* leads to asthenoteratozoospermia by affecting the inner dynein arms
Yanwei Sha, Wensheng Liu, Hua Nie, Lu Han, Chunjie Ma, Xiaoya Zhang, Ziyi Xiao, Weibing Qin, Xiaoming Jiang and Xiaoli Wei

74 Novel *HYDIN* variants associated with male infertility in two Chinese families
Hui Yu, Xiao Shi, Zhongmei Shao, Hao Geng, Senzhao Guo, Kuokuo Li, Meng Gu, Chuan Xu, Yang Gao, Qing Tan, Zongliu Duan, Huan Wu, Rong Hua, Rui Guo, Zhaolian Wei, Ping Zhou, Yunxia Cao, Xiaojin He, Liang Li, Xiaoping Zhang and Mingrong Lv

87 Effects of different sperm sources on the clinical outcomes of *in vitro* oocyte maturation cycles combined with intracytoplasmic sperm injection
Jianhua Li, Jing Chen, Shuang Tian, Tingting Jiao, Jianye Wang, Yan Wei, Yanbin Cheng, Ye Xu, Ri-Cheng Chian, Youzhu Li and Shuiwen Zhang

93 New horizons in human sperm selection for assisted reproduction
Brett Nixon, John E. Schjenken, Nathan D. Burke, David A. Skerrett-Byrne, Hanah M. Hart, Geoffry N. De Iuliis, Jacinta H. Martin, Tessa Lord and Elizabeth G. Bromfield

108 The bibliometric analysis of studies on intracytoplasmic sperm injection from 2002 to 2021
Xiaoli Shen, Tianbing Xiao, Wei Han, Hong Ye, Yuanfeng Zhang and Guoning Huang

121 The role of spermatozoa-zona pellucida interaction in selecting fertilization-competent spermatozoa in humans
Erica T. Y. Leung, Brayden K. M. Lee, Cheuk-Lun Lee, Xinyi Tian, Kevin K. W. Lam, Raymond H. W. Li, Ernest H. Y. Ng, William S. B. Yeung, Jian-Ping Ou and Philip C. N. Chiu

136 Novel mutations of *TEX11* are associated with non-obstructive azoospermia
Jian Song, Yanwei Sha, Xiaojun Liu, Xuhui Zeng and Xiuling Zhao

144 Sperm morphological abnormalities in autosomal dominant polycystic kidney disease are associated with the Hippo signaling pathway via PC1
Wei-Hui Shi, Zhi-Yang Zhou, Mu-Jin Ye, Ning-Xin Qin, Zi-Ru Jiang, Xuan-You Zhou, Nai-Xin Xu, Xian-Lin Cao, Song-Chang Chen, He-Feng Huang and Chen-Ming Xu

155 A novel mutation in *CFAP47* causes male infertility due to multiple morphological abnormalities of the sperm flagella
Mohan Liu, Siyu Dai, Jiying Zhang, Yihong Yang, Ying Shen, Hongqian Liu, Yanting Yang, Chuan Jiang and Erpo Tian

frontiers | Frontiers in Endocrinology

TYPE Editorial
PUBLISHED 15 June 2023
DOI 10.3389/fendo.2023.1231545

OPEN ACCESS

EDITED AND REVIEWED BY
Richard Ivell,
University of Nottingham, United Kingdom

*CORRESPONDENCE
Kun Li
likun@hmc.edu.cn

RECEIVED 30 May 2023
ACCEPTED 05 June 2023
PUBLISHED 15 June 2023

CITATION
Li K, Luo T and Cannarella R (2023) Editorial: Novel insights into sperm function and selection: from basic research to clinical application.
Front. Endocrinol. 14:1231545.
doi: 10.3389/fendo.2023.1231545

Editorial: Novel insights into sperm function and selection: from basic research to clinical application

Kun Li[1]*, Tao Luo[2] and Rossella Cannarella[3,4]

[1]School of Pharmacy, Hangzhou Medical College, Hangzhou, China, [2]Institute of Life Science, Nanchang University, Nanchang, China, [3]Department of Clinical and Experimental Medicine, University of Catania, Catania, Italy, [4]Glickman Urology and Kidney Institute, Cleveland Clinic Foundation, Cleveland, OH, United States

KEYWORDS

sperm, sperm function, sperm selection, sperm preparation, assisted reproductive technology (ART), male infertility, *in vitro* fertilization, intracytoplasmic sperm injection

Editorial on the Research Topic
Novel insights into sperm function and selection: from basic research to clinical application

Successful reproduction via natural fertilization depends on normal sperm function and selection. The sperm function encompasses motility, capacitation, hyperactivation, acrosome reaction, chemotaxis, thermotaxis, rheotaxis, fertilizing capacity, and so on. All these functions help the sperm to reach the place where it meets, recognizes, and fuses with the egg. Meanwhile, during natural fertilization, malfunctional sperm can be easily recognized in different positions of the female reproductive tract. Namely, sperm selection is also essential for successful reproduction. Along with technological development, selection of the most functional sperm is a key step during *in vitro* fertilization (IVF) and intracytoplasmic sperm injection (ICSI) techniques.

This Research Topic, edited by Kun Li (Hangzhou Medical College, China), Tao Luo (Nanchang University, China), and Rossella Cannarella (University of Catania, Italy, and Glickman Urology and Kidney Institute, USA), focuses on the understanding of the novel trends in sperm function and selection techniques. This Research Topic has collected 13 articles, including 11 original and 2 review articles. The volume has contributed to novel aspects from basic research to clinical application.

Identifying new gene variants involved in abnormal sperm parameters

Clinical routine testing of semen mainly includes count, motility, and morphology. Motility is included among the most important functional tests. Reduced motility or absent sperm motility, known as asthenozoospermia, often accompanies the abnormal

sperm count and/or morphology, collectively referred to as oligoasthenoteratozoospermia or asthenoteratozoospermia. Besides, azoospermia may also be found in semen examination.

New variants in pathogenic genes have been found in infertile men with abnormal sperm parameters. Bai et al. identified four X-linked hemizygous deleterious variants of *TATA-Box Binding Protein Associated Factor 7 Like* (*TAF7L*), including c.1301_1302del (p.V434Afs*5), c.699G>T (p.R233S), c.508delA (p. T170fs), and c.719dupA (p.K240fs). The findings support that *TAF7L* is one of the pathogenic genes of oligoasthenoteratozoospermia. The study by Meng et al. indicates that *Kinesin Family Member 9* (*KIF9*) associates with the central microtubules in human sperm. Bi-allelic *KIF9* loss-of-function variants cause asthenozoospermia. Sha et al. demonstrated for the first time that homozygous *Dynein Axonemal Light Intermediate Chain 1* (*DNALI1*) mutation may impair the integration of axoneme structure, affect sperm motility and cause asthenoteratozoospermia in humans. Yu et al. screened 375 asthenoteratozoospermic patients and identified two novel compound heterozygous variants of *HYDIN Axonemal Central Pair Apparatus Protein* (*HYDIN*), which significantly reduced sperm HYDIN level, damaged flagella structure, and disrupted assembly of the acrosome and neck. Xue et al. summarized the mutations of nine important genes expressed in sperm or oocytes, namely *Phospholipase C Zeta 1* (*PLCZ1*), *Actin-like protein 7A* (*ACTL7A*), *Actin-like protein 9* (*ACTL9*), *dynein axonemal heavy chain 17* (*DNAH17*), *WEE2*, *Tubulin Beta 8 Class VIII* (*TUBB8*), *NLR Family Pyrin Domain Containing 5* (*NLRP5*), *Zona Pellucida Glycoprotein 2* (*ZP2*), and *Transducin-Like Enhancer Protein 6* (*TLE6*), which can contribute to the fertilization failure of IVF/ICSI attempts. These abnormalities mainly showed Mendelian patterns of inheritance, including dominant and recessive inheritance, although *de novo* mutations were present in some cases. Song et al. revealed non-obstructive azoospermia-affected cases with *Testis-expressed gene 11* (*TEX11*) mutations (exon 5, c.313C>T: p.R105*), (exon 7, c.427A>C: p.K143Q) and (exon 29, c.2575G>A: p.G859R), that have not been previously reported. Shi et al. reported thirteen autosomal dominant polycystic kidney disease (ADPKD) males suffering from infertility and investigated the microtubule abnormalities associated with the disruption of *Polycystin-1* (*PKD1*). Their results suggested that the dysregulated Hippo signaling prominently contributed to ciliary anomalies in ADPKD and was potentially associated with axonemal defects in sperm. Liu et al. identified a novel missense mutation (c.1414G>A; p.V472M) in *Cilia and Flagella Associated Protein 47* (*CFAP47*) in two unrelated patients with asthenoteratozoospermia.

In summary, these articles focused on the gene variants involved in abnormal sperm parameters. This research field will give new clues about the etiology of unexplained infertility, which will be beneficial for the diagnosis and treatment of male infertility.

Discovering new protein biomarkers of sperm function and quality

Potential protein biomarkers were also reported to be linked with the sperm-zona pellucida (ZP)-binding ability and the quality of the frozen sperm. Leung et al. reported that heat shock protein70 2 (HSPA2) and sperm acrosome associated 3 (SPACA 3) are associated with the sperm ZP-binding ability. The results validated the possibility of applying spermatozoa-ZP interaction to select fertilization-competent spermatozoa in assisted reproductive technology (ART). Arunkumar et al. reported that the temperature equilibration process lowered the abundance of sperm proteins in bull, was involved in energy metabolism, structural integrity, and DNA repair, and increased the abundance of proteins associated with proteolysis and protein degradation. The abundance of proteins associated with signal pathways in sperm, such as metabolism, cyclic guanosine 3', 5'-monophosphate-dependent protein kinase G signaling, and regulation of the actin cytoskeleton.

Reporting new findings on ICSI at the clinical ART lab

One report showed the effect of different sperm preparation techniques on ICSI's clinical outcomes. Li et al. evaluated the effect of different sperm preparation techniques on fertilization rate, cleavage rate, embryo quality, endometrial thickness, implantation, biochemical pregnancy, clinical pregnancy, and live birth rates. They found that different sperm sources did not affect the embryo and clinical outcomes after IVM-ICSI cycles, including percutaneous epididymal sperm aspiration, testicular sperm aspiration, and ejaculated sperm.

Another report analyzed the current status and hotspots of ICSI based on 8271 publications between 2002 and 2021. Shen et al. showed that the hotspot topics of ICSI have been risks of ICSI, oocyte preservation, live birth rate, infertile men, and embryo quality in the past two decades. The top five prolific countries have been USA, China, Italy, Japan, and Belgium; the United States accounted for 22.65% of all publications in 2002; after 2018, four countries, China, UK, Italy, and Spain, increased rapidly, and China accounted for 32.10% of all publications on ICSI from 2018 to 2021. The number of publications from China grew exponentially from only five publications in 2002 to 208 publications in 2021; the top five contributing organizations were the Free University of Brussels, University of Copenhagen, University of Valencia, Ghent University, and the University of California San Francisco; the most productive and cited journals were Fertility and Sterility and Human Reproduction. This study presents a research overview of ICSI from different perspectives. These findings will contribute to a better understanding of the current status of ICSI research and provide hotspots and trends for future studies.

Discussing new developing trends in methods for sperm selection or sperm function evaluation

Nixon et al. reviewed recent developments in the understanding of sperm biology and function and highlighted the development of cutting-edge approaches for identifying and treating male infertility. In particular, the review focused on the progress toward the

implementation of precision medicine and the application of advanced technology platforms, including whole exome sequencing, proteomic analyses, advanced imaging technologies, and machine learning artificial intelligence. The review showed that the increasing novel mechanistic understanding of sperm biology and function, and the improvement of advanced technology will have a deep impact on many aspects: the uncovered and expanding potential candidate biomarkers, diagnostics, and treatments of male infertility, disrupting the fertility care paradigm, optimizing outcomes for the management of male infertility.

In conclusion, research published in this Research Topic revealed new gene variants and proteins correlated with sperm function and quality, new findings of sperm preparation, the research trends and hotspots on ICSI at clinical ART labs, and new developing trends in methods for sperm selection or function evaluation. This Research Topic has increased the insights from basic research of the genes and proteins that may affect sperm function and sperm selection to clinical application, which is beneficial for the fields of reproductive biology and reproductive medicine.

Author contributions

KL, TL, and RC drafted and revised the manuscript. All authors have read and confirmed this editorial for publication.

Acknowledgments

As Research Topic editors, we sincerely acknowledge all authors and referees for their valuable contributions to the Research Topic on the Novel Insights into Sperm Function and Selection: from Basic Research to Clinical Application.

Conflict of interest

The authors declare that the research was conducted in the absence of any commercial or financial relationships that could be construed as a potential conflict of interest.

Publisher's note

frontiers | Frontiers in Endocrinology

TYPE Original Research
PUBLISHED 09 December 2022
DOI 10.3389/fendo.2022.1064956

OPEN ACCESS

EDITED BY
Kun Li,
Hangzhou Medical College, China

REVIEWED BY
Shaharior Hossen,
Chonnam National University,
South Korea
Umut Taşdemir,
Aksaray University, Turkey

*CORRESPONDENCE
Arumugam Kumaresan
ogkumaresan@gmail.com;
A.Kumaresan@icar.gov.in

SPECIALTY SECTION
This article was submitted to Reproduction, a section of the journal Frontiers in Endocrinology

RECEIVED 09 October 2022
ACCEPTED 21 November 2022
PUBLISHED 09 December 2022

CITATION
Arunkumar R, Kumaresan A, Sinha MK, Elango K, Ebenezer Samuel King JP, Nag P, Karuthadurai T, Baithalu RK, Mohanty TK, Kumar R and Datta TK (2022) The cryopreservation process induces alterations in proteins associated with bull sperm quality: The equilibration process could be a probable critical control point. *Front. Endocrinol.* 13:1064956. doi: 10.3389/fendo.2022.1064956

The cryopreservation process induces alterations in proteins associated with bull sperm quality: The equilibration process could be a probable critical control point

Ramasamy Arunkumar[1], Arumugam Kumaresan[1]*, Manish Kumar Sinha[1], Kamaraj Elango[1], John Peter Ebenezer Samuel King[1], Pradeep Nag[1], Thirumalaisamy Karuthadurai[1], Rubina Kumari Baithalu[2], Tushar Kumar Mohanty[2], Rakesh Kumar[3] and Tirtha Kumar Datta[3]

[1]Theriogenology Laboratory, Southern Regional Station of ICAR-National Dairy Research Institute, Bengaluru, India, [2]Animal Reproduction, Gynaecology and Obstetrics, ICAR-National Dairy Research Institute, Karnal, India, [3]Animal Genomics Laboratory, Indian Council for Agricultural Research (ICAR)-National Dairy Research Institute, Karnal, India

The present study quantitatively characterized the proteomic changes in bull spermatozoa induced by the cryopreservation process. We performed high-throughput comparative global proteomic profiling of freshly ejaculated (before cryopreservation), equilibrated (refrigerated storage; during cryopreservation), and frozen (ultralow temperature; after cryopreservation) bull spermatozoa. Using the liquid chromatography–mass spectrometry (LC-MS/MS) technique, a total of 1,692, 1,415, and 1,286 proteins were identified in fresh, equilibrated, and cryopreserved spermatozoa, respectively. When the proteome of fresh spermatozoa was compared with equilibrated spermatozoa, we found that 166 proteins were differentially expressed. When equilibrated spermatozoa were compared with cryopreserved spermatozoa, we found that 147 proteins were differentially expressed between them. Similarly, we found that 156 proteins were differentially expressed between fresh and cryopreserved spermatozoa. Among these proteins, the abundance of 105 proteins was lowered during the equilibration process itself, while the abundance of 43 proteins was lowered during ultralow temperature preservation. Remarkably, the equilibration process lowered the abundance of sperm proteins involved in energy metabolism, structural integrity, and DNA repair and increased the abundance of proteins associated with proteolysis and protein degradation. The abundance of sperm proteins associated with metabolism, cGMP-PKG (cyclic guanosine 3′,5′-monophosphate-dependent protein kinase G) signaling, and regulation of the actin cytoskeleton was also

altered during the equilibration process. Collectively, the present study showed that the equilibration step in the bull sperm cryopreservation process was the critical point for sperm proteome, during which a majority of proteomic alterations in sperm occurred. These findings are valuable for developing efficient protocols to minimize protein damage and to improve the quality and fertility of cryopreserved bull spermatozoa.

KEYWORDS

proteome, stages of cryopreservation, LC-MS/MS, bioinformatics, bull spermatozoa

Introduction

Artificial insemination using cryopreserved semen has undeniably contributed to the genetic improvement and productivity enhancement of cattle (1). The long-term *ex-situ* conservation of superior germplasm by cryopreservation enables the improvement of genetic gain even after the sire's death (2). By using cryopreserved spermatozoa, the first cattle calf was produced in 1951 (3); since then, the technique was rapidly established worldwide. In spite of several developments in semen cryopreservation, a large number of spermatozoa are rendered immotile during this process; the lifespan and fertilizing potential of the motile sperm population in cryopreserved semen are also altered (4, 5). It is reasonably understood that the cryotolerance of the spermatozoa varied with individual bulls. The spermatozoa from different bulls respond differently to the changing environment during the process of cryopreservation (6, 7). Furthermore, increasing lines of evidence indicate that functional attributes like membrane integrity (8), acrosomal integrity (9), capacitation (10), and oviduct/zona binding ability (11) are altered in the cryopreserved spermatozoa. Although it is well proven that sperm functions are altered by the process of cryopreservation, the exact reason(s) for decreased fertility with cryopreserved spermatozoa still remains obscure.

The transcription and translation processes in mature spermatozoa are still debatable. Few studies evaluated the molecular alterations in cryopreserved spermatozoa and reported alterations in mRNA profiles, chromatin remodeling, DNA methylation, and post-translational histone modifications (12–14). Although genomics and transcriptomics have achieved new heights and are of extensive importance, they do not reveal temporal and spatial protein expression or protein levels and post-translational modifications (15, 16). Therefore, studies are required to identify the effect of the cryopreservation process on sperm proteins, which are indispensable for sperm binding to the oviduct or oocyte and for fertilization. Among the several molecular alterations that take place during the process of cryopreservation, sperm protein architectural alterations are extremely important. It is well proven that sperm proteins are important for timely capacitation (17), hyperactivated motility (18), acrosome reaction (19), sperm–oviduct binding, sperm–oocyte binding (20), and fertilization (21, 22). Protein alterations in the sperm could be the major cause of cryopreservation-induced premature capacitation and acrosome exocytosis, which decreases the fertilizing capacity of cryopreserved spermatozoa (23). Few studies have indicated that the cryopreservation process induces differential remodeling of the proteome in mammalian spermatozoa (24). Therefore, analysis of sperm proteomic alterations during various stages of cryopreservation is a promising way to understand the reasons behind the reduced fertility with cryopreserved spermatozoa. Furthermore, it would help us to tailor the cryopreservation protocol for bull spermatozoa with the aim to improve the quality and fertility of cryopreserved spermatozoa.

The process of cryopreservation involves several steps; the most prominent are the process of equilibration and ultralow freezing. In order to identify the critical step of cryopreservation, which induces differential remodeling of the sperm proteome, the sperm proteome needs to be analyzed at different stages of cryopreservation. Once the critical point is identified, quality control measures can be taken up for the development of an efficient cryopreservation technology that protects bull sperm proteome. With this background in mind, the aim of the current study was to find out the potential alterations of bull sperm proteome at different stages of the cryopreservation process. Using the high-throughput proteomic profiling technique, we report here the proteomic profile of fresh, equilibrated, and cryopreserved bull spermatozoa and the proteomic alterations in spermatozoa at each stage of the cryopreservation process.

Materials and methods

Experimental animals

The present investigation was conducted on Holstein Friesian crossbred bulls maintained at the Artificial Breeding

Research Centre, ICAR-National Dairy Research Institute, Karnal, India. Six ejaculates from three crossbred bulls were utilized for the study. All the experimental bulls have qualified the breeding soundness evaluation and were routinely used for artificial breeding. The age of the bulls ranged between 4 and 6 years, and they were housed under a loose housing system in individual pens (30′ × 10′) on concrete floor. The bulls were fed with 2.5 kg of concentrate ration containing 21% crude protein and 70% total digestible nutrients. Seasonal green fodders, including maize, cowpea, berseem, and jowar, as well as a blend of maize and oat silage, were made *ad libitum* to the animals. The bulls were exercised in the rotatory exerciser on the day before semen collection (twice a week), in order to preserve the sexual activity and to ensure consistent quality of semen. All the experiments were conducted in accordance with the guidelines and regulations laid down and duly approved by the Institute Animal Ethics Committee (CPCSEA/IAEC/LA/SRS-ICAR-NDRI-2019/No.04).

Semen collection and sample preparation

Ejaculates were collected from the bulls using the Danish model standard artificial vagina (AV, 14") (IMV Technologies, France). The temperature of the artificial vagina (AV) was maintained between 42°C and 45°C with sufficient pressure and proper lubrication with sterilized K-Y lubricating jelly (Johnson & Johnson Co., USA). After preliminary evaluation, two ejaculates from each bull were selected based on mass activity (+3.0 and above in the 0–5 scale), progressive motility (≥80%), and sperm concentration (>800 million/ml) and pooled before further processing. The present study was designed to analyze the proteomic profiles of fresh, equilibrated, and cryopreserved sperm samples prepared from the same animal ejaculates. In order to do that, the pooled ejaculates from each animal were divided into two aliquots. One aliquot was used as fresh, while another aliquot was processed into equilibration followed by ultralow freezing. For fresh sample preparation, seminal plasma was separated from spermatozoa by centrifugation (1,000×*g* for 15 min at 4°C), and the sperm pellet obtained was washed twice with 1 ml of PBS (pH 7.4, 10× PBS containing 1.37 M of NaCl, 27 mM of KCl, 100 mM of Na_2HPO_4, and 18 mM of KH_2PO_4) (Sigma Aldrich, USA) at 900×*g* for 5 min at 4°C. The supernatant was discarded and the pellet was purified by double layer 90%–45% discontinuous Percoll gradient centrifugation (25) to eliminate contaminating substances like epithelium cells. Protease inhibitor cocktail [1% (v/v); Amresco, USA, Cat. No. M221] was added to spermatozoa and snap-frozen in liquid nitrogen until further use (26). For the preparation of equilibrated and cryopreserved sperm samples, another aliquot of semen was extended with an egg yolk-free commercial extender (AndroMed®, Minitube Animal Reproduction Technologies, Germany, Cat. No. 13503/0201). The extended semen was filled in French mini straws (0.25 ml) with the help of an automatic straw filling and sealing machine (MRS 3, IMV France) and equilibrated in a single-layer horizontal position on the straw rack for 4 h at 5°C. After equilibration, the straws were cut and the semen sample was centrifuged at 1,000×*g* for 15 min at 4°C to remove the extender. After washing, the Percoll-selected spermatozoa were snap-frozen in liquid nitrogen after the addition of 1% (v/v) protease cocktail inhibitor. For the preparation of the cryopreserved sample, a portion of equilibrated semen straws was exposed to liquid nitrogen vapor by keeping the straws 4 cm above the liquid nitrogen level in the wide opened LN2 container for 5 min. The straws were then placed into precooled goblets using precooled forceps before being submerged in liquid nitrogen. After 24 h of cryopreservation, semen straws were thawed at 37°C for 30 s. Cryopreservation was considered successful when at least 50% of the spermatozoa remained motile after thawing. The frozen-thawed semen was washed and the Percoll-selected spermatozoa were snap-frozen in liquid nitrogen after the addition of 1% (v/v) protease cocktail inhibitor. The mean (± SE) sperm motility (%) in fresh, equilibrated, and cryopreserved semen was 83.5 ± 1.5, 71.6 ± 1.4 and 52.5 ± 1.6 percentage, respectively.

Protein extraction

For the isolation of protein, 50 million spermatozoa were taken, into which 100 µl of 50 mM NH_4HCO_3 was added and incubated at room temperature for 30 min. Then, the samples were sonicated for 10 min and centrifuged at 200×*g* for 10 min at 4°C. To these samples, sodium dodecyl sulfate (SDS) was added, and in each step, the samples were incubated at room temperature for 10 min, followed by sonication and centrifugation. The supernatant was taken further for SDS-PAGE for quality checking.

Gel electrophoresis and protein digestion

The glass plates (with 1.5 mm spacer) were cleaned thoroughly and then fixed into the casting assembly. The resolving gel (appendix) was prepared and poured in between the glass plates up to the level, 2 cm below the top, and then iso-butanol was slowly added so as to just cover the top surface of the resolving gel to avoid oxygen and to make the upper surface linear. The resolving gel was allowed to polymerize for 15 min. The iso-butanol was removed and washed twice with triple distilled water. Finally, the stacking gel (5%) solution was poured up to the top; the comb was fixed and kept for 15–20 min. The sperm proteins were separated by the SDS-PAGE method. The sample preparation involved the denaturation of proteins, by boiling the sample with 2× lysis buffer in a 1:1 ratio for 5 min in the presence of 2-mercaptoethanol and SDS. After boiling, the samples were loaded into the wells along with molecular weight markers as the reference standard. Electrophoresis was carried out at a constant

current of 100 mA in the stacking gel and at 100 mA in the resolving gel. The electrophoresis was stopped when the dye front reached about 10 mm above the bottom, and the glass plates were disassembled. The stacking gel portion was cut and the resolving gel was transferred to a fixative for 4 h, and furthermore, the gels were silver-stained to observe the bands. Finally, the gel was scanned with an Epson Expression 11000XL Scanner (Supplementary Figure 1).

For the in-solution digestion, 100 µg of the sample was taken and diluted with 50 mM of NH_4HCO_3. This sample was treated with 100 mM of DTT at 95°C for 1 h followed by 250 mM of IDA at room temperature in the dark for 45 min and then digested with trypsin and incubated overnight at 37°C. The resulting sample was vacuum-dried and dissolved in 50 µl of 0.1% formic acid in water. This solution was centrifuged at 10,000×*g*, and the supernatant was collected into a separate tube. For label-free quantitation, 3 runs per sample were carried out. The samples were cleaned up using ZipTip as per the manufacturer's protocol.

Mass spectrometry analysis of peptide mixtures

Samples (10 µl) were injected into the C18 UPLC column (Waters UPLC system). The separation of all the samples was performed on ACQUITY UPLC BEH C18 column (Waters, UK) (75 µm × 150 mm × 1.7 µm). A gradient elution program was run for the chromatographic separation with mobile phase A (0.1% formic acid in water) and mobile phase B (0.1% formic acid in acetonitrile) followed by analysis on the Q-TOF instrument for MS and MS/MS [Synapt G2 Mass Spectrometer equipped with an electrospray ionization (ESI) source]. Sample analysis was performed in the positive mode. The experimental instrument parameters include polarity- ES+, analyser-resolution mode, capillary (kV)- 3.5000, source temperature-150°C, sampling cone- 45, extraction cone- 4.5, source gas flow-30 mL/min, desolvation temperature- 350°C, cone gas flow- 30 L/Hr and desolvation gas flow- 800 L/Hr. The TOF MS setup includes a Da range from 50 to 2,000 Da and a scan time of 0.5 s. The raw data were processed by Waters MassLynx 4.1 peptide editor software to get the complete integrated sequence of the sample. The individual peptide MS/MS spectra were matched to the database sequence with the help of the ProteinLynx Global Server (PLGS) software (Waters). The peptides were loaded with buffer A and eluted with buffer B (95% acetonitrile, 0.1% formic acid) at a flow rate of 0.3 ml/min.

MS data processing

Raw data were generated and processed by MassLynx 4.1 (Waters). The individual peptide MS/MS spectra were matched to the UniProt *Bos taurus* reference proteome database sequence for protein identification on the PLGS software (Waters). The parameters used for the identification are as follows: peptide mass tolerance at the MS1 level, 50 ppm; fragment mass tolerance at the MS2 level, 100 ppm; minimum number of fragment matches for peptides, 2; minimum number of fragment matches for proteins, 5; minimum number of peptide matches for proteins, 1; and missed cleavages, 1. Carbamidomethyl on cysteine as fixed modification and oxidation of methionine and N-terminal acetylation were considered as variable modifications for database search. The score is calculated by the expression analysis extension of the PLGS software based on the relevance of the protein present in both samples being compared. Differentially expressed proteins were identified by calculating the fold change of expression values (log base2) with respect to the control samples. Differentially expressed proteins include the proteins with higher abundance (< −1 fold) and lower abundance (< −1 fold) in the treated sample. The unique proteins mentioned for each control and treated are the proteins that did not have any matching peptides or *m*/*z* values between the groups.

Gene ontology and pathway analysis of proteins

The functional annotation of the differentially expressed proteins was performed using advanced bioinformatics tools available online. Web sources like Database for Annotation, Visualization and Integrated Discovery (DAVID) version 6.8 were utilized for functional annotation and pathway analysis. Gene names were uploaded in the abovementioned software for gene ontology (GO) analysis. Furthermore, Cytoscape 3.7.1, an open-source software platform with the ClueGO plugin, was used for the visualization of protein–protein interaction networks and biological pathways at the molecular level.

Results

Global proteomic profile of fresh, equilibrated, and cryopreserved spermatozoa

A total of 1,692, 1,415, and 1,285 proteins were detected in fresh, equilibrated, and cryopreserved spermatozoa, respectively. Among these, 462 proteins were common to all three groups, while 648, 446, and 364 proteins were identified as unique to fresh, equilibrated, and cryopreserved spermatozoa, respectively (Figure 1). It was observed that 905 and 751 proteins were found to be lost during equilibration and ultralow freezing, respectively. The proteins were mapped to the chromosome, and their expression in fresh, equilibrated, and cryopreserved

10.3389/fendo.2022.1064956

sperm and their differential pattern among the groups are shown in Figure 2.

Gene ontology classification and pathway analysis of proteins detected in fresh, equilibrated, and cryopreserved spermatozoa

A total of 1,692 proteins were detected in fresh spermatozoa. DAVID software was used for gene ontology enrichment analysis, which revealed that transcription (3.53%), cytoplasm (13.14%), and ATP binding (5.41%) were the most predominant GO terms in the biological process, cellular component, and molecular function, respectively. The gene ontology of the fresh sperm proteins is depicted in Figure 3A. In equilibrated spermatozoa, 1,415 proteins were detected and the gene ontology analysis revealed that transcription (3.60%), cytoplasm (12.93%), and metal ion binding (5.30%) are the most predominant GO terms in equilibrated spermatozoa. The gene ontology of the equilibrated sperm proteins is depicted in Figure 3B. In cryopreserved spermatozoa, 1,285 proteins were detected and gene ontology analysis revealed that transcription (3.23%), cytoplasm (12.79%), and ATP binding (5.98%) were the most predominant GO terms. The gene ontology of the cryopreserved sperm proteins is depicted in Figure 3C. The protein profiles of equilibrated and cryopreserved spermatozoa indicated a reduction in the number of proteins involved in all biological processes, cellular components, and molecular functions as compared with fresh spermatozoa.

The top 10 pathways associated with the proteins expressed in fresh, equilibrated, and cryopreserved spermatozoa are depicted in Figure 4. Pathway enrichment of fresh sperm proteins (1,692) revealed the involvement of 1,079 proteins in 103 different pathways. Among these pathways, metabolic pathways and the PI3K–Akt signaling pathways were the two crucial pathways identified in fresh spermatozoa. Pathway enrichment of sperm proteins (1,415) in equilibrated spermatozoa revealed that 444 proteins were involved in 86 different pathways. The number of proteins involved in all pathways, including the metabolic pathways and the PI3K–Akt signaling pathway, was significantly lower than in fresh spermatozoa. Pathway enrichment of cryopreserved sperm proteins (1,285) revealed that 438 proteins were involved in 87 different pathways. The number of proteins involved in all enrichment pathways including major pathways was decreased as compared with fresh and equilibrated spermatozoa.

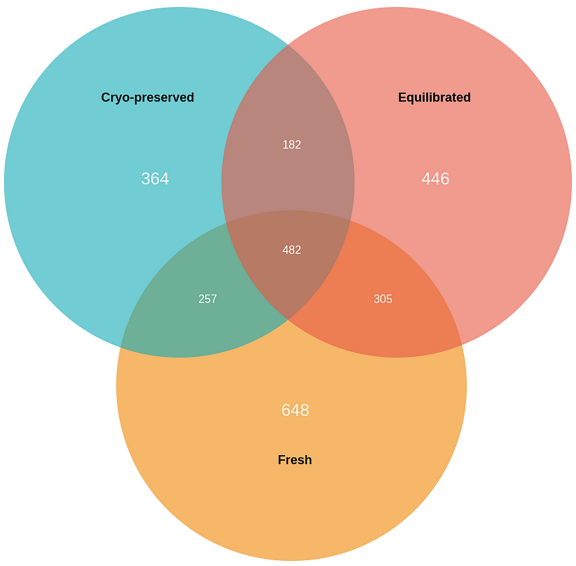

FIGURE 1
Venn diagram showing the number of unique and common proteins present in fresh, equilibrated, and cryopreserved semen samples.

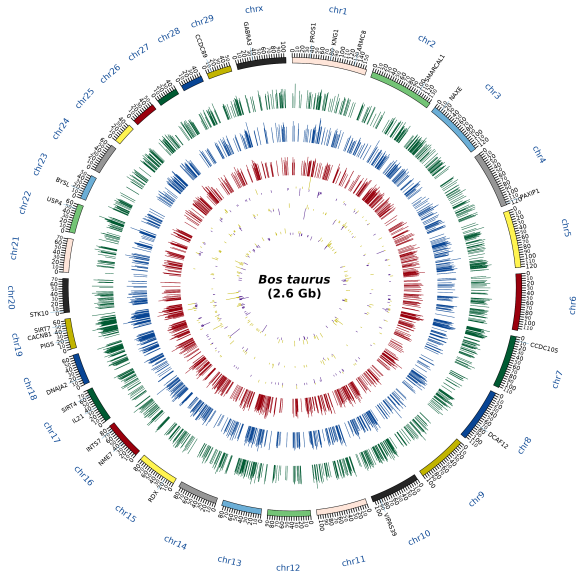

FIGURE 2
Circos plot depicting the chromosome coverage and protein expression during the different stages of cryopreservation. The outermost circle (first layer) contains the names of the abundantly dysregulated proteins. The next circle (second layer) corresponds to the chromosomal bands, the green histogram (third layer) shows the expression of the proteins in the freshly ejaculated sperm, the blue histogram (fourth layer) indicates the expression of the proteins in the equilibrated sperm, and the red histogram (fifth layer) indicates the expression of the proteins in the cryopreserved sperm. Subsequently, the differentially expressed proteins between fresh and equilibrated sperm (sixth layer), the differentially expressed proteins between equilibrated and cryopreserved sperm (seventh layer), and the differentially expressed proteins between fresh and cryopreserved sperm (eighth layer) were indicated in yellow (detected in higher abundance) and purple (detected in lower abundance) colors.

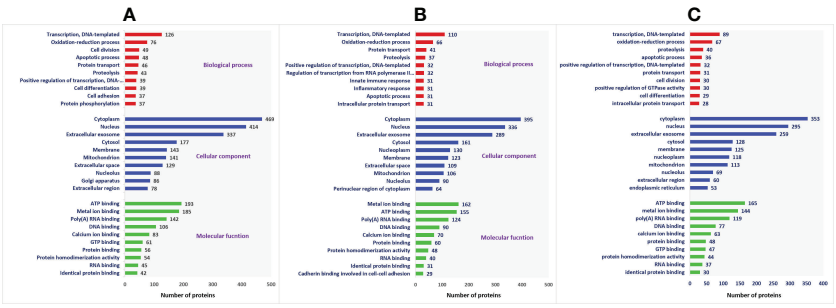

FIGURE 3
Functional classification of proteins of fresh **(A)**, equilibrated **(B)**, and cryopreserved **(C)** spermatozoa based on gene ontology terms (biological process, cellular component, molecular function).

Differentially expressed proteins between fresh and equilibrated spermatozoa

A total of 166 proteins were differentially expressed in equilibrated spermatozoa as compared with fresh spermatozoa. Of these, 61 proteins were in higher abundance and 105 proteins were in lower abundance. The heatmap of the top 10 abundantly dysregulated proteins based on their expression intensities is shown in Figure 5A. The top 10 proteins with higher abundance and lower abundance in equilibrated sperm compared with fresh sperm and their fold change are shown in Supplementary Table 1. The gene ontology of the differentially expressed proteins between

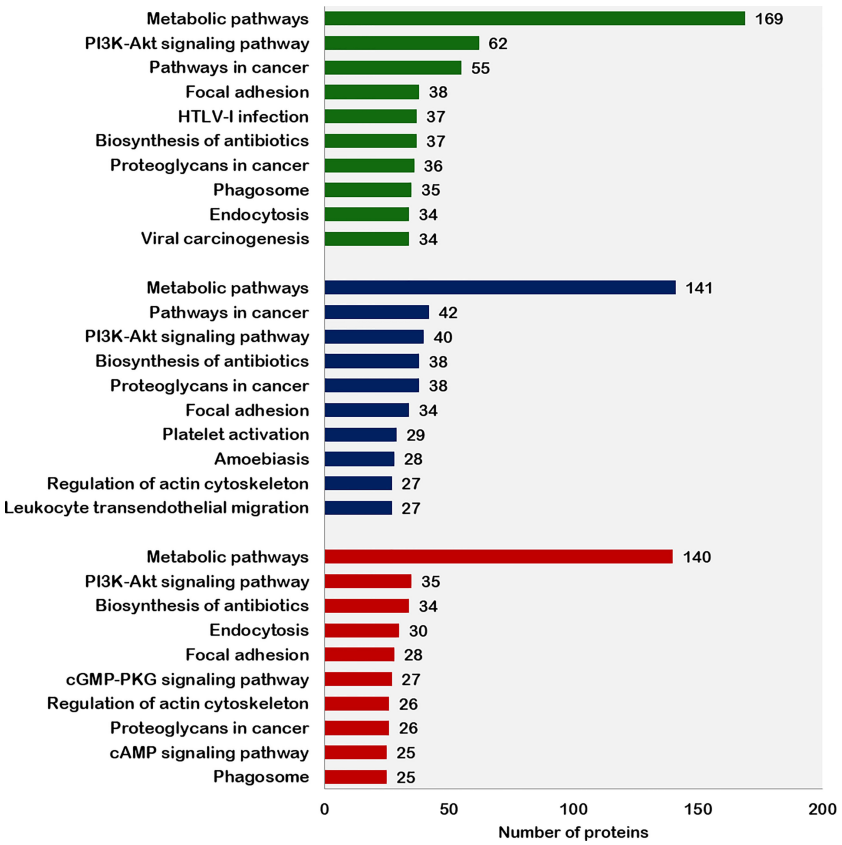

FIGURE 4
Top 10 pathways enriched with proteins from fresh, equilibrated, and cryopreserved spermatozoa.

fresh and equilibrated spermatozoa is depicted in Figure 6A. Pathway analysis of differentially expressed proteins revealed the involvement of 166 differentially expressed proteins (DEPs) in 26 different pathways. The top 10 dysregulated pathways and associated proteins are depicted in Table 1. Among the 26 dysregulated pathways, the actin cytoskeleton pathway, which is related to spermatogenesis, is highly dysregulated in equilibrated spermatozoa as compared with fresh spermatozoa.

Differentially expressed proteins between equilibrated and cryopreserved spermatozoa

A total of 147 proteins were differentially expressed in cryopreserved spermatozoa as compared with equilibrated spermatozoa. Of these, 104 proteins were in higher abundance and 43 proteins were in lower abundance in cryopreserved spermatozoa compared with equilibrated sperm. The heatmap of the top 10 abundantly dysregulated proteins based on their expression intensities is shown in Figure 5B. The top 10 proteins with higher abundance and lower abundance in cryopreserved sperm compared with equilibrated sperm and their fold change are shown in Supplementary Table 2. The gene ontology of the differentially expressed proteins between equilibrated and cryopreserved spermatozoa is depicted in Figure 6B. Pathway analysis of DEPs revealed the involvement of 147 DEPs in 6 different pathways, which are depicted with associated proteins in Table 2.

Differentially expressed proteins between fresh and cryopreserved spermatozoa

A total of 156 proteins were differentially expressed between fresh and cryopreserved spermatozoa. Of these, 84 proteins were in higher abundance and 72 proteins were in lower abundance in equilibrated spermatozoa. The heatmap of the top 10 abundantly dysregulated proteins based on their expression intensities is shown in Figure 5C. The top 10 proteins with higher abundance and lower abundance in cryopreserved sperm compared with fresh sperm and their fold change are shown in Supplementary Table 3. The gene ontology of the DEPs between fresh and cryopreserved spermatozoa is depicted in Figure 6C. Pathway analysis of DEPs revealed the involvement of 156 DEPs in 12 different pathways, in which the top 10 pathways are depicted in Table 3. Among the dysregulated pathways, the metabolic pathway and the nucleotide excision repair pathway were found to be more specific. The proteins involved in the nucleotide excision repair pathway, which is related to DNA damage, were detected in higher abundance.

The network interaction of DEPs between fresh and equilibrated spermatozoa is shown in Figure 7. It was observed that DEPs were interacting with each other and involved mainly in metabolism-related processes such as the regulation of the phospholipid metabolic process and the mucopolysaccharide metabolic process.

Discussion

The influence of the cryopreservation process on the bull sperm proteome is less explored. Studies conducted on human (26, 27), boar (24, 28), ram (29), rabbit (30), and rooster (31) showed that the process of cryopreservation may induce quantitative changes in sperm proteome. These studies indicate that the cryopreservation process alters the abundance levels of sperm proteins related to membrane permeability, metabolism, flagella structure, motility, intracellular signaling, capacitation, apoptosis, and fertilization. However, the possible cause of sperm proteome alteration and the stage of cryopreservation which is highly responsible for sperm

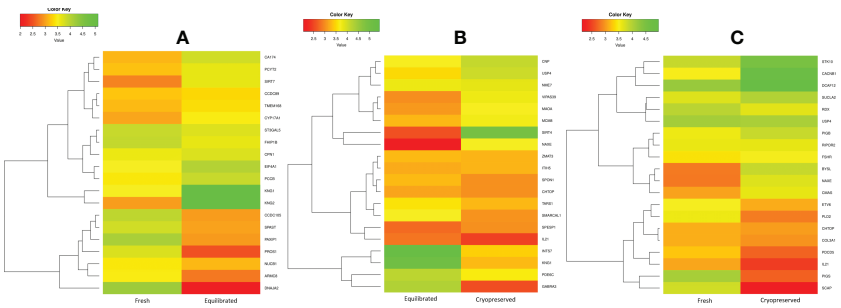

FIGURE 5
The heatmap of the top 10 abundantly differentially expressed proteins based on their expression intensities. **(A)** Differentially expressed proteins between fresh and equilibrated sperm, **(B)** differentially expressed proteins between equilibrated and cryopreserved sperm, and **(C)** differentially expressed proteins between fresh and cryopreserved sperm.

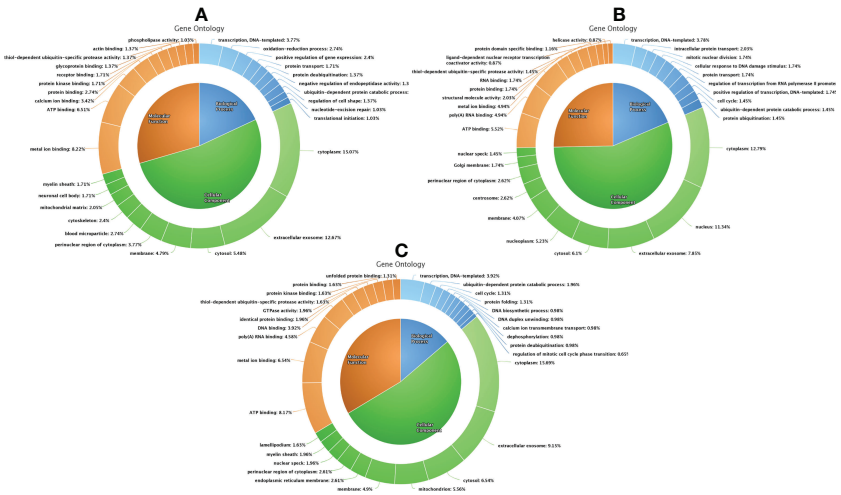

FIGURE 6
Functional classification of differentially expressed proteins between fresh and equilibrated spermatozoa **(A)**, differentially expressed proteins between equilibrated and cryopreserved sperm **(B)**, and differentially expressed proteins between fresh and cryopreserved sperm **(C)**.

proteomic changes are not fully understood. We report here that most of the quantitative proteome and functional pathway alterations occurred during the equilibration stage as compared with the ultralow freezing process.

In our study, the 905 and 751 proteins observed in freshly ejaculated sperm were not detected after equilibration and ultralow freezing, respectively, indicating that the process of equilibration may cause more alterations in the sperm protein profile than the ultralow freezing process. Although the precise reason for such loss of proteins during equilibration is not explainable with the available knowledge, it is possible that the proteins may be lost from spermatozoa during the equilibration process due to shedding, active cleavage, or degradation. However, such mechanisms have not been investigated fully. It has been reported that cold denaturation of protein occurs at a temperature range of 0°C to −20°C, and globular proteins often undergo partially reversible denaturation. Denaturation of proteins during cryopreservation results in the leakage of protease from the lysosomes found in the acrosome leading to loss of membrane integrity (32). During cryopreservation, some proteases and protease inhibitors are prematurely activated; thus, natural proteolysis regulation in cryopreserved semen is compromised (33). This may also be due to the heterogenicity of seminal plasma and sperm in the mammalian ejaculate (34) The protein changes in sperm may also be due to the difference in their responsiveness to seminal plasma (35). Another possible

TABLE 1 Top 10 dysregulated pathways between fresh and equilibrated spermatozoa and the associated proteins.

Pathways	Protein count	Proteins involved
Metabolic pathways	18	ODC1, PNLIPRP2, MAOA, CS, TKT, LTC4S, DSE, GLCE, ALAS1, CYP17A1, PLCB4, ST3GAL5, IDH1, GPT, PCYT2, PCCB, ALDH9A1, DEGS1
Pathways in cancer	8	PLCB4, ADCY7, STAT5B, ITGA3, KIT, STAT3, PIK3R2, TGFB2
Complement and coagulation cascades	6	KNG1, A2M, FGB, C1S, F7, PROS1
Amoebiasis	6	PLCB4, TLR2, ITGB2, ACTN2, PIK3R2, TGFB2
Chemokine signaling pathway	6	PLCB4, ADCY7, NCF1, STAT5B, STAT3, PIK3R2
Proteoglycans in cancer	6	TLR2, RDX, MSN, STAT3, PIK3R2, TGFB2
Biosynthesis of antibiotics	6	ODC1, CS, IDH1, TKT, PCCB, ALDH9A1
Regulation of actin cytoskeleton	6	ITGB2, RDX, ACTN2, ITGA3, MSN, PIK3R2
Pancreatic secretion	5	PNLIPRP2, CLCA1, PLCB4, ADCY7, SLC4A4
Carbon metabolism	5	CS, IDH1, GPT, TKT, PCCB

TABLE 2 Dysregulated pathways between equilibrated and cryopreserved spermatozoa and the associated proteins.

Pathways	Protein count	Proteins involved
Biosynthesis of antibiotics	5	ODC1, GFPT2, HK1, ACLY, NME7
Viral carcinogenesis	5	YWHAG, YWHAH, DDB1, YWHAB, ACTN2
Amino sugar and nucleotide sugar metabolism	4	GNPDA1, CMAS, GFPT2, HK1
Cell cycle	4	YWHAG, YWHAH, YWHAB, MCM3
Hippo signaling pathway	4	YWHAG, YWHAH, YWHAB, CDH1
Aminoacyl-tRNA biosynthesis	3	YARS, SARS, CARS2

reason, especially important to intracellular proteins, is the increased membrane sensitivity that renders these proteins to be made more accessible to lysates inside the frozen spermatozoa, which could possibly be involved in protein degradation (36). These studies support our findings on sperm protein loss during cryopreservation with possible reasons such as the shedding of proteins through an altered membrane and proteolysis. However, this may be due to the presence of these proteins in low abundance below the detection level. Despite all these factors, extenders also could affect the expression of proteins. Egg yolk-based extenders are commonly used for bull sperm cryopreservation; however, due to sanitary concerns, there has been a tendency against using egg yolk in cryoprotective media in recent years. The various extenders had affected the sperm proteins (37), and it has also been shown that altered membrane permeability enables the shedding of proteins from the spermatozoa (38). Similar to previous bull sperm protein studies (39), we also used an egg yolk-free commercial extender in this study.

On the other hand, we observed that 446 and 364 proteins that were not detected in freshly ejaculated sperm were detected after equilibration and ultralow freezing, respectively. Similar to our findings, Wang et al. found 22 proteins that became more abundant during cryopreservation, and the vast majority of them were functionally classified as intracellular proteins. The possible causes of equilibration-induced proteomic profile alteration would be cryoprotectant-induced osmotic stress which causes cell shrinkage and irreversible alteration in sperm membrane integrity (40) and potential binding of surrounding seminal plasma proteins to the spermatozoa (41). As seminal plasma is an unregulated body fluid unlike blood, its composition hugely varies. The freezability of bull sperm differs based on the difference in the composition of seminal plasma proteins between bulls. Meanwhile, the possible causes of increased protein abundance during ultralow freezing are currently not fully understood (26), although it has been suggested that increased phosphorylation could be the cause of protein abundance following cryopreservation. These proteins might have been expressed in low abundance below the detection level in fresh sperm, but the expression might have increased during cryopreservation. It may be inferred that quantitative proteomic alterations such as both the increase and decrease in protein abundance are more prevalent during equilibration than during the ultralow freezing process.

In order to elucidate the functional differences of proteome among groups, gene ontology analysis of global protein profiles and differential expression of proteins was carried out. Gene ontology analysis of individual global protein profile found that

TABLE 3 Top 10 dysregulated pathways between fresh and cryopreserved spermatozoa and the associated proteins.

Pathways	Protein count	Proteins involved
Metabolic pathways	25	PLD2, PNLIPRP2, FUT8, CMAS, MAOA, MAOB, ACLY, PIGS, LTC4S, PSPH, ACSBG1, DGKA, ATP6V1A, DHRS3, ST3GAL5, POLE3, ALDH1B1, GADL1, NT5C2, PIGB, ADSL, ATP6V0A1, SUCLA2, UGP2, DEGS1
Biosynthesis of antibiotics	6	ALDH1B1, ADSL, ACLY, PSPH, SUCLA2, UGP2
Purine metabolism	5	GUCY2F, POLE3, PDE5A, NT5C2, ADSL
Prostate cancer	4	HSP90B1, HSP90AA1, PIK3CA, CTNNB1
Estrogen signaling pathway	4	HSP90B1, HSP90AA1, GNAO1, PIK3CA
Histidine metabolism	3	ALDH1B1, MAOA, MAOB
DNA replication	3	DNA2, POLE3, MCM3
Glycine, serine, and threonine metabolism	3	MAOA, MAOB, PSPH
Nucleotide excision repair	3	POLE3, DDB1, ERCC2
Tryptophan metabolism	3	ALDH1B1, MAOA, MAOB

10.3389/fendo.2022.1064956

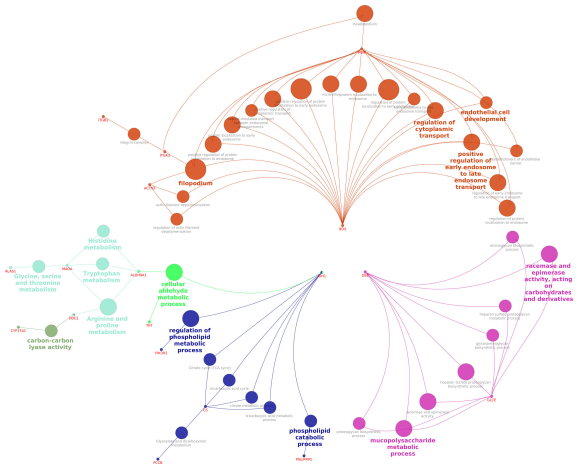

FIGURE 7
Interaction network of DEPs between fresh and equilibrated spermatozoa.

the proteins involved in inevitable biological processes such as sperm metabolism, signal transduction, energy synthesis, proteolysis, protein degradation, and apoptosis were decreased throughout the cryopreservation process. Among the pathways identified, the metabolic pathway, the PI3K–Akt signaling pathway, and the focal adhesion pathway are the crucial pathways in all three groups. The important metabolic pathways that produce cellular energy in the form of ATP are glycolysis and mitochondrial oxidative phosphorylation (42, 43). ATP is the indispensable fuel for the sperm and the facilitator of sperm motility (44, 45). The hydrolysis of ATP is essential for the sperm flagellar movement to propagate sperm (46). The PI3K–Akt pathway is an intracellular signal transduction pathway in response to extracellular signals, which promotes metabolism, proliferation, cell survival, growth, and angiogenesis (47). This pathway was reported to be critical for sperm motility and mitochondrial ROS generation (48). The focal adhesion pathway is known to form the focal adhesion protein complex in order to activate many intracellular signaling pathways in relation to capacitation and acrosome reaction. Several focal adhesion proteins such as β1-integrin, focal adhesion kinase (FAK), paxillin, vinculin, talin, and α-actinin form a protein complex that plays a vital role in the regulation of acrosomal integrity, polymerization, and remodeling of the actin cytoskeleton (49). Meanwhile, the pathway analysis of equilibrated and cryopreserved sperm proteins flaunted that the number of proteins entangled in the abovementioned crucial pathways was decreased in both equilibrated and cryopreserved spermatozoa, which may result in reduced signal transduction, energy synthesis, and acrosomal integrity in cryopreserved spermatozoa.

We found 166 DEPs during the equilibration process (vs. fresh sperm), 147 DEPs during the ultralow freezing process (vs. equilibrated sperm), and 156 DEPs throughout the cryopreservation process (vs. fresh sperm), which included both equilibration and ultralow freezing. Among these, the abundance was higher during the equilibration process with 105 proteins as compared with 43 proteins during the ultralow freezing process. The dysregulated proteins were mostly involved in cellular processes, metabolic processes, binding activities, and catalytic activities in relation to sperm function in all three comparisons. Among the biological processes observed, four proteins (USP2, USP4, USP21, and BAP1) involved in the ubiquitin–proteasome system (UPS) such as deubiquitination and ubiquitin-dependent protein catabolic process were highly abundant after the equilibration process. Ubiquitination is a post-translational modification involved in transcriptional regulation, embryonic development, preimplantation, cell cycle control, immune response, oncogenesis, apoptosis, intracellular signaling pathways, and DNA repair mechanisms such as histone ubiquitination and ubiquitin-dependent protein catabolic process in DNA damage (50). Deubiquitination is involved in protein degradation and is the terminal stage of the apoptotic process (51). Excessive levels of ubiquitinated proteins in spermatozoa represent the dysfunction of the UPS which is negatively correlated with sperm motility, morphology, and chromatin integrity (52, 53). The involvement of the UPS in fertilization is supported by substantial scientific evidence. These proteasomes are necessary for the sperm to complete the zona penetration (54–59). The CYB5R4 (Cytochrome B5 reductase) protein is involved in stress-induced ROS production (60), and the LOC784768 (Calcium-activated chloride channel) protein plays a crucial role in acrosome reaction, capacitation, and sperm motility (61). The increased abundance of these proteins during equilibration is associated with premature acrosome reaction and capacitation, which might be initiated during the equilibration process itself. Among the molecular functions observed, calcium ion binding is an essential criterion for the sperm to complete its normal capacitation and acrosome reaction (62). Among the 24 proteins commonly dysregulated in both equilibrated and cryopreserved sperm as compared with fresh sperm, the CDC37 (63), ERCC2 (64), AP2M1 (65), USP2 (58), and MAOA (66) were related to male fertility. Interestingly, all these five proteins were in lower abundance after equilibration and persisted in lower levels even after cryopreservation as compared with fresh sperm.

The pathway enrichment analysis of dysregulated/differentially expressed proteins revealed that 26, 6, and 12 pathways were altered during equilibration, ultralow freezing, and throughout the cryopreservation process, respectively. Among these pathways, the metabolic pathway and the regulation of the actin cytoskeleton pathway were found to be related to sperm functions. Though the metabolic pathway was dysregulated in both equilibrated and cryopreserved sperm, the expression of the majority of proteins (ODC1, PNLIPRP2, MAOA, TKT, DSE, GLCE, PLCB4, ST3GAL5, IDH1, and

PCCB) involved in this pathway was detected in lower abundance during the equilibration process. Fu et al. (67) also reported that metabolism-related proteins involved in glyoxylate and dicarboxylate metabolism, glycolysis/gluconeogenesis, and pyruvate metabolism were altered during cryopreservation. Metabolic pathways play a major role in energy production to maintain cellular processes like motility, hyperactivation, capacitation, and acrosome reaction (68). Spermatozoa require glycolytic energy for motility, capacitation, and acrosome reaction and mitochondrial OXPHOS for sperm cell differentiation and maturation (42, 69). An important finding of our study is that the proteins involved in major metabolic pathways such as the tricarboxylic acid (TCA) cycle, glycolysis, and the inositol phosphate pathway were in lower abundance in equilibrated spermatozoa. Since metabolic pathways play an important role in sperm functional attributes, the lower abundance levels of proteins involved in metabolic pathways may have a big impact on the ability of the sperm to fertilize. Lower abundance or loss of proteins involved in the metabolic pathway could be associated with ATP deficiency, which may lead to reduced sperm motility. Citrate synthase, an enzyme protein of the TCA cycle, delays sperm–egg fusion by initiating Ca^{2+} oscillation and negatively correlates with fertility (70), but its higher abundance during equilibration may reduce the fertility of the spermatozoa. Regarding the actin cytoskeleton pathway, the presence of actin polymerization in the tail region is necessary for sperm motility during post-testicular maturation (71) and sperm oocyte incorporation (72), and actin polymerization in the acrosomal region is necessary for capacitation and acrosomal reaction (73). The cytoskeletal proteins F-actin and β-dystrobrevin were altered by the cryopreservation process, allowing them to become more delicate (74). Similarly, Yoon et al. (75) reported that cryopreservation alters the ephrinR-actin, actin cytoskeleton assembly, and actin cytoskeleton regulatory mechanisms in epididymal spermatozoa. In our study, we observed that out of the six proteins involved in the actin cytoskeleton pathway, five proteins were detected in lower abundance in equilibrated spermatozoa, and there was no evidence of alteration during the ultralow freezing process. Therefore, we showed here that proteins involved in vital pathways such as the metabolic pathways and the regulation of the actin cytoskeleton pathway were dysregulated during the equilibration stage of cryopreservation itself.

Collectively, the quantitative and qualitative alterations in sperm proteins, which are involved in functional attributes and pathways associated with energy metabolism, motility, capacitation, and sperm membrane stability, were observed during the equilibration stage of cryopreservation. Earlier, it was thought that the sperm cryodamage during cryopreservation was due to exposure of the sperm to ultralow temperature (−196°C); however, the current study reports that the majority of the damages to sperm proteins are happening during the equilibration stage itself. Therefore, it is critical to understand how the equilibration process differs from ultralow freezing in terms of how it impacts essential sperm functional attributes, in order to tailor the cryopreservation protocols with the primary aim of preserving sperm proteome architecture by incorporating specific additives. Accordingly, the protein alterations can be minimized in the spermatozoa during cryopreservation to achieve high conception rates with frozen-thawed spermatozoa.

Data availability statement

The datasets presented in this study can be found in online repositories. The names of the repository/repositories and accession number(s) can be found below: https://repository.jpostdb.org/entry/JPST001500, PXD031895.

Ethics statement

The animal study was reviewed and approved by Institute Animal Ethics Committee.

Author contributions

RA: methodology, experiment, writing—original draft, and data curation. AK: conceptualization, project administration, supervision, funding, and writing—review and editing. MS and JK: data curation and bioinformatics analysis. PN and TK: methodology and data curation. KE: methodology and writing—original draft. RB: samples and methodology. TM: samples and methodology. RK: formal analysis and writing—review and editing. TD: formal analysis and writing—review and editing. All authors contributed to the article and approved the submitted version.

Funding

The present work was funded by the Bill and Melinda Gates Foundation (grant number OPP1154401) project entitled "Molecular markers for improving reproduction in cattle and buffaloes.

Acknowledgments

The authors are thankful to the head, Southern Regional Station of ICAR-National Dairy Research Institute, Bengaluru, and the director, ICAR-National Dairy Research Institute, Karnal, for providing the necessary facilities for conducting the experiment. The help extended by Sandor Life Sciences in proteomic analysis is duly acknowledged.

Conflict of interest

The authors declare that the research was conducted in the absence of any commercial or financial relationships that could be construed as a potential conflict of interest.

Publisher's note

All claims expressed in this article are solely those of the authors and do not necessarily represent those of their affiliated organizations, or those of the publisher, the editors and the reviewers. Any product that may be evaluated in this article, or claim that may be made by its manufacturer, is not guaranteed or endorsed by the publisher.

Supplementary material

The Supplementary Material for this article can be found online at: https://www.frontiersin.org/articles/10.3389/fendo.2022.1064956/full#supplementary-material

References

1. Foote RH. The history of artificial insemination: Selected notes and notables. *J Anim Sci* (2010) 80:1–10. doi: 10.2527/animalsci2002.80E-Suppl_21a

2. Bailey JL, Morrier A, Cormier N. Semen cryopreservation: Successes and persistent problems in farm species. *Can J Anim Sci* (2003) 83:393–401. doi: 10.4141/A03-024

3. Stewart DL. Storage of bull spermatozoa at low temperature. *Veterinary Rec* (1951) 63:65–6.

4. Watson PF. Recent developments and concepts in the cryopreservation of spermatozoa and the assessment of their post-thawing function. *Reprod Fertil Dev* (1995) 7:871–91. doi: 10.1071/RD9950871

5. Watson PF. The causes of reduced fertility with cryopreserved semen. *Anim Reprod Sci* (2000) 60-61:481–92. doi: 10.1016/S0378-4320(00)00099-3

6. Harayama H, Nishijima K, Murase T, Sakase M, Fukushima M. Relationship of protein tyrosine phosphorylation state with tolerance to frozen storage and the potential to undergo cyclic AMP dependent hyperactivation in the spermatozoa of Japanese black bulls. *Mol Reprod Dev* (2010) 77:910–21. doi: 10.1002/mrd.21233

7. Kumaresan A, Johannisson A, Bergqvist AS. Sperm function during incubation with oestrus oviductal fluid differs in bulls with different fertility. *Reprod Fertil Dev* (2016) 29:1096–106. doi: 10.1071/RD15474

8. Singh N, Cheema RS, Kumar A, Kaur M, Dhaliwal GS. Detrimental impact of cryopreservation on buffalo bull sperm motility, viability and membrane integrity due to efflux of membrane cholesterol. *Ind J Anim Reprod* (2016) 37:50–1.

9. Kumaresan A, Johannisson A, Al-Essawe EM, Morrell JM. Sperm viability, reactive oxygen species, and DNA fragmentation index combined can discriminate between above- and below-average fertility bulls. *J Dairy Sci* (2017) 100:5824–36. doi: 10.3168/jds.2016-12484

10. Bailey JL, Bilodeau JF, Cormier N. Semen cryopreservation in domestic animals: a damaging and capacitating phenomenon. *J Androl* (2000) 21:1–7. doi: 10.1002/j.1939-4640.2000.tb03268.x

11. Saraf KK, Singh RK, Kumaresan A, Nayak S, Chhillar S, Lathika S, et al. Sperm functional attributes and oviduct explant binding capacity differs between bulls with different fertility ratings in the water buffalo (Bubalus bubalis). *Reprod Fertil Dev* (2019) 31:395–403. doi: 10.1071/RD17452

12. Shangguan A, Zhou H, Sun W, Ding R, Li X , Liu J, et al. Cryopreservation induces alterations of miRNA and mRNA fragment profiles of bull sperm. *Front Genet* (2020) 11:419. doi: 10.3389/fgene.2020.00419

13. Prakash MA, Kumaresan A, Sinha MK, Kamaraj E, Mohanty TK, Datta TK. RNA-Seq analysis reveals functionally relevant coding and non-coding RNAs in crossbred bull spermatozoa. *Anim Reprod Sci* (2020) 222:106621. doi: 10.1016/j.anireprosci.2020.106621

14. Zeng C, Peng W, Ding L, He L, Zhang Y, Fang D, et al. A preliminary study on epigenetic changes during boar spermatozoa cryopreservation. *Cryobiology* (2014) 69:119–27. doi: 10.1016/j.cryobiol.2014.06.003

15. Peddinti D, Nanduri B, Kaya A, Feugang JM, Burgess SC, Memili E. Comprehensive proteomic analysis of bovine spermatozoa of varying fertility rates and identification of biomarkers associated with fertility. *BMC Syst Biol* (2008) 2:1–13. doi: 10.1186/1752-0509-2-19

16. Tomar AK, Sooch BS, Singh S, Yadav S. Differential proteomics of human seminal plasma: A potential target for searching male infertility marker proteins. *Prot Clin Appl* (2012) 6:147–51. doi: 10.1002/prca.201100084

17. Wang X, Kaya A, Memili E. Spermatozoal protein markers for Angus bull fertility. *Reprod Fertil Dev* (2010) 23:198–8. doi: 10.1071/RDv23n1Ab195

18. D'Amours O, Frenette G, Fortier M, Leclerc P, Sullivan R. Proteomic comparison of detergent-extracted sperm proteins from bulls with different fertility indexes. *Reproduction* (2010) 139:545–56. doi: 10.1530/REP-09-0375

19. Parent S, Lefièvrvcve L, Brindle Y, Sullivan R. Bull subfertility is associated with low levels of a sperm membrane antigen. *Mol Reprod Dev* (1999) 52:57–65. doi: 10.1002/(SICI)1098-2795(199901)52:1<57::AID-MRD8>3.0.CO;2-U

20. Lalancette C, Dorval V, Leblanc V, Leclerc P. Characterization of an 80-kilodalton bull sperm protein identified as PH-20. *Biol Reprod* (2001) 65:628–36. doi: 10.1095/biolreprod65.2.628

21. Aslam MK, Kumaresan A, Sharma VK. Identification of putative fertility markers in seminal plasma of crossbred bulls through differential proteomics. *Theriogenology* (2014) 82:1254–62. doi: 10.1016/j.theriogenology.2014.08.007

22. Aslam MK, Kumaresan A, Yadav S, Mohanty TK, Datta TK. Comparative proteomic analysis of high- and low-fertile buffalo bull spermatozoa for identification of fertility-associated proteins. *Reprod Dom Anim* (2019) 54:786–94. doi: 10.1111/rda.13426

23. Cormier N, Sirard MA, Bailey JL. Premature capacitation of bovine spermatozoa is initiated by cryopreservation. *J Andrology* (1997) 18(4):461–8. doi: 10.1002/j.1939-4640.1997.tb01953.x

24. Perez-Patiño C, Barranco I, Li J, Padilla L, Martinez EA, Rodriguez-Martinez H, et al. Cryopreservation differentially alters the proteome of epididymal and ejaculated pig spermatozoa. *Int J Mol Sci* (2019) 20:1791. doi: 10.3390/ijms20071791

25. McClure RD, Nunes L, Tom R. Semen manipulation: improved sperm recovery and function with a two-layer percoll gradient. *Fertil Steril* (1989) 51:874–7. doi: 10.1016/S0015-0282(16)60683-0

26. Wang S, Wang W, Xu Y, Tang M, Fang J, Sun H, et al. Proteomic characteristics of human sperm cryopreservation. *Proteomics* (2014) 14:298–310. doi: 10.1002/pmic.201300225

27. Bogle OA, Kumar K, Attardo-Parrinello C, Lewis SE, Estanyol JM, Ballescà JL. Identification of protein changes in human spermatozoa throughout the cryopreservation process. *Andrology* (2017) 5:10–22. doi: 10.1111/andr.12279

28. Chen X, Zhu H, Hu C, Hao H, Zhang J, Li K, et al. Identification of differentially expressed proteins in fresh and frozen-thawed boar spermatozoa by iTRAQ-coupled 2D LC-MS/MS. *Reproduction* (2014) 47:321–30. doi: 10.1530/REP-13-0313

29. Yuxuan H, Wang K, Zhao X, Zhang Y, Ma Y, Hu J. Differential proteome association study of freeze-thaw damage in ram sperm. *Cryobiology* (2016) 72:60–8. doi: 10.1016/j.cryobiol.2015.11.003

30. Rusco G, Słowińska M, Di Iorio M, Cerolini S, Maffione AB, Ciereszko A, et al. Proteomic analysis of rabbit fresh and cryopreserved semen provides an important insight into molecular mechanisms of cryoinjuries to spermatozoa. *Theriogenology* (2022) 191:77–95. doi: 10.1016/j.theriogenology.2022.07.018

31. Cheng CY, Chen PR, Chen CJ, Wang SH, Chen CF, Lee YP. Differential protein expression in chicken spermatozoa before and after freezing–thawing treatment. *Anim Reprod Sci* (2015) 152:99–107. doi: 10.1016/j.anireprosci.2014.11.011

32. Caldarelli G, De Los Rios P. Cold and warm denaturation of proteins. *J Biol Phys* (2001) 27:229–41. doi: 10.1023/A:1013145009949

33. Gurupriya VS, Roy SC, Dhama K, Devi G, Rekha V, Aswathi PB. Proteases and proteases inhibitors of semen – a review. *Adv Anim Vet Sci* (2014) 2:447–56. doi: 10.14737/journal.aavs/2014/2.8.447.456

34. D'Amours O, Frenette G, Bourassa S, Calvo E, Blondin P, Sullivan R. Proteomic markers of functional sperm population in bovines: comparison of low- and high-density spermatozoa following cryopreservation. *J Prot Res* (2018) 17:177–88. doi: 10.1021/acs.jproteome.7b00493

35. Höfner L, Luther AM, Palladini A, Fröhlich T, Waberski D. Tolerance of stored boar spermatozoa to autologous seminal plasma: A proteomic and lipidomic approach. *Int J Mol Sci* (2020) 21:6474. doi: 10.3390/ijms21186474

36. Schweisguth DC, Hammerstedt RH. Evaluation of plasma membrane stability by detergent-induced rupture of osmotically swollen sperm. *J Biochem Biophysi Methods* (1992) 24:81–94. doi: 10.1016/0165-022X(92)90049-G

37. Lessard C, Parent S, Leclerc P, BAILEYs JL, Sullivan R. Cryopreservation alters the levels of the bull sperm surface protein P25b. *J Androl* (2000) 21:700–7. doi: 10.1002/j.1939-4640.2000.tb02138.x

38. Pini T, Rickard JP, Leahy T, Crossett B, Druart X, De Graaf SP. Cryopreservation and egg yolk medium alter the proteome of ram spermatozoa. *J Prot* (2018) 181:73–82. doi: 10.1016/j.jprot.2018.04.001

39. Westfalewicz B, Dietrich MA, Ciereszko A. Impact of cryopreservation on bull (Bostaurus) semen proteome. *J Ani Sci* (2015) 93:5240–53. doi: 10.2527/jas.2015-9237

40. McClean R, Holt WV, Zee YP, Lisle A, Johnston SD. The effect of cryoprotectant on kangaroo sperm ultrastructure and mitochondrial function. *Cryobiology* (2008) 57:297–303. doi: 10.1016/j.cryobiol.2008.08.006

41. Roca J, Perez-Patiño C, Barranco I, Padilla LC, Martínez EA, Rodriguez-Martinez H, et al. Proteomics in fresh and preserved pig semen: recent achievements and future challenges. *Theriogenology* (2020) 150:41–7. doi: 10.1016/j.theriogenology.2020.01.066

42. Ruiz-Pesini E, Diez C, Lapena AC, Perez-Martos A, Montoya J, Alvarez E. Correlation of sperm motility with mitochondrial enzymatic activities. *Clin Chem* (1998) 44:1616–20. doi: 10.1093/clinchem/44.8.1616

43. Turner TM. Moving to the beat: a review of mammalian sperm motility regulation. *Reprod Fertil Dev* (2006) 18:25–38. doi: 10.1071/RD05120

44. Aitken RJ, Harkiss D, Buckingham D. Relationship between iron-catalysed lipid peroxidation potential and human sperm function. *Reproduction* (1993) 98:257–65. doi: 10.1530/jrf.0.0980257

45. Wise T, Lunstra DD, Rohrer GA, Ford JJ. Relationships of testicular iron and ferritin concentrations with testicular weight and sperm production in boars. *J Anim Sci* (2003) 81:503–11. doi: 10.2527/2003.812503x

46. Cosson J. ATP, the sperm movement energizer. In: *Adenosine triphosphate: Chemical properties, biosynthesis and functions in cells*. New York: Nova Publisher Inc. (2012). p. 1–46.

47. Hemmings BA, Restuccia DF. Pi3k-pkb/akt pathway. *Cold Spring Harbor Perspect Biol* (2012) 4:a011189. doi: 10.1101/cshperspect.a011189

48. Chen H, Chai R, Chen G. PI3K/AKT signaling pathway involvement in motility loss associated with prohibitin downregulation in sperm from infertile men. *Soc Reprod Fertility Annu Conference BioScientifica* (2016) Vol.3. doi: 10.1530/repabs.3.P014

49. Roa-Espitia AL, Hernández-Rendón ER, Baltiérrez-Hoyos R, Muñoz-Gotera RJ, Cote-Vélez A, Jiménez I, et al. Focal adhesion kinase is required for actin polymerization and remodelling of the cytoskeleton during sperm capacitation. *Biol Open* (2016) 5:1189–99. doi: 10.1242/bio.017558

50. Amerik AY, Hochstrasser M. Mechanism and function of deubiquitinating enzymes. *Biochim Biophys Acta (BBA)-Mol Cell Res* (2004) 1695:189–207. doi: 10.1016/j.bbamcr.2004.10.003

51. Sutovsky P, Hauser R, Sutovsky M. Increased levels of sperm ubiquitin correlate with semen quality in men from an andrology laboratory clinic population. *Hum Reprod* (2004) 19:628–38. doi: 10.1093/humrep/deh131

52. Sutovsky P, Moreno R, Ramalho-Santos J, Dominko T, Thompson WE, Schatten G. A putative, ubiquitin-dependent mechanism for the recognition and elimination of defective spermatozoa in the mammalian epididymis. *J Cell Sci* (2001) 114:1665–75. doi: 10.1242/jcs.114.9.1665

53. Hodjat M, Akhondi MA, Al-Hasani S, Mobaraki M, Sadeghi MR. Increased sperm ubiquitination correlates with abnormal chromatin integrity. *Reprod BioMed Online* (2008) 17:324–30. doi: 10.1016/S1472-6483(10)60215-5

54. Sawada H, Sakai N, Abe Y, Tanaka E, Takahashi Y, Fujino J, et al. Extracellular ubiquitination and proteasomemediated degradation of the ascidian sperm receptor. *Proc Natl Acad Sci* (2002) 99:1223–8. doi: 10.1073/pnas.032389499

55. Sutovsky P, Manandhar G, McCauley TC, Caamano JN, Sutovsky M, Thompson WE, et al. Proteasomal interference prevents zona pellucida penetration and fertilization in mammals. *Biol Reprod* (2004) 71:1625–37. doi: 10.1095/biolreprod.104.032532

56. Sakai N, Sawada MT, Sawada H. Non-traditional roles of ubiquitineproteasome system in fertilization and gametogenesis. *Int J Biochem Cell Biol* (2004) 36:776–84. doi: 10.1016/S1357-2725(03)00263-2

57. Yi YJ, Manandhar G, Sutovsky M, Li R, Jonakova V, Oko R, et al. Ubiquitin c-terminal hydrolase-activity is involved in sperm acrosomal function and anti-polyspermy defense during porcine fertilization. *Biol Reprod* (2007) 77:780–93. doi: 10.1095/biolreprod.107.061275

58. Bedard N, Yang Y, Gregory M, Cyr DG, Suzuki J, Yu X, et al. Mice lacking the USP2 deubiquitinating enzyme have severe male subfertility associated with defects in fertilization and sperm motility. *Biol Reprod* (2011) 85:594–604. doi: 10.1095/biolreprod.110.088542

59. Sawada H, Mino M, Akasaka M. Sperm proteases and extracellular ubiquitin proteasome system involved in fertilization of ascidians and sea urchins. *Adv Exp Med Biol* (2014) 759:1–11. doi: 10.1007/978-1-4939-0817-2_1

60. Yathish HM, Kumar S, Dubey PP, Modi RP, Chaudhary R, Siva Kumar A, et al. Profiling of sperm gene transcripts in crossbred (*Bos taurus* x *Bos indicus*) bulls. *Ani Reprod Sci* (2017) 177:25–34. doi: 10.1016/j.anireprosci.2016.12.003

61. Orta G, Ferreira G, José O, Treviño CL, Beltrán C, Darszon A. Human spermatozoa possess a calcium-dependent chloride channel that may participate in the acrosomal reaction. *J Physiol* (2012) 590:2659–75. doi: 10.1113/jphysiol.2011.224485

62. Breitbart H. Intracellular calcium regulation in sperm capacitation and acrosomal reaction. *Mol Cell Endocrinol* (2002) 187:139–44. doi: 10.1016/S0303-7207(01)00704-3

63. Li K, Sun P, Wang Y, Gao T, Zheng D, Liu A, et al. Hsp90 interacts with Cdc37, is phosphorylated by PKA/PKC, and regulates src phosphorylation in human sperm capacitation. *Andrology* (2021) 9:185–95. doi: 10.1111/andr.12862

64. Ji G, Gu A, Xia Y, Lu C, Liang J, Wang S, et al. ERCC1 and ERCC2 polymorphisms and risk of idiopathic azoospermia in a Chinese population. *Reprod BioMed Online* (2008) 17:36–41. doi: 10.1016/S1472-6483(10)60290-8

65. Cannarella R, Condorelli RA, Mongioì LM, La Vignera S, Calogero AE. Molecular biology of spermatogenesis: novel targets of apparently idiopathic male infertility. *Int J Mol Sci* (2020) 21:1728. doi: 10.3390/ijms21051728

66. Cortés-Rodriguez M, Royo JL, Reyes-Palomares A, Lendínez AM, Ruiz-Galdón M, Reyes-Engel A. Sperm count and motility are quantitatively affected by functional polymorphisms of HTR2A, MAOA and SLC18A. *Reprod BioMed Online* (2018) 36:560–7. doi: 10.1016/j.rbmo.2018.01.007

67. Fu L, An Q, Zhang K, Liu Y, Tong Y, Xu J, et al. Quantitative proteomic characterization of human sperm cryopreservation: using data-independent acquisition mass spectrometry. *BMC Urol* (2019) 19:1–9. doi: 10.1186/s12894-019-0565-2

68. Mukai C, Travis AJ. What sperm can teach us about energy production? *Reprod Domest Anim* (2012) 47:164–9. doi: 10.1111/j.1439-0531.2012.02071.x

69. Ford WC. Glycolysis and sperm motility: does a spoonful of sugar help the flagellum go round? *Hum Reprod Update* (2006) 12:269–74. doi: 10.1093/humupd/dmi053

70. Kang W, Harada Y, Yamatoya K, Kawano N, Kanai S, Miyamoto Y, et al. Extra-mitochondrial citrate synthase initiates calcium oscillation and supresses age-dependent sperm dysfunction. *Lab Invest* (2020) 100:583–95. doi: 10.1038/s41374-019-0353-3

71. Lin M, Hess R, Aitken JR. Induction of sperm maturation *in vitro* in epididymal cell cultures of the tammar wallaby (*Macropus eugenii*): disruption of motility initiation and sperm morphogenesis by inhibition of actin polymerization. *Reprod-cambridge* (2002) 124:107–17. doi: 10.1530/rep.0.1240107

72. Sanchez-Gutierrez M, Contreras RG, Mujica A. Cytochalasin-d retards sperm incorporation deep into the egg cytoplasm but not membrane fusion with the egg plasma membrane. *Mol Reprod Dev* (2002) 65:18–528. doi: 10.1002/mrd.10203

73. Breitbart H, Cohen G, Rubinstein S. Role of actin cytoskeleton in mammalian sperm capacitation and the acrosome reaction. *Reproduction* (2005) 129:263–8. doi: 10.1530/rep.1.00269

74. Felipe-Perez YE, Valencia J, Juarez-Mosqueda MD, Pescador N, Roa-Espitia AL, Hernandez-Gonzalez EO. Cytoskeleton proteins f-actin and beta-dystrobrevin are altered by the cryopreservation process in bull sperm. *Cryobiology* (2012) 64:103–9. doi: 10.1016/j.cryobiol.2011.12.004

75. Yoon SJ, Rahman MS, Kwon WS, Ryu DY, Park YJ, Pang MG. Proteomic identification of cryostress in epididymal spermatozoa. *J Ani Sci Biotechnol* (2016) 7:1–12. doi: 10.1186/s40104-016-0128-2

frontiers | Frontiers in Endocrinology

TYPE Review
PUBLISHED 16 December 2022
DOI 10.3389/fendo.2022.1086883

OPEN ACCESS

EDITED BY
Xiangpeng Dai,
Jilin University, China

REVIEWED BY
Lingbo Cai,
Nanjing Medical University, China
Xiaoming Jiang,
Xiamen University, China

*CORRESPONDENCE
Kun Li
likun@hmc.edu.cn

SPECIALTY SECTION
This article was submitted to Reproduction, a section of the journal Frontiers in Endocrinology

RECEIVED 01 November 2022
ACCEPTED 30 November 2022
PUBLISHED 16 December 2022

CITATION
Xue Y, Cheng X, Xiong Y and Li K (2022) Gene mutations associated with fertilization failure after *in vitro* fertilization/intracytoplasmic sperm injection.
Front. Endocrinol. 13:1086883.
doi: 10.3389/fendo.2022.1086883

Gene mutations associated with fertilization failure after *in vitro* fertilization/intracytoplasmic sperm injection

Yamei Xue[1], Xiaohong Cheng[2], Yuping Xiong[2] and Kun Li[2,3]*

[1]Assisted Reproduction Unit, Department of Obstetrics and Gynecology, Sir Run Run Shaw Hospital, School of Medicine, Zhejiang University, Hangzhou, China, [2]Institute for Reproductive Health, School of Pharmacy, Hangzhou Medical College, Hangzhou, China, [3]Zhejiang Provincial Laboratory of Experimental Animal's & Nonclinical Laboratory Studies, Hangzhou Medical College, Hangzhou, China

Fertilization failure during assisted reproductive technologies (ART) is often unpredictable, as this failure is encountered only after in vitro fertilization (IVF) and intracytoplasmic sperm injection (ICSI) have been performed. The etiology of fertilization failure remains elusive. More and more mutations of genes are found to be involved in human fertilization failure in infertile patients as high throughput sequencing techniques are becoming widely applied. In this review, the mutations of nine important genes expressed in sperm or oocytes, *PLCZ1, ACTL7A, ACTL9, DNAH17, WEE2, TUBB8, NLRP5, ZP2*, and *TLE6*, were summarized and discussed. These abnormalities mainly have shown Mendelian patterns of inheritance, including dominant and recessive inheritance, although de novo mutations were present in some cases. The review revealed the crucial roles of each reported gene in the fertilization process and summarized all known mutations and their corresponding phenotypes. The review suggested the mutations might become promising targets for precision treatments in reproductive medicine. Moreover, our work will provide some helpful clues for genetic counseling, risk prediction, and optimizing clinical treatments for human infertility by supplying the useful and timely information on the genetic causes leading to fertilization failure.

KEYWORDS

sperm, fertilization, assisted reproductive technology (ART), *in vitro* fertilization (IVF), intracytoplasmic sperm injection (ICSI), oocyte, fertilization failure, gene mutation

Introduction

Fertilization is a fundamental process of development and a hallmark event of sexual reproduction. In the process of fertilization, a sperm and a mature oocyte fuse to form a diploid zygote that will subsequently develop into a new life. Under physiological conditions, sperm pass through the vagina and uterus to migrate toward the ampulla of the oviduct.

During this transit, sperm acquire the ability to fertilize eggs through capacitation. Capacitated sperm transverse the corona radiata, penetrate the zona pellucida, bind the egg, and reach the perivitelline space. Finally, the sperm membrane and the oolemma fuse to lead to a series of changes, including the exocytosis of cortical granules, completion of the oocyte meiosis, and formation of maternal and paternal pronucleus (1, 2). Successful fertilization is assessed by the presence of the second polar body and two pronuclei.

In the treatment of *in vitro* fertilization (IVF), approximately 20% of couples with normospermia have low fertilization rates (defined as < 25%), and 5-15% have total fertilization failure (TFF) (3). In an earlier study, in 1980, Trounson AO et al. first reported an investigation into the use of IVF as a diagnostic procedure for patients with long-term infertility of unknown cause (idiopathic infertility) (4). The results indicated that fertilization failure was one of the primary causes of infertility. Barlow P et al. evaluated clinical male and female factors that might be involved in the occurrence of fertilization failure in IVF and found three main factors, including the male factors, few oocytes retrieved, and low-quality oocytes (5). The advent of intracytoplasmic sperm injection (ICSI) in 1991 has become the gold standard technique to treat male factor infertility. It was developed to allow egg-sperm fusion to bypass the natural barriers around oocytes, such as corona radiata, zona pellucida, and the oolemma (6–9). The use of ICSI technology was initially limited to serving those presenting with oligo-, astheno-, and terato-zoospermia or those with a history of unexplained TFF, and later it was also extensively used in non-male factor infertility (10). Although a drastic improvement in fertilization rate was observed in ICSI, there are still 1-5% of ICSI cycles with TTF (11). Some couples have even experienced recurrent fertilization failure after attempting ICSI for unknown reasons, despite having sperm with normal morphology, motility, and concentration (12). Fertilization failure in IVF/ICSI treatment is a most frustrating experience for patients as well as for IVF physicians.

Identification of the essential gene mutations is very important not only for understanding the mechanisms underlying fertilization failure at molecular levels but also for the treatment and diagnosis of infertile couples. Recent advances in molecular genetics have drastically accelerated the identification of novel genes responsible for fertilization. High throughput sequencing techniques have been successfully used to identify pathogenic genes related to human fertilization failure in a large individual population. Clinical researchers have attributed at least some cases of fertilization failure to the loss of function of one or more genes.

In this review, we focus on the gene mutations that can contribute to the fertilization failure of IVF/ICSI attempts and summarize the recently hereditary findings. We aim to provide useful and timely information on the genetic causes and the biomarkers of infertility for patients.

Methods

Search strategy

A computerized literature search was conducted for all publications in PubMed/Medline until December 2021 using the following MeSH or keyword terms: “Fertilization failure” or “Failed fertilization” or “Poor fertilization” or “oocyte activation deficiency” AND “*In vitro* fertilization” or “IVF” or “Intracytoplasmic sperm injection” or “ICSI” AND “Whole exome sequencing” or “WES” or “Next generation sequencing” or “NGS” or “Sanger sequencing” AND “genetic” or “gene” or “Mutation” or “Variant”. The search strategy is shown in Supplementary Table S1.

Study selection

The title, abstract, and full texts of the retrieved articles were reviewed, and the relevant articles were included. Only English-language studies or articles in other languages, but with a detailed abstract in English were enrolled. In addition, in the present systematic scoping review, we have opted to focus on the studies that discussed specific gene mutations associated with poor or failed fertilization in IVF/ICSI treatments and provided strong and convincing evidence for the roles of the genes in the corresponding phenotypes. We did not include articles regarding the association between single nucleotide polymorphisms and fertilization failure after IVF/ICSI because we believe that these studies may have a low level of evidence. Searching and screening of the articles were separately performed by two authors.

Data extraction

The details of the enrolled articles, including author, year of publication, number of individuals studied, identified genes, the identified cDNA and amino acid alterations, and fertilization results of IVF/ICSI attempts are shown in Table 1.

Results

The initial literature search yielded 669 articles from the electronic database, of which 83 studies finally remained after removing duplicates. According to the inclusion criteria, of the remaining papers, 28 studies were comprised in the current systematic scoping review. A flow diagram of the study is shown

TABLE 1 Details of included studies on gene mutations that lead to poor and failed fertilization.

Author, year	Number of patients studied (n)			Geographical origin	Identified genes	Identified cDNA alteration (Amino acid alteration)	IVF/ICSI cycles	Oocytes retrieved	Mature oocytes	Fertilized oocytes (%) #	References
	Included	Unrelated[c]	Newly tested								
Escoffier J et al., 2016	2	1	2	Tunisia	*PLCZ1*	c.1465A>T(p.Ile489Phe)	P1: ICSI = 2 P2: ICSI = 1	9, 9 14	4, 7 8	0 (0), 0 (0) 0 (0)	(13)
Torra-Massana M et al., 2019	37	37	13	Spain	*PLCZ1*	P1: c.590G>A (p.R197H) P2: c.698A>T(p.H233L) P3: c.972_973 delAG (p.V326K fs*25) P4: c.1499C>T (p.S500 L) P5: c.1499C>T (p.S500 L) P6: c.671T>C (p.L224P) P7: c.1499C>T (p.S500 L) P8: c.1499C>T (p.S500 L) P9: c.1499C>T (p.S500 L) P10: c.360C>G (p.I120M) P11: c.1499C>T (p.S500 L) P12: c.1499C>T (p.S500 L) P13: c.1499C>T (p.S500 L)	P1: ICSI=1 P2: ICSI=2 P3: ICSI=1 P4: ICSI=4 P5: ICSI=6 P6: ICSI=2 P7: ICSI=1 P8: ICSI=1 P9: ICSI=3 P10: ICSI=2 P11: ICSI=3 P12: ICSI=1 P13: ICSI=4	NA	7 2, 5 5 11, 2, 3, 3 1, 4, 3, 8, 5, 7 5,3 7 4 6, 12, 13 10, 8 3, 3, 8 7 2, 4, 4, 10	0(0) 0(0), 0(0) 0(0) 0(0), 0(0),0 (0), 2(66.7) 0(0), 0(0),2 (66.7), 0(0),0 (60.0), 0(0) 0(0), 1(33.3) 1(14.3) 0(0) 0(0),1(8.3), 0 (0) 0(0), 0(0) 1(33.3), 1 (33.3), 1 (12.5) 1(14.3) 0(0), 0(0),0 (0), 5(50.0)	(14)
Dai J et al., 2019	10	10	3	China	*PLCZ1*	P1: c.C588A (p.C196X) P2: c.T1048C (p.S350P) P3: c.C736T (p.L246F)	P1: ICSI=1, ICSI +AOA=1 P2: ICSI=1, ICSI +AOA=1 P3: ICSI=1, ICSI +AOA=1	20, 20 18, 14 14, 7	17,18 15, 6 13, 4	0(0), 16 (88.9) 0(0), 2(33.3) 1(7.7), 3 (75.0)	(15)
Yan Z et al., 2020	14	14	5	China	*PLCZ1*	P1: c.588C>A p.C196* P2: c.588C>A p.C196*, c.830T>C p.L277P P3: c.1129_1131delAAT p.N377del, c.1733T>C p.M578T P4: c.1151C>T p.A384V P5: c.570+1G>T p.V189Cfs*12, c.1344A>T p.K448N	P1: ICSI= 3 P2: ICSI= 2 P3: ICSI= 2 P4: ICSI= 1 P5: ICSI= 2	NA	29[$] 15[$] 24[$] 25[$] 24[$]	3(10.3) 0(0) 0(0) 5(20.8) 0(0)	(16)

(Continued)

10.3389/fendo.2022.1086883

TABLE 1 Continued

Author, year	Number of patients studied (n)			Geographical origin	Identified genes	Identified cDNA alteration (Amino acid alteration)	IVF/ICSI cycles	Oocytes retrieved	Mature oocytes	Fertilized oocytes (%) #	References
	Included	Unrelated[c]	Newly tested								
Yuan P et al., 2020	2	2	2	China	*PLCZ1*	P1: c.1259C>T (p.P420L), c.1733T>C (p.M578T) P2: c.1727T>C (p.L576P)	P1: IVF=1, IVF+ICSI=1 P2: IVF +ICSI=2, ICSI=1	8, 4 6, 7, 14	6, 4 6, 6, 13	0(0),0(0) 1(16.7), 2 (33.3), 6 (46.2)	(17)
Yuan P et al., 2020	1	1	1	China	*PLCZ1*	c.1658 G>C (p. R553P)	ICSI = 3	NA	22, 4, 24	0(0),0(0),0 (0)	(18)
Mu J et al., 2020	4	4	4	China	*PLCZ1*	P1: c.588C>A (p.Cys196∗) P2: c.588C>A (p.Cys196∗), c.1259C>T (p.Pro420Leu) P3: c.590G>A (p.Arg197His) P4: c.972_973delAG p.Thr324fs, c.1234delA (p.Arg412fs)	P1: IVF=1, ICSI=4, ICSI +AOA=1 P2: IVF=1, ICSI=1, ICSI +AOA=1 P3: ICSI=3, ICSI +AOA=1 P4: ICSI=5, ICSI +AOA=1	10,7,6,2,1,4 19, 16,14 5,13,25,19 12,6,5,6,1,28	10,7,6,2,1,2 17,12,8 3,8,21,10 12,6,2,2,0,26	2(20.0),1 (14.3),1 (16.7),0(0),0 (0),2(100) 1(5.9),0(0),8 (100) 2(66.7),2 (25.0),6 (28.6),9 (90.0) 0(0),0(0),0 (0),0(0), 0 (0),8(30.8)	(19)
Wang F et al., 2020	4	4	1	China	*PLCZ1*	c.588C>A (p.Cys196∗)	IVF= 1; ICSI=1; ICSI +AOA= 2	16,13,9,2	NA,10,8,2	0(0),0(0),3 (37.5),2(100)	(20)
Dai J et al., 2018	24	22	5	China	*WEE2*	P1: c.G585C (p.Lys195Asn) P2: c.1228C>T (p.Arg410Trp) P3: c.1006_1007dup (p.His337Tyrfs*24) P4: c.1006_1007dup (p.His337Tyrfs*24), c.1136-2A>G (p.Asp380Leufs*39) P5: c.1006_1007dup (p.His337Tyrfs*24)	P1: IVF=1, ICSI=1 P2: IVF=1, ICSI=1 P3: IVF=1, ICSI=1, ICSI +AOA=1 P4: IVF +ICSI=1, ICSI +AOA=1 P5: IVF +ICSI=1	9, 12 18, 21 13, 10,10 15, 8 21	7, 7 18, 16 10, 9, 8 11, 8 17	0(0),0(0) 2 (11.1),1 (6.3) 0(0),0(0),0 (0) 0(0),0(0) 0(0)	(21)

(Continued)

10.3389/fendo.2022.1086883

TABLE 1 Continued

Author, year	Number of patients studied (n)			Geographical origin	Identified genes	Identified cDNA alteration (Amino acid alteration)	IVF/ICSI cycles	Oocytes retrieved	Mature oocytes	Fertilized oocytes (%) #	References
	Included	Unrelated[c]	Newly tested								
Sang Q et al., 2018	4	4	4	China	*WEE2*	P1: c.700G>C (p.Asp234His) P2: c.1473dupA (p.Thr493Asnfs*39) P3: c.220_223delAAAG (p.Glu75Valfs*6) P4: c.1006_1007insTA (p.His337Tyrfs*24)	P1: ICSI = 2 P2: ICSI = 1 P3: IVF = 1, ICSI = 2 P4: ICSI = 1	3 [a] 11 19 [a] 20	3 8 18 20	0(0) 0(0) 0(0) 0(0)	(22)
Zhao S et al., 2018	90	90	4	China	*WEE2*	P1: c.293_294insCTGAGACACCAGCCCAACC (p.Pro98Pro fsX2) P2: c.1576T>G (p.Tyr526Asp) P3: c.991C>A (p.His331Asn), c.1304_1307delCCAA (p.Thr435Met fsX31) P4: c.341_342 del AA (p.Lys114Asn fsX20), c.864G>C (p.Gln288His) P5: c.1A>G (p.0)?, c.1261G>A (p.Gly421Arg)	P1: IVF=1, ICSI=2, IVF +ICSI=1 P2: IVF=1, ICSI=1 P3: IVF=1, ICSI=1 P4: IVF=1, ICSI=1 P5: IVF=1, ICSI=1	5, 6, 5, 5 18, 11 15,12 12, 10 6, 21	NA	1(20.0), 0(0), 0(0), 0(0) 1(5.6), 0(0) 0(0), 0(0) 0(0), 0(0) 0(0), 0(0)	(23)
Yang X et al., 2019	1	1	1	China	*WEE2*	c.619C>T (p.R207C)	Rescue ICSI =1, ICSI +AOA = 1	23,16	NA, NA	0(0), 0(0)	(24)
Zhou X et al., 2019	17	17	1	China	*WEE2*	c.598C>T (p.Arg200Ter), c.1319G>C (p.Trp440Ser)	IVF=1, ICSI =1	15, 27	NA, 22	0(0),0(0)	(25)
Tian Y et al., 2020	1	1	1	China	*WEE2*	c.1535+3A>G(p.)?, c.946C > T (p. Leu316Phe)	IVF= 1; ICSI=2; ICSI +AOA= 1	15,NA,NA, NA	NA,8,9,11	0(0),2 (25.0);0(0);0 (0)	(26)
Wang A et al., 2021	6	6	1	China	*WEE2*	c.625G>T(p.E209*), c.759-2A>G (p.)?	Rescue ICSI =1, ICSI +AOA = 1	8, 8	4,8	0(0),0(0)	(27)
Jin J et al., 2021	31	31	3	China	*WEE2*	P1: c.220_223delAAAG (p.Glu75Valfs*6), c.G585C (p.Lys195Asn) P2: c.115_116insT (p.Gln39Leufs*5), c.C1459T (p.Arg487Trp) P3: c.756_758delTGA (p. Asn252Lysfs*316), c.1006_1007insTA (p. His337Tyrfs*24)	P1: IVF=1, ICSI=1 P2: IVF=1, ICSI=1 P3: IVF=1, ICSI=2	14,14 19,17 19,18,14	14,11 19,16 12,16,9	0(0),0(0), 0(0), 3(18.8) 2(16.7), 0 (0),0(0)	(28)
Yang P et al., 2021	115	115	4[&]	China	*TUBB8*	P1: c.629T>A (p.I210K) P2: c.938C>T (p.A313V)	P1: NA P2: NA	NA NA	NA NA	Fertilization failure	(29)

(Continued)

10.3389/fendo.2022.1086883

TABLE 1 Continued

Author, year	Number of patients studied (n)			Geographical origin	Identified genes	Identified cDNA alteration (Amino acid alteration)	IVF/ICSI cycles	Oocytes retrieved	Mature oocytes	Fertilized oocytes (%) #	References
	Included	Unrelated[c]	Newly tested								
						P3: c.1130T>C (p.L377P) P4: c.1203_1204insCT (p.G402Lfs*15)	P3: NA P4: NA	NA NA	NA NA	Fertilization failure Fertilization failure Fertilization failure	
Chen B et al., 2016	1	1	1	China	*TUBB8*	c.209 C > T (p.P70L)	IVF=1, ICSI=1	NA, 25	NA, 20	0 (0),2 (10.0)	(30)
Zhao L et al., 2020	2	2	2	China	*TUBB8*	P1: c.260C>T (p.P87L) P2: c.716G>C (p.C239S)	3 cycles 2 cycles	44[$] 17[$]	NA 12	9 (NA) 2 (16.7)	(31)
Chen B et al.	4	4	4	China	*TUBB8*	P1: c.322G>A (p.E108K) P2: c.1270C>T (p.Q424*) P3: c.10A>C (p. I4L) P4: c.1228G>A (p. E410K)	2 cycles 3 cycles 3 cycles 2 cycles	27[$] 40[$] 26[$] 22[$]	20 19 21 7	2 (10.0) 0 (0) 4 (19.0) 0 (0)	(32)
Li M et al., 2020	1	1	1	China	*NLRP5*	c.1598G>C (p.Arg533Pro), c.1919T>G (p.Leu640Arg)	IVF =1, ICSI = 1	13, 11	NA, 8	0(0),0(0)	(33)
Maddirevula S et al., 2020	1	1	1	Saudi Arabia	*NLRP5*	c.2274_2275del(p.Trp759Aspfs*4)	IVF +ICSI=1, ICSI=1	28,18	NA, 6	0(0),0(0)	(34)
Wang J et al., 2021	1	1	1	China	*ACTL7A*	c.463C>T (p.Arg155Ter), c.1084G>A (p.Gly362Arg)	ICSI=1, ICSI+AOA =1	11, 13	11,13	0(0),10(76.9)	(35)
Dai J et al., 2021	21	21	3	China	*ACTL9*	P1: c.1034C>T (p.Ser345Leu) P2: c.1138G>T (p.Val380Leu) P3: c.1209C>G (p.Tyr403Ter)	P1: IVF =1, ICSI =1 P2: ICSI =1 P3: IVF =1, ICSI =2	6, 14 12 11, 20, 14	4,11 10 11,19,12	0(0),0(0) 0(0) 0(0),1(5.2),2 (16.7)	(36)
Dai C et al., 2018	2	2	2	China	*ZP2*	P1: c.1695-2A>G (p.C566H fs*5) P2: c.1691_1694dup (p.C566W fc*5)	P1: Half-ICSI=1 P2: IVF=1, Half-ICSI=1	16 17, 25	NA	8(100) [b] 0(0), 12 (80.0) [b]	(37)
Alazami A M et al., 2015	3	2	2	Saudi Arabia	*TLE6*	c.1529C > A:p.S510Y	P1: ICSI=10 P2: ICSI=2	58 19	NA NA	3 (5.2) 0(0	(38)

(Continued)

10.3389/fendo.2022.1086883

TABLE 1 Continued

Author, year	Number of patients studied (n)			Geographical origin	Identified genes	Identified cDNA alteration (Amino acid alteration)	IVF/ICSI cycles	Oocytes retrieved	Mature oocytes	Fertilized oocytes (%) #	References
	Included	Unrelated[c]	Newly tested								
Lin J et al., 2020	403	403	3	China	*TLE6*	P1: c.1226G>A(p.Arg409Gln) P2: c.1621G>A(p.Glu541Lys) P3: c.388G>A (p.Asp130Asn), c.1507G>A (p.Val503Ile)	P1: ICSI = 2 P2: IVF =1, ICSI = 4 P3: IVF =1, ICSI = 2	8,6 NA, 2, 11, 8, 8 8, 8, 14	NA	0(0),0(0) 1(NA),1 (50.0), (63.6),1 (12.5),3 (37.5) 4(50.0),7 (87.5),11 (78.6)	(39)
Jia M et al., 2021	1	1	1	China	*DNAH17*	c.1048C>T(p.Arg350*); c.3390G>A (p.Met1130Ile)	IVF=1 (rescue ICSI =1); ICSI +AOA=1	20,15	13,10	0(0),0(0)	(40)

a: indicated the total number of oocytes retrieved.
b: All mature oocytes were divided into two groups for IVF and ICSI. None of the oocytes in the IVF groups were fertilized. In ICSI group, all 8 (100%) oocytes from P1 and 12 of the 15 (80%) from P2 were fertilized.
c: indicated the number of unrelated patients among all included patients.
[$]: indicated the total number of oocytes in all cycles.
[&]: indicated the number of patients diagnosed with fertilization failure.
*: indicated stop codon (nonsense mutation).
[#]: indicated the number of fertilized oocytes (fertilization rate).
AOA, assisted oocyte activation; IVF, in vitro fertilization; ICSI, intracytoplasmic sperm injection; IVF+ICSI indicated that ICSI was performed on those oocytes that failed to fertilize in conventional IVF; ICSI+AOA indicated that AOA was performed on those oocytes that failed to fertilize in ICSI; P, patient; NA, not available.

10.3389/fendo.2022.1086883

in Figure 1. The details about the studies included are listed in Table 1. In the past decades, 9 genes (PLCZ1, ACTL7A, ACTL9, DNAH17, WEE2, TUBB8, NLRP5, ZP2, and TLE6) have been reported to be causes of fertilization failure (Figure 2). Table 2 presented all known mutations discovered in infertile patients with fertilization failure by WES and Sanger sequencing technologies. All mutations and their corresponding phenotypes were summarized in Table 3.

Discussion

Genetic alterations associated with poor or failed fertilization after IVF/ICSI attempts

Recent descriptive data obtained from whole exome sequencing (WES) and Sanger sequencing in humans have

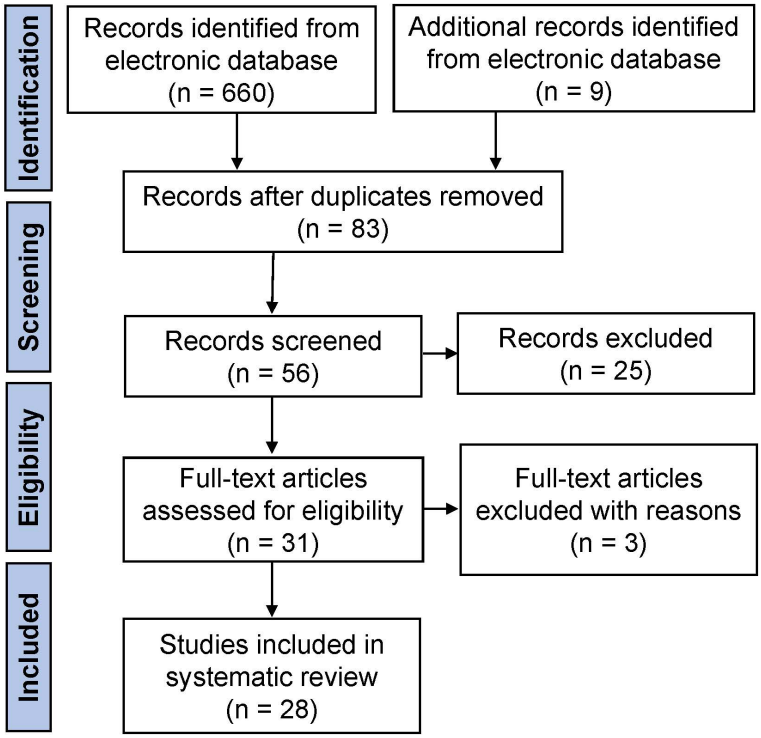

FIGURE 1
Workflow diagram of the literature review procedure.

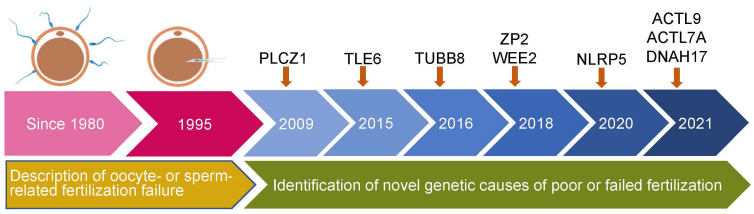

FIGURE 2
Timeline of discovery of mutations of genes that lead to poor and failed fertilization. PLCZ1, Phospholipase C zeta 1; WEE2, WEE1 Homolog 2; TUBB8, Tubulin beta 8 class VIII; NLRP5, NLR family pyrin domain containing 5; ACTL9, Actin-like 9; ACTL7A, Actin-like protein 7A; ZP2, Zona pellucida glycoprotein 2; TLE6, transducin-like enhancer of split 6; DNAH17, Dynein axonemal heavy chain 17.

TABLE 2 Genetic mutations associated with poor or failed fertilization after IVF/ICSI by WES and Sanger sequencing technologies.

Identified genes	Full name	MIM number	cDNA alteration	Amino acid alteration	Exon	Mutation	Zygosity in affected individuals	References
PLCZ1	Phospholipase C zeta 1	608075	c.1465A>T	p.Ile489Phe	Exon 13	Missense	Homozygous	(13)
			c.360C>G	p.I120M	Exon 4	Missense	Heterozygous	(14)
			c.590G>A	p.R197H	Exon 6	Missense	Heterozygous	(14)
			c.671T>C	p.L224P	Exon 6	Missense	Heterozygous	(14)
			c.698A>T	p.H233L	Exon 6	Missense	Heterozygous	(14)
			c.972_973 delAG	p.V326K fs∗25	Exon 9	Frameshift	Heterozygous	(14)
			c.1499C>T	p.S500 L	Exon 13	Missense	Homozygous	(14)
			c.588C>A	p.C196*	Exon 6	Nonsense	Homozygous	(15, 16, 19, 20)
			c.T1048C	p.S350P	Exon 10	Missense	Homozygous	(15)
			c.C736T	p.L246F	Exon 7	Missense	Homozygous	(15)
			c.830T>C p.L277P	p.L277P	Exon 7	Missense	Homozygous	(16)
			c.1129_1131delAAT	p.N377del	Exon 10	Frameshift	Compound heterozygous	(16)
			c.1733T>C	p.M578T	Exon 14	Missense	Compound heterozygous	(16)
			c.1151C>T	p.A384V	Exon 10	Missense	Homozygous	(16)
			c.570+1G>T	p.V189Cfs*12	Exon 5	Splicing	Compound heterozygous	(16)
			c.1344A>T	Heterozygous	Exon 12	Missense	Compound heterozygous	(16)
			c.1259C>T	p.P420L	Exon 11	Missense	Compound heterozygous	(17)
			c.1733T>C	p.M578T	exon 14	Missense	Compound heterozygous	(17)
			c.1727T>C	p.L576P	Exon 14	Missense	Homozygous	(17)
			c.1658 G>C	p. R553P	NM	Missense	Homozygous	(18)
			c.1259C>T	p.Pro420Leu	Exon 11	Missense	Heterozygous	(19)
			c.590G>A	p.Arg197His	Exon 6	Missense	Homozygous	(19)
			c.972_973delAG	p.Thr324fs	Exon 9	Frameshift	Compound heterozygous	(19)
			c.1234delA	p.Arg412fs	Exon 11	Frameshift	Compound heterozygous	(19)

(Continued)

10.3389/fendo.2022.1086883

TABLE 2 Continued

Identified genes	Full name	MIM number	cDNA alteration	Amino acid alteration	Exon	Mutation	Zygosity in affected individuals	References
WEE2	*WEE1 Homolog 2*	614084	c.G585C	p.Lys195Asn	Exon 3	Missense	Homozygous	(21)
			c.1228C>T	p.Arg410Trp	Exon 9	Missense	Homozygous	(21)
			c.1006_1007dup	p.His337Tyrfs*24	Exon 6	Frameshift	Compound heterozygous	(21, 22, 28)
			c.1136-2A>G	p.Asp380Leufs*39	IVS 7	Splicing	Compound heterozygous	(21)
			c.700G>C	p.Asp234His	Exon 4	Missense	Homozygous	(22)
			c.1473dupA	p.Thr493Asnfs*39	Exon 10	Frameshift	Homozygous	(22)
			c.220_223delAAAG	p.Glu75Valfs*6	Exon 1	Frameshift	Homozygous	(22)
			c.293_294insCTGAGACACCAGCCCAACC	p.Pro98Pro fsX2	Exon 1	Frameshift	Homozygous	(23)
			c.1576T>G	p.Tyr526Asp	Exon 11	Missense	Homozygous	(23)
			c.991C>A	p.His331Asn	Exon 6	Missense	Compound heterozygous	(23)
			c.1304_1307delCCAA	p.Thr435Met fsX31	Exon 9	frameshift	Compound heterozygous	(23)
			c.341_342 del AA	p.Lys114Asn fsX20	Exon 1	Frameshift	Compound heterozygous	(23)
			c.864G>C	p.Gln288His	Exon 5	Missense	Compound heterozygous	(23)
			c.1A>G	p.0?	Exon 1	Frameshift	Compound heterozygous	(23)
			c.1261G>A	p.Gly421Arg	Exon 9	Missense	Compound heterozygous	(23)
			c.619C>T	p.R207C	Exon 4	Missense	Homozygous	(24)
			c.598C>T	p.Arg200Ter	NM	Nonsense,	Compound heterozygous	(25)
			c.1319G>C	p.Trp440Ser	NM	Missense	Compound heterozygous	(25)
			c.625G>T	p.E209*	Exon 4	Nonsense	Compound heterozygous	(27)
			c.759-2A>G	p.?	Exon 5	Splicing	Compound heterozygous	(27)
			c.220_223delAAAG	p.Glu75Valfs*6	Exon 1	Frameshift	Compound heterozygous	(28)
			c.G585C	p.Lys195Asn	exon 3	Missense	Compound heterozygous	(28)
			c.115_116insT	p.Gln39Leufs*5	Exon 1	Frameshift	Compound heterozygous	(28)
			c.C1459T	p.Arg487Trp	Exon 10	Missense	Compound heterozygous	(28)

(Continued)

10.3389/fendo.2022.1086883

TABLE 2 Continued

Identified genes	Full name	MIM number	cDNA alteration	Amino acid alteration	Exon	Mutation	Zygosity in affected individuals	References
			c.756_758delTGA	p. Asn252Lysfs*316	Exon 4	Frameshift	Compound heterozygous	(28)
			c.1535+3A>G	p.?	IVS10	Splicing	Compound heterozygous	(26)
			c.946C > T	p. Leu316Phe	Exon 6	Missense	Compound heterozygous	(26)
TUBB8	Tubulin beta 8 class VIII	616768	c.629T>A	p.I210K	Exon 4	Missense	Heterozygous	(29)
			c.938C>T	p.A313V	Exon 4	Missense	Heterozygous	(29)
			c.1130T>C	p.L377P	Exon 4	Missense	Heterozygous	(29)
			c.1203_1204insCT	p.G402Lfs*15	Exon 4	Frameshift	Heterozygous	(29)
			c.613G>A	p.E205K	Exon 4	Missense	Heterozygous	(29)
			c.209 C > T	p.P70L	Exon 3	Missense	Homozygous	(30)
			c.260C>T	p.P87L	Exon 3	Missense	Heterozygous	(31)
			c.716G>C	p.C239S	Exon 4	Missense	Heterozygous	(31)
			c.322G>A	p.E108K	Exon 4	Missense	Homozygous	(32)
			c.1270C>T	p.Q424*	Exon 4	Nonsense	Compound heterozygous	(32)
			c.10A>C	p. I4L	Exon 1	Missense	Heterozygous	(32)
			c.1228G>A	p. E410K	Exon 4	Missense	Compound heterozygous	(32)
NLRP5	NLR family pyrin domain containing 5	609658	c.1598G>C	p.Arg533Pro	Exon 7	Missense	Compound heterozygous	(33)
			c.1919T>G	p.Leu640Arg	Exon 7	Missense	Compound heterozygous	(33)
			c.2274_2275del	p.Trp759Aspfs*4	NM	Frameshift	Homozygous	(34)
ACTL9	Actin like 9	619251	c.1034C>T	p.Ser345Leu	Exon 1	Missense	Homozygous	(36)
			c.1138G>T	p.Val380Leu	Exon 1	Missense	Homozygous	(36)
			c.1209C>G	p.Tyr403Ter	Exon 1	Nonsense	Homozygous	(36)
ACTL7A	Actin-like protein 7A	604303	c.463C>T	p.Arg155Ter	Exon 1	Nonsense	Compound heterozygous	(35)
			c.1084G>A	p.Gly362Arg	Exon 1	Missense	Compound heterozygous	(35)
ZP2	Zona pellucida glycoprotein 2	182888	c.1695-2A>G	p.C566H fs*5	Exon 4	Missense	Homozygous	(37)
			c.1691_1694dup	p.C566W fc*5	Exon 4	Frameshift	Homozygous	(37)

(Continued)

10.3389/fendo.2022.1086883

TABLE 2 Continued

Identified genes	Full name	MIM number	cDNA alteration	Amino acid alteration	Exon	Mutation	Zygosity in affected individuals	References
TLE6	transducin-like enhancer of split 6	612399	c.1226G>A	p.Arg409Gln	Exon 13	Missense	Homozygous	(39)
			c.1621G>A	p.Glu541Lys	Exon 17	Missense	Homozygous	(39)
			c.388G>A	p.Asp130Asn	Exon 7	Missense	Compound heterozygous	(39)
			c.1507G>A	p.Val503Ile	Exon 15	Missense	Compound heterozygous	(39)
			c.1529C > A	p.S510Y	NM	Splicing	Homozygous	(38)
DNAH17	Dynein axonemal heavy chain 17	610063	c.1048C>T	p.Arg350*	Exon 7	Nonsense	Compound heterozygous	(40)
			c.3390G>A	p.Met1130Ile	Exon 22	Missense	Compound heterozygous	(40)

NM, not mentioned.
*, indicated stop codon (nonsense mutation).

10.3389/fendo.2022.1086883

revealed gene mutations causing poor or failed fertilization after IVF/ICSI attempts (Table 2).

PLCZ1

Intracellular Ca^{2+} oscillations are a remarkable signaling phenomenon observed during the process of mammalian fertilization (41–43). Sperm-specific phospholipase C (PLC) termed PLCzeta (PLCZ1) is widely considered to be the physiological stimulus responsible for generating Ca^{2+} oscillations (44, 45). As the smallest member of the PLC family (~70 kDa in humans), PLCZ1 consists of a C-terminal C2 domain, four tandem Ca^{2+}-binding EF-hand domains, and the X and Y catalytic domains (45, 46). Each domain plays a specific role in determining the function of sperm PLCZ1 as a trigger of oocyte activation and early embryonic development (46). PLCZ1 identified in sperm from fertile men usually expressed within the equatorial, acrosomal, and post-acrosomal regions of the head (17, 47, 48).

In 2009, a point mutation (H398P) in the PLCZ1 gene [MIM: 608075] was first discovered in a non-globozoospermic case linked to defects in the ability of the sperm to induce calcium oscillations in the oocyte following ICSI (49). To date, 24 PLCZ1 variants associated with poor or failed fertilization after IVF/ICSI attempts have been identified using Sanger sequencing and WES in infertile men. Segregation analysis and family pedigrees showed that it was an autosomal recessive mode of inheritance (13–16, 19, 20, 46, 50). It was indicated that these 24 reported mutationswithin the PLCZ1 gene include missense, frameshift, splicing, and nonsense that were localized in the C2 domain, EF-hand domains, and catalytic domains. The homozygous nonsense mutation c.588C>A (p.Cys196*), which maps to the catalytic domain, has been frequently reported (13, 14, 20, 50). Interestingly, Torra-Massana et al. reported a missense variant, c.1499C>T (p.S500L), located in the C2-domain of PLCZ1, which seems to be the most frequent mutation (19). This mutation was found in nine patients with poor or failed fertilization after ICSI (19).

The pathogenicity of these identified mutations and their possible effects on PLCZ1 protein were assessed through bioinformatics analysis and revealed that these important mutations probably weakened the stability of protein function (15, 19, 20, 46, 50). PLCZ1 protein structure consists of two main regions: the catalytic domain (X- and Y-domains) and the regulatory region (EF-hands and C2- domains), suggesting that the distinct locations of identified mutations may have different effects on the PLCZ1 protein function, which may lead to different phenotypes: total or partial fertilization failure (19, 20). Additionally, microinjection with the wild-type or mutant PLCZ1 cRNA into oocytes was performed to evaluate the effect of the identified mutation on protein function. Microinjection with the mutant cRNA into oocytes failed to activate oocytes to induce the formation of pronuclear, while the injection of wild-type cRNA could effectively do, indicating that these mutations have an adverse influence on protein function (13, 15, 16, 19, 20).

The histological examination performed in PLCZ1 knockout mice revealed that loss of PLCZ1 has no deleterious effects on spermatogenesis or quality parameters associated with the ability of the sperm to penetrate, bind and fuse with the egg (18). However, PLCZ1-null sperm failed to trigger Ca^{2+} oscillations in the egg *in vitro*. In addition, the incidence of polyspermy following IVF or *in vivo* fertilization increased significantly, indicating that PLCZ1-null sperm cannot induce Ca^{2+} oscillations, which is involved in the mechanism of preventing polyspermy (18).

WEE2

WEE2 (WEE1 homolog 2, also known as WEE1B) [MIM: 614084] encodes a well-conserved oocyte-specific kinase which acts as an essential dual regulator of meiosis during prophase I and metaphase II by phosphorylating Tyr15 of the CDK1/cyclin B complex (M-phase promoting factor; MPF). In the GV stage of an oocyte, inhibition of WEE2 results in germinal vesicle breakdown (GVBD) and the resumption of meiosis. The WEE2 down-regulation leads to the failure of the MII stage exit and blockade of fertilization (51). WEE2 is predominantly expressed in the ovary of the rhesus macaque and weakly detectable in the testis, but not detected in any of the somatic tissues (52). Within the ovary, the expression of WEE2 persists in the germinal vesicle and cytoplasm of metaphase I and normal MII oocytes and reaches the highest level in preovulatory follicles (52).

In recent years, more and more evidence shows that WEE2 gene mutations may lead to fertilization failure and female infertility. Eight studies have so far reported a total of 27 mutations of WEE2 in patients with fertilization failure or poor fertilization, including 12 missense mutations, 10 frame-shift mutations, three splice-site mutations, and two nonsense mutations (21–24, 26–28, 53). The homozygous frameshift mutation c.1006_1007dup (p.His337Tyrfs*24) was repeatedly reported in three articles (27, 28, 53). Furthermore, in the study by Dai J et al., it was detected in four of nine patients, indicating that the incidence of this mutation is relatively high (53). These mutations follow an autosomal recessive pattern and proved to be truncated or loss of function, thereby reducing the protein level and disturbing the phosphorylation of WEE2 (22–24, 26–28, 53). In all reports describing female infertility linked to WEE2 mutations, nearly all the retrieved oocytes from affected individuals failed to form two pronuclei after IVF/ICSI attempts. Moreover, ICSI-AOA could not rescue fertilization failure (22, 26, 53). Interestingly, the researchers achieved phenotypic rescue by injection of WEE2 cRNA into affected oocytes, as indicated by the meiotic resumption, extrusion of the second polar body, and formation of pronuclei, embryonic development (28).

10.3389/fendo.2022.1086883

TABLE 3 Summary of gene mutations associated with poor or failed fertilization after IVF/ICSI and ART possible decision.

Gene		Phenotype in mutations				Mode of inheritance	MOAT#	ART possible decision
		Fertilization in IVF, %	Fertilization in ICSI, %	Fertilization in ICSI+AOA, %	References			
Sperm-related	*PLCZ1*	0-20.0%	0-66.7%	30.8-100%	(13–20)	AR	–	ICSI+AOA
	ACTL7A	NA	0%	76.9%	(35)	AR	NA	ICSI+AOA
	ACTL9	0%	0-16.7%	100%	(36)	AR	–	ICSI+AOA
	DNAH17	0%	0%	NA	(40)	AR	NA	ICSI+AOA or Donor sperm
Oocyte-related	*WEE2*	0-20.0%	0-25.0%	0%	(21–28)	AR	NA	Donor oocytes
	TUBB8	0-19.0%	0-19.0%	NA	(29–32)	AD, AR, *de novo*, incomplete dominance, unknown	NA	ICSI+AOA or Donor oocytes
	NLRP5	0%	0%	NA	(33, 34)	AR	NA	ICSI+AOA or Donor oocytes
	TLE6	0-50%	0-87.5%	NA	(38, 39)	AR	NA	ICSI or Donor oocytes
	ZP2	0%	80-100%	NA	(37)	AR	NA	ICSI

'-' represents a negative result, which means the percentage of two-cells is less than 20%; '+' represents a positive result, which means the percentage of two-cells is more than 90%. IVF, in vitro fertilization; ICSI, intracytoplasmic sperm injection; ICSI+AOA indicated that AOA (assisted oocyte activation) was performed on those oocytes that failed to fertilize in ICSI; MOAT, mouse oocyte activation test; FR, fertilization rate; AD, autosomal dominant; AR, autosomal recessive; ART, assisted reproductive technology; NA, not available.

TUBB8

TUBB8 (Tubulin beta 8 class VIII) [MIM:616768] encodes a highly conserved β-tubulin isotype that only exists in primates. Human β-tubulin consisted of nine isotypes, including TUBB1, TUBB2A, TUBB2B, TUBB3, TUBB4A, TUBB4B, TUBB5, TUBB6, and TUBB8 (25). TUBB8 accounts for the majority of all the β-tubulin isotype expressed in human oocytes and early embryos and play a key role in oocyte meiotic spindle assembly (54, 55). Most mutations in TUBB8 reported during recent years were associated with the maturation arrest of human oocytes and pre-implantation embryonic development abnormalities, while A few mutations in TUBB8 are responsible for poor or failed fertilization (29, 30, 32, 56).

Since 2016, 12 TUBB8 mutations associated with poor or failed fertilization have been identified using WES and Sanger sequencing. These TUBB8 mutations are paternally hereditary as an autosomal dominant, recessive inheritance or arise from *de novo*. It was indicated that 12 reported mutations in the TUBB8 gene include missense, nonsense, and frameshift. The effect of the TUBB8 mutations on microtubule dynamics, α/β tubulin heterodimeric assembly, and spindle assembly in mouse and human oocytes was evaluated by microinjection of the corresponding cRNAs (54, 55). The expression of wild-type and mutant forms of TUBB8 was measured in cultured cells (31, 54, 55). These mutations were found to interfere with α/β-tubulin heterodimeric folding, microtubule assembly, and stability, or to affect the interaction of microtubules with kinesin and potentially other microtubule-associated proteins (MAPs). The association of TUBB8 mutations with poor or failed fertilization may be due to that it results in abnormalities in the oocytes morphologically identifiable as MII, causing failure of the second polar body extrusion or zygote cleavage. The pathogenicity of these TUBB8 mutations was usually evaluated by a variety of methods, including spindle morphological observation, proband gene detection, pedigree segregation analysis, and *in vitro* experiments. However, it should be noted that due to a high prevalence of mutations in TUBB8, some of the mutations were only observed in the proband, and further *in vitro* functional verification was not carried out. Therefore, the causal relationship between these TUBB8 mutations and observed phenotypes needs to be further studied.

NLRP5

NLRP5 (NLR family, Pyrin domain containing 5) is a maternal effect gene [MIM: 609658], originally identified in

the mouse, which is exclusively expressed in the oocyte (57). The NLRP5-encoded protein belongs to the NALP protein family. Members of the NALP protein family typically consist of an amino N-terminal pyrin domain (PYD), a NACHT domain, and a carboxyl C-terminal leucine-rich repeat (LRR) region. PYD is a protein-protein interaction module, which has been identified in multiple human proteins involved in stress signaling pathways (58). The NACHT domain is presumed to bind ATP (59). LRR region is predicted to provide support for the formation of protein-protein interactions (60). As an oocyte-selective gene, NLRP5 plays a vital role in embryogenesis in mice (61), bovines (62), rhesus macaque monkeys (63), and humans (64). NLRP5 knockout female mice are infertile due to embryo development arrest at the 2-cell stage, although follicular development, oocyte maturation, and fertilization are fairly normal (61). In rhesus macaque, the NLRP5 knockout embryos had a block of embryogenesis between the 8-cell and the 16-cell stages (65). Peng H et al. reported that NLRP5 was required for preimplantation embryo development in cows, and NLRP5 knockout embryos were mainly arrested between the 2-cell and 8-cell stages (66). A recent report revealed that mutations in NLRP5 gene in human caused an early embryonic arrest (67).

NLRP5 mutations were shown to be associated with total fertilization failure after IVF/ICSI attempts. To date, two studies reported three mutations associated with fertilization failure (33, 68). In this regard, an autosomal recessive inheritance was suggested according to family pedigree. These identified mutations were missense and frameshift. The two missense variants (c.1598G>C and c.1919T>G; p.Arg533Pro and Leu640Arg), respectively located within the NACHT domain and LRR domain, are predicted to affect NLRP5 protein function, consequently, lead to total fertilization failure in IVF and ICSI cycles. Further studies are still required to reveal NLRP5 function in fertilization as well as its disruption effect on fertilization failure.

ACTL9 and ACTL7A

ACTL9 (Actin-like 9) [MIM: 619251] and ACTL7A (Actin-like 7A) [MIM: 604303] belong to the family of actin-related genes. They encode actin-like protein 9 and actin-like protein 7A, respectively. ACTL7A is an important paralog of ACTL9. ACTL9 and ACTL7A proteins are co-localized in the sub-acrosomal layer of perinuclear theca (PT) in sperm and interact with each other to maintain acrosomal anchoring to the nuclear membrane.

Two missense and one nonsense mutations in the ACTL9 gene were identified using WES and Sanger sequencing in three individuals with total fertilization failure or poor fertilization in IVF and ICSI attempts (34). ACTL9-mutated individuals exist a higher proportion of tapered-head sperm compared to those in fertile individuals. The sperm acrosome of affected individuals had an abnormal ultrastructure using transmission electron microscopy. These ACTL9 mutations were proved to weaken or lost the ability to interact with ACTL7A, resulting in the inner acrosomal membrane's detaching from the nuclear and forming a loosened perinuclear theca structure. Mutant sperm show PLCZ1 absence or abnormal localization, which leads to failure to stimulate Ca^{2+} oscillations (34).

Two compound heterozygous variants in ACTL7A were identified in a family with total fertilization failure after ICSI. Pedigree analysis indicated a recessive pattern of inheritance (36). The nonsense variant located in exon 1 of ACTL7A causes a premature stop codon and is predicted to be disease-causing. The missense variant is predicted to be damaging and disease-causing by using a silicon tool. The ultrastructure of the mutation sperm shows defects in the acrosome and perinuclear theca (36). The ACTL7A knock-in mouse model showed reduced expression and abnormal localization of PLCZ1, which could be responsible for the fertilization failure (35).

ZP2

Zona pellucida (ZP) is an extracellular glycoprotein matrix that surrounds oocytes and medicates several important roles in the acrosome reaction induction, blocking of polyspermy, and protection for the preimplantation embryo (69). ZP2 (zona pellucida glycoprotein 2) [MIM: 182888] encodes the ZP2 glycoprotein, which is a component of ZP composed of four glycoproteins (ZP1, ZP2, ZP3, and ZP4). ZP2 expression in humans was observed in oocytes and granulosa cells as early as the primordial follicle stage (70). Earlier studies on human ZP glycoproteins around the oocyte revealed that unlike ZP1, ZP3, and ZP4, ZP2 mainly binds to acrosome-reacted sperm and the N-terminus of ZP2 mediates the taxon-specific sperm-oocyte binding (71).

The human ZP2 gene, located on chromosome 16, has 19 exons and encodes a polypeptide of 745 amino acids (aa) (72). Two homozygous truncating pathogenic variants of the ZP2 gene were identified using Sanger sequencing in infertile women with IVF fertilization failure (73). The two identified variants were missense and frameshift respectively. Based on the family pedigree analysis, an autosomal recessive genetic mode of infertility was suggested. It was observed that oocytes from affected women had an abnormal ZP with a thinner matrix, and an enlarged perivitelline space compared with normal oocytes. By using transmission electron micrographs and polscope images, there was only one thin layer in the zona matrix of patient oocytes with an irregular network of filaments with large holes (73). The loss-of-function variants of the ZP2 gene led to defective ZP in gamete recognition. In conventional IVF, none of the oocytes were fertilized.

TLE6

TLE6 (Transducin-like enhancer of split 6) [MIM: 612399] is an effective gene that encodes the TLE6 protein, an essential member of the subcortical maternal complex (SCMC). The TLE6 gene is expressed only in ovaries as well as the oocytes and preimplantation embryos (37). By combining with a variety of maternal effector proteins, TLE6 protein forms SCMC has been linked to key processes occurring during the oocyte-to-embryo transition: cytoskeleton reorganization, meiotic spindle formation, and positioning, organelle redistribution, and cell division (37). Functional knockout studies of the TLE6 gene in mice showed the termination of embryo cleavage as the most phenotype (74). Several mutations within the TLE6 gene were shown to be associated with low-quality embryos (39, 75, 76). In 2015, a homozygous substitution (c.1529C > A) in TLE6 was verified by whole-exome sequencing in three infertile women (77). In 2020, a homozygous missense mutation (c.1226G>A (p.Arg409Gln) in exon 13 of TLE6 was found to be responsible for recurrent total fertilization failure in ICSI cycles (75). According to the in silico computational algorithms, this mutation is predicted to be probably damaging (75). A recessive inheritance pattern was suggested based on family pedigree analysis. Correspondingly, further studies are still required to reveal TLE6 function for the fertilization process.

DNAH17

The axoneme is the core structure of sperm flagellum and comprises an intricate network of protein complexes, where a central pair of microtubules is surrounded by nine peripheral microtubule doublets (MTDs) in the fixed order ("9 + 2" pattern). Axonemal dynein consist of the outer and inner dynein arms (ODAs and IDAs, respectively). Each dynein arm is a multi-protein ATPase complex, which is composed of light, intermediate, and heavy chain proteins. DNAH17 (Dynein axonemal heavy chain 17) [MIM: 610063], belonging to a member of the dynein axonemal heavy chains (DNAHs) family, encodes a heavy chain protein of ODAs. DNAH17 is mainly expressed in the testis and sperm. Previous reports had revealed that the biallelic mutations of DNAH17 in human sperm were associated with impaired motility and multiple morphological abnormalities of the flagella (MMAF), a rare type of asthenozoospermia which is characterized by absent, short, bent, coiled, and irregular flagella (38, 78–80). Noticeably, the knockout of DNAH17 in mice resulted in morphologically abnormal spermatozoa, showing a phenotype similar to a typical human MMAF phenotype (79).

ICSI is an effective technique used to treat infertility related to MMAF. However, two novel compound heterozygous mutations within the DNAH17 gene were identified using whole exome and Sanger sequencing in an infertile man with markedly diminished sperm motility and caused TFF after two ICSI attempts (81). The nonsense mutation results in a premature stop codon, which leads to a truncated and nonfunctional protein lacking all ATPase domains as well as a microtubule-binding region. The missense mutation was absent in population databases (EXAC, GNOMAD, 1000 Genomes Project) (81). Based on the family pedigree analysis, an autosomal recessive inheritance pattern was suggested. Briefly, mutations in DNAH17 are one of the sperm-related gene mutations associated with TFF.

Identification and treatments for sperm- or oocyte-borne activation deficiency

Human oocyte activation is characterized by a two-step pattern, called the trigger and oscillator (40). During natural fertilization, the trigger originates from the receptor-mediated interaction between the sperm and the oocyte plasma membrane. During ICSI, the trigger is replaced by a calcium influx called a 'pseudotrigger' generated by the injection procedure (40). The actions of the oscillator are described by a series of shorter calcium transients of high amplitude, resulting from the release of sperm-associated factors into the oocyte cytoplasm. The main cause of fertilization failure after IVF/ICSI is considered to be oocyte activation deficiency (OAD), which can be categorized into two kinds: oocyte-borne and sperm-borne activation deficiencies.

Several studies have tried to overcome fertilization failure through a variety of assisted oocyte activation (AOA) methods, including physical, mechanical, or chemical stimuli (82, 83). The application of ICSI combined with AOA improves fertilization rates in the majority of patients with ICSI failure (82, 83). However, not all patients benefit from AOA (84). Many reports have failed to identify which patients are candidates for AOA (85). Some cases of fertilization failure are not solely related to sperm-related OAD and may not require AOA treatment. Therefore, it is important to determine whether AOA is really necessary.

To differentiate between sperm-related OAD and oocyte-related OAD, the mouse oocyte activation test (MOAT), a heterologous ICSI model, can be used as a diagnostic tool (86). The sperm from patients was injected into mature mouse oocytes. Oocyte activation is assessed by examining the percentage of 2-cell formation. When not activated, sperm deficiency is assumed; otherwise, it is suspected that the oocyte is deficient. According to the results of the MOAT, AOA methods can be proposed to correct clear sperm-related OAD (84, 86). Due to inevitable limitations in the heterologous ICSI model, such as multiple steps, long time, and lack of reliability, the PLCZ1 screening assay was recommended to evaluate an oocyte- or sperm-related OAD by a recent study (87).

High throughput sequencing techniques have helped discover some causative gene mutations in infertile couples related to male or female factors associated with poor or failed fertilization after IVF/ICSI attempts. In recent years, a series of mutations in *PLCZ1*, *ACTL7A*, *ACTL9*, *DNAH17*, *WEE2*, *TUBB8, NLRP5, ZP2*, and *TLE6* genes have been identified as potential markers for evaluating fertilization failure in humans (Table 2). Table 3 presents that the use of AOA greatly improves fertilization rates in human cases with sperm-related mutations. However, the AOA method cannot effectively rescue the phenotypes of fertilization failure in cases with oocyte-related mutations (21, 22, 26, 32).

The reasons for fertilization failure caused by oocyte-related defects are often complicated and not easily accepted. Little is known about how to treat oocyte-borne oocyte activation failures. Tesarik J et al. reported that sperm-borne and oocyte-borne oocyte activation failures could be overcome by the use of a modified ICSI technique (40). Heindryckx B et al. recommend AOA as an efficient treatment option in cases of both oocyte- or sperm-related fertilization failure (84). However, these studies mainly focused on case reports. In a recent study, which included 114 patients with a history of extremely poor or complete fertilization failure, the modified stimulation protocol improved clinical outcomes in patients with an oocyte-related OAD (87). A large-sample investigation is needed to support the results.

Conclusions

The increasing number of IVF/ICSI cycles provides a unique opportunity to systematically evaluate the phenotype of fertilization defects. In the present review, we summarized a series of gene mutations related to poor or failed fertilization, mainly based on high throughput sequencing techniques in the past 10 years. In these studies, a portion of patients with sperm-related mutations obtained pregnancies through ICSI with AOA (13, 19, 34, 36, 46, 50). Just one couple carrying DNAH17 mutations achieved a live birth through donor sperm IVF (81). On the contrary, patients with oocyte-related mutations rarely had their babies, and it was reported that only one patient carrying ZP2 mutations gave birth after ICSI treatment. For women carrying the mutations of WEE2, TUBB8, NLRP5, and TLE6, oocyte donation is considered to be an effective strategy. These findings will help to reveal genetic causes and biomarkers behind poor or failed fertilization and provide some guidance for physicians in hereditary counseling and optimizing clinical treatments.

Author contributions

YMX and KL collected the literature and drafted the original manuscript. XHC and YPX discussed and revised the manuscript. YMX and KL designed, revised, and edited the work. All authors contributed to the article and approved the submitted version.

Funding

This work was supported by the Zhejiang Provincial Natural Science Foundation (LY22H040011), the Zhejiang Provincial Program for the Cultivation of High-level Innovative Health talents (The year 2018), and the Special Supporting Program Project for the Research Institutions of Zhejiang Province (C11920D-04).

Conflict of interest

The authors declare that the research was conducted in the absence of any commercial or financial relationships that could be construed as a potential conflict of interest.

Publisher's note

References

1. Budhwar S, Singh V, Verma P, Singh K. Fertilization failure and gamete health: Is there a link? *Front Biosci (Schol Ed)* (2017) 9(3):395–419. doi: 10.2741/s494

2. Georgadaki K, Khoury N, Spandidos DA, Zoumpourlis V. The molecular basis of fertilization (Review). *Int J Mol Med* (2016) 38(4):979–86. doi: 10.3892/ijmm.2016.2723

3. van der Westerlaken L, Helmerhorst F, Dieben S, Naaktgeboren N. Intracytoplasmic sperm injection as a treatment for unexplained total fertilization failure or low fertilization after conventional in vitro fertilization. *Fertil Steril* (2005) 83(3):612–7. doi: 10.1016/j.fertnstert.2004.08.029

4. Trounson AO, Leeton JF, Wood C, Webb J, Kovacs G. The investigation of idiopathic infertility by in vitro fertilization. *Fertil Steril* (1980) 34(5):431–8. doi: 10.1016/s0015-0282(16)45132-0

5. Barlow P, Englert Y, Puissant F, Lejeune B, Delvigne A, Van Rysselberge M, et al. Fertilization failure in ivf: Why and what next? *Hum Reprod* (1990) 5(4):451–6. doi: 10.1093/oxfordjournals.humrep.a137122

6. Palermo G, Joris H, Devroey P, Van Steirteghem AC. Pregnancies after intracytoplasmic injection of single spermatozoon into an oocyte. *Lancet* (1992) 340(8810):17–8. doi: 10.1016/0140-6736(92)92425-f

7. Van Steirteghem A, Liu J, Nagy Z, Joris H, Tournaye H, Liebaers I, et al. Use of assisted fertilization. *Hum Reprod* (1993) 8(11):1784–5. doi: 10.1093/oxfordjournals.humrep.a137934

8. Van Steirteghem AC, Liu J, Joris H, Nagy Z, Janssenswillen C, Tournaye H, et al. Higher success rate by intracytoplasmic sperm injection than by subzonal insemination. report of a second series of 300 consecutive treatment cycles. *Hum Reprod* (1993) 8(7):1055–60. doi: 10.1093/oxfordjournals.humrep.a138191

9. Van Steirteghem AC, Nagy Z, Joris H, Liu J, Staessen C, Smitz J, et al. High fertilization and implantation rates after intracytoplasmic sperm injection. *Hum Reprod* (1993) 8(7):1061–6. doi: 10.1093/oxfordjournals.humrep.a138192

10. Li Z, Wang AY, Bowman M, Hammarberg K, Farquhar C, Johnson L, et al. Icsi does not increase the cumulative live birth rate in non-Male factor infertility. *Hum Reprod* (2018) 33(7):1322–30. doi: 10.1093/humrep/dey118

11. Yeste M, Jones C, Amdani SN, Patel S, Coward K. Oocyte activation deficiency: A role for an oocyte contribution? *Hum Reprod Update* (2016) 22 (1):23–47. doi: 10.1093/humupd/dmv040

12. Yanagida K. Complete fertilization failure in icsi. *Hum Cell* (2004) 17 (4):187–93. doi: 10.1111/j.1749-0774.2004.tb00042.x

13. Mu J, Zhang Z, Wu L, Fu J, Chen B, Yan Z, et al. The identification of novel mutations in Plcz1 responsible for human fertilization failure and a therapeutic intervention by artificial oocyte activation. *Mol Hum Reprod* (2020) 26(2):80–7. doi: 10.1093/molehr/gaaa003

14. Wang F, Zhang J, Kong S, Li C, Zhang Z, He X, et al. A homozygous nonsense mutation of Plcz1 cause Male infertility with oocyte activation deficiency. *J Assist Reprod Genet* (2020) 37(4):821–8. doi: 10.1007/s10815-020-01719-4

15. Escoffier J, Lee HC, Yassine S, Zouari R, Martinez G, Karaouzène T, et al. Homozygous mutation of Plcz1 leads to defective human oocyte activation and infertility that is not rescued by the ww-binding protein pawp. *Hum Mol Genet* (2016) 25(5):878–91. doi: 10.1093/hmg/ddv617

16. Yuan P, Yang C, Ren Y, Yan J, Nie Y, Yan L, et al. A novel homozygous mutation of phospholipase c zeta leading to defective human oocyte activation and fertilization failure. *Hum Reprod* (2020) 35(4):977–85. doi: 10.1093/humrep/dez293

17. Grasa P, Coward K, Young C, Parrington J. The pattern of localization of the putative oocyte activation factor, phospholipase czeta, in uncapacitated, capacitated, and ionophore-treated human spermatozoa. *Hum Reprod* (2008) 23 (11):2513–22. doi: 10.1093/humrep/den280

18. Hachem A, Godwin J, Ruas M, Lee HC, Ferrer Buitrago M, Ardestani G, et al. Plcζ is the physiological trigger of the Ca(2+) oscillations that induce embryogenesis in mammals but conception can occur in its absence. *Development* (2017) 144(16):2914–24. doi: 10.1242/dev.150227

19. Torra-Massana M, Cornet-Bartolomé D, Barragán M, Durban M, Ferrer-Vaquer A, Zambelli F, et al. Novel phospholipase c zeta 1 mutations associated with fertilization failures after icsi. *Hum Reprod* (2019) 34(8):1494–504. doi: 10.1093/humrep/dez094

20. Yan Z, Fan Y, Wang F, Yan Z, Li M, Ouyang J, et al. Novel mutations in Plcz1 cause Male infertility due to fertilization failure or poor fertilization. *Hum Reprod* (2020) 35(2):472–81. doi: 10.1093/humrep/dez282

21. Wang A, Huang S, Liu M, Wang B, Wu F, Zhu D, et al. Clinical exome sequencing identifies novel compound heterozygous mutations of the Wee2 gene in primary infertile women with fertilization failure. *Gynecol Endocrinol* (2021) 37 (12):1096–101. doi: 10.1080/09513590.2021.1916458

22. Tian Y, Wang G, Wang J, Mu X, Chen H, Song X, et al. Novel compound heterozygous mutation in Wee2 is associated with fertilization failure: Case report of an infertile woman and literature review. *BMC Womens Health* (2020) 20(1):246. doi: 10.1186/s12905-020-01111-5

23. Zhou X, Zhu L, Hou M, Wu Y, Li Z, Wang J, et al. Novel compound heterozygous mutations in Wee2 causes female infertility and fertilization failure. *J Assist Reprod Genet* (2019) 36(9):1957–62. doi: 10.1007/s10815-019-01553-3

24. Zhao S, Chen T, Yu M, Bian Y, Cao Y, Ning Y, et al. Novel Wee2 gene variants identified in patients with fertilization failure and female infertility. *Fertil Steril* (2019) 111(3):519–26. doi: 10.1016/j.fertnstert.2018.11.018

25. Sirajuddin M, Rice LM, Vale RD. Regulation of microtubule motors by tubulin isotypes and post-translational modifications. *Nat Cell Biol* (2014) 16 (4):335–44. doi: 10.1038/ncb2920

26. Yang X, Shu L, Cai L, Sun X, Cui Y, Liu J. Homozygous missense mutation Arg207cys in the Wee2 gene causes female infertility and fertilization failure. *J Assist Reprod Genet* (2019) 36(5):965–71. doi: 10.1007/s10815-019-01418-9

27. Jin J, Tong X, Zhang YL, Yang W, Ma Y, Ren P, et al. Novel Wee2 compound heterozygous mutations identified in patients with fertilization failure or poor fertilization. *J Assist Reprod Genet* (2021) 38(11):2861–9. doi: 10.1007/s10815-021-02285-z

28. Sang Q, Li B, Kuang Y, Wang X, Zhang Z, Chen B, et al. Homozygous mutations in Wee2 cause fertilization failure and female infertility. *Am J Hum Genet* (2018) 102(4):649–57. doi: 10.1016/j.ajhg.2018.02.015

29. Zhao L, Guan Y, Wang W, Chen B, Xu S, Wu L, et al. Identification novel mutations in Tubb8 in female infertility and a novel phenotype of Large polar body in oocytes with Tubb8 mutations. *J Assist Reprod Genet* (2020) 37(8):1837–47. doi: 10.1007/s10815-020-01830-6

30. Chen B, Wang W, Peng X, Jiang H, Zhang S, Li D, et al. The comprehensive mutational and phenotypic spectrum of Tubb8 in female infertility. *Eur J Hum Genet* (2019) 27(2):300–7. doi: 10.1038/s41431-018-0283-3

31. Yao Z, Zeng J, Zhu H, Zhao J, Wang X, Xia Q, et al. Mutation analysis of the Tubb8 gene in primary infertile women with oocyte maturation arrest. *J Ovarian Res* (2022) 15(1):38. doi: 10.1186/s13048-022-00971-9

32. Yang P, Yin C, Li M, Ma S, Cao Y, Zhang C, et al. Mutation analysis of tubulin beta 8 class viii in infertile females with oocyte or embryonic defects. *Clin Genet* (2021) 99(1):208–14. doi: 10.1111/cge.13855

33. Maddirevula S, Awartani K, Coskun S, AlNaim LF, Ibrahim N, Abdulwahab F, et al. A genomics approach to females with infertility and recurrent pregnancy loss. *Hum Genet* (2020) 139(5):605–13. doi: 10.1007/s00439-020-02143-5

34. Dai J, Zhang T, Guo J, Zhou Q, Gu Y, Zhang J, et al. Homozygous pathogenic variants in Actl9 cause fertilization failure and Male infertility in humans and mice. *Am J Hum Genet* (2021) 108(3):469–81. doi: 10.1016/j.ajhg.2021.02.004

35. Xin A, Qu R, Chen G, Zhang L, Chen J, Tao C, et al. Disruption in Actl7a causes acrosomal ultrastructural defects in human and mouse sperm as a novel Male factor inducing early embryonic arrest. *Sci Adv* (2020) 6(35):eaaz4796. doi: 10.1126/sciadv.aaz4796

36. Wang J, Zhang J, Sun X, Lin Y, Cai L, Cui Y, et al. Novel bi-allelic variants in Actl7a are associated with Male infertility and total fertilization failure. *Hum Reprod* (2021) 36(12):3161–9. doi: 10.1093/humrep/deab228

37. Bebbere D, Albertini DF, Coticchio G, Borini A, Ledda S. The subcortical maternal complex: Emerging roles and novel perspectives. *Mol Hum Reprod* (2021) 27(7):gaab043. doi: 10.1093/molehr/gaab043

38. Sha Y, Wei X, Ding L, Mei L, Huang X, Lin S, et al. Dnah17 is associated with asthenozoospermia and multiple morphological abnormalities of sperm flagella. *Ann Hum Genet* (2020) 84(3):271–9. doi: 10.1111/ahg.12369

39. Liu J, Tan Z, He J, Jin T, Han Y, Hu L, et al. Two novel mutations in Padi6 and Tle6 genes cause female infertility due to arrest in embryonic development. *J Assist Reprod Genet* (2021) 38(6):1551–9. doi: 10.1007/s10815-021-02194-1

40. Tesarik J, Rienzi L, Ubaldi F, Mendoza C, Greco E. Use of a modified intracytoplasmic sperm injection technique to overcome sperm-borne and oocyte-borne oocyte activation failures. *Fertil Steril* (2002) 78(3):619–24. doi: 10.1016/s0015-0282(02)03291-0

41. Runft LL, Jaffe LA, Mehlmann LM. Egg activation at fertilization: Where it all begins. *Dev Biol* (2002) 245(2):237–54. doi: 10.1006/dbio.2002.0600

42. Stricker SA. Comparative biology of calcium signaling during fertilization and egg activation in animals. *Dev Biol* (1999) 211(2):157–76. doi: 10.1006/dbio.1999.9340

43. Tesarik J, Sousa M. Mechanism of calcium oscillations in human oocytes: A two-store model. *Mol Hum Reprod* (1996) 2(6):383–6. doi: 10.1093/molehr/2.6.383

44. Cuthbertson KS, Cobbold PH. Phorbol ester and sperm activate mouse oocytes by inducing sustained oscillations in cell Ca2+. *Nature* (1985) 316 (6028):541–2. doi: 10.1038/316541a0

45. Kashir J. Increasing associations between defects in phospholipase c zeta and conditions of Male infertility: Not just icsi failure? *J Assist Reprod Genet* (2020) 37 (6):1273–93. doi: 10.1007/s10815-020-01748-z

46. Yuan P, Zheng L, Liang H, Lin Q, Ou S, Zhu Y, et al. Novel mutations in the Plcz1 gene associated with human low or failed fertilization. *Mol Genet Genom Med* (2020) 8(10):e1470. doi: 10.1002/mgg3.1470

47. Saleh A, Kashir J, Thanassoulas A, Safieh-Garabedian B, Lai FA, Nomikos M. Essential role of sperm-specific plc-zeta in egg activation and Male factor infertility: An update. *Front Cell Dev Biol* (2020) 8:28. doi: 10.3389/fcell.2020.00028

48. Yeste M, Jones C, Amdani SN, Yelumalai S, Mounce G, da Silva SJ, et al. Does advancing Male age influence the expression levels and localisation patterns of phospholipase c zeta (Plcζ) in human sperm? *Sci Rep* (2016) 6:27543. doi: 10.1038/srep27543

49. Heytens E, Parrington J, Coward K, Young C, Lambrecht S, Yoon SY, et al. Reduced amounts and abnormal forms of phospholipase c zeta (Plczeta) in spermatozoa from infertile men. *Hum Reprod* (2009) 24(10):2417–28. doi: 10.1093/humrep/dep207

50. Dai J, Dai C, Guo J, Zheng W, Zhang T, Li Y, et al. Novel homozygous variations in Plcz1 lead to poor or failed fertilization characterized by abnormal

localization patterns of plcζ in sperm. *Clin Genet* (2020) 97(2):347–51. doi: 10.1111/cge.13636

51. Hanna CB, Mudaliar D, John K, Allen CL, Sun L, Hawkinson JE, et al. Development of Wee2 kinase inhibitors as novel non-hormonal female contraceptives that target meiosisdagger. *Biol Reprod* (2020) 103(2):368–77. doi: 10.1093/biolre/ioaa097

52. Hanna CB, Yao S, Patta MC, Jensen JT, Wu X. Wee2 is an oocyte-specific meiosis inhibitor in rhesus macaque monkeys. *Biol Reprod* (2010) 82(6):1190–7. doi: 10.1095/biolreprod.109.081984

53. Dai J, Zheng W, Dai C, Guo J, Lu C, Gong F, et al. New biallelic mutations in Wee2: Expanding the spectrum of mutations that cause fertilization failure or poor fertilization. *Fertil Steril* (2019) 111(3):510–8. doi: 10.1016/j.fertnstert.2018.11.013

54. Feng R, Sang Q, Kuang Y, Sun X, Yan Z, Zhang S, et al. Mutations in Tubb8 and human oocyte meiotic arrest. *N Engl J Med* (2016) 374(3):223–32. doi: 10.1056/NEJMoa1510791

55. Feng R, Yan Z, Li B, Yu M, Sang Q, Tian G, et al. Mutations in Tubb8 cause a multiplicity of phenotypes in human oocytes and early embryos. *J Med Genet* (2016) 53(10):662–71. doi: 10.1136/jmedgenet-2016-103891

56. Chen B, Li B, Li D, Yan Z, Mao X, Xu Y, et al. Novel mutations and structural deletions in Tubb8: Expanding mutational and phenotypic spectrum of patients with arrest in oocyte maturation, fertilization or early embryonic development. *Hum Reprod* (2017) 32(2):457–64. doi: 10.1093/humrep/dew322

57. Tong ZB, Nelson LM, Dean J. Mater encodes a maternal protein in mice with a leucine-rich repeat domain homologous to porcine ribonuclease inhibitor. *Mamm Genome* (2000) 11(4):281–7. doi: 10.1007/s003350010053

58. Kohl A, Grutter MG. Fire and death: The pyrin domain joins the death-domain superfamily. *C R Biol* (2004) 327(12):1077–86. doi: 10.1016/j.crvi.2004.08.006

59. Koonin EV, Aravind L. The nacht family - a new group of predicted ntpases implicated in apoptosis and mhc transcription activation. *Trends Biochem Sci* (2000) 25(5):223–4. doi: 10.1016/s0968-0004(00)01577-2

60. Kobe B, Kajava AV. The leucine-rich repeat as a protein recognition motif. *Curr Opin Struct Biol* (2001) 11(6):725–32. doi: 10.1016/s0959-440x(01)00266-4

61. Tong ZB, Gold L, Pfeifer KE, Dorward H, Lee E, Bondy CA, et al. Mater, a maternal effect gene required for early embryonic development in mice. *Nat Genet* (2000) 26(3):267–8. doi: 10.1038/81547

62. Ponsuksili S, Brunner RM, Goldammer T, Kuhn C, Walz C, Chomdej S, et al. Bovine Nalp5, Nalp8, and Nalp9 genes: Assignment to a qtl region and the expression in adult tissues, oocytes, and preimplantation embryos. *Biol Reprod* (2006) 74(3):577–84. doi: 10.1095/biolreprod.105.045096

63. McDaniel P, Wu X. Identification of oocyte-selective nlrp genes in rhesus macaque monkeys (Macaca mulatta). *Mol Reprod Dev* (2009) 76(2):151–9. doi: 10.1002/mrd.20937

64. Tschopp J, Martinon F, Burns K. Nalps: A novel protein family involved in inflammation. *Nat Rev Mol Cell Biol* (2003) 4(2):95–104. doi: 10.1038/nrm1019

65. Wu X. Maternal depletion of Nlrp5 blocks early embryogenesis in rhesus macaque monkeys (Macaca mulatta). *Hum Reprod* (2009) 24(2):415–24. doi: 10.1093/humrep/den403

66. Peng H, Liu F, Li W, Zhang W. Knockdown of Nlrp5 arrests early embryogenesis in sows. *Anim Reprod Sci* (2015) 163:151–6. doi: 10.1016/j.anireprosci.2015.11.004

67. Mu J, Wang W, Chen B, Wu L, Li B, Mao X, et al. Mutations in Nlrp2 and Nlrp5 cause female infertility characterised by early embryonic arrest. *J Med Genet* (2019) 56(7):471–80. doi: 10.1136/jmedgenet-2018-105936

68. Li M, Jia M, Zhao X, Shi R, Xue X. A new Nlrp5 mutation causes female infertility and total fertilization failure. *Gynecol Endocrinol* (2021) 37(3):283–4. doi: 10.1080/09513590.2020.1832069

69. Lefievre L, Conner SJ, Salpekar A, Olufowobi O, Ashton P, Pavlovic B, et al. Four zona pellucida glycoproteins are expressed in the human. *Hum Reprod* (2004) 19(7):1580–6. doi: 10.1093/humrep/deh301

70. Gook DA, Edgar DH, Borg J, Martic M. Detection of zona pellucida proteins during human folliculogenesis. *Hum Reprod* (2008) 23(2):394–402. doi: 10.1093/humrep/dem373

71. Tsubamoto H, Hasegawa A, Nakata Y, Naito S, Yamasaki N, Koyama K. Expression of recombinant human zona pellucida protein 2 and its binding capacity to spermatozoa. *Biol Reprod* (1999) 61(6):1649–54. doi: 10.1095/biolreprod61.6.1649

72. Gupta SK. Human zona pellucida glycoproteins: Binding characteristics with human spermatozoa and induction of acrosome reaction. *Front Cell Dev Biol* (2021) 9:619868. doi: 10.3389/fcell.2021.619868

73. Dai C, Hu L, Gong F, Tan Y, Cai S, Zhang S, et al. Zp2 pathogenic variants cause in vitro fertilization failure and female infertility. *Genet Med* (2019) 21(2):431–40. doi: 10.1038/s41436-018-0064-y

74. Feng M, Bai Y, Chen Y, Wang K. Knockout of the transducin-like enhancer of split 6 gene affects the proliferation and cell cycle process of mouse spermatogonia. *Int J Mol Sci* (2020) 21(16):5827. doi: 10.3390/ijms21165827

75. Lin J, Xu H, Chen B, Wang W, Wang L, Sun X, et al. Expanding the genetic and phenotypic spectrum of female infertility caused by Tle6 mutations. *J Assist Reprod Genet* (2020) 37(2):437–42. doi: 10.1007/s10815-019-01653-0

76. Mao B, Jia X, Liu H, Xu X, Zhao X, Yuan Y, et al. A novel Tle6 mutation, C.541+1g>a, identified using whole-exome sequencing in a Chinese family with female infertility. *Mol Genet Genom Med* (2021) 9(8):e1743. doi: 10.1002/mgg3.1743

77. Alazami AM, Awad SM, Coskun S, Al-Hassan S, Hijazi H, Abdulwahab FM, et al. Tle6 mutation causes the earliest known human embryonic lethality. *Genome Biol* (2015) 16:240. doi: 10.1186/s13059-015-0792-0

78. Whitfield M, Thomas L, Bequignon E, Schmitt A, Stouvenel L, Montantin G, et al. Mutations in Dnah17, encoding a sperm-specific axonemal outer dynein arm heavy chain, cause isolated Male infertility due to asthenozoospermia. *Am J Hum Genet* (2019) 105(1):198–212. doi: 10.1016/j.ajhg.2019.04.015

79. Zhang B, Ma H, Khan T, Ma A, Li T, Zhang H, et al. A Dnah17 missense variant causes flagella destabilization and asthenozoospermia. *J Exp Med* (2020) 217(2):e20182365. doi: 10.1084/jem.20182365

80. Zheng R, Sun Y, Jiang C, Chen D, Yang Y, Shen Y. A novel mutation in Dnah17 is present in a patient with multiple morphological abnormalities of the flagella. *Reprod BioMed Online* (2021) 43(3):532–41. doi: 10.1016/j.rbmo.2021.05.009

81. Jia M, Shi R, Xue X. Novel Dnah17 mutations associated with fertilization failures after icsi. *Gynecol Endocrinol* (2021) 37(8):769–71. doi: 10.1080/09513590.2021.1937979

82. Nasr-Esfahani MH, Deemeh MR, Tavalaee M. Artificial oocyte activation and intracytoplasmic sperm injection. *Fertil Steril* (2010) 94(2):520–6. doi: 10.1016/j.fertnstert.2009.03.061

83. Vanden Meerschaut F, Nikiforaki D, Heindryckx B, De Sutter P. Assisted oocyte activation following icsi fertilization failure. *Reprod BioMed Online* (2014) 28(5):560–71. doi: 10.1016/j.rbmo.2014.01.008

84. Heindryckx B, van der Elst J, De Sutter P, Dhont M. Treatment option for sperm- or oocyte-related fertilization failure: Assisted oocyte activation following diagnostic heterologous icsi. *Hum Reprod* (2005) 20(8):2237–41. doi: 10.1093/humrep/dei029

85. Rubino P, Vigano P, Luddi A, Piomboni P. The icsi procedure from past to future: A systematic review of the more controversial aspects. *Hum Reprod Update* (2016) 22(2):194–227. doi: 10.1093/humupd/dmv050

86. Rybouchkin A, Dozortsev D, Pelinck MJ, De Sutter P, Dhont M. Analysis of the oocyte activating capacity and chromosomal complement of round-headed human spermatozoa by their injection into mouse oocytes. *Hum Reprod* (1996) 11(10):2170–5. doi: 10.1093/oxfordjournals.humrep.a019071

87. Cheung S, Xie P, Parrella A, Keating D, Rosenwaks Z, Palermo GD. Identification and treatment of men with phospholipase czeta-defective spermatozoa. *Fertil Steril* (2020) 114(3):535–44. doi: 10.1016/j.fertnstert.2020.04.044

frontiers | Frontiers in Endocrinology

TYPE Original Research
PUBLISHED 04 January 2023
DOI 10.3389/fendo.2022.1091107

OPEN ACCESS

EDITED BY
Tao Luo,
Nanchang University, China

REVIEWED BY
Ying Chen,
Nanchang University, China
Hao Wu,
Center for Excellence in Molecular Cell Science, Chinese Academy of Sciences (CAS), China
Rui Guo,
Anhui Medical University, China

*CORRESPONDENCE
Hong Li
hongli@njmu.edu.cn
Yibo Wu
moliaty@aliyun.com
Jinxing Lv
szdalv@163.com

†These authors have contributed equally to this work

SPECIALTY SECTION
This article was submitted to Reproduction, a section of the journal Frontiers in Endocrinology

RECEIVED 06 November 2022
ACCEPTED 14 December 2022
PUBLISHED 04 January 2023

CITATION
Meng Z, Meng Q, Gao T, Zhou H, Xue J, Li H, Wu Y and Lv J (2023) Identification of bi-allelic *KIF9* loss-of-function variants contributing to asthenospermia and male infertility in two Chinese families. *Front. Endocrinol.* 13:1091107. doi: 10.3389/fendo.2022.1091107

Identification of bi-allelic *KIF9* loss-of-function variants contributing to asthenospermia and male infertility in two Chinese families

Zhixiang Meng[1†], Qingxia Meng[2†], Tingting Gao[3†], Hui Zhou[4], Jiajia Xue[1], Hong Li[2*], Yibo Wu[4*] and Jinxing Lv[1*]

[1]Center for Reproduction, Suzhou Dushu Lake Hospital (Dushu Lake Hospital Affiliated to Soochow University), Suzhou, China, [2]State Key Laboratory of Reproductive Medicine, Center for Reproduction and Genetics, Suzhou Municipal Hospital, The Affiliated Suzhou Hospital of Nanjing Medical University, Gusu School, Nanjing Medical University, Suzhou, China, [3]Changzhou Maternal and Child Health Care Hospital, Changzhou Medical Center, Nanjing Medical University, Changzhou, China, [4]Human Reproductive and Genetic Center, Affiliated Hospital of Jiangnan University, Wuxi, China

Introduction: Asthenozoospermia (AZS) is a leading cause of male infertility, affecting an estimated 18% of infertile patients. Kinesin proteins function as molecular motors capable of moving along microtubules. The highly conserved kinesin family member 9 (*KIF9*) localizes to the central microtubule pair in the flagella of *Chlamydomonas* cells. The loss of KIF9 expression in mice has been linked to AZS phenotypes.

Methods: Variant screening was performed by whole exome sequencing from 92 Chinese infertile patients with AZS. Western blot was used to was used for analyzing of candidate proteins expression. Patients' sperm samples were stained with immunofluorescent to visualise proteins localization and were visualised by transmission electron microscopy (TEM) to determine axoneme structures. Co-immunoprecipitation assay was used to verify the binding proteins of KIF9. In vitro fertilization (IVF) was used to evaluate the efficiency of clinical treatment.

Results: Bi-allelic *KIF9* loss-of-function variants were identified in two unrelated Chinese males exhibiting atypical sperm motility phenotypes. Both of these men exhibited typical AZS and suffered from infertility together with the complete absence of *KIF9* expression. In contrast to these KIF9-deficient patients, positive *KIF9* staining was evident throughout the flagella of sperm from normal control individuals. *KIF9* was able to interact with the microtubule central pair (CP) component hydrocephalus-inducing protein homolog (HYDIN) in human samples. And *KIF9* was undetectable in spermatozoa harboring CP deletions. The morphologicy of *KIF9*-deficient spermatozoa appeared normal under gross examination and TEM. Like in mice, *in vitro* fertilization was sufficient to overcome the fertility issues for these two patients

10.3389/fendo.2022.1091107

Discussion: These findings indicate that KIF9 associates with the central microtubules in human sperm and that it functions to specifically regulate flagellar swinging. Overall, these results offer greater insight into the biological functions of KIF9 in the assembly of the human flagella and its role in male fertility.

KEYWORDS

male infertility, asthenozoospermia, KIF9, HYDIN, flagellum

Introduction

Infertility, which is defined as the inability to achieve a successful pregnancy despite regular sexual intercourse for at least 12 months, is estimated to impact at least 12% of couples (1). Asthenospermia (AZS) is among the most prevalent of the male infertility-related phenotypes, and is characterized by poor sperm motility, defined by either < 40% total motility or < 32% forward motility (2). The majority of AZS phenotypes are not solely associated with aberrant sperm motility, and instead arise from some combination of AZS and oligo- and/or teratozoospermia referred to as oligo-astheno-teratozoospermia (OAT), including instances of multiple morphological abnormalities of the sperm flagella (MMAF) (3, 4). However, the spermatozoa of roughly 25% of AZS patients do not exhibit any clear structural defects (5).

Sperm flagella consist of an evolutionarily conserved axoneme core, composed of nine outer microtubule doublets (DMTs) and a central pair (CP) of microtubules in a 9 + 2 structure. The flagella also include periaxonemal structures, including the mitochondrial sheath (MS) and fibrous sheath (FS) in the midpiece and principal piece regions, respectively, as well as outer dense fibers (ODFs) present in both the midpiece and proximal principal piece regions (6). To date, many single-gene variants have been shown to cause AZS and associated morphological defects by damaging the integrity of these flagellar structures (7–12). In addition to these structures, other smaller functional flagellar components that are difficult to distinguish under transmission electron microscopy also play important roles in flagellar function, including the tektins which consist of bundles of helical tektin filaments (13, 14). Mutations that damage these structures can result in AZS without having any significant impact on the overt flagellar structure (13–16). Nevertheless, spermatozoa motility relies upon all of these structures.

Kinesins are motor proteins that generally move in an anterograde fashion along microtubules. To date, 45 human kinesin superfamily (KIF) proteins have been identified and shown to exhibit a diverse range of functions. Of these, *KIF9* is a highly conserved kinesin that is enriched in the testes of mice and has been shown to interact with hydrocephalus-inducing protein homolog (HYDIN) and to localize to the axonemal CP (17, 18). Deletion of murine *Kif9* impairs flagellar motility of sperm, resulting in male infertility (18). KIF9 is also reportedly important for ciliary beating and the maintenance of the integrity of the distal end of axonemal structures including the dynein arms, radial spokes, and CP in contrast to the somewhat subtle phenotypes reported in murine sperm flagella (18, 19). The present study was designed in part to explore the impact of the loss of KIF9 expression on the function and structural characteristics of human spermatozoa.

Here, a whole exome sequencing (WES) approach led to the identification of two unrelated human males with AZS harboring pathological homozygous variants in *KIF9* (NM_001134878.3). *KIF9* consists of 22 exons and is encoded on chromosome 3. These homozygous *KIF9* variants resulted in significant downregulation of the gene in spermatozoa. Further analysis revealed that KIF9 is expressed on the CP in the flagella of healthy human spermatozoa where it functions as a regulator of flagellar swing. Notably, *in vitro* fertilization (IVF) was able to successfully overcome the infertility issues facing these two *KIF9*-deficient patients. These results offer a theoretical foundation for the treatment of patients diagnosed with AZS resulting from *KIF9* variations.

Materials and methods

Subjects and clinical investigation

Ninety-two men of Han Chinese ethnicity who had been diagnosed with primary infertility and AZS were recruited from Suzhou Municipal Hospital. Details regarding the history of infertility and related information were collected for all patients, and samples of peripheral whole blood were isolated for WES analyses. Clinical assessment indicated that the probands discussed in this study were able to achieve a normal erection and exhibited intact ejaculatory function, proper external development of the male genitalia, appropriate secondary sexual characteristics and bilateral testicular size, and hormone levels within the expected range. All patients were karyotypically normal (46; XY) with no evidence of Y chromosome microdeletions.

Genetic analyses

DNA for sequencing of the protein-coding genes was prepared from the whole-blood samples using a TIANamp Blood DNA Kit (TIANGEN Biotech, Beijing, China), according to the provided instructions. Exon capture and sequencing were performed with an AlExome Enrichment kit V1 (iGeneTech, Beijing, China) and a Hiseq2000 platform (Illumina, CA, USA), respectively. The reads were aligned to the hg19 (GRCh37) human reference genome using default Burrows-Wheeler Aligner (http://bio-bwa.sourceforge.net/) parameters. Genomic variant calling was performed with the Genome Analysis Toolkit HaplotypeCaller (http://www.broadinstitute.org/gatk/), after which ANNOVAR was used for filtering and annotation (https://annovar.openbioinformatics.org/en/latest/).

Variants with a gnomAD (http://gnomad-sg.org/) allele frequency > 1% were excluded, as were variants in upstream, downstream, or intronic regions. Any frameshift, nonsense, key splice-site, or potentially deleterious missense variants identified using PolyPhen-2, Mutation Taster, and SIFT were retained for further evaluation. Any genes harboring two potentially deleterious missense or loss-of-function mutations were retained, and these candidate genes were cross- referenced with genes known to be enriched in the testis and associated with AZS phenotypes. Positive variant candidates were additionally investigated *via* Sanger sequencing.

Sanger sequencing

The target genomic regions of interest were amplified with appropriate primers (Supplementary Table S1) and PhantaTM Super-Fidelity DNA Polymerase (Vazyme, P501) *via* PCR with the following settings: 95°C for 2 min; 35 cycles of 95°C for 10 s, 58°C for 15 s, 72°C for 8 min, and 72°C for 10 min. An ABI Prism Big Dye Terminator Cycle Sequencing Ready Reaction kit was then used for direct sequencing of these amplicons using an ABI 3100 Genetic Analyzer (Applied Biosystems, CA, USA), and the resultant PCR products (214/264 bp) were analyzed *via* by 2% agarose gel electrophoresis. DNA sequence alignment was performed with SnapGene (v 3.2.1).

Semenological and sperm analyses

Semen samples were collected from study participants after sexual abstinence for 2-7 days and analyzed after liquefaction at 37°C for 30 min. Liquefaction was completed within an hour. The semen parameters were analyzed by a computer-assisted analysis system (CASA) device using IVOS software (version 12, Hamilton-Thorne Biosciences). Up to 10 sequels, 10s long were acquired for each sample. The sample volumes, sperm concentrations, and sperm motility were assessed according to the WHO guidelines (20). H&E staining was performed to evaluate sperm morphology. A minimum of 200 spermatozoa per patient were analyzed to assess the frequency of morphologically abnormal cells as per WHO guidelines.

Sperm hyperactivity assay

As described elsewhere (21), human sperm cells (10^7 cells/ml) were incubated in capacitation medium (Ham's F-10) supplemented with 3 mg/ml BSA for 3 h at 37°C in 5% CO_2. The semen parameters were then analyzed by CASA. A minimum of 100 sperm cells were analyzed each time. The proportion of hyperactivated (HA) spermatozoa in each sample was determined using the SORT function of the CASA instrument. In human spermatozoa, HA motility is defined by curvilinear velocity (VCL) > 100 μm/s, linearity (LIN) < 60%, and lateral head displacement (ALH) > 5 μm.

Western immunoblotting

Western immunoblotting was performed as previously described (22) with some modifications. Initially, the spermatozoa were lysed with buffer containing 7 M urea, 2M thiourea, 2% (w/v) DTT), and 1% (v/v) protease inhibitors (Pierce Biotechnology). The lysates were centrifuged and proteins in the supernatants were separated by SDS-PAGE and transferred to PVDF membranes. The blots were blocked with 5% skim milk in TBST at room temperature for 2 h and were then incubated overnight at 4°C with appropriate primary antibodies (Supplementary Table S2). The protein bands were then detected using the SuperSignalWest Femto Chemiluminescent Substrate system (Thermo Scientific).

Immunofluorescent staining

The spermatozoa were rinsed three times with PBS, spread on microscope slides, and allowed to air dry. The cells were then fixed with 1% paraformaldehyde for 10 min, rinsed three times using PBST (10 minutes per wash), blocked with 1% BSA for 1 h, and probed overnight using appropriate primary antibodies at 4°C. Samples were then probed with secondary antibodies for 2 h, nuclei were counterstained for 5 min using Hoechst 33342, rinsed with PBS, mounted with Immu-Mount or VectaShield, and imaged with an ORCA Flash4.0 digital monochrome camera (Hamamatsu Photonics) on a Leica DM5500B microscope (Leica Microsystems).

Transmission electron microscopy

Transmission electron microscopy (TEM) was performed by initial fixation of spermatozoa in 2.5% phosphate-buffered

glutaraldehyde. The cells were then rinsed three times with 0.1 mol/L phosphate buffer (PB, pH 7.2), treated for 60-90 min with 1% osmium tetroxide in 0.1 mol/L PB at 4°C, and dehydrated in an ethanol gradient (50, 70, 80, 95, and 100%), followed by 100% acetone. The samples were then treated overnight with 1:1 acetone and SPI-Chem resin containing dodecyl succinic anhydride, N-methylacetamide, SPI-Pon 812, and DMP-30 at 37°C and embedded in Epon 812. Ultrathin sections were cut and stained with lead citrate and uranyl acetate before TEM imaging (TECNAI-10, Philips) at an accelerating voltage of 80 kV.

Immunoprecipitation

HEK293T cells were co-transfected with the *PcDNA3.1-KIF9-Flag* and *pcDNA3.1-HYDIN-HA* or *pcDNA3.1-SPAG6 \16-HA* constructs. The cells were then lysed in IP lysis buffer (20 mM Tris, pH 7.4, 2 mM EGTA, 1% NP-40) containing a protease inhibitor cocktail (Roche, 04693132001) for 30 min on ice. The lysates were then centrifuged for 15 min at 13000 g and the supernatants were incubated overnight with anti-FLAG at 4° C followed by incubation for 2 h with protein A-Sepharose (GE, 17-1279-03) at 4°C. The precipitates were then rinsed twice in IP buffer and mixed with 1% SDS sample buffer *via* before separation on SDS-PAGE and immunoblotting as described above.

Results

Identification of deleterious bi-allelic *KIF9* variants in two male AZS patients

In this study, 92 Chinese males with AZS underwent WES analyses. Two unrelated members of this cohort exhibiting abnormal sperm motility were found to harbor homozygous *KIF9* variants, as confirmed *via* by Sanger sequencing (Figures 1A–C). One of the homozygous *KIF9* variants was a frameshift mutation (c.1433delinsA: p.N478Tfs*39) detected in proband A021 II-1, a member of the consanguineous family A021. Both of the patient's parents were heterozygous carriers for the variant (Figure 1A). The second homozygous *KIF9* variant detected in proband II-1 from family A062 was a stop-gain variant (c.1861A>T: p.K621X) in the C-terminus of *KIF9*. This patient's mother was a heterozygous carrier for this variant (Figure 1A). Analysis of the prevalence of these variants by gnomAD showed that they were largely absent in the general population, indicating that they were rare variants (Table 1). The two variants were thus identified as deleterious bi-allelic *KIF9* variants present in males with AZS.

The nonsense-mediated decay process facilitates the selective degradation of mRNAs harboring premature stop codons (23, 24). If not degraded, these mRNAs generally produce truncated proteins that result in either damaging gain-of-function phenotypes or dominant-negative characteristics (23, 24). To understand the potential pathogenicity of the detected variants, western immunoblotting and immunofluorescence were used to assess the abundance and localization of KIF9 within spermatozoa. This showed the presence of a KIF9-specific protein band at ~100 kDa in control spermatozoa that was absent in the sperm of the two probands (Figure 1D), indicating a loss of KIF9 expression. Immunofluorescent staining also confirmed that KIF9 was present in control spermatozoa but was undetectable in the sperm flagella from the two probands (Figure 1E). These findings thus indicated that an absence of KIF9 expression in the probands harboring the identified bi-allelic *KIF9* variants.

Analyses of AZS phenotypes in males harboring bi-allelic *KIF9* variants

Routine semenological analyses were next performed in accordance with the WHO guidelines. This showed that the semen from both probands was normal with respect to color, pH, volume, and smell (Table 2). Both samples contained sperm concentrations and motility levels above the reference value (Table 2). However, the percentages of forward motile sperm in the samples from the probands were just 13.4% and 18.6%, respectively (normal: ≥32%; 25), consistent with an AZS phenotype (Table 2). Both probands produced sufficient numbers of morphologically normal sperm (65% and 55%, respectively). Further, sperm cells of A021 II-1 were incubated in capacitation medium for 3 h, and the percentage of hyperactive cells was evaluated. The data showed no sperm hyperactivation (Table 2). These results suggest that *KIF9*-deficient spermatozoa from the two AZS patients were morphologically normal but exhibited impaired forward movement. KIF9 functions as a protein that can specifically regulate flagellar beating.

IVF can successfully treat *KIF9*-associated male infertility

To determine whether assisted reproductive technologies could overcome the AZS-related infertility observed in the two patients, both impacted couples (which included F1: II- 1 and F2: II- 1) underwent IVF treatment at our hospital. One round of IVF for the couple including the A021 patient led to the retrieval of 8 MII oocytes which achieved a 62.5% fertilization rate. All 8 of these embryos underwent cleavage and developed to the blastocyst stage. The couple carried one of these embryos to term, giving birth in 2021 (Table 3). In total, 15 MII oocytes were retrieved for A062, with a 60% fertilization rate and 9 embryos that developed into blastocysts. After undergoing an embryo transfer, the wife

10.3389/fendo.2022.1091107

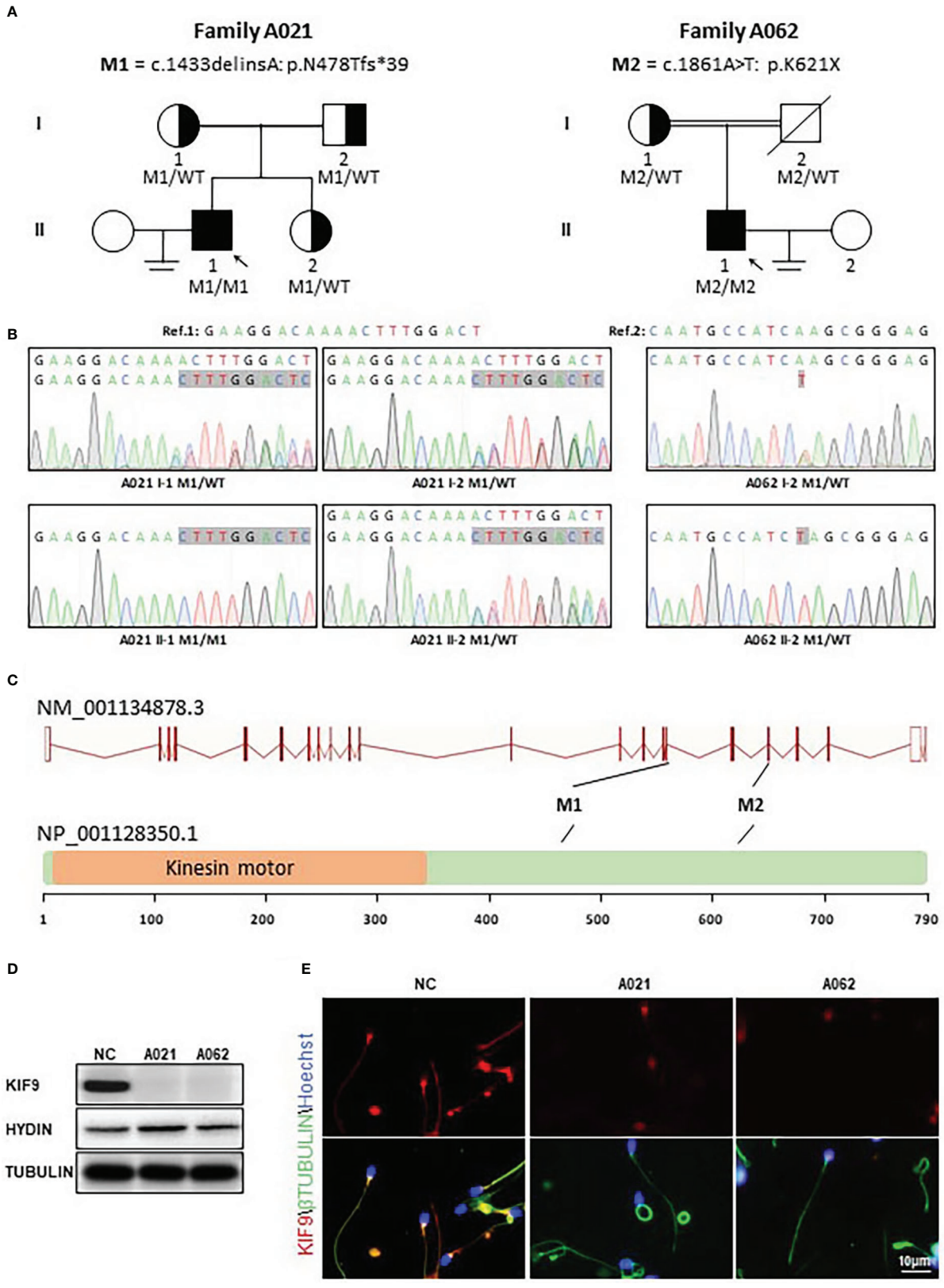

FIGURE 1 (Continued)

FIGURE 1 (Continued)
Identification of bi-allelic *KIF9* variants in two unrelated male AZS patients. **(A)** Pedigree analyses were performed for the families of the probands identified as harboring bi-allelic *KIF9* variants *via* WES. Filled black squares denote infertile males. **(B)** *KIF9* variants were confirmed by Sanger sequencing, revealing homozygous variants in both probands, whereas their parents were heterozygous carriers for these deleterious alleles. Red arrows and boxes are used to indicate mutated positions. **(C)** Variant locations within the genome and the structure of the KIF9 protein. *KIF9* is predicted to encode a protein that is 786 amino acids in length and contains a kinesin motor domain. Variants identified herein are denoted with black lines. The exons identified by NCBI are indicated by red squares, while the kinesin motor domain identified by UniProt is marked with an orange square. **(D)** *KIF9* expression is absent in the spermatozoa of the two probands harboring bi-allelic mutations in the gene. **(E)** Immunofluorescent staining was performed to detect KIF9 in spermatozoa from these two probands and a control fertile individual. Cells were stained with anti-KIF9 (red) and Hoechst dye (blue) as a nuclear counterstain.

TABLE 1 Detailed description of the biallelic variants in *KIF9* identified in two infertile men with AZS.

Subjects	*KIF9* Variants			Affected Allele	Allele Frequency in Population (gnomAD)
	cDNA Mutation	Protein Alteration	Mutation Type		
A021 II-1	c.1433del	p.N478Tfs*39	frameshift	homozygous	0
A062 II-1	c.1861A>T	p.K621X	stop-gain	homozygous	0

39, the number of the stop in the new reading frame is calculated starting at the first amino acid that is changed by the frame shift, ending at the stop codon (#). NCBI accession number of KIF9 is NM_001134878.3. GnomAD, the Genome Aggregation Database.

TABLE 2 Semen data of the patient.

Semen parameters	P01	P02	Normal values
Color	gray-white	gray-white	Milk-white, gray-white, yellowwish
Semen volume(ml)	3.5	4.8	≥1.5
pH	7.4	7.8	7.2–8.5
Sperm concentration (M/ml)	34.6	65.3	≥15
Progressive motility (%)	13.4	18.6	≥32
Motility	46.5	55.8	≥40
Morphologically normal sperm (%)	65	55	>4
VCL (μm/s)	42.5	38.9	
VSL (μm/s)	18.6	13.5	
VAP (μm/s)	26.9	24	
LIN (%)	38.9	34.4	
STR (%)	42.6	71	
WOB (%)	61.5	64	
ALH (μm)	2.0	1.8	
BCF (Hz)	8.4	7.8	
Sperm showing hyperactivation after capacitation (%)	0	–	

Normal Values based on the World Health Organization, 2015; M, million; VCL, curvilinear velocity; VSL, straight line velocity; VAP, average path velocity; LIN, linearity; STR, straightness; WOB, wobble; ALH, amplitude of lateral head displacement; BCF, beat cross frequency.

10.3389/fendo.2022.1091107

TABLE 3 Outcomes of IVF.

	A021	A062
Male age (year)	35	30
Female age (year)	32	28
Number of MII	8	15
Number (and rate) of fertilized oocytes	5 (62.5%)	9 (60%)
Number (and rate) of blastocyst	4 (50%)	9 (60%)
Implantation rate	100%	100%
Clinical pregnancy rate	100%	100%

gave birth to a child in 2021 (Table 3). These results were consistent with findings in mice in which *Kif9*-deficient sperm could still fertilize eggs, albeit at lower efficiency (18).

No obvious structural abnormalities were detected in the *KIF9*-deficient spermatozoa

To clarify the mechanisms whereby *KIF9* deficiency contributed to the observed AZS phenotypes in humans, the structural characteristics of the spermatozoa from the two probands were next analyzed. H&E staining showed that the spermatozoa appeared similar to controls, consistent with the results of the semenological analyses (Figure 2A). Immunofluorescent staining for the flagellum (α-tubulin), acrosome (PNA), MS (TOMM20), and FS (AKAP4) confirmed the presence of these components with no abnormalities in both probands (Figures 2B–D).

As the deletion of axonemal proteins frequently disrupts the structural integrity of the axoneme (6, 11, 26), TEM was next used to assess the ultrastructural characteristics of the flagella (Figure 3). Midpiece sections from both a normal control donor and the two *KIF9*-deficient probands showed mitochondria forming an outer layer with a central axoneme surrounded by ODFs. Moreover, the axoneme, ODF, and FS were clearly visible in samples from both control donors and probands, with the membrane wrapping around the filaments in the principal piece. These intact structures were in line with previous observation on sperm from *Kif9*-deficient mice.

KIF9 exhibits CP localization and interacts with the axonemal CP protein HYDIN *in vitro*

KIF9/KLP1 have been reported to localize to the axonemal CP in both mice and *Chlamydomonas*, associating with the CP protein HYDIN (18, 27). To test whether similar interactions also occurred in human cells, HA-HYDIN and FLAG-KIF9 expression plasmids were generated and the two genes were co-expressed in HEK293T cells. Subsequent immunoprecipitation analysis confirmed the interaction of these two proteins (Figure 4A). HA-tagged plasmids encoding SPAG6 and SPAG16, which are also CM components, were also generated but KIF9 failed to interact with either of these proteins (Figure 4A).

Knockdown of *HYDIN* in *Chlamydomonas* results in a marked drop in KLP1 expression (27), and *Hydin*-KO mice also lack KIF9 in the spermatozoa (18). As human spermatozoa lacking *HYDIN* were unavailable, immunofluorescent staining was instead used to detect KIF9 in sperm deficient in *SPAG6*, which lack a CP, as evident in ultrastructural cross-sections prepared from the sperm flagella (11, 12). No KIF9 staining was detectable in these *SPAG6*-deficient sperm (Figure 4B). Moreover, KIF9 staining was performed in sperm lacking *DNAH10*, which retain the CP but exhibit MMAF phenotypes (10). KIF9 expression was observed in the tails of the *DNAH10*-deficient spermatozoa even though they were abnormally short and curly (Figure 4B). In addition, we detected the level of HYDIN in the *KIF9*-deficient spermatozoa, and no difference was detected between the samples (Figure 1D). These analyses indicated that KIF9 is potentially associated with HYDIN and localized to the axonemal CP in humans.

Loss of KIF9 has no adverse impact on flagellar proximal-to-distal patterning of the radial spokes or inner dynein arms

In cilia, KIF9 deficiency has been linked to altered proximal-to-distal radial spoke and inner dynein arm patterning (19). Given the high degree of structural conservation observed between respiratory cilia and sperm flagella, RSPH3 and DNALI1 expression was next evaluated in the spermatozoa from the two probands. These proteins were selected as RSPH3 is a radial spoke protein (28), whereas the DNALI1 is

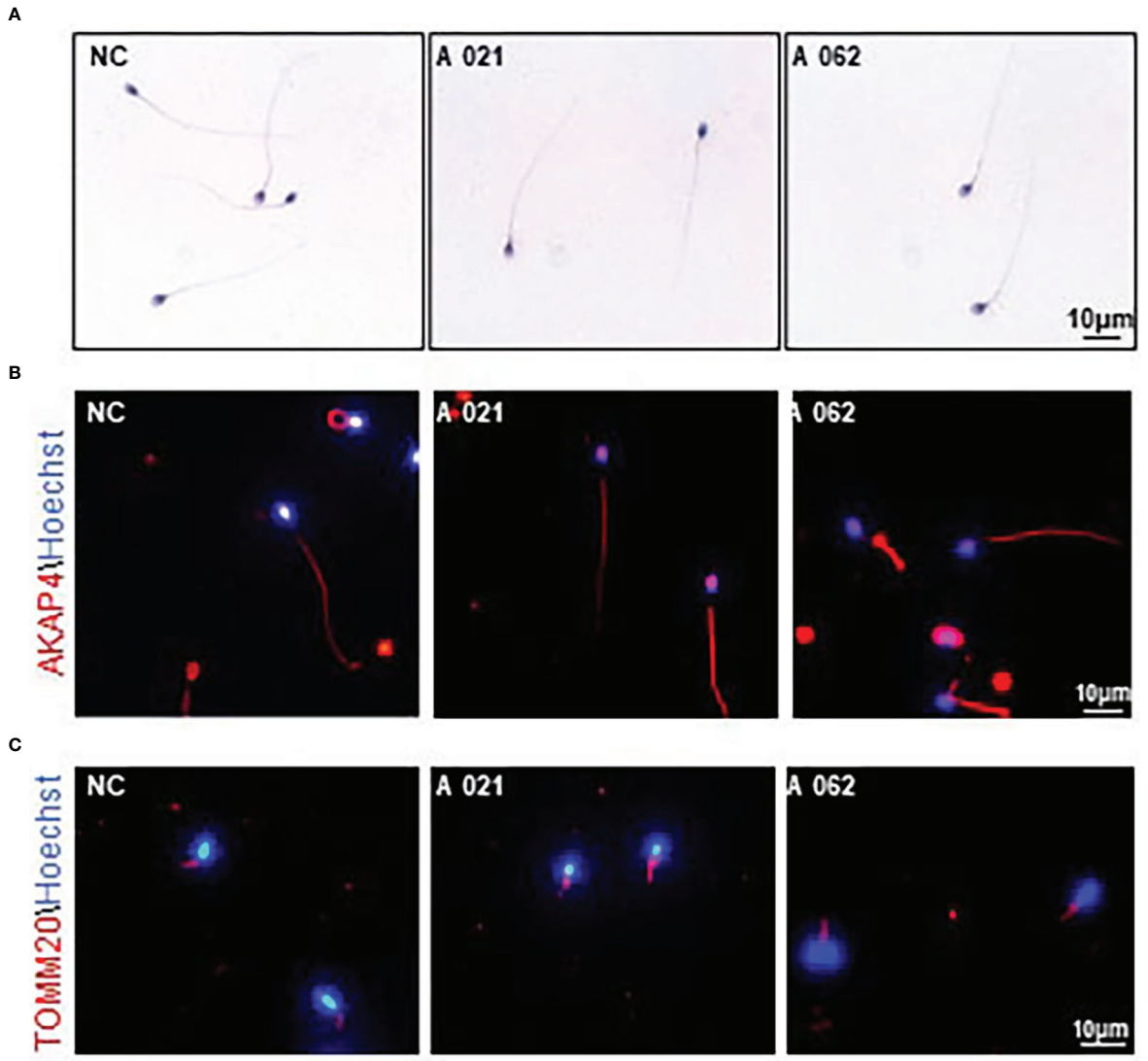

FIGURE 2
Morphology and *KIF9* deficiency of spermatozoa from control subjects and men with biallelic *KIF9* variants. **(A)** Morphological findings for spermatozoa from the two probands harboring bi-allelic *KIF9* variants and a fertile control individual. **(B, C)** Anti-TUBULIN, anti-TOMM20, and anti-AKAP4 antibodies were used to identify these proteins in spermatozoa from the probands harboring bi-allelic *KIF9* variants and a fertile control, revealing that the majority of flagellum from these probands with AZS exhibited normal flagellar morphology.

found in association with the inner dynein arm (29). No significant changes in the lengths or distributions of radial spokes or inner dynein arms were observed between the control and *KIF9*-deficient spermatozoa (Figures 5A, B). Although it is possible that measurements of flagellar length could be inaccurate due to their extended length and tendency to curl. Western immunoblotting confirmed that there were no significant reductions in DNALI1 or RSPH3 levels in *KIF9*-deficient spermatozoa (Figure 5C), indicating that the loss of KIF9 has no adverse impact on the patterning of the radial spoke or inner dynein arm domains of human flagella.

Discussion

Although AZS is among the most common causes of infertility in males. Its etiology is poorly understood and thought to arise from several contributing factors (3). The

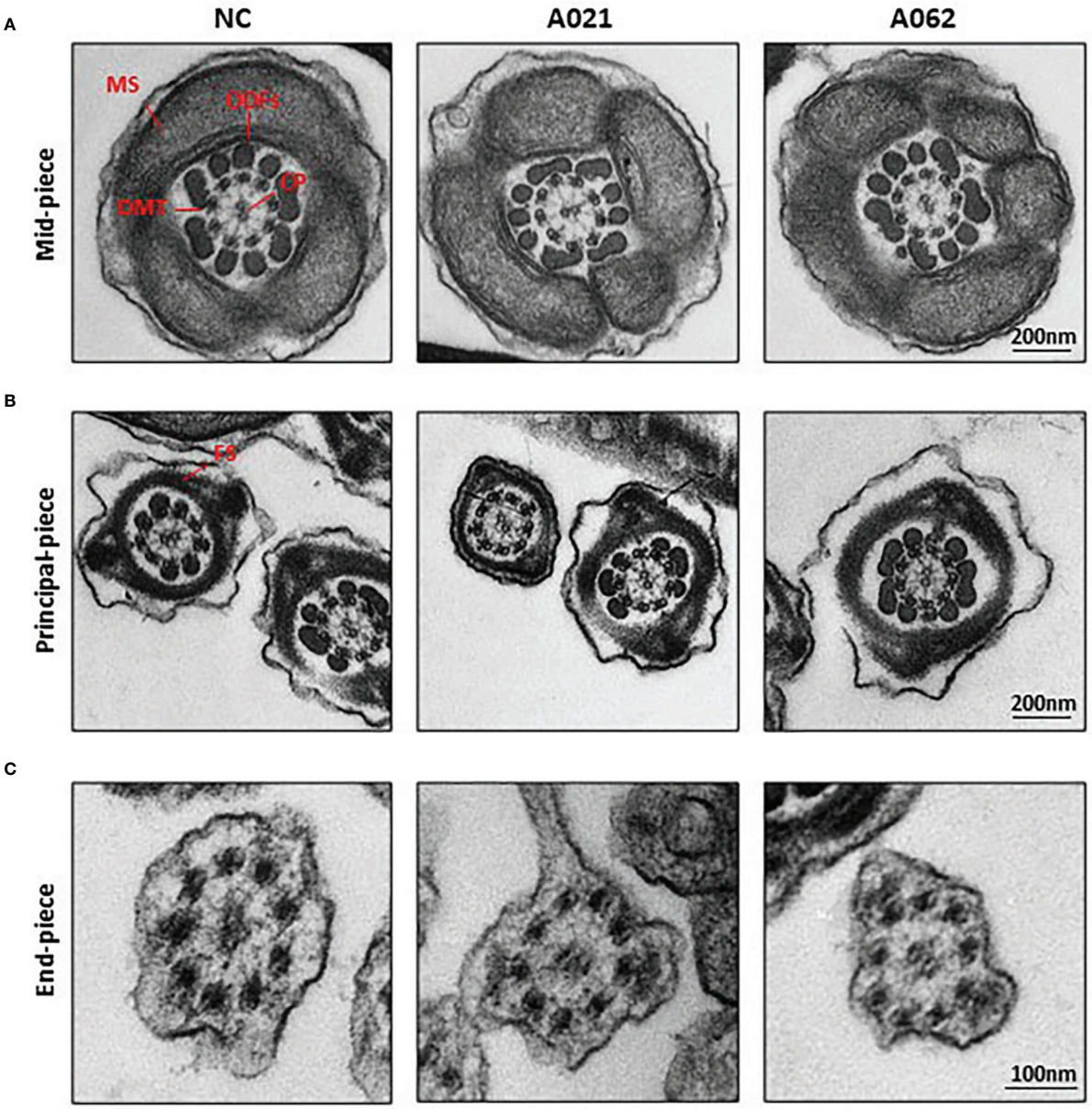

FIGURE 3
KIF9-deficient spermatozoa do not exhibit any obvious ultrastructural abnormalities. Transmission electron microscopy was used to visualize the midpiece **(A)**, principal piece **(B)**, and end piece **(C)** regions of spermatozoa in the cauda epididymis. The axoneme consists of nine peripheral microtubule doublets (DMTs) surrounding a central pair (CP) of microtubules in a 9 + 2 arrangement, surrounded by periaxonemal structures including a fiber sheath (FS), nine outer dense fibers (ODFs), and helical mitochondrial sheath (MS).

present study describes the findings from two unrelated male AZS patients with spermatozoa that were apparently free of structural defects despite exhibiting poor sperm motility. WES analyses of these patients revealed the presence of bi-allelic *KIF9* variants resulting in the production of a truncated version of this kinesin. No other variants in known AZS-related genes were identified in the WES analyses. The identified deleterious *KIF9* variants were subsequently found to be present at very low frequencies in the general population consistent with an autosomal recessive inheritance pattern. Additional staining revealed the absence of KIF9 in the spermatozoa from these two men harboring bi-allelic *KIF9* variants. Consistent with the

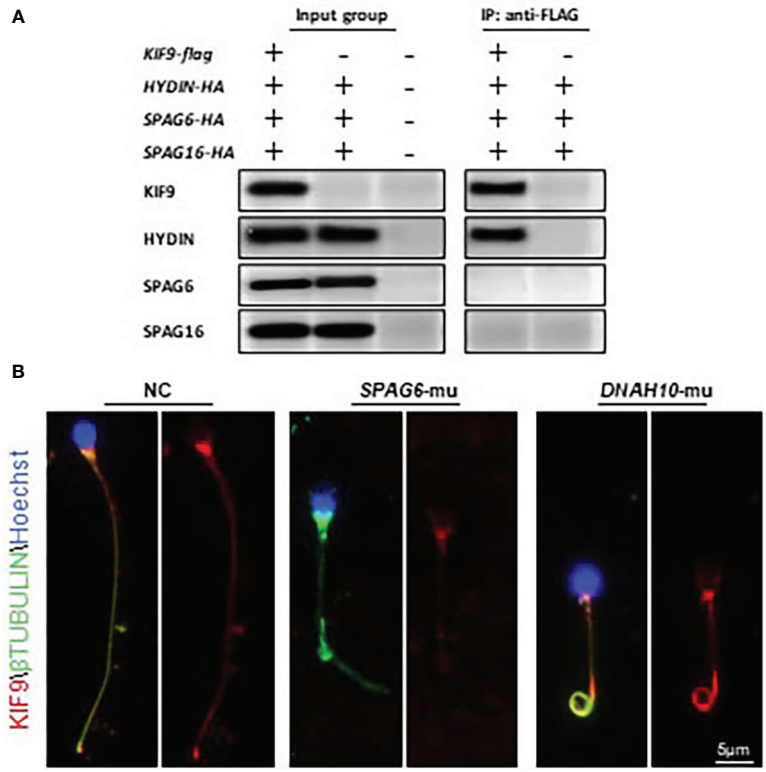

FIGURE 4
KIF9 localizes to the CP in human spermatozoa. **(A)** HEK293T cells were co-transfected with *KIF9* and individual components of the CP followed by immunoprecipitation with FLAG-KIF9, resulting in HA-HYDIN co-precipitation. **(B)** KIF9 staining was performed in spermatozoa from a *SPAG6*-deficient individual, a *DNAH10*-deficient individual, and a normal fertile control.

reports of mice lacking *Kif9* expression (18), the loss of *KIF9* function was further found to be associated with normal sperm morphology but a reduction in progressive motility. As such, the observed bi-allelic *KIF9* loss-of-function variants are likely the cause of the AZS phenotypes in these patients individuals.

Intraflagellar transport (IFT) is essential for the formation of flagella and cilia, and relies on microtubules to facilitate the bi-directional movement of particular cargos. Impaired IFT activity impairs flagellar development and leads to short sperm tail domains in both mice and humans (30–32). Kinesins are responsible for the anterograde movement of IFT cargos to the tip of the flagella. Murine KIF9 has been shown to be an important mediator of progressive spermatozoa motility and the maintenance of male fertility. *Kif9*-knockout mice exhibit abnormal symmetric flagellar motility waveform patterns consistent with the impairment of the switching of microtubule sliding (18). Here, spermatozoa from both analyzed probands exhibited reductions in progressive motility, even those that were morphologically normal, consistent with the findings in *Kif9*-knockout mice. KIF9 is thus likely to specifically regulate flagellar swing patterns in an evolutionary conserved manner in both humans and mice. HYDIN localizes to the C2 CP microtubule in both *Chlamydomonas* and mice, where it is believed to play a critical role in the switching of bending directionality through the control of dynein arm activity (18, 27). KIF9 may thus influence human flagellar switching *via* interactions with HYDIN.

Another member of the kinesin superfamily, KIF3B, has also been found to be mutated in some cases of male infertility (33). The function of KIF3B has been studied in the context of intracellular transport and spermatogenesis in many species (34–36). A human A>T variant in OAT patients was linked to decreased KIF3B expression resulting in impaired male fertility (33). Other kinesins have also been reported to influence spermatogenesis by regulating IFT and intramanchette

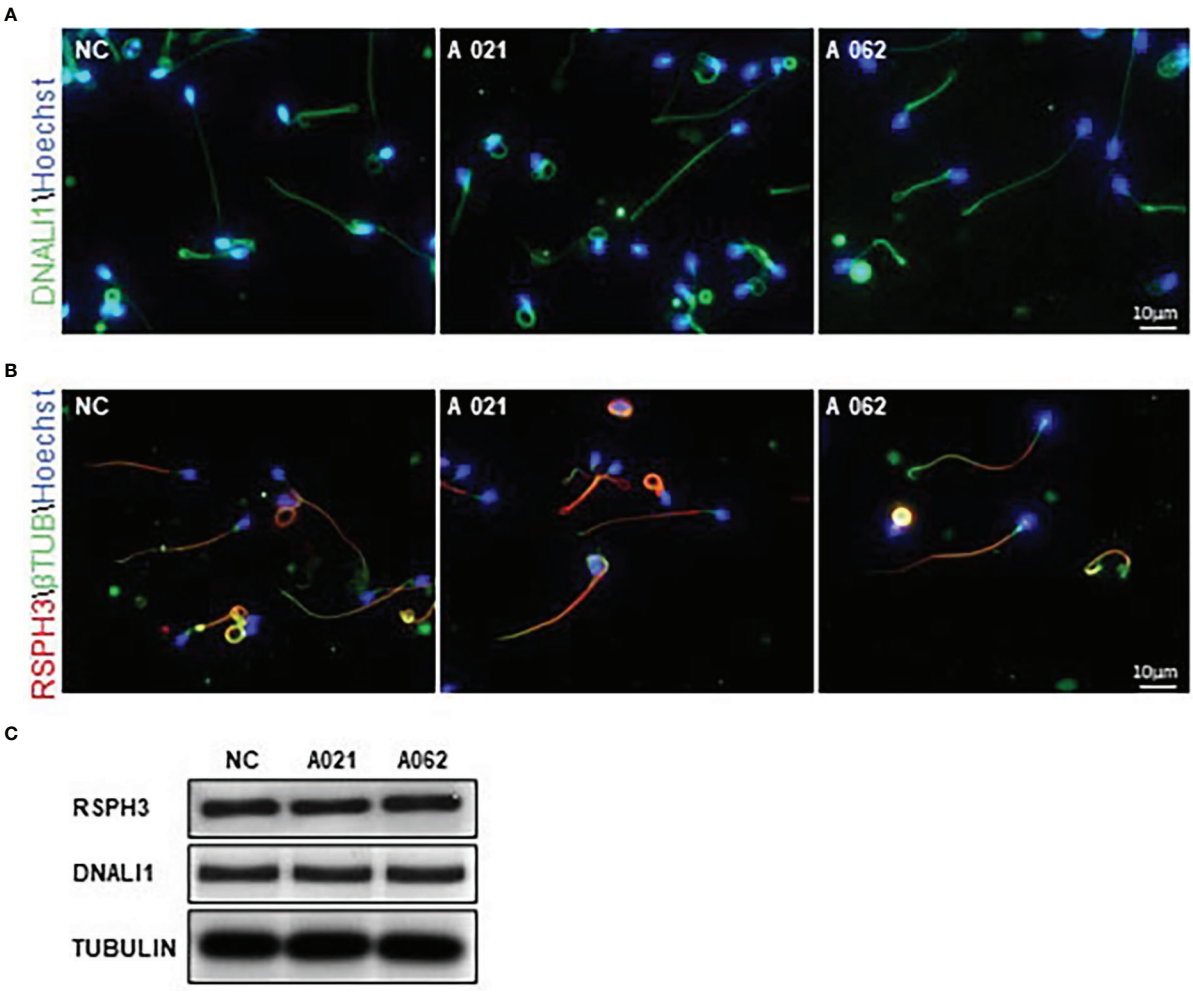

FIGURE 5
KIF9-deficient spermatozoa do not exhibit any significant radial spoke or inner dynein arm distal end abnormalities. **(A, B)** Spermatozoa from *KIF9*-deficient and fertile control individuals were imaged by confocal microscopy to assess the localization of the radial spoke stalk component RSPH9 and the inner dynein arm component DNALI1. Comparisons were performed for 15 straightened sperm pairs. **(C)** Western immunoblotting revealed no differences in RSPH9 and DNALI1 levels when comparing *KIF9*-deficient and control spermatozoa.

transport processes (37–39). In one recent analysis, KIF9 was posited to contribute to the integrity of the distal tip of motile axonemes, with altered cilial proximal-to-distal patterning for radial spokes and outer/inner dynein arms in the absence of Kif9 expression (19). However, possibly due to differences in the tip and axonemal structures between cilia and flagella, no apparent differences in the radial spokes or dynein arms of human spermatozoa were observed in the absence of *KIF9* expression. Indeed, these *KIF9*-deficient spermatozoa appeared ultrastructurally normal upon TEM analysis, suggesting that KIF9 instead plays a more nuanced or specific role in the regulation of the sperm flagella.

In summary, the present results highlight the characteristization of spermatozoa from two males harboring bi-allelic loss-of-function variants in the *KIF9* gene identified from among a cohort of 92 Chinese males diagnosed with AZS. This study is the first report demonstrating a link between *KIF9* variants and the incidence of male infertility among humans, thus expanding the known catalog of AZS-related genes. These results will be of value for genetic and reproductive counseling aimed at males affected by AZS.

Data availability statement

The datasets presented in this study can be found in online repositories. The names of the repository/repositories and accession number(s) can be found in the article/Supplementary Material.

Ethics statement

The study was conducted in accordance with the Declaration of Helsinki, and approved by the Institutional Review Board (or Ethics Committee) of Suzhou Municipal Hospital, China (No. 2020190). All participants provided written informed consent for study participation.

Author contributions

Conceptualization, JL, YW, and HL; methodology, ZM, QM, and TG; validation, ZM, QM, and TG; formal analysis, ZM, QM, and TG; resources, HZ and JX; data curation, HZ; writing—original draft preparation, ZM; writing—review and editing, JL, YW, and HL; visualization, JX; supervision, HL; project administration, YW; funding acquisition, JL, YW, and HL. All authors contributed to the article and approved the submitted version.

Funding

This work was supported by the National Natural Science Foundation of China (82201762), the Suzhou Science and Technology Development Plan (SS202060, LCZX202109 and SZM2021010), the Introduce Project of Clinical Medicine Experts of Suzhou Industrial Park (SZYQTD202104), the Science and Technology Project of Changzhou (CJ20220143), and the Top Talent Support Program for Young and Middle-aged people of Wuxi Health Committee (BJ2020047).

Acknowledgments

The authors would like to thank the families of all of the patients and the individuals who participated in this study. We would also like to thank the genetic counselling team at the Suzhou Municipal Hospital and the clinicians who referred the patients for the clinical study.

Conflict of interest

The authors declare that the research was conducted in the absence of any commercial or financial relationships that could be construed as a potential conflict of interest.

Publisher's note

All claims expressed in this article are solely those of the authors and do not necessarily represent those of their affiliated organizations, or those of the publisher, the editors and the reviewers. Any product that may be evaluated in this article, or claim that may be made by its manufacturer, is not guaranteed or endorsed by the publisher.

Supplementary material

The Supplementary Material for this article can be found online at: https://www.frontiersin.org/articles/10.3389/fendo.2022.1091107/full#supplementary-material

References

1. Ombelet W, Cooke I, Dyer S, Serour G, Devroey P. Infertility and the provision of infertility medical services in developing countries. *Hum Reprod Update* (2008) 14:605–21. doi: 10.1093/humupd/dmn042

2. Curi SM, Ariagno JI, Chenlo PH, Mendeluk GR, Pugliese MN, Sardi Segovia LM, et al. Asthenozoospermia: analysis of a large population. *Arch Androl.* (2003) 49:343–9. doi: 10.1080/01485010390219656

3. Colpi G, Francavilla S, Haidl G, Link K, Behre H, Goulis D, et al. European Academy of andrology guideline management of oligo-astheno-teratozoospermia. *Andrology* (2018) 6:513–24. doi: 10.1111/andr.12502

4. Jiao SY, Yang YH, Chen SR. Molecular genetics of infertility: loss-of-function mutations in humans and corresponding knockout/mutated mice. *Hum Reprod Update* (2021) 27:154–89. doi: 10.1093/humupd/dmaa034

5. Wilton LJ, Temple-Smith PD, de Kretser DM. Quantitative ultrastructural analysis of sperm tails reveals flagellar defects associated with persistent asthenozoospermia. *Hum Reprod* (1992) 7:510–6. doi: 10.1093/oxfordjournals.humrep.a137681

6. Hu T, Meng L, Tan C, Luo C, He WB, Tu C, et al. Biallelic CFAP61 variants cause male infertility in humans and mice with severe oligoasthenoteratozoospermia. *J Med Genet* (2022) 6. doi: 10.1136/jmedgenet-2021-108249

7. Auguste Y, Delague V, Desvignes JP, Longepied G, Gnisci A, Besnier P, et al. Loss of calmodulin- and radial-Spoke-Associated complex protein CFAP251 leads to immotile spermatozoa lacking mitochondria and infertility in men. *Am J Hum Genet* (2018) 103:413–20. doi: 10.1016/j.ajhg.2018.07.013

8. He X, Liu C, Yang X, Lv M, Ni X, Li Q, et al. Bi-allelic loss-of-function variants in CFAP58 cause flagellar axoneme and mitochondrial sheath defects and asthenoteratozoospermia in humans and mice. *Am J Hum Genet* (2020) 107:514–26. doi: 10.1016/j.ajhg.2020.07.010

9. Liu C, Shen Y, Tang S, Wang J, Zhou Y, Tian S, et al. Homozygous variants in AKAP3 induce asthenoteratozoospermia and male infertility. *J Med Genet* (2022) 28. doi: 10.1136/jmedgenet-2021-108271

10. Tu C, Cong J, Zhang Q, He X, Zheng R, Yang X, et al. Bi-allelic mutations of DNAH10 cause primary male infertility with asthenoteratozoospermia in humans and mice. *Am J Hum Genet* (2021) 108:1466–77. doi: 10.1016/j.ajhg.2021.06.010

11. Wu H, Wang J, Cheng H, Gao Y, Liu W, Zhang Z, et al. Patients with severe asthenoteratospermia carrying SPAG6 or RSPH3 mutations have a positive pregnancy outcome following intracytoplasmic sperm injection. *J assisted Reprod Genet* (2020) 37:829–40. doi: 10.1007/s10815-020-01721-w

12. Xu C, Tang D, Shao Z, Geng H, Gao Y, Li K, et al. Homozygous SPAG6 variants can induce nonsyndromic asthenoteratozoospermia with severe MMAF. *Reprod Biol Endocrinol* (2022) 20:41. doi: 10.1186/s12958-022-00916-3

13. Roy A, Lin YN, Agno JE, DeMayo FJ, Matzuk MM. Absence of tektin 4 causes asthenozoospermia and subfertility in male mice. *FASEB J* (2007) 21:1013–25. doi: 10.1096/fj.06-7035com

14. Roy A, Lin YN, Agno JE, DeMayo FJ, Matzuk MM. Tektin 3 is required for progressive sperm motility in mice. *Mol Reprod Dev* (2009) 76:453–9. doi: 10.1002/mrd.20957

15. Castaneda JM, Hua R, Miyata H, Oji A, Guo Y, Cheng Y, et al. TCTE1 is a conserved component of the dynein regulatory complex and is required for motility

and metabolism in mouse spermatozoa. *Proc Natl Acad Sci United States America* (2017) 114:E5370–8. doi: 10.1073/pnas.1621279114

16. Zhou S, Wu H, Zhang J, He X, Liu S, Zhou P, et al. Bi-allelic variants in human TCTE1/DRC5 cause asthenospermia and male infertility. *Eur J Hum Genet* (2022) 30:721–9. doi: 10.1038/s41431-022-01095-w

17. Miyata H, Oyama Y, Kaneda Y, Ikawa M. The motor domain of testis-enriched kinesin KIF9 is essential for its localization in the mouse flagellum. *Exp Anim* (2022) 71:46–52. doi: 10.1538/expanim.21-0082

18. Miyata H, Shimada K, Morohoshi A, Oura S, Matsumura T, Xu Z, et al. Testis-enriched kinesin KIF9 is important for progressive motility in mouse spermatozoa. *FASEB J* (2020) 34:5389–400. doi: 10.1096/fj.201902755R

19. Konjikusic MJ, Lee C, Yue Y, Shrestha BD, Nguimtsop AM, Horani A, et al. Kif9 is an active kinesin motor required for ciliary beating and proximodistal patterning of motile axonemes. *J Cell Sci Mar* (2023) 1:136. doi: 10.1242/jcs.259535

20. Cooper TG, Noonan E, von Eckardstein S, Auger J, Baker HW, Behre HM, et al. World health organization reference values for human semen characteristics. *Hum Reprod Update* (2010) 16:231–45. doi: 10.1093/humupd/dmp048

21. Chan PJ, Corselli JU, Patton WC, Jacobson JD, Chan SR, King A. A simple comet assay for archived sperm correlates DNA fragmentation to reduced hyperactivation and penetration of zona-free hamster oocytes. *Fertility sterility* (2001) 75:186–92. doi: 10.1016/S0015-0282(00)01655-1

22. Zheng B, Zhao D, Zhang P, Shen C, Guo Y, Zhou T, et al. Quantitative proteomics reveals the essential roles of stromal interaction molecule 1 (STIM1) in the testicular cord formation in mouse testis. *Mol Cell Proteomics* (2015) 14:2682–91. doi: 10.1074/mcp.M115.049569

23. Chang YF, Imam JS, Wilkinson MF. The nonsense-mediated decay RNA surveillance pathway. *Annu Rev Biochem* (2007) 76:51–74. doi: 10.1146/annurev.biochem.76.050106.093909

24. Mühlemann O. Spermatogenesis studies reveal a distinct nonsense-mediated mRNA decay (NMD) mechanism for mRNAs with long 3'UTRs. *PloS Genet* (2016) 12:e1005979. doi: 10.1371/journal.pgen.1005979

25. World Health Organization (2022). *WHO Laboratory Manual for the Examination and Processing of Human Semen. 6th* edn. (Geneva, Swtizerland: World Health Organization)

26. Zhang J, He X, Wu H, Zhang X, Yang S, Liu C, et al. Loss of DRC1 function leads to multiple morphological abnormalities of the sperm flagella and male infertility in human and mouse. *Hum Mol Genet* (2021) 30:1996–2011. doi: 10.1093/hmg/ddab171

27. Lechtreck K, Witman G. Chlamydomonas reinhardtii hydin is a central pair protein required for flagellar motility. *J Cell Biol* (2007) 176:473–82. doi: 10.1083/jcb.200611115

28. Jeanson L, Copin B, Papon JF, Dastot-Le Moal F, Duquesnoy P, Montantin G, et al. RSPH3 mutations cause primary ciliary dyskinesia with central-complex defects and a near absence of radial spokes. *Am J Hum Genet* (2015) 97:153–62. doi: 10.1016/j.ajhg.2015.05.004

29. Rashid S, Breckle R, Hupe M, Geisler S, Doerwald N, Neesen J. The murine Dnali1 gene encodes a flagellar protein that interacts with the cytoplasmic dynein heavy chain 1. *Mol Reprod Dev* (2006) 73:784–94. doi: 10.1002/mrd.20475

30. Lorès P, Kherraf ZE, Amiri-Yekta A, Whitfield M, Daneshipour A, Stouvenel L, et al. A missense mutation in IFT74, encoding for an essential component for intraflagellar transport of tubulin, causes asthenozoospermia and male infertility without clinical signs of bardet-biedl syndrome. *Hum Genet* (2021) 140:1031–43. doi: 10.1007/s00439-021-02270-7

31. San Agustin JT, Pazour GJ, Witman GB. Intraflagellar transport is essential for mammalian spermiogenesis but is absent in mature sperm. *Mol Biol Cell* (2015) 26:4358–72. doi: 10.1091/mbc.E15-08-0578

32. Zhang Z, Li W, Zhang Y, Zhang L, Teves ME, Liu H, et al. Intraflagellar transport protein IFT20 is essential for male fertility and spermiogenesis in mice. *Mol Biol Cell* (2016) 27:3705–16. doi: 10.1091/mbc.e16-05-0318

33. Heydari R, Seresht-Ahmadi M, Mirshahvaladi S, Sabbaghian M, Mohseni-Meybodi A. KIF3B gene silent variant leading to sperm morphology and motility defects and male infertility†. *Biol Reprod* (2022) 106:766–74. doi: 10.1093/biolre/ioab226

34. Abad C, Amengual M, Gosálvez J, Coward K, Hannaoui N, Benet J, et al. Effects of oral antioxidant treatment upon the dynamics of human sperm DNA fragmentation and subpopulations of sperm with highly degraded DNA. *Andrologia* (2013) 45:211–6. doi: 10.1111/and.12003

35. Shen H, Xiao Y, She Z, Tan F, Yang W. A novel role of KIF3b in the seminoma cell cycle. *Exp Cell Res* (2017) 352:95–103. doi: 10.1016/j.yexcr.2017.01.023

36. Zhao Y, Mu D, Wang D, Han Y, Hou C, Zhu J. Analysis of the function of KIF3A and KIF3B in the spermatogenesis in boleophthalmus pectinirostris. *Fish Physiol Biochem* (2018) 44:769–88. doi: 10.1007/s10695-017-0461-1

37. Kierszenbaum A. Intramanchette transport (IMT): managing the making of the spermatid head, centrosome, and tail. *Mol Reprod Dev* (2002) 63:1–4. doi: 10.1002/mrd.10179

38. Lehti MS, Kotaja N, Sironen A. KIF3A is essential for sperm tail formation and manchette function. *Mol Cell Endocrinol* (2013) 377:44–55. doi: 10.1016/j.mce.2013.06.030

39. Miller M, Mulholland D, Vogl A. Rat testis motor proteins associated with spermatid translocation (dynein) and spermatid flagella (kinesin-II). *Biol Reprod* (1999) 60:1047–56. doi: 10.1095/biolreprod60.4.1047

frontiers | Frontiers in Endocrinology

TYPE Original Research
PUBLISHED 11 January 2023
DOI 10.3389/fendo.2022.1099270

OPEN ACCESS

EDITED BY
Tao Luo,
Nanchang University, China

REVIEWED BY
Yang Xiaoyu,
Nanjing Medical University, China
Houyang Chen,
Jiangxi Maternal and Child Health Hospital, China

*CORRESPONDENCE
Chencheng Yao
yaochencheng@126.com
Zheng Li
lizhengboshi@163.com
Erlei Zhi
zhzzer1985@alumni.sjtu.edu.cn

†These authors have contributed equally to this work and share first authorship

SPECIALTY SECTION
This article was submitted to Reproduction, a section of the journal Frontiers in Endocrinology

RECEIVED 15 November 2022
ACCEPTED 05 December 2022
PUBLISHED 11 January 2023

CITATION
Bai H, Sha Y, Tan Y, Li P, Zhang Y, Xu J, Xu S, Ji Z, Wang X, Chen W, Zhang J, Yao C, Li Z and Zhi E (2023) Deleterious variants in TAF7L cause human oligoasthenoteratozoospermia and its impairing histone to protamine exchange inducing reduced *in vitro* fertilization. *Front. Endocrinol.* 13:1099270. doi: 10.3389/fendo.2022.1099270

Deleterious variants in TAF7L cause human oligoasthenoteratozoospermia and its impairing histone to protamine exchange inducing reduced *in vitro* fertilization

Haowei Bai[1†], Yanwei Sha[2†], Yueqiu Tan[3†], Peng Li[1], Yuxiang Zhang[1], Junwei Xu[1], Shuai Xu[1], Zhiyong Ji[1], Xiaobo Wang[1], Wei Chen[1], Jianxiong Zhang[1], Chencheng Yao[1*], Zheng Li[1*] and Erlei Zhi[1*]

[1]Department of Andrology, Center for Men's Health, Department of ART, Institute of Urologic Medical Center, Shanghai General Hospital, Shanghai Key Lab of Reproductive Medicine, Shanghai Jiao Tong University School of Medicine, Shanghai, China, [2]Department of Andrology, Women and Children's Hospital, School of Medicine, Xiamen University, Xiamen, Fujian, China, [3]Institute of Reproductive and Stem Cell Engineering, School of Basic Medical Science, Central South University, Changsha, China

Introduction: Oligoasthenoteratozoospermia (OAT) is a major cause of infertility in males. Only a few pathogenic genes of OAT have been clearly identified till now. A large number of OAT-affected cases remain largely unknown.

Methods: Here, Whole-exome sequencing (WES) in 725 idiopathic OAT patients was performed. Ejaculated spermatozoa by OAT patients were microinjected into mouse oocytes to estimate fertilization potential. Diff-quick staining and transmission electron microscopy were performed to evaluate sperm morphology and ultrastructure. The protein expression level and localization In vitro were detected by Western Blotting and Immunocytochemistry.

Results: We identified four X-linked hemizygous deleterious variants of TAF7L —namely, c.1301_1302del;(p.V434Afs*5), c.699G>T;(p.R233S), c.508delA; (p.T170fs), c.719dupA;(p.K240fs) —in five probands. Intracytoplasmic sperm injection (ICSI) were carried out in M1, M2-1and M3 patient's wife. However only M1 patient's wife became pregnant after embryo transfer. In vitro study demonstrated significantly reduced fertilization ability in patient with TAF7L mutation. The TAF7L mutation let to abnormal sperm head and impaired histone-to protamine exchange. Variant 719dupA (p. K240fs) resulted in producing a truncated TAF7L protein and localized massively within the

nucleus. In addition, TAF7L expression were not able to be detected due to variants c.1301_1302del (p. V434Afs*5) and c.508delA (p. T170fs) In vitro.

Conclusion: Our findings support that TAF7L is one of pathogenic genes of OAT and deleterious mutations in TAF7L may cause impaired histone-to-protamine affected the chromatin compaction of sperm head.

KEYWORDS

TAF7L, hemizygous variant, oligoasthenoteratozoospermia, ICSI, male infertility

Introduction

Infertility affects about 15% of couples worldwide and a male infertility associated factor could be found in approximately half of all the couples (1, 2). Clinical manifestations of male infertility are mainly as follows, oligozoospermia, asthenozoospermia, teratozospermia, astheno-teratozospemia and oligoasthenoteratozoospermia (OAT) (3, 4). Varicocele, poor drug delivery, Y chromosomal microdeletion, and genetic abnormalities all contribute to male infertility (5).

Genetic research of male infertility related defect spermiogenesis has achieved some progress in recent years. Based on the above researches, different pathogenic genes have been classified as two specific phenotypes, including sperm head malformations (*AURKC, SPATA16*, *DPY19L2*, *PICK1*, *IQCN*), and multiple morphological abnormalities of the sperm flagella (*DNAH1*, *CFAP65*, *CFAP47, CFAP44*, *CFAP43*, *CFAP251, DZIP1, DNAH8, DNAH10*) (3, 6–14). However, the discovery of different pathogenic genes indicates that there is great genetic heterogeneity in male infertility, and abnormal sperm with the same morphology may also be caused by different genes. Therefore, the discovery of more pathogenic genes has an important role in the genetic analysis of male infertility.

Sex chromosomes not only determine the sex of a baby but also play a vital part in fertility. According to previous research, most of the genes that are expressed predominantly in testes were identified on sex chromosomes (15). Deletion mutations in certain genes can cause male infertility (16). It is well known that microdeletions in the Y chromosome play important role in the infertility of males, however, only a few genes present on the X chromosome are known to cause male infertility. For instance, it has been found that the hemizygous *TEX11* variant causes meiosis arrest, giving rise to non-obstructive azoospermia (NOA) (17, 18). Also, hemizygous *ADGRG2* variants were identified in obstructive azoospermia (OA)-affected patients (19). Hemizygous *CFAP47* variants induced OAT and primary male infertility (12). However, many other X-linked genes responsible for male infertility related defect spermatogenesis are yet to be identified.

Another X-linked gene, *TAF7L* (also known as *CT40*), was linked to OAT and male infertility in the current study, and four X-linked hemizygous deleterious variations of *TAF7L* were detected in probands, but with significantly reduced *in vitro* fertilization. The results of this study will help in genetic counselling and treatments of infertility.

Abbreviations: OAT, Oligoasthenoteratozoospermia; WES, Whole-exome sequencing; NOA, non-obstructive azoospermia; HCG, human chorionic gonadotropin; CZB, Chatot-Ziomek-Bavister; PNA, peanut agglutinin; TEM, Transmission electron microscopy analysis; ICSI, Intracytoplasmic sperm injection.

Material and methods

Study participants

In the current study, 725 idiopathic OAT patients were recruited. According to the WHO Laboratory Manual for the Examination and Processing of Human Semen (5th edition), OAT was defined as sperm concentration $<15\times10^6$/mL, progressive motility <32% and normal sperm morphology <4% with two times of semen analyses. 126 infertile men were recruited in the Department of Andrology, Urologic Medical Center, Shanghai General Hospital, Shanghai Jiao Tong University (Shanghai, China). 479 male infertile individuals were recruited in the Reproductive and Genetic Hospital of CITIC-Xiangya (Changsha, Hunan, China) and 120 in the Department of Reproductive Medicine, Xiamen Maternity and Child Care Hospital, Xiamen. (Fujian, Xiamen, China).

Patients with congenital diseases, deletions in the AZF gene, or factors linked to OAT, testicular cancer, cryptorchidism, or orchitis were excluded from the study. Patients who received chemotherapy or radiation were also excluded. The family histories of the patients were collected. For the control group, 20 healthy and fertility men from the Han Chinese ethnic group with a similar background of genetic makeup were included.

Subjects of the control group exhibited normal semen analysis and they fathered one or more healthy babies.

Prior to participation, each participant signed a written informed consent form. The research was approved by the corresponding ethics committees of the Shanghai General Hospital, Shanghai Jiao Tong University(2021-SQ-112), the Reproductive and Genetic Hospital of CITIC Xiangya (LL-SC-2017-025 and LL-SC-2019-034), and the Xiamen Maternity and Child Care Hospital, Xiamen (Permit Number: 2020SQ199, KY-2019-060).

Whole-exome sequencing

The manufacturer's protocol was followed to extract whole DNA from blood samples of patients using TIANamp Blood DNA (TIANGEN Biotech, Beijing, China). Covaris focused ultrasonication was used for DNA fragmentation. xGen Exome Research Panel (Integrated DNA Technologies, Coralville, IA, USA) was used for capturing known exons and boundaries of the exon-intron followed by preparation of DNA sequences libraries according to the manufacturer's protocol.

DNA was sequenced on a HiSeq X10 platform (Illumina, San Diego, CA, USA). Burrows-Wheeler Aliigner (BWA) was employed for the alignment of the sequencing reads with the human genome (GRCh37/hg19). GATK, VarSCan, Platypus, LoFreq, SNVer, Freebayes, VarDict and SAM tools were used for calling SNVs as well as indels within the intervals of captured coding exons. ANNOVAR software was used to filter and annotate variants. Those genetic variants were excluded which had higher than 1% allelic frequencies as per 1000 Gnomes Project and ExAC Browser while removing upstream, downstream and intronic variants. Frameshift, Nonsense, essential splice-site and missense variants with deleterious potential (SIFT, Mutation Taster and Polyphen-2) were retained for later analysis. Additionally, candidate genes were compared with pathogenic genes in mice (http://www.informatics.jax.org/mgihome/homepages/) and testis enriched genes in the database (http://www.proteinatlas.org/). The bioinformatic analysis and sequencing were performed with the collaboration of the Nuprobe company.

Semen analysis, testicular biopsy for sperm extraction and ICSI treatment

Semen samples were collected from patients by asking them for masturbation, 3-7 days post-sexual intercourse. Analysis of the samples was performed in a laboratory as per 5th WHO guidelines. The morphology of sperm was analyzed with examination using Diff-Quick staining. Ejaculated sperm of one patient (family 1, M1: II-1) without enough spermatozoa were recovered by testicular biopsy on the day of oocyte retrieval. H&E staining was performed on testicular tissue to assess spermatogenesis.

Viable sperm for ICSI were selected by laser, the tips of immotile sperm were targeted with a laser beam of approximately 200 μJ with an irradiation time of about 2 ms. Those spermatozoa which presented with curling of the tails after the laser shot were regarded as viable, while others which did not curling of the tails were considered to be non-viable. And assisted oocyte activation (AOA) has been done to activate oocytes. After ICSI treatment, outcomes were obtained from three different hospitals. Results of the following parameters were included: the number of injected oocytes, fertilized oocytes, ICSI cycles, rate of embryos cleavage, 8 cells, blastocysts, transfer cycles, per cycle transferred embryos, rate of implantation, pregnancies and miscarriage.

Transmission electron microscopy analysis

Spermatozoa were fixed routinely as previously (5). After being embedded in Epon, ultrathin sections of sperm were stained with uranyl acetate, then photographed by TEM. At least 50 flagella with cross sections and several longitudinal sections were counted.

ICSI derived from human ejaculated spermatozoa into mouse oocytes

To further prove the different capacity of ejaculated spermatozoa between patients with *TAF7L* variants and healthy men, microinjection of spermatozoa into the mice oocytes were performed using a previously described procedure (20). For superovulation, mice were injected with 5 IU of equine chorionic gonadotropin. Mice were then given 5 IU of human chorionic gonadotropin (HCG) after 48 hours. After 16 hours of HCG injection, cumulus-oocyte complexes were harvested from oviducts and transferred to HEPES Chatot-Ziomek-Bavister (CZB) medium. To disperse cells of cumulus, they were treated with hyaluronidase (0.1%). Oocytes were rinsed two times and then transferred to fresh CZB drop. They were given at least 15 min incubation in plain CZB media. To artificially activate the oocytes, they were kept for 1 hour in CZB free of Ca2+ and supplemented with SrCL2 (10mM) followed by washing two times again. For resuming incubation, they were again transferred to a CZB medium. 100 sperm from each group were microinjected into the eggs with piezoelectric elements. To examine the formation of pronucleus and *in vitro* development, the oocytes in the CZB medium were kept for incubation at 37 °C and 5% CO2.

Immunofluorescence staining

The spermatozoa of the proband (family 1, M1: II-1) and normal control were stained by immunofluorescent. The samples were fixed with 4% paraformaldehyde for 20 min. After 10 min washes with PBS, heat-induced antigen retrieval was carried out by boiling the slides in 10 mM citrate buffer (pH 6.0) with a microwave oven for 10 min. After three 10 min washes with 0.1% Triton X-100 in PBS, the slides were blocked with 5% BSA diluted in PBST for 1h and then the slides were incubated with anti-histone H3 (1:100; CST), anti-PRM2(1:100; Atlas) in PBST overnight, samples were incubated with fluorescein isothiocyanate-conjugated anti-rabbit IgG (1:200; Invitrogen), and peanut agglutinin (PNA) (1:300; Invitrogen) for 30 min at room temperature. The samples were washed three times in PBS and incubated 10-min with Hoechst33342(1:200; Invitrogen), imaged by fluorescence microscopy.

RNA extraction and reverse transcriptase polymerase chain reaction

According to the manufacturer's instruction, testicular RNA of patient (Family 1, M1: II-1) was extracted using the kit (Qiagen, USA). The purity was assessed by the A260/A280 ratio. Then we carried out the reverse transcription under the following conditions: 37 °C for 15 min, followed by 85 °C for 5 s. The products were performed under the following conditions: 95 °C for 30s, 40 cycles of 95 °C for 10 s, 60 °C for 30 s, and 95 °C 15s, 60°C for 60s, 95°C for 15s. GAPDH was used as an internal control and primers for real-time quantitative PCR are listed in Table S1.

Expression plasmid construction and transfection

Full-length cDNA encoding human *TAF7L* was amplified and cloned into pCMV7.1 vector with N-terminal FLAG tag. Site-directed mutagenesis was accomplished using a ClonExpress Ultra One Step Cloning Kit (C115-01, Vazyme, China). The wild-type and mutant clones were confirmed by Sanger sequencing. HEK293T cells were cultured in DMEM/high glucose (SH30243.FS, Cytiva) with 10% FBS (10099141C, Gibco) and 1% penicillin/streptomycin (15140122, Gibco) at 37°C in 5% CO2. *TAF7L* wild-type and mutant plasmids were transfected into HEK293T cells using the lipofectamine 3000 (L3000015, Invitrogen) according to the manufacturer's protocol.

Western blot

48 h after transfection, the cells were lysed by RIPA lysis buffer (89901, Thermo Fisher Scientific) on ice 20 min, followed by centrifugation at 14,000 × g for 15 min at 4°C to isolate the protein, which was quantified by BCA assay (23225, Thermo Fisher Scientific) and separated by 10% sodium dodecyl sulfate polyacrylamide gels and were transferred to a 0.22 μm PVDF membrane (ISEQ00010, Millipore). The membranes were blocked with 5% not fat milk in TBST buffer 1h. After washing three times with TBST for 5 min, then incubated at 4°C overnight with anti-FLAG rabbit monoclonal antibodies (dilution: 1:5,000; catalogue number: F1804, Sigma) or β-actin (dilution: 1:10,000; 66009-1-Ig, Proteintech). The membranes were washed with TBST three times and incubated with anti-Mouse IgG HRP (dilution: 1:5,000; sc-516102, Santa Cruz Biotechnology) for 1 h at room temperature followed by washing again with TBST three times. Finally, the blots were imaged on AI600 imager (GE healthcare)

Results

Clinical characteristics

In this study, WES of 725 idiopathic OAT patients was performed. Four X-linked hemizygous deleterious variants of *TAF7L* were identified in five probands (0.68%,5/725).

Patients were examined for physical parameters and they exhibited normal epididymis, scrotum, prostate, penis and testes development. Semen analysis revealed OAT phenotype as per the 5th edition of WHO guidelines. All patients had normal sex hormones, sex chromosomes and autosomal chromosomes. No Y chromosome microdeletions and no history of cancer, cryptorchidism, hypogonadism, alcoholism, or smoking were found.

Identification of hemizygous *TAF7L* variants in men with OAT

To identify candidate genes that could be potentially associated with OAT, WES was performed. The workflow of data processing and analyses was described in Supplementary Figure 1. After excluding the polymorphisms, which were reported in previous studies. We found four deleterious variants X-Linked *TAF7L* variants in five Chinese OAT patients, the hemizygous frameshift [c.1301_1302del; (p.V434Afs*5)] in M1(Figure 1A; Table 1), a hemizygous

10.3389/fendo.2022.1099270

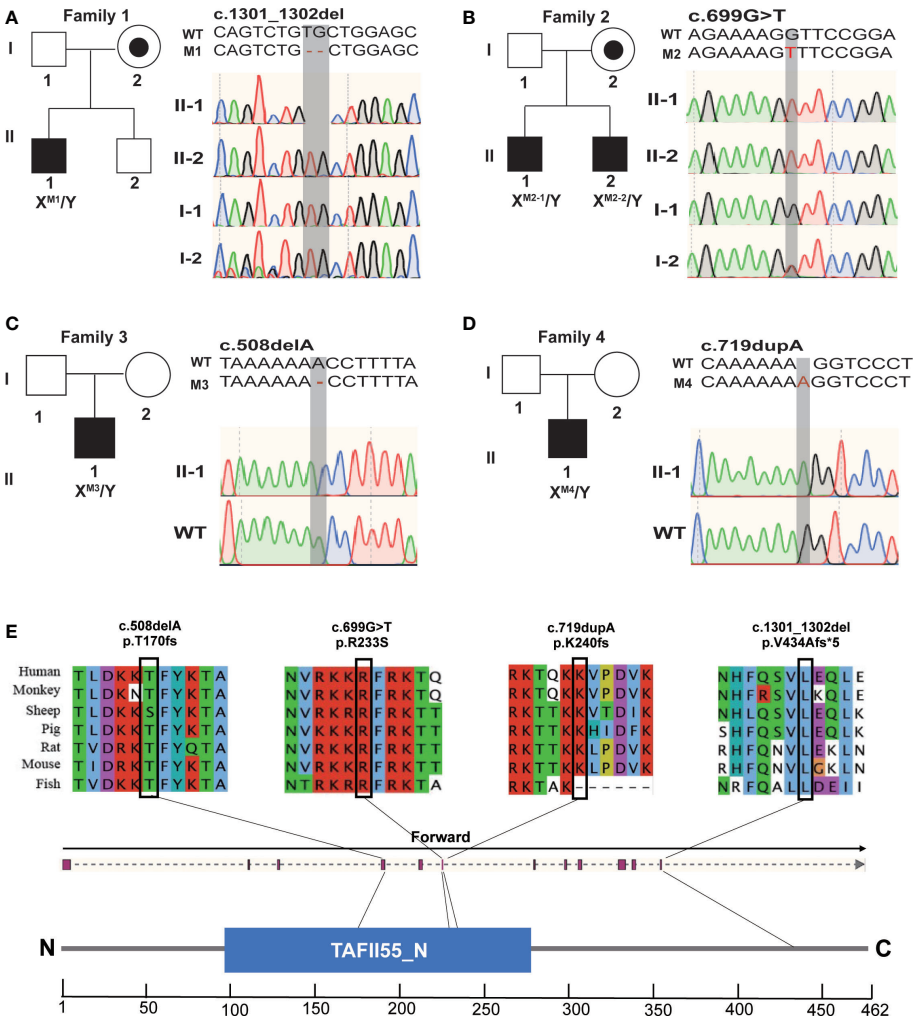

FIGURE 1
Hemizygous mutations in *TAF7L* identified in patients with OAT. **(A–D)** Pedigree analysis of the four patients affected by X-linked *TAF7L* Hemizygous variants that were identified by WES. Black filled squares indicate infertile men in these families. Sanger sequencing results are shown to the right of the pedigrees. The mutated positions are indicated by red words and black shadow boxes. **(E)** The genomic structure of *TAF7L*, with variants mapped to isoform 1 (GenBank accession number, NM_024885) The positions of the novel *TAF7L* variants identified in this study are indicated by black lines. Locations of the mutated sites in the exon structure of *TAF7L*(upper); Locations of the affected amino acids in the protein domain map of TAF7L (bottom). Sequence alignment shows conservation of the mutated residues among different species. Blue squares stand for TAFII55 protein conserved region according to the NCBI.

missense mutation [c.699G>T;(p.R233S)] in M2-1 and M2-2, which was inherited from their parents (Figure 1B; Table 1). We also found the hemizygous frameshift [c.508delA; (p. T170fs)] in M3, the hemizygous frameshift [c.719dupA;(p.K240fs)] in M4 (Figures 1C, D; Table 1).

These hemizygous *TAF7L* variants were not detected in human population genome databases, including gnomAD and the 1000 Genomes Project (Table 1). *In silico* analysis of all these variants predicted them to be deleterious (SIFT, PolyPhen-2, M-CAP and CADD tools) (Table 1). Hence, these variants were classified as pathogenic following the American College of Medical Genetics and Genomics criteria (ACMG). All corresponding variant residues are highly conserved in many organisms (Figure 1E).

ICSI treatment may rescue the damaged male fertility carrying *TAF7L* mutation with sperm of testes

It is suggested that ICSI treatment can be effective in overcoming the physical problems faced by sperm from patients. The couples underwent ICSI by using spermatozoa of the subjects carrying hemizygous *TAF7L* mutation. Hence,

TABLE 1 Hemizygous deleterious *TAF7L* variants induce OAT in Chinese men.

TAF7L variants	M1	M2-1/M2-2	M3	M4
cDNA alteration	c.1301_1302del	c.699G>T	c.508delA	c.719dupA
Variant allele	Hemizygous	Hemizygous	Hemizygous	Hemizygous
Protein alteration	p. V434Afs*5	p. R233S	p. T170fs	p. K240fs
Variant type	Frameshift	Missense	Frameshift	Frameshift
Allele frequency in human population				
1000 Genomes Project	0	0	0	0
East Asians in gnomAD	0	0	0	0
All individuals in gnomAD	0	0	0	0
Function prediction				
Mutation Taster	Damaging	Damaging	Damaging	Damaging
SIFT	N/A	Damaging	N/A	N/A
PolyPhen-2	N/A	Damaging	N/A	N/A

NCBI reference sequence number of TAF7L in GenBank: NM_024885. N/A, not available.
*means stop.

the patients with *TAF7L* variants got fewer two-cell embryos and blastocysts than the control. These five patients with *TAF7L* variants didn't get clinical pregnancy using ejaculated sperm, two of them chose donor's sperm for ICSI treatment.

One patient (Family 1, M1: II-1), who had previously undergone seven ICSI cycles without conceiving with ejaculated sperm. In this time, ejaculated sperm of patient without enough spermatozoa were recovered by testicular biopsy on the day of oocyte retrieval. The couple got the successful clinical pregnancy with sperm of testes at the time of writing (Table 2).

As contrast normal spermatogenesis, histological analysis of testis revealed that this patient (Family 1, M1: II-1) showed post meiotic arrest at the first stage of spermiogenesis, which revealed dramatically decreased elongated spermatids (Figure 2).

TABLE 2 Clinical outcomes of ICSI cycles using the spermatozoa from men harboring hemizygous *TAF7L* variants.

Subject	M1	M2-1	M2-2	M3	M4
Male age (years)	32	34	27	33	35
Female age (years)	29	31	-	32	-
Number of ICSI cycles	3	4	N/A	2	N/A
Number of oocytes injected	15	21	-	13	-
Number (and rate) of fertilized oocytes	6 (40%)	4 (19%)	–	5 (38%)	–
Number (and rate) of cleavage embryos	2 (33%)	1 (25%)	-	0	-
Number (and rate) of 8-cells	N/A	N/A	–	–	–
Number (and rate) of blastocysts	N/A	N/A	-	-	-
Number of transfer cycles	N/A	N/A	-	-	-
Number of embryos transferred per cycle	1	1	-	-	-
Implantation rate	1	1	-	-	-
Clinical pregnancy rate	1	0	-	0	-
Miscarriage rate	1	-	-	-	-

–, not applicable; N/A, not available

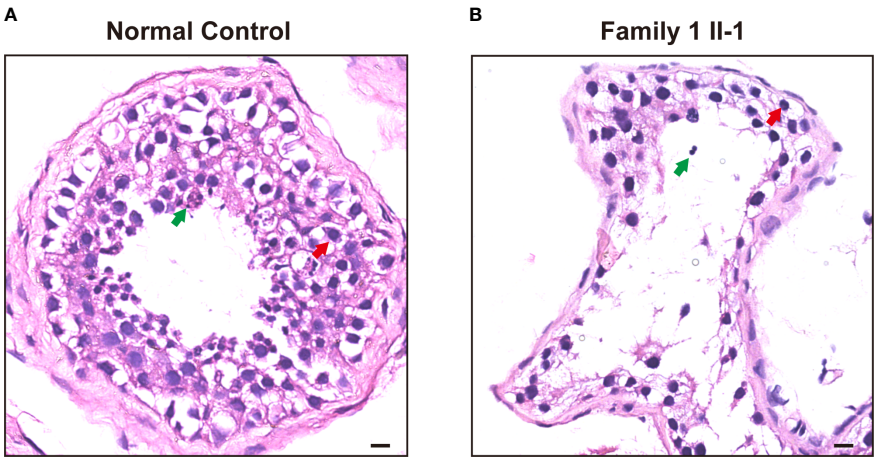

FIGURE 2
H&E staining of cross-sections in the subjects carrying hemizygous mutations in *TAF7L* and a patient with OA. **(A)** H&E staining of cross-sections of testicular biopsy from a patient with OA as the positive control and **(B)** the Family 1 II-1patient. Red arrows mark the spermatocyte. Green arrows mark the spermatozoa. Scale bars: 10μm.

Reduced *in-vitro* fertilization capacity from patients with *TAF7L* variants

To ascertain the fertilization capacity of sperm from patients with *TAF7L* variants, microinjection of spermatozoa into the mice oocytes were performed to demonstrate the capacity of spermatozoa derived from OAT-affected patients with *TAF7L* variants. Notably, the embryos from both *TAF7L* variants and control could develop into the two-cell stage. However, the two-cell rate was significantly reduced compared with the control (10% *vs* 64%) (Figure 3). Collectively, it is illustrated that the sperm from OAT affected patients with *TAF7L* variants showed reduced fertilization capacity compared to the normal sperm.

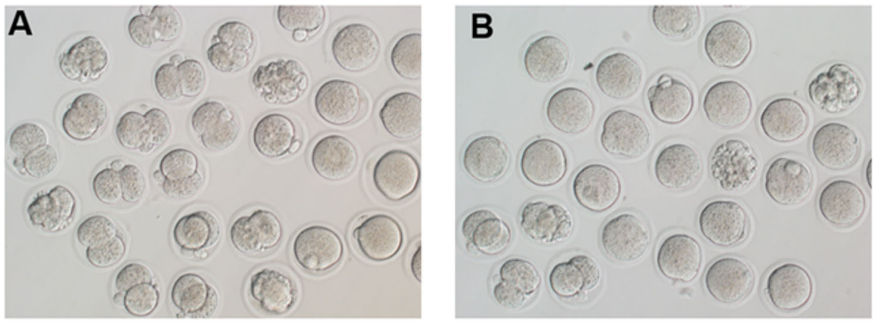

C

	Number of 2-cells	Number of 1-cells	Fragmented cells	Unfertilized cells
NC group (n=50)	32(64%)	4(8%)	6(12%)	7(14%)
TAF7L mut (n=50)	5(10%)	1(2%)	4(8%)	40(80%)

FIGURE 3
Embryos developmental potentials from oocytes of mouse fertilized with sperm carrying hemizygous mutations in *TAF7L* and the healthy man. **(A)** Two cells embryo formation from the ejaculated of healthy man. **(B)** Two cells embryo formation from ejaculated of the patient (Family 1 II-1) presented with OAT phenotype. **(C)** Statistics of pregnancy outcome from the healthy man and patient. NC: normal control.

10.3389/fendo.2022.1099270

Defective chromatin compaction in men carrying hemizygous *TAF7L* variants

The parameters for semen analysis of *TAF7L* variants were obtained from laboratories according to the WHO^{5th} guidelines. Semen analysis indicated severe reduced sperm concentration in all of five men harboring hemizygous *TAF7L* variants (Table 3). Furthermore, Diff-Quik staining displayed sperm head deformity (Figure 4A). Moreover, their nuclei were more efficiently stained with acidic aniline (Figure 4A), implying less condensed chromatin in these sperm head. TEM verified that the heads of sperm were less condensed in comparison with the controls (Figure 4B). These observations indicated of defective chromatin compaction in the heads of sperm.

Abnormal histone-to-protamine during spermiogenesis

To figure out the potential causes underlying defective chromatin compaction in the heads of sperm. Immunofluorescence staining verified abnormal retention of histone H3, and conversely, drastic reduced levels of protamine PRM2 in the heads of sperm (Family 1, M1: II-1) contrast to control (Figure 5).

Subsequently, As shown in Figure 6, RT-PCR analysis revealed that the testicular tissue of patient (Family 1, M1: II-1) had significantly reduced expression of protamine *PRM2* mRNA ($p < 0.001$). And these experiments indicated impaired histone-to-protamine exchange during spermiogenesis.

In vitro protein expression of *TAF7L* variants

To determine the functional phenotypes of missense and LoF variants of human *TAF7L* variants *in vitro*. 293T cells were transiently transfected with the *TAF7L* wild-type and four mutant *TAF7L* plasmids with 3×FLAG tagged. Compared to wild-type, Immunofluorescence analysis showed that variant c.1301_1302del (p. V434Afs*5) and c.508delA (p. T170fs) had no immunofluorescence signal was detected above the background (Figures 7A, B, D), c. 719dupA (p. K240fs) signal was localized massively within the nucleus (Figure 7E). But variant c.699G>T;(p. R233S) location were no different compared to WT (Figure 7C). The WB data were similar with the IF results. The c. 1301_1302del (p. V434Afs*5), c. 508delA (p. T170fs) and c.719dupA (p. K240fs) mutations yielded a truncated protein, c. 1301_1302del (p. V434Afs*5) and c.508delA (p. T170fs) showed nearly undetectable expression protein level and that the c.719dupA (p. K240fs) mutation generated a normal expression truncated protein. There was no change in protein level for the c. 699G>T (p. R233S) mutation (Figure 7F).

Discussion

As discussed above, we found hemizygous mutations of *TAF7L* among five non-related OAT patients (0.68%,5/725). The samples were collected from three different hospitals. The WES results showed that the subjects did not carry any other known pathogenic

TABLE 3 Semen characteristics and sperm morphology in men harboring hemizygous *TAF7L* variants.

Subject	M1	M2-1	M2-2	M3	M4	Reference Limits
Semen parameter						
Semen volume (mL)	2.0	2.0	1.5	1.5	1.5	1.5[a]
Sperm concentration (10^6/mL)	<1.0	<1.0	<1.0	<1.0	<1.0	15.0[a]
Motility (%)	0	0	0	0	0	40.0[a]
Progressive motility (%)	0	0	0	0	0	32[a]
Sperm morphology						
Head defects (%)	95	92	94	97	89	>4[b]
Neck and midpiece defects (%)	5	8	6	3	11	
Tail defects (%)	0	0	0	0	0	
Excess residual cytoplasm (%)	0	0	0	0	0	
Irregular caliber (%)	100	100	100	100	100	

N/A, not available.
[a]Reference limits according to the WHO standards.
[b]Reference limits according to the WHO standards: Normal sperm morphology rate

10.3389/fendo.2022.1099270

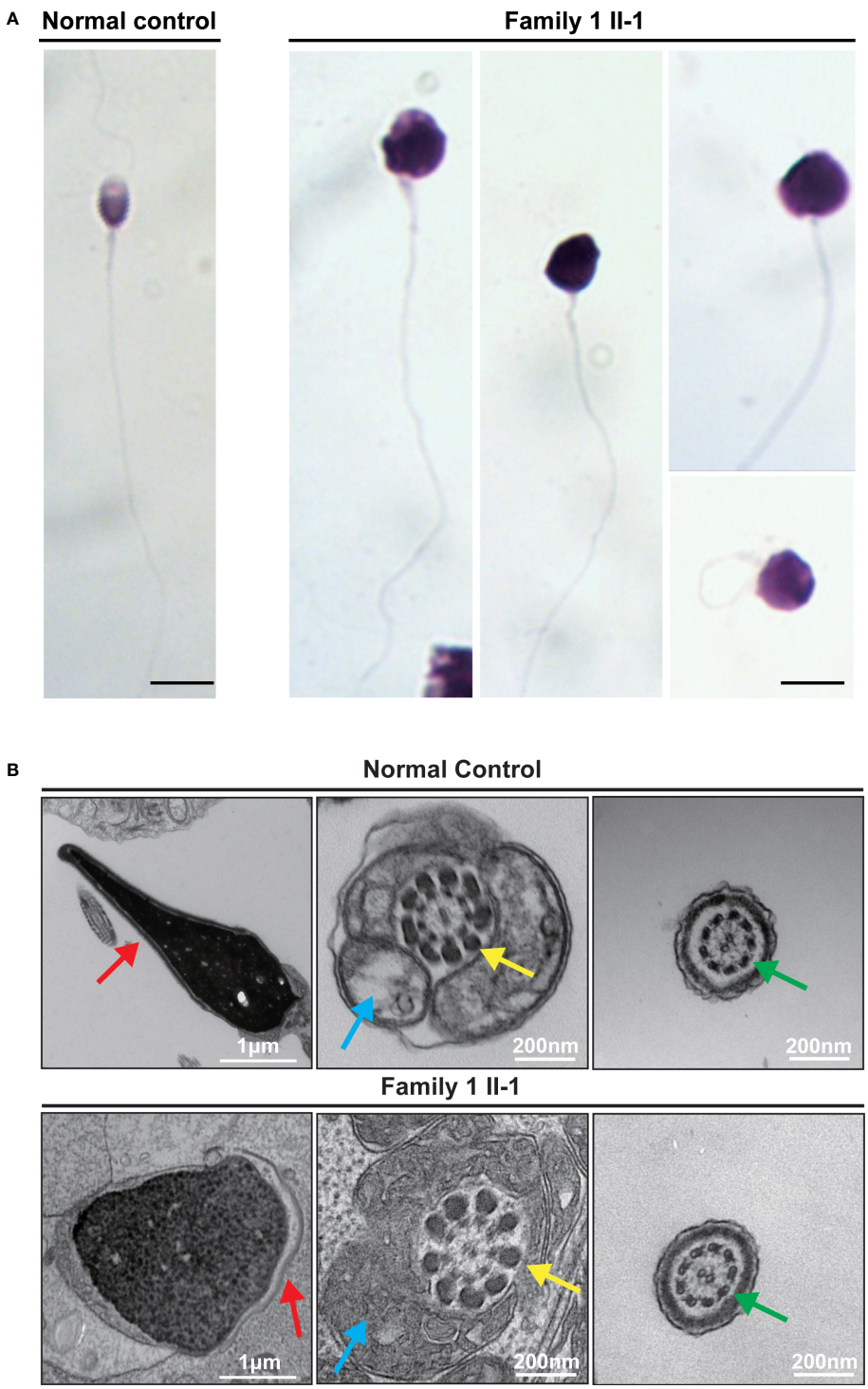

FIGURE 4
Sperm morphology and Ultrastructure Analysesin for the subjects carrying hemizygous mutations in *TAF7L*. **(A)** The morphology of the spermatozoa from a fertile control individual and subject Family 1 II-1 under light microscopy. Multiple images were taken, and typical features of abnormal spermatozoa are exemplified, such as abnormal head. Scale bars: 10 μm. **(B)** The longitudinal sections of sperm flagellar of a control individual. The normal sperm had a symmetrical mid-piece with smooth axoneme surrounding with a regularly arranged mitochondrial sheath. Family 1 II-1 sperm showed the less condensed head. Red arrows mark the acrosome. Blue arrows mark the mitochondrial sheath. Green arrows mark the axoneme. Yellow arrows mark the outer dense fibers.

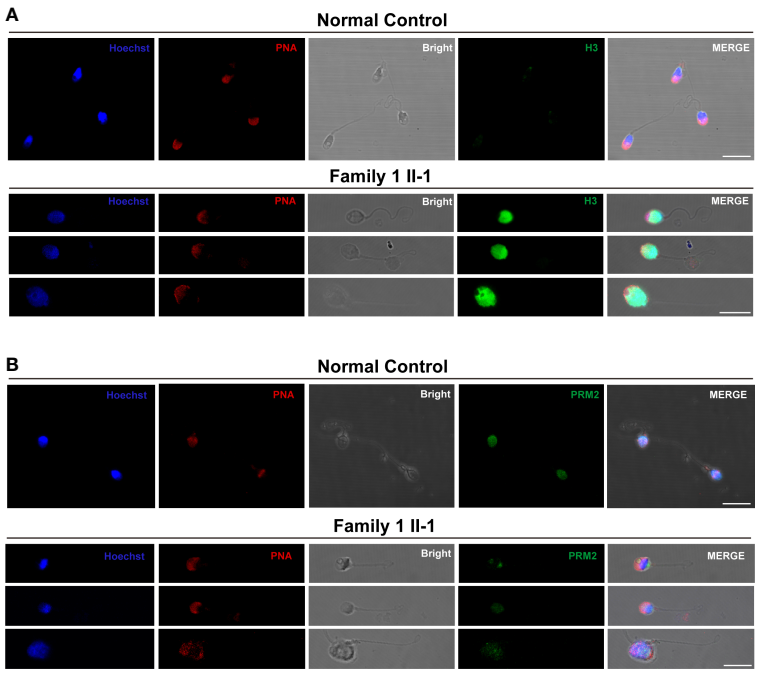

FIGURE 5
The Histone-to-Protamine Exchange Is Impaired during Spermiogenesis in the subjects carrying hemizygous mutations in *TAF7L*. **(A)** Representative confocal images of immunostaining with Hoechst (blue), PNA (red), Bright, and anti-H3 antibody (green) on sperm from *TAF7L* variants -affected patients and normal man. Scale bars: 10μm. **(B)** Representative confocal images of immunostaining with Hoechst (blue), PNA (red), Bright, and anti-PRM2 antibody (green) on sperm from *TAF7L* variants -affected patients and normal man. Scale bars: 10μm.

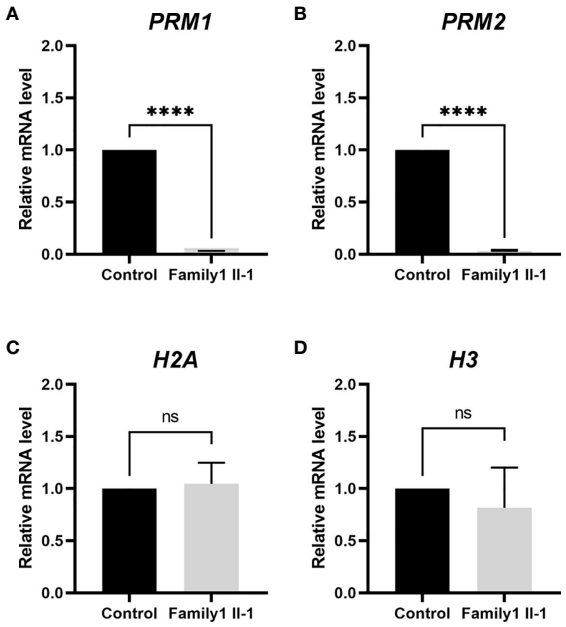

FIGURE 6
Differential abundance of the *PRM1*, *PRM2*, *H2A* and *H3* transcripts in the subject carrying hemizygous mutations in *TAF7L* and normal men. **(A–D)** The mRNA content of *PRM1* and *PRM2* is significantly lower in *TAF7L* variants -affected patient compared with normal man. *H2A* and *H3* mRNA ratio in *TAF7L* variants -affected patient samples are close to normal man. NS, not significant; **** indicates p <0.0001.

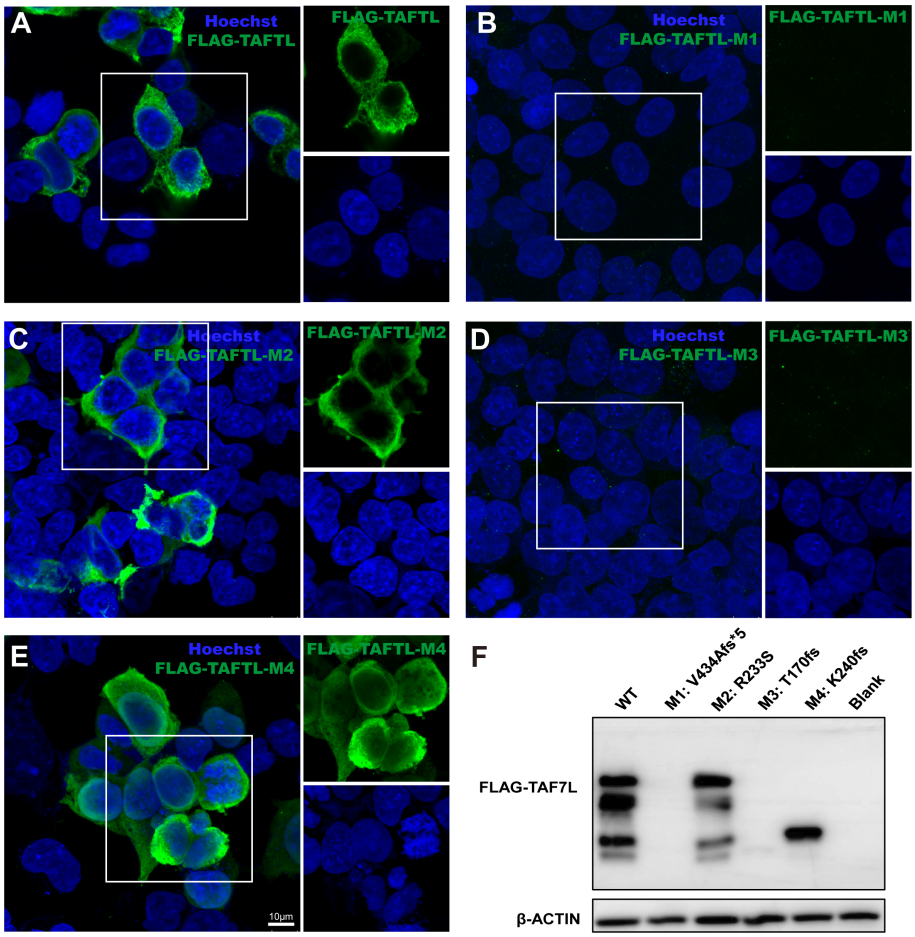

FIGURE 7
Effects of the *TAF7L* variants in *in vitro*. **(A–E)** Immunofluorescence analysis of TAF7L expression in HEK293T cell transfected with FLAG-tagged wild-type and mutant plasmids. **(F)** Western blot analysis of TAF7L-3×FLAG protein level in HEK293T transfected with wild-type and mutant plasmids.

variant related to OAT genes except the hemizygous *TAF7L* mutation. Remarkably, all the *TAF7L* mutations were either completely missing in the public databases (1000 Genomes and gnomAD) or they showed low allelic frequencies. They were indicated to be potentially pathogenic by *in-silico* study. Therefore, it is needed to explore the OAT phenotypes in such cases by hemizygous deleterious variants in *TAF7L*.

TAF7L (also known as CT40) is a paralogue of *TAF7* which is a subunit of TFIID and is specific to germ cells. *TAF7L* encodes a protein associated with transcription factors and is mainly expressed in testis (21). Previously it was found that mice deficient with *TAF7L* exhibited low fertility, abnormal morphology of sperm and reduced motility (22).Previous study mutation frequencies in *Taf7l* gene were likely to be polymorphisms in human. Only one study previously reported a deleterious mutation (D136G) in the X-linked *TAF7L* gene as a potential cause of oligozoospermia in men, but the morphology of sperm was not described in this study. And the corresponding D144G substitution in the mouse *Taf7l* gene does not affect male fertility (23).Therefore, this is a great clinical heterogeneity in man with *Taf7l* variants.

Herein, we identified four deleterious variants *TAF7L* in human. Instead of causing oligozoospermia, the mutation causes OAT, including a hemizygous frameshift mutation of *TAF7L* [c. 1301_1302del;(p. V434Afs*5)] in M1(Figure 1A), one hemizygous missense mutation [c. 699G>T;(p. R233S)] in M2-1 and M2-2, it

was confirmed that this variant was inherited from their parents (Figure 1B). We also found the hemizygous frameshift mutation [c. 508delA;(p. T170fs), c. 719dupA;(p. K240fs)] in M3 and M4, respectively, (Figures 1C, D; Table 1). These four *TAF7L* variants were not found in the control group of human population genome databases and *in silico* analysis predicted as deleterious. *In vitro* tests confirmed the protein-truncating mutation c. 1301_1302del; (p. V434Afs*5), c. 508delA;(p. T170fs), c. 719dupA;(p. K240fs) causes abnormal expression of TAF7L.

No medicine is available for the treatment of OAT patients which can improve the quality of the ejaculated spermatozoa, which renders ICSI as the only solution for conception. However, studies have found that different mutations in various genes cause OAT with various types of clinical outcomes. For instance, biallelic mutations of CEP135 (MIM: 301057) resulted in pregnancy failure, while oligozoospermia due to CFAP47 (MIM:301057) mutation showed good clinical results (12). In this study, the outcomes of the ICSI treatment from three different hospitals showed that the number of blastocysts and two cells embryo formation by *TAF7L* variants was lower compared to the control.

In the current study, these three patients with *TAF7L* variants didn't get clinical pregnancy using ejaculated sperm, two of them chose donor's sperm for ICSI treatment. Ejaculated sperm of patient (Family 1, M1: II-1) without enough spermatozoa were recovered by testicular biopsy on the day of oocyte retrieval. The couple got successful clinical pregnancy at the time of writing (Table 2). Based on the current clinical evaluation of female fertility, we believe that their fertility were normal. Hence, this study supports the idea that male infertility could be because of hemizygous *TAF7L* variants due to the low fertilization capacity of sperm.

To further prove this hypothesis that the capacity of low spermatozoa derived from OAT patients with *TAF7L* variants, microinjection of spermatozoa into the mice oocytes was performed. The two-cell rate was significantly reduced than the control (10% *vs* 64%). This indicated the sperm from OAT patients with *TAF7L* variants showed reduced *in-vitro* fertilization capacity through ICSI treatment.

Why the low capacity of spermatozoa derived from OAT patients with *TAF7L* variants? In this study, we confirmed that the defective chromatin compaction in sperm head of proband (Family 1, M1: II-1). Previous study indicated that Taf7l and Trf2 coregulate the expression of protamine 1/2 (*Prm1/2*) genes, and ChIP-qPCR analysis confirmed dramatically diminished in Taf7l-null testes at target protamine 1/2 (*Prm1/2*) promoters (24). In this study, we found that abnormal retention of histone *H3* and reduced levels of protamine *PRM2* were in the heads of sperm. RT-PCR analysis revealed that the testicular tissue of patient (Family 1, M1: II-1) had significantly reduced expression of protamine *PRM2* mRNA, So we speculated that the abnormal of histone-to-protamine exchange may induce the defective chromatin compaction of sperm head. Because the histone-to-protamine exchange is crucial for producing functional sperm, these results implied that a defect histone-to-protamine exchange may underlie the capacity deficiency of *TAF7L* variants sperm.

Data availability statement

The datasets for this article are not publicly available due to concerns regarding participant/patient anonymity. Requests to access the datasets should be directed to the corresponding authors.

Ethics statement

The research was approved by the corresponding ethics committees of the Shanghai General Hospital, Shanghai Jiao Tong University(2021-SQ-112), the Reproductive and Genetic Hospital of CITIC Xiangya (LL-SC-2017-025 and LL-SC-2019-034), and the Xiamen Maternity and Child Care Hospital, Xiamen (Permit Number: 2020SQ199, KY-2019-060)

Author contributions

CY, ZL and EZ designed the study, directed and supervised the research. HB, YS and YT collected the data. YZ, JX, SX, performed experiments. PL and ZJ have drafted the work. XW, WC, JZ enrolled the patients and collected clinical information. HB wrote the manuscript, with input from others. CY, ZL and EZ substantively revised it. All authors contributed to the article and approved the submitted version.

Funding

This study was supported by National Natural Science Foundation of China (Grant Nos. 82171586, 82071697, 32271163 and 81871200), the Medical Innovation Project of Fujian Province (Grant No. 2020CXB051).

Acknowledgments

We thank the patients and their family members for their support during this research study, and all the individuals who participated in and supported this research.

Conflict of interest

The authors declare that the research was conducted in the absence of any commercial or financial relationships that could be construed as a potential conflict of interest.

Publisher's note

All claims expressed in this article are solely those of the authors and do not necessarily represent those of their affiliated organizations, or those of the publisher, the editors and the reviewers. Any product that may be evaluated in this article, or claim that may be made by its manufacturer, is not guaranteed or endorsed by the publisher.

Supplementary material

The Supplementary Material for this article can be found online at: https://www.frontiersin.org/articles/10.3389/fendo.2022.1099270/full#supplementary-material

References

1. Curi SM, Ariagno JI, Chenlo PH, Mendeluk GR, Pugliese MN, Sardi Segovia LM, et al. Asthenozoospermia: Analysis of a large population. *Arch Androl* (2003) 49(5):343–9. doi: 10.1080/01485010390219656

2. Coutton C, Escoffier J, Martinez G, Arnoult C, Ray PF. Teratozoospermia: spotlight on the main genetic actors in the human. *Hum Reprod Update* (2015) 21 (4):455–85. doi: 10.1093/humupd/dmv020

3. Tang S, Wang X, Li W, Yang X, Li Z, Liu W, et al. Biallelic mutations in CFAP43 and CFAP44 cause Male infertility with multiple morphological abnormalities of the sperm flagella. *Am J Hum Genet* (2017) 100(6):854–64. doi: 10.1016/j.ajhg.2017.04.012

4. McLachlan RI. Approach to the patient with oligozoospermia. *J Clin Endocrinol Metab* (2013) 98(3):873–80. doi: 10.1210/jc.2012-3650

5. Liu C, He X, Liu W, Yang S, Wang L, Li W, et al. Bi-allelic mutations in TTC29 cause Male subfertility with asthenoteratospermia in humans and mice. *Am J Hum Genet* (2019) 105(6):1168–81. doi: 10.1016/j.ajhg.2019.10.010

6. Ghedir H, Gribaa M, Mamai O, Ben Charfeddine I, Braham A, Amara A, et al. Macrozoospermia: screening for the homozygous c.144delC mutation in AURKC gene in infertile men and estimation of its heterozygosity frequency in the Tunisian population. *J Assist Reprod Genet* (2015) 32(11):1651–8. doi: 10.1007/s10815-015-0565-4

7. ElInati E, Fossard C, Okutman O, Ghedir H, Ibala-Romdhane S, Ray PF, et al. A new mutation identified in SPATA16 in two globozoospermic patients. *J Assist Reprod Genet* (2016) 33(6):815–20. doi: 10.1007/s10815-016-0715-3

8. Shang YL, Zhu FX, Yan J, Chen L, Tang WH, Xiao S, et al. Novel DPY19L2 variants in globozoospermic patients and the overcoming this male infertility. *Asian J Androl* (2019) 21(2):183–9. doi: 10.4103/aja.aja_79_18

9. Ben Khelifa M, Coutton C, Zouari R, Karaouzene T, Rendu J, Bidart M, et al. Mutations in DNAH1, which encodes an inner arm heavy chain dynein, lead to male infertility from multiple morphological abnormalities of the sperm flagella. *Am J Hum Genet* (2014) 94(1):95–104. doi: 10.1016/j.ajhg.2013.11.017

10. Sha Y, Chen Y, Wang X, Meng R, Yang X, Li Y, et al. Biallelic mutations in IQCN, encoding a novel acroplaxome protein, lead to fertilization failure and male infertility with defects in the acrosome and shaping of the spermatid head in humans and mice. *Life Med* (2022) lnac050. doi: 10.1093/lifemedi/lnac050

11. Liu C, Miyata H, Gao Y, Sha Y, Tang S, Xu Z, et al. Bi-allelic DNAH8 variants lead to multiple morphological abnormalities of the sperm flagella and primary Male infertility. *Am J Hum Genet* (2020) 107(2):330–41. doi: 10.1016/j.ajhg.2020.06.004

12. Liu C, Tu C, Wang L, Wu H, Houston BJ, Mastrorosa FK, et al. Deleterious variants in X-linked CFAP47 induce asthenoteratozoospermia and primary male infertility. *Am J Hum Genet* (2021) 108(2):309–23. doi: 10.1016/j.ajhg.2021.01.002

13. Lv M, Liu W, Chi W, Ni X, Wang J, Cheng H, et al. Homozygous mutations in DZIP1 can induce asthenoteratospermia with severe MMAF. *J Med Genet* (2020) 57(7):445–53. doi: 10.1136/jmedgenet-2019-106479

14. Tu C, Cong J, Zhang Q, He X, Zheng R, Yang X, et al. Bi-allelic mutations of DNAH10 cause primary male infertility with asthenoteratozoospermia in humans and mice. *Am J Hum Genet* (2021) 108(8):1466–77. doi: 10.1016/j.ajhg.2021.06.010

15. Vockel M, Riera-Escamilla A, Tuttelmann F, Krausz C. The X chromosome and male infertility. *Hum Genet* (2021) 140(1):203–15. doi: 10.1007/s00439-019-02101-w

16. Vogt PH, Edelmann A, Kirsch S, Henegariu O, Hirschmann P, Kiesewetter F, et al. Human y chromosome azoospermia factors (AZF) mapped to different subregions in Yq11. *Hum Mol Genet* (1996) 5(7):933–43. doi: 10.1093/hmg/5.7.933

17. Boroujeni PB, Sabbaghian M, Totonchi M, Sodeifi N, Sarkardeh H, Samadian A, et al. Expression analysis of genes encoding TEX11, TEX12, TEX14 and TEX15 in testis tissues of men with non-obstructive azoospermia. *JBRA Assist Reprod* (2018) 22(3):185–92. doi: 10.5935/1518-0557.20180030

18. Yatsenko AN, Georgiadis AP, Ropke A, Berman AJ, Jaffe T, Olszewska M, et al. X-Linked TEX11 mutations, meiotic arrest, and azoospermia in infertile men. *N Engl J Med* (2015) 372(22):2097–107. doi: 10.1056/NEJMoa1406192

19. Zhang DL, Sun YJ, Ma ML, Wang YJ, Lin H, Li RR, et al. Gq activity- and beta-arrestin-1 scaffolding-mediated ADGRG2/CFTR coupling are required for male fertility. *Elife* (2018) 7:e33432. doi: 10.7554/eLife.33432

20. Yang S, Ping P, Ma M, Li P, Tian R, Yang H, et al. Generation of haploid spermatids with fertilization and development capacity from human spermatogonial stem cells of cryptorchid patients. *Stem Cell Rep* (2014) 3 (4):663–75. doi: 10.1016/j.stemcr.2014.08.004

21. Akinloye O, Gromoll J, Callies C, Nieschlag E, Simoni M. Mutation analysis of the X-chromosome linked, testis-specific TAF7L gene in spermatogenic failure. *Andrologia* (2007) 39(5):190–5. doi: 10.1111/j.1439-0272.2007.00789.x

22. Pointud JC, Mengus G, Brancorsini S, Monaco L, Parvinen M, Sassone-Corsi P, et al. The intracellular localisation of TAF7L, a paralogue of transcription factor TFIID subunit TAF7, is developmentally regulated during male germ-cell differentiation. *J Cell Sci* (2003) 116(Pt 9):1847–58. doi: 10.1242/jcs.00391

23. Ling L, Li F, Yang P, Oates RD, Silber S, Kurischko C, et al. Genetic characterization of a missense mutation in the X-linked TAF7L gene identified in an oligozoospermic man. *Biol Reprod* (2022) 107(1):157–67. doi: 10.1093/biolre/ioac093

24. Zhou H, Grubisic I, Zheng K, He Y, Wang PJ, Kaplan T, et al. Taf7l cooperates with Trf2 to regulate spermiogenesis. *Proc Natl Acad Sci USA* (2013) 110(42):16886–91. doi: 10.1073/pnas.1317034110

frontiers | Frontiers in Endocrinology

TYPE Original Research
PUBLISHED 16 January 2023
DOI 10.3389/fendo.2022.1058651

OPEN ACCESS

EDITED BY
Tao Luo,
Nanchang University, China

REVIEWED BY
Yang Xiaoyu,
Nanjing Medical University, China
Shenmin Yang,
Suzhou Municipal Hospital, China

*CORRESPONDENCE
Xiaoli Wei
xiaoli@ynu.edu.cn
Xiaoming Jiang
keaishmily@126.com
Weibing Qin
guardqin@163.com

†These authors have contributed equally to this work

SPECIALTY SECTION
This article was submitted to Reproduction, a section of the journal Frontiers in Endocrinology

RECEIVED 30 September 2022
ACCEPTED 25 October 2022
PUBLISHED 16 January 2023

CITATION
Sha Y, Liu W, Nie H, Han L, Ma C, Zhang X, Xiao Z, Qin W, Jiang X and Wei X (2023) Homozygous mutation in *DNALI1* leads to asthenoteratozoospermia by affecting the inner dynein arms. *Front. Endocrinol.* 13:1058651. doi: 10.3389/fendo.2022.1058651

Homozygous mutation in *DNALI1* leads to asthenoteratozoospermia by affecting the inner dynein arms

Yanwei Sha[1,2,3†], Wensheng Liu[4†], Hua Nie[4†], Lu Han[4], Chunjie Ma[4], Xiaoya Zhang[5], Ziyi Xiao[6], Weibing Qin[4*], Xiaoming Jiang[7*] and Xiaoli Wei[6*]

[1]Department of Andrology, Women and Children's Hospital, School of Medicine, Xiamen University, Xiamen, Fujian, China, [2]Fujian Provincial Key Laboratory of Reproductive Health Research, School of Medicine, Xiamen University, Xiamen, Fujian, China, [3]State Key Laboratory of Molecular Vaccinology and Molecular Diagnostics, School of Public Health, Xiamen University, Xiamen, Fujian, China, [4]National Health Commission (NHC) Key Laboratory of Male Reproduction and Genetics, Guangdong Provincial Reproductive Science Institute (Guangdong Provincial Fertility Hospital), Guangzhou, China, [5]School of Pharmaceutical Sciences, State Key Laboratory of Cellular Stress Biology, Xiamen University, Xiamen, Fujian, China, [6]School of Medicine, Yunnan University, Kunming, Yunnan, China, [7]Reproductive Medicine Center, Xiamen University Affiliated Chenggong Hospital, Xiamen, Fujian, China

Asthenozoospermia is the most common cause of male infertility. Dynein protein arms play a crucial role in the motility of sperm flagella and defects in these proteins generally impair the axoneme structure and affect sperm flagella function. In this study, we performed whole exome sequencing for a cohort of 126 infertile patients with asthenozoospermia and identified homozygous *DNALI1* mutation in one patient from a consanguineous family. This identified homozygous mutation was verified by Sanger sequencing. *In silico* analysis showed that this homozygous mutation is very rare, highly pathogenic, and very conserved. Sperm routine analysis confirmed that the motility of the spermatozoa from the patient significantly decreased. Further sperm morphology analysis showed that the spermatozoa from the patient exhibited multiple flagella morphological defects and a specific loss in the inner dynein arms. Fortunately, the patient was able to have his child *via* intracytoplasmic sperm injection treatment. Our study is the first to demonstrate that homozygous *DNALI1* mutation may impair the integration of axoneme structure, affect sperm motility and cause asthenoteratozoospermia in human beings.

KEYWORDS

asthenoteratozoospermia, whole-exome sequencing, *DNALI1*, inner dynein arms, intracytoplasmic sperm injection

Abbreviations: DNALI1, dynein axonemal light intermediate chain 1; WES, whole exome sequencing; MTD, microtubule doublets; TEM, transmission electron microscopy; ICSI, intracytoplasmic sperm injection; IDA, inner dynein arm; ODA, outer dynein arm; CASA, computer-assisted sperm analysis; EXAC, exome aggregation consortium; ACMG, American college of medical genetics and genomics.

Background

More than 80% of male infertility cases exhibit asthenozoospermia, which is caused by the dysfunction of sperm motility, such as reduced or completely absent sperm motility in the ejaculated (1, 2). Many factors, such as infection, varicocele, and pollution exposure, may predispose to asthenozoospermia. However, the genetic factors underlying asthenozoospermia cannot be ignored (3, 4).

The sperm flagellum plays an essential role in sperm motility through its conserved axonemal structure (5). Sperm axonemes consist of highly ordered "9+2" microtubules characterized by a central pair of microtubules surrounded by nine peripheral microtubule doublets (MTD) (6). There are various protein complexes, such as radial spokes, nexin-dynein regulatory complex, central complex, and dynein arms, as major components of the axoneme (7). Among these important complexes, dynein arms consisting of an inner and an outer dynein arm (IDA and ODA, respectively) are attached to each of the nine MTDs, which are essential for generating the beating forces of sperm flagellum (8). Strikingly, each dynein arm possesses a similar molecular composition: several light-chain proteins, at least two heavy-chain proteins, and at least two intermediate-chain proteins (9–11).

Dynein axonemal light intermediate chain 1 (*DNALI1*), also called *P28*, encodes a flagellar protein that is essential for the assembly of the inner dynein arm (12). Previous studies have shown that *p28* mutation disrupted dynein heavy chain composition in *Tetrahymena thermophila*, leading to defects in beat frequency and waveform patterns of cilia (13). Furthermore, DNALI1 is strongly expressed in spermatocytes, spermatids, and flagella of mature sperm in the murine testis, indicating its potential function in male reproduction (12). Based on structural analysis, DNALI1 was found to be linked to the C-terminus of DNAH1, and infertile patients with *DNAH1* mutations also presented DNALI1 defect in human beings (12, 14). Unfortunately, the role of DNALI1 in male reproduction has not been reported.

In the present study, we conducted whole-exome sequencing on 126 patients with asthenozoospermia and identified a homozygous mutation in *DNALI1* from an infertile patient. The spermatozoa of this patient showed motility and morphological defects, as well as a significant loss of the internal dynein arms. Our findings proposed that mutation in *DNALI1* is novel genetic pathogenesis of asthenoteratozoospermia and this infertile defect can be overcome by ICSI for the first time. These results demonstrate that DNALI1 plays an important role in the motility of sperm flagellum, which may extend the spectrum of etiological genes and provide new insight into the diagnosis and treatment of patients with asthenoteratozoospermia.

Methods

Subjects

We recruited 126 patients who were infertile due to asthenozoospermia for genetic analysis and 60 fertile healthy men as control subjects. The parents of the *DNALI1* mutated patient had consanguineous marriage. All infertile patients included in the study were excluded for abnormal karyotype, translocations, Y chromosome microdeletions, etc. We performed a routine analysis of semen for the participants.

Ethical approval

This study was approved by the Ethics Committee of Women and Children's Hospital of Xiamen University. All subjects participating in the study signed a written informed consent form.

Whole-exome sequencing and Sanger sequencing

Whole-exome sequencing (WES) was performed on these asthenozoospermia patients as previously described (15). Briefly, genomic DNA for each patient was isolated from the peripheral blood sample and processed for exome enrichment using the TruSeq Exome Enrichment kit according to the manufacturer's protocol. DNA sequencing was performed on an Illumina Hiseq 2000 sequencer and sequence reads were aligned to the human genome reference (hg19) using Burrows-Wheeler Aligner and sorted by Picard software. Candidate variants were annotated by using ANNOVAR and other bioinformatics databases. Further Sanger sequencing was performed to validate the selected mutation site in the *DNALI1* mutated patient. We were unable to validate this mutation site in his parents because both of his parents passed away.

Transmission electron microscopy

Transmission electron microscopy (TEM) was performed at the core facility of biomedical sciences of Xiamen University as

described elsewhere (16). Briefly, the fresh spermatozoa were first fixed by incubation in 2.5% glutaraldehyde. The samples were washed twice with 0.1M phosphate buffer and resuspended in 0.2 M sodium cacodylate buffer. After embedding with Epon 812, the ultrathin sections were stained with uranyl acetate and lead citrate and observed by TEM (JEM-1400, Jeol, Japan).

Intracytoplasmic sperm injection

Intracytoplasmic sperm injection (ICSI) treatment for assisted fertilization was performed as described previously (17). The percentage of fertilization was evaluated by the presence of two polar bodies and two pronuclei. Then the embryos were individually cultured in Vitrolife G-SERIES culture media. Serum HCG levels were measured 14 days after embryo transfer and clinical pregnancy was confirmed by ultrasound performed 28 days after embryo transfer.

Results

Identification of homozygous *DNALI1* mutation in a patient with asthenoteratozoospermia

We performed WES and bioinformatic analyses to reveal the genetic etiology of 126 patients with asthenozoospermia and identified the homozygous *DNALI1* mutation NM_003462.5: c.691_693del in a patient from a consanguineous family (Figure 1A). This homozygous *DNALI1* mutation in this patient was further confirmed by Sanger sequencing (Figure 1B). Among

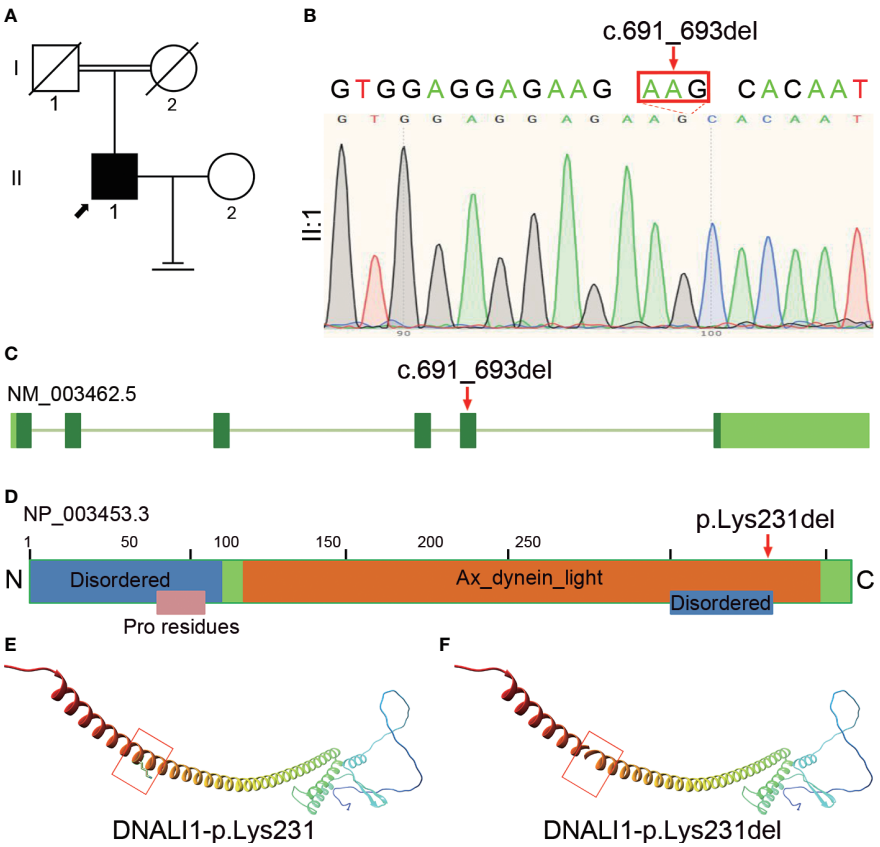

FIGURE 1
Identification of homozygous *DNALI1* mutation in an infertile man with asthenoteratozoospermia. **(A)** Pedigree chart of the patient with asthenoteratozoospermia. The black square and the black arrow represent the proband. **(B)** Sanger sequencing verified the variant in the patient. The mutated bases are indicated by the red arrow and red rectangle. **(C)** The location of the mutated bases on the genome of *DNALI1*. **(D)** The position of the amino acid substitution on the domain map of DNALI1. The blue rectangle represents the "Disordered" domain, the orange rectangle represents the "Ax_dynein_light" domain, and the pink rectangle represents the "Pro residues" domain. **(E)** The position of the affected amino acid on the three-dimensional structure of the wild-type DNALI1. The red rectangle shows p.Lys231 of DNALI1. **(F)** Effect of the deletion mutation on DNALI1 three-dimensional structure. The red rectangle shows the site of the deleted amino acid.

all homozygous or compound heterozygous mutated genes in this patient, no genes that have been reported to be associated with asthenozoospermia, teratozoospermia, or structural components of spermatozoa were identified. Among the testis-specific or highly expressed genes, also only the DNALI1 gene was mutated and has been associated with primary ciliary dyskinesia. The ultrastructural defects of the inner dynein arms could be found. In *Chlamydomonas*, mutations in this gene exhibits similar defects. Moreover, by TEM, we also observed a defect in the inner dynein arms of axonemes in this patient. Based on these evidences, we hypothesize that *DNALI1* mutation is likely responsible for asthenoteratozoospermia in this patient.

This patient had some symptoms of suspected PCD such as cough, chronic sinusitis, and recurrent upper respiratory tract infections. Based on this, we hypothesized that this patient is a suspected PCD patient. This patient had a history of infertility for 5 years after marriage, but his parents had normal fertility with only one child. Although further verification was not available due to the passing of his parents, we hypothesized that the patient's parents were heterozygous carriers of this mutation and that the patient's homozygous mutation locus was likely inherited from his parents who had a consanguineous marriage.

In silico analysis of the identified homozygous *DNALI1* mutation

The homozygous *DNALI1* mutation was further evaluated using *in silico* analysis. This *DNALI1* mutation NM_003462.5: c.691_693del (p.Lys231del) is very rare in the EXAC, 1000 genome, ESP6500, and gnomAD databases of the human population. This variant is classified as of uncertain significance with minor pathogenic evidence according to the ACMG Classification.

This homozygous NM_003462.5:c.691_693del (p.Lys231del) mutation is located at the fifth exon of the *DNALI1* genome (Figure 1C) and results in the deletion of the 231th amino acid in the Ax_dynein_light and the Disordered domains (Figure 1D). We then aligned the amino acid sequences of DNALI1 from *Homo sapiens* to that of *Drosophila melanogaster* and found that the amino acid affected by the NM_003462.5:c.691_693del (p.Lys231del) mutation is highly conserved among these species from human beings to fruit fly (Supplementary Figure 1). In addition, we constructed the mutated protein structure using SWISS-MODEL and found that this mutation affected the three-dimensional structure of DNALI1. Compared to the original DNALI1 three-dimensional structure (Figure 1E), the NM_003462.5:c.691_693del (p.Lys231del) mutation resulted in the deletion of Lysine at the 231th (Figure 1F). Lysine is a positively charged basic hydrophilic essential amino acid of the basic amino acid class. This change could significantly affect the nearby steric hindrance and the three-dimensional structure of DNALI1, possibly affecting its stability and function.

Spermatozoa defects of the patient with *DNALI1* deficiency

Clinical examination showed that the *DNALI1*-mutated patient had normal physical development. No significant abnormalities were found in the development of organs or accessory glands of the reproductive system. Serum hormone levels were within the normal range, with only a slight increase in PRL values (Table 1). Routine semen analysis was performed for the patient, and the results showed that the patient had normal sperm concentration. However, the percentages of progressive motility and non-progressive motility were significantly decreased, and the percentage of normal morphology sperm was also lower than the reference value (Table 2). We performed CASA on the patient's spermatozoa, and the results showed that the patients had significantly lower sperm parameters (Table 3).

Compared with the normal morphology of the spermatozoa from the control subject, the results of Papanicolaou staining showed that the patient's spermatozoa exhibited multiple flagellar defects, including absent or coiled flagella (Figure 2A). The results of field emission scanning electron microscopy further confirmed the morphological defects of the patient's spermatozoa (Figure 2B). In addition, TEM analysis was performed to explore ultrastructural defects, and it was found that the cross-section of the control sample showed a typical "9 +2" axoneme structure, but the cross-sections of the patient's spermatozoa exhibited specific inner dynein arm defects (Figure 2C).

TABLE 1 Clinical data of the patient harboring homozygous *DNALI1* mutation.

	Patient	Reference
Age (year)	32	–
Infertility (year)	5	
Height (cm)	166	–
Body weight (kg)	60	–
BMI	22.58	–
Testicular volume (Left/Right, ml)	12/12	10-15ml
FSH (mIU/ml)	10.18	1.27~18.96
LH (mIU/ml)	8.23	1.24~8.62
Testosterone (ng/ml)	4.51	4.14-7.26
PRL (ng/ml)	14.38	2.64~13.13
E2 (pg/ml)	22	20~75

TABLE 2 Semen parameters of the patient with asthenoteratozoospermia.

Patient	Volume (ml)	PH	Concentration (10^6/ml)	Total sperm (10^6)	PR (%)	NP (%)	PR+NP (%)	IM (%)	Normal forms (%)
First	3.0	7.20	16.42	49.25	15.67	0.75	16.42	83.58	3
Second	3.0	7.30	9.80	29.40	6.25	1.25	7.5	92.50	3
Reference	≥1.5	≥7.2	≥15	≥39	≥32	–	≥40	–	≥4

PR, progressive motility; NP, non-progressive motility; IM, immotility.

Prognosis of the *DNALI1*-mutated patient following ICSI treatment

This couple underwent two cycles of ICSI treatment. In the first cycle, we retrieved 18 oocytes, 14 of which were in the MII stage. All these 14 oocytes at the MII stage were injected with the proband's sperm and nine of them were fertilized. After embryo culture, only one blastocyst was formed on day 3. This embryo was transferred, but his wife failed to be conceived. In the second cycle, 14 oocytes were retrieved, nine of which were in the MII stage. All nine of these MII oocytes were injected with the proband's sperm and all of them were fertilized. After embryo culture, two blastocysts were formed and transferred. The embryos were successfully implanted and his wife had a clinically successful pregnancy.

Discussion

In this study, we recruited 126 infertile patients due to asthenozoospermia and detected a homozygous *DNALI1* mutation from one patient with asthenoteratozoospermia. This homozygous mutation in *DNALI1* resulted in the deletion of the inner dynein arms, which severely impairs sperm motility. These data suggest that *DNALI1* is a novel gene associated with sperm flagellar function and defects in this gene may contribute to asthenoteratozoospermia in humans.

The formation and function of sperm flagellum are essential for sperm motility (18). Typically, the sperm flagellum has a highly organized axoneme portion consisting of nine outer doublet microtubules and a central pair microtubule, called the "9+2" structure (19). Axonemal dyneins, including ODA and IDA, are observed on outer doublet microtubules, which play a central role in the beating and motility of sperm flagellum (20). Indeed, mutations in genes associated with the formation of the sperm tail are responsible for sperm motility and fertility defect (18). For example, mutations in IDA and ODA genes, such as *DNAH1*, *DNAH2*, *DNAH8*, and *DNAH10*, cause male infertility due to asthenozoospermia with multiple morphological abnormalities of the sperm flagella (21). However, mutations in *DNAH5*, *DNAH11*, and *DNAI1* also lead to male infertility due to isolated non-syndromic asthenozoospermia (22, 23). In this study, we identified for the first time homozygous *DNALI1* mutation as potential pathogenesis for asthenoteratozoospermia.

DNALI1 is a kind of axonemal IDA protein and is mainly expressed in the human ciliated tissues, including the testis, ovary, and lung (12). *DNALI1* mutation altered dynein heavy chain composition, which further resulted in defects in beat frequency and waveform patterns of cilia in *Tetrahymena thermophila* (13). In the present study, spermatozoa from the *DNALI1*-mutated patient exhibited specific inner dynein arm loss, resulting in a significant decrease in progressive and non-progressive motility. Moreover, CASA results further demonstrated that the motility parameters of the patient's sperm were significantly reduced. In addition to the motility of spermatozoa, the flagella morphology of the patient's sperm also exhibited various abnormalities characterized by absent or coiled flagella. These findings suggest that defects in *DNALI1* may

TABLE 3 Semen parameters of CASA of the patient with asthenoteratozoospermia.

Patient	VCL (μm/s)	VSL (μm/s)	VAP (μm/s)	ALH (μm)	LIN (%)	WOB (%)	STR (%)	BCF (Hz)	MAD (°)
First	26.98	22.62	23.13	1.80	83.28	85.56	96.87	5.25	35.85
Second	28.75	20.58	22.26	3.66	68.73	77.10	84.10	5.30	33.29

1. VCL, curvilinear velocity (m/s). The time-averaged velocity of a sperm head along its actual curvilinear path, as perceived in two dimensions in the microscope. A measure of cell vigor.
2. VSL, straight-line (rectilinear) velocity (m/s). The time-averaged velocity of a sperm head along the straight line between its first detected position and its last.
3. VAP, average path velocity (m/s). The time-averaged velocity of a sperm head along its average path. This path is computed by smoothing the curvilinear trajectory according to algorithms in the CASA instrument; these algorithms vary between instruments, so values may not be comparable among systems.
4. ALH, the amplitude of lateral head displacement (m). The magnitude of lateral displacement of a sperm head about its average path. It can be expressed as a maximum or an average of such displacements. Different CASA instruments compute ALH using different algorithms, so values may not be comparable among systems.
5. LIN, linearity. The linearity of a curvilinear path, VSL/VCL.
6. WOB, wobble. A measure of oscillation of the actual path about the average path, VAP/VCL.
7. STR, straightness. Linearity of the average path, VSL/VAP.
8. BCF, beat-cross frequency (Hz). The average rate at which the curvilinear path crosses the average path.
9. MAD, mean angular displacement (degrees). The time-averaged absolute values of the instantaneous turning angle of the sperm head along its curvilinear trajectory.

10.3389/fendo.2022.1058651

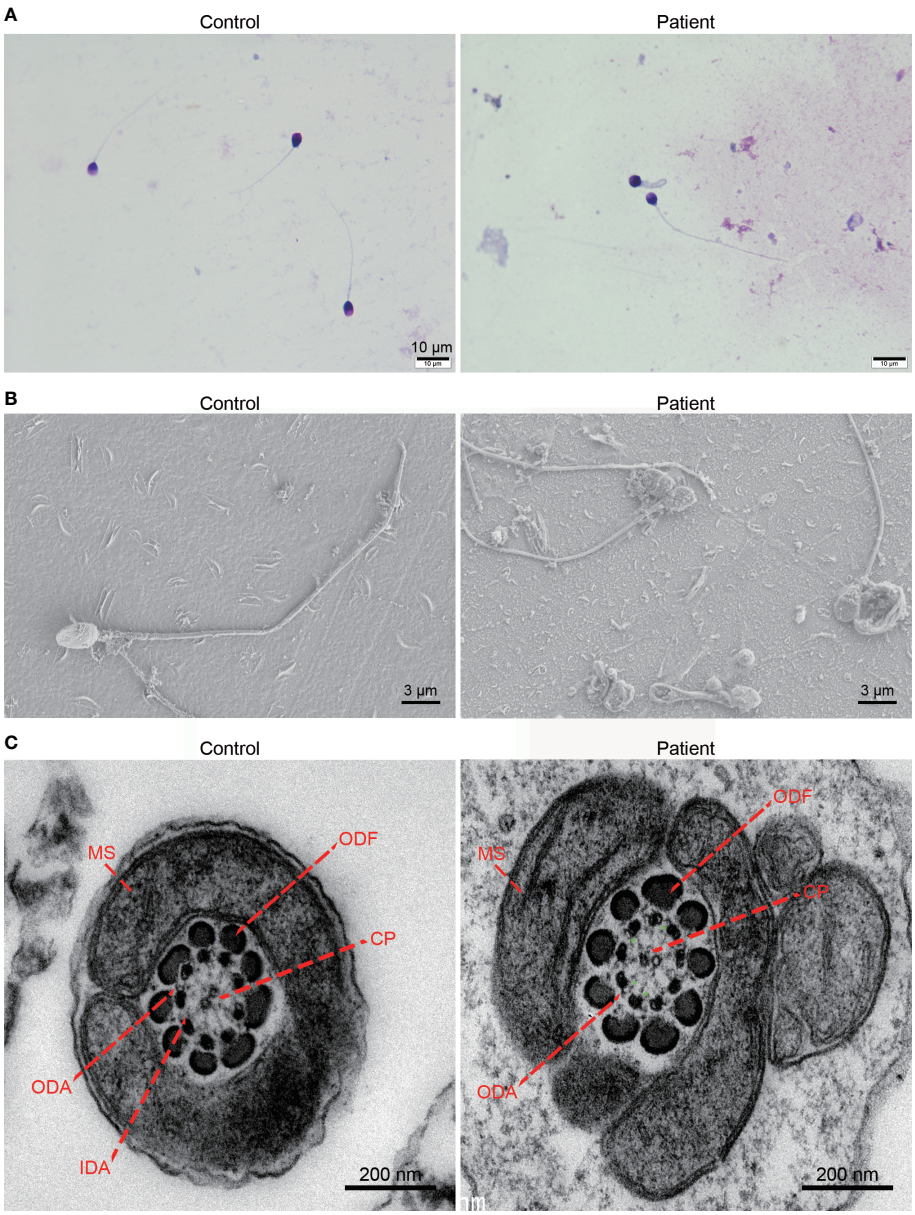

FIGURE 2
Morphological and ultrastructural analysis of the spermatozoa from the *DNALI1*-mutated patient. **(A)** Morphological analysis of the spermatozoa from a control subject and the patient with homozygous *DNALI1* mutation. Scale bar: 10 μm. **(B)** Morphological analysis of the patient's spermatozoa by field emission scanning electron microscopy. Scale bar: 3 μm. **(C)** Ultrastructure analysis of the spermatozoa from the patient at the midpiece. The green "*" indicates the loss of IDA. Scale bar: 200 nm. CP, central pair of microtubules; ODF, outer dense fiber; MS, mitochondrial sheath; ODA, outer dynein arm; IDA, inner dynein arm.

affect IDA assembly during flagellar axoneme formation, leading to IDA deficiency, sperm flagellar morphology anomalous, and asthenozoospermia.

ICSI is the preferred clinical treatment for patients with asthenoteratozoospermia (24). However, for some patients with idiopathic asthenoteratozoospermia, multiple attempts are often required and some do not end up with satisfactory results (25). Therefore, reports on assisted reproduction are of clinical importance when studying infertility due to genetic defects. In this study, the patient underwent two cycles of ICSI treatment

and obtained a clinical pregnancy, which could provide a reference for other infertility due to *DNALI1* deficiency.

Conclusions

In summary, our work demonstrates that genetic defects of *DNALI1* severely impair sperm motility and contribute to the human azoospermia phenotype, for which ICSI treatment is an effective remedy for the first time. Our results prove the importance of DNALI1 in the structure and function of the sperm axoneme, which provides novel evidence for a comprehensive understanding of the axonemal assembly and function of sperm flagellum.

Data availability statement

The datasets presented in this article are not readily available because the CNGB regulations. Requests to access the datasets should be directed to Y-WS, shayanwei928@126.com.

Ethics statement

The studies involving human participants were reviewed and approved by the Ethics Committee of Women and Children's Hospital of Xiamen University. The patients/participants provided their written informed consent to participate in this study.

Author contributions

XW and XJ designed this study. XW and WL drafted the manuscript. YS, WQ, and HN performed bioinformatic analysis. XZ and ZX performed molecular genetics experiments. YS and XJ conducted clinical phenotyping. LH and CM interpreted the data. All authors approved the final manuscript.

Funding

This work was supported by the following grants: the National Natural Science Foundation of China (82071697, and 81871200), the Medical Innovation Project of Fujian Province (2020-CXB-051), the open project of NHC Key Laboratory of Male Reproduction and Genetics in Guangzhou (KF202004).

Acknowledgments

We express our deepest gratitude to the participants for their cooperation.

Conflict of interest

The authors declare that the research was conducted in the absence of any commercial or financial relationships that could be construed as a potential conflict of interest.

Publisher's note

Supplementary material

The Supplementary Material for this article can be found online at: https://www.frontiersin.org/articles/10.3389/fendo.2022.1058651/full#supplementary-material

References

1. Curi SM, Ariagno JI, Chenlo PH, Mendeluk GR, Pugliese MN, Sardi Segovia LM, et al. Asthenozoospermia: analysis of a large population. *Arch Androl* (2003) 49:343–9. doi: 10.1080/01485010390219656

2. Sha Y, Wei X, Ding L, Mei L, Huang X, Lin S, et al. DNAH17 is associated with asthenozoospermia and multiple morphological abnormalities of sperm flagella. *Ann Hum Genet* (2020) 84:271–9. doi: 10.1111/ahg.12369

3. Tu C, Wang W, Hu T, Lu G, Lin G, Tan YQ. Genetic underpinnings of asthenozoospermia. *Best Pract Res Clin Endocrinol Metab* (2020) 34:101472. doi: 10.1016/j.beem.2020.101472

4. Shahrokhi SZ, Salehi P, Alyasin A, Taghiyar S, Deemeh MR. Asthenozoospermia: Cellular and molecular contributing factors and treatment strategies. *Andrologia* (2020) 52:e13463. doi: 10.1111/and.13463

5. Inaba K. Sperm flagella: comparative and phylogenetic perspectives of protein components. *Mol Hum Reprod* (2011) 17:524–38. doi: 10.1093/molehr/gar034

6. Linck RW, Chemes H, Albertini DF. The axoneme: the propulsive engine of spermatozoa and cilia and associated ciliopathies leading to infertility. *J Assist Reprod Genet* (2016) 33:141–56. doi: 10.1007/s10815-016-0652-1

7. Heuser T, Raytchev M, Krell J, Porter ME, Nicastro D. The dynein regulatory complex is the nexin link and a major regulatory node in cilia and flagella. *J Cell Biol* (2009) 187:921–33. doi: 10.1083/jcb.200908067

8. Sui H, Downing KH. Molecular architecture of axonemal microtubule doublets revealed by cryo-electron tomography. *Nature* (2006) 442:475–8. doi: 10.1038/nature04816

9. Mische S, He Y, Ma L, Li M, Serr M, Hays TS. Dynein light intermediate chain: an essential subunit that contributes to spindle checkpoint inactivation. *Mol Biol Cell* (2008) 19:4918–29. doi: 10.1091/mbc.e08-05-0483

10. Asai DJ, Wilkes DE. The dynein heavy chain family. *J Eukaryot Microbiol* (2004) 51:23–9. doi: 10.1111/j.1550-7408.2004.tb00157.x

11. Ide T, Owa M, King SM, Kamiya R, Wakabayashi K. Protein-protein interactions between intermediate chains and the docking complex of chlamydomonas flagellar outer arm dynein. *FEBS Lett* (2013) 587:2143–9. doi: 10.1016/j.febslet.2013.05.058

12. Rashid S, Breckle R, Hupe M, Geisler S, Doerwald N, Neesen J. The murine Dnali1 gene encodes a flagellar protein that interacts with the cytoplasmic dynein heavy chain 1. *Mol Reprod Dev* (2006) 73:784–94. doi: 10.1002/mrd.20475

13. Subramanian A, Kabi A, Gray SF, Pennock D. p28 dynein light chains and ciliary motility in tetrahymena thermophila. *Cytoskeleton (Hoboken)* (2016) 73:197–208. doi: 10.1002/cm.21295

14. Ben Khelifa M, Coutton C, Zouari R, Karaouzene T, Rendu J, Bidart M, et al. Mutations in DNAH1, which encodes an inner arm heavy chain dynein, lead to male infertility from multiple morphological abnormalities of the sperm flagella. *Am J Hum Genet* (2014) 94:95–104. doi: 10.1016/j.ajhg.2013.11.017

15. Sha Y, Liu W, Huang X, Li Y, Ji Z, Mei L, et al. EIF4G1 is a novel candidate gene associated with severe asthenozoospermia. *Mol Genet Genomic Med* (2019) 7: e807. doi: 10.1002/mgg3.807

16. Liu W, Sha Y, Li Y, Mei L, Lin S, Huang X, et al. Loss-of-function mutations in SPEF2 cause multiple morphological abnormalities of the sperm flagella (MMAF). *J Med Genet* (2019) 56:678–84. doi: 10.1136/jmedgenet-2018-105952

17. Sha YW, Zhang Q, Ding L, Li P. First successful pregnancy outcome after intracytoplasmic sperm injection with short-tailed sperm from an infertile han Chinese man. *Asian J Androl* (2017) 19:613–4. doi: 10.4103/1008-682X.182395

18. Lehti MS, Sironen A. Formation and function of sperm tail structures in association with sperm motility defects. *Biol Reprod* (2017) 97:522–36. doi: 10.1093/biolre/iox096

19. King SM. Axonemal dyneins winch the cilium. *Nat Struct Mol Biol* (2010) 17:673–4. doi: 10.1038/nsmb0610-673

20. Satir P, Christensen ST. Overview of structure and function of mammalian cilia. *Annu Rev Physiol* (2007) 69:377–400. doi: 10.1146/annurev.physiol.69.040705.141236

21. Tu C, Cong J, Zhang Q, He X, Zheng R, Yang X, et al. Et al: Bi-allelic mutations of DNAH10 cause primary male infertility with asthenoteratozoospermia in humans and mice. *Am J Hum Genet* (2021) 108:1466–77. doi: 10.1016/j.ajhg.2021.06.010

22. He J, Li L, Yu Y, Hu X, Zhang H, Liu R, et al. Two mutations in the axonemal dynein heavy chain gene 5 in a Chinese asthenozoospermia patient: A case report. *Med (Baltimore)* (2020) 99:e20813. doi: 10.1097/MD.0000000000020813

23. Zuccarello D, Ferlin A, Cazzadore C, Pepe A, Garolla A, Moretti A, et al. Mutations in dynein genes in patients affected by isolated non-syndromic asthenozoospermia. *Hum Reprod* (2008) 23:1957–62. doi: 10.1093/humrep/den193

24. Colpi GM, Francavilla S, Haidl G, Link K, Behre HM, Goulis DG, et al. European Academy of andrology guideline management of oligo-astheno-teratozoospermia. *Andrology* (2018) 6:513–24. doi: 10.1111/andr.12502

25. Ortega C, Verheyen G, Raick D, Camus M, Devroey P, Tournaye H. Absolute asthenozoospermia and ICSI: what are the options? *Hum Reprod Update* (2011) 17:684–92. doi: 10.1093/humupd/dmr018

frontiers | Frontiers in Endocrinology

TYPE Original Research
PUBLISHED 18 January 2023
DOI 10.3389/fendo.2023.1118841

OPEN ACCESS

EDITED BY
Tao Luo,
Nanchang University, China

REVIEWED BY
Ying Shen,
Sichuan University, China
Yimin Cheng,
Yichun University, China
Shenmin Yang,
Suzhou Municipal Hospital, China

*CORRESPONDENCE
Mingrong Lv
lvmingrong2016@163.com

†These authors have contributed equally to this work

SPECIALTY SECTION
This article was submitted to Reproduction, a section of the journal Frontiers in Endocrinology

RECEIVED 08 December 2022
ACCEPTED 03 January 2023
PUBLISHED 18 January 2023

CITATION
Yu H, Shi X, Shao Z, Geng H, Guo S, Li K, Gu M, Xu C, Gao Y, Tan Q, Duan Z, Wu H, Hua R, Guo R, Wei Z, Zhou P, Cao Y, He X, Li L, Zhang X and Lv M (2023) Novel *HYDIN* variants associated with male infertility in two Chinese families. *Front. Endocrinol.* 14:1118841. doi: 10.3389/fendo.2023.1118841

Novel *HYDIN* variants associated with male infertility in two Chinese families

Hui Yu[1,2†], Xiao Shi[3†], Zhongmei Shao[1,2†], Hao Geng[2,4,5†], Senzhao Guo[2,4,5], Kuokuo Li[2,4,5], Meng Gu[2,4,5], Chuan Xu[2,4,5], Yang Gao[2,4,5], Qing Tan[2,6], Zongliu Duan[2,4,5], Huan Wu[2,4,5], Rong Hua[4,5], Rui Guo[4,5], Zhaolian Wei[2,4,5], Ping Zhou[2,4,5], Yunxia Cao[2,4,5], Xiaojin He[2,4,5], Liang Li[1], Xiaoping Zhang[1] and Mingrong Lv[1,2,4,5*]

[1]Department of Obstetrics and Gynecology, Fuyang Hospital of Anhui Medical University, Fuyang, China, [2]Reproductive Medicine Center, Department of Obstetrics and Gynecology, First Affiliated Hospital of Anhui Medical University, Hefei, China, [3]Department of Respiratory and Critical Care Medicine, Second Affiliated Hospital of Anhui Medical University, Hefei, China, [4]National Health Commission (NHC) Key Laboratory of Study on Abnormal Gametes and Reproductive Tract (Anhui Medical University), Hefei, China, [5]Key Laboratory of Population Health Across Life Cycle (Anhui Medical University), Ministry of Education of the People's Republic of China, Hefei, China, [6]Anhui Provincial Human Sperm Bank, First Affiliated Hospital of Anhui Medical University, Hefei, China

Introduction: Infertility is a major disease affecting human life and health, among which male factors account for about half. Asthenoteratozoospermia accounts for the majority of male infertility. High-throughput sequencing techniques have identified numerous variants in genes responsible for asthenoteratozoospermia; however, its etiology still needs to be studied.

Method: In this study, we performed whole-exome sequencing on samples from 375 patients with asthenoteratozoospermia and identified two *HYDIN* compound heterozygous variants, a primary ciliary dyskinesia (PCD)-associated gene, in two unrelated subjects. H&E staining, SEM were employed to analyze the varies on sperm of patients, further, TEM was employed to determine the ultrastructure defects. And westernblot and immunostaining were chose to evaluate the variation of structural protein. ICSI was applied to assist the mutational patient to achieve offspring.

Result: We identified two HYDIN compound heterozygous variants. Patient AY078 had novel compound heterozygous splice variants (c.5969-2A>G, c.6316+1G>A), altering the consensus splice acceptor site of *HYDIN*. He was diagnosed with male infertility and PCD, presenting with decreased sperm progressive motility and morphological abnormalities, and bronchial dilatation in the inferior lobe. Compared to the fertile control, HYDIN levels, acrosome and centrosome markers (ACTL7A, ACROSIN, PLCζ1, and Centrin1), and flagella components (TOMM20, SEPT4, SPEF2, SPAG6, and RSPHs) were significantly reduced in *HYDIN*-deficient patients. Using intracytoplasmic sperm injection (ICSI), the patient successfully achieved clinical pregnancy. AY079 had deleterious compound heterozygous missense variants, c.9507C>G (p. Asn3169Lys) and c.14081G>A (p. Arg4694His), presenting with infertility; however, semen samples and PCD examination were unavailable.

Discussion: Our findings provide the first evidence that the loss of *HYDIN* function causes asthenoteratozoospermia presenting with various defects in the flagella structure and the disassembly of the acrosome and neck. Additionally, ICSI could rescue this failure of insemination caused by immobile and malformed sperm induced by *HYDIN* deficiency.

KEYWORDS

male infertility, asthenoteratozoospermia, whole-exome sequencing, *HYDIN*, acrosome, ICSI

Introduction

Reproductive health is crucial for the continuation of human civilization; however, approximately 12% of couples experience infertility and fail to conceive offspring, with males accounting for approximately 50% of all cases (1, 2). Based on semen evaluation (3), male infertility can be classified into azoospermia, oligozoospermia, teratozoospermia, asthenozoospermia, or two or three types of these combined. Asthenoteratozoospermia is characterized by attenuated sperm motility and flagellar abnormalities, accounting for ~ 81.84% of male infertility cases (4).

Cilia and flagella are highly conserved microtubule-based structures that have evolved from single-celled algae to human organelles, are found in many organs and systems, and play crucial roles in normal embryogenesis and organ homeostasis (5). According to their ultrastructure and function, microtubule-based organelles in the human body can be described as motile or immotile "9+2" or "9 +0" cilia (6, 7). Sperm flagella are motile 9 + 2 structures that are assembled by nine peripheral microtubule doublets (DMTs) surrounding a central microtubule pair (CP) (8). The CP is an asymmetrical structure that consists of two microtubules, C1 and C2, each with two projections: C1a, C1b, C2a, and C2b. The radial spoke complexes that connect DMTs and CPs are thought to be crucial for mechanochemical signal transduction that governs ciliary waveforms (9). Deficiencies in components of each of these structures have been reported to cause primary ciliary dyskinesia (PCD) or male infertility. For instance, *SPEF2*, *RSPH4A*, or *RSPH9* variants cause intermittent CP loss, leading to PCD and/or infertility (10–12). Previous studies have reported that 75% of male patients with PCD are also diagnosed as male infertility (13). To date, mutations in approximately 50 genes have been associated with PCD; most of which are highly expressed in the testis, and half have been linked to male infertility and immobile sperm (14, 15).

HYDIN variations were commonly observed in primary ciliary dyskinesia(PCD), which caused deficiencies in the ultrastructure of cilia (16–18). Using *hydin*-deficient unicellular green Chlamydomonas algae, it was shown that the HYDIN protein is localized at the C2b projection and is anchored to the C1 microtubule through C1b projection and CPC1 protein (19). Additionally, in the *Hydin*-deficient mice and *HYDIN*-mutant humans (16, 17), the mammalian ortholog of CPC1 and SPEF2 were also absent in the *HYDIN*-mutant axonemes of ciliated respiratory cells (20–22). Olbrich et al. found that most sperm tails were immotile in an adult PCD man harboring *HYDIN* variants; no other phenotypes were reported (16). Many exome screening studies have reported that *HYDIN* is a common pathogenic gene in children diagnosed with PCD, but little attention was paid to study the influence on the reproductive system in adult men induced by *HYDIN* variants (11, 23).

In this study, we identified two compound heterozygous *HYDIN* variants in two infertile patients with asthenoteratozoospermia from unrelated families and demonstrated that *HYDIN* deficiency causes abnormalities in sperm head, neck, and flagella morphology and ultrastructures. Therefore, we explored the role of *HYDIN* in sperm morphology and motility, as well as the relationship between *HYDIN* and male infertility.

Materials and methods

Samples from subjects with asthenoteratozoospermia

A total of 375 infertile Chinese men with asthenoteratozoospermia were enrolled in this study from the First Affiliated Hospital of the Anhui Medical University. Patients with aberrant somatic karyotypes and Y chromosome microdeletions were eliminated. Some mutated genes were discovered in this cohort, including *CFAP58* (24), *CFAP69* (25), *SLC26A8* (26), *TTC21A* (27), *DNAH9* (28), and *DNAH10* (29). In addition, we identified candidate genes related to male infertility. All study subjects and their family members, as well as fertile control subjects, provided informed consent. This study was approved by the Ethics Committee of Anhui Medical University, Hefei, China.

Semen parameters and sperm morphological analysis

Semen samples were collected from patients and normal controls through masturbation after 2–7 days of sexual abstinence. Samples were evaluated after liquefaction at 37 °C for 30 min in accordance with World Health Organization (WHO) guidelines (6^{th} Edition) (30). Sperm morphology was analyzed after hematoxylin and eosin (H&E) staining by an experienced experimenter. More than 200 spermatozoa were counted to assess the percentage of morphologically abnormal spermatozoa. Unfortunately, semen samples were not available for patient AY079.

Bioinformatic analysis

Genomic DNA was extracted from the peripheral blood samples of asthenoteratozoospermic individuals for whole-exome sequencing (WES). DNA was sheared into fragments, enriched using a SureSelect XT Human All Exon Kit, and sequenced using an Illumina HiSeq X-TEN platform. Sequenced reads were mapped to the human reference GRCh38/hg38 genome using Burrows-Wheeler Aligner (BWA) software (31). After low-quality reads and PCR duplications had been removed, all variants were annotated and filtered as described previously (32). *HYDIN* variants were identified using WES and verified using Sanger sequencing. The PCR primers used for sequencing *HYDIN* are listed in Table S1.

Real-time quantitative PCR (RT-qPCR) and statistical analysis

Total RNA was extracted from semen samples of the AY078 proband and fertile men using TRIzol reagent (Invitrogen, Carlsbad, CA92008 USA) and converted into cDNA using a PrimeScript RT Reagent Kit (Takara, Shiga, Japan). cDNA was amplified using transcript-specific primers (Table S2) for RT-qPCR analysis using a LightCycler 480 SYBR Green I Master (Roche), with β-actin as an internal control. Raw data were analyzed using the $2^{-\Delta\Delta Ct}$ method in GraphPad Prism to determine *HYDIN* mRNA expression.

Scanning electron microscopy (SEM) and transmission electron microscopy (TEM)

Spermatozoa from AY078 and fertile controls were washed three times with 1× phosphate-buffered saline (PBS) at 2500 rpm at 25°C and then fixed with 2.5% glutaraldehyde (pH 6.9) for more than 2 h at 4°C.

For SEM, fixed samples were dehydrated using an ethanol gradient (30, 50, 70, 80, 90, and 100%; ×2), dried with a Quorum K850 Critical Point Dryer (Quorum Technology, Lewes, UK) after the ethanol had been replaced with hexamethyldisilamane, coated with a Cressington 108 Auto Sputter Carbon Coater (Cressington Scientific Instruments, Watford, UK), and observed using a ZEISS GeminiSEM 300 instrument (ZEISS, Oberkochen, Germany).

For TEM, fixed spermatozoa were post-fixed for 2 h at 4°C using 1% osmium tetroxide, dyed with 2% uranium acetate, dehydrated using a gradient, embedded in EPON 812 epoxy resin, cut into 100-nm sections using a Leica EM UC7 microtome (Leica, Wetzlar, Germany), stained with lead citrate, and examined using a Talos L120C G2 TEM (Thermo Fisher Scientific, Waltham, MA, USA).

Immunofluorescence (IF) assays

IF was performed after samples had been pre-processed as described previously (32) using rabbit polyclonal anti-HYDIN (HPA067155, Sigma, Castle Hill, NSW, Australia, 1:100), rabbit polyclonal anti-SPEF2 (HPA040343, Sigma, Castle Hill, NSW, Australia, 1:100), rabbit polyclonal anti-PLCζ1 (pab0367-P, Covalab, USA, 1:100), rabbit polyclonal anti-ACTL7A (HPA021624, Sigma, Castle Hill, NSW, Australia, 1:100), rabbit polyclonal anti-ACROSIN (NBP2-14260, Novus Biologicals, Colorado, USA, 1:200), rabbit polyclonal anti-RSPH1 (HPA017382, Sigma, Castle Hill, NSW, Australia, 1:100), rabbit polyclonal anti-RSPH3 (17603-1-AP, Proteintech, Rosemont, IL, USA, 1:100), as well as mouse monoclonal anti-acetylated α-tubulin (T6793, Sigma, Castle Hill, NSW, Australia,1:500) antibodies and secondary anti-mouse Alexa Fluor 488 (Yeasen Biotechnology, USA, 34106ES60, 1:500) and anti-rabbit Alexa Fluor 594 antibodies (Jackson ImmunoResearch, USA, 111–585-003, 1:500). DNA was stained using Hoechst 33342 (Thermo Fisher Scientific, USA, 62,249, 1:1000).

Western blot (WB) analysis

Human spermatozoa from AY078 and control fertile groups were washed three times with PBS, dissolved using 1×SDS loading buffer (Beyotime Biotechnology,China), and denatured at 100°C to avoid protein loss due to inadequate lysis. Proteins were separated using 10% sodium dodecyl sulfate-polyacrylamide gel electrophoresis, transferred onto polyvinylidene fluoride membranes, and incubated with the following primary antibodies overnight at 4°C: rabbit polyclonal anti-SPEF2 (HPA040343, Sigma, Castle Hill, NSW, Australia, 1:1000), rabbit polyclonal anti-PLCζ1 (pab0367-P, Covalab, USA, 1:1000), rabbit polyclonal anti-SPAG6 (HPA038440, Sigma, Castle Hill, NSW, Australia, 1:1000), rabbit polyclonal anti-ACTL7A (HPA021624, Sigma, Castle Hill, NSW, Australia, 1:1000), rabbit polyclonal anti-ACROSIN (NBP2-14260, Novus Biologicals, Colorado, USA, 1:1000), rabbit polyclonal anti-RSPH1 (HPA017382, Sigma, Castle Hill, NSW, Australia, 1:1000), rabbit polyclonal anti-RSPH3 (17603-1-AP, Proteintech, Rosemont, IL, USA, 1:1000), and mouse polyclonal anti-β-actin (TA-09, ZSGB-Bio, China). After incubation with secondary antibodies at 37°C for 2 h, blots were visualized and analyzed(Tanon 5200,China).

Statistical analyses

All data in this study were obtained from at least in three independent experiments. The data of RT-qPCR was analyzed using GraphPad Prism (GraphPad Software, San Diego, CA, USA). Differences were analyzed by Student's t-tests compared with control groups, and P-values < 0.05 were considered significant.

Results

Identification of two bi-allelic *HYDIN* variants in men with asthenoteratozoospermia

In this study, WES and bioinformatic analyses were performed in a cohort of 375 men with asthenoteratozoospermia, according to a

previously described procedure (32). Two heterozygous *HYDIN* splicing variants of c.5969-2A>G and c.6316+1G>A were identified in patient AY078, and two heterozygous *HYDIN* missense variants of c.9507C>G (p.N3169K) and c.14081G>A (p.R4694H) were identified in patient AY079. Sanger sequencing validated that the heterozygous c.6316+1G>A variant was inherited from the patient's AY078's mother, while his father's DNA was not available. For patient AY079, heterozygous missense variants c.9507C>G (p.N3169K) and c.14081G>A (p.R4694H) were respectively inherited from his heterozygous parents (Figure 1A). The variants were absent or infrequent (allele frequency <1%) in the human genetic variant databases 1000 Genomes Project and the Genome Aggregation Database, and were annotated using bioinformatic databases including SIFT, PolyPhen-2, and Mutation Taster. Functional predictions were not available for M1 and M2, and mutations in M3 and M4 were predicted to be weakly deleterious (Table 1). The amino acids at the mutation sites were relatively conserved among species and the mutated amino acids were located behind the ASPH-SPD-2-Hydin (ASH)and Hydin adenylate kinase-like (ADK) domains (Figure 1B).

The clinical features of AY078 were consistent with those of PCD syndrome, presenting with bronchial dilatation in the inferior lobe of the left lung. Information concerning PCD syndrome was not available for AY079. Despite having normal sexual relationships, the partners of both AY078 (31 years old) and AY079 (32 years old) were unable to achieve pregnancy for over 2 years. Routine semen examinations indicated that semen volume and concentration were unaffected, yet sperm motility and progressive motility decreased dramatically (Table 2), suggesting that the variants of *HYDIN* we found may cause infertility and PCD.

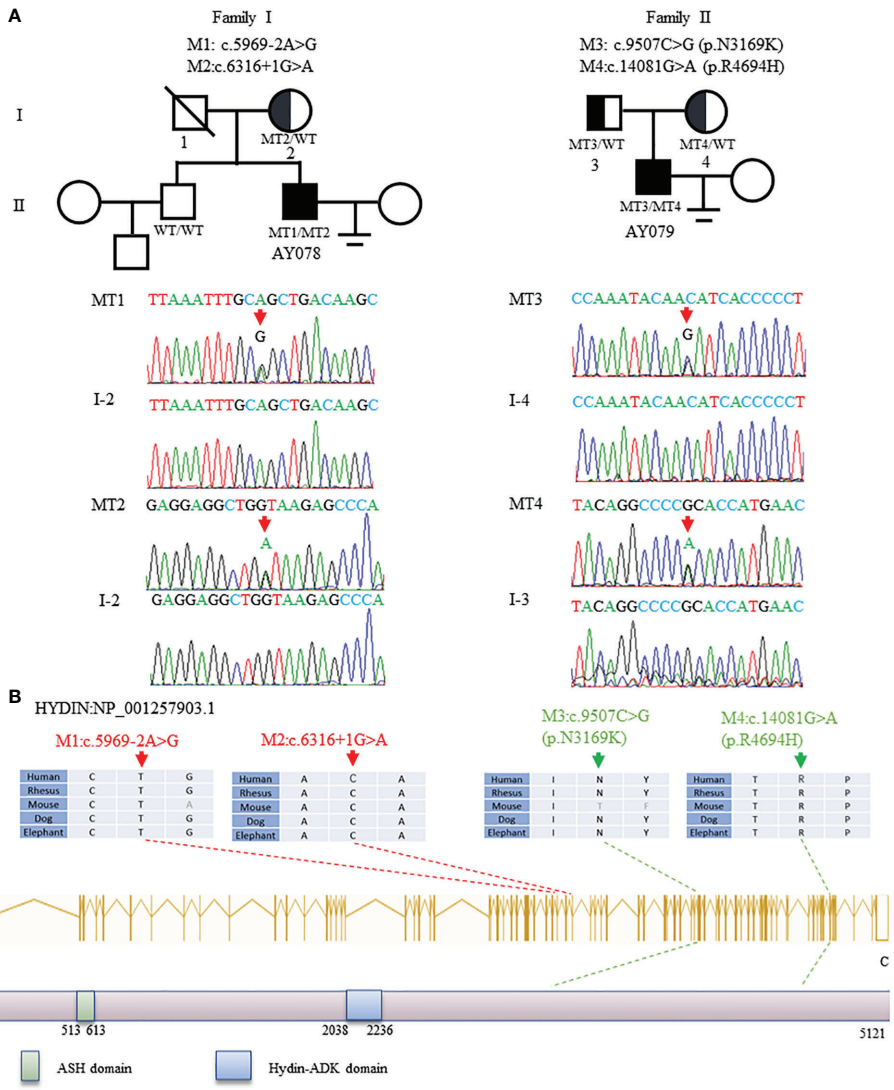

FIGURE 1
Identification and Bioinformation Analysis of *HYDIN* Mutations in Two unrelated families. **(A)**Two compound heterozygous mutations (M1-M4) of *HYDIN* were identified in two subjects with asthenoteratozoospemia. M2 of patient AY078 was inherited from heterozygous parents. Because the bioinformation of P1's father was incapable gained, M1 in AY078 was undetermined whether is inherited from his father or is new. M3 and M4 of patient 2 AY079 were obviously inherited from his heterozygous parents. The mutational positions were indicated with red arrow under Sanger sequencing results below. **(B)** Schematic representation of *HYDIN* exons and protein product. The conservation of variant residues among different species were verified by sequence alignment. The positions of variants were indicated in dots lines. Green square represents typical ASH (ASPH-SPD-2-Hydin) domain, blue square stands for Hydin-ADK domain, according to the NCBI browser.

10.3389/fendo.2023.1118841

TABLE 1 Bi-allelic variants of *HYDIN* variants identified in Chinese men.

HYDIN Variant	M1	M2	M3	M4
cDNA alteration	c.5969-2A>G	c.6316+1G>A	c.9507C>G	c.14081G>A
Variant allele	Het	Het	Het	Het
Protein alteration	–	–	N3169K	R4694H
Variant type	Splicing	Splicing	Missense	Missense
Allele Frequency in Human Population				
1000 Genomes				
East Asians in gnomAD_exome	0	0	0.001	0.001
All individuals in gnomAD	NA	NA	0.000199680511182109	0.00019968051118
Function Prediction				
SIFT	NA	NA	Tolerate	Tolerate
PolyPhen-2	NA	NA	Benign	Possibly damaging
CADD	10.98	23.8	16.84	24.8

The accession number of human HYDIN is GenBank: NM_001270974.2.
Full-length HYDIN has 5121 amino acids.
Het, heterozygous; NA, not available.

TABLE 2 Semen routine parameters and sperm morphology in men harboring homozygous *HYDIN* variants.

Subject	P1	P2	Reference Limits
Age	31	32	
Semen Parameter			
Semen volume (mL)	3.75	2.50	>1.5[a]
Semen concentration (10^6/mL)	13.45	67.83	>15.0 [a]
Motility (%)	14.0	17.06	>40.0 [a]
Progressive motility (%)	0.65	15.05	>32.0 [a]
Sperm Morphology			
Sperm Head			
Normal head (%)	14.4	/	
Amorphous head (%)	64.2	/	
Vacuolar head (%)	5.0	/	
Pear-shaped head (%)	8.5	/	
Pyramid head (%)	15.4	/	
Acrosome≥(70%)	5.5	/	
Small acrosome (%)	10.4	/	
Sperm Tail			
Normal flagella (%)	10.9	/	>23.0 [b]
Absent flagella (%)	4.4	/	<5.0 [b]
Short flagella (%)	21.3	/	<1.0 [b]
Coiled flagella (%)	51.5	/	<17.0 [b]
Angulation (%)	11.4	/	<13.0 [b]
Thick (%)	0.5	/	<2.0 [b]

[a] Reference limits according to the 6th WHO standards (30).
[b] limits according to the classification of morphologically normal spermatozoa observed in 926 fertile individuals (33).

Sperm malformations in a subject harboring compound heterozygous *HYDIN* variants

Next, we analyzed the morphology of sperm from AY078 using H&E staining, according to WHO guidelines. Unfortunately, semen specimens from AY079 could not be used for these molecular experiments. Fertile control individuals had regular, smooth, and oval-shaped sperm heads, whereas AY078 sperm had a high rate (~80%) of head malformation, including amorphous, pyramidal, and small acrosome heads (orange arrowhead). In addition, we observed the absence of a structure between mid- and principal regions (yellow arrowhead) in approximately one-third of sperm from AY078. AY078 sperm also displayed various flagellar deformities, including coiled (51.5%), short (21.3%), and angulated flagella (11.4%; Figure 2A and Table 2). Similar phenotypes were also observed by SEM: most AY078 spermatozoa displayed abnormal (amorphous and pyramid) head morphology with few normal acrosome forms, as well as a thin bent neck and short coiled flagella (Figure 2B).

To investigate the effect of compound heterozygous *HYDIN* variants on the ultrastructure of the sperm head and neck, we performed TEM. In normal controls, the acrosome covered two-thirds of the sperm head, with an intact outer acrosomal membrane and inner acrosomal membrane containing acrosomal contents. In AY078, diverse malformations were observed in the sperm acrosome and mid-region. As shown in Figure 3A, most acrosomes were damaged and stripped from the nuclear envelope, with more than one large nuclear vacuole, a deep depression on the surface of the nucleus, and low nuclear concentration in some severely impaired sperm. Furthermore, the sperm head-tail junction structure was damaged in AY078 sperm, with head and tail separation and a bare, thin structure at the end of the mid-region (Figure 3A).

Sperm flagella are strictly organized into 9 + 2 microtubule structures that consist of a central pair of microtubules surrounded by nine peripheral doublets supported by nine radial spoke complexes. It has been reported that *HYDIN*-mutant cilia have subtle CP defects. Meanwhile, we examined TEM cross-section images of the mid-, principal and end-flagella regions of sperm from AY078. Most sperm lacked CP axonemal composition and were characterized by "9+0" and "9+1" axonemes, and with no other obvious abnormalities in the mitochondrial sheath (MS), outer dense fibers (ODF), or doublets of microtubules (DMT) structures were observed (Figure 3B). These observations indicate that *HYDIN* plays an important role in spermiogenesis.

10.3389/fendo.2023.1118841

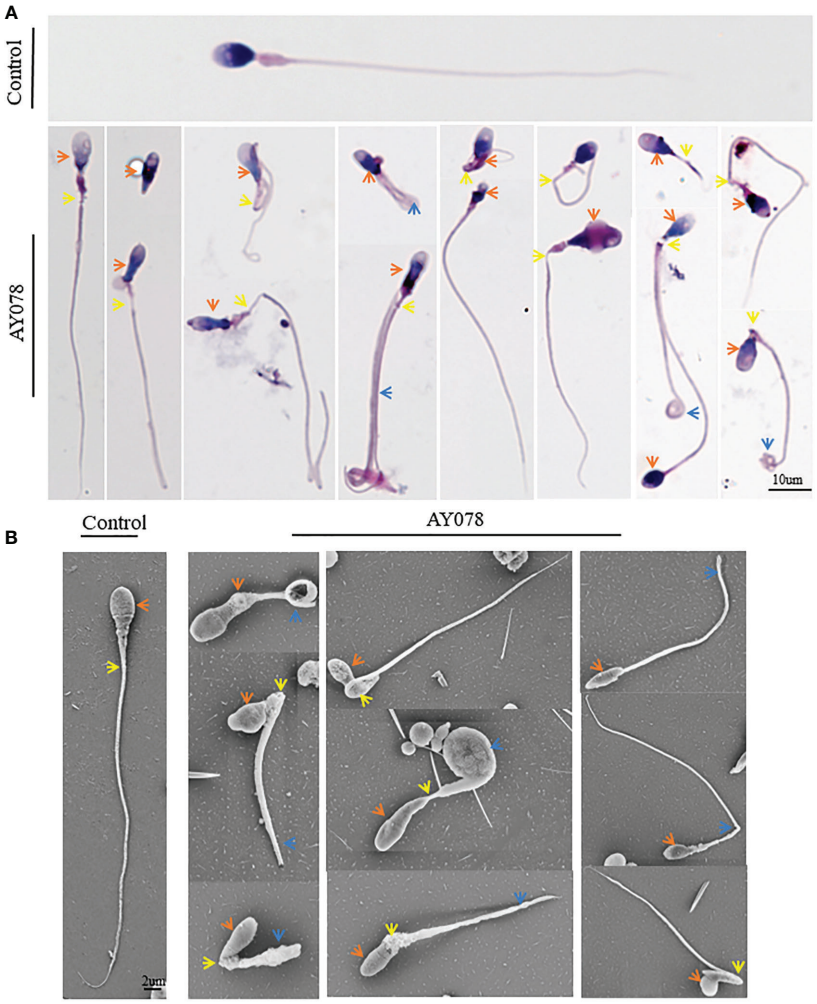

FIGURE 2
Morphology analysis of sperm from *HYDIN*-deficient patient AY078. **(A, B)** Morphology analysis showed various defects in head, neck and flagella of sperm from AY078 *via* H&E staining and SEM. Comparing with normal-shaped head that nucleus capped by acrosome, long and smooth flagella in control spermatozoa, the amorphous head, pyramid head and abnormal acrosome (orange arrowhead), the short and coiled flagella were observed in P1. Scale bar: 10μm in **(A)**, 2μm in **(B)**.

Sperm component defects in a subject harboring compound heterozygous *HYDIN* variants

To confirm the pathological manifestations associated with the *HYDIN* variants, we performed IF and RT-qPCR analyses of sperm samples from fertile controls and infertile patient. We found that HYDIN signals were concentrated in the acrosomal region and neck of normal sperm, with limited protein signals distributed along the entire flagella. In a subject harboring the *HYDIN* variant, significantly fewer HYDIN signals were distributed on the sperm acrosomal region and neck, while signals on the flagella were comparable to the control (Figure 4A). *HYDIN* mRNA expression levels were significantly reduced in spermatozoa from AY078, indicating that compound heterozygous splicing had a negative influence on *HYDIN* expression in AY078 (Figure 4B).

To further investigate the molecular defects observed in sperm head ultrastructure, we analyzed the location and expression levels of various acrosome components, including ACTL7A, acrosin, and PLCζ1, using WB and IF. ACTL7A and acrosin signals were almost absent in AY078 spermatozoa, while abnormal localization and significantly reduced signals were observed for PLCζ1 compared to the normal control (Figures 5A–C). Consistently, immunoblot analysis showed that ACTL7A, acrosin, and PLCζ1 were absent or dramatically downregulated in spermatozoa from AY078 (Figure 5D). Together, these findings suggest that the compound heterozygous *HYDIN* mutations resulted in a reduced or altered ACTL7A, acrosin, and PLCζ1 distribution, which could be responsible for the sperm head malformations observed using H&E, SEM, and TEM.

Some defects were also observed in the neck and mid-region of AY078 sperm. Since HYDIN is an ASH-containing protein concentrated on the neck, which may be related to centrosome and mid-region formation, we examined the localization and levels of components of the centrosome, mitochondrial sheath, and annulus ring. As shown in Figure 6, the numbers of centrosomes, mitochondrial sheaths, and annulus rings were decreased to different degrees, and the levels of Centrin1, TOMM20, and SEPT4

10.3389/fendo.2023.1118841

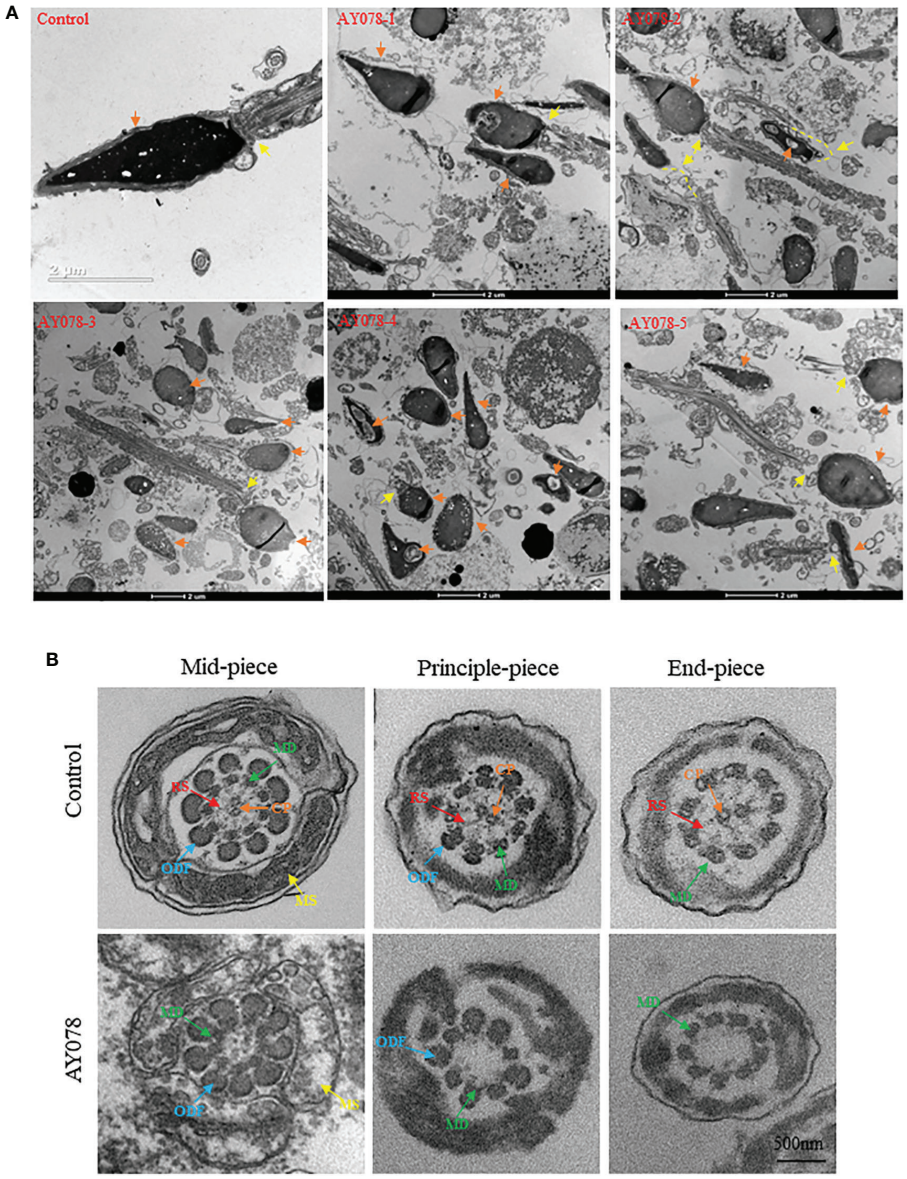

FIGURE 3
Ultrastructural deficiency in sperm in *HYDIN*-deficient AY078 comparing with normal control. **(A)** Magnification of longitudinal section of sperm showed that the anterior two thirds of nucleus was covered by acrosome, which was packaged with OAM and IAM (orange arrow), and firm linkage between head and tail in normal-shaped sperm (yellow arrow). While, it was showed that various malformations in AY078: uneven nuclear concentration, damaged and exposed acrosomal contents accompanied the outer acrosomal membrane stripped from the nucleus (orange arrow), abnormal or desultory connection between head and flagella (yellow arrow). Scale bar: 2μm. **(B)** TEM analysis of cross-section ultrastructure within flagella of AY078 and normal sperm. Typical axoneme and peri-axoneme: ODF, MS in mid-piece or FS in principle-piece surrounded the "9+2" structure, that nine MDs and one pair CP, were showed in cross-section of mid-piece, principle-piece and end-piece of sperm flagella from control man. The projection of RS also was captured lightly through TEM in three cross-section of control sperm. It was found that the dramatically reduction of CP and RS complex and destroy on mitochondrial sheath in AY078 flagella. CP, central pair; MD, microtubules doublet; RS, radical spoke; ODF, outer dense fiber; MS, mitochondrial sheath; FS, fibrous sheath. Scale bar: 500 nm.

were also decreased in sperm from AY078, indicating that *HYDIN* deficiency may contribute to these defects.

A previous study found that the CP-associated protein SPEF2 is absent in *HYDIN*-mutant cells. Here, IF and WB assays revealed that the levels of SPEF2 and another CP marker, SPAG6, were significantly reduced in sperm from AY078 (Figures 7A, D and Figures S1A, D). STRING analysis further indicated that HYDIN may be highly associated with RSPH4A (Figure 7B). To investigate the potential association between these two proteins, we performed IF and WB assays using commercial antibodies against RSPH4A on spermatozoa from AY078. RSPH4A immunostaining was localized along the entire flagella in normal sperm, whereas RSPH4A signals and levels were markedly decreased (Figures 7C, D). We also examined the abundance and location of other components of the radical spoke complexes, RSPH1 and RSPH3, which were significantly reduced, similar to those of RSPH4A (Figures S1B–D). Together, these experimental observations suggest that compound heterozygous *HYDIN* variants could cause defects in the structure of sperm flagella, especially for the CP and RS of the axoneme in humans.

10.3389/fendo.2023.1118841

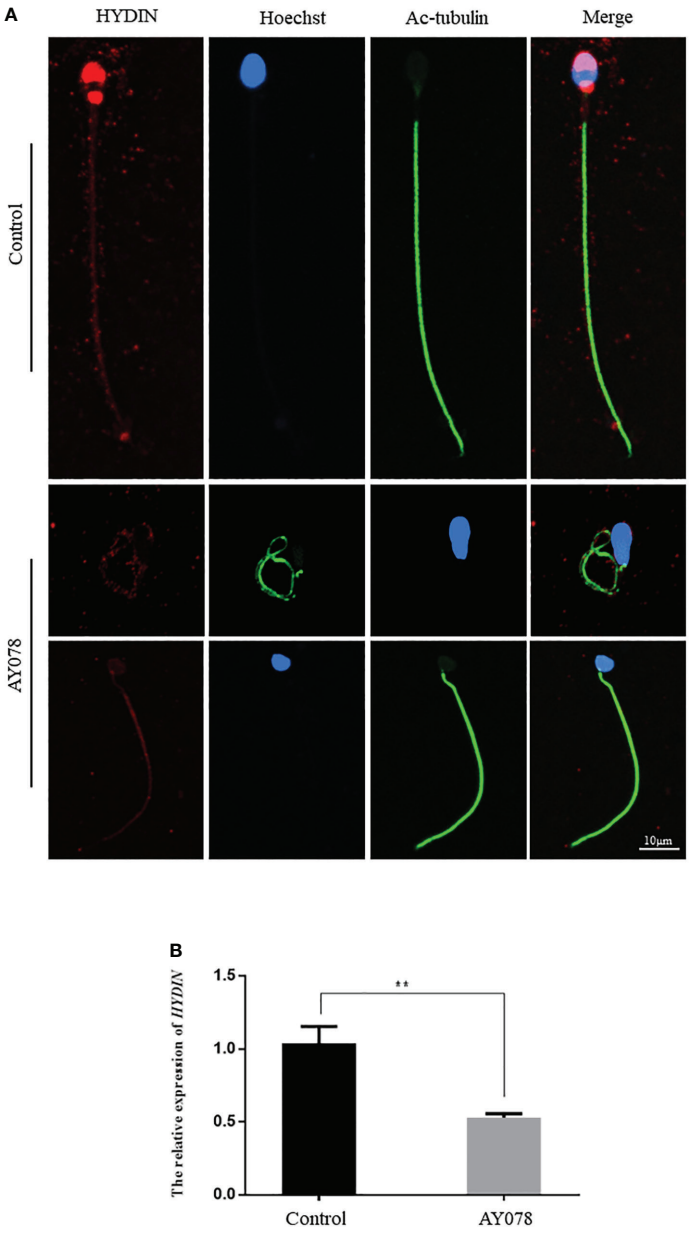

FIGURE 4
The IF and RT-qPCR assays in patient AY078 and fertile individuals. **(A)** IF analysis of HYDIN in sperm from control man and AY078. In the fertile individual, signals of HYDIN localized along the sperm flagella, besides this, were clear found in the neck and anterior head (acrosome). By contrast, the HYDIN staining was dramatically reduced or absent in sperm of P1 harboring *HYDIN* variants. Scale bar: 10μm. **(B)** The relative mRNA expression level of HYDIN in AY078 and control individual. The HYDIN mRNA level of HYDIN-deficient subjects was significantly reduced compared with that in the control. ** $P < 0.01$.

Successful outcomes of ICSI for a man with *HYDIN* variants

The partners of the two individuals harboring compound heterozygous *HYDIN* variants had been unable to conceive spontaneously without contraception for over two years. Since the partner of AY078 had regular menstrual cycles and normal basal gonadal hormone concentrations, she was treated with a gonadotropin-releasing hormone (GnRH) agonist to induce ovulation. Due to the acrosome and flagella defects observed in the sperm of AY078 with *HYDIN* mutations, intracytoplasmic sperm injection (ICSI) was conducted to improve insemination. All ten oocytes retrieved from the partner of AY078 following GnRH treatment were successfully microinjected; however, only four were fertilized. One blastocyst and two poor blastocysts were obtained on the 5th and 6th days, respectively, and all were frozen awaiting transfer. After one freeze-thaw blastocyst transfer, the partner of AY078 achieved pregnancy (Table 3). Although we were unable to obtain information on the assisted reproductive cycle of AY079, the successful outcome in AY078 suggests that ICSI could be a clinical treatment option for patients with PCD carrying *HYDIN* variants.

Discussion

In this study, we identified two compound heterozygous variants of *HYDIN*, a PCD-related gene, in two patients from a cohort of 375

10.3389/fendo.2023.1118841

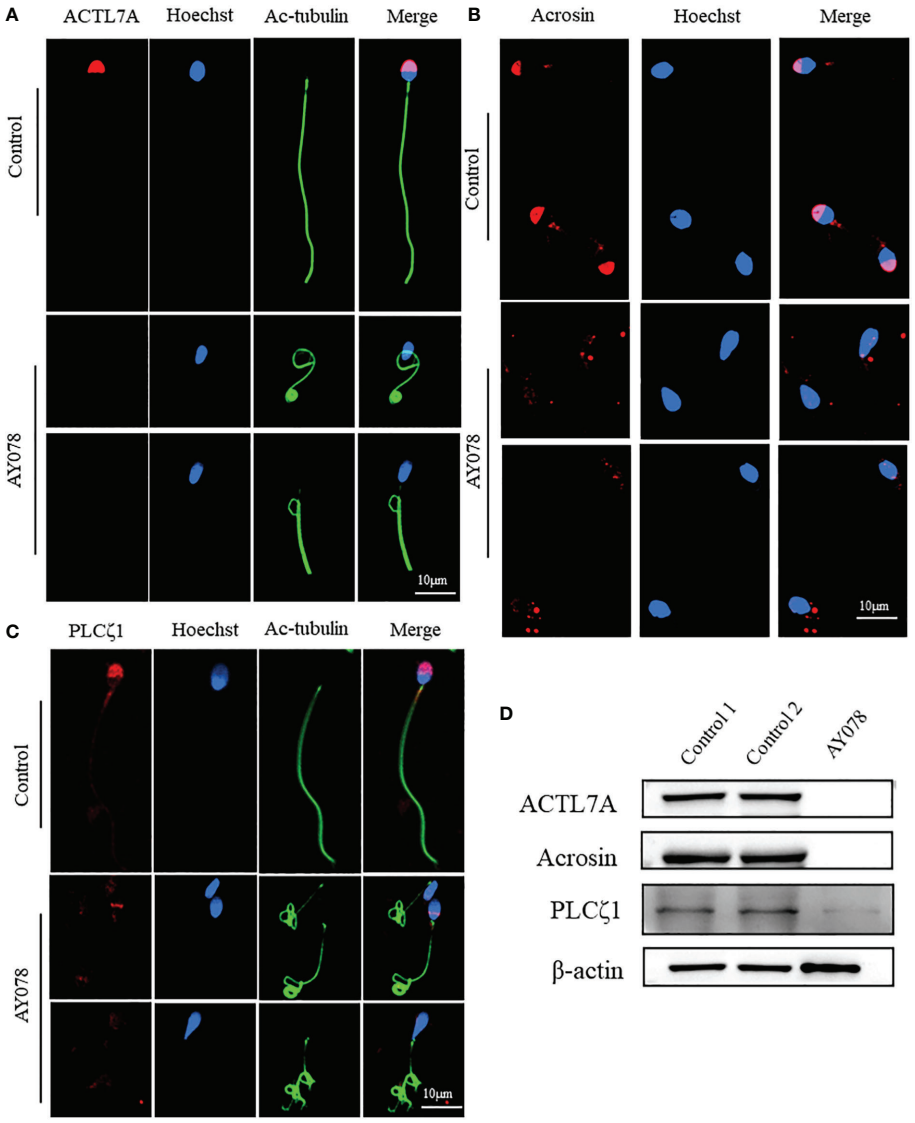

FIGURE 5
The distribution and expression of acrosomal associated proteins in AY078 and control individual. **(A–C)** Immunofluorescence staining assays were performed on the sperm of AY078 and normal subject using anti-ACTL7A(red in A), anti-ACROSIN (red in B) and anti-PLCz1 (red in C). Compared with cap-like staining of ACTL7A and ACROSIN, localized on anterior head in normal sperm, the signal in P1 of those proteins were absent from acrosome. The PLCz1 normally localized in cap-like area of acrosome, while was absent, decreased and dispersive from normal region. Anti-ac-tubulin (green) marked the sperm flagella, Hoechst (blue) marked the nucleus of spermatozoa. Scale bars: 10mm. **(D)** WB assays analysis the expression levels of ALTL7A, ACROSIN and PLCz1 in sperm obtained from P1 and normal control. The results of WB assays were accordance with those of immunofluorescence assays described above. b-actin was used as internal reference.

men with asthenoteratozoospermia. One of the affected individuals, AY078, presented with PCD syndrome and bronchial dilatation in the inferior lobe of the left lung. Unfortunately, information on PCD syndrome was not available for the other patient (AY079); however, both patients had been infertile for more than two years and presented with asthenoteratozoospermia. Using H&E and SEM, we observed various defects in sperm from AY078, which had amorphous, pyramidal, and small acrosomes in the head; thin and folded necks; and coiled, short, and angulated flagella. In addition, sperm nuclei with exfoliated acrosomal membranes, or nuclei with vacuoles, indentations, and loose condensation were clearly visualized by TEM, as well as damaged head-tail junction structure, separated heads and tails, and a bare, thin structure at the end of the mid-piece. Notably, this study is the first to report the association between these structural sperm defects and *HYDIN* mutations.

HYDIN is a large, evolutionarily conserved protein that contains ASH (ASPH-SPD-2-Hydin) and Hydin adenylate kinase-like domains (Figure 1B). The ASH domain is a homologous member of the immunoglobulin (Ig)-like 7-stranded beta sandwich fold superfamily that includes major sperm protein, Pap-D, and usher-chaperone domains (34–38), and has shown highly conserved secondary and tertiary structures despite having little primary sequence similarity *via* PSI-BLAST (39). A computational study identified that thirteen human ASH-containing proteins were confined to the centrosome, Golgi apparatus, and cilia/flagella subcellular fractions (35). In silico analysis confirmed that the ASH domain is located in centrosomes and centrosome-associated

10.3389/fendo.2023.1118841

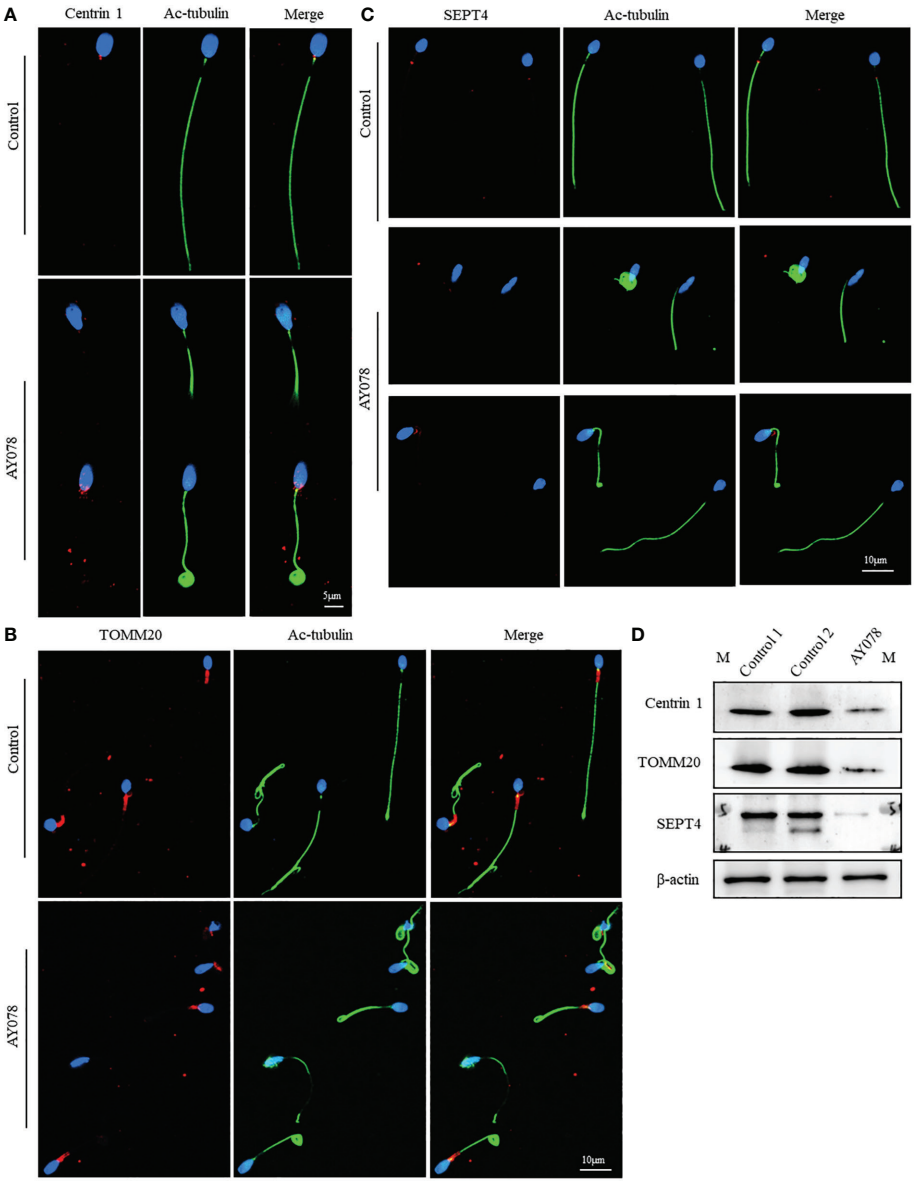

FIGURE 6
The distribution and expression of proteins related to centrosome and middle piece formation in AY078 and control individual. **(A–C)** IF results on the sperm of AY078 and normal subject using anti-Centrin1(red in **A)**, anti-TOMM20 **(**red in **B)** and anti-SEPT4 **(**red in **C)**. It was demonstrated that Centrin1 express at centriole, TOMM20 locate at mitochondrial sheath, and SEPT4 distribute on annulus ring in normal sperm. While, it was found that different degrees of reduction of Centrin1, TOMM20 and SEPT4 in sperm from AY078. Anti-ac-tubulin (green) marked the sperm flagella, Hoechst (blue) marked the nucleus of spermatozoa. Scale bars: 5μm in **(A)**, 10μm in **(B–D)** WB assays analysis the expression levels of Centrin1, TOMM20 and SEPT4 in sperm obtained from AY078 and normal control. The results of WB assays were accordance with those of immunofluorescence assays described above. β-actin was used as internal reference.

microtubules, suggesting that it may be involved in cellular signaling, trafficking events, and ciliary functions (35, 39). Interestingly, we found that HYDIN signals localized in the acrosome, neck, and tail of mature sperm, indicating that HYDIN plays an important role in sperm differentiation. However, in AY078, HYDIN signals were almost absent in the sperm acrosome and neck. Spermatozoa are specialized cells with a unique membranous organelle, known as the acrosome, which is thought to be generated through the trafficking and fusion of Golgi-derived vesicles and lysosomes (40–42). The acrosome is formed from proacrosomal vesicles synthesized on the Golgi apparatus and receives cargo through the fusion of lysosomes and endosomes (43, 44), which may be disrupted both structurally and functionally once the Golgi apparatus and/or lysosomes are broken. Although similar microtubule and lysosomal damage have been observed in other ASH domain-containing proteins, few studies have examined the Golgi; therefore, we cannot rule out the possibility that the Golgi is destroyed in *HYDIN*-deficient sperm (36, 37, 45). Additionally, *OCRL* is located on the mother centriole, which acts as the basal body on the primary cilium *via* the ASH domain and is important for centrosomal microtubule nucleation and lysosomal positioning (37). Centrosomal proteins have various functions, including centriole duplication, microtubule nucleation, and structural roles (46). Therefore, we hypothesized that the ASH-containing protein, HYDIN, acts as a centrosome-associated microtubule protein in acrosome development. The *HYDIN* splice

10.3389/fendo.2023.1118841

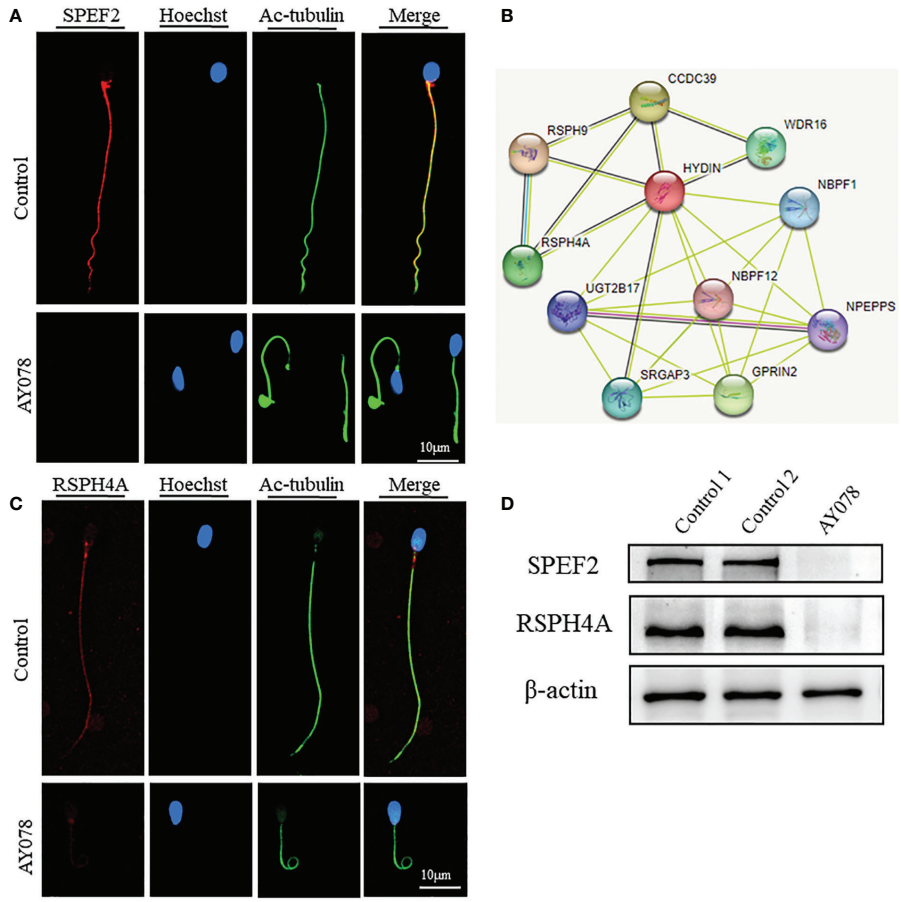

FIGURE 7
Deficiency of axoneme and appendages in sperm from AY078. **(A, C)** The immunofluorescence assays of flagella associated proteins SPEF2 (Sperm Flagellar2) and RSPH4A. Anti- SPEF2 **(**red in **B)** and Anti- RSPH4A **(**red in **C)** normally localized along the sperm flagella in the control sperm. However, expressions of SPEF2 and RSPH4A were almost absent in sperm obtained from AY078 harboring *HYDIN* variants. Anti-ac-tubulin (green) marked the sperm flagella. Hoechst (blue) labeled the nucleus of spermatozoa. Scale bars: 10μm **(B)** STRING analysis towards *HYDIN*. Evidently, it was indicated that *HYDIN* may be highly connected with *RSPH4A*. **(D)** The expression levels of SPEF2 and RSPH4A in spermatozoa were analyzed by western blot from normal individual and *HYDIN*-deficient subjects. The results showed obviously decrease of those proteins. β-actin was used as internal reference.

TABLE 3 The clinical outcomes of *HYDIN* mutated subject AY078.

	HYDIN Mutated Subject (AY078)
No. of couples	1
Male age (years)	31
Female age (years)	32
No. of ICSI	1
No. of oocytes retrieved	10
No. of oocytes injected	9
Fertilization rate (%)	55.56(5/9)
Cleavage rate (%)	80(4/5)
8-Cell formation rate (%)	60(3/5)
Blastocyst formation rate (%)	60(3/5)
High quality blastocyst rate (%)	66.7(2/3)
No. of transfer cycles	1
Implantation rate (%)	100(1/1)
Miscarriage rate (%)	0

variations caused HYDIN protein deficiency concentrated in the acrosome and neck, leading to the absence of the acrosome proteins ACTL7A and acrosin, a reduction in PLCζ1, and a decrease in the centrosome marker protein centrin1, which induces various malformations in the head and neck of sperm from AY078. However, further studies are required to clarify the specific molecular mechanisms.

The axoneme structures of sperm flagella and lung cilia are highly conserved among species and consist of nine DMTs surrounding the CP, an asymmetrical structure consisting of two microtubules (C1 and C2), with two patterns of projections attached to each (C1a, C1b, C2a, and C2b). Previous studies have reported that HYDIN localizes to the C2b projection and that PCD patients, *Hydin*-KO mice, and *Hydin*-deficient Chlamydomonas algae/Trypanosoma lack the CP apparatus projection C2b in *HYDIN*-mutant cilia. In addition, *HYDIN* mutant sperm tails appeared rigid and sperm motility was markedly decreased in PCD subjects carrying *HYDIN* variants (16–18, 20, 47), but the morphological and ultrastructural alterations of spermatozoa in *HYDIN* mutant patients were not explored further. In our study, we found that sperm motility was significantly reduced in the absence of CP and RS in the axoneme ultrastructure of most

HYDIN mutant sperm, and to a greater degree than previously reported in *HYDIN*-mutant cilia (17–19, 47). *SPEF2*, the mammalian ortholog of CPC1 positioned at the C1b projection, interacts with Hydin in Chlamydomonas and has been reported to connect with HYDIN in a cohort study of humans with PCD (19, 20). Here, we observed the absence of SPEF2 and a significant decrease in the levels of another CP marker, SPAG6, in sperm from AY078, consistent with the finding that CP-associated SPEF2 is absent in HYDIN-mutant cells from PCD patients. STRING analysis further indicated that HYDIN may be highly correlated with RSPH4A, while RSPH4A protein levels were markedly decreased in sperm from AY078, consistent with the abundance of other components of the radical spoke complexes RSPH1 and RSPH3. Together, these experimental observations suggest that the absence of HYDIN leads to the failed anchoring of CP and RS component proteins, resulting in abnormal sperm flagella axoneme assembly.

Like other patients with asthenoteratozoospermia, the subject harboring an *HYDIN* variant (AY078) also achieved pregnancy after ICSI; however, failed pregnancies have been reported in subjects carrying the centriole-associated gene *DZIP1* or *CEP135* variants due to centriole assembly defects (32, 48). In this study, despite the reduction in centrin1 protein level observed in sperm from AY078, the fertilization and blastocyst formation rates were not severely affected. Therefore, ICSI could be recommended for treating *HYDIN*-associated asthenoteratozoospermia. Although *HYDIN* variants have been reported in patients with PCD, mice, Chlamydomonas algae, and Trypanosoma, these variants have mainly been studied in cilia. To our knowledge, this study is therefore the first to report a new phenotype of male infertility caused by novel *HYDIN* variants associated with asthenoteratozoospermia. Unfortunately, the lack of semen samples from AY079 limited the sample size of this study, and future investigations should screen a greater number of patients with asthenoteratozoospermia.

Conclusion

In summary, we identified two compound heterozygous variants of *HYDIN* in infertile male patients and demonstrated that the splicing variants from AY078 cause defects in the sperm head, neck, and flagella, leading to asthenoteratozoospermia and PCD, which improve our understanding of the new phenotype of patients carrying *HYDIN* variants. Furthermore, our findings suggest that ICSI could be recommended for patients with infertility caused by *HYDIN* variants.

Data availability statement

The datasets presented in this study can be found in online repositories. The names of the repository/repositories and accession number(s) can be found in the article/Supplementary Material.

Ethics statement

The studies involving human participants were reviewed and approved by the ethics committee of Anhui Medical University. The patients/participants provided their written informed consent to participate in this study. Written informed consent was obtained from the individual(s) for the publication of any potentially identifiable images or data included in this article.

Author contributions

HY, XS, ZS, and HG contributed equally to this work and shared first authorship. HY, XS, ZS, HG, and ML participated in the design of the experiments. HY, SG, MG, and JT performed the experiments. KL, YG, RH, and RG analyzed the data. CX, ZD, and HW conducted the sample collection. ZW, PZ, YC, XH, LL, and XZ worked on the revision of the article. HY, ZS, and ML contributed to the writing of the paper. ML had overall supervision and conceived of the project. All authors contributed to the article and approved the submitted version.

Funding

This work was supported by the National Natural Science Foundation of China (82071705), University Outstanding Youth Program of Anhui Provincial Education Department (2022AH030113) and the University Outstanding Young Talents Support Program (gxyq2021174).

Acknowledgments

We are grateful to the patients and their families, as well as the fertile men who provided semen samples for this study. We would also like to thank Zhenhai Tang and Haijian Cai at the Center for Scientific Research of Anhui Medical University for assisting with SEM and TEM. We would like to thank Editage (www.editage.cn) for English language editing.

Conflict of interest

The authors declare that the research was conducted in the absence of any commercial or financial relationships that could be construed as a potential conflict of interest.

Publisher's note

Supplementary material

The Supplementary Material for this article can be found online at: https://www.frontiersin.org/articles/10.3389/fendo.2023.1118841/full#supplementary-material

References

1. Vander Borght M, Wyns C. Fertility and infertility: Definition and epidemiology. *Clin Biochem* (2018) 62:2–10. doi: 10.1016/j.clinbiochem.2018.03.012

2. Agarwal A, Baskaran S, Parekh N, Cho CL, Henkel R, Vij S, et al. Male Infertility. *Lancet* (2021) 397:319–33. doi: 10.1016/S0140-6736(20)32667-2

3. Practice Comm Amer Soc Reprod, M. Diagnostic evaluation of the infertile male: a committee opinion. *Fertility sterility* (2015) 103:E18–25. doi: 10.1016 j.fertnstert.2014.12.103

4. Curi SM, Ariagno JI, Chenlo PH, Mendeluk GR, Pugliese MN, Sardi Segovia LM, et al. Asthenozoospermia: analysis of a large population. *Arch Androl* (2003) 49:343–9. doi: 10.1080/01485010390219656

5. Satir P, Mitchell DR, Jekely G. How did the cilium evolve? *Curr Top Dev Biol* (2008) 85:63–82. doi: 10.1016/S0070-2153(08)00803-X

6. Fliegauf M, Benzing T, Omran H. When cilia go bad: cilia defects and ciliopathies. *Nat Rev Mol Cell Biol* (2007) 8:880–93. doi: 10.1038/nrm2278

7. Cardenas-Rodriguez M, Badano JL. Ciliary biology: understanding the cellular and genetic basis of human ciliopathies. *Am J Med Genet C Semin Med Genet* (2009) 151C:263–80. doi: 10.1002/ajmg.c.30227

8. Mitchison HM, Valente EM. Motile and non-motile cilia in human pathology: from function to phenotypes. *J Pathol* (2017) 241:294–309. doi: 10.1002/path.4843

9. Pigino G, Bui KH, Maheshwari A, Lupetti P, Diener D, Ishikawa T. Cryoelectron tomography of radial spokes in cilia and flagella. *J Cell Biol* (2011) 195:673–87. doi: 10.1083/jcb.201106125

10. Tu C, Nie H, Meng L, Wang W, Li H, Yuan S, et al. Novel mutations in SPEF2 causing different defects between flagella and cilia bridge: the phenotypic link between MMAF and PCD. *Hum Genet* (2020a) 139:257–71. doi: 10.1007/s00439-020-02110-0

11. Demir Eksi D, Yilmaz E, Basaran AE, Erduran G, Nur B, Mihci E, et al. Novel gene variants associated with primary ciliary dyskinesia. *Indian J Pediatr* (2022) 89:682–91. doi: 10.1007/s12098-022-04098-z

12. Mabrouk I, Al-Harthi N, Mani R, Montantin G, Tissier S, Lagha R, et al. Combining RSPH9 founder mutation screening and next-generation sequencing analysis is efficient for primary ciliary dyskinesia diagnosis in Saudi patients. *J Hum Genet* (2022) 67:381–6. doi: 10.1038/s10038-021-01006-9

13. Vanaken GJ, Bassinet L, Boon M, Mani R, Honore I, Papon JF, et al. Infertility in an adult cohort with primary ciliary dyskinesia: phenotype-gene association. *Eur Respir J* (2017) 50(5):1700314. doi: 10.1183/13993003.00314-2017

14. Jayasena CN, Sironen A. Diagnostics and management of Male infertility in primary ciliary dyskinesia. *Diagnostics (Basel)* (2021) 11(9):1550. doi: 10.3390/diagnostics11091550

15. Backman K, Mears WE, Waheeb A, Beaulieu Bergeron M, Mcclintock J, De Nanassy J, et al. A splice site and copy number variant responsible for TTC25-related primary ciliary dyskinesia. *Eur J Med Genet* (2021) 64:104193. doi: 10.1016/j.ejmg.2021.104193

16. Olbrich H, Schmidts M, Werner C, Onoufriadis A, Loges NT, Raidt J, et al. Recessive HYDIN mutations cause primary ciliary dyskinesia without randomization of left-right body asymmetry. *Am J Hum Genet* (2012) 91:672–84. doi: 10.1016/j.ajhg.2012.08.016

17. Lechtreck KF, Delmotte P, Robinson ML, Sanderson MJ, Witman GB. Mutations in hydin impair ciliary motility in mice. *J Cell Biol* (2008) 180:633–43. doi: 10.1083/jcb.200710162

18. Davy BE, Robinson ML. Congenital hydrocephalus in hy3 mice is caused by a frameshift mutation in hydin, a large novel gene. *Hum Mol Genet* (2003) 12:1163–70. doi: 10.1093/hmg/ddg122

19. Lechtreck KF, Witman GB. Chlamydomonas reinhardtii hydin is a central pair protein required for flagellar motility. *J Cell Biol* (2007) 176:473–82. doi: 10.1083/jcb.200611115

20. Cindric S, Dougherty GW, Olbrich H, Hjeij R, Loges NT, Amirav I, et al. SPEF2- and HYDIN-mutant cilia lack the central pair-associated protein SPEF2, aiding primary ciliary dyskinesia diagnostics. *Am J Respir Cell Mol Biol* (2020) 62:382–96. doi: 10.1165/rcmb.2019-0086OC

21. Sironen A, Hansen J, Thomsen B, Andersson M, Vilkki J, Toppari J, et al. Expression of SPEF2 during mouse spermatogenesis and identification of IFT20 as an interacting protein. *Biol Reprod* (2010) 82:580–90. doi: 10.1095/biolreprod.108.074971

22. Ostrowski LE, Andrews K, Potdar P, Matsuura H, Jetten A, Nettesheim P. Cloning and characterization of KPL2, a novel gene induced during ciliogenesis of tracheal epithelial cells. *Am J Respir Cell Mol Biol* (1999) 20:675–83. doi: 10.1165/ajrcmb.20.4.3496

23. Kilinc AA, Cebi MN, Ocak Z, Cokugras HC. The relationship between genotype and phenotype in primary ciliary dyskinesia patients. *Sisli Etfal Hastan Tip Bul* (2021) 55:188–92. doi: 10.14744/SEMB.2020.22567

24. He X, Liu C, Yang X, Lv M, Ni X, Li Q, et al. Bi-allelic loss-of-function variants in CFAP58 cause flagellar axoneme and mitochondrial sheath defects and asthenoteratozoospermia in humans and mice. *Am J Hum Genet* (2020) 107:514–26. doi: 10.1016/j.ajhg.2020.07.010

25. He X, Li W, Wu H, Lv M, Liu W, Liu C, et al. Novel homozygous CFAP69 mutations in humans and mice cause severe asthenoteratospermia with multiple morphological abnormalities of the sperm flagella. *J Med Genet* (2019) 56:96–103. doi: 10.1136/jmedgenet-2018-105486

26. Gao Y, Wu H, Xu Y, Shen Q, Xu C, Geng H, et al. Novel biallelic mutations in SLC26A8 cause severe asthenozoospermia in humans owing to midpiece defects: Insights into a putative dominant genetic disease. *Hum Mutat* (2021) 43(3):434–43. doi: 10.1002/humu.24322

27. Liu W, He X, Yang S, Zouari R, Wang J, Wu H, et al. Bi-allelic mutations in TTC21A induce asthenoteratospermia in humans and mice. *Am J Hum Genet* (2019) 104:738–48. doi: 10.1016/j.ajhg.2019.02.020

28. Tang D, Sha Y, Gao Y, Zhang J, Cheng H, Zhang J, et al. Novel variants in DNAH9 lead to nonsyndromic severe asthenozoospermia. *Reprod Biol Endocrinol* (2021) 19:27. doi: 10.1186/s12958-021-00709-0

29. Li K, Wang G, Lv M, Wang J, Gao Y, Tang F, et al. Bi-allelic variants in DNAH10 cause asthenoteratozoospermia and male infertility. *J Assist Reprod Genet* (2022) 39:251–9. doi: 10.1007/s10815-021-02306-x

30. Bjorndahl L, Kirkman Brown JOther Editorial Board Members Of The, W. H. O. L. M. F. T. E and Processing Of Human, S. The sixth edition of the WHO laboratory manual for the examination and processing of human semen: ensuring quality and standardization in basic examination of human ejaculates. *Fertil Steril* (2022) 117:246–51. doi: 10.1016/j.fertnstert.2021.12.012

31. Li H, Durbin R. Fast and accurate short read alignment with burrows-wheeler transform. *Bioinformatics* (2009) 25:1754–60. doi: 10.1093/bioinformatics/btp324

32. Lv M, Liu W, Chi W, Ni X, Wang J, Cheng H, et al. Homozygous mutations in DZIP1 can induce asthenoteratospermia with severe MMAF. *J Med Genet* (2020) 57:445–53. doi: 10.1136/jmedgenet-2019-106479

33. Auger J, Jouannet P, Eustache F. Another look at human sperm morphology. *Hum Reprod* (2016) 31:10–23. doi: 10.1093/humrep/dev251

34. Tarr DE, Scott AL. MSP domain proteins. *Trends Parasitol* (2005) 21:224–31. doi: 10.1016/j.pt.2005.03.009

35. Ponting CP. A novel domain suggests a ciliary function for ASPM, a brain size determining gene. *Bioinformatics* (2006) 22:1031–5. doi: 10.1093/bioinformatics/btl022

36. Schou KB, Morthorst SK, Christensen ST, Pedersen LB. Identification of conserved, centrosome-targeting ASH domains in TRAPPII complex subunits and TRAPPC8. *Cilia* (2014) 3:6. doi: 10.1186/2046-2530-3-6

37. Wang B, He W, Prosseda PP, Li L, Kowal TJ, Alvarado JA, et al. OCRL regulates lysosome positioning and mTORC1 activity through SSX2IP-mediated microtubule anchoring. *EMBO Rep* (2021) 22:e52173. doi: 10.15252/embr.202052173

38. Verdier P, Morthorst SK, Pedersen LB. Targeting of ASH domain-containing proteins to the centrosome. *Methods Mol Biol* (2016) 1454:15–33. doi: 10.1007/978-1-4939-3789-9_2

39. Murph M, Singh S, Schvarzstein M. A combined in silico and *in vivo* approach to the structure-function annotation of SPD-2 provides mechanistic insight into its functional diversity. *Cell Cycle* (2022) 21:1958–79. doi: 10.1080/15384101.2022.2078458

40. Berruti G. Towards defining an 'origin'-the case for the mammalian acrosome. *Semin Cell Dev Biol* (2016) 59:46–53. doi: 10.1016/j.semcdb.2016.01.013

41. Gioria M, Pasini ME, Berruti G. Dynamic of contribution of UBPy-sorted cargo to acrosome biogenesis: effects of its derailment in a mouse model of globozoospermia, the infertile Vps54 (L967Q) mutant. *Cell Tissue Res* (2017) 369:413–27. doi: 10.1007/s00441-017-2592-1

42. Jiao SY, Yang YH, Chen SR. Molecular genetics of infertility: loss-of-function mutations in humans and corresponding knockout/mutated mice. *Hum Reprod Update* (2021) 27:154–89. doi: 10.1093/humupd/dmaa034

43. Guidi LG, Holloway ZG, Arnoult C, Ray PF, Monaco AP, Molnar Z, et al. AU040320 deficiency leads to disruption of acrosome biogenesis and infertility in homozygous mutant mice. *Sci Rep* (2018) 8:10379. doi: 10.1038/s41598-018-28666-6

44. Han F, Liu C, Zhang L, Chen M, Zhou Y, Qin Y, et al. Globozoospermia and lack of acrosome formation in GM130-deficient mice. *Cell Death Dis* (2017) 8:e2532. doi: 10.1038/cddis.2016.414

45. Erdmann KS, Mao Y, Mccrea HJ, Zoncu R, Lee S, Paradise S, et al. A role of the Lowe syndrome protein OCRL in early steps of the endocytic pathway. *Dev Cell* (2007) 13:377–90. doi: 10.1016/j.devcel.2007.08.004

46. Amargant F, Pujol A, Ferrer-Vaquer A, Durban M, Martinez M, Vassena R, et al. The human sperm basal body is a complex centrosome important for embryo preimplantation development. *Mol Hum Reprod* (2021) 27(11):gaab062. doi: 10.1093/molehr/gaab062

47. Dawe HR, Shaw MK, Farr H, Gull K. The hydrocephalus inducing gene product, hydin, positions axonemal central pair microtubules. *BMC Biol* (2007) 5:33. doi: 10.1186/1741-7007-5-33

48. Sha YW, Xu X, Mei LB, Li P, Su ZY, He XQ, et al. A homozygous CEP135 mutation is associated with multiple morphological abnormalities of the sperm flagella (MMAF). *Gene* (2017) 633:48–53. doi: 10.1016/j.gene.2017.08.033

frontiers | Frontiers in Endocrinology

TYPE Original Research
PUBLISHED 20 February 2023
DOI 10.3389/fendo.2023.1115210

OPEN ACCESS

EDITED BY
Tao Luo,
Nanchang University, China

REVIEWED BY
Zhuqing Wang,
The Lundquist Institute, United States
Ying Chen,
Nanchang University, China

*CORRESPONDENCE
Ri-Cheng Chian
rchian@126.com
Youzhu Li
liyouzhu2006@sina.com
Shuiwen Zhang
zhang180308@163.com

†These authors have contributed equally to this work

SPECIALTY SECTION
This article was submitted to Reproduction, a section of the journal Frontiers in Endocrinology

RECEIVED 03 December 2022
ACCEPTED 03 February 2023
PUBLISHED 20 February 2023

CITATION
Li J, Chen J, Tian S, Jiao T, Wang J, Wei Y, Cheng Y, Xu Y, Chian R-C, Li Y and Zhang S (2023) Effects of different sperm sources on the clinical outcomes of *in vitro* oocyte maturation cycles combined with intracytoplasmic sperm injection. *Front. Endocrinol.* 14:1115210. doi: 10.3389/fendo.2023.1115210

Effects of different sperm sources on the clinical outcomes of *in vitro* oocyte maturation cycles combined with intracytoplasmic sperm injection

Jianhua Li[1†], Jing Chen[2†], Shuang Tian[1], Tingting Jiao[1], Jianye Wang[1], Yan Wei[1], Yanbin Cheng[1], Ye Xu[1], Ri-Cheng Chian[3*], Youzhu Li[2*] and Shuiwen Zhang[1*]

[1]Reproductive Medical Center, Department of Obstetrics and Gynecology, Seventh Medical Center of PLA General Hospital, Beijing, China, [2]Reproductive Medicine Center, The First Affiliated Hospital of Xiamen University, Xiamen, China, [3]Center for Reproductive Medicine, Shanghai Tenth People's Hospital of Tongji University, Shanghai, China

Objectives: To evaluate the embryonic developments and clinical outcomes of different sperm sources with cycles of intracytoplasmic sperm injection (ICSI) and *in vitro* maturation (IVM).

Methods: This retrospective study was approved by the hospital ethics committee and conducted in the hospital *in vitro* fertilization (IVF) clinic. From January 2005 to December 2018, 239 infertile couples underwent IVM–ICSI cycles and were divided into three groups according to different sperm sources. Group 1 comprised patients with percutaneous epididymal sperm aspiration (PESA; n = 62, 62 cycles), group 2 comprised patients with testicular sperm aspiration (TESA; n = 51, 51 cycles), and group 3 comprised patients with ejaculated sperm (n = 126, 126 cycles). We calculated the following outcomes: 1) outcomes per IVM–ICSI cycle: fertilization rate, cleavage rate, and embryo quality; 2) outcomes per embryo transfer cycle: endometrial thickness, implantation rate, biochemical pregnancy rate, clinical pregnancy rate, and live birth rate.

Results: There was no difference in basic characteristics among the three groups, such as the female partner's age, basal follicle-stimulating hormone (FSH), basal luteinizing hormone (LH), and antral follicle count ($p > 0.1$). There were no statistically significant differences according to the IVM–ICSI cycle among the three groups in fertilization rate, cleavage rate, and rate of good-quality embryos ($p > 0.05$). The results were similar among cycles regarding the number of transfer embryos and endometrial thickness per embryo transfer cycle among the three groups ($p > 0.05$). There were also similar clinical outcomes per embryo transfer cycle among the three groups, such as the biochemical pregnancy rate, clinical pregnancy rate, and live birth rate ($p > 0.05$).

Conclusions: Different sperm sources, percutaneous epididymal sperm aspiration, testicular sperm aspiration, and ejaculated sperm, do not affect the embryo and clinical outcomes after IVM–ICSI cycles.

KEYWORDS

percutaneous epididymal sperm aspiration (PESA), testicular sperm aspiration (TESA), ejaculated sperm, *in vitro* maturation (IVM), intracytoplasmic sperm injection (ICSI)

1 Introduction

Azoospermia refers to the absence of sperm in semen after three consecutive semen examinations and accounts for 15% of cases of male infertility (1). Sperm is initially generated in the seminiferous tubules of the testis, collected through these tubules, and temporarily stored in the epididymis. During ejaculation, sperm is discharged from the body through the vas deferens, ejaculatory ducts, and urethra. Azoospermia can be divided into obstructive azoospermia (OA) and non-obstructive azoospermia (NOA) according to the etiology. Non-obstructive azoospermia is a severe impairment or loss of testicular spermatogenesis function, while obstructive azoospermia refers to when the sperm production of the testicle is normal but the delivery pipeline (the epididymis or vas deferens) is blocked or absent.

Intracytoplasmic sperm injection (ICSI) can assist fertility by directly injecting sperm into an oocyte. This method has been the mainstream technique to help azoospermia patients produce genetic offspring (1). Percutaneous epididymal sperm aspiration (PESA) and testicular sperm aspiration (TESA) are common surgical methods for azoospermia patients to retrieve sperm for further ICSI (1). Recent research shows that sperm may carry genetic information that affects the development of offspring and control the early development of embryos (2). Sperm first shows two peaks of piRNA production in the testis and then experiences a large loss of piRNAs and an increase of tRNA fragments in the process of post-testicular maturation. Finally, sperm matures in the cauda (tail) epididymis with stronger forward movement ability and fertilization ability (3).

Small RNAs and microRNA changes mainly occur from the caput to the cauda of the epididymis. The sperm in the caput epididymis carries higher loads of tRF-Glu-CTC and tRF-Gly-GCC than sperm in the cauda epididymis, while sperm in the cauda epididymis has ten times more tRF-Val-CAC than sperm in the caput epididymis. MicroRNAs also dramatically vary during sperm maturation. For example, sperm in the cauda epididymis has a higher level of miR-17-92 oncomir clusters than sperm in the caput epididymis (4).

In vitro maturation (IVM) of the immature oocyte is an alternative to controlled ovarian hyperstimulation (COH). IVM can improve the utilization rate of oocytes, reduce the risk of ovarian hyperstimulation, and reduce cost (5). Due to the limited application of IVM in *in vitro* fertilization (IVF) laboratories, although there is no contraindication for IVM, it is still very difficult for couples with azoospermia and other types of male infertility to choose TESA–IVM or PESA–IVM. However, it is easier for such couples to make IVM decisions due to the risk of ovarian hyperstimulation syndrome (OHSS) and repeat IVF failure cycles, as well as the advantages of IVM, such as low cost, no OHSS risk, and repeatability in a short period after the failure of a traditional IVF cycle.

The maturity of sperm obtained from the testis, the epididymis, or ejaculation is different, and further clarification is needed in regard to whether these differences ultimately affect fertilization, embryo development, and clinical pregnancy. There is limited research on TESA–IVM and PESA–IVM cycles, and only a limited number of studies have reported on IVM oocytes fertilized by sperm from male patients with azoospermia in the ICSI cycle (6, 7). It is still debatable whether the source of sperm affects outcomes in the ICSI cycle or the IVM–ICSI cycle (1, 8). Therefore, we used different sperm sources (percutaneous epididymal sperm aspiration, testicular sperm aspiration, and ejaculated sperm) to analyze outcomes after ICSI in IVM cycles.

2 Materials and methods

2.1 Design and patients

This retrospective study was approved by the ethics committee at the Seventh Medical Centre of PLA General Hospital IVF clinic, where the study was conducted. Patients who underwent an IVM–ICSI cycle from January 2005 to December 2018 were included. The inclusion criteria were a normal karyotype of the female, normal uterine cavity and bilateral ovaries, fallopian tubes free of hydrosalpinx, and more than seven antral follicles. Azoospermia was diagnosed if no sperm was found in the male partner in three semen examinations and microscopic examinations after centrifugation and sedimentation. For a male with azoospermia, if the karyotype and azoospermic factor gene (AZF) were normal, on the day of oocyte retrieval, an andrologist checked the azoospermia patient and determined whether there was obstructive azoospermia (OA) or non-obstructive azoospermia (NOA) according to the history of obstruction, testicular volume, and hormone level.

All enrolled cases were undergoing an IVM–ICSI cycle for the first time. On the day of the female partner's oocyte retrieval, the patients were classified by temporary semen extraction. OA patients whose sperm was aspirated from the corpus of the epididymis by PESA were classified as the PESA group (group 1). If PESA did not obtain sperm, then TESA was performed to extract sperm, and such patients were classified as the TESA group. Patients with NOA for whom TESA was performed directly were also considered as part of the TESA group (group 2). Group 3 was made up of male patients whose semen could be obtained directly by ejaculation. There were 26

cases in the PESA group and 31 cases in the TESA group, and all patients gave written informed consent.

2.2 Oocyte collection and IVM

On day 3 of menstruation, the number of follicles was monitored by vaginal ultrasound, excluding cyst formation. The monitoring was repeated 7–9 days after menstruation. When the dominant follicles reached 12–14 mm or the endometrial thickness was ≥6 mm, human chorionic gonadotropin (hCG) was triggered (10,000 IU), and then oocytes were collected 36 h later. The maturation of oocytes was evaluated under an anatomical microscope, and immature oocytes in metaphase I (MI) and germinal vesicle (GV) stages were matured in the IVM medium *in vitro* (5).

2.3 Sperm preparation and ICSI

Sperm was prepared using ejaculated sperm, caput epididymal sperm obtained by PESA, or testicular sperm obtained by TESA. For PESA, after applying local anesthesia, a fine needle was used to puncture the epididymal head with a 1-ml sperm-washing syringe. The sperm was aspirated and analyzed under an optical microscope. If no sperm was recovered, TESA was immediately performed by percutaneous puncture of testicular tissue with a needle, extraction of a convoluted seminiferous tubule with fiber tweezers, and microscopic examination of sufficient sperm. If necessary, the operation was repeated until there was enough sperm for ICSI. For patients with NOA, TESA was performed directly. Then, the *in vitro* matured oocytes were inseminated with sperm by ICSI.

2.4 Embryo culture and transfer

At 17 to 19 h after ICSI, fertilization was evaluated by the appearance of two pronuclei (2PN). Embryos with six cells on day 3 after ICSI and <20% fragments with regular morphology were evaluated as good-quality embryos. On day 3 after ICSI, the embryo was transferred. This study only counted the pregnancy data of fresh embryo transfers. Biochemical pregnancy was determined by the serum hCG on day 14 after embryo transfer. Clinical pregnancy was determined by the presence of an intrauterine gestational sac by ultrasound after 14 days of biochemical pregnancy.

2.5 Statistical analysis

SPSS 20.0 (IBM, Armonk, New York, USA) was used for statistical analysis. The Kruskal–Wallis test was used to statistically analyze data. P-values of less than 0.05 were considered statistically significant, and the results were expressed as the mean standard error.

3 Results

From January 2005 to December 2018, 239 infertile couples underwent ICSI–IVM cycles and were divided into group 1 (PESA, n = 62, 62 cycles), group 2 (TESA, n = 51, 51 cycles), and group 3 (n = 126, 126 cycles). There was no difference in basic characteristics among the three groups, such as the female partner's age, basal follicle-stimulating hormone (FSH), basal luteinizing hormone (LH), and antral follicle count ($p > 0.1$, Table 1). There was no statistically significant difference per ICSI–IVM cycle among the three groups in fertilization rate, cleavage rate, and rate of good-quality embryos ($p > 0.05$, Table 1).

There were two cases in group 2 with no embryos available, so the total number of embryo transfer cycles in that group was 49. The total number of transplants in group 1 was 62, and that in group 3 was 126. The results were similar among cycles regarding the number of transfer embryos and endometrial thickness per embryo transfer cycle among the three groups ($p > 0.05$, Table 2). There were also similar clinical outcomes per embryo transfer cycle among the three groups, such as the biochemical pregnancy rate, clinical pregnancy rate, and live birth rate ($p > 0.05$, Table 2).

TABLE 1 Patient characteristics and embryology information of different sperm sources in IVM–ICSI cycle.

Variable	Sperm origin			p-Value
	PESA	TESA	Ejaculated	
No. of IVM–ICSI cycles (no. of patients)	62	51	126	
Female partner's age (years)	28.76 ± 4.19	29.61 ± 3.92	29.85 ± 2.92	0.15
Basal FSH (IU/ml)	6.25 ± 3.35	6.05 ± 2.08	5.78 ± 1.89	0.66
Basal LH (IU/ml)	3.25 ± 2.28	2.89 ± 1.74	2.73 ± 2.00	0.25
Antral follicle count	14.73 ± 5.84	15.39 ± 6.01	14.11 ± 4.37	0.766
Fertilization rate/per oocyte for ICSI	82.44 ± 16.49	79.64 ± 22.72	86.66 ± 13.47	0.193
Cleavage rate/per fertility	86.23 ± 19.49	82.65 ± 25.02	82.80 ± 18.83	0.313
No. of embryo/cycle	2.74 ± 1.11	3.22 ± 1.73	2.97 ± 0.77	0.082
good quality embryo rate/cycle	16.67 ± 28.94	21.78 ± 26.88	21.16 ± 29.24	0.249

Numbers are mean ± SD unless otherwise indicated.
No., number; IVM, in vitro maturation; ICSI, intracytoplasmic sperm injection; PESA, percutaneous epididymal sperm aspiration; TESA, testicular sperm aspiration; FSH, follicle-stimulating hormone; LH, luteinizing hormone.

4 Discussion

When couples are infertile due to male factors, such as azoospermia, they often question the impact of surgical sperm retrieval on the pregnancy rate and birth rate. It may also present significant challenges for them to choose a method of assisted pregnancy, and some people will even give up the chance to have genetic offspring because of too much anxiety (9). Due to the progress of science and technology, surgical sperm retrieval has enabled more and more men with azoospermia to have offspring. Previous research showed that ICSI using ejaculated or surgically retrieved sperm produced similar fertilization rates and pregnancy rates (10). However, there are few reports of successful pregnancies using surgically retrieved spermatozoa for ICSI cycles to fertilize IVM immature oocytes (6, 7).

In vitro maturation is a good choice for infertile women with normal ovarian function because they have a certain number of antral follicles in their ovaries, which can reduce the risk of the ovarian hyperstimulation syndrome. In addition, *in vitro* maturation can significantly reduce the required dosage of FSH and the cost of treatment (11). Due to the time efficiency, cost efficiency, and convenience of IVM, it has become a mature technique in our laboratory. The clinical pregnancy rate of IVM in our center is 30%–40% (12, 13), and the cumulative live birth rate is 66%–69% (12). These results have driven men who suffer from azoospermia to be inclined to surgical sperm retrieval combined with IVM. However, there are few reports on its clinical outcome (14, 15). In this study, we used different sperm sources to analyze the outcomes of ICSI using surgical sperm retrieval combined with IVM cycles, which may help patients make informed decisions.

Conine et al. inferred that caput sperm cannot undergo full-term maturation in FVB mice. They aspirated sperm from the caput and cauda of the epididymis in FVB mice and used them for fertilization by ICSI, and they found that multiple genetic materials (RNA) were highly expressed in zygotes fertilized by caput sperm, but the implantation rate was lower than in the cauda sperm group (2). Zygote fertilized by caput sperm began from the four-cell stage and continued to the blastocyst stage of development and expressed about 50 genes mainly encoding the regulation of RNA-binding protein and chromatin-related genes. In addition, purifying the small RNAs from cauda sperm and then injecting them into embryos formed by caput sperm can remedy the defects of the early embryo gene regulation and post-implantation development (2). However, other research showed that caput sperm is completely capable of full-term development in 129Sv/Ev, BDF1, C57BL/6NHsd, FVB, and CD1 mice (16–18). Our study also supports that no obvious differences were found among different sperm sources on fertilization rate and clinical pregnancy rate.

Some researchers found that compared with the sperm from TESA, the sperm from PESA is more likely to lead to fertilization and produce more usable blastocysts. However, its euploid rate is similar, and the pregnancy rate of the first embryo transfer cycle also has no significant difference when compared with the ejaculation group and TESA group (19). Multiple cumulative transplantation cycles were required to observe the clinical outcome. We have come to the same conclusion since sperm recovered by PESA and TESA had similar clinical pregnancy rates and birth rates, and there was no significant difference compared to the ejaculation group. Another study found that the rate of high-quality blastocysts in the TESA group (82.56%) was significantly higher than that in the PESA group (71.82%), but the embryo implantation rate, pregnancy rate, and miscarriage rate of spermatozoa from the PESA and TESA groups were similar during the ICSI cycle (1).

Sperm obtained by TESA is fresh sperm in testicular tissue, while sperm obtained by PESA is stored in the caput of the epididymis for a long time, resulting in high DNA fragmentation of the sperm, which ultimately affects the quality of embryos (20). Another analysis showed that the DNA fragmentation rate of testicular sperm was lower than that of ejaculatory sperm, and the live yield of TESA-ICSI was higher than that of ejaculatory ICSI (21). Although the embryo quality of the PESA

TABLE 2 Comparison of clinical and obstetric outcomes based on different sperm sources in IVM–ICSI cycle.

Variable	Sperm origin			p-Value
	PESA	TESA	Ejaculated	
No. of embryo transfer cycle	62	49	126	
No. of embryo transfer/cycle	2.50 ± 0.62	2.55 ± 0.58	2.70 ± 0.46	0.084
Endometrial thickness (mm)	7.27 ± 1.15	7.24 ± 1.44	7.45 ± 1.39	0.53
Implantation rate/cycle	18.01 ± 25.83	24.49 ± 35.69	21.43 ± 31.96	0.819
Biochemical pregnancy rate/cycle	28 (45.16%)	23 (46.93%)	58 (46.03%)	0.983
Miscarriage/cycle	3	2	8	
Clinical pregnancy/cycle	24 (38.71%)	20 (40.81%)	50 (39.68%)	0.975
Live birth (ongoing pregnancy)/cycle	22 (35.48%)	18 (36.73%)	45 (35.71%)	0.989
Singleton/cycle	18 (29.03%)	14 (28.57%)	31 (24.60%)	
Twins/cycle	4 (6.45%)	4 (8.16%)	14 (11.11%)	
Birthweight (g)				
Singleton	3,377 ± 465	3,565 ± 353	3,325 ± 263	0.101
Twins	2,341 ± 420	2,655 ± 250	2,450 ± 412	0.246

Numbers are mean ± SD unless otherwise indicated.
No.: number; IVM, in vitro maturation; ICSI, intracytoplasmic sperm injection; PESA, percutaneous epididymal sperm aspiration; TESA, testicular sperm aspiration.

group was slightly poor, the best embryo quality was routinely selected for transfer in the first transfer cycle, so there was no significant difference in the clinical pregnancy rate and abortion rate.

As the sperm obtained by PESA and TESA is processed in the laboratory, sperm with good shape and vitality are selected for ICSI, so as long as the woman's age, endometrium, and other conditions are good, there is no significant impact on the pregnancy outcome (1). In addition, no abnormal increase of DNA was found in sperm cells of epididymis by using the TdT-mediated dUTP nick-end labeling assay, and ICSI combined with PESA and TESA did not increase the birth rate, malformation rate, and abortion rate (22). Based on the physiological and biochemical characteristics of testicular sperm, it is immature. However, they are completely adequate from the perspective of ICSI fertilization (23). Our research data support this, suggesting that the fertilization rate, pregnancy rate, and birth rate of testicular sperm are not significantly different from those of epididymal sperm and ejaculatory sperm.

One limitation of our study is that the sample size was not large enough. Also, we did not carry out euploid analysis on embryos, and we were unable to judge the quality of embryos at the genetic level. Finally, we only followed up on the birth of children but did not examine the deformity rate of children over the long term. Therefore, more comprehensive and larger samples and longer follow-up periods are needed to confirm the results.

In conclusion, infertile couples with azoospermia alone can achieve satisfactory outcomes regardless of whether the sperm is from the testis or epididymis. There were no significant differences in fertilization rate, clinical pregnancy rate, and birth rate in the IVM cycle between these types of sperm, and the rates were also equivalent to those of the ejaculated sperm group. In clinical practice, most doctors will choose PESA due to its advantages, such as less trauma, less bleeding, rapid recovery, and fewer complications (24). Therefore, for men with azoospermia, the source of sperm has no significant impact on the IVM cycle, and the selection of TESA or PESA should be considered comprehensively. The advantages and disadvantages of multiple factors should be weighed to determine the actual prognosis to make the most appropriate and reasonable treatment plan.

Data availability statement

The original contributions presented in the study are included in the article/Supplementary Material. Further inquiries can be directed to the corresponding authors.

Ethics statement

This study was approved by the Ethics Committee of the Seventh Medical Center of PLA General Hospital. The patients/participants provided their written informed consent to participate in this study.

Author contributions

SZ, YL, and R-CC conceived and designed the study. JL, JC, JW, ST, and YX performed the experiments and analyzed the data. TJ, YW, and YC collected the data. JL and JC wrote and revised the manuscript. All authors contributed to the article and approved the submitted version.

Funding

This work was supported by the National Natural Science Foundation of China (grant no. 81401271).

Acknowledgments

We thank all the patients who agreed to participate in this study.

Conflict of interest

The authors declare that the research was conducted in the absence of any commercial or financial relationships that could be construed as a potential conflict of interest.

Publisher's note

References

1. Li L, Liao H, Li M, Xiao J, Wu L. Comparative clinical study of percutaneous epididymal sperm aspiration and testicular biopsy in the outcome of ICSI-assisted fertility treatment in patients with obstructive azoospermia. *Front Surg* (2022) 9:901601. doi: 10.3389/fsurg.2022.901601

2. Conine CC, Sun F, Song L, Rivera-Pérez JA, Rando OJ. Small RNAs gained during epididymal transit of sperm are essential for embryonic development in mice. *Dev Cell* (2018) 46(4):470–80.e3. doi: 10.1016/j.devcel.2018.06.024

3. Sharma U, Sun F, Conine CC, Reichholf B, Kukreja S, Herzog VA, et al. Small RNAs are trafficked from the epididymis to developing mammalian sperm. *Dev Cell* (2018) 46 (4):481–94.e6. doi: 10.1016/j.devcel.2018.06.023

4. Sharma U, Conine CC, Shea JM, Boskovic A, Derr AG, Bing XY, et al. Biogenesis and function of tRNA fragments during sperm maturation and fertilization in mammals. *Science* (2016) 351(6271):391–6. doi: 10.1126/science.aad6780

5. Li J, Chen J, Sun T, Zhang S, Jiao T, Chian RC, et al. Chromosome aneuploidy analysis in embryos derived from *in vivo* and *in vitro* matured human oocytes. *J Transl Med* (2021) 19(1):416. doi: 10.1186/s12967-021-03080-1

6. González-Ortega C, Piña-Aguilar RE, Cancino-Villareal P, Gutiérrez-Gutiérrez AM. Birth after human chorionic gonadotropin-primed oocyte in vitro maturation and fertilization with testicular sperm in a normo-ovulatory patient. *J Hum Reprod Sci* (2016) 9(3):210–2. doi: 10.4103/0974-1208.192076

7. Zhang S, Li J, Zhou G, Qin S, Xin N, Guo J, et al. Infertility treatment for azoospermic patients with a history of infectious parotitis (mumps) using combined techniques. *Hum Fertil (Camb)* (2013) 16(4):266–8. doi: 10.3109/14647273.2013.840392

8. Javed A, Ramaiah MK, Talkad MS. ICSI using fresh and frozen PESA-TESA spermatozoa to examine assisted reproductive outcome retrospectively. *Obstet Gynecol Sci* (2019) 62(6):429–37. doi: 10.5468/ogs.2019.62.6.429

9. Yu X, Lu S, Yuan M, Ma G, Li X, Zhang T, et al. Does ICSI outcome in obstructive azoospermia differ according to the origin of retrieved spermatozoa or the cause of epididymal obstruction? a comparative study. *Int Urol Nephrol* (2022) 54(12):3087–95. doi: 10.1007/s11255-022-03350-x

10. Ghazzawi IM, Sarraf MG, Taher MR, Khalifa FA. Comparison of the fertilizing capability of spermatozoa from ejaculates, epididymal aspirates and testicular biopsies using intracytoplasmic sperm injection. *Hum Reprod* (1998) 13(2):348–52. doi: 10.1093/humrep/13.2.348

11. Akbari H, Mohammadi M. Effect of ovarian growth factors on ultra-structural maturation in frozen human immature oocytes after in vitro maturation: A comparative study. *Reprod Health* 2022 19(1):215. doi: 10.1186/s12978-022-01521-8

12. Li JH, Sun TC, Zhang SW, Jiao TT, Cheng YB, Dong P, et al. Effect of dominant follicle status at the time of retrieval on the clinical outcomes in natural cycle IVF combined with immature oocyte treatment. *Aging (Albany NY)* (2022) 14(11):4728–38. doi: 10.18632/aging.204106

13. Lim JH, Yang SH, Xu Y, Yoon SH, Chian RC. Selection of patients for natural cycle *in vitro* fertilization combined with *in vitro* maturation of immature oocytes. *Fertil Steril* (2009) 91(4):1050–5. doi: 10.1016/j.fertnstert.2008.01.066

14. Fernandes BD, Dos Santos FA, Bezerra LGP, de Brito PD, de Macêdo LB, da Silva AR, et al. Development of a microfluidic system structured on a modified polydimethylsiloxane device for the selection of bovine epididymal spermatozoa. *Reprod Toxicol* (2022) 110:1–8. doi: 10.1016/j.reprotox.2022.03.005

15. Bry-Gauillard H, Belin F, Vinolas C, Renoult-Pierre P, Massin N, Young J, et al. Live birth after in-vitro maturation of oocytes in a patient with specific ovarian insufficiency caused by long-term mitotane treatment for adrenocortical carcinoma. *Reprod BioMed Online* (2022) 44(2):304–9. doi: 10.1016/j.rbmo.2021.10.004

16. Suganuma R, Yanagimachi R, Meistrich ML. Decline in fertility of mouse sperm with abnormal chromatin during epididymal passage as revealed by ICSI. *Hum Reprod* (2005) 20(11):3101–8. doi: 10.1093/humrep/dei169

17. Zhou D, Suzuki T, Asami M, Perry ACF. Caput epididymidal mouse sperm support full development. *Dev Cell* (2019) 50(1):5–6. doi: 10.1016/j.devcel.2019.05.012

18. Wang Y, Yamauchi Y, Wang Z, Zheng H, Yanagimachi R, Ward MA, et al. Both cauda and caput epididymal sperm are capable of supporting full-term development in FVB and CD-1 mice. *Dev Cell* (2020) 55(6):675–6. doi: 10.1016/j.devcel.2020.11.022

19. Morin SJ, Hanson BM, Juneau CR, Neal SA, Landis JN, Scott RT, et al. A comparison of the relative efficiency of ICSI and extended culture with epididymal sperm versus testicular sperm in patients with obstructive azoospermia. *Asian J Androl* (2020) 22(2):222–6. doi: 10.4103/aja.aja_58_19

20. Zhang J, Xue H, Qiu F, Zhong J, Su J. Testicular spermatozoon is superior to ejaculated spermatozoon for intracytoplasmic sperm injection to achieve pregnancy in infertile males with high sperm DNA damage. *Andrologia* (2019) 51(2):e13175. doi: 10.1111/and.13175

21. Esteves SC, Roque M, Bradley CK, Garrido N. Reproductive outcomes of testicular versus ejaculated sperm for intracytoplasmic sperm injection among men with high levels of DNA fragmentation in semen: systematic review and meta-analysis. *Fertil Steril* (2017) 108(3):456–67.e1. doi: 10.1016/j.fertnstert.2017.06.018

22. Woldringh GH, Horvers M, Janssen AJ, Reuser JJ, de Groot SA, Steiner K, et al. Follow-up of children born after ICSI with epididymal spermatozoa. *Hum Reprod* (2011) 26(7):1759–67. doi: 10.1093/humrep/der136

23. Kawwass JF, Chang J, Boulet SL, Nangia A, Mehta A, Kissin DM. Surgically acquired sperm use for assisted reproductive technology: trends and perinatal outcomes, USA, 2004-2015. *J Assist Reprod Genet* (2018) 35(7):1229–37. doi: 10.1007/s10815-018-1178-5

24. Dozortsev D, Neme R, Diamond MP, Abdelmassih S, Abdelmassih V, Oliveira F, et al. Embryos generated using testicular spermatozoa have higher developmental potential than those obtained using epididymal spermatozoa in men with obstructive azoospermia. *Fertil Steril* (2006) 86(3):606–11. doi: 10.1016/j.fertnstert.2006.01.036

frontiers | Frontiers in Endocrinology

TYPE Review
PUBLISHED 22 February 2023
DOI 10.3389/fendo.2023.1145533

OPEN ACCESS

EDITED BY
Kun Li,
Hangzhou Medical College, China

REVIEWED BY
Stuart A. Meyers,
University of California, Davis, United States
Enrica Bianchi,
University of York, United Kingdom

*CORRESPONDENCE
Brett Nixon
brett.nixon@newcastle.edu.au

SPECIALTY SECTION
This article was submitted to Reproduction, a section of the journal Frontiers in Endocrinology

RECEIVED 16 January 2023
ACCEPTED 08 February 2023
PUBLISHED 22 February 2023

CITATION
Nixon B, Schjenken JE, Burke ND, Skerrett-Byrne DA, Hart HM, De Iuliis GN, Martin JH, Lord T and Bromfield EG (2023) New horizons in human sperm selection for assisted reproduction. *Front. Endocrinol.* 14:1145533. doi: 10.3389/fendo.2023.1145533

New horizons in human sperm selection for assisted reproduction

Brett Nixon[1,2]*, John E. Schjenken[1,2], Nathan D. Burke[1,2], David A. Skerrett-Byrne[1,2], Hanah M. Hart[1,2], Geoffry N. De Iuliis[1,2], Jacinta H. Martin[1,2], Tessa Lord[1,2] and Elizabeth G. Bromfield[1,2]

[1]Priority Research Centre for Reproductive Science, School of Environmental and Life Sciences, The University of Newcastle, Callaghan, NSW, Australia, [2]Infertility and Reproduction Research Program, Hunter Medical Research Institute, New Lambton Heights, NSW, Australia

Male infertility is a commonly encountered pathology that is estimated to be a contributory factor in approximately 50% of couples seeking recourse to assisted reproductive technologies. Upon clinical presentation, such males are commonly subjected to conventional diagnostic andrological practices that rely on descriptive criteria to define their fertility based on the number of morphologically normal, motile spermatozoa encountered within their ejaculate. Despite the virtual ubiquitous adoption of such diagnostic practices, they are not without their limitations and accordingly, there is now increasing awareness of the importance of assessing sperm quality in order to more accurately predict a male's fertility status. This realization raises the important question of which characteristics signify a high-quality, fertilization competent sperm cell. In this review, we reflect on recent advances in our mechanistic understanding of sperm biology and function, which are contributing to a growing armory of innovative approaches to diagnose and treat male infertility. In particular we review progress toward the implementation of precision medicine; the robust clinical adoption of which in the setting of fertility, currently lags well behind that of other fields of medicine. Despite this, research shows that the application of advanced technology platforms such as whole exome sequencing and proteomic analyses hold considerable promise in optimizing outcomes for the management of male infertility by uncovering and expanding our inventory of candidate infertility biomarkers, as well as those associated with recurrent pregnancy loss. Similarly, the development of advanced imaging technologies in tandem with machine learning artificial intelligence are poised to disrupt the fertility care paradigm by advancing our understanding of the molecular and biological causes of infertility to provide novel avenues for future diagnostics and treatments.

KEYWORDS

andrology diagnosis, biomarker, assisted reproductive technologies (ART), male infertility, sperm function assay, sperm

1 Introduction

Infertility is a relatively common condition afflicting upwards of 15% of couples of reproductive age. Male factors are uniquely responsible for an estimated 30% of couples experiencing difficulty conceiving and beyond this, are a recognized contributor in approximately 50% of all cases of infertility (1). In the four decades since the report of the first successful human *in vitro* fertilization (IVF) (2), considerable gains have been made toward improving the effectiveness of male subfertility treatments. In particular, the advent of gamete micromanipulation techniques, such as intracytoplasmic sperm injection (ICSI), have reframed the field of assisted reproduction by effectively mitigating the need for the fertilizing spermatozoon to exhibit progressive motility, be capable of recognizing an oocyte or completing acrosomal exocytosis (3). Indeed, so profound has the impact of ICSI been in permitting men with defective sperm parameters to reproduce, that it has become the favored choice for fertilization irrespective of the underlying etiology (4). As such, ICSI now features in approximately two thirds of all cycles of assisted reproduction undertaken in countries such as Australia; well beyond that of its initial indication (5). Despite this strategy, worldwide clinical pregnancy and live birth rates resulting from this procedure have remained stubbornly modest at only 26.8% and 20% per initiated cycle, respectively (3). Notwithstanding confounders, recent epidemiological data has also raised concern regarding the prospect of an increased risk of birth defects and the propagation of substandard semen profiles in men conceived using ICSI compared to that of their naturally conceived peers (6, 7). Such findings affirm the need for cautious utilization of ICSI beyond its intended application for men with severely compromised semen parameters and present a strong case for exploring new diagnostic approaches for sperm selection, patient stratification, and therapeutic treatment options for sub/infertile males (8). In this review, we give consideration to current and future directions in male infertility research that are helping address the long-standing question of how to personalize and improve the clinical management of infertile patients.

2 Diagnostic andrology

Traditional approaches to diagnostic andrology are grounded in the principle that a male's fertility can be assessed using routine descriptive criteria of the semen profile, with emphasis being placed on sperm count, sperm morphology and sperm motility parameters (Figure 1). Unfortunately, this conventional clinical strategy sheds little light on the underlying infertility etiology or the functional integrity of a patient's spermatozoa and has thus proven to be of limited utility in predicting fertilization success (9). Indeed, despite iterative improvements in the semen assessment guidelines curated by the WHO (10–12), a substantial proportion of infertile men (~15%) still present with 'normal' semen profiles according to WHO criteria (13). Such cases of unexplained, or idiopathic, infertility have led us to appreciate that there are many different pathologies that contribute to male sub/infertility, each of which impose different clinical implications for patient management and help account for the relatively weak prognostic value of routine andrological assessment pipelines (14). Similarly, although advances have been made toward the automation of sperm morphology assessment *via* the coupling of ultra-high magnification with machine learning [i.e., 'motile sperm organelle morphology examination' (MSOME)], with the goal of standardizing the detection of morphological anomalies, it remains uncertain which elements of sperm structure define the functionality of this highly specialized cell. Thus, despite the potential of improving reproductive outcomes associated with using MSOME in tandem with ICSI (i.e., intracytoplasmic morphologically selected sperm injection; IMSI) (15), there remains insufficient evidence to support a positive effect of IMSI on either clinical pregnancy, live birth or miscarriage rates (16). While such pitfalls could theoretically be addressed by the application of selective stains to discriminate key features of sperm structure and quality (e.g., fluorophores that differentially label spermatozoa according to their viability, acrosomal status, capacitation status, mitochondrial membrane potential, generation of reactive oxygen species (ROS), peroxidation of membrane lipids, apoptosis and the integrity of their DNA), the use of such probes is currently prohibited in clinical practice; and will likely remain so until such time as the development of alternative stains that can achieve the non-destructive labeling of sperm structures in a manner that is either reversible or biologically inert.

As a descriptive stalwart of conventional semen profiling, the assessment of sperm motility offers some promise, especially when this assay is performed with objective computer aided semen analysis (CASA) systems that accurately measure the kinematics of swimming spermatozoa (17). It follows that positive correlations have been reported between the concentration of progressively motile spermatozoa and the outcome of human sperm-cervical mucus interaction tests (18) as well as overall fertility (19). Unfortunately, since the sperm motility profile is not static, such correlations are often weak. Indeed, under the influence of the differing physiological environments that spermatozoa encounter during their passage to the site of fertilization, they variably display forward progressive motility, complete quiescence (permissive of the formation of a storage reservoir in the isthmus of the fallopian tubes), and a characteristic high-frequency high-amplitude, asymmetric flagellar beat known as hyperactivated motility (20, 21). Whilst CASA measurements can discriminate these alternate forms of sperm motility (17), their intermittent nature limits their application as robust diagnostic criteria in a clinical setting. This phenomenon also likely contributes to the situation whereby the application of 'swim up' techniques to select motile spermatozoa have failed to deliver improved pregnancy rates compared to that of the most widely utilized colloidal silica density gradient preparation methods (22–24). With the intention of providing a more complete appraisal of sperm motility characteristics, new acquisition methods are in development that enable high-resolution reconstruction of three-dimensional sperm trajectories (i.e., *via* real-time tracking of the position of the whole flagellum in three-dimensional space), with some also featuring simultaneous analysis of the morphological characteristics of individual free swimming sperm cells (25–28). One

such recently described application exploited a high-speed off-axis holographic system to map the three-dimensional refractive-index profile of the sperm head, in tandem with the dynamic flagellum localization during free swim (29). The four-dimensional reconstructed profile so generated enabled the specimen's natural movement to be tracked together with detailed volumetric data on internal organelle structures (such as the nucleus housing the paternal genome); all without an attendant need for cell staining (29). Notwithstanding the considerable promise afforded by these new developments, both in the context of biological assays and clinical use, it remains uncertain whether they will be able to resolve the limitations associated with the continuum of motility profiles displayed by the fertilizing spermatozoon.

3 Strategies to improve diagnostic andrology

It is clear that there is a pressing need for new modalities of fertility diagnosis and the selection of spermatozoa for use in ART. In terms of addressing the limitations and variability inherent in current methodologies, we have much to learn from studying both the molecular basis of sperm dysfunction and equally, the features of functionally competent spermatozoa that can successfully ascend the female reproductive tract to reach the site of fertilization and complete the sequence of cellular interactions that precede natural conception (Figures 1, 2). This latter, highly selected subset of spermatozoa not only possess the requisite motility to gain entry into the oviducts but also the competence to engage in capacitation; a complex suite of biochemical and biophysical changes that prime spermatozoa for interaction with the cumulus oophorus and zona pellucida (ZP) surrounding the ovulated oocyte (30). These interactions are orchestrated by specialized membrane domains adorning the anterior sperm head (31, 32), which are formed during spermatogenesis before being extensively modified coincident with sperm transit of both the male and female reproductive tracts (33, 34). It therefore stands to reason that the development of sperm selection protocols that mimic the stringency of the barriers that fertilizing spermatozoa naturally encounter have obvious appeal (Figure 2).

3.1 Sperm-hyaluronic acid binding

Among an ever-expanding list of emerging sperm selection technologies designed to impose the physiological stringency of natural sperm selection barriers are protocols that exploit the hyaluronic acid (HA) binding properties of spermatozoa. These

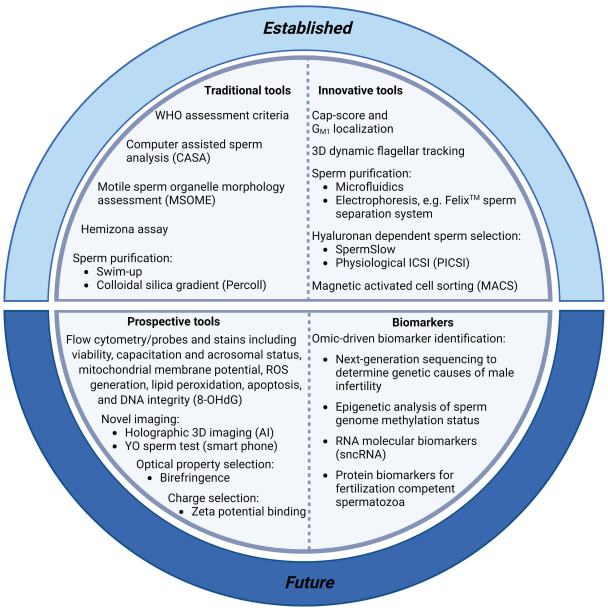

FIGURE 1
Summary of current and prospective tools for sperm selection and the clinical diagnosis of male infertility. Conventional protocols for the diagnosis of male infertility include assessment of sperm morphology, motility and concentration [including World Health Organisation (WHO) assessment criteria (35), computer assisted sperm analysis (CASA) (17), and motile sperm organelle morphology assessment (MSOME)] (16). These protocols are facilitated by the purification of sperm cells from seminal plasma with swim-up techniques or, more commonly, with density gradient centrifugation based on the use of colloidal silica suspensions. More innovative sperm selection strategies including microfluidics (36) and electrophoresis (Felix^{TM}; (37)) are also showing promise for use in clinical settings. Recent additions to the armoury of sperm selection tools include assays with the ability to determine DNA integrity and fertilization capacity [including the Cap-Score test (38), hyaluronan-based sperm immobilization methods (39), and high-throughput flow cytometry assays to detect DNA integrity [e.g., probes for the oxidized base 8-hydroxyl-2-deoxyguanosine (8-OHdG) (40)]. Further, smart phone technology is making semen analyses more accessible with at home YO sperm tests (41), and artificial intelligence (AI) advances have enabled new holographic 3D sperm imaging (28) and sperm quality assessment. Finally, technological advancements in omics platforms (34, 42) are permitting the identification of molecular biomarkers with which to stratify infertile patients, allowing enhanced evaluation of subfertility phenotypes, aiding our understanding of the genetic and epigenetic causes of male infertility, and potentially revolutionising fertility treatment with personalized therapeutic regimens.

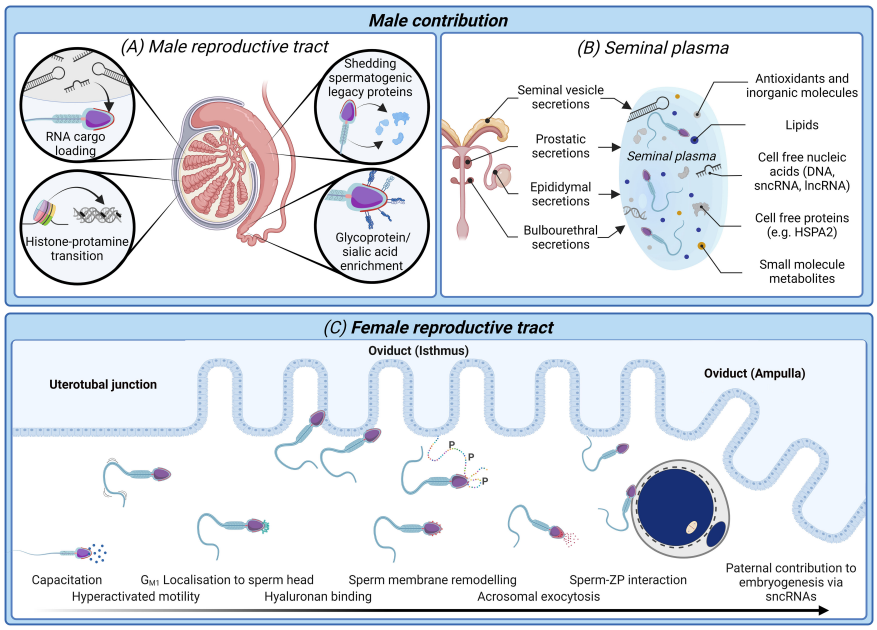

FIGURE 2
The biological processes and biomarkers of sperm production and functional maturation; an untapped resource for diagnostic tools of male infertility and sperm selection techniques. **(A)** In the male reproductive tract sperm nuclear compaction transitions from histone packaging to one characterized by predominantly protamines (43). Developing spermatozoa are simultaneously loaded with regulatory RNA cargo (42, 44) while also shedding excess cytoplasm and spermatogenic legacy proteins (34). Mature spermatozoa are identifiable upon completion of epididymal transit by an enrichment glycosylated surface proteins (34) and dynamic changes in their small non-coding RNAs (sncRNA) profile (45, 46). **(B)** Seminal plasma conveys not only spermatozoa to the female reproductive tract, but also several non-cellular components including antioxidants, lipids, and cell-free nucleic acids and proteins (47). Many of these non-cellular features offer high potential as biomarkers of a healthy, fertile human ejaculate. **(C)** After spermatozoa are deposited in the female reproductive tract they must successively negotiate the uterus and uterotubal junction before progressing through the oviduct isthmus and ampulla to contact the ovulated oocyte. Thereafter, spermatozoa must undergo a process termed capacitation, which is accompanied by dynamic protein phosphorylation events giving rise to altered patterns of motility (hyperactivated motility) and substantial membrane remodeling to facilitate the presentation/unmasking of the sperm surface receptors that orchestrate cumulus matrix (hyaluronan) and sperm-zona pellucida adhesion and penetration (30, 48). Finally, spermatozoa undergo an acrosome reaction leading to release of their acrosomal contents and remodeling of the sperm head architecture compatible with downstream gamete membrane fusion and fertilization (49). Beyond the delivery of the paternal genome, there is now compelling evidence that sperm convey epigenetic factors including sncRNAs to influence the trajectory of pre-implantation embryogenesis (50, 51).

techniques harness the principle that functionally competent spermatozoa are endowed with HA binding sites that permit their adherence to, and digestion of, the HA-rich cumulus oophorus matrix (52). Two dominant protocols have been marketed under the umbrella of HA sperm selection, i.e., physiological intracytoplasmic sperm injection (PICSI; which features the use of HA immobilized on a solid support) and SpermSlow (which features HA suspended within a viscous medium). Such systems immobilize or retard sperm movement, theoretically enabling the positive selection of mature spermatozoa in preparation for ICSI (52). Notwithstanding the appeal and clinical interest in such interventions, current evidence appears insufficient to support their ability to improve either clinical pregnancy or live birth rates resulting from ART (53–55). Meta analyses have also concluded current evidence is inadequate to exclude adverse effects or differentiate the efficacy of SpermSlow versus PICSI HA binding systems (53). On the contrary, recent re-analysis of data from a parallel, two-group, randomized trial (i.e., HABSelect) has now reported that the use of PICSI is positively associated with a reduction in the rate of miscarriages, particularly in the subset of women aged over 35 (39, 55). Such an effect has been attributed to PICSI selection of spermatozoa with reduced levels of DNA damage.

In terms of offering a biological explanation for the lack of consensus regarding the clinical outcomes of sperm selection achieved using HA-based systems, there is now compelling evidence that the surface architecture of a human spermatozoon undergoes a substantial capacitation-associated remodeling in preparation of oocyte interaction (30, 33, 56–59). This event is characterized by a reduction in the proportion of sperm cells with surface exposed hyaluronidase enzymes [such as sperm adhesion molecule 1, (SPAM1)] (48, 60–62) and a reciprocal increase in those cells presenting ZP receptors on their surface (56). These receptors include arylsulfatase A (ARSA), an enzyme that is predominantly expressed on the surface of capacitated human spermatozoa where it displays affinity for the sulfated sugar ligands adorning the ZP (58, 62, 63). Importantly, recent work has demonstrated that sperm dysfunction may be due to the ubiquitination of ARSA on the sperm surface leading to an altered sperm surface glycosylation profile which, in turn, may negatively impact sperm-oocyte recognition (64). Thus, HA adhesion may favor the selection of the subset of spermatozoa that have yet to complete capacitation.

However, whether this delay is reflective of underlying lesions in capacitation-associated signaling remains to be determined. Irrespective, the importance of capacitation as a predictive measure of fertility success is highlighted by recent developments such as the Cap-Score Sperm Function Test (65). As discussed below (please see Section 3.4.3: Sperm lipid biomarkers), this assay is formulated to assess sperm capacitation based on evaluation of the spatial distribution of the dominant sperm ganglioside, G_{M1}.

3.2 Sperm-zona pellucida binding

After penetration of the HA-rich cumulus oophorus, spermatozoa encounter their final physiological barrier to fertilization in the form of the ZP (Figure 2); a glycoprotein matrix that envelops the ovulated oocyte (66). It is well established that an inability to bind and penetrate the ZP ranks among the most common defects recorded in the spermatozoa of infertile male patients (67). Thus, ~10% of men diagnosed with idiopathic infertility present with a failure of sperm-ZP adhesion (68). However, defects in sperm-ZP adhesion are commonly a matter of degree and upon quantification using techniques such as the hemizona assay (HZA), provide the highest discriminatory power for both *in vitro* and *in vivo* fertilization success of any sperm parameter (69). These findings have been taken as putative evidence that the ZP serves an important role in the selection of high quality spermatozoa (33, 66), a notion that resonates with multiple reports that the ZP preferentially binds spermatozoa that display superior motility, morphology, high levels of DNA integrity and lower global DNA methylation levels than that of their unbound counterparts (70–73). In accounting for this phenomenon, it is perhaps notable that each of these functional parameters are acutely sensitive to elevated levels of reactive oxygen species, the excessive production of which is a common etiology in the spermatozoa of infertile males (74). Indeed, work in our own laboratory has shown that molecular chaperone proteins (i.e., heat shock protein A2; HSPA2), which coordinate capacitation-associated membrane remodeling, are highly vulnerable to adduction by reactive lipid aldehydes [including 4-hydroxynonenal (4HNE)] formed as a consequence of oxidative-stress induced membrane lipid peroxidation (75–77). Such adductions disrupt HSPA2-client protein interactions and consequently limit the surface presentation of ZP receptors in capacitated spermatozoa (63).

As an extension of these findings, it has been shown that the use of ZP binding as a tool for selecting spermatozoa for downstream use in ICSI is associated with the production of higher quality embryos as well as improved implantation and clinical pregnancy rates compared to spermatozoa selected by conventional subjective criteria (71, 78, 79). Despite the biological importance of ZP binding, the advent of ICSI to bypass this physiological barrier has effectively diverted attention away from research into the molecular basis by which spermatozoa recognize and engage in productive interactions with the ZP (32). Nevertheless, the balance of clinical evidence as well as that compiled from animal studies indicates that this event likely involves contributions from both protein-protein and lectin-like interactions (80–84). Such observations raise the prospect of using ZP ligands to harvest superior quality, fertilization competent spermatozoa. Although the use of native ZP holds obvious appeal in this regard, ethical and resourcing limitations prohibit the use of this resource. Nevertheless, complex carbohydrate surrogates, such as fucoidan and neoglycoproteins decorated with the sialyl-Lewisx (sLex) sequence, have been identified that possess the ability to competitively inhibit human gamete interactions (81, 85). Similarly, agarose beads coated in recombinant human ZP2 peptides have shown promise in the selection of high-quality human spermatozoa (84). Taken together, these data support the tenant that specific carbohydrate and/or ZP peptide motifs can be harnessed as sperm selection strategies to enhance the success of downstream ART applications. Building on this principle, below we briefly discuss several other advanced sperm selection techniques that are in development based on exploiting the surface characteristics of functionally viable spermatozoa; including those that discriminate sperm on the basis of the degree of negative surface charge, exteriorization of apoptotic markers, and birefringence properties (Figures 1, 2). Notably, however, while several of these technologies have shown promise in a pre-clinical setting, additional high quality randomized evidence is required before advocating for their widespread clinical adoption (53, 54, 86).

3.3 Sperm surface characteristics

In common with their somatic cell counterparts, the surface of a human spermatozoon is furnished with a complex glycocalyx comprising a diversity of carbohydrates linked to membrane protein and lipid anchors (87, 88). Moreover, this acellular coat is substantially remodeled during the consecutive stages of sperm maturation, such that those spermatozoa that have successfully completed their epididymal maturation are characterized by an enrichment of glycoproteins with terminal sialic acid residues (89). This gradient of increasing sialylation is now a well-recognized hallmark of sperm maturity and one that has been associated with the protection of spermatozoa from immune surveillance within the female reproductive tract (89). However, beyond masking the allogeneic properties of the sperm cell, the accompanying increase in electronegativity brought about by sialyation has formed the basis of electrophoretic separation techniques designed to rapidly fractionate mature spermatozoa away from other deleterious ejaculate contaminates (i.e., immature germ cells, bacteria, and leucocytes) (90) (Figure 1). One such recent development, now marketed under the trademark of the Felix Sperm Separation System, has shown promise for the isolation of suspensions of viable, morphologically normal spermatozoa with high levels of total and progressive motility, and low levels of DNA damage (37, 90–93). Clinical compatibility has also been demonstrated with biopsied material, snap-frozen sperm suspensions and cryostored semen, and the first report of a human pregnancy and live birth using electrophoretically isolated spermatozoa (91). Alternate electrokinetic properties of mature spermatozoa including the ~ -16 to -20 mV charge differential across their plasma membrane (i.e.

their zeta potential) have also been exploited as a means by which to capture these cells following their adherence to positively charged support matrices (94). Akin to electrophoretic separation methods, methods exploiting zeta potential have been reported to select mature sperm cells with enhanced levels of normal morphology, kinematic parameters and DNA integrity, and accordingly, have been associated with improved fertilization and pregnancy success following ART (95).

Among the leading non-genetic etiologies causally linked to male infertility is oxidative stress, a pathology that arises as a consequence of elevated levels of reactive oxygen species (ROS) within the male germline (74). Sperm cells are highly vulnerable to oxidative stress owing to an abundance of oxidizable substrates (including high levels of polyunsaturated fatty acids) combined with the fact that they possess limited capacity to protect themselves against oxidative attack or to enact repair once they sustain damage (74). Instead, spermatozoa revert to an apoptotic cascade upon the induction of oxidative stress, a situation that eliminates their fertilization potential and presumably promotes their phagocytosis without the propagation of an attendant inflammatory response within the female reproductive tract (96). One of the late hallmarks of the apoptotic sperm membrane is the externalization of phosphatidylserine resides, the detection of which forms the basis of negative selection protocols, including glass wool separation and magnetic activated cell sorting (MACS)-annexin V technologies, designed to remove senescent spermatozoa from within an ejaculate prior to ART (53, 54, 97–100). One potential flaw in this otherwise laudable approach is that the superficial exposure of phosphatidylserine has recently been reported in the head region of viable and motile mouse spermatozoa (101). Indeed, the surface presentation of phosphatidylserine is reported to progressively increase during sperm transit through the epididymis and again upon the capacitation of these cells. Moreover, the masking of sperm surface phosphatidylserine residues potently inhibited fertilization, thus identifying this ligand as a potential key player in sperm-oocyte fusion (101). Such findings raise the prospect that the loss of phospholipid asymmetry within the sperm plasma membrane is not simply a signature of apoptotic cells but rather one associated with the level of sperm functional maturity. As an important caveat however, it remains to be determined whether this model also holds true in the case of human spermatozoa. It is thus premature to conclude whether this is an extenuating factor that has limited the clinical utility of MACS-annexin V selection protocols (53, 54).

Apart from measurable differences in the macromolecular composition of the sperm surface that herald changes in their functional status, maturing sperm cells are also characterized by changes in their birefringence optical properties. Birefringence is a phenomenon exhibited by certain materials in which an incoming (incident) ray of light is split by polarization into two rays each assuming slightly different paths and travelling at different velocities. The extent of this so called 'bi'refraction (i.e., birefringence) is determined by the non-uniform spatial (i.e., anisotropic) properties of the material; which in the case of human spermatozoa, originate from a combination of longitudinally orientated protein filaments residing within the subacrosomal, nuclear, and axonemal domains, each of which refract light differently (102–104). Accordingly, the use of polarized light microscopy has drawn attention as a diagnostic tool with which to evaluate the structural integrity of spermatozoa with applications extending to the selection of viable cells with normal morphology and low levels of DNA damage in preparation for ICSI (105, 106). However, the clinical utility of this technology has yet to be investigated in randomized trials (53).

3.4 Sperm biomarkers

As discussed above, there are numerous inherent limitations associated with existing strategies for sperm selection and defining male fertility. These limitations have, in turn, fueled renewed interest in the identification of non-invasive biomarkers that accurately predict fertilization outcome and provide molecular insight into underlying infertility pathophysiology (107). Such approaches have been aided by rapid technological advances in analytical 'omic' platforms leading to a recent proliferation in studies seeking to define the macromolecular signatures (e.g. lipidomic, metabolomic, proteomic, and epigenomic) of semen and spermatozoa from fertile males versus those produced by subfertile/infertile men (57, 108–112).

3.4.1 Sperm protein biomarkers

Due to their inability to engage in *de novo* protein synthesis, the functional maturation of human spermatozoa is reliant on changes associated with two phases of post-testicular maturation, namely: (i) the incorporation of new proteins encountered during their descent through the male reproductive tract (epididymis), and (ii) the processing and/or post-translational modification of their intrinsic proteome that occurs during post-ejaculatory capacitation (33, 34, 57) (Figure 2). These characteristics highlight the importance of proteomic tools for studying the molecular changes that drive the acquisition of sperm functionality (57, 110, 111). It follows that considerable research effort has been directed to cataloging the sperm proteome in addition to the seminal fluid and innumerable extracellular vesicles in which they are bathed (108, 109, 111, 113–116). In the context of spermatozoa, this growing proteomic resource has been assembled into a comprehensive reference library of 6,198 proteins; an inventory that accounts for ~80% of the estimated 7,500 proteins that are represented in human spermatozoa (117). Notably, recent work from our own laboratory has demonstrated that alongside proteins that are either gained and/or modified during post-testicular sperm maturation, the shedding of proteins also constitutes a major part of the proteomic changes that contribute to producing a fertilization competent sperm cell (34). Such proteins, which are underrepresented in the mature spermatozoon, have been shown to map to several infertility phenotypes and could thus represent negative selection markers to potentially identify poor quality spermatozoa. Amid the remaining challenges to realizing the transformative impact of this information are the investigation of protein interaction networks,

characterization of those proteins whose function is influenced by post-translational modifications (e.g. phosphorylation, proteolytic cleavage, acetylation, glycosylation), and defining anomalies in protein abundance that signify specific defects in sperm function (57, 109).

Advances are being made toward these goals through the application of advanced mass spectrometry technology platforms to deliver new insight into the proteomic features of spermatozoa in different functional states (i.e., fertile *vs.* infertile, immature *vs.* mature, and non-capacitated *vs.* capacitated) (34, 61, 118–122). Such strategies are helping to shed light on specific proteomic elements that are of functional significance and facilitating improved interpretation of the spectrum of post-translational modifications necessary for generating a fertilization competent spermatozoon (57). Illustrative of this potential, mass spectrometry based proteomic analyses have been used to identify specific defects in human sperm cells associated with their failure of ZP recognition (61). Among the subset of proteins significantly under-represented in the spermatozoa of infertile patients, this study identified the molecular chaperone, HSPA2 (61). Such unbiased findings align with independent evidence that the overall abundance of HSPA2 in human spermatozoa provides a robust discriminative index of their fertilizing potential (52). By way of a biological explanation, HSPA2 appears to be a critical component of the machinery that orchestrates sperm plasma membrane remodeling events during spermiogenesis and capacitation (56, 59, 62, 123–125). Thus, an under-representation of HSPA2 likely has functional consequences in terms of the functional priming of ZP binding domains on the mature sperm surface. Moreover, the under-representation of HSPA2 within the sperm proteome has been causally linked to oxidative stress (63), thus reinforcing the concept that the fidelity of sperm-ZP interactions can be used to sensitively monitor the legacy of this pathophysiological challenge.

Aside from HSPA2, a subset of other sperm proteins have been identified as targets for damage brought about by the formation of oxidative 4HNE adducts (126–128), including A-kinase anchor protein 4 (AKAP4); a sperm-specific protein that localizes to the fibrous sheath of the flagellum, where it fulfils indispensable roles in spermatogenesis and subsequently in the support of sperm motility, capacitation-associated signaling and chemotaxis (129, 130). Data from our own laboratory have shown that both the AKAP4 protein and its precursor (proAKAP4), are targeted for 4HNE adduction in primary cultures of round spermatids and in mature mouse and human spermatozoa (127). We further demonstrated that exogenous 4HNE challenge of round spermatids and spermatozoa leads to a significant reduction in the detectable levels of both proAKAP4 and AKAP4 and a concomitant compromise of capacitation-associated phosphotyrosine expression in human spermatozoa; the latter putatively being caused dysregulation of the signaling network assembled around the AKAP4 scaffold. Such data affirm the utility of proAKAP4/AKAP4 as markers of sperm function and identify the measurement of proAKAP4/AKAP4 abundance as a promising approach to evaluate semen quality in male infertility disorders (131–133).

3.4.2 Sperm nucleic acid biomarkers

In addition to sperm proteins, alternative macromolecular features such as the sperm RNA signature and the integrity of the paternal genome have also attracted attention as prospective markers of fertilization success (134, 135). With regard to the latter, it has long been of interest to understand the principles, and biological consequences, associated with the packaging of approximately two meters of DNA into the sperm nucleus to create a structure far more compact than that of its somatic cell counterparts. It is now understood that this remarkable feat is accomplished by substantial remodeling of the chromatin during spermiogenesis linked to replacement of the majority of DNA packaging histones with protamines; effectively reducing the paternal DNA to a quasi-crystalline state approaching the physical limits of compaction (136) (Figure 2). In addition to streamlining the morphological profile of the spermatozoon, this strategy has attendant consequences in terms of reducing the exposure of the paternal genome to damaging agents yet effectively silencing transcription such that human spermatozoa possess limited capacity to enact DNA repair if they sustain damage to the paternal genome (137, 138). When attacks to the paternal genome do occur, they are commonly oxidatively induced as evidenced by the formation of the 8-hydroxy-2'-deoxyguanosine (8OHdG) DNA base adduct (139–141). Notably, such lesions are not randomly dispersed across the genome in mature spermatozoa but rather are targeted, with chromosome 15 being particularly susceptible to oxidative stress (142); a phenomenon potentially linked to its position within the nuclear matrix (143). Moreover, areas of vulnerability to oxidative attack are commonly associated with inter-linker regions (142); short (<1000 bp) non-protein bound segments interspersed between protamine-bound DNA toroids (43, 144, 145) and retained histone-bound DNA units that affix DNA to the nuclear matrix (146–148). Notably, these regions of vulnerability are of clinical relevance owing to the fact that they have been shown to harbor oxidative damage in the spermatozoa of infertile male patients (142). It follows that such defects (in addition to those associated with genetic mutations, exposure to environmental agents and disruption of chromatin proteins) have been causally linked to natural reproductive failures including reductions in fertilization rates, pregnancy rates, embryo quality, and increased rates of spontaneous abortion (149–151). However, it remains uncertain to what extent the evasion of natural conception barriers by directly injecting spermatozoa with damaged DNA into an oocyte, accounts for the increased risk of birth defects associated with assisted conception technologies such as ICSI (7, 152–154). Moreover, the retention of histones in approximately 4-15% of the sperm nuclear genome, contributes to a scenario in which epigenetic marks can endure reprogramming events (138, 155) thereby enabling transcriptional memory with potential implications extending across generations (156).

Accordingly, a battery of diagnostic assays have been brought to market that evaluate sperm DNA fragmentation such as the sperm chromatin structure assay (SCSA) (157), the single cell gel electrophoresis (Comet) assay (158), the terminal deoxynucleotidyl transferase mediated deoxyuridine triphosphate nick end labeling

(TUNEL) assay (159), the chromomycin A3 test (160), *in situ* nick translation (161), the sperm chromatin dispersion (SCD) test (162, 163), and protamine ratio analysis (164). Regrettably, none of these report on the epigenetic state of the genome, and similarly, current evidence linking sperm DNA damage with outcomes of ART interventions is controversial. Thus, although some literature reports a strong negative association between sperm DNA fragmentation and pregnancy outcomes to justify the incorporation of sperm DNA testing into routine clinical tests (165, 166), other systematic reviews and meta-analyses suggest that our current armory of DNA damage assays have limited ability to predict pregnancy outcomes in the context of ART (167, 168). Thus, despite the potential benefits, there remains insufficient impetus to foster the routine application of sperm DNA damage testing in the management of couples seeking recourse to ART. We do, however, advocate for the continuation of high-quality research into the predictive value of sperm DNA fragmentation assays for both the success of pregnancy and for the choice of ART treatment.

Beyond the implications of sperm DNA damage and histone modifications, several classes of regulatory RNA species have also been implicated in epigenetic inheritance, including multiple sub-types of sperm-borne small non-coding RNAs (sncRNAs). Indeed, despite their transcriptionally and translationally inert state, it is well documented that mature spermatozoa convey a heterogenous cargo of RNA transcripts, including, mRNA, long non-coding RNA (lncRNA), and sncRNA (169). Moreover, a subset of the latter have been linked with regulation of the trajectory of pre-implantation embryo development and consequently, influencing the lifetime health of offspring (170). Thus, rather than being insignificant vestiges of spermatogenesis, sperm-borne sncRNAs are gaining attention for their potential prognostic value in evaluating sperm quality linked to male infertility (169). Growing interest has also focused on sperm-borne sncRNAs as diagnostic markers of a male's exposure to environmental stressors and the fidelity of sperm production (134, 169). In this regard, mounting evidence has drawn links between an array of environmental stressors (e.g. dietary challenges, stress hormone administration, imposition of psychological stress, and exposure to environmental pollutants such as cigarette smoke) and pronounced alterations in the sperm sncRNA profile of exposed males (51, 171, 172). Of concern is that each of these changes can potentially contribute to sperm dysfunction and may account, at least in part, for the observation that the sperm sncRNA signature of idiopathic infertile males is evidently different from that of fertile individuals (169, 173–176). Notwithstanding the interest these studies have generated, the distinctive features of sperm biology pose several hurdles to utilizing RNA cargo for diagnostic purposes. Key among these are the low yield and the highly degraded nature of sperm RNA, yet it is hoped that these limitations will, in time, be circumvented by continued optimization of RNA isolation protocols (177). Such advances are necessary to realize the translational potential of data collected from pre-clinical animal studies and ensure the reproducibility of clinical assessments of male fertility using RNA biomarkers. Ultimately, the cataloging of human sperm RNA, similar to that achieved for the sperm proteome, may herald new opportunities to assess the effects of environmental, physical and chemical factors on semen quality with a level of unparalleled sensitivity.

3.4.3 Sperm lipid biomarkers

As integral components of the sperm surface, the composition, orientation and distribution of membrane lipids have also attracted attention as diagnostic biomarkers of male fertility. Illustrative of this potential are the MACs sperm selection technologies described previously, which exploit the externalization of phosphatidylserine in moribund cells (discussed above). However, recent developments have also seen a renewed focus on alternative lipids such as monosialotetrahexosylganglioside (G_{M1}), which features as the target of assays marketed under the trademark of the Cap-Score Sperm Function Test (178, 179). In principle, Cap-Scores provide an indication of the percentage of capacitated spermatozoa within a given sample as determined by the localization of G_{M1}; an integral component of sperm membrane rafts and one that becomes progressively concentrated within the vicinity of the anterior domain of the sperm head as capacitation proceeds (178, 180, 181). It follows that the re-localization of G_{M1} differs in the spermatozoa of cohorts of fertile and potentially infertile men, giving credence to the utility of Cap-Score. Indeed, Cap-Score has shown promise in predicting the success, or failure, of intrauterine insemination (IUI) in both retrospective (178) and prospective contexts (38, 65). Notably, Cap-Scores appear highly reproducible among ejaculates from a single individual and reliably identify those cells competent of completing an acrosome reaction induced by either an ionophore (179) or progesterone challenge (182); yet they have limited relationship with conventional semen analysis criteria (178). These data identify the utility of the Cap-Score as a predictive measure of male fertility and, if borne out across larger cohort studies, a strategy with important clinical applications in patient stratification. For a comprehensive summary of lipids that may be further developed as biomarkers of male infertility see (112, 183).

3.5 Seminal plasma biomarkers

Beyond the sperm component of the ejaculate, the seminal plasma in which they are bathed is also recognized as comprising a rich variety of biomolecules; many of which could potentially serve as non-invasive biomarkers of a male's fertility status [e.g. proteins (125, 184, 185), small-molecule metabolites (186), lipids (187), cell-free nucleic acid (DNA, sncRNA and lncRNA) (188–191), as well as antioxidant agents and inorganic chemicals (ions) (192)]. Indeed, seminal plasma is an elaborate nutrient-rich fluid generated by the accessory glands of the male reproductive tract, which constitutes as much as 95% of human semen (193). Contrary to the long-held belief that seminal plasma acts solely as a transport medium for spermatozoa, a compelling body of data now supports key physiological roles in the promotion of early pregnancy success (47, 194). Such functions are attributed to direct communication with the female reproductive tract at insemination, effectively modulating cellular, molecular and immunological adaptions of the uterine environment to accommodate the semi-allogeneic

conceptus and optimize pregnancy outcomes (47, 194). While it is apparent that human conception can proceed in the absence of seminal plasma, emerging clinical evidence (195–197) in tandem with data arising from pre-clinical animal models (198–201) suggests that an absence of seminal plasma exposure at conception results in suboptimal embryonic development and placentation; changes that can, in turn, manifest in pathological consequences for offspring. Such findings have prompted mounting interest in the active signaling factors present within seminal fluid (47) as well as the susceptibility of these factors to paternal stressors (202–204). Moreover, beyond those molecules with putative roles in modulating the female response, it is emerging that the components of seminal plasma may bear witness to the legacy of defective sperm production. Illustrative of this potential is HSPA2, a molecular chaperone protein previously discussed in relation to its role in the capacitation associated remodeling of the sperm surface, and one that is intimately associated with spermatogenesis. Recent work has also documented the presence of sperm-free HSPA2 in seminal plasma wherein its relative abundance is positively correlated with spermatogenic status (125). It follows that sub-classes of infertile males, such as cryptozoospermic patients, have low to non-detectable seminal plasma HSPA2; likely reflective of an almost total meiosis arrest. Additional work toward characterizing the molecular composition of seminal plasma and its relationship with a male's fertility status is certainly warranted to help realize the potential of this easily accessible suspension as a source of biomarkers capable of predicting the potential success or failure of ART procedures.

4 Implications for therapeutic interventions

With ongoing limitations associated with the accurate diagnosis of male infertility, it is not surprising that a majority of the therapeutic interventions that have been clinically successful have been targeted to the treatment of pathologies with an obvious phenotype. Examples of these successful strategies lie in the treatment of varicocele through surgical means (205), the use of aromatase inhibitors in patients with abnormal testosterone-to-estradiol ratios (206), and extensive developments in ART procedures, such as ICSI (3), that have assisted patients with poor semen parameters, or those with an absence of sperm in the ejaculate through a combination of testicular sperm extraction (TESE) and ICSI.

In the case of varicocele, although the prevalence of the condition remains high at up to 20% of the male population, clinical varicocele now ranks as the most common correctable cause of male infertility (205). Varicocele repair is aimed at the dilation of the pampiniform plexus, a venous network located in the spermatic cord, to relieve the causative retrograde blood flow through the internal spermatic vein. In current practice, surgical approaches to repair varicocele, including ligation and resection of the dilated vessels by open surgery or microsurgery, are preferred. Further, the ability to tailor interventions to the grade and condition of each patient has led to a large array of treatment options (205). These innovations have had a significant impact on the recovery of fertility in patients that have undergone varicocelectomy. However, complications due to the inflammation and testicular heating paradigms associated with this condition have led to the suggestion that varicocele may be a progressive pathological condition, with implications extending to both structural and functional damage within the testis (207). Particularly concerning is that even in varicocele patients with normal semen parameters, or those with improved fertility post-surgery, the condition is commonly accompanied by an increased prevalence of sperm DNA fragmentation (208). Thus, issues associated with reduced paternal DNA integrity may persist in embryos generated through either natural conception or through ART interventions after varicocelectomy.

Although the nature of the sperm DNA damage experienced in varicocele patients is not entirely understood, one hypothesis is that excessive production of ROS in varicocele testes may contribute oxidative DNA lesions in spermatozoa and/or damaged chromatin in developing germ cells (205). One option for the management of these patients, pre- and post-surgery, is the administration of oral antioxidants to reduce the presence of ROS. While there is obvious theoretical appeal to this strategy and sound evidence from recent animal models that report the efficacy of targeted antioxidant strategies to reduce DNA damage (209), the use of oral antioxidants in a clinical setting has been met with mixed success. Recent reviews have highlighted just five oral antioxidant supplements that have resulted in increases in clinical pregnancy rates and live birth rates (76, 210), namely: astaxanthin, L-carnitine in combination with L-acetyl carnitine, zinc sulphate, vitamin E, and Menevit. Despite the initial promise of these therapeutic candidates, there have been few reports regarding the longevity of this success or follow up studies on the consistency of improved pregnancy outcomes following administration of these antioxidants. Moreover, throughout the analysis of 29 clinical studies of antioxidants targeted to men experiencing fertility problems, extensive variation in outcomes was observed with some studies reporting profound improvement in several semen parameters and some reporting no effect using the same oral antioxidant (210).

Certainly, some of this variability can be attributed to disparities in the intrinsic design of clinical trials, with potential confounders including variations in dose regimens, methodology and the duration of treatment. However, recent reports have also highlighted a lack of selectivity in the patient populations that are recruited for each trial (210, 211). Regrettably, very few antioxidant trials have been performed with cohorts of patients specifically selected based on the presentation of oxidative defects in their spermatozoa or high levels of ROS in their ejaculate. Moreover, the measures of success for these trials, while encompassing important outcomes such as improved semen parameters and time-to-conception, do not commonly include assessments to ensure a complete resolution of ROS levels or DNA damage in the patient's spermatozoa (210). This has led to a concerning inability to account for why individual antioxidant trials have not been successful and

also compromises our future ability to improve on formulations that may be beneficial in stratified patient cohorts.

The reasons for omitting crucial patient selection procedures are undoubtedly complex, though difficulties in the diagnosis of ROS-driven fertility issues and the accurate quantification of oxidative DNA damage remain major clinical roadblocks. Here, despite extensive validation of a number of reliable biomarkers for lipid peroxidation products, ROS, and oxidative DNA damage (211), there are still major challenges associated with the cost-efficiency and accuracy of these tools. Consideration should be given to the development of these common laboratory tools to form clinically applicable markers that can be employed for the high throughput analysis of ROS and oxidative DNA damage in human spermatozoa. Working toward this goal, validation has now been performed across several protocols to assess human DNA oxidation levels using 8-hydroxy-2'-deoxyguanosine (8-OHdG) antibodies in tandem with flow cytometry to discriminate patients with poor semen quality (40). Indeed, this study has helped to establish a consensus for a clinically applicable protocol that allows for the stratification of patients based on 8-OHdG fluorescence. Moreover, great care has been taken to provide evidence of the repeatability and accuracy of the assay, and a rationale for its use as part of routine diagnostics in ART clinics (40). It remains to be seen whether the clinical application of this technique will aid in the selection of patients for oral antioxidant trials. However, this approach is a step towards the development of better management strategies for patients with oxidative-stress derived infertility.

The examples provided here serve to highlight the necessity of a continuum between accurate diagnostics to stratify male reproductive pathologies and the successful development of appropriate treatment and management strategies. While there are many exceptions to this rule, such as the management of patients with non-obstructive azoospermia for which there are no current treatment options despite the clarity of the condition, gaining an advanced mechanistic understanding of male reproductive pathologies is essential to improve diagnostic and therapeutic strategies. In this context, the field of reproductive science stands to benefit from diagnostic innovations and personalized treatment strategies that are currently disrupting the standard of care for other clinical pathologies. Indeed, the current key gap in activity regarding precision medicine approaches to optimize ART commits couples to a standard trial-and-error treatment paradigm that is both inefficient and costly. The case for improved treatment selection tools is only further justified by ongoing research and big data efforts, which continue to uncover potential new fertility biomarkers, but we remain some way from actualizing these into novel therapeutic strategies. While most activity is currently focused on female infertility, notable recent efforts discussed above to address male infertility include the introduction of the Cap-Score to assess sperm capacitation, curation of big data arising from the application of omic-based approaches, broader adoption of sperm DNA fragmentation analyses earlier in diagnostic workups, novel imaging tools (e.g. holographic 3D imaging) that leverage artificial intelligence (AI) to improve the accuracy and speed of gamete selection for ART, and at-home smartphone-based semen testing (e.g., the FDA-approved YO Sperm Test).

5 Conclusions

Despite males accounting for a substantial proportion of human infertility, we currently lack the tools to accurately diagnose and treat this distressing condition. Traditional diagnostic approaches often overlook the subtleties associated with day-to-day variations in sperm production and have increasingly been found to be inadequate predictors of fertilization outcome and live birth rates. These shortcomings underscore an urgent need to develop improved diagnostic tools to more accurately inform patient stratification, improve sperm selection and identify valid therapeutic treatment options for males afflicted with subfertility and infertility. In terms of realizing these ambitious goals, we have much to gain from continued research into the molecular mechanisms that govern normal sperm function and an improved understanding of how sperm cell biology becomes dysregulated in infertile males. In particular, dissection of the highly specialized sequence of changes that accompany sperm production and their functional maturation during their transit of the male and female reproductive tracts promises to yield novel insights into how these cells behave during *in vitro* interventions (Figures 1, 2). Moreover, with the growing realization that poorer-quality sperm may impact offspring health, we have an obligation to define those contributions of the fertilizing spermatozoon that limit the possibility of an adverse outcome after ART interventions. The development of specific sperm biomarkers for this purpose remains a significant goal as does defining the biological signatures indicative of the stress (ors) that the male may have experienced; information that may eventually provide additional clinical decision support to guide ART treatment strategies and maximize success rates.

Author contributions

BN, JS, NB, DS-B, HH, GD, JM, TL and EB contributed to conception and design of this article. BN and EB wrote the first draft of the manuscript. JS, NB, DS-B, HH, GDI, JM, and TL each wrote sections of the manuscript. All authors contributed to manuscript revision, read, and approved the submitted version.

Funding

BN is supported by a National Health and Medical Research Council of Australia (NHMRC) Senior Researcher Fellowship (Grant number: APP1154837). EB is supported by an Australian Research Council (ARC) Discovery Early Career Researcher Award (Grant number: DE210100103). TL is supported by an Australian Research Council Discovery Early Career Research Award (DE220100032).

Conflict of interest

The authors declare that this review article has been prepared in the absence of any commercial or financial relationships that could be construed as a potential conflict of interest.

Publisher's note

References

1. Kolettis PN. Evaluation of the subfertile man. *Am Fam Physician* (2003) 67:2165–72.

2. Niederberger C, Pellicer A. Introduction: IVF's 40th world birthday. *Fertil Steril* (2018) 110:4. doi: 10.1016/j.fertnstert.2018.05.017

3. O'Neill CL, Chow S, Rosenwaks Z, Palermo GD. Development of ICSI. *Reproduction* (2018) 156:F51–8. doi: 10.1530/REP-18-0011

4. Esteves SC. Who cares about oligozoospermia when we have ICSI. *Reprod BioMed Online* (2022) 44:769–75. doi: 10.1016/j.rbmo.2021.11.026

5. Fitzgerald O, Harris K, Paul RC, Chambers CG. *Assisted reproductive technology in Australia and new Zealand 2015*. Sydney: National Perinatal Epidemiology & Statistics Unit, University of New Sotuth Wales (2017).

6. Belva F, Bonduelle M, Roelants M, Michielsen D, Van Steirteghem A, Verheyen G, et al. Semen quality of young adult ICSI offspring: the first results. *Hum Reprod* (2016) 31:2811–20. doi: 10.1093/humrep/dew245

7. Davies MJ, Rumbold AR, Moore VM. Assisted reproductive technologies: a hierarchy of risks for conception, pregnancy outcomes and treatment decisions. *J Dev Orig Health Dis* (2017) 8:443–7. doi: 10.1017/S2040174417000526

8. Simopoulou M, Gkoles L, Bakas P, Giannelou P, Kalampokas T, Pantos K, et al. Improving ICSI: A review from the spermatozoon perspective. *Syst Biol Reprod Med* (2016) 62:359–71. doi: 10.1080/19396368.2016.1229365

9. Barratt CLR, De Jonge CJ, Sharpe RM. 'Man up': the importance and strategy for placing male reproductive health centre stage in the political and research agenda. *Hum Reprod* (2018) 33:541–5. doi: 10.1093/humrep/dey020

10. Bjorndahl L. A paradigmatic shift in the care of male factor infertility: how can the recommendations for basic semen examination in the sixth edition of the WHO manual and the ISO 23162:2021 standard help? *Reprod BioMed Online* (2022) 45:731–6. doi: 10.1016/j.rbmo.2022.03.011

11. Bjorndahl L, Kirkman Brown J, other Editorial Board Members of the WHO Laboratory Manual for the Examination and Processing of Human Semen. The sixth edition of the WHO laboratory manual for the examination and processing of human semen: ensuring quality and standardization in basic examination of human ejaculates. *Fertil Steril* (2022) 117:246–51. doi: 10.1016/j.fertnstert.2021.12.012

12. Chung E, Arafa M, Boitrelle F, Kandil H, Henkel R, Saleh R, et al. The new 6th edition of the WHO laboratory manual for the examination and processing of human semen: is it a step toward better standard operating procedure? *Asian J Androl* (2022) 24:123–4. doi: 10.4103/aja2021118

13. Esteves SC. Evolution of the world health organization semen analysis manual: where are we? *Nat Rev Urol* (2022) 19:439–46. doi: 10.1038/s41585-022-00593-2

14. Pozzi E, Ramasamy R, Salonia A. Initial andrological evaluation of the infertile Male. *Eur Urol Focus.* (2022) 9:51–4. doi: 10.1016/j.euf.2022.09.012

15. Setti AS, Paes De Almeida Ferreira Braga D, Iaconelli AJr., Aoki T, Borges EJr. Twelve years of MSOME and IMSI: a review. *Reprod BioMed Online* (2013) 27:338–52. doi: 10.1016/j.rbmo.2013.06.011

16. Teixeira DM, Barbosa MA, Ferriani RA, Navarro PA, Raine-Fenning N, Nastri CO, et al. Regular (ICSI) versus ultra-high magnification (IMSI) sperm selection for assisted reproduction. *Cochrane Database Syst Rev* (2013) (7):CD010167. doi: 10.1002/14651858.CD010167.pub2

17. Mortimer D, Mortimer ST. Computer-aided sperm analysis (CASA) of sperm motility and hyperactivation. *Methods Mol Biol* (2013) 927:77–87. doi: 10.1007/978-1-62703-038-0_8

18. Mortimer D, Pandya IJ, Sawers RS. Relationship between human sperm motility characteristics and sperm penetration into human cervical mucus *in vitro*. *J Reprod Fertil* (1986) 78:93–102. doi: 10.1530/jrf.0.0780093

19. Hirano Y, Shibahara H, Obara H, Suzuki T, Takamizawa S, Yamaguchi C, et al. Relationships between sperm motility characteristics assessed by the computer-aided sperm analysis (CASA) and fertilization rates *in vitro*. *J Assist Reprod Genet* (2001) 18:213–8. doi: 10.1023/A:1009420432234

20. Tung CK, Suarez SS. Co-Adaptation of physical attributes of the mammalian female reproductive tract and sperm to facilitate fertilization. *Cells* (2021) 10:1297. doi: 10.3390/cells10061297

21. Zaferani M, Suarez SS, Abbaspourrad A. Mammalian sperm hyperactivation regulates navigation *via* physical boundaries and promotes pseudo-chemotaxis. *Proc Natl Acad Sci U.S.A.* (2021) 118:e2107500118. doi: 10.1073/pnas.2107500118

22. Allamaneni SS, Agarwal A, Rama S, Ranganathan P, Sharma RK. Comparative study on density gradients and swim-up preparation techniques utilizing neat and cryopreserved spermatozoa. *Asian J Androl* (2005) 7:86–92. doi: 10.1111/j.1745-7262.2005.00008.x

23. Karamahmutoglu H, Erdem A, Erdem M, Mutlu MF, Bozkurt N, Oktem M, et al. The gradient technique improves success rates in intrauterine insemination cycles of unexplained subfertile couples when compared to swim up technique; a prospective randomized study. *J Assist Reprod Genet* (2014) 31:1139–45. doi: 10.1007/s10815-014-0274-4

24. Baldini D, Ferri D, Baldini GM, Lot D, Catino A, Vizziello D, et al. Sperm selection for ICSI: Do we have a winner? *Cells* (2021) 10:3566. doi: 10.3390/cells10123566

25. Silva-Villalobos F, Pimentel JA, Darszon A, Corkidi G. Imaging of the 3D dynamics of flagellar beating in human sperm. *Annu Int Conf IEEE Eng Med Biol Soc* (2014) 2014:190–3. doi: 10.1109/EMBC.2014.6943561

26. Bukatin A, Kukhtevich I, Stoop N, Dunkel J, Kantsler V. Bimodal rheotactic behavior reflects flagellar beat asymmetry in human sperm cells. *Proc Natl Acad Sci U.S.A.* (2015) 112:15904–9. doi: 10.1073/pnas.1515159112

27. Daloglu MU, Luo W, Shabbir F, Lin F, Kim K, Lee I, et al. Label-free 3D computational imaging of spermatozoon locomotion, head spin and flagellum beating over a large volume. *Light Sci Appl* (2018) 7:17121. doi: 10.1038/lsa.2017.121

28. Gong A, Rode S, Gompper G, Kaupp UB, Elgeti J, Friedrich BM, et al. Reconstruction of the three-dimensional beat pattern underlying swimming behaviors of sperm. *Eur Phys J E Soft Matter* (2021) 44:87. doi: 10.1140/epje/s10189-021-00076-z

29. Dardikman-Yoffe G, Mirsky SK, Barnea I, Shaked NT. High-resolution 4-d acquisition of freely swimming human sperm cells without staining. *Sci Adv* (2020) 6:eaay7619. doi: 10.1126/sciadv.aay7619

30. Aitken RJ, Nixon B. Sperm capacitation: a distant landscape glimpsed but unexplored. *Mol Hum Reprod* (2013) 19:785–93. doi: 10.1093/molehr/gat067

31. Nixon B, Aitken RJ, Mclaughlin EA. New insights into the molecular mechanisms of sperm-egg interaction. *Cell Mol Life Sci* (2007) 64:1805–23. doi: 10.1007/s00018-007-6552-x

32. Dun MD, Mitchell LA, Aitken RJ, Nixon B. Sperm-zona pellucida interaction: molecular mechanisms and the potential for contraceptive intervention. *Handb Exp Pharmacol* (2010) 198:139–78. doi: 10.1007/978-3-642-02062-9_9

33. Nixon B, Cafe SL, Eamens AL, De Iuliis GN, Bromfield EG, Martin JH, et al. Molecular insights into the divergence and diversity of post-testicular maturation strategies. *Mol Cell Endocrinol* (2020) 517:110955. doi: 10.1016/j.mce.2020.110955

34. Skerrett-Byrne DA, Anderson AL, Bromfield EG, Bernstein IR, Mulhall JE, Schjenken JE, et al. Global profiling of the proteomic changes associated with the post-testicular maturation of mouse spermatozoa. *Cell Rep* (2022) 41:111655. doi: 10.1016/j.celrep.2022.111655

35. World Health Organization. *WHO laboratory manual for the examination and processing of human semen, sixth edition*. Geneva: World Health Organization (2021).

36. Heydari A, Zabetian Targhi M, Halvaei I, Nosrati R. A novel microfluidic device with parallel channels for sperm separation using spermatozoa intrinsic behaviors. *Sci Rep* (2023) 13:1185. doi: 10.1038/s41598-023-28315-7

37. Villeneuve P, Saez F, Hug E, Chorfa A, Guiton R, Schubert B, et al. Spermatozoa isolation with Felix TM outperforms conventional density gradient centrifugation preparation in selecting cells with low DNA damage. *Andrology* (2023). doi: 10.1111/andr.13384

38. Sharara F, Seaman E, Morris R, Schinfeld J, Nichols J, Sobel M, et al. Multicentric, prospective observational data show sperm capacitation predicts male fertility, and cohort comparison reveals a high prevalence of impaired capacitation in men questioning their fertility. *Reprod BioMed Online* (2020) 41:69–79. doi: 10.1016/j.rbmo.2020.03.011

39. West R, Coomarasamy A, Frew L, Hutton R, Kirkman-Brown J, Lawlor M, et al. Sperm selection with hyaluronic acid improved live birth outcomes among older couples and was connected to sperm DNA quality, potentially affecting all treatment outcomes. *Hum Reprod* (2022) 37:1106–25. doi: 10.1093/humrep/deac058

40. Vorilhon S, Brugnon F, Kocer A, Dollet S, Bourgne C, Berger M, et al. Accuracy of human sperm DNA oxidation quantification and threshold determination using an 8-OHdG immuno-detection assay. *Hum Reprod* (2018) 33:553–62. doi: 10.1093/humrep/dey038

41. Onofre J, Geenen L, Cox A, van der AuwerA I, Willendrup F, Andersen E, et al. Simplified sperm testing devices: a possible tool to overcome lack of accessibility and inconsistency in male factor infertility diagnosis. an opportunity for low- and middle-income countries. *Facts Views Vis Obgyn* (2021) 13:79–93. doi: 10.52054/FVVO.13.1.011

42. Nixon B, Stanger SJ, Mihalas BP, Reilly JN, Anderson AL, Tyagi S, et al. The microRNA signature of mouse spermatozoa is substantially modified during epididymal maturation. *Biol Reprod* (2015) 93:91. doi: 10.1095/biolreprod.115.132209

43. Wykes SM, Krawetz SA. The structural organization of sperm chromatin. *J Biol Chem* (2003) 278:29471–7. doi: 10.1074/jbc.M304545200

44. Hutcheon K, Mclaughlin EA, Stanger SJ, Bernstein IR, Dun MD, Eamens AL, et al. Analysis of the small non-protein-coding RNA profile of mouse spermatozoa reveals specific enrichment of piRNAs within mature spermatozoa. *RNA Biol* (2017) 14:1776–90. doi: 10.1080/15476286.2017.1356569

45. Conine CC, Sun F, Song L, Rivera-Perez JA, Rando OJ. Small RNAs gained during epididymal transit of sperm are essential for embryonic development in mice. *Dev Cell* (2018) 46:470–480 e3. doi: 10.1016/j.devcel.2018.06.024

46. Sharma U, Sun F, Conine CC, Reichholf B, Kukreja S, Herzog VA, et al. Small RNAs are trafficked from the epididymis to developing mammalian sperm. *Dev Cell* (2018) 46:481–494 e6. doi: 10.1016/j.devcel.2018.06.023

47. Schjenken JE, Robertson SA. The female response to seminal fluid. *Physiol Rev* (2020) 100:1077–117. doi: 10.1152/physrev.00013.2018

48. Bromfield EG, Nixon B. The function of chaperone proteins in the assemblage of protein complexes involved in gamete adhesion and fusion processes. *Reproduction* (2013) 145:R31–42. doi: 10.1530/REP-12-0316

49. Zhou W, Anderson AL, Turner AP, De Iuliis GN, Mccluskey A, Mclaughlin EA, et al. Characterization of a novel role for the dynamin mechanoenzymes in the regulation of human sperm acrosomal exocytosis. *Mol Hum Reprod* (2017) 23:657–73. doi: 10.1093/molehr/gax044

50. Trigg NA, Skerrett-Byrne DA, Xavier MJ, Zhou W, Anderson AL, Stanger SJ, et al. Acrylamide modulates the mouse epididymal proteome to drive alterations in the sperm small non-coding RNA profile and dysregulate embryo development. *Cell Rep* (2021) 37:109787. doi: 10.1016/j.celrep.2021.109787

51. Lee GS, Conine CC. The transmission of intergenerational epigenetic information by sperm microRNAs. *Epigenomes* (2022) 6:12. doi: 10.3390/epigenomes6020012

52. Huszar G, Jakab A, Sakkas D, Ozenci CC, Cayli S, Delpiano E, et al. Fertility testing and ICSI sperm selection by hyaluronic acid binding: clinical and genetic aspects. *Reprod BioMed Online* (2007) 14:650–63. doi: 10.1016/S1472-6483(10)61060-7

53. Mcdowell S, Kroon B, Ford E, Hook Y, Glujovsky D, Yazdani A. Advanced sperm selection techniques for assisted reproduction. *Cochrane Database Syst Rev* (2014) (10):CD010461. doi: 10.1002/14651858.CD010461.pub2

54. Lepine S, Mcdowell S, Searle LM, Kroon B, Glujovsky D, Yazdani A. Advanced sperm selection techniques for assisted reproduction. *Cochrane Database Syst Rev* (2019) 7:CD010461. doi: 10.1002/14651858.CD010461.pub3

55. Miller D, Pavitt S, Sharma V, Forbes G, Hooper R, Bhattacharya S, et al. Physiological, hyaluronan-selected intracytoplasmic sperm injection for infertility treatment (HABSelect): a parallel, two-group, randomised trial. *Lancet* (2019) 393:416–22. doi: 10.1016/S0140-6736(18)32989-1

56. Nixon B, Bromfield EG, Cui J, De Iuliis GN. Heat shock protein A2 (HSPA2): Regulatory roles in germ cell development and sperm function. *Adv Anat Embryol Cell Biol* (2017) 222:67–93. doi: 10.1007/978-3-319-51409-3_4

57. Nixon B, Dun MD, Aitken RJ. Proteomic analysis of human spermatozoa. In: Krause WKH, Naz RK, editors. *Immune infertility: The impact of immune reactions on human infertility*. Heidelberg, Germany: Springer Publishing Company (2017).

58. Gomez-Torres MJ, Huerta-Retamal N, Robles-Gomez L, Saez-Espinosa P, Aizpurua J, Aviles M, et al. Arylsulfatase a remodeling during human sperm *In vitro* capacitation using field emission scanning electron microscopy (FE-SEM). *Cells* (2021) 10:222. doi: 10.3390/cells10020222

59. Huerta-Retamal N, Saez-Espinosa P, Robles-Gomez L, Aviles M, Romero A, Aizpurua J, et al. Human sperm chaperone HSPA2 distribution during *in vitro* capacitation. *J Reprod Immunol* (2021) 143:103246. doi: 10.1016/j.jri.2020.103246

60. Aitken RJ, Nixon B, LIN M, Koppers AJ, Lee YH, Baker MA. Proteomic changes in mammalian spermatozoa during epididymal maturation. *Asian J Androl* (2007) 9:554–64. doi: 10.1111/j.1745-7262.2007.00280.x

61. Redgrove KA, Anderson AL, Dun MD, Mclaughlin EA, O'bryan MK, Aitken RJ, et al. Involvement of multimeric protein complexes in mediating the capacitation-dependent binding of human spermatozoa to homologous zonae pellucidae. *Dev Biol* (2011) 356:460–74. doi: 10.1016/j.ydbio.2011.05.674

62. Redgrove KA, Anderson AL, Mclaughlin EA, O'bryan MK, Aitken RJ, Nixon B. Investigation of the mechanisms by which the molecular chaperone HSPA2 regulates the expression of sperm surface receptors involved in human sperm-oocyte recognition. *Mol Hum Reprod* (2013) 19:120–35. doi: 10.1093/molehr/gas064

63. Bromfield EG, Aitken RJ, Anderson AL, Mclaughlin EA, Nixon B. The impact of oxidative stress on chaperone-mediated human sperm-egg interaction. *Hum Reprod* (2015) 30:2597–613. doi: 10.1093/humrep/dev214

64. Kelsey KM, Zigo M, Thompson WE, Kerns K, Manandhar G, Sutovsky M, et al. Reciprocal surface expression of arylsulfatase a and ubiquitin in normal and defective mammalian spermatozoa. *Cell Tissue Res* (2020) 379:561–76. doi: 10.1007/s00441-019-03144-1

65. Schinfeld J, Sharara F, Morris R, Palermo GD, Rosenwaks Z, Seaman E, et al. Cap-score prospectively predicts probability of pregnancy. *Mol Reprod Dev* (2018) 85:654–64. doi: 10.1002/mrd.23057

66. Bedford JM. Enigmas of mammalian gamete form and function. *Biol Rev Camb Philos Soc* (2004) 79:429–60. doi: 10.1017/S146479310300633X

67. Muller CH. Rationale, interpretation, validation, and uses of sperm function tests. *J Androl* (2000) 21:10–30. doi: 10.1002/j.1939-4640.2000.tb03270.x

68. Liu DY, Baker HW. Defective sperm-zona pellucida interaction: a major cause of failure of fertilization in clinical *in-vitro* fertilization. *Hum Reprod* (2000) 15:702–8. doi: 10.1093/humrep/15.3.702

69. Oehninger S, Franken DR, Ombelet W. Sperm functional tests. *Fertil Steril* (2014) 102:1528–33. doi: 10.1016/j.fertnstert.2014.09.044

70. Liu DY, Baker HW. Human sperm bound to the zona pellucida have normal nuclear chromatin as assessed by acridine orange fluorescence. *Hum Reprod* (2007) 22:1597–602. doi: 10.1093/humrep/dem044

71. Liu DY. Could using the zona pellucida bound sperm for intracytoplasmic sperm injection (ICSI) enhance the outcome of ICSI? *Asian J Androl* (2011) 13:197–8. doi: 10.1038/aja.2010.179

72. Ganeva R, Parvanov D, Velikova D, Vasileva M, Nikolova K, Stamenov G. Sperm morphology and DNA fragmentation after zona pellucida selection. *Reprod Fertil* (2021) 2:221–30. doi: 10.1530/RAF-21-0041

73. Wang L, Chen M, Yan G, Zhao S. DNA Methylation differences between zona pellucida-bound and manually selected spermatozoa are associated with autism susceptibility. *Front Endocrinol (Lausanne)* (2021) 12:774260. doi: 10.3389/fendo.2021.774260

74. Aitken RJ, Baker MA, De Iuliis GN, Nixon B. New insights into sperm physiology and pathology. *Handb Exp Pharmacol* (2010) 198:99–115. doi: 10.1007/978-3-642-02062-9_7

75. Walters JLH, De Iuliis GN, Dun MD, Aitken RJ, Mclaughlin EA, Nixon B, et al. Pharmacological inhibition of arachidonate 15-lipoxygenase protects human spermatozoa against oxidative stress. *Biol Reprod* (2018) 98:784–94. doi: 10.1093/biolre/ioy058

76. Walters JLH, De Iuliis GN, Nixon B, Bromfield EG. Oxidative stress in the male germline: A review of novel strategies to reduce 4-hydroxynonenal production. *Antioxid (Basel)* (2018) 7:132. doi: 10.3390/antiox7100132

77. Walters JLH, Anderson AL, Martins da Silva SJ, Aitken RJ, De Iuliis GN, Sutherland JM, et al. Mechanistic insight into the regulation of lipoxygenase-driven lipid peroxidation events in human spermatozoa and their impact on Male fertility. *Antioxid (Basel)* (2020) 10:43. doi: 10.3390/antiox10010043

78. Paes Almeida Ferreira De Braga D, Iaconelli A Jr., Cassia Savio De Figueira R, Madaschi C, Semiao-Francisco L, Borges E Jr.. Outcome of ICSI using zona pellucida-bound spermatozoa and conventionally selected spermatozoa. *Reprod BioMed Online* (2009) 19:802–7. doi: 10.1016/j.rbmo.2009.09.020

79. Jin R, Bao J, Tang D, Liu F, Wang G, Zhao Y, et al. Outcomes of intracytoplasmic sperm injection using the zona pellucida-bound sperm or manually selected sperm. *J Assist Reprod Genet* (2016) 33:597–601. doi: 10.1007/s10815-016-0676-6

80. Clark GF. The molecular basis of mouse sperm-zona pellucida binding: a still unresolved issue in developmental biology. *Reproduction* (2011) 142:377–81. doi: 10.1530/REP-11-0118

81. Pang PC, Chiu PC, Lee CL, Chang LY, Panico M, Morris HR, et al. Human sperm binding is mediated by the sialyl-lewis(x) oligosaccharide on the zona pellucida. *Science* (2011) 333:1761–4. doi: 10.1126/science.1207438

82. Avella MA, Xiong B, Dean J. The molecular basis of gamete recognition in mice and humans. *Mol Hum Reprod* (2013) 19:279–89. doi: 10.1093/molehr/gat004

83. Avella MA, Baibakov B, Dean J. A single domain of the ZP2 zona pellucida protein mediates gamete recognition in mice and humans. *J Cell Biol* (2014) 205:801–9. doi: 10.1083/jcb.201404025

84. Avella MA, Baibakov BA, Jimenez-Movilla M, Sadusky AB, Dean J. ZP2 peptide beads select human sperm *in vitro*, decoy mouse sperm *in vivo*, and provide reversible contraception. *Sci Transl Med* (2016) 8:336ra60.

85. Oehninger S, Clark GF, Fulgham D, Blackmore PF, Mahony MC, Acosta AA, et al. Effect of fucoidin on human sperm-zona pellucida interactions. *J Androl* (1992) 13:519–25.

86. Martin C, Woodland E. Sperm selection technology in ART. *Semin Reprod Med* (2021) 39:200–6. doi: 10.1055/s-0041-1732313

87. Schroter S, Osterhoff C, Mcardle W, Ivell R. The glycocalyx of the sperm surface. *Hum Reprod Update* (1999) 5:302–13. doi: 10.1093/humupd/5.4.302

88. Lan R, Xin M, Hao Z, You S, Xu Y, Wu J, et al. Biological functions and Large-scale profiling of protein glycosylation in human semen. *J Proteome Res* (2020) 19:3877–89. doi: 10.1021/acs.jproteome.9b00795

89. Tecle E, Gagneux P. Sugar-coated sperm: Unraveling the functions of the mammalian sperm glycocalyx. *Mol Reprod Dev* (2015) 82:635–50. doi: 10.1002/mrd.22500

90. Ainsworth C, Nixon B, Aitken RJ. Development of a novel electrophoretic system for the isolation of human spermatozoa. *Hum Reprod* (2005) 20:2261–70. doi: 10.1093/humrep/dei024

91. Ainsworth C, Nixon B, Jansen RP, Aitken RJ. First recorded pregnancy and normal birth after ICSI using electrophoretically isolated spermatozoa. *Hum Reprod* (2007) 22:197–200. doi: 10.1093/humrep/del351

92. Ainsworth CJ, Nixon B, Aitken RJ. The electrophoretic separation of spermatozoa: an analysis of genotype, surface carbohydrate composition and potential for capacitation. *Int J Androl* (2011) 34:e422–34. doi: 10.1111/j.1365-2605.2011.01164.x

93. Shapouri F, Mahendran T, Govindarajan M, Xie P, Kocur O, Palermo GD, et al. A comparison between the Felix electrophoretic system of sperm isolation and conventional density gradient centrifugation: a multicentre analysis. *J Assist Reprod Genet* (2022) 40:83-95. doi: 10.1007/s10815-022-02680-0

94. Said TM, Land JA. Effects of advanced selection methods on sperm quality and ART outcome: a systematic review. *Hum Reprod Update* (2011) 17:719–33. doi: 10.1093/humupd/dmr032

95. Simon L, Ge SQ, Carrell DT. Sperm selection based on electrostatic charge. *Methods Mol Biol* (2013) 927:269–78. doi: 10.1007/978-1-62703-038-0_25

96. Aitken RJ, De Iuliis GN, Gibb Z, Baker MA. The simmet lecture: new horizons on an old landscape–oxidative stress, DNA damage and apoptosis in the male germ line. *Reprod Domest Anim* (2012) 47 Suppl 4:7–14. doi: 10.1111/j.1439-0531.2012.02049.x

97. Pacheco A, Blanco A, Bronet F, Cruz M, Garcia-Fernandez J, Garcia-Velasco JA. Magnetic-activated cell sorting (MACS): A useful sperm-selection technique in cases of high levels of sperm DNA fragmentation. *J Clin Med* (2020) 9:3976. doi: 10.3390/jcm9123976

98. Pedrosa ML, Furtado MH, Ferreira MCF, Carneiro MM. Sperm selection in IVF: the long and winding road from bench to bedside. *JBRA Assist Reprod* (2020) 24:332–9. doi: 10.5935/1518-0557.20190081

99. Gil Julia M, Hervas I, Navarro-Gomez Lechon A, Quintana F, Amoros D, Pacheco A, et al. Sperm selection by magnetic-activated cell sorting before microinjection of autologous oocytes increases cumulative live birth rates with limited clinical impact: A retrospective study in unselected males. *Biol (Basel)* (2021) 10:430. doi: 10.3390/biology10050430

100. El Fekih S, Gueganic N, Tous C, Ali HB, Ajina M, Douet-Guilbert N, et al. MACS-annexin V cell sorting of semen samples with high TUNEL values decreases the concentration of cells with abnormal chromosomal content: a pilot study. *Asian J Androl* (2022) 24:445–50. doi: 10.4103/aja202197

101. Rival CM, Xu W, Shankman LS, Morioka S, Arandjelovic S, Lee CS, et al. Phosphatidylserine on viable sperm and phagocytic machinery in oocytes regulate mammalian fertilization. *Nat Commun* (2019) 10:4456. doi: 10.1038/s41467-019-12406-z

102. Koike-Tani M, Tani T, Mehta SB, Verma A, Oldenbourg R. Polarized light microscopy in reproductive and developmental biology. *Mol Reprod Dev* (2015) 82:548–62. doi: 10.1002/mrd.22221

103. Omidi M, Faramarzi A, Agharahimi A, Khalili MA. Noninvasive imaging systems for gametes and embryo selection in IVF programs: a review. *J Microsc* (2017) 267:253–64. doi: 10.1111/jmi.12573

104. Ribeiro MA, Broi MGD, Rose MB, Garolla A, Foresta C, Bragheto A, et al. Sperm selection by birefringence: a promising non-invasive tool to improve ICSI outcomes. *JBRA Assist Reprod* (2022). doi: 10.5935/1518-0557.20220055

105. Gianaroli L, Magli MC, Collodel G, Moretti E, Ferraretti AP, Baccetti B. Sperm head's birefringence: a new criterion for sperm selection. *Fertil Steril* (2008) 90:104–12. doi: 10.1016/j.fertnstert.2007.05.078

106. Vermey BG, Chapman MG, Cooke S, Kilani S. The relationship between sperm head retardance using polarized light microscopy and clinical outcomes. *Reprod BioMed Online* (2015) 30:67–73. doi: 10.1016/j.rbmo.2014.09.011

107. Singh Jamwal VD. A systematic review identifying fertility biomarkers in semen: a clinical approach through omics to diagnose male infertility. *Fertil Steril* (2023) 119:158. doi: 10.1016/j.fertnstert.2022.10.031

108. Jodar M, Sendler E, Krawetz SA. The protein and transcript profiles of human semen. *Cell Tissue Res* (2016) 363:85–96. doi: 10.1007/s00441-015-2237-1

109. Jodar M, Soler-Ventura A, Oliva R, Molecular Biology of R, Development Research G. Semen proteomics and male infertility. *J Proteomics* (2017) 162:125–34. doi: 10.1016/j.jprot.2016.08.018

110. Agarwal A, Baskaran S, Panner Selvam MK, Barbarosie C, Master K. Unraveling the footsteps of proteomics in male reproductive research: A scientometric approach. *Antioxid Redox Signal* (2020) 32:536–49. doi: 10.1089/ars.2019.7945

111. Agarwal A, Panner Selvam MK, Baskaran S. Proteomic analyses of human sperm cells: Understanding the role of proteins and molecular pathways affecting Male reproductive health. *Int J Mol Sci* (2020) 21:1621. doi: 10.3390/ijms21051621

112. Walters JLH, Gadella BM, Sutherland JM, Nixon B, Bromfield EG. Male Infertility: Shining a light on lipids and lipid-modulating enzymes in the Male germline. *J Clin Med* (2020) 9:327. doi: 10.3390/jcm9020327

113. Zhou W, De Iuliis GN, Dun MD, Nixon B. Characteristics of the epididymal luminal environment responsible for sperm maturation and storage. *Front Endocrinol (Lausanne)* (2018) 9:59. doi: 10.3389/fendo.2018.00059

114. Zhou W, Stanger SJ, Anderson AL, Bernstein IR, De Iuliis GN, Mccluskey A, et al. Mechanisms of tethering and cargo transfer during epididymosome-sperm interactions. *BMC Biol* (2019) 17:35. doi: 10.1186/s12915-019-0653-5

115. Nixon B, De Iuliis GN, Hart HM, Zhou W, Mathe A, Bernstein IR, et al. Proteomic profiling of mouse epididymosomes reveals their contributions to post-testicular sperm maturation. *Mol Cell Proteomics* (2019) 18:S91–S108. doi: 10.1074/mcp.RA118.000946

116. Tamessar CT, Trigg NA, Nixon B, Skerrett-Byrne DA, Sharkey DJ, Robertson SA, et al. Roles of male reproductive tract extracellular vesicles in reproduction. *Am J Reprod Immunol* (2021) 85:e13338. doi: 10.1111/aji.13338

117. Amaral A, Castillo J, Ramalho-Santos J, Oliva R. The combined human sperm proteome: cellular pathways and implications for basic and clinical science. *Hum Reprod Update* (2014) 20:40–62. doi: 10.1093/humupd/dmt046

118. Ayaz A, Agarwal A, Sharma R, Kothandaraman N, Cakar Z, Sikka S. Proteomic analysis of sperm proteins in infertile men with high levels of reactive oxygen species. *Andrologia* (2018) 50:e13015. doi: 10.1111/and.13015

119. Dias TR, Samanta L, Agarwal A, Pushparaj PN, Panner Selvam MK, Sharma R. Proteomic signatures reveal differences in stress response, antioxidant defense and proteasomal activity in fertile men with high seminal ROS levels. *Int J Mol Sci* (2019) 20:203. doi: 10.3390/ijms20010203

120. Panner Selvam MK, Agarwal A, Pushparaj PN, Baskaran S, Bendou H. Sperm proteome analysis and identification of fertility-associated biomarkers in unexplained Male infertility. *Genes (Basel)* (2019) 10:522. doi: 10.3390/genes10070522

121. Martins AD, Panner Selvam MK, Agarwal A, Alves MG, Baskaran S. Alterations in seminal plasma proteomic profile in men with primary and secondary infertility. *Sci Rep* (2020) 10:7539. doi: 10.1038/s41598-020-64434-1

122. Panner Selvam MK, Baskaran S, Agarwal A, Henkel R. Protein profiling in unlocking the basis of varicocele-associated infertility. *Andrologia* (2021) 53:e13645. doi: 10.1111/and.13645

123. Huszar G, Stone K, Dix D, Vigue L. Putative creatine kinase m-isoform in human sperm is identifiedas the 70-kilodalton heat shock protein HspA2. *Biol Reprod* (2000) 63:925–32. doi: 10.1095/biolreprod63.3.925

124. Bromfield E, Aitken RJ, Nixon B. Novel characterization of the HSPA2-stabilizing protein BAG6 in human spermatozoa. *Mol Hum Reprod* (2015) 21:755–69. doi: 10.1093/molehr/gav041

125. Nowicka-Bauer K, Malcher A, Wloczkowska O, Kamieniczna M, Olszewska M, Kurpisz MK. Evaluation of seminal plasma HSPA2 protein as a biomarker of human spermatogenesis status. *Reprod Biol* (2022) 22:100597. doi: 10.1016/j.repbio.2021.100597

126. Baker MA, Weinberg A, Hetherington L, Villaverde AI, Velkov T, Baell J, et al. Defining the mechanisms by which the reactive oxygen species by-product, 4-hydroxynonenal, affects human sperm cell function. *Biol Reprod* (2015) 92:108. doi: 10.1095/biolreprod.114.126680

127. Nixon B, Bernstein IR, Cafe SL, Delehedde M, Sergeant N, Anderson AL, et al. A kinase anchor protein 4 is vulnerable to oxidative adduction in Male germ cells. *Front Cell Dev Biol* (2019) 7:319. doi: 10.3389/fcell.2019.00319

128. Netherton JK, Hetherington L, Ogle RA, Gavgani MM, Velkov T, Villaverde AIB, et al. Mass spectrometry reveals new insights into the production of superoxide anions and 4-hydroxynonenal adducted proteins in human sperm. *Proteomics* (2020) 20:e1900205. doi: 10.1002/pmic.201900205

129. Miki K, Willis WD, Brown PR, Goulding EH, Fulcher KD, Eddy EM. Targeted disruption of the Akap4 gene causes defects in sperm flagellum and motility. *Dev Biol* (2002) 248:331–42. doi: 10.1006/dbio.2002.0728

130. Fang X, Huang LL, Xu J, Ma CQ, Chen ZH, Zhang Z, et al. Proteomics and single-cell RNA analysis of Akap4-knockout mice model confirm indispensable role of Akap4 in spermatogenesis. *Dev Biol* (2019) 454:118–27. doi: 10.1016/j.ydbio.2019.06.017

131. Luconi M, Cantini G, Baldi E, Forti G. Role of a-kinase anchoring proteins (AKAPs) in reproduction. *Front Biosci (Landmark Ed)* (2011) 16:1315–30. doi: 10.2741/3791

132. Jumeau F, Sigala J, Dossou-Gbete F, Frimat K, Barbotin AL, Buee L, et al. A-kinase anchor protein 4 precursor (pro-AKAP4) in human spermatozoa. *Andrology* (2018) 6:854–9. doi: 10.1111/andr.12524

133. Carracedo S, Briand-Amirat L, Dordas-Perpinya M, Ramos Escuredo Y, Delcombel R, Sergeant N, et al. ProAKAP4 protein marker: Towards a functional approach to male fertility. *Anim Reprod Sci* (2022) 247:107074. doi: 10.1016/j.anireprosci.2022.107074

134. Jenkins TG, Aston KI, James ER, Carrell DT. Sperm epigenetics in the study of male fertility, offspring health, and potential clinical applications. *Syst Biol Reprod Med* (2017) 63:69–76. doi: 10.1080/19396368.2016.1274791

135. Simon L, Emery BR, Carrell DT. Review: Diagnosis and impact of sperm DNA alterations in assisted reproduction. *Best Pract Res Clin Obstet Gynaecol* (2017) 44:38–56. doi: 10.1016/j.bpobgyn.2017.07.003

136. Johnson GD, Lalancette C, Linnemann AK, Leduc F, Boissonneault G, Krawetz SA. The sperm nucleus: chromatin, RNA, and the nuclear matrix. *Reproduction* (2011) 141:21–36. doi: 10.1530/REP-10-0322

137. Braun RE. Packaging paternal chromosomes with protamine. *Nat Genet* (2001) 28:10–2. doi: 10.1038/ng0501-10

138. Hammoud SS, Nix DA, Zhang H, Purwar J, Carrell DT, Cairns BR. Distinctive chromatin in human sperm packages genes for embryo development. *Nature* (2009) 460:473–8. doi: 10.1038/nature08162

139. Aitken RJ, De Iuliis GN. Origins and consequences of DNA damage in male germ cells. *Reprod BioMed Online* (2007) 14:727–33. doi: 10.1016/S1472-6483(10)60676-1

140. De Iuliis GN, Thomson LK, Mitchell LA, Finnie JM, Koppers AJ, Hedges A, et al. DNA Damage in human spermatozoa is highly correlated with the efficiency of chromatin remodeling and the formation of 8-hydroxy-2'-deoxyguanosine, a marker of oxidative stress. *Biol Reprod* (2009) 81:517–24. doi: 10.1095/biolreprod.109.076836

141. Aitken RJ, De Iuliis GN. On the possible origins of DNA damage in human spermatozoa. *Mol Hum Reprod* (2010) 16:3–13. doi: 10.1093/molehr/gap059

142. Xavier MJ, Nixon B, Roman SD, Scott RJ, Drevet JR, Aitken RJ. Paternal impacts on development: identification of genomic regions vulnerable to oxidative DNA damage in human spermatozoa. *Hum Reprod* (2019) 34:1876–90. doi: 10.1093/humrep/dez153

143. Noblanc A, Damon-Soubeyrand C, Karrich B, Henry-Berger J, Cadet R, Saez F, et al. DNA Oxidative damage in mammalian spermatozoa: where and why is the male nucleus affected? *Free Radic Biol Med* (2013) 65:719–23. doi: 10.1016/j.freeradbiomed.2013.07.044

144. Balhorn R, Brewer L, Corzett M. DNA Condensation by protamine and arginine-rich peptides: analysis of toroid stability using single DNA molecules. *Mol Reprod Dev* (2000) 56:230–4. doi: 10.1002/(SICI)1098-2795(200006)56:2+<230::AID-MRD3>3.0.CO;2-V

145. Conwell CC, Vilfan ID, Hud NV. Controlling the size of nanoscale toroidal DNA condensates with static curvature and ionic strength. *Proc Natl Acad Sci U.S.A.* (2003) 100:9296–301. doi: 10.1073/pnas.1533135100

146. Zalenskaya IA, Bradbury EM, Zalensky AO. Chromatin structure of telomere domain in human sperm. *Biochem Biophys Res Commun* (2000) 279:213–8. doi: 10.1006/bbrc.2000.3917

147. Van Der Heijden GW, Ramos L, Baart EB, Van Den Berg IM, Derijck AA, van der Vlag J, et al. Sperm-derived histones contribute to zygotic chromatin in humans. *BMC Dev Biol* (2008) 8:34. doi: 10.1186/1471-213X-8-34

148. Ward WS. Function of sperm chromatin structural elements in fertilization and development. *Mol Hum Reprod* (2010) 16:30–6. doi: 10.1093/molehr/gap080

149. Boe-Hansen GB, Fedder J, Ersboll AK, Christensen P. The sperm chromatin structure assay as a diagnostic tool in the human fertility clinic. *Hum Reprod* (2006) 21:1576–82. doi: 10.1093/humrep/del019

150. Cebesoy FB, Aydos K, Unlu C. Effect of sperm chromatin damage on fertilization ratio and embryo quality post-ICSI. *Arch Androl* (2006) 52:397–402. doi: 10.1080/01485010600666953

151. Bungum M, Humaidan P, Axmon A, Spano M, Bungum L, Erenpreiss J, et al. Sperm DNA integrity assessment in prediction of assisted reproduction technology outcome. *Hum Reprod* (2007) 22:174–9. doi: 10.1093/humrep/del326

152. Davies MJ, Moore VM, Willson KJ, Van Essen P, Priest K, Scott H, et al. Reproductive technologies and the risk of birth defects. *N Engl J Med* (2012) 366:1803–13. doi: 10.1056/NEJMoa1008095

153. Seggers J, De Walle HE, Bergman JE, Groen H, Hadders-Algra M, Bos ME, et al. Congenital anomalies in offspring of subfertile couples: a registry-based study in the northern Netherlands. *Fertil Steril* (2015) 103:1001–1010 e3. doi: 10.1016/j.fertnstert.2014.12.113

154. Wijers CH, Van Rooij IA, Rassouli R, Wijnen MH, Broens PM, Sloots CE, et al. Parental subfertility, fertility treatment, and the risk of congenital anorectal malformations. *Epidemiology* (2015) 26:169–76. doi: 10.1097/EDE.0000000000000226

155. Brykczynska U, Hisano M, Erkek S, Ramos L, Oakeley EJ, Roloff TC, et al. Repressive and active histone methylation mark distinct promoters in human and mouse spermatozoa. *Nat Struct Mol Biol* (2010) 17:679–87. doi: 10.1038/nsmb.1821

156. Lim JP, Brunet A. Bridging the transgenerational gap with epigenetic memory. *Trends Genet* (2013) 29:176–86. doi: 10.1016/j.tig.2012.12.008

157. Evenson DP, Darzynkiewicz Z, Melamed MR. Relation of mammalian sperm chromatin heterogeneity to fertility. *Science* (1980) 210:1131–3. doi: 10.1126/science.7444440

158. Singh NP, Mccoy MT, Tice RR, Schneider EL. A simple technique for quantitation of low levels of DNA damage in individual cells. *Exp Cell Res* (1988) 175:184–91. doi: 10.1016/0014-4827(88)90265-0

159. Gorczyca W, Gong J, Darzynkiewicz Z. Detection of DNA strand breaks in individual apoptotic cells by the *in situ* terminal deoxynucleotidyl transferase and nick translation assays. *Cancer Res* (1993) 53:1945–51.

160. Manicardi GC, Bianchi PG, Pantano S, Azzoni P, Bizzaro D, Bianchi U, et al. Presence of endogenous nicks in DNA of ejaculated human spermatozoa and its relationship to chromomycin A3 accessibility. *Biol Reprod* (1995) 52:864–7. doi: 10.1095/biolreprod52.4.864

161. Sakkas D, Urner F, Bianchi PG, Bizzaro D, Wagner I, Jaquenoud N, et al. Sperm chromatin anomalies can influence decondensation after intracytoplasmic sperm injection. *Hum Reprod* (1996) 11:837–43. doi: 10.1093/oxfordjournals.humrep.a019263

162. Fernandez JL, Muriel L, Rivero MT, Goyanes V, Vazquez R, Alvarez JG. The sperm chromatin dispersion test: a simple method for the determination of sperm DNA fragmentation. *J Androl* (2003) 24:59–66. doi: 10.1002/j.1939-4640.2003.tb02641.x

163. Fernandez JL, Muriel L, Goyanes V, Segrelles E, Gosalvez J, Enciso M, et al. Simple determination of human sperm DNA fragmentation with an improved sperm chromatin dispersion test. *Fertil Steril* (2005) 84:833–42. doi: 10.1016/j.fertnstert.2004.11.089

164. Aoki VW, Emery BR, Liu L, Carrell DT. Protamine levels vary between individual sperm cells of infertile human males and correlate with viability and DNA integrity. *J Androl* (2006) 27:890–8. doi: 10.2164/jandrol.106.000703

165. Simon L, Zini A, Dyachenko A, Ciampi A, Carrell DT. A systematic review and meta-analysis to determine the effect of sperm DNA damage on *in vitro* fertilization and intracytoplasmic sperm injection outcome. *Asian J Androl* (2017) 19:80–90. doi: 10.4103/1008-682X.182822

166. Ribas-Maynou J, Yeste M, Becerra-Tomas N, Aston KI, James ER, Salas-Huetos A. Clinical implications of sperm DNA damage in IVF and ICSI: updated systematic review and meta-analysis. *Biol Rev Camb Philos Soc* (2021) 96:1284–300. doi: 10.1111/brv.12700

167. Collins JA, Barnhart KT, Schlegel PN. Do sperm DNA integrity tests predict pregnancy with *in vitro* fertilization? *Fertil Steril* (2008) 89:823–31. doi: 10.1016/j.fertnstert.2007.04.055

168. Zini A, Sigman M. Are tests of sperm DNA damage clinically useful? pros and cons. *J Androl* (2009) 30:219–29. doi: 10.2164/jandrol.108.006908

169. Jodar M, Selvaraju S, Sendler E, Diamond MP, Krawetz SA, Reproductive Medicine N. The presence, role and clinical use of spermatozoal RNAs. *Hum Reprod Update* (2013) 19:604–24. doi: 10.1093/humupd/dmt031

170. Burl RB, Clough S, Sendler E, Estill M, Krawetz SA. Sperm RNA elements as markers of health. *Syst Biol Reprod Med* (2018) 64:25–38. doi: 10.1080/19396368.2017.1393583

171. Sharma U. Paternal contributions to offspring health: Role of sperm small RNAs in intergenerational transmission of epigenetic information. *Front Cell Dev Biol* (2019) 7:215. doi: 10.3389/fcell.2019.00215

172. Trigg NA, Eamens AL, Nixon B. The contribution of epididymosomes to the sperm small RNA profile. *Reproduction* (2019) 157:R209–23. doi: 10.1530/REP-18-0480

173. Kiani M, Salehi M, Mogheiseh A. MicroRNA expression in infertile men: its alterations and effects. *Zygote* (2019) 27:263–71. doi: 10.1017/S0967199419000340

174. Alves MBR, Celeghini ECC, Belleannee C. From sperm motility to sperm-borne microRNA signatures: New approaches to predict Male fertility potential. *Front Cell Dev Biol* (2020) 8:791. doi: 10.3389/fcell.2020.00791

175. Salas-Huetos A, James ER, Aston KI, Carrell DT, Jenkins TG, Yeste M. The role of miRNAs in male human reproduction: a systematic review. *Andrology* (2020) 8:7–26. doi: 10.1111/andr.12714

176. Barbu MG, Thompson DC, Suciu N, Voinea SC, Cretoiu D, Predescu DV. The roles of MicroRNAs in Male infertility. *Int J Mol Sci* (2021) 22:2910. doi: 10.3390/ijms22062910

177. Bianchi E, Stermer A, Boekelheide K, Sigman M, Hall SJ, Reyes G, et al. High-quality human and rat spermatozoal RNA isolation for functional genomic studies. *Andrology* (2018) 6:374–83. doi: 10.1111/andr.12471

178. Cardona C, Neri QV, Simpson AJ, Moody MA, Ostermeier GC, Seaman EK, et al. Localization patterns of the ganglioside G(M1) in human sperm are indicative of male fertility and independent of traditional semen measures. *Mol Reprod Dev* (2017) 84:423–35. doi: 10.1002/mrd.22803

179. Moody MA, Cardona C, Simpson AJ, Smith TT, Travis AJ, Ostermeier GC. Validation of a laboratory-developed test of human sperm capacitation. *Mol Reprod Dev* (2017) 84:408–22. doi: 10.1002/mrd.22801

180. Nixon B, Aitken RJ. The biological significance of detergent-resistant membranes in spermatozoa. *J Reprod Immunol* (2009) 83:8–13. doi: 10.1016/j.jri.2009.06.258

181. Nixon B, Mitchell LA, Anderson AL, Mclaughlin EA, O'Bryan M K, Aitken RJ. Proteomic and functional analysis of human sperm detergent resistant membranes. *J Cell Physiol* (2011) 226:2651–65. doi: 10.1002/jcp.22615

182. Ostermeier GC, Cardona C, Moody MA, Simpson AJ, Mendoza R, Seaman E, et al. Timing of sperm capacitation varies reproducibly among men. *Mol Reprod Dev* (2018) 85:387–96. doi: 10.1002/mrd.22972

183. Shan S, Xu F, Hirschfeld M, Brenig B. Sperm lipid markers of Male fertility in mammals. *Int J Mol Sci* (2021) 22:8767. doi: 10.3390/ijms22168767

184. Drabovich AP, Jarvi K, Diamandis EP. Verification of male infertility biomarkers in seminal plasma by multiplex selected reaction monitoring assay. *Mol Cell Proteomics* (2011) 10:M110 004127. doi: 10.1074/mcp.M110.004127

185. Korbakis D, Schiza C, Brinc D, Soosaipillai A, Karakosta TD, Legare C, et al. Preclinical evaluation of a TEX101 protein ELISA test for the differential diagnosis of male infertility. *BMC Med* (2017) 15:60. doi: 10.1186/s12916-017-0817-5

186. Lazzarino G, Listorti I, Muzii L, Amorini AM, Longo S, Di Stasio E, et al. Low-molecular weight compounds in human seminal plasma as potential biomarkers of male infertility. *Hum Reprod* (2018) 33:1817–28. doi: 10.1093/humrep/dey279

187. Gamidov SI, Shatylko TV, Tambiev AK, Tokareva AO, Chagovets VV, Bitsoev TB, et al. [Prognostic ability of seminal plasma lipidomic analysis in predicting the success of microTESE in men with azoospermia]. *Urologiia* (2022) 4:32–7. doi: 10.18565/urology.2022.4.32-37

188. Li HG, Huang SY, Zhou H, Liao AH, Xiong CL. Quick recovery and characterization of cell-free DNA in seminal plasma of normozoospermia and azoospermia: implications for non-invasive genetic utilities. *Asian J Androl* (2009) 11:703–9. doi: 10.1038/aja.2009.65

189. Hong Y, Wang C, Fu Z, Liang H, Zhang S, Lu M, et al. Systematic characterization of seminal plasma piRNAs as molecular biomarkers for male infertility. *Sci Rep* (2016) 6:24229. doi: 10.1038/srep24229

190. Zhi EL, Liang GQ, Li P, Chen HX, Tian RH, Xu P, et al. Seminal plasma miR-192a: a biomarker predicting successful resolution of nonobstructive azoospermia following varicocele repair. *Asian J Androl* (2018) 20:396–9. doi: 10.4103/aja.aja_8_18

191. Xu Y, Zhang Y, Yang Y, Liu X, Chen Y. Seminal plasma miR-210-3p is a biomarker for screening dyszoospermia caused by varicocele. *Andrologia* (2019) 51: e13244. doi: 10.1111/and.13244

192. Wang F, Yang W, Ouyang S, Yuan S. The vehicle determines the destination: The significance of seminal plasma factors for male fertility. *Int J Mol Sci* (2020) 21:8499. doi: 10.3390/ijms21228499

193. Bromfield JJ. Seminal fluid and reproduction: much more than previously thought. *J Assist Reprod Genet* (2014) 31:627–36. doi: 10.1007/s10815-014-0243-y

194. Robertson SA, Sharkey DJ. Seminal fluid and fertility in women. *Fertil Steril* (2016) 106:511–9. doi: 10.1016/j.fertnstert.2016.07.1101

195. Kho EM, Mccowan LM, North RA, Roberts CT, Chan E, Black MA, et al. Duration of sexual relationship and its effect on preeclampsia and small for gestational age perinatal outcome. *J Reprod Immunol* (2009) 82:66–73. doi: 10.1016/j.jri.2009.04.011

196. Crawford G, Ray A, Gudi A, Shah A, Homburg R. The role of seminal plasma for improved outcomes during *in vitro* fertilization treatment: review of the literature and meta-analysis. *Hum Reprod Update* (2015) 21:275–84. doi: 10.1093/humupd/dmu052

197. Saccone G, Di Spiezio Sardo A, Ciardulli A, Caissutti C, Spinelli M, Surbek D, et al. Effectiveness of seminal plasma in *in vitro* fertilisation treatment: a systematic review and meta-analysis. *BJOG* (2019) 126:220–5. doi: 10.1111/1471-0528.15004

198. Chan OC, Chow PH, O WS. Total ablation of paternal accessory sex glands curtails developmental potential in preimplantation embryos in the golden hamster. *Anat Embryol (Berl)* (2001) 204:117–22. doi: 10.1007/s004290100186

199. Wong CL, Lee KH, Lo KM, Chan OC, Goggins W, O WS, et al. Ablation of paternal accessory sex glands imparts physical and behavioural abnormalities to the progeny: an *in vivo* study in the golden hamster. *Theriogenology* (2007) 68:654–62. doi: 10.1016/j.theriogenology.2007.04.062

200. Wong CL, Chan OC, Lee KH, O WS, Chow PH. Absence of paternal accessory sex glands dysregulates preimplantation embryo cell cycle and causes early oviductal-uterine transit in the golden hamster *in vivo*. *Fertil Steril* (2008) 89:1021–4. doi: 10.1016/j.fertnstert.2007.04.038

201. Bromfield JJ, Schjenken JE, Chin PY, Care AS, Jasper MJ, Robertson SA. Maternal tract factors contribute to paternal seminal fluid impact on metabolic phenotype in offspring. *Proc Natl Acad Sci U.S.A.* (2014) 111:2200–5. doi: 10.1073/pnas.1305609111

202. Skerrett-Byrne DA, Nixon B, Bromfield EG, Breen J, Trigg NA, Stanger SJ, et al. Transcriptomic analysis of the seminal vesicle response to the reproductive toxicant acrylamide. *BMC Genomics* (2021) 22:728. doi: 10.1186/s12864-021-07951-1

203. Skerrett-Byrne DA, Trigg NA, Bromfield EG, Dun MD, Bernstein IR, Anderson AL, et al. Proteomic dissection of the impact of environmental exposures on mouse seminal vesicle function. *Mol Cell Proteomics* (2021) 20:100107. doi: 10.1016/j.mcpro.2021.100107

204. Smyth SP, Nixon B, Anderson AL, Murray HC, Martin JH, Macdougall LA, et al. Elucidation of the protein composition of mouse seminal vesicle fluid. *Proteomics* (2022) 22:e2100227. doi: 10.1002/pmic.202100227

205. Zavattaro M, Ceruti C, Motta G, Allasia S, Marinelli L, Di Bisceglie C, et al. Treating varicocele in 2018: current knowledge and treatment options. *J Endocrinol Invest* (2018) 41:1365–75. doi: 10.1007/s40618-018-0952-7

206. Khourdaji I, Lee H, Smith RP. Frontiers in hormone therapy for male infertility. *Transl Androl Urol* (2018) 7:S353–66. doi: 10.21037/tau.2018.04.03

207. Jung A, Schuppe HC. Influence of genital heat stress on semen quality in humans. *Andrologia* (2007) 39:203–15. doi: 10.1111/j.1439-0272.2007.00794.x

208. Moazzam A, Sharma R, Agarwal A. Relationship of spermatozoal DNA fragmentation with semen quality in varicocele-positive men. *Andrologia* (2015) 47:935–44. doi: 10.1111/and.12360

209. Gharagozloo P, Gutierrez-Adan A, Champroux A, Noblanc A, Kocer A, Calle A, et al. A novel antioxidant formulation designed to treat male infertility associated with oxidative stress: promising preclinical evidence from animal models. *Hum Reprod* (2016) 31:252–62. doi: 10.1093/humrep/dev302

210. Majzoub A, Agarwal A. Systematic review of antioxidant types and doses in male infertility: Benefits on semen parameters, advanced sperm function, assisted reproduction and live-birth rate. *Arab J Urol* (2018) 16:113–24. doi: 10.1016/j.aju.2017.11.013

211. Aitken RJ. Not every sperm is sacred; a perspective on male infertility. *Mol Hum Reprod* (2018) 24:287–98. doi: 10.1093/molehr/gay010

frontiers | Frontiers in Endocrinology

TYPE Original Research
PUBLISHED 14 March 2023
DOI 10.3389/fendo.2023.1109623

OPEN ACCESS

EDITED BY
Tao Luo,
Nanchang University, China

REVIEWED BY
Ying Chen,
Nanchang University, China
Jichun Tan,
Shengjing Hospital of China Medical University, China

*CORRESPONDENCE
Yuanfeng Zhang
304100@cqmu.edu.cn
Guoning Huang
gnhuang217@sina.com

†These authors have contributed equally to this work and share first authorship

SPECIALTY SECTION
This article was submitted to Reproduction, a section of the journal Frontiers in Endocrinology

RECEIVED 07 December 2022
ACCEPTED 28 February 2023
PUBLISHED 14 March 2023

CITATION
Shen X, Xiao T, Han W, Ye H, Zhang Y and Huang G (2023) The bibliometric analysis of studies on intracytoplasmic sperm injection from 2002 to 2021. *Front. Endocrinol.* 14:1109623. doi: 10.3389/fendo.2023.1109623

The bibliometric analysis of studies on intracytoplasmic sperm injection from 2002 to 2021

Xiaoli Shen[1†], Tianbing Xiao[2†], Wei Han[1], Hong Ye[1], Yuanfeng Zhang[3*] and Guoning Huang[1*]

[1]Center for Reproductive Medicine, Chongqing Key Laboratory of Human Embryo Engineering, Chongqing Health Center for Women and Children, Women and Children's Hospital of Chongqing Medical University Chongqing, Chongqing, China, [2]Department of Urology, People's Hospital of Fengjie, Chongqing, China, [3]Department of Urology, The Second Affiliated Hospital of Chongqing Medical University, Chongqing, China

Background: Infertility is estimated to occur in 1 out of every 4–7 couples. Intracytoplasmic sperm injection (ICSI), a type of assisted reproduction introduced in 1992, has been used across the world for almost all indications of infertility, yielding high pregnancy rates. There is a growing concern worldwide about ICSI since semen quality has declined in recent years, accompanied with the potential risks of this technology. This study aims to analyze the current status and hotspots of ICSI *via* a bibliometric analysis.

Methods: We retrieved publications on ICSI from the Web of Science Core Collection database from 2002 to 2021. CiteSpace was used to summarize knowledge mapping of subject categories, keywords, and co-citation relationships with the strongest citation bursts. VOSviewer was used to explore co-citation and co-occurrence relationships for countries, organizations, references, authors, and keywords.

Results: A total of 8271 publications were analyzed between 2002 and 2021. The major findings are as follows: the USA, China, Italy, Japan, and Belgium are the top five prolific countries. The Free University of Brussels, University of Copenhagen, University of Valencia, Ghent University, and the University of California San Francisco are the top five contributing organizations. *Fertility and Sterility* and *Human Reproduction* are the most productive and cited journals. The hotspot topics are risks of ICSI, oocyte preservation, live birth rate, infertile men, and embryo quality in the past two decades.

Conclusion: This study presents a research overview of ICSI from different perspectives. These findings will contribute to a better understanding of the current status of ICSI research and provide hotspots and trends for future studies.

KEYWORDS

intracytoplasmic sperm injection (ICSI), bibliometric analysis, infertility, research hotspots, data visualization, assisted reproductive technology

Introduction

Infertility is defined as failure to achieve a clinical pregnancy after one year of unprotected sexual intercourse. It is estimated that 8% to 12% of reproductive-aged couples are affected by infertility worldwide (1, 2), with male problems accounting for approximately 50% of sterility cases (3, 4). Assisted reproductive technology (ART) includes all fertility treatments in which either eggs or embryos are manipulated to accomplish successful pregnancy. In general, ART comprises *in vitro* fertilization (IVF) and intracytoplasmic sperm injection (ICSI). ICSI involves a single sperm being microinjected into an oocyte. It has become increasingly employed as a form of infertility therapy. Compared to traditional IVF, ICSI appears to be more successful in helping infertile men to be parents. ICSI is usually performed when the sperm is unable to fertilize the egg. Only about 5% of infertile men could be treated without ICSI (5). Therefore, ICSI restores the fertilization rate to normal in couples with unexpectedly low fertilization rates due to a decline in semen quality. However, issues regarding the health of offspring obtained *via* ICSI have been discussed for years. There are minor potential risks of congenital and epigenetic disorders in infants who were conceived through ICSI (6, 7). Given the importance of the sperm epigenome to early embryogenesis, ICSI technology might increase the frequency of imprinting disorders and change epigenetic reprogramming, eventually adversely affect embryo evolution and long-life health of offspring by using immature spermatozoa that may not have been adequately imprinted or methylated (8, 9). Some evidences demonstrated the severity of male factor infertility does not seem to impact on cognitive development in early childhood among children conceived with ICSI, while many studies are limited by small sample size and the potential for ICSI by itself to influence cognitive outcomes requires elucidation (10, 11). During the last two decades, substantial progress has been made in ART research. Although the number of ICSI procedures has been increasing year by year, the associated birth defects are still not only one of the frontier problems but also the focus of research (12).

Bibliometric analysis was used to summarize qualitative and quantitative contributions in a specific research field; for instance, the numbers of citations and publications of authors, journals, countries, institutions, keywords, and influential articles (13). Furthermore, a bibliometric analysis could also reflect research hotspots and study trends through keyword and item analyses (14). To date, there is still no bibliometric study that illustrates hotspots and summarizes the research status in the ICSI field during the past 20 years.

This study aimed to quantitatively explore the publishing trend, authors, institutions, cited articles, countries, journals, and keywords with the strongest citation burst detection in the field of ICSI research. The resultant analysis should characterize the insight into the most influential articles in the field of ICSI. This study also attempted to identify potential future hotspots and trends in this area *via* the overlay map of co-occurring keywords and clustering visualization analyses.

Materials and methods

Data sources and search strategy

The Web of Science Core Collection (WoSCC) database was used as the data source. The citation indexes include 'Science Citation Index Expanded,' 'Current Chemical Reactions,' and 'Index Chemicus'. Study data were retrieved by using the following index terms during the 2002–2021 period: TS = ("Intracytoplasmic Sperm Injection" or "ICSI"). The data source was extracted on September 28, 2022. The publication type included articles and reviews but excluded meeting abstracts, letters, reports, news, etc. The language was limited to English. The search results were exported with "full records and full contents" stored in "txt" format as the input source for CiteSpace and VOSviewer. The database was searched and screened independently by W. Han and Y. Zhang. Differences in viewpoints between these two were resolved *via* discussions with the whole author team until a consensus was reached. In the end, a total of 8271 publications were extracted for analysis.

Data extraction and analytical methods

Several bibliometric analysis software packages with different capabilities and limitations have been used; for example, Perish, CiteSpace, HistCite, BibExcel, and VOSviewer. For the objectivity of ICSI research results, we used CiteSpace 6.1.R3, VOSviewer 1.6.18, and an online platform of literature metrology analysis (https://bibliometric.com/) to perform bibliometric analyses (15, 16).

CiteSpace was used to analyze the keywords and trends in this research area. We used VOSviewer to visualize the number of publications, identify those with the most citations, and classify publications by author, organization, country, and journal. Next, we summarized the number of citations, article title, first author's name, year, journal of publication, and country of the corresponding author using Microsoft Excel 2010 and online platforms for literature metrology analysis. The 2021 impact factor (IF) of each journal was extracted from the latest Journal Citation Reports (JCR, 2021) using Clarivate Analytics. The keyword bursts were used to identify the hotspots and trends in the field of ICSI research. In the visualization of CiteSpace and VOSviewer, the node size represents the number of publications while the line thickness indicates the strength of the relationship. The parameters of CiteSpace were set as follows: time slicing (2002–2021), years per slice '3', term source (all selection), and visualization (cluster view/time zone view). The main steps for setting up a bibliometric analysis were operated as follows (1): importing the publications and formatting the data (2), restricting the term sources (3), setting the selection criteria or the minimum number of co-occurrence and co-citations.

Results

General study data

Based on the screening criteria, a total of 15,618 publications were identified using the index terms "intracytoplasmic sperm injection" or "ICSI" from January 1, 2002, to December 31, 2021. After excluding non-English manuscripts (n=250) and the irrelevant publications (n=4622), there were 10746 publications. Duplicate publications were excluded by CiteSpace. Finally, 8271 publications (7081 articles and 1190 reviews) were selected for analysis per the above screening conditions (Figure 1). A total of 5932 of these publications were cited more than 10 times.

The number of ICSI research publications increased from 309 in 2002 to 648 in 2021 as indexed by the WoSCC (Figure 2A). The rate of production of publications grew fast between 2018 and 2021. The top fifteen most cited publications ranged from 458 to 1337 citations as shown in Table 1. The most cited article was a recommendation published in 2006 in *Journal of Clinical Oncology* by Stephanie J. Lee et al. from the American Society of Clinical Oncology, with 1337 citations (17).

Distribution and contribution of countries

The United States accounted for 22.65% of all publications (n=309) in 2002. In the early stages, the United States, Belgium, Japan, Italy, and the UK contributed the majority of studies on ICSI, both in terms of number and citation rate. After 2018, these parameters increased rapidly in China, the UK, Italy, and Spain, with China accounting for 32.10% of all publications on ICSI from 2018 to 2021. All these results are presented in Figure 2A and Figure 2B. Next, we compared the two countries with the highest numbers of publications; i.e., the United States and China. The number of studies conducted in the United States has remained fairly constant in the past 20 years. However, China grew exponentially from only five publications in 2002 to 208 publications in 2021 as shown in Figure 3A. Consequently, we analyzed the collaboration between different countries using VOSviewer, CiteSpace, and online resources. The results show that the USA, China, Japan, and Belgium collaborate closely in the field of ICSI research (Figures 3B–D).

Contribution of institutions

There are many institutions that contribute constantly to the ICSI field. Institutional contributions may vary, as the CiteSpace and VOSviewer algorithms include the addresses of all authors that appear in the same articles. Some articles appeared in two related units at the same time, such as the University of Copenhagen and Copenhagen University Hospital, or different languages of the same correspondence address, for example, the Free University of Brussels apnd *Vrije Universiteit Brussel*. These discrepancies could make the contributions of the same unit discrete. To solve this problem, we united similar addresses to a consolidated institution. The Free University of Brussels had a total of 23547 citations in the past 20 years, the average number of citations of each paper (ACP) was 97.71. The University of California San Francisco was the most cited organization in the North American area, as it was cited 3071 times and its ACP was 63.98 in the field of ICSI research. The Free University of Brussels, University of Copenhagen, University of Valencia, and Ghent University had the most citations in ICSI research in Europe (Table 2). The Shanghai Jiao Tong University had the most citations among Asian countries, with a total of 2366 citations; however, the ACP was 20.05. The Free University of Brussels was the most productive institution, with 241 manuscripts published in the past two decades, followed by the University of

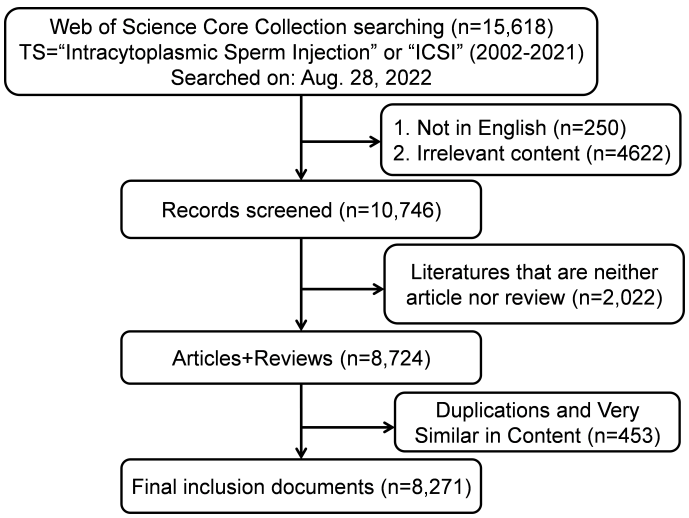

FIGURE 1
Flow chart of data screening and bibliometric analysis on ICSI research.

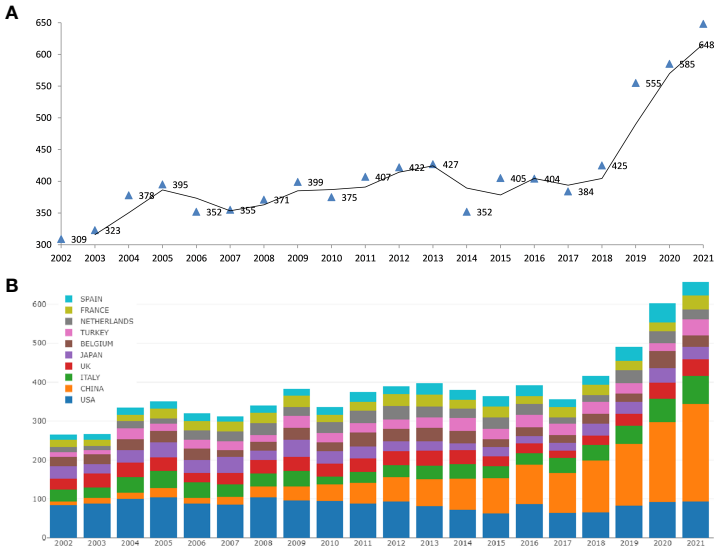

FIGURE 2
The number of ICSI research publications indexed by the WoSCC from 2002 to 2021. Distribution trends of publications by year **(A)** and country **(B)**.

TABLE 1 Top 15 high-cited references in the field of ICSI research from 2002-2021.

First Author	TC	Journal	Title	Institution	Year
Lee, Stephanie J	1337	Journal of Clinical Oncology	American Society of Clinical Oncology recommendations on fertility preservation in cancer patients	Cornell University	2006
Kuwayama, M	878	Reproductive Biomedicine Online	Highly efficient vitrification method for cryopreservation of human oocytes	Aarhus University	2005
Jackson, RA	818	Obstetrics & Gynecology	Perinatal outcomes in singletons following *in vitro* fertilization: A meta-analysis	University of California San Francisco	2004
Broekmans, F. J.	781	Human Reproduction Update	A systematic review of tests predicting ovarian reserve and IVF outcome	Vrije University Amsterdam	2006
Hansen, M	762	New England Journal of Medicine	The risk of major birth defects after intracytoplasmic sperm injection and *in vitro* fertilization.	University of Leicester	2002
DeBaun, MR	674	American Journal of Human Genetics	Association of *in vitro* fertilization with Beckwith-Wiedemann syndrome and epigenetic alterations of LIT1 and H19	Johns Hopkins University	2003
Inhorn, Marcia C	623	Human Reproduction Update	Infertility around the globe: new thinking on gender, reproductive technologies and global movements in the 21st century	Yale University	2015
Lanfranco, F	575	Lancet	Klinefelter's syndrome	University of Munster	2004
AmerSocReprod Med	553	Fertility and Sterility	Mature oocyte cryopreservation: a guideline	AmerSocReprod Med	2013
Wallace, WHB	537	Lancet Oncology	Fertility preservation for young patients with cancer: who is at risk and what can be offered?	University of Edinburgh	2005
Meseguer, Marcos	529	Human Reproduction	The use of morphokinetics as a predictor of embryo implantation	University of Valencia	2011
Cox, GF	518	American Journal of Human Genetics	Intracytoplasmic sperm injection may increase the risk of imprinting defects	Harvard University	2002
Davies, MJ	514	New England Journal of Medicine	Reproductive Technologies and the Risk of Birth Defects	University of Adelaide	2012
Bungum, M	458	Human Reproduction	Sperm DNA integrity assessment in prediction of assisted reproduction technology outcome	Lund University	2007
Hansen, M	458	Human Reproduction	Assisted reproductive technologies and the risk of birth defects - a systematic review	University of Western Australia	2005

TC, total citations.

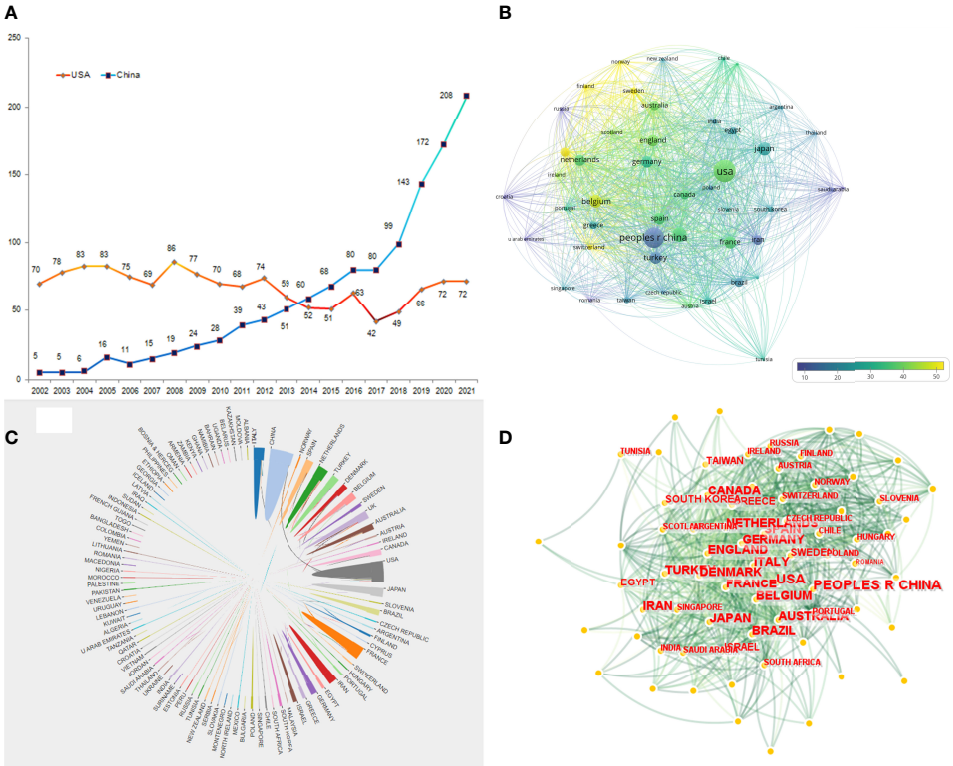

FIGURE 3
Distribution of country-specific studies in the dataset; Trends of publications between China and USA were compared during past two decades **(A)**. The co-occurrence of citations among different countries was visualized from VOSviewer **(B)** and CiteSpace **(D)**. The cooperation network of different regions was drawn by online bibliometric analysis **(C)**. Node size indicates the number of publications.

Copenhagen (n=146), Ghent University (n=125), Tel Aviv University (124), and Shanghai Jiao Tong University (n=118); these are the top five institutions (Table 3). The network knowledge map among institutions was generated using VOSviewer as shown in Figure 4A.

Top contributing authors

Knowledge mapping provides information on potential productive and influential scholars. The top three authors with the largest number of publications were Tournaye Herman (n=97), Devroey Paul (n=92), and De Sutter Petra (n=69). The details of the most productive authors are shown in Table 4. On the other hand, the authors with the most citations were Devroey Paul from the Free University of Brussels with 6358 total citations and an average of 69.11 citations per paper, followed by Van Steirteghem A, also from the Free University of Brussels, with 4873 total citations and an average of 85.49 citations per publication. The top 15 most cited authors are summarized in Table 5. The authors' cooperation network was visualized by VOSviewer. The size of a node represents the number of publications and different colors represent the authors of a given cluster. Further network mapping was presented by VOSviewer to identify the co-citation related to ICSI research in the last two decades. These results show the most active and fruitful authors in the field of ICSI research (Figure 4B).

Top cited articles

The most cited articles are usually considered landmarks because of their referential value. The co-citation analysis revealed that 5932 publications were cited more than ten times. The online database, WoSCC, revealed that 605 publications were cited more than 100 times. We concluded on the top 15 cited articles which are related to ICSI items (Table 1). The most cited publication was *"American Society of Clinical Oncology recommendations on fertility preservation in cancer patients."* In this paper, Lee et al. mentioned the topic of fertility preservation and talked about how to choose an appropriate plan to preserve fertility in cancer patients. They recommended that sperm and embryo cryopreservation are considered standard practice and were widely available for reproduction *via* ICSI (17). These highly-cited publications could provide a reliable reference for researchers, and ICSI had an important role in the fields of reproductive medicine. Four out of 15 publications, which concentrated on fertility preservation, were cited at a high frequency. In addition, the risk of birth defects after ICSI was a hotly-debated subject. Six studies were highly cited among the top 15 publications. The results indicated that researchers paid close attention to fertility preservation and the risks of birth defects during the past 20 years. The landmark articles and coocurrence on ICSI research can be found in Figure 4D. To track the concentration in different stages, the top 15 references with strongest citation bursts was visualized in Figure 5D.

TABLE 2 Top 15 most cited affiliations in the field of ICSI research.

Rank	Affiliation	Documents	Citations	TLS	ACP
1	Free University of Brussels	241	23547	4930	97.71
2	University of Copenhagen	146	8043	3246	55.09
3	University of Valencia	101	5423	1957	53.69
4	Ghent University	125	3719	2845	29.75
5	University of California San Francisco	48	3071	1034	63.98
6	University of Pennsylvania	35	2961	703	84.60
7	Harvard University	64	2813	956	43.95
8	University of Adelaide	52	2631	985	50.60
9	Yale University	49	2549	859	52.02
10	Tel Aviv University	124	2476	1243	19.97
11	ESHRE Central Office	18	2449	638	136.06
12	Shanghai Jiao Tong University	118	2366	1236	20.05
13	University of Bologna	52	2352	846	45.23
14	European Hospital	38	2278	974	59.95
15	University of Helsinki	38	2245	711	59.08

ACP, average citations per publication; TLS, total link strength.

Top contributing and core journals

The numbers of publications and citations indicate the impact of a journal in a given research field. The top 15 most productive journals published 4702 (56.85%) manuscripts on ICSI between 2002 and 2021 as shown in Table 6, alongside their 2021 impact factor and JCR category. Of these journals, *Human Reproduction* and *Fertility and Sterility* published the most papers on ICSI research (1051/8271, 12.71% and 1046/8271, 12.65%, respectively), and they were the most cited journals. The results suggested these two journals were the core journals of the field of ICSI research. Most of the top publishing journals were categorized

TABLE 3 Top 15 most prolific affiliations in terms of ICSI research.

Rank	Affiliation	Documents	Citations	TLS	ACP
1	Free University of Brussels	241	23547	4930	97.71
2	University Of Copenhagen	146	8043	3246	55.09
3	Ghent University	125	3719	2845	29.75
4	Tel Aviv University	124	2476	1243	19.97
5	Shanghai Jiao Tong University	118	2366	1236	20.05
6	University of Valencia	101	5423	1957	53.69
7	Academic Center for Education, Culture and Research (ACECR)	91	1176	1219	12.92
8	Peking University	85	1162	880	13.67
9	Shandong University	85	1096	706	12.89
10	Zhengzhou University	78	585	753	7.50
11	Sun YatSen University	77	1203	640	15.62
12	Mcgill University	74	2193	814	29.64
13	Cairo University	74	1313	489	17.74
14	University of Amsterdam	70	1730	971	24.71
15	Tehran University of Medical Sciences	70	961	422	13.73

ACP, average citations per publication; TLS, total link strength.

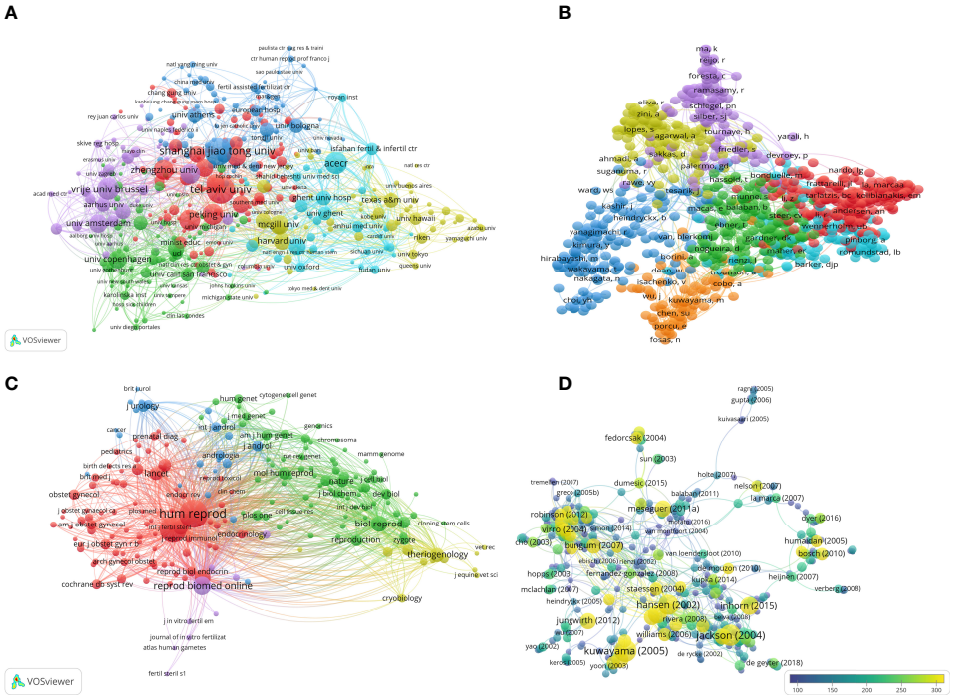

FIGURE 4
The co-citation map and cooperation network of institutions **(A)**, authors **(B)** and journals **(C)** based on VOSviewer analysis. Node size indicates the number of publications **(A, C)**. The most cited publications were visualized by VOSviewer **(D)**, different color means the range of citation times. The higher the centrality of a node, the more influential and important it is **(C, D)**.

TABLE 4 Top 15 most productive authors in the field of ICSI research.

Author	Documents	Citations	TLS	Organizations
Tournaye, Herman	97	4271	93	Free University of Brussels
Devroey, Paul	92	6358	91	Free University of Brussels
De Sutter, Petra	69	2426	60	Ghent University
Borges, Edson, Jr.	60	1118	59	Fertility Medical Group & Sapientiae Institute, Sao Paulo
Andersen, Anders Nyboe	59	4832	50	University of Copenhagen
Van Steirteghem, A	57	4873	55	Free University of Brussels
Iaconelli, Assumpto, Jr.	56	1026	56	Fertility Medical Group & Sapientiae Institute, Sao Paulo
Pellicer, Antonio	46	2464	40	University of Valencia
Setti, Amanda Souza	46	674	26	Fertility Medical Group & Sapientiae Institute, Sao Paulo
Kuang, Yanping	44	1183	42	Shanghai Jiao Tong University
Qiao, Jie	44	557	42	Peking University
Remohi, Jose	43	3061	43	University of Valencia
De Almeida Ferreira Braga, Daniela Paes	40	687	40	Fertility Medical Group & Sapientiae Institute, Sao Paulo
Meseguer, Marcos	40	2829	36	University of Valencia
Wakayama, Teruhiko	37	1040	34	University of Hawaii System

TLS, total link strength.

TABLE 5 Top 15 most influential authors involved in ICSI research.

Author	Documents	Citations	TLS	Organizations
Devroey, Paul	92	6358	91	Free University of Brussels
Van Steirteghem, A	57	4873	55	Free University of Brussels
Andersen, Anders Nyboe	59	4832	50	University of Copenhagen
Tournaye, Herman	97	4271	93	Free University of Brussels
De Mouzon, Jacques.	26	3136	25	National Institute of Health and Medical Research (INSERM)
Liebaers, Inge	41	3119	41	Free University of Brussels
Remohi, Jose	43	3061	43	University of Valencia
Meseguer, Marcos	40	2829	36	University of Valencia
Ferraretti, Anna P.	22	2466	20	SISMeRReprod Med Unit, Bologna
Pellicer, Antonio	46	2464	40	University of Valencia
Camus, Michel	32	2435	32	Free University of Brussels
De Sutter, Petra	69	2426	60	Ghent University
Tesarik, Jan	29	2374	26	ClinicaMargen Infertility clinic in Granada
Goossens, V.	12	2283	12	ESHRE Central Office
Greco, Ermanno	37	2267	34	Center for Reproductive Medicine, Villa Mafalda, Rome,

TLS, total link strength.

as reproductive biology, obstetrics & gynecology, and andrology journals (Figure 4C).

Mapping and analysis of keywords

The highest frequency of keywords can be mapped based on their frequency of occurrence, and keywords were classified based on their number of appearances by VOSviewer (Figure 5A). A keyword analysis is used to identify current hotspots and get insight into the overview of a field; moreover, it can also determine the trends and future directions (18). To determine the evolution of the research hotspots, the strongest citation bursts of keywords were illustrated by CiteSpace in Figure 5B. The outcome of the pregnancy and the live birth rate have appeared consistently from 2014 to 2021, indicating that more and more studies have focused on improving embryonic quality and newborn health since 2014. Figures 5C, E show the co-occurrence analysis of the most frequent keywords. The different colors represented the clusters revealed by the VOSviewer analysis. The size of the node represents the frequency use of the keyword, and the thickness of the connecting line represented the strength of the relationship between these keywords. According to the frequency of occurrence, the pregnancy rate and male infertility were constant foci of attention. In the past two decades, ICSI, as an important component of ART, had been greatly promoted and clinically applied. However, the development characteristics are different in certain stages. More studies have focused on embryonic quality and reproductive health in recent years. With the deepening understanding of this technology, ICSI has become an effective weapon against male infertility. However, we need to pay more attention to the risks of live birth.

Research shared between ICSI and COVID-19

In late 2019, the first case of Coronavirus disease 2019 (COVID-19) was reported in Wuhan, China. The World Health Organization (WHO) declared the outbreak of the epidemic an international emergency on January 30, 2020 (19). The rapid human-to-human transmission of the disease *via* direct contact or droplets has been confirmed. The epidemic had many negative impacts on medical systems. Especially, the suspicious sequelae of those severe cases should be followed up carefully for a long time. To know if COVID-19 could have disadvantages on the outcomes of ICSI or ART, we extracted relevant references from the WoSCC database by using the search terms "ICSI" and "COVID" to explore the database from 2019 to 2021. There were only nine publications that focused on the relationship between ICSI and COVID-19. The major topics have been observing whether COVID-19 would affect the number of fertility consultations, successful pregnancy rates, and protective measures from the virus' hazard throughout the medical procedure. The overall results show that COVID-19 had minimal impact on ICSI outcomes and no negative impact on implantation rates or on live births (Table 7). The quality of the patient's semen and embryos did not decrease due to COVID-19 (20–22). More data and longer follow-ups are needed to validate the previous conclusions.

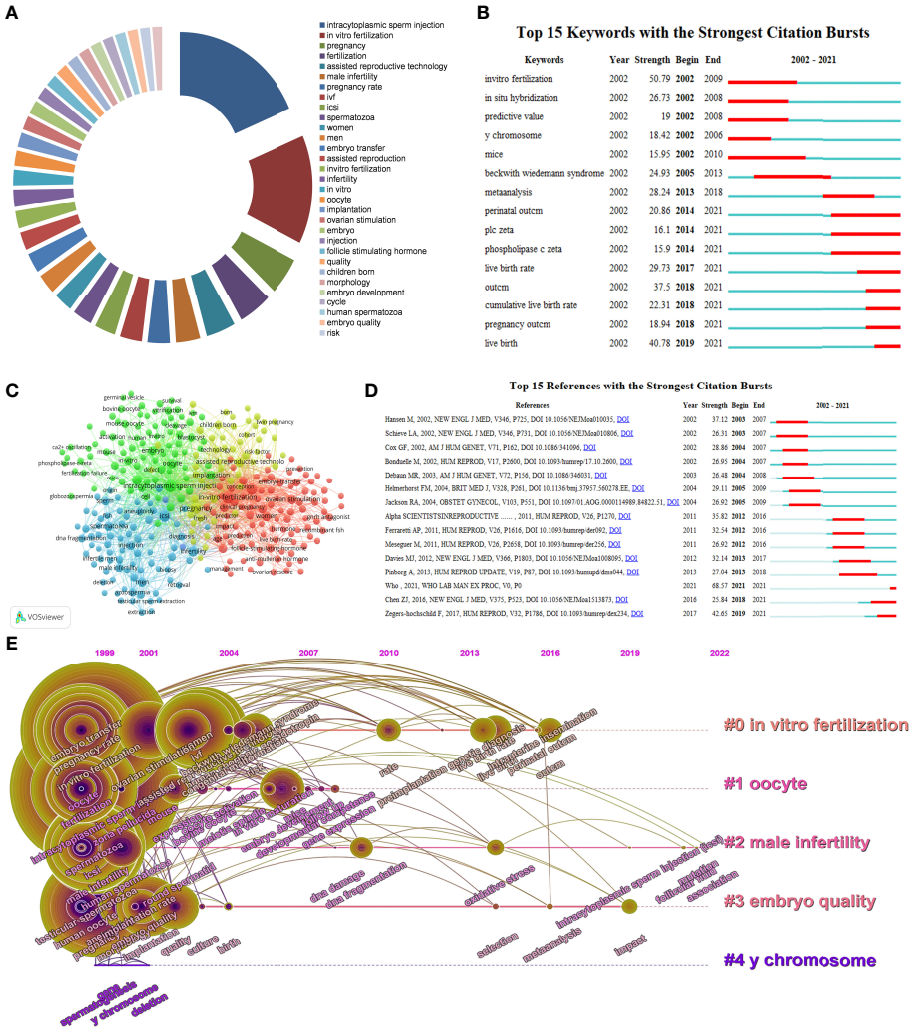

FIGURE 5
Visual cluster analysis of co-occurrence among keywords of ICSI. Top keywords in terms of their frequency in ICSI research **(A)**.Top 15 keywords with the strongest citation bursts from 2002 to 2021. The red bar means that researchers in that time highly emphasize the keyword **(B)**. The frequency of occurrence and co-occurrence were displayed by VOSviewer **(C)**. The strongest citations bursts of references in different stages were concluded by CiteSpace **(D)**. The strength value indicates the degree of a burst **(B, D)**. Keywords were grouped in five clusters, timeline distribution of the top 5 clusters and keywords trends by year were visualized from CiteSpace **(E)**.

Latest reviews in the field of ICSI research

Literature reviews are comprehensive summaries of previous research on a specific topic. They are essential to learning current research topics and are the keystone of evidence-based medicine. A literature review is able to summarize and synthesize the existing scholarly research on a particular topic. It critically analyses the information gathered by identifying areas that require further research and reviewing areas of controversy. The following data included the top 15 most cited reviews on ICSI during the past 12 months (Table 8). The *'Human Reproduction Update'* journal was the most prolific source of reviews on ICSI. Four main subfields were focused on: sperm quality and male infertility, dosage regimens of ovarian stimulation, preferential oocyte and embryo quality, and updated guidelines on the diagnosis and management of infertility. Six publications were assigned to the subfield "sperm quality and male infertility." The results suggested that ICSI remains a crucial treatment for male infertility. Furthermore, how to improve the quality of the sperm, oocyte, and embryo is still a hotspot in the field of ICSI research.

Discussion

The increase in the prevalence of infertility is a serious health problem. There are about 50 million couples experiencing fertility-related issues worldwide, and 30%-50% of them are caused by male factors (23, 24). The reductions in male sperm concentration, motility, and morphology, which have occurred over the past few years, were related to environmental pollution, obesity, unhealthy diet, and work stress. Women's ovarian reserves are also declining due to work stress, delayed childbearing, and so on (25). The frequency of use of ART has been increasing over the past two

TABLE 6 Top 15 most cited journals in ICSI research.

Journal	Documents	Citations	TLS	2021 IF	JCR Category
Human Reproduction	1051	57118	12213	6.353	Obstetrics & Gynecology - Scie(Q1); Reproductive Biology - Scie (Q1)
Fertility And Sterility	1046	47414	11378	7.49	Reproductive Biology - Scie(Q1)
Reproductive Biomedicine Online	623	18814	6723	4.567	Reproductive Biology - Scie(Q1); Obstetrics & Gynecology - Scie (Q1)
Journal Of Assisted Reproduction And Genetics	596	8916	4737	3.357	Obstetrics & Gynecology - Scie(Q2); Genetics & Heredity - Scie (Q3); Reproductive Biology - Scie(Q3)
Gynecological Endocrinology	187	1738	992	2.277	Obstetrics & Gynecology - Scie(Q3); Endocrinology & Metabolism - Scie(Q4)
Andrologia	181	2078	1341	2.532	Andrology - Scie(Q3)
European Journal Of Obstetrics & Gynecology And Reproductive Biology	151	2621	1042	2.831	Reproductive Biology - Scie(Q3); Obstetrics & Gynecology - Scie (Q3)
Theriogenology	147	3532	1182	2.923	Veterinary Sciences - Scie(Q1); Reproductive Biology - Scie(Q3)
Reproductive Biology And Endocrinology	130	2467	1203	4.982	Reproductive Biology - Scie(Q1); Endocrinology & Metabolism - Scie(Q2)
Biology Of Reproduction	129	5702	1144	4.161	Reproductive Biology - Scie(Q2)
Archives Of Gynecology And Obstetrics	112	1319	804	2.493	Obstetrics & Gynecology - Scie(Q3)
Zygote	96	794	712	1.818	Reproductive Biology - Scie(Q4); Cell Biology - Scie(Q4); Developmental Biology - Scie(Q4)
Clinical And Experimental Obstetrics & Gynecology	89	243	359	0.192	Obstetrics & Gynecology - Scie(Q4)
Frontiers In Endocrinology	86	484	595	6.055	Endocrinology & Metabolism - Scie(Q1)
Andrology	78	941	823	4.456	Andrology - Scie(Q1)

TLS, total link strength; IF, impact factor; JCR; journal citation of reports.

decades, with more than 2.5 million cycles being operated every year (26). During the ART cycle, a selected subpopulation of 25,000–150,000 sperms is placed around an oocyte to initiate fertilization in IVF. Unlike IVF, ICSI requires more careful manipulation of a single sperm that is injected into an oocyte in the laboratory. ICSI was introduced as an efficient form of ART in 1992 for the treatment of male infertility. With ICSI, Men with severe oligozoospermia or azoospermia have the opportunity to produce genetically-linked offspring due to ICSI (27). The percentage of IVF cycles with the use of ICSI increased dramatically from 11.0% in 1995 to 57.5% in 2004 in the United States, while the percentage of infertility attributed to male factors remained constant (28).

The present bibliometric analysis explored the contributions, impact, research hotspots, and trends in the ICSI field during the last two decades. The main research areas, according to the WoSCC database, were 'Reproductive Biology', 'Obstetrics and Gynecology', 'Genetics Heredity' and 'Andrology'. The number of publications increased quickly from 2018 onward, suggesting a generally increasing interest in research on ICSI area. However, the present study has some limitations. Firstly, similar to other bibliometric analyses, the documents were extracted only from the WoSCC database because of the rules of the system algorithm. Secondly, the authors' addresses were not written normatively, certain institutions' contributions may have been dispersive, and the rankings were influenced slightly. Lastly, the synonyms of keywords could affect the emergence analysis of keywords, although we tried to remove these heterogeneities as much as possible to reduce the resultant bias.

The United States, Belgium, Japan, Italy, and the UK contributed the majority of publications and were responsible for the highest quote rates in ICSI studies from 2002 to 2011. After 2018, the number of publications from Chinese institutions increased rapidly, with publications from Chinese academic institutions accounting for 32.10% of the total number of publications in the field of ICSI research from 2018 to 2021. By contrast, the number of American studies has remained fairly constant in the past 20 years. However, the number of Chinese publications increased exponentially from 5 in 2002 to 208 in 2021. The most influential institution in the field of ICSI research was the Free University of Brussels.

Human Reproduction and *Fertility and Sterility* were the core sources of publications. These two journals had the most citations and publications in ICSI research. The top three most cited papers were "American Society of Clinical Oncology recommendations on fertility preservation in cancer patients," "Highly efficient vitrification method for cryopreservation of human oocytes," and "Perinatal outcomes in singletons following *in vitro* fertilization: A meta-analysis." The results indicated that researchers focused a lot

TABLE 7 The research between ICSI and COVID-19.

First Author	Article Title	Journal	Year	Corresponding Orgnazation
Jacobs, Emily;	Fresh Embryo Transfer Cycle Characteristics and Outcomes Following *In Vitro* Fertilization *via* Intracytoplasmic Sperm Injection Among Patients With and Without COVID-19 Vaccination	Jama Network Open	2021	University of Iowa
Kolanska, Kamila	Mild COVID-19 infection does not alter the ovarian reserve in women treated with ART	Reproductive Biomedicine Online	2021	INSERM
Alviggi, Carlo	COVID-19 and assisted reproductive technology services: repercussions for patients and proposal for individualized clinical management	Reproductive Biology and Endocrinology	2020	University of Naples Federico II
Li, Fei	Controlled Ovarian Hyperstimulation Protocol in Infertile Patients During the COVID-19 Pandemic	Frontiers in Physiology	2021	Zhengzhou University
Cutting, Elizabeth	The impact of COVID-19 mitigation measures on fertility patients and clinics around the world	Reproductive Biomedicine Online	2021	Monash University
Rajput, Sandeep K	Absence of SARS-CoV-2 (COVID-19 virus) within the IVF laboratory using strict patient screening and safety criteria	Reproductive Biomedicine Online	2021	CCRM Fertility Network, Lone Tree CO.
Wang, Meng	Investigating the impact of SARS-CoV-2 infection on basic semen parameters and *in vitro* fertilization/intracytoplasmic sperm injection outcomes: a retrospective cohort study	Reproductive Biology and Endocrinology	2021	Huazhong University of Science and Technology
Porcu, Eleonora	High-security closed devices are efficient and safe to protect human oocytes from potential risk of viral contamination during vitrification and storage especially in the COVID-19 pandemic	Journal of Assisted Reproduction and Genetics	2021	University of Bologna
Porcu, Eleonora	Successful Pregnancies, Births, and Children Development Following Oocyte Cryostorage in Female Cancer Patients During 25 Years of Fertility Preservation	Cancers	2021	University of Bologna

on the preservation of oocytes, sperms, or embryos during the past 20 years. The outcomes and risks of pregnancy always drew the attention of clinicians. These topics will continue to be debated in the next few years.

The latest reviews were extracted for tracking the focused issues of ICSI between 2021 and 2022. *Human Reproduction Update'* had the highest number of ICSI reviews. These four subfields were focused on: sperm quality and male infertility, dosage regimens of ovarian stimulation, preferential oocyte and embryo quality, and updated guidelines for the diagnosis and management of infertility. After that, the authors searched all publications that focused on the relationship between ICSI and COVID-19, and there were only nine of such publications. The results of these highly-cited articles suggested that COVID-19 has neither a substantial influence on the outcomes of ICSI nor an effect on infertile couples' consultation for now.

As the indications have expanded and the number of cycles of ICSI has increased, more attention has been focused on the safety and stability of this technology. As of 2020, an estimated 8 million children had been conceived *via* ART. The American Society of Reproductive Medicine declared ICSI might be a safe and effective technology for the management of male infertility in 1994. Generally, ICSI is considered as a safe alternative for couples who would be unable to achieve a successful pregnancy (29, 30). There were potential controversies regarding offspring obtained *via* ICSI in the following aspects: the obstetrical outcomes of pregnancies, chromosomal abnormalities associated with the offspring obtained *via* ICSI, congenital malformations of the newborns resulting from ICSI procedures, and developmental abnormalities in postnatal children resulting from ICSI (29). With the increased incidence of preterm birth and low birth weight associated with ART, there have been concerns about postnatal growth. Theoretically, there are potential risks from ICSI manipulation. The injection of the oocyte might cause damage to the ooplasm or meiotic spindle apparatus. The external substances and contaminants could affect the microenvironment of the oocyte. The male gamete might also bring hazards because of potentially risky sperm, which include structural defects, Y-chromosome deletions, DNA fragments or breaks, and aneuploidy that could be injected into a healthy oocyte. The process of genomic imprinting might be changed during gametogenesis or maintained incompletely during embryonic development (31). The outcome data of childhood and growth into early adulthood are the potential hotspots and trends of ICSI. Continuous follow-up into later life needs to be investigated and confirmed (32). Recent studies suggested a small excess of birth defects and low birth weight in children conceived *via* ART. Furthermore, several studies have reported an increased frequency of ART conceptions associated with Beckwith–Wiedemann syndrome or Angelman syndrome caused by an imprinting defect (32, 33). The keywords with the strongest citation burst result indicated the focus and hotspots of ICSI research, concentrating on the outcomes of pregnancy and risks

TABLE 8 Top 15 high-cited reviews in ICSI research during the latest 12 months .

Author	Article Title	Journal	Citations
Agarwal, Ashok	Male infertility	Lancet	150
Carson, Sandra Ann	Diagnosis and Management of Infertility A Review	Jama	49
Zaat, Tjitske	Fresh versus frozen embryo transfers in assisted reproduction (Review)	Cochrane Database of Systematic Reviews	26
Nirgianakis, Konstantinos	Fertility, pregnancy and neonatal outcomes of patients with adenomyosis: a systematic review and meta-analysis	Reproductive Biomedicine Online	20
Datta, Adrija Kumar	Mild versus conventional ovarian stimulation for IVF in poor, normal and hyper-responders: a systematic review and meta-analysis	Human Reproduction Update	18
Ribas-Maynou, Jordi	Clinical implications of sperm DNA damage in IVF and ICSI: updated systematic review and meta-analysis	Biological Reviews	18
Sang, Qing	Genetic factors as potential molecular markers of human oocyte and embryo quality	Journal of Assisted Reproduction and Genetics	17
Nikshad, Aylin	Advances of microfluidic technology in reproductive biology	Life Sciences	14
Gualtieri, Roberto	Sperm Oxidative Stress during *In Vitro* Manipulation and Its Effects on Sperm Function and Embryo Development	Antioxidants	12
Coticchio, Giovanni	Plasticity of the human preimplantation embryo: developmental dogmas, variations on themes and self-correction	Human Reproduction Update	12
Capalbo, Antonio	Preconception genome medicine: current state and future perspectives to improve infertility diagnosis and reproductive and health outcomes based on individual genomic data	Human Reproduction Update	12
Allen, Christopher P.	Outcomes of pregnancies using donor sperm compared with those using partner sperm: systematic review and meta-analysis	Human Reproduction Update	12
Andrade, Danilo L.	Differential Diagnosis of Azoospermia in Men with Infertility	Journal of Clinical Medicine	11
Diaz-Hernandez, Indra	Uterine natural killer cells: from foe to friend in reproduction	Human Reproduction Update	10
Dai, Changsheng	Advances in sperm analysis: techniques, discoveries and applications	Nature Reviews Urology	9

of live birth from 2014 onward. In addition, the clinical pregnancy rate and outcomes of frozen–thawed embryo transfer or fresh embryo transfer and how to improve the quality of semen for ICSI, are hotspots and issues from keyword analysis results. Nowadays, ICSI is a frequently procedure applied worldwide to treat infertile couples. As an invasive method, ICSI surpasses all the process of physiological events in normal fertilization, thus is frequently debated as potentially increasing risk in future generations. Despite the above observations, the evidence concerning an increased risk of diseases in ICSI offspring remains confusing. It's always worth to keep an eye on this field. More studies are needed to evaluate the safety of ICSI on long-term health and developmental outcomes in offspring.

Conclusion

To the authors' knowledge, this is the first study to assess the ICSI research status *via* a bibliometric analysis. In this study, a systematic view of ICSI research hotspots, future directions, most cited authors, journals, and institutions was conducted using CiteSpace or VOSviewer. The results would help researchers to better understand the current situation, trends and hotspots, and future development of this field. European institutions are the most impactful in the world regarding the study of ICSI. Research hotspot analyses suggested that male fertility, fertility preservation and risks of live birth remain major concerns in the next few years. International collaboration, which helps researchers to easily keep up with academic progress, was common in this area.

Data availability statement

The original contributions presented in the study are included in the article/Supplementary Material. Further inquiries can be directed to the corresponding authors.

Author contributions

YZ and GH designed the study. WH, TX, and HY searched the database. XS, TX, and GH analyzed the data. Manuscript was written by XS. and GH. All authors contributed to the article and approved the submitted version.

Funding

This study was supported by the National Natural Science Foundation of China (grant no. 81901487).

Conflict of interest

The authors declare that the research was conducted in the absence of any commercial or financial relationships that could be construed as a potential conflict of interest.

Publisher's note

References

1. Vander Borght M, Wyns C. Fertility and infertility: Definition and epidemiology. *Clin Biochem* (2018) 62:2–10. doi: 10.1016/j.clinbiochem.2018.03.012

2. Inhorn MC, Patrizio P. Infertility around the globe: New thinking on gender, reproductive technologies and global movements in the 21st century. *Hum Reprod Update* (2015) 21(4):411–26. doi: 10.1093/humupd/dmv016

3. The role and place of antioxidants in the treatment of Male infertility caused by varicocele. *J Clin Med* (2022) 11(21). doi: 10.3390/jcm11216391

4. Agarwal A, Baskaran S, Parekh N, Cho CL, Henkel R, Vij S, et al. Male Infertility. *Lancet* (2021) 397(10271):319–33. doi: 10.1016/S0140-6736(20)32667-2

5. Bibi R, Jahan S, Afsar T, Almajwal A, Hammadeh ME, Alruwaili NW, et al. The influence of paternal overweight on sperm chromatin integrity, fertilization rate and pregnancy outcome among males attending fertility clinic for Ivf/Icsi treatment. *BMC pregnancy childbirth* (2022) 22(1):620. doi: 10.1186/s12884-022-04953-z

6. Sciorio R, Esteves SC. Contemporary use of icsi and epigenetic risks to future generations. *J Clin Med* (2022) 11(8). doi: 10.3390/jcm11082135

7. Fauser BC, Devroey P, Diedrich K, Balaban B, Bonduelle M, Delemarre-van de Waal HA, et al. Health outcomes of children born after Ivf/Icsi: A review of current expert opinion and literature. *Reprod biomedicine Online* (2014) 28(2):162–82. doi: 10.1016/j.rbmo.2013.10.013

8. Esteves SC, Roque M, Bedoschi G, Haahr T, Humaidan P. Intracytoplasmic sperm injection for Male infertility and consequences for offspring. *Nat Rev Urol* (2018) 15(9):535–62. doi: 10.1038/s41585-018-0051-8

9. Laprise SL. Implications of epigenetics and genomic imprinting in assisted reproductive technologies. *Mol Reprod Dev* (2009) 76(11):1006–18. doi: 10.1002/mrd.21058

10. Rumbold AR, Moore VM, Whitrow MJ, Oswald TK, Moran LJ, Fernandez RC, et al. The impact of specific fertility treatments on cognitive development in childhood and adolescence: A systematic review. *Hum Reprod* (2017) 32(7):1489–507. doi: 10.1093/humrep/dex085

11. Catford SR, McLachlan RI, O'Bryan MK, Halliday JL. Long-term follow-up of icsi-conceived offspring compared with spontaneously conceived offspring: A systematic review of health outcomes beyond the neonatal period. *Andrology* (2018) 6(5):635–53. doi: 10.1111/andr.12526

12. Davies MJ, Moore VM, Willson KJ, Van Essen P, Priest K, Scott H, et al. Reproductive technologies and the risk of birth defects. *New Engl J Med* (2012) 366(19):1803–13. doi: 10.1056/NEJMoa1008095

13. Park S, Blackledge K, Ananth C, Sauer M, Brandt J. Altmetric and bibliometric analysis of influential articles in reproductive biology, 1980-2019. *Reprod biomedicine Online* (2022) 45(2):384–90. doi: 10.1016/j.rbmo.2022.04.005

14. Ellegaard O, Wallin JA. The bibliometric analysis of scholarly production: How great is the impact? *Scientometrics* (2015) 105(3):1809–31. doi: 10.1007/s11192-015-1645-z

15. Chen C, Song M. Visualizing a field of research: A methodology of systematic scientometric reviews. *PloS One* (2019) 14(10):e0223994. doi: 10.1371/journal.pone.0223994

16. van Eck NJ, Waltman L. Software survey: Vosviewer, a computer program for bibliometric mapping. *Scientometrics* (2010) 84(2):523–38. doi: 10.1007/s11192-009-0146-3

17. Lee SJ, Schover LR, Partridge AH, Patrizio P, Wallace WH, Hagerty K, et al. American Society of clinical oncology recommendations on fertility preservation in cancer patients. *J Clin Oncol Off J Am Soc Clin Oncol* (2006) 24(18):2917–31. doi: 10.1200/JCO.2006.06.5888

18. Zhang X, Hui L, Wei L, Song F, Hu F. A bibliometric analysis of human-machine interaction methodology for electric-powered wheelchairs driving from 1998 to 2020. *Int J Environ Res Public Health* (2021) 18(14). doi: 10.3390/ijerph18147567

19. Adetuyi BO, Olajide PA, Awoyelu EH, Adetuyi OA, Adebisi OA, Oloke JK. Epidemiology and treatment options for covid-19: A review. *Afr J Reprod Health* (2020) 24(s1):142–53. doi: 10.29063/ajrh2020/v24i2s.18

20. Kolanska K, Hours A, Jonquiere L, Mathieu d'Argent E, Dabi Y, Dupont C, et al. Mild covid-19 infection does not alter the ovarian reserve in women treated with art. *Reprod biomedicine Online* (2021) 43(6):1117–21. doi: 10.1016/j.rbmo.2021.09.001

21. Cutting E, Catt S, Vollenhoven B, Mol BW, Horta F. The impact of covid-19 mitigation measures on fertility patients and clinics around the world. *Reprod biomedicine Online* (2022) 44(4):755–63. doi: 10.1016/j.rbmo.2021.12.016

22. Wang M, Hu J, Huang B, Yang Q, Liu S, Li Z, et al. Investigating the impact of sars-Cov-2 infection on basic semen parameters and in vitro Fertilization/Intracytoplasmic sperm injection outcomes: A retrospective cohort study. *Reprod Biol Endocrinol RB&E* (2022) 20(1):46. doi: 10.1186/s12958-022-00918-1

23. Mascarenhas MN, Flaxman SR, Boerma T, Vanderpoel S, Stevens GA. National, regional, and global trends in infertility prevalence since 1990: A systematic analysis of 277 health surveys. *PloS Med* (2012) 9(12):e1001356. doi: 10.1371/journal.pmed.1001356

24. Bashamboo A, Ferraz-de-Souza B, Lourenco D, Lin L, Sebire NJ, Montjean D, et al. Human Male infertility associated with mutations in Nr5a1 encoding steroidogenic factor 1. *Am J Hum Genet* (2010) 87(4):505–12. doi: 10.1016/j.ajhg.2010.09.009

25. You JB, McCallum C, Wang Y, Riordon J, Nosrati R, Sinton D. Machine learning for sperm selection. *Nat Rev Urol* (2021) 18(7):387–403. doi: 10.1038/s41585-021-00465-1

26. Fauser BC. Towards the global coverage of a unified registry of ivf outcomes. *Reprod biomedicine Online* (2019) 38(2):133–7. doi: 10.1016/j.rbmo.2018.12.001

27. Hodes-Wertz B, Mullin CM, Adler A, Noyes N, Grifo JA, Berkeley AS. Is intracytoplasmic sperm injection overused? *J Urol* (2012) 187(2):602–6. doi: 10.1016/j.juro.2011.09.151

28. Jain T, Gupta RS. Trends in the use of intracytoplasmic sperm injection in the united states. *New Engl J Med* (2007) 357(3):251–7. doi: 10.1056/NEJMsa070707

29. Retzloff MG, Hornstein MD. Is intracytoplasmic sperm injection safe? *Fertility sterility* (2003) 80(4):851–9. doi: 10.1016/s0015-0282(03)01014-8

30. Zhang L, Yan LY, Zhi X, Yan J, Qiao J. Female fertility: Is it safe to "Freeze?". *Chin Med J* (2015) 128(3):390–7. doi: 10.4103/0366-6999.150115

31. Woldringh GH, Kremer JA, Braat DD, Meuleman EJ. Intracytoplasmic sperm injection: A review of risks and complications. *BJU Int* (2005) 96(6):749–53. doi: 10.1111/j.1464-410X.2005.05708.x

32. Graham ME, Jelin A, Hoon AH Jr, Wilms Floet AM, Levey E, Graham EM. Assisted reproductive technology: Short- and long-term outcomes. *Dev Med Child Neurol* (2023) 65(1):38–49. doi: 10.1111/dmcn.15332

33. Maher ER. Imprinting and assisted reproductive technology. *Hum Mol Genet* (2005) 14 Spec No 1:R133–8. doi: 10.1093/hmg/ddi107

frontiers | Frontiers in Endocrinology

TYPE Original Research
PUBLISHED 20 March 2023
DOI 10.3389/fendo.2023.1135973

OPEN ACCESS

EDITED BY
Kun Li,
Hangzhou Medical College, China

REVIEWED BY
Lucia Rocco,
University of Campania Luigi Vanvitelli, Italy
Miguel Betancourt,
Metropolitan Autonomous University, Mexico

*CORRESPONDENCE
Philip C. N. Chiu
pchiucn@hku.hk
Jian-Ping Ou
oujp3@mail.sysu.edu.cn

SPECIALTY SECTION
This article was submitted to Reproduction, a section of the journal Frontiers in Endocrinology

RECEIVED 02 January 2023
ACCEPTED 07 March 2023
PUBLISHED 20 March 2023

CITATION
Leung ETY, Lee BKM, Lee C-L, Tian X, Lam KKW, Li RHW, Ng EHY, Yeung WSB, Ou J-P and Chiu PCN (2023) The role of spermatozoa-zona pellucida interaction in selecting fertilization-competent spermatozoa in humans.
Front. Endocrinol. 14:1135973.
doi: 10.3389/fendo.2023.1135973

The role of spermatozoa-zona pellucida interaction in selecting fertilization-competent spermatozoa in humans

Erica T. Y. Leung[1], Brayden K. M. Lee[1], Cheuk-Lun Lee[1,2], Xinyi Tian[1], Kevin K. W. Lam[1,2], Raymond H. W. Li[1,2], Ernest H. Y. Ng[1,2], William S. B. Yeung[2], Jian-Ping Ou[1,3]* and Philip C. N. Chiu[1,2]*

[1]Department of Obstetrics and Gynaecology, Li Ka Shing Faculty of Medicine, The University of Hong Kong, Hong Kong, Hong Kong SAR, China, [2]Shenzhen Key Laboratory of Fertility Regulation, The University of Hong Kong – Shenzhen Hospital, Shenzhen, China, [3]Center for Reproductive Medicine, The Third Affiliated Hospital, Sun Yat-sen University, Guangzhou, China

Human fertilization begins when a capacitated spermatozoon binds to the zona pellucida (ZP) surrounding a mature oocyte. Defective spermatozoa-ZP interaction contributes to male infertility and is a leading cause of reduced fertilization rates in assisted reproduction treatments (ARTs). Human ejaculate contains millions of spermatozoa with varying degrees of fertilization potential and genetic quality, of which only thousands of motile spermatozoa can bind to the ZP at the fertilization site. This observation suggests that human ZP selectively interacts with competitively superior spermatozoa characterized by high fertilizing capability and genetic integrity. However, direct evidence for ZP-mediated sperm selection process is lacking. This study aims to demonstrate that spermatozoa-ZP interaction represents a crucial step in selecting fertilization-competent spermatozoa in humans. ZP-bound and unbound spermatozoa were respectively collected by a spermatozoa-ZP coincubation assay. The time-course data demonstrated that ZP interacted with a small proportion of motile spermatozoa. Heat shock 70 kDa protein 2 (HSPA2) and sperm acrosome associated 3 (SPACA 3) are two protein markers associated with the sperm ZP-binding ability. Immunofluorescent staining indicated that the ZP-bound spermatozoa had significantly higher expression levels of HSPA2 and SPACA3 than the unbound spermatozoa. ZP-bound spermatozoa had a significantly higher level of normal morphology, DNA integrity, chromatin integrity, protamination and global methylation when compared to the unbound spermatozoa. The results validated the possibility of applying spermatozoa-ZP interaction to select fertilization-competent spermatozoa in ART. This highly selective interaction might also provide diagnostic information regarding the fertilization potential and genetic qualities of spermatozoa independent of those derived from the standard semen analysis.

KEYWORDS

zona pellucida, human spermatozoa, sperm selection, DNA integrity, methylation, protamination, HSPA2, SPACA3

1 Introduction

Infertility is a public health concern affecting approximately 15% of reproductive-aged couples worldwide (1). Assisted reproduction technologies (ARTs) including *in vitro* fertilization (IVF), intrauterine insemination (IUI), intracytoplasmic sperm injection (ICSI) are provided to infertile couples who wish to conceive. Despite major technological advancements, the live birth rate following ART is only about 30% (2).

Sperm quality is a major factor contributing to fertilization success following ARTs (3, 4). During migration through the female reproductive tract, only the fertilization-competent spermatozoa survive the natural selection mechanisms involving anatomical, biochemical, and physiological barriers in a highly specialized microenvironment (5). In ART, the motile and morphologically normal spermatozoa are routinely isolated by either the swim-up or density gradient centrifugation (DGC) according to their motility and density, respectively for subsequent procedures. However, these two surrogate markers lack the discriminatory power to select high-quality spermatozoa according to their fertilization potential and genetic quality (5–10).

Advanced sperm selection methods have been developed to enrich high-quality spermatozoa aiming to improve the fertilization and clinical outcomes (11–14). Two approaches are being used to develop sperm selection methods. One approach is to focus on the intrinsic properties of spermatozoa, such as surface charges and apoptotic status of spermatozoa (15, 16). Another approach is to replicate the natural selection mechanisms such as thermotactic and chemotactic responses in a controlled environment to isolate fertilization-competent spermatozoa in a manner similar to those observed in the female reproductive tract (5, 17, 18). However, contradicting results have been reported on the clinical significance of these methods on ART outcomes (5). In addition, many of these new techniques are small-scaled, which can only process a small volume of sample per run (5). These findings highlight the need for new approaches to sperm selection in ART.

In the fallopian tubes, the capacitated spermatozoa bind to the zona pellucida (ZP) surrounding the released oocyte and undergo acrosome reaction which facilitates the subsequent penetration process for gamete fusion. Defective sperm-ZP binding (DSZPB) is a leading cause of male-factor infertility and fertilization failure in IVF (19–22). Spermatozoa-ZP binding is a highly species specific event that occurs when the specific ligands on the ZP are recognized by the protein receptors located on the capacitated spermatozoa (23). The receptor(s) are multimeric protein complex(es) assembled during capacitation (24). Fertile male ejaculate contains millions of spermatozoa, of which only 14% of the motile spermatozoa are capable of binding to the ZP (25) and only 48% of the ZP-bound spermatozoa can then undergo ZP-induced acrosome reaction (26). These observations suggest that human ZP selectively interacts with high-quality spermatozoa possessing superior genetic integrity and fertilizing capability. However, direct evidence for the existence of this ZP-mediated sperm selection process in humans is lacking. Therefore, the objective of this study is to validate the functional role of human ZP in selecting fertilization-competent spermatozoa.

2 Materials and methods

2.1 Semen and oocyte collection

The research protocol of this study was approved by the Institutional Review Board of the University of Hong Kong/Hospital Authority Hong Kong West Cluster. Semen samples were collected from men attending the Family Planning Association of Hong Kong for premarital checkup after obtaining informed written consent. The residual portion after the routine test was collected for research use. Normal semen samples were selected for research use according to the World Health Organization (WHO) criteria, fifth edition (27): total volume > 1.5 mL, total motility > 40%, progressive motility > 32%, total sperm number > 39×10^6 per ejaculate, concentration > 15×10^6/mL, and viability > 58%, normal morphology > 4%. Direct swim-up method was used to isolate motile and viable spermatozoa from the seminal plasma. In this method, 1.0 mL of thoroughly mixed semen was overlaid by 1.5 mL of Earle Balanced Salt Solution (EBSS; Flow Laboratories, Irvine, United Kingdom) supplemented with 0.3% bovine serum albumin (BSA), 0.3 mmol/l sodium pyruvate, 0.16 mmol/L penicillin G, 0.05 mmol/l streptomycin sulfate, and 14 mmol/L sodium bicarbonate (all from Sigma, MO, USA) (EBSS/0.3% BSA). The tube was then placed at a 45° angle and incubated at 37°C with 5% CO_2 for one hour to allow motile spermatozoa to migrate from the seminal plasma into the overlaying medium. 1 mL of the top layer of the medium was collected, transferred into a sterile 15 mL centrifuge tube, and centrifuged at 500g for 5 min twice. The washed pellet was then resuspended with EBSS/0.3% BSA and diluted to the appropriate concentrations (1×10^6 or 2×10^6 spermatozoa/ml). All processed spermatozoa were incubated in EBSS supplemented with 3% BSA (EBSS/3%BSA) to induce capacitation for the spermatozoa-ZP coincubation assays (28).

Oocytes were collected from infertile women attending IVF treatment at the Queen Mary Hospital, Hong Kong. Immature oocytes (germinal vesicle/metaphase I oocytes) or mature metaphase II oocytes that failed to achieve fertilization following conventional insemination were donated from patients with informed consent and stored in high-salt oocyte storage buffer containing 1.5 M $MgCl_2$, 0.1% polyvinyl pyrrolidone (PVP) and 40 mM HEPES with pH 7.2. Morphologically abnormal oocytes were discarded.

2.2 Evaluation of sperm motility

Sperm motility was assessed by the computer-assisted sperm analysis (CASA) system (CEROS system, Hamilton Thorne, MA, USA). For each measurement, 10 µL of sperm sample was transferred on a glass slide (Hamilton Thorne, USA) specifically made for the CASA system equipped with a warmed stage at 37°C. A minimum of 200 spermatozoa per sample in randomly selected fields were examined to analyze the following sperm motion parameters: 1) Progressive motility (%), 2) average path velocity (VAP, µm/s), 3) straight line velocity (VSL; µm/s), 4) curvilinear

velocity (VCL, μm/s), 5) lateral amplitude (μm), 6) beat frequency (Hz), 7) straightness (%), 8) linearity (%), 9) elongation of sperm head (%), and 10) area (μm).

2.3 Evaluation of sperm viability

Sperm viability was assessed by the trypan blue exclusion assay. Spermatozoa were thoroughly mixed with an equal volume of trypan blue dye (1:1 ratio) on a sterile glass slide and kept at 37°C for 5 min prior to examination. The mixture was then evaluated under a light microscope with a magnification of 400x. Viable spermatozoa appeared transparent whilst non-viable spermatozoa with disrupted plasma membranes were stained blue. A minimum of 200 spermatozoa per sample in randomly selected fields were quantified to determine the overall viability.

2.4 ZP-bound spermatozoa collection

ZP-bound spermatozoa were collected by a modified spermatozoa-ZP coincubation assay (25). In brief, 4 human oocytes were transferred into a 30 μL droplet of EBSS/3% BSA containing 2×10^6 spermatozoa covered with mineral oil for coincubation at 37°C in 5% CO_2 for 30 min unless stated otherwise. After incubation, the oocytes were successively washed with 3 droplets of EBSS/no BSA to dislodge loosely bound spermatozoa. The ZP-bound spermatozoa were then removed from the surface of the oocytes through vigorous aspiration using a glass pipette in a confined area containing 10 μL of EBSS/no BSA on a sterile glass slide for further analysis.

2.5 ZP-unbound spermatozoa collection

ZP-unbound spermatozoa were collected by a modified continuous spermatozoa-ZP coincubation assay (25). In this method, 4 human oocytes were transferred into a 20 μL droplet of EBSS/3%BSA containing 1×10^6 spermatozoa for a 6-h incubation at 37°C in 5% CO_2. The following procedures were performed at intervals of 2, 4 and 6 h. The oocytes were successively washed with 3 droplets of EBSS/no BSA to dislodge any loosely bound spermatozoa and transferred into a fresh droplet of EBSS/no BSA for observation under a light microscope. Only spermatozoa tightly bound to the ZP with their sperm heads were quantified whilst those bound to the ZP with their tails, or any other regions were omitted. The ZP-bound spermatozoa were then removed from the ZP as described above and the oocytes were transferred back into the original sperm droplet for further coincubation. All spermatozoa remaining in the sperm droplet after 6 h of coincubation were considered as unbound spermatozoa, which were subsequently collected for further analysis.

2.6 Evaluation of the acrosomal status of spermatozoa

The acrosomal status of spermatozoa was evaluated by the fluorescein isothiocyanate conjugated *Pisum sativum* (FITC-PSA) (Sigma) staining. 20 μL of ZP-bound and unbound spermatozoa were allowed to air-dry in a small area on a sterile glass slide at 37°C. The slide was then washed with distilled water thrice. The spermatozoa were incubated with 50 μL of FITC-PSA (20 μg/mL) for 1 h at 37°C in the dark. The slides were rinsed with distilled water twice and mounted with DAKO mounting solution (Dako, CA, USA). The stained spermatozoa were observed under a fluorescence microscope (Zeiss, Oberkochen, Germany) at a magnification of 600x using excitation/emission wavelengths of 495 nm/515 nm. Acrosome-intact spermatozoa were stained with bright green, fluorescent signals in no less than half of the acrosomal regions whilst acrosome-reacted spermatozoa only had fluorescent signals at the equatorial region or completely lacked fluorescent signals in the acrosomal region. A minimum of 100 spermatozoa/sample was quantified to determine the acrosome reaction rates.

2.7 Immunodetection of protein expressions on spermatozoa

Capacitated sperm suspensions were fixed with 0.4% paraformaldehyde for 10 min and washed with EBSS/no BSA twice. The fixed spermatozoa were individually incubated with the primary antibodies against heat shock 70 kDa protein 2 (HSPA2) (Sigma) or sperm acrosome associated 3 (SPACA 3) (Abcam, Cambridge, UK) diluted at 1:100 for 1 h at 37°C in 5% CO_2. The samples were then centrifuged twice at 500g for 5 min and incubated with Alexa Fluro 488 conjugated goat anti-rabbit IgG for one hour at 37°C in 5% CO_2. (1:1000; Invitrogen, MA, USA). The samples were centrifuged twice at 500g for 5 min and resuspended into EBSS/ no BSA for flow consistency (Beckman Coulter, CA, USA). Data were analyzed using FlowJo v10.0.7 software (Copyright Tree Star, Inc. Stanford Jr. University).

ZP-bound and unbound spermatozoa were allowed to air-dry in a small area on a sterile glass slide at 37°C. The slides were gently rinsed with distilled water thrice. The samples were individually incubated with primary antibodies against HSPA2 (Sigma) or SPACA3 (Abcam) diluted at 1:100 overnight at 4°C. The slides were gently rinsed with distilled water twice. The samples were then incubated with Alexa Fluro 555 conjugated goat anti-rabbit IgG for one hour at 37°C in 5% CO_2. (1:1000; Invitrogen), rinsed gently with distilled water twice and immediately mounted with fluorescent mounting medium (Dako). The stained spermatozoa were observed under a fluorescence microscope (Nikon Eclipse Ti, Tokyo, Japan) at a magnification of 600x or a Carl Zeiss LSM 880 with Ariyscan 2 at a magnification of 630x (Carl Zeiss, NY, USA) using excitation/emission wavelengths of 555 nm/580 nm. A minimum of 100 spermatozoa/sample with positive signals across their head regions was quantified to determine the expression patterns. The fluorescence intensities were evaluated using Image J analysis software (Version 1.48 v; NIH, USA)

2.8 Evaluation of sperm morphology

ZP-bound and unbound spermatozoa were smeared on a glass slide and allowed to air-dry at 37°C. The slides were then gently

rinsed with distilled water once. The samples were fixed with the fixative solution (methanol-based solution) for 15 s and stained with the staining solution 1 (buffered solution of Eosin Y) for 10 s followed by the staining solution 2 (buffered solution of thiazine dyes) for 10 s. The excess solution was allowed to drip off the slides between steps. The samples were gently rinsed with distilled water once and allowed to air-dry. Spermatozoa were assessed manually under oil immersion using a light microscope (Zeiss, Gottingen, Germany) at a magnification of 1000x. A minimum of 100 spermatozoa/sample was quantified according to the WHO strict criteria (27) to determine the percentage of normal morphology.

2.9 Evaluation of DNA fragmentation rates by terminal deoxynucleotidyl transferase dUTP nick end labelling

ZP-bound and unbound spermatozoa were allowed to air-dry in a small area on a sterile glass slide at 37°C. The slides were then gently rinsed with distilled water thrice. The washed spermatozoa were fixed with 2% paraformaldehyde for 1 h at room temperature and gently rinsed with PBS twice. After fixation, the spermatozoa were permeabilized with freshly prepared 0.1% Triton X-100 in sodium citrate for 2 min at 4°C and rinsed with PBS twice. The permeabilized spermatozoa were incubated in 50 µL of reaction mixture containing terminal deoxynucleotidyl transferase (TdT) and fluorescein- dUTP (*In Situ* cell death detection kit, fluorescein, Sigma-Aldrich, MA, USA) in a 1:9 ratio for 1 hour at 37°C in the dark. The slide was then rinsed with PBS twice and mounted with fluorescent mounting medium (Dako). The TUNEL-positive spermatozoa were observed under a fluorescence microscope (Nikon Eclipse Ti, Tokyo, Japan) at a magnification of 600x using excitation/emission wavelengths of 488nm/530nm. A minimum of 100 spermatozoa/sample was quantified to determine the percentage of DNA fragmentation rates [(number of TUNEL-positive spermatozoa with bright, green fluorescence over the head regions/total number of spermatozoa) x 100%].

2.10 Evaluation of DNA damages by comet assay

ZP-bound and unbound spermatozoa were mixed with the molten low-melting point agarose (Trevigen, MD, USA) at 1:5 ratio (V/V) on a Comet slide (Trevigen). The mixture was allowed to solidify at 4°C in the dark for 10 min. The slides were then immersed in cold lysis buffer (Trevigen) at 4°C for 30 min. After removing the excess buffer, the slides were incubated in freshly prepared alkaline solution (pH~13) for 30 min. The slides were then transferred into a horizontal electrophoresis tank containing freshly prepared alkaline buffer for electrophoresis at 21V for 30 min. The slides were washed in distilled water twice for 10 min followed by 70% ethanol for 5 min. The samples were allowed to air-dry at 37°C. The dried samples were then incubated with SYBR Green I (Molecular Probes, OR, USA) at room temperature in the dark for 5 min. After removing the excess staining solution, the COMET-positive spermatozoa were observed under a fluorescence microscope (Nikon Eclipse Ti, Tokyo, Japan) at a magnification of 600x using excitation/emission wavelengths of 488nm/530nm. The extent of DNA damage in a minimum of 100 spermatozoa/sample was determined by measuring the percentage of tail DNA ((tail intensity/total intensity) x 100%) and the tail moment (%DNA in the comet tail x tail length) using the COMET assay II software (Perceptive Instruments, Haverhill, UK).

2.11 Evaluation of chromatin integrity by acridine orange staining

Air-dried and washed ZP-bound and unbound spermatozoa in a small area on a sterile glass slide as described above were fixed with Carnoy's solution (acetic acid-methanol in a 3:1 ratio) overnight at 4°C. The slides were gently rinsed with PBS twice and allowed to air-dry prior to the staining procedure. The AO staining solution was prepared daily by adding 1% AO stock solution (Thermofisher, MA, USA) to a mixture of 0.1M citric acid and 0.3M Na_2HPO_4, pH 2.5. The spermatozoa were incubated with the staining solution for 5 min at 37°C in the dark and gently rinsed with distilled water twice. The stained spermatozoa were immediately observed under a fluorescence microscope (Nikon Eclipse Ti, Tokyo, Japan) at a magnification of 600x using excitation/emission wavelengths of 488nm/530nm. The percentage of spermatozoa with normal/abnormal chromatin structure was determined by scoring a minimum of 100 spermatozoa/sample with bright, green fluorescence (double-stranded DNA) and those with orange/yellow fluorescence (single-stranded DNA).

2.12 Evaluation of protamine deficiency by chromomycin A3 staining

Air-dried and washed ZP-bound and unbound spermatozoa were fixed with Carnoy's solution (acetic acid-methanol in a 3:1 ratio) at 37°C for 10 min. The fixed spermatozoa were incubated with 0.25mg/ml CMA_3 (Sigma) in Mcllvaine buffer 0.1M citric acid and Na_2HPO_4•$7H_2O$, pH 7.0, containing 10 mM $MgCl_2$ for 20 min at room temperature. The slides were gently rinsed with PBS and mounted with fluorescent mounting medium (Dako). The stained spermatozoa were observed under a fluorescence microscope (Nikon Eclipse Ti, Tokyo, Japan) at a magnification of 600x using excitation/emission wavelengths of 488nm/580nm. The degree of protamine deficiency was determined by quantifying the overall signal intensity of a minimum of 100 spermatozoa with yellow fluorescence (CMA3-positive).

2.13 Evaluation of methylation level by immunostaining

Air-dried and washed ZP-bound and unbound spermatozoa were fixed with Carnoy's solution (acetic acid- methanol in a 3:1

ratio) at 4°C for 20 min and gently rinsed with PBS with 0.5% Tween twice. For sperm decondensation, the fixed spermatozoa were incubated with 1M Tris-HCl, pH 9.5, containing 25 mM dithiothreitol (DTT) for 20 min at room temperature and gently rinsed with PBS twice. The decondensed spermatozoa are denatured by incubation with 6N HCl for 15 min and gently rinsed with PBS twice. The denatured spermatozoa were stained with anti-5-methylcytosine (5-mC) (Abcam) overnight at 4°C and gently rinsed with PBS twice. The samples were then incubated with Alexa Fluro 488 conjugated goat anti-mouse IgG for one hour at 37°C (1:1000; Invitrogen), rinsed gently with distilled water twice and immediately mounted with fluorescent mounting medium (Dako). The stained spermatozoa were observed under a fluorescence microscope (Nikon Eclipse Ti, Tokyo, Japan) at a magnification of 600x using excitation/emission wavelengths of 488 nm/525 nm. The level of methylation in spermatozoa was determined by quantifying the overall signal intensity of a minimum of 100 spermatozoa with green fluorescence (5-Mc-positive).

2.14 Data analysis

All experimental data were expressed as mean ± standard deviation (Mean ± SD) or median (range). Statistical software (GraphPad Prism 9.1.0, GraphPad software, CA, USA) was used to analyze the data. Two tailed unpaired t-test was used to examine the differences between the ZP-bound and unbound sperm subpopulations. If the data failed the normality test, Mann-Whitney (non-parametric) test was used to perform statistical analysis. A probability value of < 0.05 was considered as statistically significant.

3 Results

3.1 Retrieval of ZP-bound human spermatozoa by continuous spermatozoa-ZP coincubations

The total number of spermatozoa tightly bound to the ZP per assay was quantified at 2 h intervals during the 6 h continuous coincubation (Figure 1A). An average of 150 ZP-bound spermatozoa was retrieved per assay within the first 2 h of coincubation. The time-course study showed that the total number of ZP-bound spermatozoa gradually decreased over time and eventually plateaued at 20 h (Figure 1A). Approximately 0.03% of the motile spermatozoa in the incubation droplet containing $1x10^6$ spermatozoa/mL bound to the ZP within the first 6-h incubation period. Incubation of spermatozoa for up to 6-h had no adverse effects on sperm viability, motility and DNA integrity (Figures 1B-D). The number of ZP-bound spermatozoa in two continuous assays with or without the replacement of oocyte at 4-h was comparable (Figure 1E), suggesting that reusing the same group of oocytes throughout the entire incubation period did not impair the binding interaction.

3.2 Immunodetection of acrosome reaction and protein markers on ZP-bound spermatozoa

The acrosome reaction rates of ZP-bound spermatozoa recovered at 15 and 30 min (15.7% ± 4.2 and 14.5% ± 2.7) (Figure 2) were comparable to the spontaneous acrosome reaction rates of those in the control without prior exposure to the ZP. The ZP-bound spermatozoa recovered at 60 and 120 min (63.7% ± 10.1 and 70.9% ± 4.4 vs. 26.3% ± 11.7, $p<0.05$) (Figure 2) had higher acrosome reaction rates than the unbound ones.

The expression of HSPA2 and SPACA3 on capacitated human spermatozoa were individually evaluated by flow cytometry. The protein markers were positively present (HSPA2: 36.3 ± 6.5% and SPACA3: 17.9 ± 0.5%) (Supplementary Figure 1) on the capacitated human spermatozoa. Confocal microscopy revealed markedly granular pattern of staining for these molecules on capacitated spermatozoa (Figures 3A, B). HSPA2 and SPACA3 localized to the head regions of capacitated human spermatozoa (Figures 3C, D). To examine their expression solely on the plasma membrane, the optimal time-point to recover acrosome-intact, ZP-bound spermatozoa was 30 min. Approximately 86% of the ZP-bound spermatozoa recovered at 30 min were HSPA2- or SPACA3-positive (Figures 3E, F). ZP-bound spermatozoa recovered at 30 min had a higher percentage of positive HSPA2 (85.8% vs. 45.9%, $p<0.05$) and SPACA3 signals (86.3% vs. 30.5%, $p<0.05$) than the unbound ones (Figure 3). The signal intensities of both markers were stronger in the ZP-bound spermatozoa recovered at 30 min than the unbound ones ($p<0.05$) (Figures 3G, H).

3.3 Morphology evaluation of ZP-bound and unbound spermatozoa

The number of morphologically normal spermatozoa was significantly higher in the ZP-bound spermatozoa recovered at 30 min than in the unbound ones (Figure 4), indicating a relationship between the morphology and ZP-binding ability of spermatozoa.

3.4 Evaluation of genetic quality of ZP-bound and unbound spermatozoa

Comet and TUNEL assays (Supplementary Figures 2A, B) were used to evaluate DNA fragmentation rates of ZP-bound and unbound spermatozoa. In the comet assay, the ZP-bound spermatozoa had a significantly lower level of tail DNA (27.6% vs. 40.2%, $p<0.05$) (Figure 5A) and tail moment (15.4% vs 22.1%, $p<0.05$) (Figure 5A) than the unbound ones. Consistently, the number of TUNEL-positive spermatozoa was significantly lower in the ZP-bound than in the unbound sperm subpopulations (4.1% vs. 15.5%, $p<0.05$) (Figure 5B), correlating the ZP-binding ability and DNA integrity of spermatozoa. A high proportion of ZP-bound spermatozoa with intact DNA was found in all sample groups, even

10.3389/fendo.2023.1135973

A

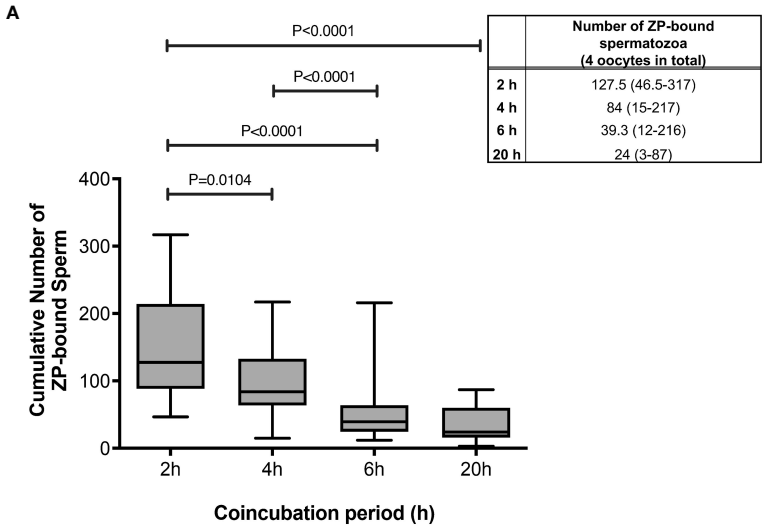

	Number of ZP-bound spermatozoa (4 oocytes in total)
2 h	127.5 (46.5-317)
4 h	84 (15-217)
6 h	39.3 (12-216)
20 h	24 (3-87)

B

Time	0 h	2 h	4 h	6 h
Total Number of sperm	253.0± 66.4	263.8± 39.6	248.4± 30.9	255.8± 34.8
Motility %	93.6± 5.6	91.2± 7.8	94.0± 5.6	94.8± 5.8
Progressive motility %	85.2± 6.8	82.6± 8.4	82.0± 9.8	84.2± 3.3
Non-progressive motiltiy %	10.2± 4.3	10.0± 3.0	13.2± 9.6	12.8± 3.1
immotility %	4.8± 4.7	7.4± 7.3	4.8± 2.9	3.0± 2.0
Average path velocity (VAP) μm/s	25.1± 1.7	25.2± 1.5	26.3± 3.0	25.6± 1.5
Straight line velocity (VSL) μm/s	10.8± 1.8	10.6± 0.4	10.8± 1.8	11.0± 2.6
Curvilinear velocity (VCL) μm/s	92.8± 13.2	95.6± 5.1	101.6± 8.8	100.7± 7.9
Lateral Amplitude μm	3.5± 0.7	3.7± 1.1	4.1± 2.1	3.8± 0.9
Beat Frequency Hz	54.1± 1.8	53.1± 1.4	54.7± 2.3	54.9± 1.4
Straightness %	43.6± 7.8	41.0± 2.5	40.0± 3.2	42.2± 6.1
Linearity %	15.8± 4.2	15.0± 2.5	15.4± 4.5	16.0± 6.5
Elongation of sperm head %	65.8± 2.4	63.4± 3.2	63.4± 1.8	64.6± 3.7
Area μm	5.9± 0.8	5.7± 0.5	5.7± 1.0	5.2± 0.8

C D E

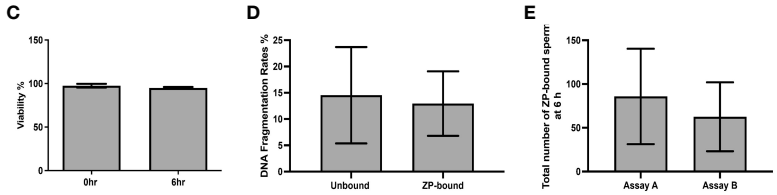

FIGURE 1
The total number of ZP-bound spermatozoa over the 6-h and 20-h incubation. **(A)** The number of spermatozoa tightly bound to the oocytes was counted at 2 h intervals during the 6-h incubation. There was a large variation in the number of ZP-bound spermatozoa, but the decreasing trend persisted in all samples. All data are represented as median (range) (n=24 for 6-h; n=6 for 20-h, p<0.05). **(B)** Effects of prolonged incubation on sperm motility at intervals of 0, 2, 4, 6 h. **(C, D)** Effects of prolonged incubation on sperm viability and DNA integrity at 0 and 6 hr. **(E)** The total number of ZP-bound spermatozoa with (Assay A) /without (Assay B) the replacement of fresh oocytes at 4 hr. All data are represented as mean ± SD (n=5).

in raw semen with a high DNA fragmentation rate of 19.1% (Supplementary Figure 3). AO staining (Supplementary Figure 2C) was used to evaluate the chromatin structure and to differentiate spermatozoa with normal double-stranded DNA from those with abnormal single-stranded DNA. The number of spermatozoa with green fluorescence was significantly higher in the ZP-bound than the unbound spermatozoa (93.1% vs. 64.3%, p<0.05) (Figure 5C). There was a small proportion of ZP-bound spermatozoa with red fluorescence (6.4% on average) in both swim-up and raw sample groups (Supplementary Figure 3), indicating a correlation between the ZP-binding ability and chromatin integrity of spermatozoa.

3.5 Evaluation of protamination and methylation of ZP-bound and unbound spermatozoa

CMA3 staining (Supplementary Figure 2D)was used to indirectly evaluate the degree of protamination in spermatozoa. CMA3 is a fluorochrome that specifically binds to the same location as protamines at the GC-rich sequences. Spermatozoa with protamine deficiency appeared bright yellow whilst those with proper protamination fluoresced light yellow with different degrees of signal intensity (Figure 5D). The level of CMA3 positivity was significantly lower in ZP-bound than in the

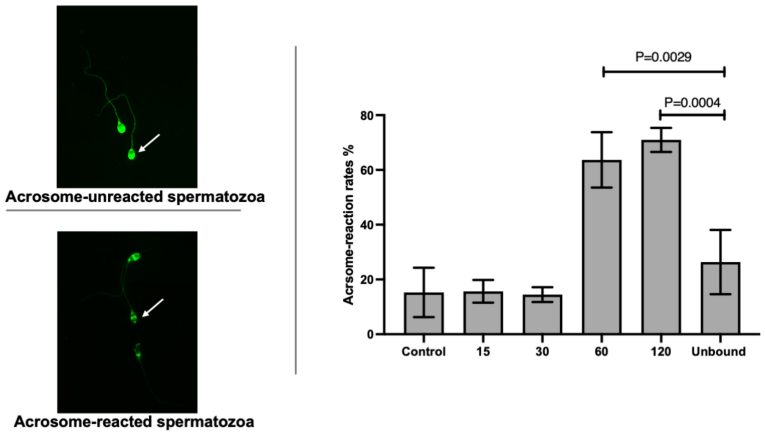

FIGURE 2
Time-course study of acrosome-reaction rates in ZP-bound spermatozoa. Acrosomal status of the control, unbound spermatozoa, ZP-bound spermatozoa (recovered at 15, 30, 60 and 120min) was determined by FITC-PSA. All data are represented as mean ± SD (n=4, p<0.05).

unbound spermatozoa ($p<0.05$) (Figure 5D), suggesting that the human ZP selectively bound to spermatozoa with high degree of protamination. Immunofluorescent staining for the methylated regions (Supplementary figure 2E) was used to evaluate the overall methylation level of ZP-bound and unbound spermatozoa. Spermatozoa displayed varying degrees of green fluorescence depending on the DNA methylation level (Figure 5E). The overall methylation level was higher in ZP-bound than in the unbound spermatozoa (Figure 5E), as reflected by the signal intensity.

4 Discussion

Spermatozoa-ZP binding assay was first established by Overstreet and Hembree to examine the interaction between the non-viable oocytes and spermatozoa *in vitro* (29). Considering the small number of motile spermatozoa with ZP-binding ability in fertile donors (25, 30), it is logical to assume that this species-specific interaction might shed light on the potential use of ZP to select high-quality spermatozoa *in vitro*. In this study, the ZP-bound spermatozoa were found with higher rates of normal morphology, acrosome reaction rates, and DNA integrity when compared with the controls, consistent with previous studies demonstrating the selective nature of ZP to spermatozoa to fertilization-competent spermatozoa (31–33). Clinical studies using ZP-selected spermatozoa demonstrated minimal advantages on the fertilization and implantation rates but greatly improved the embryo qualities and pregnancy rates (34–37).

In this study, a modified continuous coincubation assay was used to collect spermatozoa without ZP-binding ability by gradually removing the ZP-bound spermatozoa from the incubation droplet at 2-h intervals over a 6-h period. Our results demonstrated that the total number of ZP-bound spermatozoa varied distinctively among samples, consistent with previous findings reporting on the differences in the number of motile spermatozoa with ZP-binding ability between fertile and infertile men (25). The time-course data indicated that about 50% of the motile spermatozoa with ZP-binding ability bound to the ZP within the first 2 h and gradually decreased over time until the end of coincubation at 6 hr. In comparison with a previous study (25), the overall percentage of ZP-bound spermatozoa recovered by our protocol was significantly lower (0.03% vs. 14.0% in fertile men). The discrepancy is likely due to the difference in protein concentration of BSA or other specific molecules related to ZP-binding ability. The number of ZP-bound spermatozoa is higher in culture medium supplemented with human serum than with BSA (38). Liu et al. also reported that the number of ZP-bound spermatozoa exponentially increased over 6 h, which differed from our results. Capacitation is a time-dependent process (39). It is possible that the components of the culture medium could affect capacitation during which the spermatozoa acquire ZP-binding ability (40), although human spermatozoa tend to complete capacitation within 3 h (41, 42). We also performed additional tests to confirm that the repeated uses of oocytes did not affect the ZP-binding results and that the extended incubation had no negative impact on the sperm parameters, excluding the possibility that the low ZP-binding efficiency was caused by progressive loss of functional and/or structural properties of the ZP and spermatozoa during incubation.

Spermatozoa-ZP binding interaction involves the recognition of ligands by the protein receptors on the plasma membrane of capacitated spermatozoa. Ultrasensitive analysis by mass spectrometry revealed that human ZP glycans are terminated with a high abundance of Siayl-LewisX (SLeX) sequences (43). Treatment targeting against SLeX sequences inhibits approximately 70% of spermatozoa-ZP binding (43). Moreover, recombinant human ZP-proteins with glycosylation different from their native counterparts are capable of binding to human spermatozoa (44, 45). The results suggested that both glycan-protein and protein-protein interactions are involved in spermatozoa-ZP binding. Proteomic studies identified a list of potential ZP receptors located on the plasma membrane of capacitated spermatozoa (46–48). During capacitation, dynamic changes occur on the sperm proteome to facilitate conformational modifications or exposure of ZP receptors located on the plasma

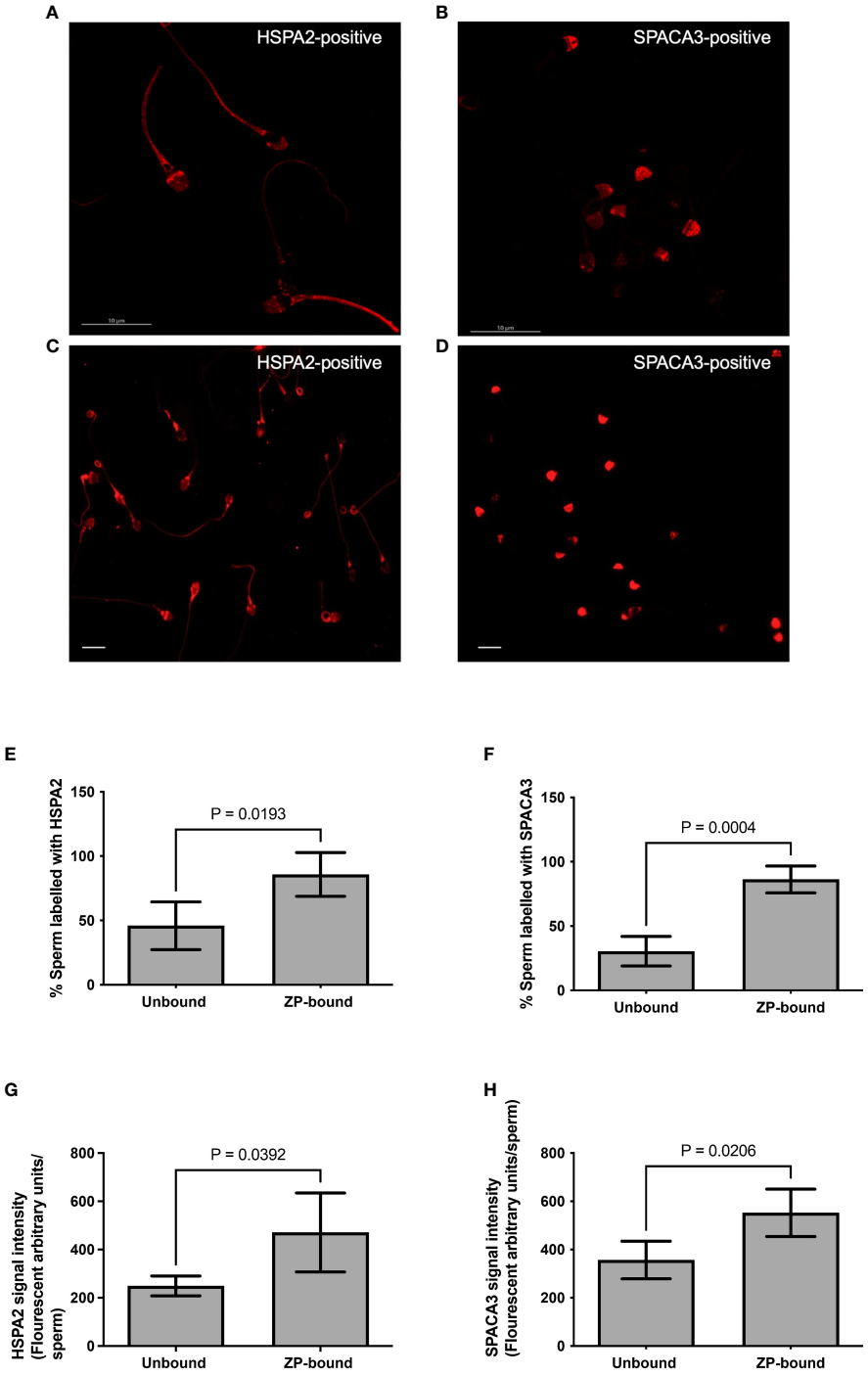

FIGURE 3
Immunolocalization of HSPA2 and SPACA3 on capacitated human spermatozoa. **(A, B)** Capacitated spermatozoa were labelled with anti-HSPA2 and SPACA3 antibodies (diluted 1:100) respectively followed by Alexa-555 secondary antibodies. The images captured using confocal microscopy showed granular staining patterns of HSPA2 and SPACA3 on spermatozoa. Scale bar = 10 μM. **(C)** HSPA2 was localized to the peri-acrosomal region, equatorial segment, post-acrosomal region, mid-piece and the sperm tail. **(D)** SPACA3 was localized to the acrosomal region. Scale bar=200 uM. **(E, F)** Quantification of ZP-bound recovered at 30 min and unbound spermatozoa showing positive staining with HSPA2 and SPACA3 at the head regions. All data are represented as mean ± SD (n=4, $p<0.05$). **(G, H)** Fluorescence intensity analysis of each protein marker was performed by the Image J software. All data are represented as mean ± SD (n=4, $p<0.05$).

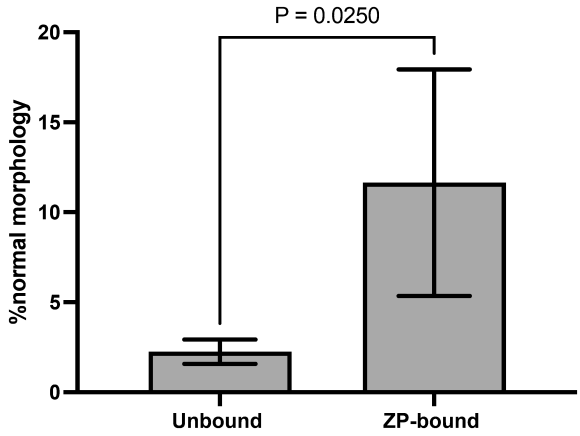

FIGURE 4
Morphology evaluation of ZP-bound and unbound spermatozoa. ZP-bound and unbound spermatozoa were classified as having normal or abnormal morphology according to the WHO strict criteria. All data are represented as mean ± SD (n=5, $p<0.05$).

membrane of acrosome-intact spermatozoa (49, 50). Soon after ZP-binding, acrosome reaction is initiated in ZP-bound spermatozoa to facilitate the subsequent penetration through the ZP. Thus, the acrosomal status is an indirect evaluation of sperm fertilization potential. Many membrane proteins, such as sperm adhesion molecule 1 (also known as PH-20), are also found on the inner acrosomal region of spermatozoa, which become exposed after the ZP binding interaction (51). In this study, we determined the optimal time-point to collect acrosome-intact, ZP-bound spermatozoa. Acrosome reaction is a time-dependent process. Consistently, after binding to the ZP, mouse spermatozoa remain acrosome-unreacted for approximately 40 min before commencing acrosome-reaction (52). Using the time-lapse fluorescence microscopy, it has been demonstrated that calcium ionophore (A23187) and progesterone induce acrosome reaction in human spermatozoa within 12 min (53). There is a lack of time-lapse study on the acrosome reaction rates of ZP-bound spermatozoa in humans. Our results demonstrated that majority of spermatozoa bound to the ZP for less than 30 min were acrosome-intact and approximately 60% of the ZP-bound spermatozoa became acrosome-reacted after 60 min. The ZP-bound spermatozoa recovered at 60 and 120 min had significantly higher acrosome reaction rates than the unbound ones.

In this study, the ZP-bound spermatozoa were recovered within 30 min to maximize the possibility of collecting acrosome-intact spermatozoa. The expression levels of HSPA2 and SPACA3 were about two times higher on the ZP-bound spermatozoa than on the unbound ones. HSPA2 is a testis-enriched member of the 70 kDa heat shock proteins (HSP-70) family, which promotes proper protein folding, translocation of intracellular proteins, and assembly of multimeric protein complexes (54). In humans, the HSPA2 gene expression is downregulated in men with azoospermia (55), varicocele and oligozoospermia (56), and idiopathic oligoteratozoospermia (57). The expression level of HSPA2 is positively correlated with maturity (58, 59), ability of binding to ZP and cumulus complexes (58, 60), and fertilization potential (58, 61–63) of human spermatozoa. Emerging studies suggest that HSPA2 remains predominantly intracellular in human spermatozoa, which serves as a chaperone to mediate the assembly of multimeric protein complexes located on the anterior region of the sperm head for ZP binding (64–66). During capacitation, HSPA2 is translocated from the inner to the outer leaflet of the plasma membrane, leading to an increased level of HSPA2 on spermatozoa (62, 67). HSPA2 interacts with the sperm adhesion molecule 1 (SPAM1) and arylsulfatase A (ARSA) to form an acrosomal domain for spermatozoa-ZP recognition. A lack of HSPA2 is found in infertile patients with defective ZP-binding ability (64). In this study, our results suggested that the expression level of HSPA2 on spermatozoa was reflective of their ZP-binding ability.

SPACA3, also known as SLLP1, is highly homologous with c-lysozyme and retains the putative substrate-binding residues conserved across mammals, such as humans and mice, for the binding to oligosaccharides of N-acetylglucosamine (GlcNAc) (68, 69). In mice, SLLP1 specifically binds to the receptors within the perivitelline space and on the plasma membrane of oocyte *in vitro* (70). The recombinant SLLP1 and antibodies directed against SLLP1 suppress the binding of spermatozoa to cumulus intact and ZP-free oocytes (70). This observation implies a functional role of SLLP1 in spermatozoa-oolemma interaction during fertilization. It is logical to assume that SLLP1 can participate in the spermatozoa-ZP binding interaction since GlcNAc has been identified on mammalian ZP (71–73). Partial inhibition of spermatozoa-ZP binding occurs when capacitated spermatozoa are pre-treated with GlcNAc or ZP is pre-incubated with glycosidase N-acetylglucosaminidase *in vitro* prior to hemizona assay (74, 75). The involvement of SLLP1 in spermatozoa-ZP interaction was further supported by a modified spermatozoa-ZP binding assay in which the calcium ions in the culture and co-incubation medium were replaced by the strontium ions to ensure that the spermatozoa were allowed to undergo capacitation required for ZP- binding, but not acrosome reaction following the binding interaction (76). This experimental condition demonstrated the inhibitory effects of exogenous GlcNAc specifically on

10.3389/fendo.2023.1135973

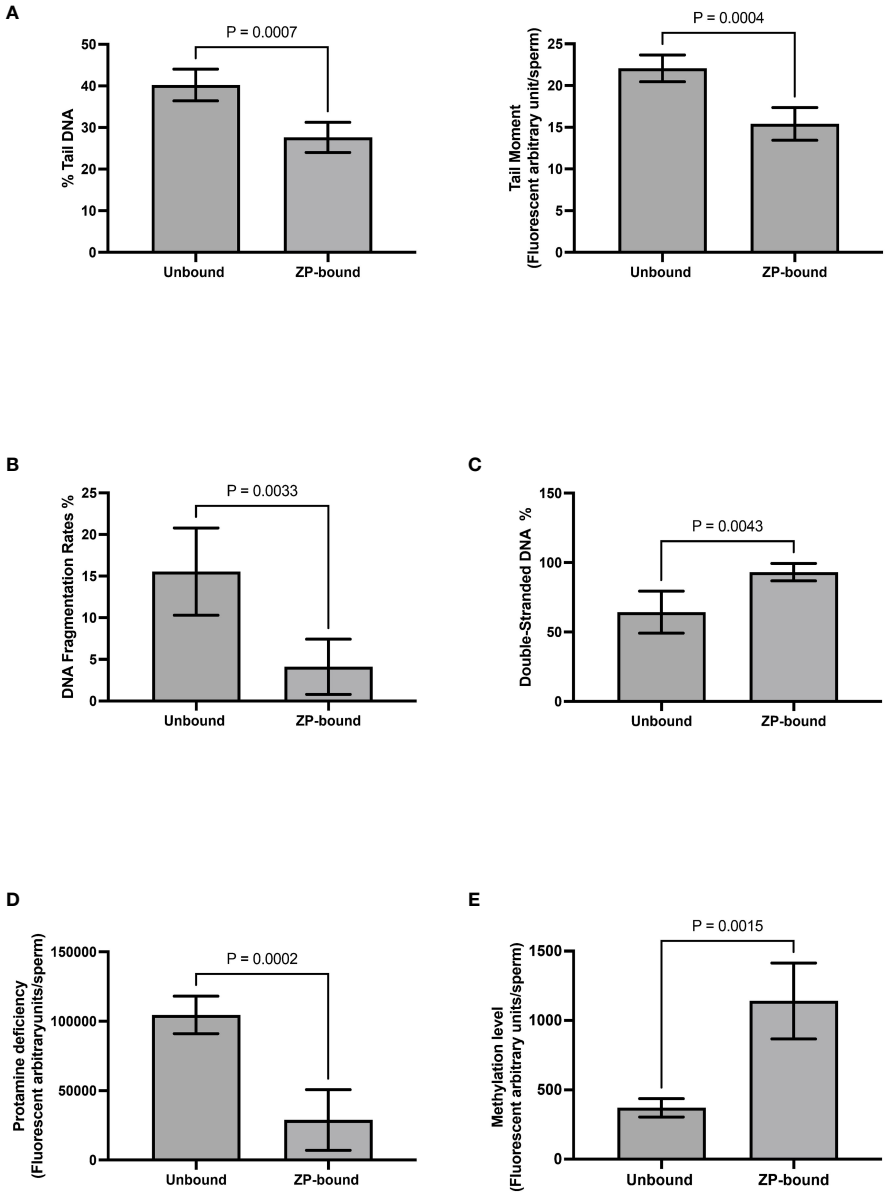

FIGURE 5
Evaluation of genetic qualities and epigenetic profile of ZP-bound and unbound spermatozoa. Quantification of **(A)** Comet-positive spermatozoa with different levels of DNA damages as reflected by the (Left) %tail DNA and (Right) tail moment **(B)** TUNEL-positive spermatozoa **(C)** AO-stained spermatozoa with double-stranded DNA in green fluorescence **D)** CMA3-positive spermatozoa with different levels of protamine deficiency as reflected by the yellow fluorescence intensity. **(E)** 5-Mc-positive spermatozoa with different levels of methylation as reflected by the green fluorescence intensity. All data are represented as mean ± SD (n=5 for **(A–E)**, $p<0.05$).

spermatozoa- ZP binding (76). According to our results, neither HSPA2 nor SPACA3 were uniformly expressed on the entire population of ZP-bound spermatozoa, corroborating previous findings that the absence of a single protein receptor is highly unlikely to cause complete failure of spermatozoa-ZP binding because the ZP-receptor is a multimolecular structure assembled during capacitation (23, 77). Nevertheless, the expression level of a single marker could reflect the ability of spermatozoa acquiring the appropriate molecules required for ZP-binding during transit through the reproductive tract. The fluorescence intensity of protein markers can serve as an additional surrogate marker relevant to sperm fertilizing capability and genetic quality, which might in turn increase the discriminating power of the conventional semen analysis. If the protein markers are to become useful as diagnostic tools, clinical samples with varying degrees of ZP-binding ability should be collected to establish clinical thresholds of protein expressions.

DNA damages in spermatozoa are primarily induced by abortive apoptosis during spermatogenesis, chromatin remodeling during spermiogenesis, and oxidative stress during migration through the male reproductive tract (78). Under physiological circumstances, a low level of reactive oxygen species (ROS) is needed for physiological functions such as cellular activities and signaling pathways in spermatozoa (79). Oxidative stress as a result

of excessive ROS production is closely related to male infertility (80). In some cases, spermatozoa with genetic abnormalities can retain their fertilizing ability leading to fertilization success, but the genetic defects might later manifest themselves as late paternal effects (81), resulting in a higher rate of suboptimal embryo development, pregnancy failure and pregnancy complications (82, 83). The level of DNA fragmentation is associated with lower pregnancy rates in IVF cycles following conventional insemination but not in intracytoplasmic sperm injection cycles (84), although increased miscarriage rates (84) and reduced live birth rates (85) are observed in both conventional insemination and intracytoplasmic sperm injection cycles. The ZP-binding ability of spermatozoa was closely related to their DNA integrity and chromatin status. Both alkaline Comet and TUNEL assays are developed to examine the overall level of DNA damages in spermatozoa. Alkaline Comet assay is a relatively sensitive method for measurement of single and double-strand breaks in spermatozoa. In this method, the fragmented DNA migrate out of the sperm head towards the anode forming a comet tail under an applied electrical field. The degree of DNA fragmentation is reflected by the fluorescence intensity and the length of the Comet tail. A high degree of DNA fragmentation measured by the comet assay is correlated with the lower rates of fertilization, good embryo development and implantation (86). TUNEL assay involves the attachment of fluorescently modified nucleotide to the free 3'- OH terminal of single- and double-stranded DNA mediated by TdT (87). The DNA fragmentation index is negatively correlated with inferior sperm parameters in terms of concentration, viability, motility, and morphology (88, 89). In this study, both methods demonstrated that the number of spermatozoa with fragmented DNA was significantly lower in ZP-bound spermatozoa than the unbound ones, implicating the relationship between the ZP-binding ability and genetic quality of spermatozoa.

AO intercalates into normal double-stranded DNA as a monomer and fluoresces green as opposed to binding to the denatured, single-stranded DNA as an aggregate which fluoresces yellow to red depending on the extent of the damages (90). The number of spermatozoa with green fluorescence was significantly higher in the ZP-bound spermatozoa than in the unbound ones, suggesting that the spermatozoa-ZP interaction is highly selective for spermatozoa with normal, double-stranded DNA. In contrast to the TUNEL results, the AO staining results demonstrated that the swim-up method failed to eliminate spermatozoa with abnormal genetic integrity; the number of spermatozoa with yellow-red fluorescence in post-swim-up samples was comparable to those in raw samples, consistent with previous findings that showed the lack of correlation between motility and chromatin integrity of spermatozoa (91).

In addition to genetic integrity, the epigenetic patterns of spermatozoa have been linked to embryonic development, implantation success, and the offspring health following ICSI (92, 93). Spermatozoa undergo epigenetic modifications including chromatin remodeling, DNA methylation, and non-coding RNAs to regulate transcriptional activities and gene expression at post-transcriptional level (94, 95). Aberrant epigenetic profiles in spermatozoa have been implicated in male idiopathic infertility. Protamine protein 1 and 2 (P1 and 2) are equally distributed in spermatozoa of healthy men. P1/2 imbalance is associated with poor sperm parameters and male infertility (96–99). Furthermore, abnormal methylation patterns at specific loci, such as H-19 and mesoderm-specific transcript (MEST), have been found in men with male-factor infertility (100–103). Aberrant global methylation levels are associated with suboptimal sperm parameters (104–106) and male infertility (107, 108). Our results indicated that the ZP-binding ability of spermatozoa was closely related to their epigenetic patterns in terms of protamination degree and global methylation level. The examination of methylation status at specific loci might definitively answer the question as to whether hypomethylation or hypermethylation is the major factor leading to suboptimal ZP-binding ability. To pinpoint the specific locus associated with ZP-binding ability, future investigation is needed to examine the DNA methylation profile of ZP-bound spermatozoa by single-cell bisulfite sequencing (109, 110). While the complicated staining and quantification procedures restrict wide application of genetic evaluation in clinical settings, future investigation should seek to develop a highly robust, indirect evaluation of sperm quality metrics by image analysis of sperm morphology associated with genetic integrity (111) and epigenetic pattern to establish a comprehensive profile of clinical samples.

5 Conclusion

Although conventional semen analysis is useful for establishing a fertility profile of men, it fails to provide diagnostic information regarding the sperm fertilization potential. The spermatozoa-ZP interaction serves as an integral part of the natural sperm selection mechanisms *in vivo*, which can potentially be used for sperm evaluation and selection in clinical settings. An early detection of defective ZP-binding ability in men with normal semen parameters could be offered intracytoplasmic sperm injection instead of conventional insemination, preventing them from financial and psychological sufferings caused by the low or no fertilization rates following conventional insemination. HPSPA2 and SPACA3 are the protein markers associated with the ZP-binding ability of spermatozoa. There was a quantitative difference in the expression level of HSPA2 and SPACA3 between acrosome intact, ZP-bound and unbound spermatozoa. Although the ZP-receptor is likely a multi-molecular structure, the expression level of a single marker could reflect the ability of spermatozoa acquiring the appropriate molecules required for ZP-binding during transit through the reproductive tract. Our results demonstrated that the ZP-binding ability of spermatozoa was closely related to their genetic quality in terms of DNA integrity, chromatin structure, protamination degree and global methylation level. Human ZP was highly selective for genetically normal spermatozoa with distinct epigenetic profiles. If the spermatozoa-ZP interaction is to become useful as a clinical tool, clinical samples with varying degrees of ZP-binding ability should be collected to establish a representative database for identification of high-quality spermatozoa by image analysis of sperm morphology. Taken together, the development of a robust and reproducible selection method incorporating the ZP-

binding ability of spermatozoa might improve the overall workflow and the pregnancy outcomes in ART.

Data availability statement

The original contributions presented in the study are included in the article/Supplementary Material. Further inquiries can be directed to the corresponding authors.

Ethics statement

The studies involving human participants were reviewed and approved by Institutional Review Board of the University of Hong Kong/Hospital Authority Hong Kong West Cluster. The patients/participants provided their written informed consent to participate in this study.

Author contributions

WY and PC conceived and designed the project. EL, BL, and KL collected samples and conducted experiments. EL and BL analyzed and interpreted the collected data. EL and PC wrote the first draft of the manuscript. C-LL, XT, KL, RL, EN, WY, and J-PO revised the manuscript. All authors contributed to the article and approved the submitted version.

Funding

This work was supported in part by the Health and Medical Research Fund, the Food and Health Bureau, The Government of the HKSAR (07182446), the High Level-Hospital Program, Health Commission of Guangdong Province, China (HKUSZH201902015), and HKU-SZH Fund for Shenzhen Key Medical Discipline (SZXK2020089).

Acknowledgments

We appreciated all participants of this study and the assistance from the andrology laboratory at Family Planning Association of Hong Kong and the IVF laboratory at Queen Mary Hospital, Hong Kong.

Conflict of interest

The authors declare that the research was conducted in the absence of any commercial or financial relationships that could be construed as a potential conflict of interest.

Publisher's note

Supplementary material

The Supplementary Material for this article can be found online at: https://www.frontiersin.org/articles/10.3389/fendo.2023.1135973/full#supplementary-material

References

1. Agarwal A, Mulgund A, Hamada A, Chyatte MR. A unique view on male infertility around the globe. *Reprod Biol Endocrinol* (2015) 13:37. doi: 10.1186/s12958-015-0032-1

2. Kushnir VA, Barad DH, Albertini DF, Darmon SK, Gleicher N. Systematic review of worldwide trends in assisted reproductive technology 2004-2013. *Reprod Biol Endocrinol* (2017) 15(1):6. doi: 10.1186/s12958-016-0225-2

3. Simon L, Proutski I, Stevenson M, Jennings D, McManus J, Lutton D, et al. Sperm DNA damage has a negative association with live-birth rates after IVF. *Reprod BioMed Online* (2013) 26(1):68–78. doi: 10.1016/j.rbmo.2012.09.019

4. Chapuis A, Gala A, Ferrières-Hoa A, Mullet T, Bringer-Deutsch S, Vintejoux E, et al. Sperm quality and paternal age: effect on blastocyst formation and pregnancy rates. *Bas Clin Androl* (2017) 27:2. doi: 10.1186/s12610-016-0045-4

5. Leung ETY, Lee CL, Tian X, Lam KKW, Li RHW, Ng EHY, et al. Simulating nature in sperm selection for assisted reproduction. *Nat Rev Urol* (2022) 19(1):16–36. doi: 10.1038/s41585-021-00530-9

6. Stevanato J, Bertolla RP, Barradas V, Spaine DM, Cedenho AP, Ortiz V. Semen processing by density gradient centrifugation does not improve sperm apoptotic deoxyribonucleic acid fragmentation rates. *Fertil Steril* (2008) 90(3):889–90. doi: 10.1016/j.fertnstert.2007.01.059

7. Muratori M, Tarozzi N, Cambi M, Boni L, Iorio AL, Passaro C, et al. Variation of DNA fragmentation levels during density gradient sperm selection for assisted reproduction techniques: A possible new Male predictive parameter of pregnancy? *Med (Baltimore)* (2016) 95(20):e3624. doi: 10.1097/md.0000000000003624

8. Shirota K, Yotsumoto F, Itoh H, Obama H, Hidaka N, Nakajima K, et al. Separation efficiency of a microfluidic sperm sorter to minimize sperm DNA damage. *Fertil Steril* (2016) 105(2):315–21. doi: 10.1016/j.fertnstert.2015.10.023

9. Quinn MM, Jalalian L, Ribeiro S, Ona K, Demirci U, Cedars MI, et al. Microfluidic sorting selects sperm for clinical use with reduced DNA damage compared to density gradient centrifugation with swim-up in split semen samples. *Hum Reprod* (2018) 33(8):1388–93. doi: 10.1093/humrep/dey239

10. Zhang H, Xuan X, Yang S, Li X, Xu C, Gao X. Selection of viable human spermatozoa with low levels of DNA fragmentation from an immotile population using density gradient centrifugation and magnetic-activated cell sorting. *Andrologia* (2018) 50(1):e12821. doi: 10.1111/and.12821

11. Nasr-Esfahani MH, Deemeh MR, Tavalaee M. New era in sperm selection for ICSI. *Int J Androl* (2012) 35(4):475–84. doi: 10.1111/j.1365-2605.2011.01227.x

12. Sakkas D. Novel technologies for selecting the best sperm for *in vitro* fertilization and intracytoplasmic sperm injection. *Fertil Steril* (2013) 99(4):1023–9. doi: 10.1016/j.fertnstert.2012.12.025

13. Vaughan DA, Sakkas D. Sperm selection methods in the 21st century. *Biol Reprod* (2019) 101(6):1076–82. doi: 10.1093/biolre/ioz032

14. Marzano G, Chiriacò MS, Primiceri E, Dell'Aquila ME, Ramalho-Santos J, Zara V, et al. Sperm selection in assisted reproduction: A review of established methods and cutting-edge possibilities. *Biotechnol Adv* (2020) 40:107498. doi: 10.1016/j.biotechadv.2019.107498

15. Chan PJ, Jacobson JD, Corselli JU, Patton WC. A simple zeta method for sperm selection based on membrane charge. *Fertil Steril* (2006) 85(2):481–6. doi: 10.1016/j.fertnstert.2005.07.1302

16. Gil M, Sar-Shalom V, Melendez Sivira Y, Carreras R, Checa MA. Sperm selection using magnetic activated cell sorting (MACS) in assisted reproduction: a systematic review and meta-analysis. *J Assist Reprod Genet* (2013) 30(4):479–85. doi: 10.1007/s10815-013-9962-8

17. Sakkas D, Ramalingam M, Garrido N, Barratt CL. Sperm selection in natural conception: what can we learn from mother nature to improve assisted reproduction outcomes? *Hum Reprod Update* (2015) 21(6):711–26. doi: 10.1093/humupd/dmv042

18. Yan Y, Zhang B, Fu Q, Wu J, Liu R. A fully integrated biomimetic microfluidic device for evaluation of sperm response to thermotaxis and chemotaxis. *Lab Chip* (2021) 21(2):310–8. doi: 10.1039/d0lc00845a

19. Liu DY, Clarke GN, Martic M, Garrett C, Baker HW. Frequency of disordered zona pellucida (ZP)-induced acrosome reaction in infertile men with normal semen analysis and normal spermatozoa-ZP binding. *Hum Reprod* (2001) 16(6):1185–90. doi: 10.1093/humrep/16.6.1185

20. Liu DY, Baker HW. Frequency of defective sperm-zona pellucida interaction in severely teratozoospermic infertile men. *Hum Reprod* (2003) 18(4):802–7. doi: 10.1093/humrep/deg164

21. Liu DY, Baker HW. High frequency of defective sperm-zona pellucida interaction in oligozoospermic infertile men. *Hum Reprod* (2004) 19(2):228–33. doi: 10.1093/humrep/deh067

22. Liu DY, Liu ML, Garrett C, Baker HW. Comparison of the frequency of defective sperm-zona pellucida (ZP) binding and the ZP-induced acrosome reaction between subfertile men with normal and abnormal semen. *Hum Reprod* (2007) 22(7):1878–84. doi: 10.1093/humrep/dem087

23. Chiu PC, Lam KK, Wong RC, Yeung WS. The identity of zona pellucida receptor on spermatozoa: an unresolved issue in developmental biology. *Semin Cell Dev Biol* (2014) 30:86–95. doi: 10.1016/j.semcdb.2014.04.016

24. Redgrove KA, Anderson AL, Dun MD, McLaughlin EA, O'Bryan MK, Aitken RJ, et al. Involvement of multimeric protein complexes in mediating the capacitation-dependent binding of human spermatozoa to homologous zonae pellucidae. *Dev Biol* (2011) 356(2):460–74. doi: 10.1016/j.ydbio.2011.05.674

25. Liu DY, Garrett C, Baker HW. Low proportions of sperm can bind to the zona pellucida of human oocytes. *Hum Reprod* (2003) 18(11):2382–9. doi: 10.1093/humrep/deg456

26. Liu DY, Stewart T, Baker HW. Normal range and variation of the zona pellucida-induced acrosome reaction in fertile men. *Fertil Steril* (2003) 80(2):384–9. doi: 10.1016/s0015-0282(03)00603-4

27. WHO. *WHO laboratory manual for the examination and processing of human semen. 5th ed*. Geneva: World Health Organization (2011).

28. Chiu PC, Liao S, Lam KK, Tang F, Ho JC, Ho PC, et al. Adrenomedullin regulates sperm motility and oviductal ciliary beat *via* cyclic adenosine 5'-monophosphate/protein kinase a and nitric oxide. *Endocrinology* (2010) 151 (7):3336–47. doi: 10.1210/en.2010-0077

29. Overstreet JW, Hembree WC. Penetration of the zona pellucida of nonliving human oocytes by human spermatozoa *in vitro*. *Fertil Steril* (1976) 27(7):815–31. doi: 10.1016/S0015-0282(16)41959-X

30. Liu DY, Lopata A, Johnston WI, Baker HW. A human sperm-zona pellucida binding test using oocytes that failed to fertilize *in vitro*. *Fertil Steril* (1988) 50(5):782–8. doi: 10.1016/s0015-0282(16)60316-3

31. Bastiaan HS, Windt ML, Menkveld R, Kruger TF, Oehninger S, Franken DR. Relationship between zona pellucida-induced acrosome reaction, sperm morphology, sperm-zona pellucida binding, and *in vitro* fertilization. *Fertil Steril* (2003) 79(1):49–55. doi: 10.1016/s0015-0282(02)04548-x

32. Liu DY, Baker HW. Human sperm bound to the zona pellucida have normal nuclear chromatin as assessed by acridine orange fluorescence. *Hum Reprod* (2007) 22 (6):1597–602. doi: 10.1093/humrep/dem044

33. Liu DY, Liu ML, Clarke GN, Baker HW. Hyperactivation of capacitated human sperm correlates with the zona pellucida-induced acrosome reaction of zona pellucida-bound sperm. *Hum Reprod* (2007) 22(10):2632–8. doi: 10.1093/humrep/dem245

34. Braga DPd.AF, Iaconelli A, Figueira R, d. CS, Madaschi C, Semião-Francisco L, et al. Outcome of ICSI using zona pellucida-bound spermatozoa and conventionally selected spermatozoa. *Reprod BioMed Online* (2009) 19(6):802–7. doi: 10.1016/j.rbmo.2009.09.020

35. Black M, Liu DY, Bourne H, Baker HWG. Comparison of outcomes of conventional intracytoplasmic sperm injection and intracytoplasmic sperm injection using sperm bound to the zona pellucida of immature oocytes. *Fertil Steril* (2010) 93 (2):672–4. doi: 10.1016/j.fertnstert.2009.08.063

36. Liu F, Qiu Y, Zou Y, Deng Z-H, Yang H, Liu DY. Use of zona pellucida–bound sperm for intracytoplasmic sperm injection produces higher embryo quality and implantation than conventional intracytoplasmic sperm injection. *Fertil Steril* (2011) 95(2):815–8. doi: 10.1016/j.fertnstert.2010.09.015

37. Jin R, Bao J, Tang D, Liu F, Wang G, Zhao Y, et al. Outcomes of intracytoplasmic sperm injection using the zona pellucida-bound sperm or manually selected sperm. *J Assist Reprod Genet* (2016) 33(5):597–601. doi: 10.1007/s10815-016-0676-6

38. Yao YQ, Yeung WS, Ho PC. The factors affecting sperm binding to the zona pellucida in the hemizona binding assay. *Hum Reprod* (1996) 11(7):1516–9. doi: 10.1093/oxfordjournals.humrep.a019429

39. Ward CR, Storey BT. Determination of the time course of capacitation in mouse spermatozoa using a chlortetracycline fluorescence assay. *Dev Biol* (1984) 104(2):287–96. doi: 10.1016/0012-1606(84)90084-8

40. Hinrichs K, Love CC, Brinsko SP, Choi YH, Varner DD. *In vitro* fertilization of *in vitro*-matured equine oocytes: effect of maturation medium, duration of maturation, and sperm calcium ionophore treatment, and comparison with rates of fertilization *in vivo* after oviductal transfer. *Biol Reprod* (2002) 67(1):256–62. doi: 10.1095/biolreprod67.1.256

41. Ostermeier GC, Cardona C, Moody MA, Simpson AJ, Mendoza R, Seaman E, et al. Timing of sperm capacitation varies reproducibly among men. *Mol Reprod Dev* (2018) 85(5):387–96. doi: 10.1002/mrd.22972

42. Puga Molina LC, Luque GM, Balestrini PA, Marín-Briggiler CI, Romarowski A, Buffone MG. Molecular basis of human sperm capacitation. *Front Cell Dev Biol* (2018) 6:72. doi: 10.3389/fcell.2018.00072

43. Pang P-C, Chiu PCN, Lee C-L, Chang L-Y, Panico M, Morris HR, et al. Human sperm binding is mediated by the sialyl-lewis(x) oligosaccharide on the zona pellucida. *Science* (2011) 333(6050):1761. doi: 10.1126/science.1207438

44. Chakravarty S, Kadunganattil S, Bansal P, Sharma RK, Gupta SK. Relevance of glycosylation of human zona pellucida glycoproteins for their binding to capacitated human spermatozoa and subsequent induction of acrosomal exocytosis. *Mol Reprod Dev* (2008) 75(1):75–88. doi: 10.1002/mrd.20726

45. Chirinos M, Cariño C, González-González ME, Arreola E, Reveles R, Larrea F. Characterization of human sperm binding to homologous recombinant zona pellucida proteins. *Reprod Sci* (2011) 18(9):876–85. doi: 10.1177/1933719111398146

46. Byrne K, Leahy T, McCulloch R, Colgrave ML, Holland MK. Comprehensive mapping of the bull sperm surface proteome. *Proteomics* (2012) 12(23-24):3559–79. doi: 10.1002/pmic.201200133

47. Wong CW, Lam KKW, Lee CL, Yeung WSB, Zhao WE, Ho PC, et al. The roles of protein disulphide isomerase family a, member 3 (ERp57) and surface thiol/disulphide exchange in human spermatozoa-zona pellucida binding. *Hum Reprod* (2017) 32(4):733–42. doi: 10.1093/humrep/dex007

48. Wang Y, Zhao W, Mei S, Chen P, Leung TY, Lee CL, et al. Identification of sialyl-Lewis(x)-Interacting protein on human spermatozoa. *Front Cell Dev Biol* (2021) 9:700396. doi: 10.3389/fcell.2021.700396

49. Reid AT, Redgrove K, Aitken RJ, Nixon B. Cellular mechanisms regulating sperm-zona pellucida interaction. *Asian J Androl* (2011) 13(1):88–96. doi: 10.1038/aja.2010.74

50. Baker MA, Naumovski N, Hetherington L, Weinberg A, Velkov T, Aitken RJ. Head and flagella subcompartmental proteomic analysis of human spermatozoa. *Proteomics* (2013) 13(1):61–74. doi: 10.1002/pmic.201200350

51. Sabeur K, Cherr GN, Yudin AI, Primakoff P, Li MW, Overstreet JW. The PH-20 protein in human spermatozoa. *J Androl* (1997) 18(2):151–8.

52. Jin M, Fujiwara E, Kakiuchi Y, Okabe M, Satouh Y, Baba SA, et al. Most fertilizing mouse spermatozoa begin their acrosome reaction before contact with the zona pellucida during *in vitro* fertilization. *Proc Natl Acad Sci U.S.A.* (2011) 108 (12):4892–6. doi: 10.1073/pnas.1018202108

53. Harper CV, Cummerson JA, White MR, Publicover SJ, Johnson PM. Dynamic resolution of acrosomal exocytosis in human sperm. *J Cell Sci* (2008) 121(Pt 13):2130–5. doi: 10.1242/jcs.030379

54. Mayer MP, Bukau B. Hsp70 chaperones: cellular functions and molecular mechanism. *Cell Mol Life Sci* (2005) 62(6):670–84. doi: 10.1007/s00018-004-4464-6

55. Son WY, Han CT, Hwang SH, Lee JH, Kim S, Kim YC. Repression of hspA2 messenger RNA in human testes with abnormal spermatogenesis. *Fertil Steril* (2000) 73 (6):1138–44. doi: 10.1016/s0015-0282(00)00496-9

56. Lima SB, Cenedeze MA, Bertolla RP, Filho PA, Oehninger S, Cedenho AP. Expression of the HSPA2 gene in ejaculated spermatozoa from adolescents with and without varicocele. *Fertil Steril* (2006) 86(6):1659–63. doi: 10.1016/j.fertnstert.2006.05.030

57. Cedenho AP, Lima SB, Cenedeze MA, Spaine DM, Ortiz V, Oehninger S. Oligozoospermia and heat-shock protein expression in ejaculated spermatozoa. *Hum Reprod* (2006) 21(7):1791–4. doi: 10.1093/humrep/del055

58. Huszar G, Stone K, Dix D, Vigue L. Putative creatine kinase m-isoform in human sperm is identifiedas the 70-kilodalton heat shock protein HspA2. *Biol Reprod* (2000) 63(3):925–32. doi: 10.1095/biolreprod63.3.925

59. Huszar G, Ozenci CC, Cayli S, Zavaczki Z, Hansch E, Vigue L. Hyaluronic acid binding by human sperm indicates cellular maturity, viability, and unreacted acrosomal status. *Fertil Steril* (2003) 79:1616–24. doi: 10.1016/s0015-0282(03)00402-3

60. Huszar G, Ozkavukcu S, Jakab A, Celik-Ozenci C, Sati GL, Cayli S. Hyaluronic acid binding ability of human sperm reflects cellular maturity and fertilizing potential:

selection of sperm for intracytoplasmic sperm injection. *Curr Opin Obstet Gynecol* (2006) 18(3):260–7. doi: 10.1097/01.gco.0000193018.98061.2f

61. Ergur AR, Dokras A, Giraldo JL, Habana A, Kovanci E, Huszar G. Sperm maturity and treatment choice of *in vitro* fertilization (IVF) or intracytoplasmic sperm injection: diminished sperm HspA2 chaperone levels predict IVF failure. *Fertil Steril* (2002) 77(5):910–8. doi: 10.1016/s0015-0282(02)03073-x

62. Motiei M, Tavalaee M, Rabiei F, Hajihosseini R, Nasr-Esfahani MH. Evaluation of HSPA2 in fertile and infertile individuals. *Andrologia* (2013) 45(1):66–72. doi: 10.1111/j.1439-0272.2012.01315.x

63. Heidari M, Darbani S, Darbandi M, Lakpour N, Fathi Z, Zarnani AH, et al. Assessing the potential of HSPA2 and ADAM2 as two biomarkers for human sperm selection. *Hum Fertil (Camb)* (2020) 23(2):123–33. doi: 10.1080/14647273.2018.1534277

64. Redgrove KA, Nixon B, Baker MA, Hetherington L, Baker G, Liu DY, et al. The molecular chaperone HSPA2 plays a key role in regulating the expression of sperm surface receptors that mediate sperm-egg recognition. *PloS One* (2012) 7(11):e50851. doi: 10.1371/journal.pone.0050851

65. Redgrove KA, Anderson AL, McLaughlin EA, Bryan MK, Aitken RJ, Nixon B. Investigation of the mechanisms by which the molecular chaperone HSPA2 regulates the expression of sperm surface receptors involved in human sperm-oocyte recognition. *Mol Hum Reprod* (2013) 19(3):120–35. doi: 10.1093/molehr/gas064

66. Gómez-Torres MJ, Huerta-Retamal N, Robles-Gómez L, Sáez-Espinosa P, Aizpurua J, Avilés M, et al. Arylsulfatase a remodeling during human sperm *In vitro* capacitation using field emission scanning electron microscopy (FE-SEM). *Cells* (2021) 10(2):222. doi: 10.3390/cells10020222

67. Huerta-Retamal N, Sáez-Espinosa P, Robles-Gómez L, Avilés M, Romero A, Aizpurua J, et al. Human sperm chaperone HSPA2 distribution during *in vitro* capacitation. *J Reprod Immunol* (2021) 143:103246. doi: 10.1016/j.jri.2020.103246

68. Mandal A, Klotz KL, Shetty J, Jayes FL, Wolkowicz MJ, Bolling LC, et al. SLLP1, a unique, intra-acrosomal, non-bacteriolytic, c lysozyme-like protein of human spermatozoa. *Biol Reprod* (2003) 68(5):1525–37. doi: 10.1095/biolreprod.102.010108

69. Zheng H, Mandal A, Shumilin IA, Chordia MD, Panneerdoss S, Herr JC, et al. Sperm lysozyme-like protein 1 (SLLP1), an intra-acrosomal oolemmal-binding sperm protein, reveals filamentous organization in protein crystal form. *Andrology* (2015) 3(4):756–71. doi: 10.1111/andr.12057

70. Herrero MB, Mandal A, Digilio LC, Coonrod SA, Maier B, Herr JC. Mouse SLLP1, a sperm lysozyme-like protein involved in sperm-egg binding and fertilization. *Dev Biol* (2005) 284(1):126–42. doi: 10.1016/j.ydbio.2005.05.008

71. Wassarman PM. Zona pellucida glycoproteins. *Annu Rev Biochem* (1988) 57:415–42. doi: 10.1146/annurev.bi.57.070188.002215

72. Sinowatz F, Töpfer-Petersen E, Kölle S, Palma G. Functional morphology of the zona pellucida. *Anat Histol Embryol* (2001) 30(5):257–63. doi: 10.1046/j.1439-0264.2001.00337.x

73. Jiménez-Movilla M, Avilés M, Gómez-Torres MJ, Fernández-Colom PJ, Castells MT, de Juan J, et al. Carbohydrate analysis of the zona pellucida and cortical granules of human oocytes by means of ultrastructural cytochemistry. *Hum Reprod* (2004) 19(8):1842–55. doi: 10.1093/humrep/deh311

74. Miranda PV, Gonzalez-Echeverría F, Marín-Briggiler CI, Brandelli A, Blaquier JA, Tezón JG. Glycosidic residues involved in human sperm-zona pellucida binding *in vitro*. *Mol Hum Reprod* (1997) 3(5):399–404. doi: 10.1093/molehr/3.5.399

75. Miranda PV, González-Echeverría F, Blaquier JA, Mahuran DJ, Tezón JG. Evidence for the participation of beta-hexosaminidase in human sperm-zona pellucida interaction *in vitro*. *Mol Hum Reprod* (2000) 6(8):699–706. doi: 10.1093/molehr/6.8.699

76. Zitta K, Wertheimer E, Miranda PV. Analysis of the participation of n-acetylglucosamine in the different steps of sperm-zona pellucida interaction in hamster. *Mol Hum Reprod* (2004) 10(12):925–33. doi: 10.1093/molehr/gah122

77. Petit FM, Serres C, Bourgeon F, Pineau C, Auer J. Identification of sperm head proteins involved in zona pellucida binding. *Hum Reprod* (2013) 28(4):852–65. doi: 10.1093/humrep/des452

78. Panner Selvam MK, Ambar RF, Agarwal A, Henkel R. Etiologies of sperm DNA damage and its impact on male infertility. *Andrologia* (2021) 53(1):e13706. doi: 10.1111/and.13706

79. Ford WC. Regulation of sperm function by reactive oxygen species. *Hum Reprod Update* (2004) 10(5):387–99. doi: 10.1093/humupd/dmh034

80. Aitken RJ, Baker MA. The role of genetics and oxidative stress in the etiology of Male infertility-a unifying hypothesis? *Front Endocrinol (Lausanne)* (2020) 11:581838. doi: 10.3389/fendo.2020.581838

81. Tesarik J. Late, but not early, paternal effect on human embryo development is related to sperm DNA fragmentation. *Hum Reprod* (2004) 19(3):611–5. doi: 10.1093/humrep/deh127

82. Twigg JP, Irvine DS, Aitken RJ. Oxidative damage to DNA in human spermatozoa does not preclude pronucleus formation at intracytoplasmic sperm injection. *Hum Reprod* (1998) 13(7):1864–71. doi: 10.1093/humrep/13.7.1864

83. Zini A, Meriano J, Kader K, Jarvi K, Laskin CA, Cadesky K. Potential adverse effect of sperm DNA damage on embryo quality after ICSI. *Hum Reprod* (2005) 20(12):3476–80. doi: 10.1093/humrep/dei266

84. Zhao J, Zhang Q, Wang Y, Li Y. Whether sperm deoxyribonucleic acid fragmentation has an effect on pregnancy and miscarriage after *in vitro* fertilization/intracytoplasmic sperm injection: a systematic review and meta-analysis. *Fertil Steril* (2014) 102(4):998–1005.e1008. doi: 10.1016/j.fertnstert.2014.06.033

85. Osman A, Alsomait H, Seshadri S, El-Toukhy T, Khalaf Y. The effect of sperm DNA fragmentation on live birth rate after IVF or ICSI: a systematic review and meta-analysis. *Reprod BioMed Online* (2015) 30(2):120–7. doi: 10.1016/j.rbmo.2014.10.018

86. Simon L, Liu L, Murphy K, Ge S, Hotaling J, Aston KI, et al. Comparative analysis of three sperm DNA damage assays and sperm nuclear protein content in couples undergoing assisted reproduction treatment. *Hum Reprod* (2014) 29(5):904–17. doi: 10.1093/humrep/deu040

87. Sharma R, Masaki J, Agarwal A. Sperm DNA fragmentation analysis using the TUNEL assay. *Methods Mol Biol* (2013) 927:121–36. doi: 10.1007/978-1-62703-038-0_12

88. Cohen-Bacrie P, Belloc S, Ménézo YJ, Clement P, Hamidi J, Benkhalifa M. Correlation between DNA damage and sperm parameters: a prospective study of 1,633 patients. *Fertil Steril* (2009) 91(5):1801–5. doi: 10.1016/j.fertnstert.2008.01.086

89. Nijs M, De Jonge C, Cox A, Janssen M, Bosmans E, Ombelet W. Correlation between male age, WHO sperm parameters, DNA fragmentation, chromatin packaging and outcome in assisted reproduction technology. *Andrologia* (2011) 43(3):174–9. doi: 10.1111/j.1439-0272.2010.01040.x

90. Tejada RI, Mitchell JC, Norman A, Marik JJ, Friedman S. A test for the practical evaluation of male fertility by acridine orange (AO) fluorescence. *Fertil Steril* (1984) 42(1):87–91. doi: 10.1016/s0015-0282(16)47963-x

91. Eggert-Kruse W, Rohr G, Kerbel H, Schwalbach B, Demirakca T, Klinga K, et al. The acridine orange test: a clinically relevant screening method for sperm quality during infertility investigation? *Hum Reprod* (1996) 11(4):784–9. doi: 10.1093/oxfordjournals.humrep.a019255

92. Georgiou I, Syrrou M, Pardalidis N, Karakitsios K, Mantzavinos T, Giotitsas N, et al. Genetic and epigenetic risks of intracytoplasmic sperm injection method. *Asian J Androl* (2006) 8(6):643–73. doi: 10.1111/j.1745-7262.2006.00231.x

93. Sharma R, Agarwal A, Rohra VK, Assidi M, Abu-Elmagd M, Turki RF. Effects of increased paternal age on sperm quality, reproductive outcome and associated epigenetic risks to offspring. *Reprod Biol Endocrinol* (2015) 13:35. doi: 10.1186/s12958-015-0028-x

94. Donkin I, Barrès R. Sperm epigenetics and influence of environmental factors. *Mol Metab* (2018) 14:1–11. doi: 10.1016/j.molmet.2018.02.006

95. Åsenius F, Danson AF, Marzi SJ. DNA Methylation in human sperm: a systematic review. *Hum Reprod Update* (2020) 26(6):841–73. doi: 10.1093/humupd/dmaa025

96. de Yebra L, Ballescá JL, Vanrell JA, Corzett M, Balhorn R, Oliva R. Detection of P2 precursors in the sperm cells of infertile patients who have reduced protamine P2 levels. *Fertil Steril* (1998) 69(4):755–9. doi: 10.1016/s0015-0282(98)00012-0

97. Aoki VW, Liu L, Jones KP, Hatasaka HH, Gibson M, Peterson CM, et al. Sperm protamine 1/protamine 2 ratios are related to *in vitro* fertilization pregnancy rates and predictive of fertilization ability. *Fertil Steril* (2006) 86(5):1408–15. doi: 10.1016/j.fertnstert.2006.04.024

98. Oliva R. Protamines and male infertility. *Hum Reprod Update* (2006) 12(4):417–35. doi: 10.1093/humupd/dml009

99. Nanassy L, Liu L, Griffin J, Carrell DT. The clinical utility of the protamine 1/protamine 2 ratio in sperm. *Protein Pept Lett* (2011) 18(8):772–7. doi: 10.2174/092986611795713934

100. Boissonnas CC, Abdalaoui HE, Haelewyn V, Fauque P, Dupont JM, Gut I, et al. Specific epigenetic alterations of IGF2-H19 locus in spermatozoa from infertile men. *Eur J Hum Genet* (2010) 18(1):73–80. doi: 10.1038/ejhg.2009.117

101. Hammoud SS, Purwar J, Pflueger C, Cairns BR, Carrell DT. Alterations in sperm DNA methylation patterns at imprinted loci in two classes of infertility. *Fertil Steril* (2010) 94(5):1728–33. doi: 10.1016/j.fertnstert.2009.09.010

102. Cui X, Jing X, Wu X, Yan M, Li Q, Shen Y, et al. DNA Methylation in spermatogenesis and male infertility. *Exp Ther Med* (2016) 12(4):1973–9. doi: 10.3892/etm.2016.3569

103. Santi D, De Vincentis S, Magnani E, Spaggiari G. Impairment of sperm DNA methylation in male infertility: a meta-analytic study. *Andrology* (2017) 5(4):695–703. doi: 10.1111/andr.12379

104. Bahreinian M, Tavalaee M, Abbasi H, Kiani-Esfahani A, Shiravi AH, Nasr-Esfahani MH. DNA Hypomethylation predisposes sperm to DNA damage in individuals with varicocele. *Syst Biol Reprod Med* (2015) 61(4):179–86. doi: 10.3109/19396368.2015.1020116

105. Montjean D, Zini A, Ravel C, Belloc S, Dalleac A, Copin H, et al. Sperm global DNA methylation level: association with semen parameters and genome integrity. *Andrology* (2015) 3(2):235–40. doi: 10.1111/andr.12001

106. Santana VP, James ER, Miranda-Furtado CL, Souza MF, Pompeu CP, Esteves SC, et al. Differential DNA methylation pattern and sperm quality in men with varicocele. *Fertil Steril* (2020) 114(4):770–8. doi: 10.1016/j.fertnstert.2020.04.045

107. Rahiminia T, Yazd EF, Fesahat F, Moein MR, Mirjalili AM, Talebi AR. Sperm chromatin and DNA integrity, methyltransferase mRNA levels, and global DNA methylation in oligoasthenoteratozoospermia. *Clin Exp Reprod Med* (2018) 45(1):17–24. doi: 10.5653/cerm.2018.45.1.17

108. Laqqan M, Ahmed I, Yasin M, Hammadeh ME, Yassin M. Influence of variation in global sperm DNA methylation level on the expression level of protamine genes and human semen parameters. *Andrologia* (2020) 52(1):e13484. doi: 10.1111/and.13484

109. Clark SJ, Smallwood SA, Lee HJ, Krueger F, Reik W, Kelsey G. Genome-wide base-resolution mapping of DNA methylation in single cells using single-cell bisulfite sequencing (scBS-seq). *Nat Protoc* (2017) 12(3):534–47. doi: 10.1038/nprot.2016.187

110. Wang L, Chen M, Yan G, Zhao S. DNA Methylation differences between zona pellucida-bound and manually selected spermatozoa are associated with autism susceptibility. *Front Endocrinol (Lausanne)* (2021) 12:774260. doi: 10.3389/fendo.2021.774260

111. McCallum C, Riordon J, Wang Y, Kong T, You JB, Sanner S, et al. Deep learning-based selection of human sperm with high DNA integrity. *Commun Biol* (2019) 2(1):250–10. doi: 10.1038/s42003-019-0491-6

112. Anbari F, Khalili MA, Sultan Ahamed AM, Mangoli E, Nabi A, Dehghanpour F. Sabour M. Microfluidic sperm selection yields higher sperm quality compared to conventional method in ICSI program: A pilot study. *Syst Biol Reprod Med* (2021) 67 (2):137–43. doi: 10.1080/19396368.2020.1837994

frontiers | Frontiers in Endocrinology

TYPE Original Research
PUBLISHED 14 April 2023
DOI 10.3389/fendo.2023.1159723

OPEN ACCESS

EDITED BY
Kun Li,
Hangzhou Medical College, China

REVIEWED BY
Ying Shen,
Sichuan University, China
Singh Rajender,
Central Drug Research Institute (CSIR), India

*CORRESPONDENCE
Xuhui Zeng
zengxuhui@ntu.edu.cn
Xiuling Zhao
zhaoxiuling@ntu.edu.cn

†These authors have contributed equally to this work

SPECIALTY SECTION
This article was submitted to Reproduction, a section of the journal Frontiers in Endocrinology

RECEIVED 06 February 2023
ACCEPTED 20 March 2023
PUBLISHED 14 April 2023

CITATION
Song J, Sha Y, Liu X, Zeng X and Zhao X (2023) Novel mutations of *TEX11* are associated with non-obstructive azoospermia. *Front. Endocrinol.* 14:1159723. doi: 10.3389/fendo.2023.1159723

Novel mutations of *TEX11* are associated with non-obstructive azoospermia

Jian Song[1,2†], Yanwei Sha[3,4,5†], Xiaojun Liu[2], Xuhui Zeng[2*] and Xiuling Zhao[2*]

[1]Affiliated Hospital of Nantong University, School of Medicine, Nantong University, Nantong, China, [2]School of Medicine, Nantong University, Nantong, China, [3]Department of Andrology, Women and Children's Hospital, School of Medicine, Xiamen University, Xiamen, Fujian, China, [4]Fujian Provincial Key Laboratory of Reproductive Health Research, School of Medicine, Xiamen University, Xiamen, Fujian, China, [5]State Key Laboratory of Molecular Vaccinology and Molecular Diagnostics, School of Public Health, Xiamen University, Xiamen, Fujian, China

Non-obstructive azoospermia (NOA) affects 10% of infertile men worldwide, and genetic studies revealed that there are plenty of monogenic mutations that responsible for a part of idiopathic NOA cases. Testis-expressed gene 11 (*TEX11*) is an X-linked meiosis-specific gene, many pathogenic variants in *TEX11* have been detected in NOA patients, and the deficiency of this gene can cause abnormal meiotic recombination and chromosomal synapsis. However, many NOA-affected cases caused by *TEX11* mutation remain largely unknown. This study reported three novel *TEX11* mutations (exon 5, c.313C>T: p.R105*), (exon 7, c.427A>C: p.K143Q) and (exon 29, c.2575G>A: p.G859R). Mutations were screened using whole-exome sequencing (WES) and further verified by amplifying and sequencing the specific exon. Histological analysis of testicular biopsy specimens revealed a thicker basement membrane of the seminiferous tubules and poorly developed spermatocytes, and no post-meiotic round spermatids or mature spermatozoa were observed in the seminiferous tubules of patients with *TEX11* mutation.

Conclusion: This study presents three novel variants of *TEX11* as potential infertility alleles that have not been previously reported. It expanded the variant spectrum of patients with NOA, which also emphasizes the necessity of this gene screening for the clinical auxiliary diagnosis of patients with azoospermia.

KEYWORDS

azoospermia, TEX11 mutation, meiosis, infertility, WES

Abbreviations: FISH, Fluorescent *in situ* hybridization; PCR, Polymerase chain reaction; WES, Whole-exome sequencing; TEX11, Testis-expressed gene 11.

Introduction

Infertility affects approximately 15% of couples worldwide, males accounts for half to infertility (1). Non-obstructive azoospermia (NOA) is defined by absence of spermatozoa in the seminal fluid, and 80% of male infertility with NOA were thought to be idiopathic (2–4). Genetic testing is an important tool in the diagnosis of severe male infertility due of the high prevalence of genetic abnormalities in these patients (5). Numerous attempts have been made to link the gene mutations and azoospermia, the genetic basis of NOA is still unknown in the majority of infertile men. New technological advances for genetic diagnosis has enabled a substantial increase in our understanding about the etiology of male infertility. Research in the mutations involved in male infertility will help us to identify potential molecular targets for contraception, it can also improve genetic counseling for infertility patients seeking for effective treatments in humans.

Meiosis is a specialized cell division program, homologous chromosomes undergo pairing, synapsis, recombination, and faithful segregation in the process (6). Defects in meiosis is one of the important etiologies of infertility and birth defects in humans (6). Although numerous genes involved in meiosis have been specifically identified in the regulation of fertility (7–11), efforts to discover single-gene mutations that contribute to human spermatogenic failure have been mostly unavailing. As an X-chromosome encoded meiosis-specific protein, TEX11 was reported to be present in late-pachytene spermatocytes and in round and elongated spermatids (4), and the high expression of TEX11 in spermatogonia and spermatocytes indicates a critical role of TEX11 in the early stage of germ cell development. Extensive classic experiments using mice models have contributed significantly to how we understand the role of TEX11 in chromosomal synapsis and meiotic recombination (12, 13). TEX11 was proved to be an important component of meiotic nodules needed for recombination, and in *TEX11* mutant mice, spermatogenesis is impaired due to delayed repair of double-strand breaks (DSB) and decreased crossover formation in spermatocytes (14). More specifically, TEX11 may provide a physical link between chromosomal synapsis and meiotic recombination by interacting with SYCP2 *in vivo*, which is an indispensable component of the synaptonemal complex lateral elements, and defects in TEX11 caused apoptosis of spermatocytes at the pachytene stage and male infertility (6).

The homology of amino acid sequences in human and mouse indicates the similarity of function in spermatogenesis. Recently, X-linked *TEX11* mutations have been identified in azoospermic men (3, 4). Yatsenko et al. identified six different *TEX11* mutations, including a deletion mutation of 79 amino acids within the meiosis-specific sporulation domain SPO22, three splicing mutations and two missense mutations, theses mutations were occurred in 2.4% of men with azoospermia and 15% of azoospermia patients with meiotic arrest (4). Yang et al. reported 18 singleton variants in azoospermic men, which included a frameshift mutation, five missense mutations, two silent mutations and the remaining 10 were intronic mutations in *TEX11*. Specifically, the incidence of mutation in men with spermatogenic failure is higher than in controls (7.3% vs 1.7%) (3). Moreover, another recent study of *TEX11* mutations in patient with NOA, they identified seven potential pathogenic mutations, and 1.5% of the 479 patients with NOA carried *TEX11* mutations (15). Given the high incidence of *TEX11* mutations, this gene could be a significant candidate for the clinical evaluation of azoospermia.

In the present study, we reported three novel *TEX11* mutations in the patients with severe non-obstructive azoospermia and analyzed the genetic causes by WES. In addition, we summarized the mutations of *TEX11* related to male infertility.

Methods and results

Subjects

Pedigrees of the three families were recruited from the Reproductive Medicine Center of the Maternal and Child Care Hospital of Xiamen. Proband semen analysis was performed according to the guidelines of the World Health Organization 2010 guidelines for patients, who were diagnosed with NOA and confirmed using testicular fine needle aspiration.

Ethical approval

All procedures involving human participants were performed in accordance with the ethical standards of the Ethics Committee of the Maternal and Child Care Hospital of Xiamen. Written informed consents were obtained from all participants.

Karyotype and AZF deletion analysis

Karyotype analysis was carried out as described previously, peripheral blood lymphocytes (PBL) were collected to confirm the chromosomal status and cytogenetic chromosomal karyotype. PBL were treated with 20 mg/mL colcemid for 1 h to stay at metaphase. G-banding of metaphase chromosomes was performed by Giemsa staining. A total of 20-100 metaphase cells were counted and described by the G-banding method according to the international system for chromosome nomenclature. According to the result of karyotype analysis, the karyotype of all patients was normal (46, XY), and no gonadal mosaicism was observed. PCR was used to detect Y chromosome microdeletions in azoospermia factor regions (AZFa, b, and c). Genomic DNA (gDNA) was isolated from peripheral blood lymphocytes using a QIAamp Blood Mini Kit (Qiagen, Hilden, Germany). The gDNA was amplified using markers (sY84, sY127, sY255, sY86, sY134, and sY254) to detect AZF microdeletions, *SRY* gene was used as internal quantity control, the primers used for PCR were listed in Supplementary Table 1, and no microdeletions were detected at AZF loci in either patient. Moreover, the endocrine hormone levels of patients were normal (Table 1).

TABLE 1 The clinicopathological variables of four infertile patients.

Infertility-related examination of affected individuals				
Study participants	P1	P2	P3	P4
Age at last visit (y)	26	24	32	31
Infertility duration (y)	2.5	1.5	3.5	3
Height at last visit (cm)	170	168	171	166
Weight at last visit (kg)	74	72	76	70
Testicular volume (mL)	10	10	12	10
Hormone levels				
FSH (IU/L)	5.02	6.31	6.12	5.60
LH (IU/L)	5.64	5.23	5.84	5.21
T (ng/mL)	4.06	4.28	5.06	4.68
PRL(ng/mL)	12.15	11.85	13.15	9.15
Genetic investigation Karyotype	46, XY	46, XY	46, XY	46, XY
Y-chromosome microdeletion	No	No	No	No

Whole-exome sequencing

Genomic DNA samples from the three families were extracted from peripheral blood using a QIAamp DNA Blood Midi Kit (Qiagen, Hilden, Germany). WES was performed by Beijing Genome Institute at Shenzhen in the HiSeq2000 sequencing platform (Illumina, San Diego, CA, USA) as described elsewhere (16). Sequencing data were analyzed using Genome Analysis Toolkit Best Practices. (https://software.broadinstitute.org/gatk/best-practices/). Here, we sequenced the whole exome of azoospermia patients with meiotic arrest and found three novel *TEX11* mutations. (exon 29, c.2575G>A) in patient 1, 2 (P1, 2) and (exon 7, c.427A>C) in patient 4 (P4) were missense mutation, and (exon 5, c.313C>T) in patient 3 (P3) was nonsense mutation. Single nucleotide variation of c.427A>C was occurred in 0.0106% of humans according to GnomAD database, and the clinical significance was thought to be benign. And the other two missense mutations were not determined up to now. PCR and Sanger sequencing were used to validate the mutations detected by WES. Primer sequences used for detection of these mutations are shown in Supplementary Table 2. In this study, we identified three novel mutations, c.313C>T, c.427A>C and c.2575G>A (Figure 1), all of which were inherited from their mother (Figure 2), and no pathogenic biallelic or other mutations were found. This suggests

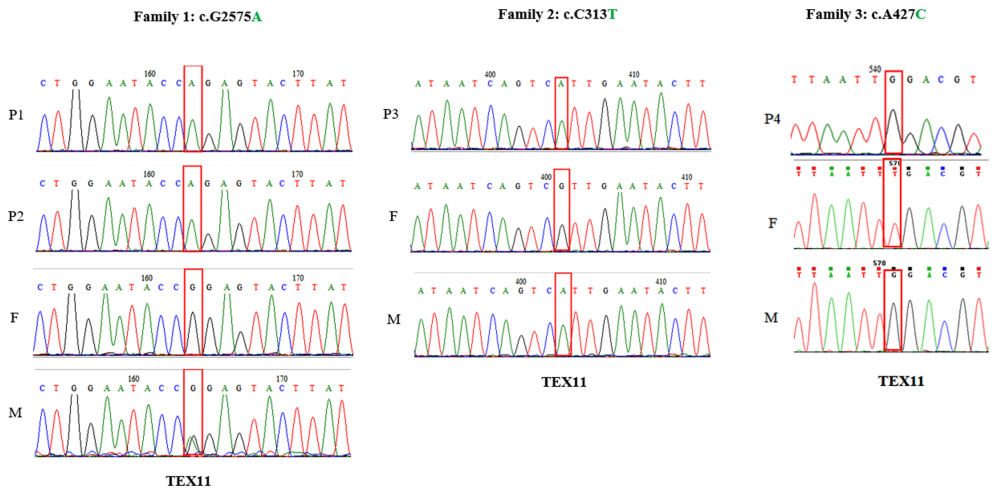

FIGURE 1
Analysis of the TEX11 variants, the red box indicates the mutation site. Family 1 shows the pedigrees of two brothers (P1, P2) with azoospermia and the inherited TEX11 missense mutation locate in exon 29, c.G2575A; Family 2 shows the pedigrees of P3 inherited TEX11 nonsense mutation locate in exon5, c. C313T; Family 3 shows the pedigrees of P4 inherited TEX11 missense mutation locate in exon7, c.A427C.

that mutations in *TEX11* carried by the proband may underlie their infertility.

Histological analysis

To characterize the nature of azoospermia patients, histological examination and TEX11 staining in testicular biopsy were performed. For histology, testicular tissues were obtained by testicular fine needle aspiration from the patient and immediately fixed in Bouin fixative at 4°C overnight, dehydrated in graded ethanol, embedded in paraffin, and cut into 4-μm-thick sections. To examine testicular histology, the sections were deparaffinized in xylene, rehydrated in graded ethanol, and stained with hematoxylin and eosin (H&E), stained sections were examined microscopically. Spermatogenesis was scored according to Johnsen's scoring system. As for the tubule structure, pathological examination of the patient showed a thicker basement membrane of the seminiferous tubules and poorly developed spermatocytes, no post-meiotic round spermatids or mature spermatozoa. Immunohistochemical staining of TEX11 indicated positive staining spermatogonia, spermatocytes, round spermatids, and mature spermatozoa in the seminiferous tubules of normal testis; TEX11 was detected in spermatogonia and spermatocytes, and absence of staining in post-meiotic round spermatids or mature spermatozoa of mutant seminiferous tubules for the impaired meiosis process in the testicular biopsies (Figure 3).

Discussion and conclusion

Infertility affects a great number of couples worldwide, and male infertility accounts for nearly half of reproductive health problem. The majority of causes of non-obstructive azoospermia in humans are deemed to be idiopathic, and genetic defects are postulated to be the underlying causes. Spermatogenesis is a complex and continuous process controlled by thousands of genes, and any change in the expression or function of these genes may impair the process of spermatogenesis and lead to male infertility (17, 18). It has been reported that genetic variations are probably associated with idiopathic male infertility (19), and identification of stage-specific genes and investigation of novel mutations involved in spermatogenesis are crucial for uncovering the mechanism of male infertility. Sex chromosomes play a key role in germ cell development in men. An increasing number of genes located on the X chromosome have been found to be involved in meiosis. In addition, many X-derived retrogenes such as *Utp14b* (20), *Pgk2* (21), *Cetn1* (22), *Rpl10l* (23), and *Cstf2t* (24) have been confirmed to initiate transcription during male meiosis, and alterations of meiotic proteins results in failure of gametogenesis, which lead to partial or complete sterility. To date, a large amount of singletons had been identified in patients with azoospermia, including exonic missense mutations, exonic frameshift mutations, and intronic mutations.

As an X-linked testis-specific gene, TEX11 expression is present in late-pachytene spermatocytes and in round and elongated spermatids (4), nevertheless, TEX11 staining can be seen in spermatogonia, spermatocytes and post-meiotic sperm in the seminiferous tubules in our study. The difference may arise from the antibody specificity and the different mutation site of TEX11. *TEX11* mutations have been identified in many patients with azoospermia (25). Yu et al. reported a deletion mutation in exon 3 in infertile patients with meiotic arrest, representing a 2.5% incidence (26). Yatsenko et al. identified three splicing mutations and two missense mutations in infertile men (4); Yang et al. verified one frameshift mutation of *TEX11* in two brothers with azoospermia, and heterozygous mutations were also found in his mother (6). Clinic-pathological variables of infertile patients with *TEX11* mutation in the published literatures and our study are shown in Table 2. The high frequency of *TEX11* mutations in men with azoospermia suggests a critical role in human spermatogenesis, and deficiency in *TEX11* causes meiotic arrest and male infertility. The abundance of *TEX11* mutations may be a great help in auxiliary analysis of male infertility, however, it also increases the difficulty of identifying causal mutations for male infertility.

TEX11 was reported to be an X-linked meiosis-specific gene, and contain a meiosis-specific sporulation (SPO22) domain (175-402AA) and repetitive tetratricopeptide repeat (TPR) domains (402-436AA and 441-471AA) (Figure 4A), which are commonly observed in scaffold proteins and exhibit a wide range of molecular recognition modes (28, 29). Extensive studies revealed that TEX11 plays an essential role in meiotic recombination, the repair of DNA double-strand breaks, meiotic crossover and chromosomal synapsis (6, 14, 30). Mutations in SPO22/ZIP4, which are the homologues of TEX11 in budding yeast and Arabidopsis, led to defects in meiosis

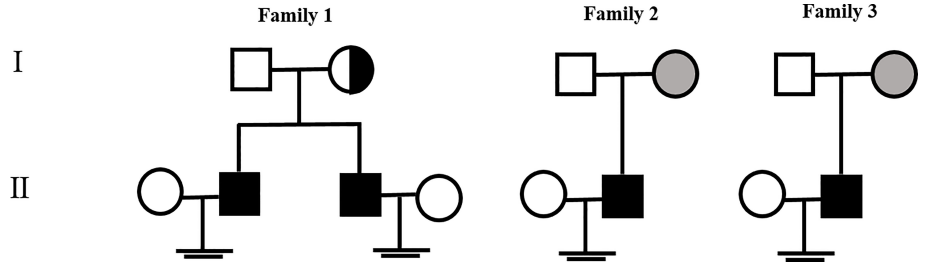

FIGURE 2
Family pedigree of the proband affected by NOA with a TEX11 mutation. The gray symbols indicate the patient's mother who is the homozygous carrier of the TEX11 mutation, and the dotted-circle symbols indicate the patient's mother who is the heterozygous carrier of the TEX11 mutation.

10.3389/fendo.2023.1159723

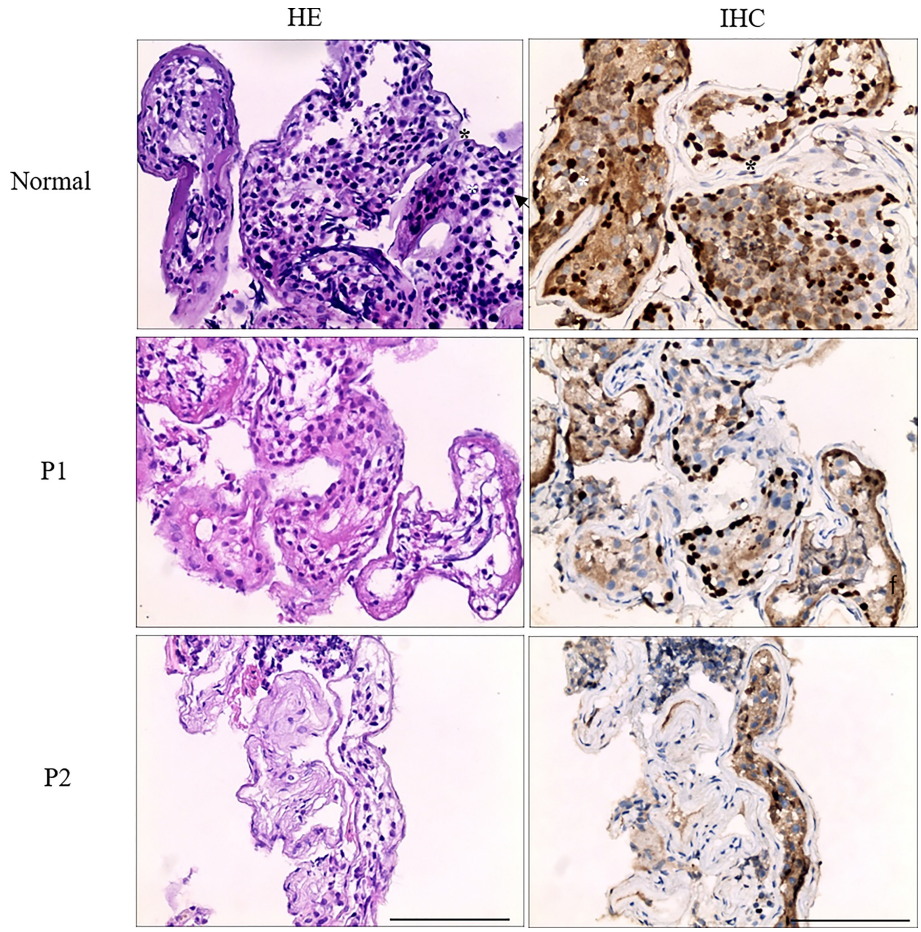

FIGURE 3
Analysis of testis biopsy samples from family 1 (P1, P2) and normal control. Primary spermatocytes and round spermatids were observed in the normal seminiferous tubules of the testis. Histologic sections showing a thicker basement membrane of the seminiferous tubules and poorly developed spermatocytes, no post-meiotic round spermatids or mature spermatozoa were observed in the seminiferous tubules of patient 1 and patient 2, in contrast with the normal testicular histology. Black asterisk denotes spermatogonia, white asterisk denotes spermatocytes, and arrowhead denotes round spermatids. Scale bar = 100 μm.

TABLE 2 Mutations of TEX11 reported for azoospermia patients in published literature and our data.

Position	Nucleotide change	Protein/RNA change	Testicular sperm	Patients (n)	Reference
Exon 6	405C>T	Silent mutation, A135spl d[b]	Few sperm	1	(4)
Exon 7	466A>G	Missense mutation, M156V	No sperm	1	(4)
Exon 9-11	607del237bp	203del79aa	Few sperm	2	(4)
Intron 10	748+1G>A[c]	L249spl d[b]	No sperm	1	(4)
Intron 21	1793+1G>C[c]	R597spl d[b]	No sperm	1	(4)
Exon 24	2047G>A	Missense mutation, A683T	Few sperm	1	(4)
Exon 6	349T>A	Missense mutation, W117R	No sperm	1	(3)
Exon 6	405C>T	Silent mutation	No sperm	1	(3)
Exon 7	424G>A	Missense mutation, V142I	No sperm	1	(3)
Exon 7	515A>G	Missense mutation, Q172R	No sperm	1	(3)
Exon 10	731C>T	Missense mutation, T244I	No sperm	1	(3)

(Continued)

TABLE 2 Continued

Position	Nucleotide change	Protein/RNA change	Testicular sperm	Patients (n)	Reference
Exon 16	1258Ins (TT)	Frameshift mutation, 1258GATG→TTGGTA	No sperm	1	(3)
Exon 26	2243T>C	Missense mutation, V748A	No sperm	1	(3)
Exon 27	2319T>C	Silent mutation	No sperm	1	(3)
Intron 3	-17T>C[c]	Intronic alteration	No sperm	1	(3)
Intron 5	-48G>A[c]	Intronic alteration	No sperm	1	(3)
Intron 10	+42C>A[c]	Intronic alteration	No sperm	1	(3)
Intron 12	-28T>C[c]	Intronic alteration	No sperm	1	(3)
Intron 15	-64G>A[c]	Intronic alteration	No sperm	1	(3)
Intron 21	-1G>A[c]	Intronic alteration	No sperm	1	(3)
Intron 22	-37A>G[c]	Intronic alteration	No sperm	1	(3)
Intron 24	+119G>A[c]	Intronic alteration	No sperm	1	(3)
Intron 27	-55A>C[c]	Intronic alteration	No sperm	1	(3)
Intron 28	-44A>G[c]	Intronic alteration	No sperm	1	(3)
Exon 29	2568G>T	Missense mutation, W856C	No sperm	2	(25)
Exon 3	151_154del	D51 frame-shift mutation	No sperm	1	(26)
Intron 21	1796 + 2T > G	Splicing mutation, 599K spl d	No sperm	2	(15)
Intron 16	1426-1C > T	Splicing mutation, 476A spl d	No sperm	6	(15)
Exon 30	2613G > T	Missense mutation, W871C	No sperm	2	(15)
Exon 12	1051G > T	Nonsense mutation, E351*	No sperm	1	(15)
Exon 16	1254dupA	Frameshift mutation, N418K fs*10	No sperm	1	(15)
Exon 5	298delG	Frameshift mutation, V85L fs*5	No sperm	1	(15)
Exon 12	857delA	Frameshift mutation K286R fs*5	No sperm	1	(15)
Exon 26	2240C>A	Missense mutation p.S747X	No sperm	1	(27)
Exon 16	1337G>T	Missense mutation p.R446M	No sperm	1	(27)
Exon 16	1246C>T	Missense mutation p.Q416X	No sperm	1	(27)
Exon 5	313C>T	Nonsense mutation, R105* p.R105*	No sperm	1	This study
Exon 7	427A>C	Missense mutation, K143Q K143Q	No sperm	1	This study
Exon 29	2575G>A	Missense mutation, G859R G859R	No sperm	2	This study

[a]TEX11 mutations were mapped to isoform 2 (GenBank accession number, NM_031276); [b]The term spl d represents the splicing donor sit; [c]+1 refers to the first base of a given intron, and -1 denotes the last base. TEX11: testis expressed 11; del: deletion; bp: base pair; Ins: insertion.

(31, 32). Therefore, the function of TEX11 in meiosis is highly conserved from budding yeast to humans. Moreover, TPRs is composed of helix-turn-helix repeats that typically appear in tandem and pack with each other to form super-helical structures with various curvatures. In brief, TPRs are protein-protein interaction modules that can provide docking surfaces for other molecules (4). What's more, some TPR proteins orchestrate different activities by integrating signals from multiple interacting partners (33). TEX11 was reported to contain repetitive TPR domains, which may provide docking surfaces for SYCP2 to form synaptonemal complex, and involved in chromosomal synapsis and crossover formation in meiosis. In the present study, we identified

10.3389/fendo.2023.1159723

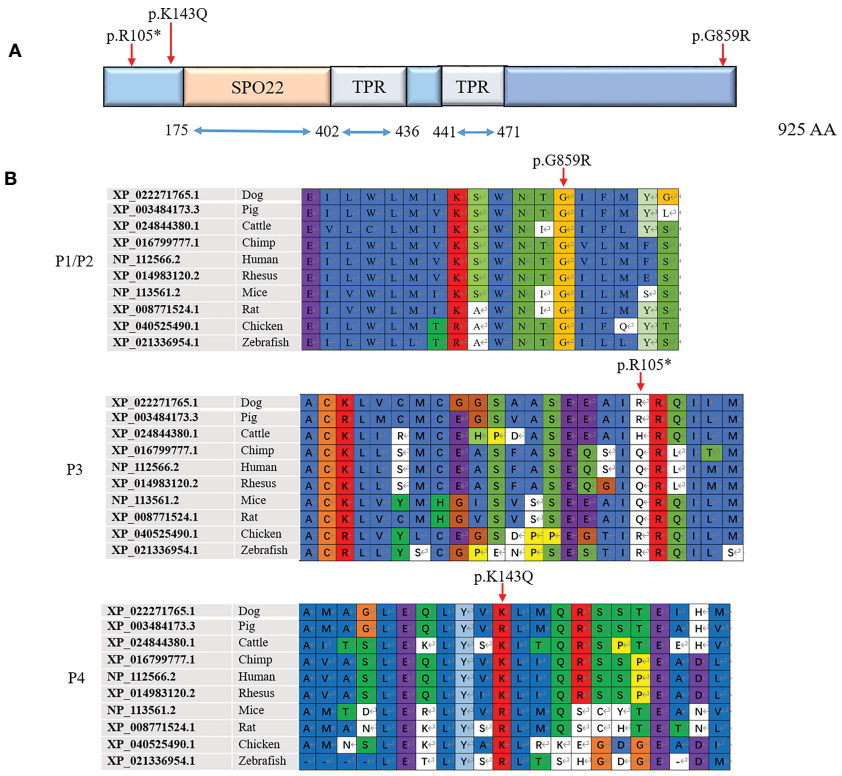

FIGURE 4
Three novel mutations identified in the TEX11 gene. **(A)** Predicted TEX11 domains with a SPO22 motif (amino acid positions 175-402) and multiple TPR-containing regions. The mutations found were shown under the predicted protein domains for TEX11. **(B)** Amino acid sequence alignment of TEX11 from different species. The red arrow indicates the mutated amino acid. TEX11, testis expressed 11; SPO22, sporulation domain; TPR, tetratricopeptide repeat; WT, wild type; AA, amino acid.

three novel *TEX11* mutations in patients and their mother. The *TEX11* p.R105* mutation displayed in our current study resulted in spermatogenic failure for loss of SPO22 and TPR domains; the other two missense mutations (p.G859R and p.K143Q) identified in our report were neither in SPO22 nor TPR domains; however, the Gly859 residue was found to be highly conserved across several species (Figure 4B) and histological analysis of testis biopsy obtained from the patient with Gly859 missense mutation showed meiotic arrest and no post-meiotic germ cells were observed in the seminiferous tubules. The testicular histology of two brothers carrying p.G859R mutation suggested that this mutation caused meiotic arrest. The mutations of p.G859R and p.K143Q are not in the known functional domains of TEX11, and how it affects meiosis is unclear. What is known is that TEX11 forms distinct foci on homologous chromosomes that synapse with each other, therefore these mutations may affect the tertiary structure, disrupting its function or stability. Further study will be necessary to clarify the molecular determinants that control TEX11 function and the connection between function domain and function.

In conclusion, the current report presents three pathogenic mutations in *TEX11* gene in four patients which are possibly associated with male infertility. All patients presented with azoospermia at reproductive age without any other manifestations. This study provides novel *TEX11* mutations in infertile men with meiotic arrest, which not only helps to ascertain the exact genetic cause in each patient but also facilitates the counseling of family members about their reproductive health. While we presented *TEX11* mutations in infertile men, causality of these variants has not been definitively proven.

Data availability statement

The original contributions presented in the study are included in the article/Supplementary Material. Further inquiries can be directed to the corresponding authors.

Author contributions

JS: Conceptualization, methodology, investigation, data curation. YS: Methodology, investigation, funding acquisition. XL: Data curation, writing-review. XuZ: Visualization and writing-review. XiZ: Methodology, writing-review, and editing. All authors contributed to the article and approved the submitted version.

Funding

This work was supported by grants from the National Natural Science Foundation of China (Grant Nos. 82071697 and 81871200),

the Medical Innovation Project of Fujian Province (Grant Nos. 2019CXB35 and 2020CXB051) and the Natural Science Foundation of Jiangsu Province (BK20210840).

Acknowledgments

We sincerely thank all the participants and their families for their support and cooperation.

Conflict of interest

The authors declare that the research was conducted in the absence of any commercial or financial relationships that could be construed as a potential conflict of interest.

Publisher's note

Supplementary material

The Supplementary Material for this article can be found online at: https://www.frontiersin.org/articles/10.3389/fendo.2023.1159723/full#supplementary-material

References

1. Mueller JL, Mahadevaiah SK, Park PJ, Warburton PE, Page DC, Turner JM. The mouse X chromosome is enriched for multicopy testis genes showing postmeiotic expression. *Nat Genet* (2008) 40 6:794–9. doi: 10.1038/ng.126

2. Zheng K, Yang F, Wang PJ. Regulation of male fertility by X-linked genes. *J Androl* (2010) 31 1:79–85. doi: 10.2164/jandrol.109.008193

3. Yang F, Silber S, Leu NA, Oates RD, Marszalek JD, Skaletsky H, et al. TEX11 is mutated in infertile men with azoospermia and regulates genome-wide recombination rates in mouse. *EMBO Mol Med* (2015) 7 9:1198–210. doi: 10.15252/emmm.201404967

4. Yatsenko AN, Georgiadis AP, Röpke A, Berman AJ, Jaffe T, Olszewska M, et al. X-Linked TEX11 mutations, meiotic arrest, and azoospermia in infertile men. *N Engl J Med* (2015) 372 22:2097–107. doi: 10.1056/NEJMoa1406192

5. Xie C, Chen X, Liu Y, Wu Z, Ping P. Multicenter study of genetic abnormalities associated with severe oligospermia and non-obstructive azoospermia. *J Int Med Res* (2018) 46 1:107–14. doi: 10.1177/0300060517718771

6. Yang F, Gell K, van der Heijden GW, Eckardt S, Leu NA, Page DC, et al. Meiotic failure in male mice lacking an X-linked factor. *Genes Dev* (2008) 22 5:682–91. doi: 10.1101/gad.1613608

7. Choi Y, Jeon S, Choi M, Lee MH, Park M, Lee DR, et al. Mutations in SOHLH1 gene associate with nonobstructive azoospermia. *Hum Mutat* (2010) 31 7:788–93. doi: 10.1002/humu.21264

8. Miyamoto T, Hasuike S, Yogev L, Maduro MR, Ishikawa M, Westphal H, et al. Azoospermia in patients heterozygous for a mutation in SYCP3. *Lancet* (2003) 362 9397:1714–9. doi: 10.1016/S0140-6736(03)14845-3

9. Ropke A, Tewes AC, Gromoll J, Kliesch S, Wieacker P, Tuttelmann F. Comprehensive sequence analysis of the NR5A1 gene encoding steroidogenic factor 1 in a large group of infertile males. *Eur J Hum Genet* (2013) 21 9:1012–5. doi: 10.1038/ejhg.2012.290

10. Imken L, Rouba H, El Houate B, Louanjli N, Barakat A, Chafik A, et al. Mutations in the protamine locus: association with spermatogenic failure? *Mol Hum Reprod* (2009) 15 11:733–8. doi: 10.1093/molehr/gap056

11. Mou L, Wang Y, Li H, Huang Y, Jiang T, Huang W, et al. A dominant-negative mutation of HSF2 associated with idiopathic azoospermia. *Hum Genet* (2013) 132 2:159–65. doi: 10.1007/s00439-012-1234-7

12. Hu Z, Xia Y, Guo X, Dai J, Li H, Hu H, et al. A genome-wide association study in Chinese men identifies three risk loci for non-obstructive azoospermia. *Nat Genet* (2011) 44 2:183–6. doi: 10.1038/ng.1040

13. Hu Z, Li Z, Yu J, Tong C, Lin Y, Guo X, et al. Association analysis identifies new risk loci for non-obstructive azoospermia in Chinese men. *Nat Commun* (2014) 5:3857. doi: 10.1038/ncomms4857

14. Adelman CA, Petrini JH. ZIP4H (TEX11) deficiency in the mouse impairs meiotic double strand break repair and the regulation of crossing over. *PloS Genet* (2008) 4 3:e1000042. doi: 10.1371/journal.pgen.1000042

15. Ji Z, Yao C, Yang C, Huang C, Zhao L, Han X, et al. Novel hemizygous mutations of TEX11 cause meiotic arrest and non-obstructive azoospermia in Chinese han population. *Front Genet* (2021) 12:741355. doi: 10.3389/fgene.2021.741355

16. Tan YQ, Tu C, Meng L, Yuan S, Sjaarda C, Luo A, et al. Loss-of-function mutations in TDRD7 lead to a rare novel syndrome combining congenital cataract and nonobstructive azoospermia in humans. *Genet Med* (2019) 21 5:1209–17. doi: 10.1038/gim.2017.130

17. Cooke HJ, Saunders PT. Mouse models of male infertility. *Nat Rev Genet* (2002) 3 10:790–801. doi: 10.1038/nrg911

18. Tamowski S, Aston KI, Carrell DT. The use of transgenic mouse models in the study of male infertility. *Syst Biol Reprod Med* (2010) 56 3:260–73. doi: 10.3109/19396368.2010.485244

19. Eggers S, DeBoer KD, van den Bergen J, Gordon L, White SJ, Jamsai D, et al. Copy number variation associated with meiotic arrest in idiopathic male infertility. *Fertil Steril* (2015) 103 1:214–9. doi: 10.1016/j.fertnstert.2014.09.030

20. Rohozinski J, Bishop CE. The mouse juvenile spermatogonial depletion (jsd) phenotype is due to a mutation in the X-derived retrogene, mUtp14b. *Proc Natl Acad Sci U.S.A.* (2004) 101 32:11695–700. doi: 10.1073/pnas.0401130101

21. Danshina PV, Geyer CB, Dai Q, Goulding EH, Willis WD, Kitto GB, et al. Phosphoglycerate kinase 2 (PGK2) is essential for sperm function and male fertility in mice. *Biol Reprod* (2010) 82 1:136–45. doi: 10.1095/biolreprod.109.079699

22. Avasthi P, Scheel JF, Ying G, Frederick JM, Baehr W, Wolfrum U. Germline deletion of Cetn1 causes infertility in male mice. *J Cell Sci* (2013) 126(Pt 14):3204–13. doi: 10.1242/jcs.128587

23. Jiang L, Li T, Zhang X, Zhang B, Yu C, Li Y, et al. RPL10L is required for Male meiotic division by compensating for RPL10 during meiotic sex chromosome inactivation in mice. *Curr Biol* (2017) 27 10:1498-1505.e6. doi: 10.1016/j.cub.2017.04.017

24. Tardif S, Akrofi AS, Dass B, Hardy DM, MacDonald CC. Infertility with impaired zona pellucida adhesion of spermatozoa from mice lacking TauCstF-64. *Biol Reprod* (2010) 83 3:464–72. doi: 10.1095/biolreprod.109.083238

25. Sha Y, Zheng L, Ji Z, Mei L, Ding L, Lin S, et al. A novel TEX11 mutation induces azoospermia: a case report of infertile brothers and literature review. *BMC Med Genet* (2018) 19 1:63. doi: 10.1186/s12881-018-0570-4

26. Yu XC, Li MJ, Cai FF, Yang SJ, Liu HB, Zhang HB. A new TEX11 mutation causes azoospermia and testicular meiotic arrest. *Asian J Androl* (2021) 23 5:510–5. doi: 10.4103/aja.aja_8_21

27. An M, Liu Y, Zhang M, Hu K, Jin Y, Xu S, et al. Targeted next-generation sequencing panel screening of 688 Chinese patients with non-obstructive azoospremia. *J Assost Reprod Genet* (2021) 38(8):1997–2005.

28. D'Andrea LD, Regan L. TPR proteins: the versatile helix. *Trends Biochem Sci* (2003) 28 12:655–62. doi: 10.1016/j.tibs.2003.10.007

29. Perez-Riba A, Itzhaki LS. The tetratricopeptide-repeat motif is a versatile platform that enables diverse modes of molecular recognition. *Curr Opin Struct Biol* (2019) 54:43–9. doi: 10.1016/j.sbi.2018.12.004

30. Dapper AL, Payseur BA. Molecular evolution of the meiotic recombination pathway in mammals. *Evolution* (2019) 73 12:2368–89. doi: 10.1111/evo.13850

31. Chelysheva L, Gendrot G, Vezon D, Doutriaux MP, Mercier R, Grelon M. Zip4/Spo22 is required for class I CO formation but not for synapsis completion in arabidopsis thaliana. *PloS Genet* (2007) 3 5:e83. doi: 10.1371/journal.pgen.0030083

32. Tsubouchi T, Zhao H, Roeder GS. The meiosis-specific zip4 protein regulates crossover distribution by promoting synaptonemal complex formation together with zip2. *Dev Cell* (2006) 10 6:809–19. doi: 10.1016/j.devcel.2006.04.003

33. Pyatnitskaya A, Andreani J, Guerois R, De Muyt A, Borde V. The Zip4 protein directly couples meiotic crossover formation to synaptonemal complex assembly. *Genes Dev* (2022) 36 1-2:53–69. doi: 10.1101/gad.348973.121

frontiers | Frontiers in Endocrinology

TYPE Original Research
PUBLISHED 19 April 2023
DOI 10.3389/fendo.2023.1130536

OPEN ACCESS

EDITED BY
Kun Li,
Hangzhou Medical College, China

REVIEWED BY
Martin Prince,
NewYork-Presbyterian, United States
Mengcheng Luo,
Wuhan University, China

*CORRESPONDENCE
He-Feng Huang
huanghefg@hotmail.com
Chen-Ming Xu
chenming_xu2006@163.com

†These authors have contributed equally to this work

SPECIALTY SECTION
This article was submitted to Reproduction, a section of the journal Frontiers in Endocrinology

RECEIVED 23 December 2022
ACCEPTED 27 March 2023
PUBLISHED 19 April 2023

CITATION
Shi W-H, Zhou Z-Y, Ye M-J, Qin N-X, Jiang Z-R, Zhou X-Y, Xu N-X, Cao X-L, Chen S-C, Huang H-F and Xu C-M (2023) Sperm morphological abnormalities in autosomal dominant polycystic kidney disease are associated with the Hippo signaling pathway via PC1. *Front. Endocrinol.* 14:1130536. doi: 10.3389/fendo.2023.1130536

Sperm morphological abnormalities in autosomal dominant polycystic kidney disease are associated with the Hippo signaling pathway via PC1

Wei-Hui Shi[1†], Zhi-Yang Zhou[1†], Mu-Jin Ye[2], Ning-Xin Qin[3], Zi-Ru Jiang[1], Xuan-You Zhou[1], Nai-Xin Xu[2], Xian-Lin Cao[1], Song-Chang Chen[1], He-Feng Huang[1,2,4*] and Chen-Ming Xu[1,2*]

[1]Obstetrics and Gynecology Hospital, Institute of Reproduction and Development, Fudan University, Shanghai, China, [2]International Peace Maternity and Child Health Hospital, Shanghai Jiao Tong University School of Medicine, Shanghai, China, [3]Department of Assisted Reproductive Medicine, Shanghai First Maternity and Infant Hospital, Tongji University School of Medicine, Shanghai, China, [4]Research Units of Embryo Original Diseases, Chinese Academy of Medical Sciences (No. 2019RU056), Shanghai, China

Background: Autosomal dominant polycystic kidney disease (ADPKD) is a hereditary kidney disorder mostly caused by mutations in *PKD1* or *PKD2* genes. Here, we report thirteen ADPKD males with infertility and investigated the sperm morphological defects associated with PC1 disruption.

Methods: Targeted next-generation sequencing was performed to detect *PKD1* variants in patients. Sperm morphology was observed by immunostaining and transmission electron microscopy, and the sperm motility was assessed using the computer-assisted sperm analysis system. The Hippo signaling pathway was analyzed with by quantitative reverse transcription polymerase chain reaction (qPCR) and western blotting *in vitro*.

Results: The ADPKD patients were infertile and their sperm tails showed morphological abnormalities, including coiled flagella, absent central microtubules, and irregular peripheral doublets. In addition, the length of sperm flagella was shorter in patients than in controls of in in. *In vitro*, ciliogenesis was impaired in *Pkd1*-depleted mouse kidney tubule cells. The absence of PC1 resulted in a reduction of MST1 and LATS1, leading to nuclear accumulation of YAP/TAZ and consequently increased transcription of *Aurka*. which might promote HDAC6-mediated ciliary disassembly.

Conclusion: Our results suggest the dysregulated Hippo signaling significantly contributes to ciliary abnormalities in and may be associated with flagellar defects in spermatozoa from ADPKD patients.

KEYWORDS

autosomal dominant polycystic kidney disease, *PKD1*, male infertility, sperm flagella, the Hippo pathway

1 Introduction

Autosomal dominant polycystic kidney disease (ADPKD) is one of the most common monogenic kidney disorders with an estimated prevalence of one in 1000 live births. ADPKD is characterized by bilateral renal cysts and extra-renal manifestations, including aortic aneurysm, intracranial aneurysm and cysts in the liver, pancreas, seminal vesicles, epididymides and testes (1, 2). Mutations in *PKD1* (OMIM 601313) and *PKD2* (OMIM 173910) are the most common causes of ADPKD, which account for 80-85% and 10-15% of cases, respectively (3). Polycystin-1 (PC1), a 4303 amino acid product of *PKD1* gene, acts as a transmembrane glycoprotein with a large extracellular amino terminus, 11 membrane-spanning domains and a short intracellular carboxy terminus. Polycystin-2 (PC2), encoded by *PKD2*, functions as a non-selective cation channel permeable for to calcium ions, which co-localizes with PC1 at the primary cilia of the renal epithelia and plays a vital role in mechanosensation (4, 5).

Since the first case of a 32-year-old man with ADPKD suffering from infertility and seminal vesicle cysts was reported in 1995, male infertility in ADPKD has gradually gained attention (6–10). It has recently been reported that seminal megavesicles are found in 31% of patients with *PKD1* mutations and may be associated with the male infertility observed in ADPKD patients (11, 12). Primary cilia in the kidney are microtubule-based organelles that protrude from the surface of epithelial cells. Disruption of PC1 or PC2 causes defects in primary cilia, leading to the development of ADPKD. Similar to primary cilia, the sperm flagellum is a ciliary organelle with nine peripheral microtubule doublets and two central microtubule singlets (9 + 2 axoneme) that whip back and forth to propel the sperm, which is essential for male fertility. *Pkd2* has been reported to be highly expressed in mature sperms of Drosophila (13) and PC1 has also been observed in on human sperm proteomics studies (14). Moreover, Okada et al. discovered that four infertile men with immotile spermatozoa and abnormal flagellar ultrastructure were all diagnosed with ADPKD, suggesting that PC1 and PC2 may play a vital role in the structure of sperm flagella.

The Hippo signaling pathway, initially identified by genetic mosaic screens for suppressor genes associated with tissue overgrowth in Drosophila, regulates cell proliferation, death and differentiation to maintain organ size and tissue homeostasis (15). The components of this pathway are highly conserved in mammals and consist of MST1/2, LATS1/2, SAV1, MOB1, and YAP/TAZ (16). When upstream stimuli, such as mechanotransduction, cell polarity, and G-protein-coupled receptor signals, trigger the of the Hippo pathway kinase cascade, the kinase activity of MST1/2 which phosphorylates SAV1, LATS1/2, and MOB1, is enhanced (17, 18). Activated LATS1/2, accelerated by interaction with MOB1, directly phosphorylates the transcriptional co-activators YAP/TAZ, leading to their sequestration in the cytoplasm. It has recently been reported that depletion of *Yap* or *Taz* leads to ciliary abnormalities in zebrafish and renal cysts in mice respectively, suggesting that the Hippo signaling pathway may promote ciliogenesis and cyst formation (19, 20).

In this study, we identified thirteen ADPKD patients with mutations in *PKD1* using targeted next-generation sequencing (NGS) and observed poor semen quality and abnormal sperm morphology. *In vitro*, we found that the defect of *Pkd1* resulted in decreased in MST1 and LATS1, which promoted ciliary disassembly via the AURKA/HDAC6 complex. Our results suggest that suppressed Hippo signaling in lead to a boost in ciliary disassembly, which may also be a mechanism of impaired sperm flagella in ADPKD.

2 Methods

2.1 Subjects

All the subjects of in this study were recruited from the reproductive outpatient department of the International Peace Maternity and Child Health Hospital (IPMCH), Shanghai Jiao Tong University School of Medicine from January 2018 to September 2022. Genomic DNA of was extracted from peripheral blood samples of all subjects. A gene panel related to polycystic kidney diseases (PKD), containing *VHL*, *TSC1*, *TSC2*, *UMOD*, *PKD1*, *PKD2*, *MUC1*, and *PKHD1* genes, was detected by NGS as previously described (21). Detected variants were confirmed with by Sanger sequencing and interpreted and classified according to the ACMG guideline (22).

2.2 Semen analysis

Sperm samples from all subjects were collected by masturbation after 3 days of sexual abstinence. After liquefaction, sperm concentration and motility were assessed using the computer-assisted sperm analysis (CASA) system according to the World Health Organization laboratory manual (23). Semen smears were prepared by spreading the sperm suspension on a microscope the slide for subsequent sperm immunofluorescence staining.

2.3 Transmission electron microscopy (TEM)

Semen samples were centrifuged at 800 g for 15 minutes and washed three times with 0.01M phosphate buffered saline (PBS, pH 7.4). After fixation with pre- cooled 2.5% glutaraldehyde (in 0.1 M PBS buffer) for two hours, samples were washed twice in PBS (10 minutes each time) and post-fixed with osmium tetroxide for two hours at 4°C. Samples were dehydrated with in cold 30%, 50%, 70%, 80%, 95% and 100% ethanol for 10 minutes (100% ethanol repeated once). After being embedded with resin, the samples were cut with into thin sections and stained with lead citrate. Images were captured with a PHILIP CM-120 transmission electron microscope.

2.4 Cell culture

Pkd1-depleted mouse kidney tubule cell lines ($Pkd1^{+/-}$ and $Pkd1^{-/-}$ cells) (a kind gift from Dr. Changlin Mei of Changzheng Hospital, Second Military Medical University, Shanghai, China)

were cultured in Dulbecco's modified Eagle's medium/Ham's F-12 medium (DMEM/F12) (Gibco) supplemented with 2% fetal bovine serum (Gibco), Insulin-Transferrin-Selenium (41400045, Gibco), triiodothyronine (2 x 10^{-9} M, T5516, Sigma) and recombinant γ-interferon (10 units/ml, Sigma) at 33°C. For cilia formation, cells were transferred to 37°C and grown in γ-interferon-free medium for 7 days.

2.5 Cell growth detection

Cells were cultured with in equal amounts (1 x 10^4 per well) and counted daily for 7 days using a hemocytometer. Experiments were carried out in triplicate.

2.6 Bromodeoxyuridine (BrdU) cell proliferation assay

Cells were grown on the coverslips in a 24-well plate to 70-90% confluence. BrdU (10μM) was added for two hours at 33°C. The cells were then washed three times with 0.01 M PBS and fixed with 4% paraformaldehyde. After washing three times again with PBS, the cells were incubated in 2 mol/L HCL for 30 minutes and then neutralized with 0.1 M sodium borate buffer three times for 15 minutes each. BrdU staining was followed by standard immunofluorescence protocols as described below.

2.7 Real-time quantitative reverse transcription polymerase chain reaction (qPCR)

Total RNA was isolated with RNAiso Plus (No.9108Q, Takara, Japan) and reversed to cDNA with using a PrimeScript™ RT reagent Kit with gDNA Eraser (No. RR047Q, Takara, Japan) according to the manufacturer's instructions. Quantitative PCR (qPCR) was performed with using TB Green™ Premix Ex Taq™ (Tli RNaseH Plus) (No. RR420Q, Takara, Japan).

2.8 Western blotting

For western blotting analysis, cells and sperms were lysed on ice with RIPA buffer (No. P0013B; Beyotime, Shanghai, China) supplemented with InStabTM Phosphatase Inhibitor Cocktail (No.20109ES05, Yeasen, Shanghai, China) and InStabTM Protease Cocktail (No.20124ES03, Yeasen) for 30 minutes and cleared by centrifugation at 4°C, 12,000 rpm for 10 minutes. Protein concentrations were quantified by Pierce™ BCA Protein Assay Kit (No.23225, Thermo Fisher, USA). After denaturation, total protein was fractionated by SDS-polyacrylamide gel electrophoresis and transferred to polyvinylidene difluoride (PVDF) membranes. Membranes were blocked with 5% non-fat milk in TBST buffer for one hour and incubated with primary antibodies overnight at 4°C. Horseradish peroxide- conjugated secondary antibodies (Cell Signaling Technology, 1:1000) were incubated for one hour at room temperature and blots were visualized by ECL Chemiluminescent Substrate Kit (No.36222ES76, Yeasen). Primary antibodies used in for western blotting included acetylated α-tubulin (T6973, Sigma, 1:2000), α-tubulin (11224-1-AP, Proteintech, 1:1000), phospho-YAP (4911, Cell Signaling Technology, 1:1000), YAP (4912, Cell Signaling Technology, 1:1000), TAZ (4883, Cell Signaling Technology, 1:1000), MST1 (3682, Cell Signaling Technology, 1:1000), MST2 (3952, Cell Signaling Technology, 1:1000), MOB1 (13730, Cell Signaling Technology, 1:1000), phospho-MOB1 (8699, Cell Signaling Technology, 1:1000), SAV1 (13301, Cell Signaling Technology, 1:1000), LATS1 (3477, Cell Signaling Technology, 1:1000), AURKA (610938, BD Biosciences, 1:1000), PRM1 (HPA055150, Sigma, 1:500), and GAPDH (2118, Cell Signaling Technology, 1:1000).

2.9 Immunofluorescence staining

Cells grown on coverslips or spermatozoa on semen smears were fixed with 4% paraformaldehyde for 15 minutes at room temperature. After the fixation, samples were washed three times in 1 x PBS for 5 minutes each and then blocked in 1 x PBS with 0.3% Triton™ X-100 and 5% normal serum for one hour. Primary antibodies were incubated overnight at 4°C. Alexa Fluor 488 or 594 conjugated secondary antibodies (Invitrogen) were incubated at for one hour at room temperature. Cell nuclei were stained with DAPI (Vector labs H-1200). Images were captured using an the SP8 confocal microscope (Leica Microsystems, Wetzlar, Germany). Primary antibodies used for immunofluorescence staining included acetylated a-tubulin (T7451, Sigma, 1:250), ZO-1 (339100, Invitrogen, 1:100), YAP/TAZ (8418, Cell Signaling Technology, 1:150).

2.10 Data analysis

The length of cell cilia or sperm flagella and protein bands from western blotting were measured or quantified with using Image J. T wo-tailed *P* values were calculated with unpaired Student's *t*-test. The significance level of was set at 0.05. Graphs were generated with GraphPad Prism software.

3 Results

3.1 Genetic diagnosis and semen analysis of thirteen ADPKD patients

In our reproductive genetics department, thirteen patients with renal cysts or a family history of cystic kidney disease were highly suspected of having polycystic kidney disease. Targeted NGS was performed to detect variants associated with the symptoms. After variant calling and annotation, nine pathogenic and four likely pathogenic *PKD1* variants were identified in these patients

(Table 1). In particular, one patient (No. 8) harbored two variants that were classified as likely pathogenic and variants of uncertain significance (VUS) according to the ACMG-AMP guidelines (22).

These patients all suffered from male infertility. Two patients (Nos. 8 and 11 in Table 1) had severe oligospermia and three patients (Nos. 9, 10 and 12 in Table 1) had azoospermia. Semen samples from the other eight patients and sixteen age-matched controls were analyzed by CASA (Table 2). Compared to controls, the percentage of sperm with progressive motility (PR, %) and sperm with normal morphology in ADPKD patients was apparently less ($P < 0.001$) and below the reference limit (Table 2). In addition, the parameters of sperm curvilinear velocity (VCL), straight-line velocity (VSL), average path velocity (VAP), and amplitude of lateral head displacement (ALH) were also significantly lower in ADPKD patients than that in healthy controls ($P < 0.05$).

3.2 Morphological defects of spermatozoa in ADPKD patients

To further investigate the sperm abnormalities in ADPKD patients, we observed sperm morphology by acetylated α-tubulin immunostaining, a protein specific for flagellar microtubules. In *PKD1*-mutant patients, spermatozoa showed a high rate of coiled flagella and some had small heads (Figure 1A). Moreover, the length of acetylated α-tubulin staining on sperm flagella of was shorter in patients than that of in control s and the expression of acetylated α-tubulin was also lower in ADPKD patients (Figures 1B–D).

Detected by TEM, the normal ultrastructure of sperm flagella was shown in controls, including nine microtubular doublets and two central singlets along the entire tail, the mitochondrial sheath and outer dense fibers (ODFs) in the middle piece, as well as the fibrous sheath in the principal piece (Figures 1Ea-g). However, longitudinal sections of sperm from ADPKD patients showed coiled flagella wrapped around the heads forming a loop (Figures 1Fa, b). Additionally, the intrinsic structure of the axonemes was dramatically disrupted in of. In transverse sections, the absence of central singlets and irregular arrangements or a decrease in the number of doublet microtubules and ODFs were frequently observed in different pieces of sperm flagella (Figures 1Fc-f).

3.3 Compromised ciliogenesis in *Pkd1*-depleted mouse kidney tubule cells

PC1, encoded by *PKD1*, is one of the structural components of primary cilia. To evaluate the ciliogenesis of *Pkd1*-depleted mouse kidney tubule cells, the cells were grown at 37°C for 7 days without interferon-γ. After induction, the number of ciliated cells labeled with acetylated α-tubulin of in homozygous *Pkd1*-depleted ($Pkd1^{-/-}$) cells with less than that in heterozygous *Pkd1*-depleted ($Pkd1^{+/-}$) cells (Figures 2A, B). Furthermore, the length of cilia of in $Pkd1^{-/-}$ cells was significantly shorter than that in $Pkd1^{+/-}$ cells (Figures 2C, D). In addition, the acetylation level of α-tubulin in $Pkd1^{-/-}$ cells was lower compared to $Pkd1^{+/-}$ cells after ciliogenesis, whereas there was no significant difference between $Pkd1^{-/-}$ and $Pkd1^{+/-}$ cells before ciliogenesis (Figures 2E, F). These results suggest an important role of *PKD1* in ciliogenesis, the underlying mechanism of which may be similar to the defects in sperm flagella in ADPKD.

TABLE 1 Genetic information of the ADPKD patients.

Patients	Gene	Exon/ Intron	Nucleotide change	Amino acid change	Zygosity	De novo/Inherited	Variant Classification
1	*PKD1*	EX18	c.7288C>T	p. Arg2430Ter	heterogeneous	inherit	pathogenic
2	*PKD1*	EX14	c.6465_6466delGC	p. Leu2155fs18Ter	heterogeneous	inherit	pathogenic
3	*PKD1*	EX15	c.3670G>T	p. Glu1224Ter	heterogeneous	*de novo*	pathogenic
4	*PKD1*	EX5	c.937G>T	p. Glu313Ter	heterogeneous	inherit	pathogenic
5	*PKD1*	EX46	c.12448C>T	p. Arg4150Cys	heterogeneous	inherit	likely pathogenic
6	*PKD1*	EX28	c.9578C>T	p. Pro3193Leu	heterogeneous	inherit	likely pathogenic
7	*PKD1*	EX10	c.1987C>T	p. Gln663Ter	heterogeneous	inherit	pathogenic
8	*PKD1*	EX3	c.350T>C	p. Leu117Ser	heterogeneous	*de novo*	likely pathogenic
	PKD1	EX46	c.12455A>C	p. Lys4152Thr	heterogeneous	inherit	VUS
9	*PKD1*	EX13	c.3067C>T	p. Gln1023Ter	heterogeneous	inherit	pathogenic
10	*PKD1*	EX45	c.12366G>A	p. Trp4122Ter	heterogeneous	inherit	pathogenic
11	*PKD1*	EX46	c.12712C>T	p. Gln4238Ter	heterogeneous	NA	pathogenic
12	*PKD1*	EX15	c.4997G>A	p. Trp1666Ter	heterogeneous	inherit	pathogenic
13	*PKD1*	EX15	c.6890A>C	p. His2297Pro	heterogeneous	NA	likely pathogenic

NA, not available; VUS, Variant of uncertain significance.

TABLE 2 Sperm characteristics of ADPKD patients and age-matched healthy controls.

Parameters	Male controls (n=16)	ADPKD patients (n=8)	*P* value
Age	37.56 ± 5.39	37.50 ± 6.16	0.980
Semen volume (ml)	3.25 ± 1.41	2.41 ± 1.29	0.173
Sperm concentration (10^6 per ml)	60.36 ± 30.27	66.96 ± 61.19	0.724
Normal forms (%)	5.63 ± 1.41	2.75 ± 1.91	<0.001
Progressive motility (PR, %)	50.77 ± 10.59	17.23 ± 13.17	<0.001
Non-progressive motility (NP, %)	7.15 ± 4.44	13.22 ± 16.03	0.325
Immotile spermatozoa (IM, %)	42.81 ± 10.63	70.60 ± 15.62	<0.001
Curvilinear velocity (VCL, μm/s)	101.15 ± 23.90	56.09 ± 24.04	<0.001
Straight-line velocity (VSL, μm/s)	46.72 ± 5.85	28.37 ± 11.44	<0.001
Average path velocity (VAP, μm/s)	60.36 ± 8.88	35.61 ± 14.23	<0.001
Linearity (LIN, %)	49.63 ± 8.89	56.10 ± 9.35	0.113
Amplitude of lateral head displacement (ALH, μm)	5.34 ± 1.56	3.38 ± 1.38	0.006
Straightness (STR, %)	77.71 ± 7.82	80.90 ± 7.69	0.354
Beat-cross frequency (BCF, Hz)	23.74 ± 2.72	22.62 ± 4.04	0.426
Wobble (WOB, %)	61.87 ± 5.45	67.45 ± 6.18	0.034

3.4 Increased nuclear accumulation of YAP/TAZ in the absence of PC1

Several studies on in animal models have shown that YAP/TAZ, known as transcriptional coactivators that promote cell proliferation, are critical for ciliogenesis and kidney development (16, 17). Since YAP/TAZ may be involved in the pathogenesis of ADPKD, we detected the expression of YAP and TAZ in *Pkd1*-depleted kidney tubule cells. It was shown that the expression patterns of total YAP/TAZ were qualitatively parallel, with no difference between $Pkd1^{+/-}$ cells and $Pkd1^{-/-}$ cells (Figures 3A, B). Nevertheless, the both phospho-YAP and phospho-TAZ were reduced in homozygous cells. Moreover, YAP/TAZ were prone to accumulate in the nuclei in of $Pkd1^{-/-}$ cells (Figure 3C), which would enhance their growth-promoting function. Indeed, $Pkd1^{-/-}$ cells were found to proliferate faster than $Pkd1^{+/-}$ cells detected by the cell growth curve and BrdU assay (Figures S1A–C).

3.5 Disruption of PC1 restrained the Hippo signaling pathway

The activation of YAP/TAZ is mainly regulated by the Hippo kinase cascade. To further explore the cause of reduced phospho-YAP/TAZ, we detected core components in of the Hippo signaling pathway. It was found that both MST1 and LATS1 were reduced in $Pkd1^{-/-}$ cells (Figures 4A–E), with a significant difference compared with to in $Pkd1^{+/-}$ cells. Moreover, phospho-MOB1, which is regulated by MST1, appeared to be reduced in $Pkd1^{-/-}$ cells in concordance with the reduction of MST1 (Figure 4F). The scaffold protein SAV1, which is also phosphorylated by MST1 and complexes with MST1 to activate LATS1/2 and MOB1, was not significantly different between the two cell types (Figure 4G). Activated YAP/TAZ drives the transcription factor TEAD4 to bind to the promoter region of the Aurora A kinase (*Aurka*), which has been demonstrated to promote ciliary disassembly by activating the histone deacetylase 6 (HDAC6) (24). We found a significantly increased expression of AURKA in the absence of PC1 (Figures 4H–J), suggesting that the enhanced ciliary disassembly contributes to the compromised ciliary integrity in *Pkd1*-depleted cells.

4 Discussion

The sperm tail is the propulsion system, so the abnormal structures of the flagella are responsible for sperm immobility, which is also a typical feature of male infertility (25). Accumulating evidence suggests that sperm motility is associated with pathologies of the sperm tail, including defects in the mitochondrial sheath, the outer dense fiber, the fibrous sheath or the axoneme (26). For instance, SPAG6 is a scaffold protein that localized in the central microtubules of flagellar axonemes. The male *Spag6* knockout mice were infertile and characterized by abnormal sperm flagella, such as the loss of central microtubules, disorganized ODFs and disrupted fiber sheaths (27).In a study of 247 patients with asthenospermia, flagellar abnormalities were frequently detected (28). In this study, we found that men with ADPKD, an inherited cystic kidney disease, were associated with male infertility. The spermatozoa of these patients had obvious flagellar defects, such as coiled and short flagella, missing central microtubules, and irregular peripheral doublets. Primary ciliary dyskinesia (PCD), another ciliopathy, was also associated with male infertility. In an adult cohort of PCD, 37 males out of 49

10.3389/fendo.2023.1130536

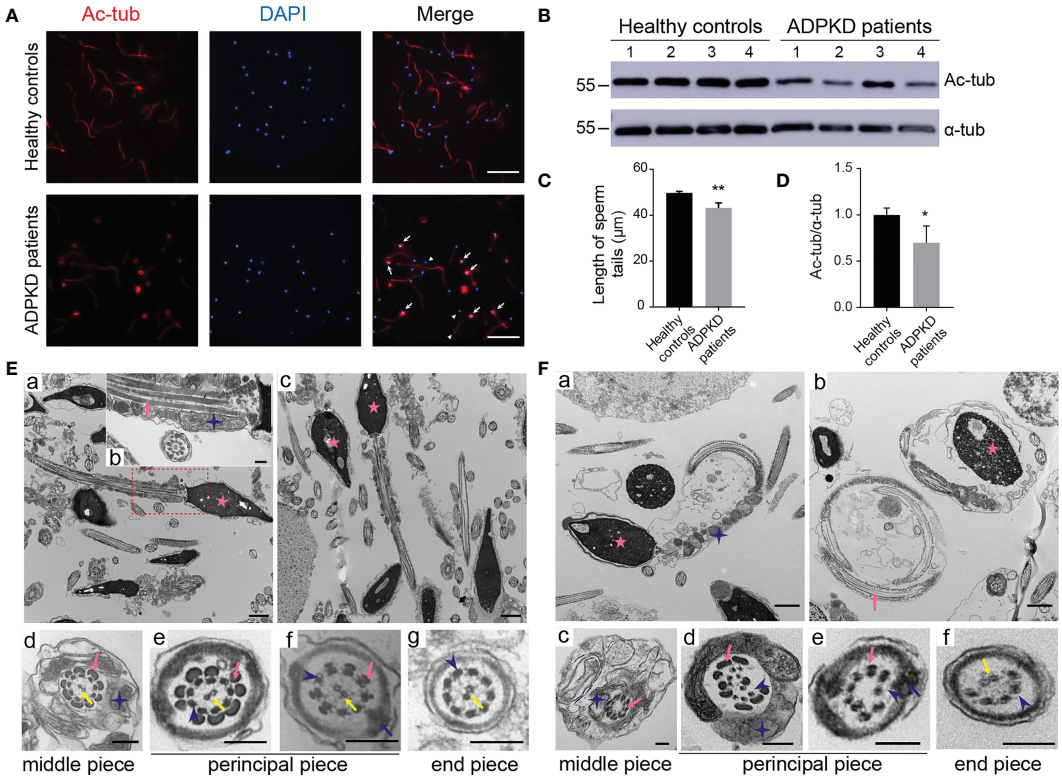

FIGURE 1
Morphology of sperm from healthy controls and ADPKD patients. **(A)** Immunofluorescence staining of sperms. White arrows indicate curled sperm flagella stained with acetylated α-tubulin (red signal) in ADPKD patients. White arrowheads indicate small sperm heads stained with 4′,6-diamidino-2-phenylindole (DAPI) (blue signal). Scale bar: 50μm. **(B)** Representative western blotting images of acetylated α-tubulin and α-tubulin in sperms from healthy controls and ADPKD patients (n=4). **(C)** Comparison of sperm tail length between controls and ADPKD patients (n=4). At least 30 sperms were counted from each individual observed from three random fields per slide. **(D)** Relative intensities of acetylated α-tubulin/α-tubulin in sperms. **(E)** Ultrastructure of sperm flagella from healthy controls. (a, c) Longitudinal sections of normal spermatozoa with straight sperm tails. (b) Magnification of the dotted area in (a). (d-g) Cross-sections of spermatozoa at various levels with regular arrangement of axonemes. **(F)** Ultrastructure of sperm flagella from ADPKD patients. (a, b) Sperm flagella in ADPKD patients are coiled and wrapped around the heads. (c-f) Disruption of axonemes or outer dense fibers in the cross-section of sperm tails. Blue stars indicate mitochondria, pink arrows indicate outer dense fibers, blue arrows indicate fibrous sheath, yellow arrows indicate central axoneme; blue arrowheads indicate peripheral axonemes, and pink stars indicate nuclei. Scale bars: Ea, Ec, Fa, Fb: 1μm; Eb, Ed-g, Fc-f: 200nm. Error bars indicate standard deviation of three independent experiments (*P < 0.05, **P < 0.01; Student's t test).

(75.5%) PCD patients were infertile (29). Thus, the sterile manifestations of ciliopathies may be due to a similar mechanism of ciliogenesis and flagellogenesis.

The core of the sperm flagellum is the axoneme, which consists of a central pair of singlet microtubules and nine surrounding microtubular doublets (30). Two major components of microtubules, α-tubulin and β-tubulin, undergo various post-translational modifications (PTMs), including acetylation, tyrosination, glutamylation, and glycation (31). As the most common PTM, acetylation of α-tubulin, first identified in axonemes of Chlamydomonas at the of lysine 40 (32), is a marker of stable microtubules, such as cilia and flagella. Acetylated α-tubulin is involved in many cellular processes, including cilium assembly, cellular signal and intracellular transport (33, 34). In semen samples of from ADPKD patients, we observed that the acetylation level of α-tubulin was significantly reduced. Intriguingly, a similar downward trend in the ratio of sperm acetylated α-tubulin/α-tubulin has been reported in individuals with asthenospermia compared with to controls (35). Moreover, the sperm flagella immunostained with acetylated α-tubulin were shorter in ADPKD patients. It suggested that the shortened flagella may contribute to poor sperm motility in ADPKD males.

The Hippo signaling pathway, which is highly conserved in mammals, is essential for controlling organ size and plays a vital role in cancer (36). Recently, it has been shown that YAP, one of the core components of the Hippo signaling, is associated with primary cilia growth (37–40). To investigate whether the Hippo signaling pathway is relevant to the pathogenesis of ADPKD, we detected YAP/TAZ expression in *Pkd1*-depleted mouse kidney tubule cells. It was found that phosphorylation level of YAP/TAZ was apparently reduced in $Pkd1^{-/-}$ cells, which promoted the of YAP/TAZ translocation to the nucleus. Consequentially, proliferation of $Pkd1^{-/-}$ cells was accelerated and the level of AURKA, a cilium disassembly-related protein, was obviously elevated under the regulation of nuclear YAP/TAZ. To further investigate the altered Hippo signaling, it was identified that MST1 and LATS1, the upstream kinases of YAP/TAZ, were both prominently decreased in the absence of PC1. Notably, it was reported that Hippo signaling

10.3389/fendo.2023.1130536

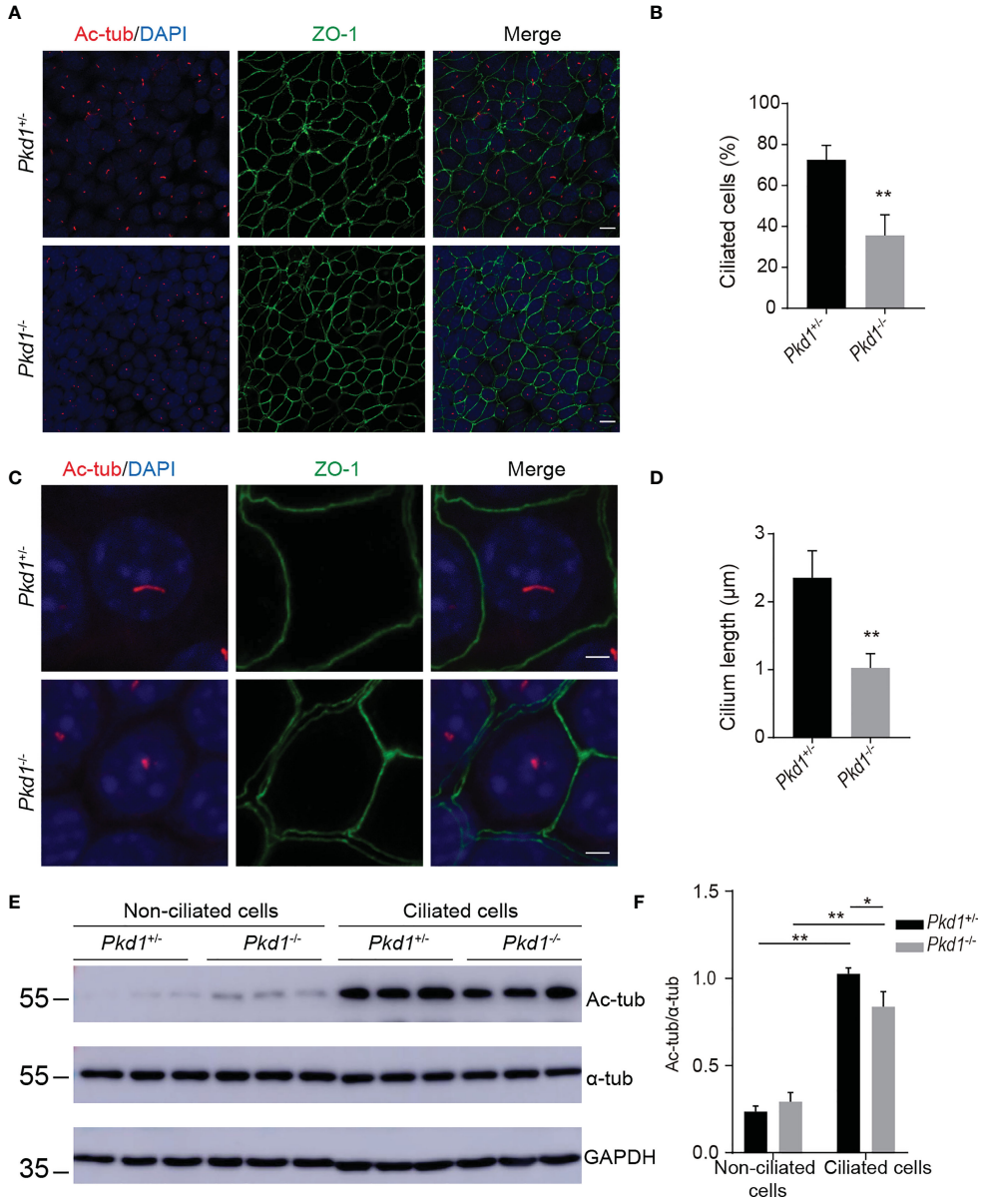

FIGURE 2
Compromised ciliary integrity in *Pkd1*-depleted mouse kidney tubule cells. **(A)** Immunofluorescence images of homozygous or heterozygous *Pkd1*-knockout cells. Cilia and tight junctions were stained with acetylated α-tubulin (red) and ZO-1 (green), respectively. Nuclei were stained with DAPI (blue). Scale bar: 25μm. **(B)** Percentage of ciliated cells in $Pkd1^{+/-}$ or $Pkd1^{-/-}$ cells. At least 200 cells were counted from three random fields per slide. **(C)** Ciliary morphology in $Pkd1^{+/-}$ or $Pkd1^{-/-}$ cells. Scale bar: 2.5μm. **(D)** Quantifications of cilia length in $Pkd1^{+/-}$ or $Pkd1^{-/-}$ cells. At least 50 cells were counted from three random fields per slide. **(E)** Representative western blotting images of acetylated α-tubulin (Ac-tub) and α-tubulin (α-tub) with GAPDH loading control in non-ciliated and ciliated *Pkd1*-depleted mouse kidney tubule cells. **(F)** Relative intensities of acetylated α-tubulin/α-tubulin in cells. Error bars indicate standard deviation of three independent experiments (*$P < 0.05$, **$P < 0.01$; Student's *t* test).

pathway promotes ciliogenesis through preventing AURKA from forming the complex with the HDAC6 to stabilize the ciliary axoneme (41, 42). HDAC6 has been recognized to exacerbate cyst growth in ADPKD through enhancing cAMP signaling and upregulating epidermal growth factor receptor (EGFR) activity (43). As a result of reduced of MST1 and increased AURKA in the *Pkd1*-depleted cells, the function of HDAC6 would be enhanced, which would subsequently promote the ciliary disassembly (Figure 5).

Nevertheless, there are some limitations to this study. First, limited to ADPKD patients recruited from the reproductive outpatient department, it must be acknowledged that there was a selection bias and all of ADPKD subjects had abnormal semen parameters. We did not encounter ADPKD subjects without infertility as a control group to further verify the association of flagellar abnormalities with infertility. Although, it is difficult to conclude that all male patients with ADPKD are infertile, a certain proportion of infertility in male patients with ADPKD has been

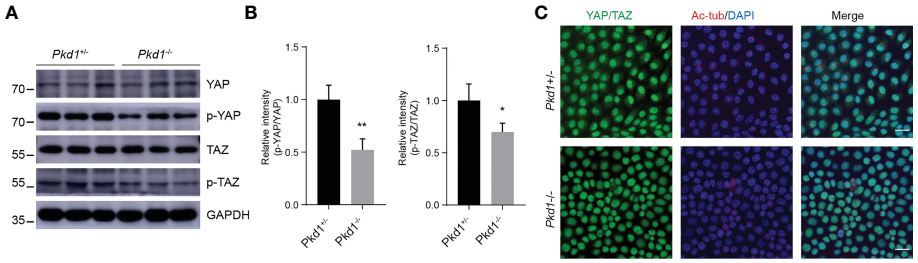

FIGURE 3
Increased nuclear accumulation of YAP/TAZ in the absence of PC1. **(A)** Representative western blotting images of YAP, phospho-YAP, TAZ and phospho-TAZ in ciliated *Pkd1*$^{+/-}$ and *Pkd1*$^{-/-}$ cells. **(B)** Relative intensities of phospho-Yap to Yap and phospho-TAZ to TAZ. Error bars indicates standard deviation of three independent experiments (*P < 0.05, **P < 0.01; Student's t test). **(C)** Immunofluorescence staining of YAP/TAZ (green), acetylated α-tubulin (red), and DAPI (blue). Scale bar: 25μm.

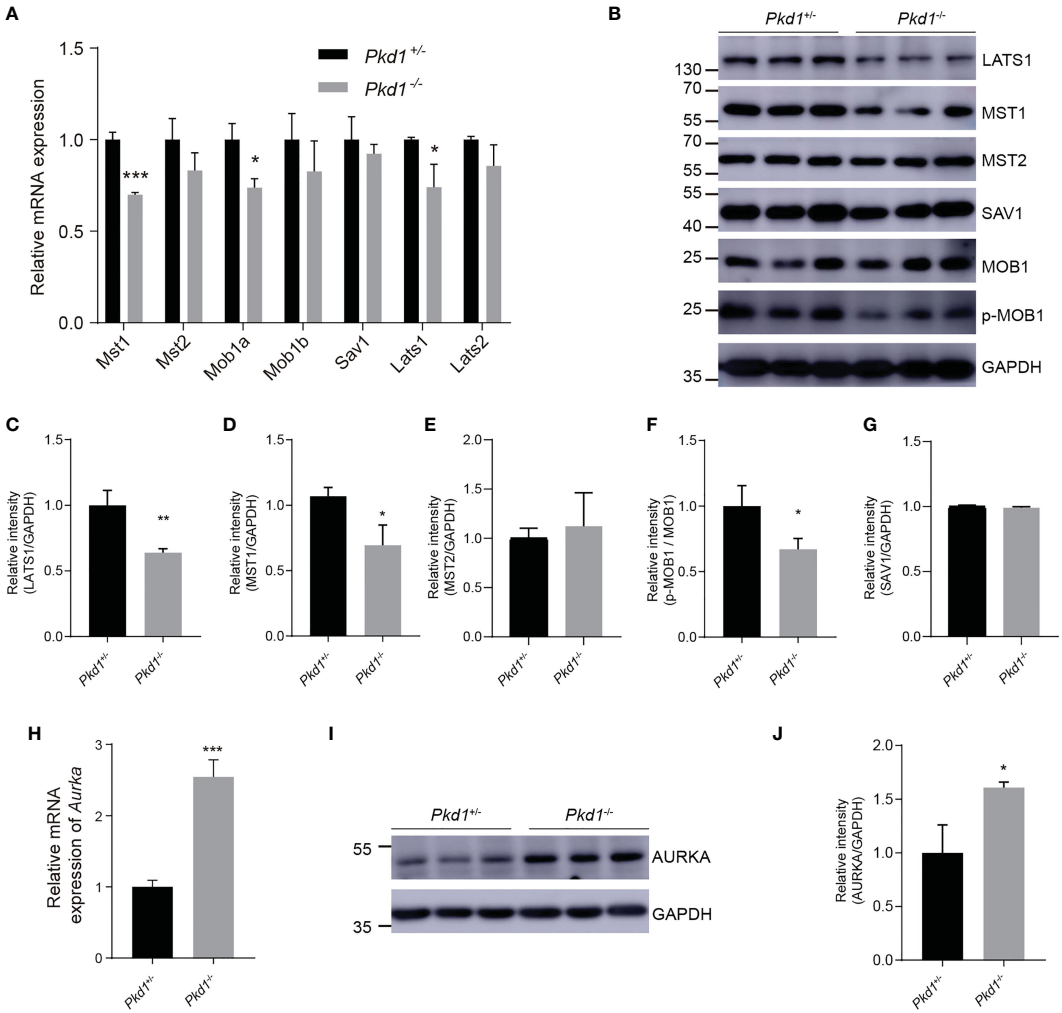

FIGURE 4
The restrained Hippo signaling pathway and increased AURKA. **(A)** Relative mRNA expression of core components of the Hippo kinase cascade. **(B)** Representative western blotting images of core components of the Hippo signaling pathway with GAPDH as the loading control. **(C–G)** Relative intensities of LATS1, MST1, MST2, p-MOB1, and SAV1, respectively. **(H)** Relative mRNA expression of *Aurka* in *Pkd1*$^{+/-}$ and *Pkd1*$^{-/-}$ cells. **(I)** Representative western blotting images of AURKA. **(J)** Relative intensity of AURKA. All error bars indicate standard deviation of three independent experiments (*P < 0.05, **P < 0.01, ***P < 0.001; Student's t test).

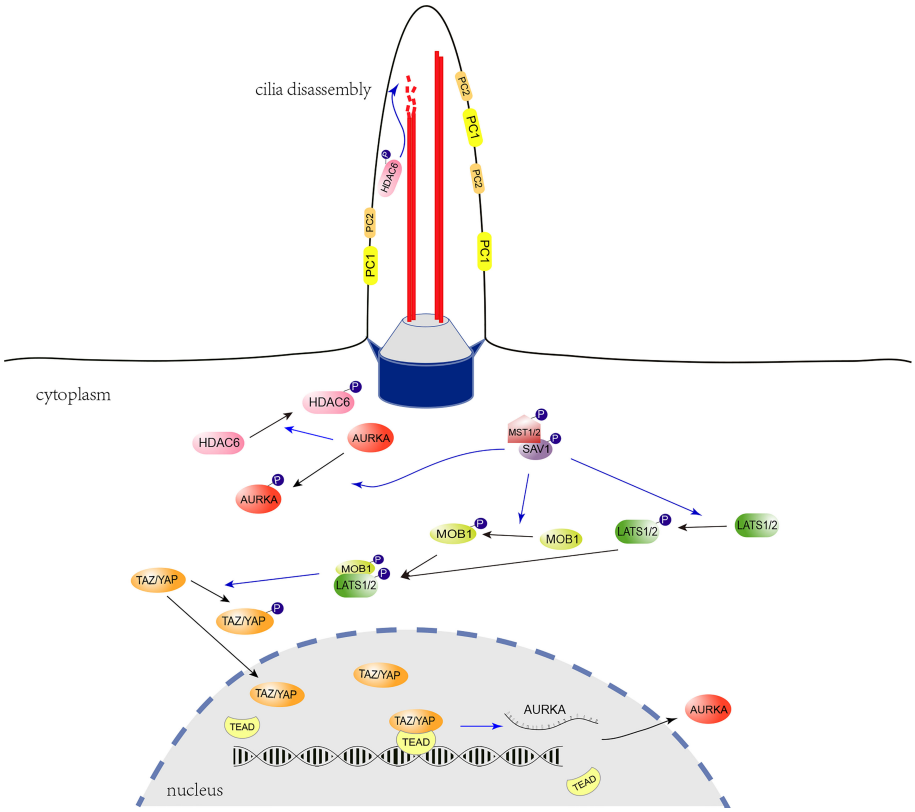

FIGURE 5
Regulatory role of the Hippo signaling pathway in ciliogenesis. The cilium is indicated with two microtubule doublets (red robs) bounded with the ciliary membrane, the transition zone (grey trapezoidal cylinder), and the basal body (blue cylinder) formed with the mother centriole. In the Hippo signaling pathway, Activated LATS1/2 phosphorylate and inhibit the translocation of YAP/TAZ from the cytoplasm to the nucleus. LATS1/2 is activated by MST1/2 through direct phosphorylation, which is promoted by the scaffold protein, phosphorylated SAV1. The YAP/TAZ act as transcriptional coactivators and interact with the TEAD transcription factor 4 (TEAD 4) to regulate the expression of *Aurka*. The AURKA phosphorylates and activates the tubulin deacetylase HDAC6 to promote ciliary disassembly. In the absence of PC1, decreased MST1 and LATS1 may promote YAP/TAZ nuclear translocation, facilitate *Aurka* transcription and subsequent ciliary disassembly. The blue-arrow lines indicate positive regulation.

reported (7, 9, 44). Second, the structure of spermatozoa was not detected in all patients due to the limited sperm samples in 5 patients (Nos. 9-13). Thus, the flagellar abnormalities identified in this study may partially explain male infertility in ADPKD, but cannot account for the manifestations of infertility in all ADPKD patients, which warrants further investigation.

5 Conclusions

In conclusion, we highlighted the association between ADPKD and male infertility. Male ADPKD patients showed defects in the sperm morphology and shortened length of in sperm flagella. In the absence of PC1, MST1 and LATS1, the upstream components of the Hippo signaling pathway, were apparently reduced, which not only led to hyperactivation of YAP/TAZ, but also promoted AURKA/HDAC6-dependent ciliary disassembly. Our results demonstrated that the restrained Hippo signaling played a vital role in abnormal ciliogenesis and was potentially involved in the pathogenesis of flagellar defects in ADPKD.

Data availability statement

The datasets presented in this study can be found in online repositories. The names of the repository/repositories and accession number(s) can be found in the article/Supplementary Material.

Ethics statement

This study was prospectively approved by the ethics review committee of IPMCH. The patients/participants provided their written informed consent to participate in this study.

Author contributions

C-MX and H-FH conceived the study and edited the paper. W-HS and Z-YZ carried out cell experiments and drafted the paper. M-JY, N-XQ, and Z-RJ collected semen samples and conducted sperm analysis. N-XX, X-YZ, X-LC, and S-CC analyzed the data. Z-YZ and

M-JY made the figures. All authors contributed to the article and approved the submitted version.

Funding

This work is supported by the National Natural Science Foundation of China (Nos. 8197060221, 82171677), National Key R&D Program (2021YFC2701002, 2022YFC2703701), Shanghai Municipal Health Commission (No.GW-10.1-XK07), the Shanghai Municipal Commission of Science and Technology Program (21Y21901002, 22S31901500), CAMS Innovation Fund for Medical Sciences (2019-I2M-5-064), Collaborative Innovation Program of Shanghai Municipal Health Commission (2020CXJQ01).

Acknowledgments

We thank all the participants in this research. We also appreciate the support provided by the Youth Science and Technology Innovation Studio, Shanghai Jiao Tong University School of Medicine.

Conflict of interest

The authors declare that the research was conducted in the absence of any commercial or financial relationships that could be construed as a potential conflict of interest.

Publisher's note

Supplementary material

The Supplementary Material for this article can be found online at: https://www.frontiersin.org/articles/10.3389/fendo.2023.1130536/full#supplementary-material

References

1. Simms RJ. Autosomal dominant polycystic kidney disease. *BMJ (Clinical Res ed)* (2016) 352:i679. doi: 10.1136/bmj.i679

2. Torres VE, Harris PC, Pirson Y. Autosomal dominant polycystic kidney disease. *Lancet (London England)* (2007) 369(9569):1287–301. doi: 10.1016/S0140-6736(07)60601-1

3. Ong AC, Devuyst O, Knebelmann B, Walz G. Autosomal dominant polycystic kidney disease: the changing face of clinical management. *Lancet (London England)* (2015) 385(9981):1993–2002. doi: 10.1016/S0140-6736(15)60907-2

4. Nauli SM, Alenghat FJ, Luo Y, Williams E, Vassilev P, Li X, et al. Polycystins 1 and 2 mediate mechanosensation in the primary cilium of kidney cells. *Nat Genet* (2003) 33(2):129–37. doi: 10.1038/ng1076

5. Park JH, Woo YM, Ko JY, Kim DY. Autosomal dominant polycystic kidney disease induced by ciliary defects. In: Li X, editor. *Polycystic kidney disease*. Brisbane (AU: Codon Publications (2015).

6. Van der Linden EF, Bartelink AK, Ike BW, van Leeuwaarden B. Polycystic kidney disease and infertility. *Fertil Steril* (1995) 64(1):202–3. doi: 10.1016/S0015-0282(16)57683-3

7. Kanagarajah P, Ayyathurai R, Lynne CM. Male Infertility and adult polycystic kidney disease–revisited: case report and current literature review. *Andrologia* (2012) 44 Suppl 1:838–41. doi: 10.1111/j.1439-0272.2011.01221.x

8. Nie X, Arend LJ. Pkd1 is required for male reproductive tract development. *Mech Dev* (2013) 130(11-12):567–76. doi: 10.1016/j.mod.2013.07.006

9. Shefi S, Levron J, Nadu A, Raviv G. Male Infertility associated with adult dominant polycystic kidney disease: a case series. *Arch Gynecol Obstet* (2009) 280 (3):457–60. doi: 10.1007/s00404-008-0916-9

10. Torra R, Sarquella J, Calabia J, Martí J, Ars E, Fernández-Llama P, et al. Prevalence of cysts in seminal tract and abnormal semen parameters in patients with autosomal dominant polycystic kidney disease. *Clin J Am Soc Nephrol CJASN.* (2008) 3 (3):790–3. doi: 10.2215/CJN.05311107

11. Reig B, Blumenfeld J, Donahue S, Prince MR. Seminal megavesicle in autosomal dominant polycystic kidney disease. *Clin Imag* (2015) 39(2):289–92. doi: 10.1016/j.clinimag.2014.10.016

12. Zhang W, Stephens CJ, Blumenfeld JD, Behzadi AH, Donahue S, Bobb WO, et al. Relationship of seminal megavesicles, prostate median cysts, and genotype in autosomal dominant polycystic kidney disease. *J Magn Reson Imag* (2019) 49(3):894–903. doi: 10.1002/jmri.26289

13. Gao Z, Ruden DM, Lu X. PKD2 cation channel is required for directional sperm movement and male fertility. *Curr Biol* (2003) 13(24):2175–8. doi: 10.1016/j.cub.2003.11.053

14. Amaral A, Castillo J, Ramalho-Santos J, Oliva R. The combined human sperm proteome: cellular pathways and implications for basic and clinical science. *Hum Reprod Update* (2014) 20(1):40–62. doi: 10.1093/humupd/dmt046

15. Yu FX, Zhao B, Guan KL. Hippo pathway in organ size control, tissue homeostasis, and cancer. *Cell* (2015) 163(4):811–28. doi: 10.1016/j.cell.2015.10.044

16. Yu FX, Guan KL. The hippo pathway: regulators and regulations. *Genes Dev* (2013) 27(4):355–71. doi: 10.1101/gad.210773.112

17. Gumbiner BM, Kim NG. The hippo-YAP signaling pathway and contact inhibition of growth. *J Cell Sci* (2014) 127(Pt 4):709–17. doi: 10.1242/jcs.140103

18. Zhao B, Wei X, Li W, Udan RS, Yang Q, Kim J, et al. Inactivation of YAP oncoprotein by the hippo pathway is involved in cell contact inhibition and tissue growth control. *Genes Dev* (2007) 21(21):2747–61. doi: 10.1101/gad.1602907

19. He L, Xu W, Jing Y, Wu M, Song S, Cao Y, et al. Yes-associated protein (Yap) is necessary for ciliogenesis and morphogenesis during pronephros development in zebrafish (Danio rerio). *Int J Biol Sci* (2015) 11(8):935–47. doi: 10.7150/ijbs.11346

20. Hossain Z, Ali SM, Ko HL, Xu J, Ng CP, Guo K, et al. Glomerulocystic kidney disease in mice with a targeted inactivation of Wwtr1. *Proc Natl Acad Sci USA* (2007) 104(5):1631–6. doi: 10.1073/pnas.0605266104

21. Chen SC, Xu XL, Zhang JY, Ding GL, Jin L, Liu B, et al. Identification of PKD2 mutations in human preimplantation embryos *in vitro* using a combination of targeted next-generation sequencing and targeted haplotyping. *Sci Rep* (2016) 6:25488. doi: 10.1038/srep25488

22. Richards S, Aziz N, Bale S, Bick D, Das S, Gastier-Foster J, et al. Standards and guidelines for the interpretation of sequence variants: a joint consensus recommendation of the American college of medical genetics and genomics and the association for molecular pathology. *Genet Med* (2015) 17(5):405–24. doi: 10.1038/gim.2015.30

23. World Health Organization DoRHaR. *WHO laboratory manual for the examination and processing of human semen fifth edition*. (2010). p. 287.

24. Gerstein MB, Kundaje A, Hariharan M, Landt SG, Yan KK, Cheng C, et al. Architecture of the human regulatory network derived from ENCODE data. *Nature* (2012) 489(7414):91–100. doi: 10.1038/nature11245

25. Escalier D. Knockout mouse models of sperm flagellum anomalies. *Hum Reprod Update* (2006) 12(4):449–61. doi: 10.1093/humupd/dml013

26. Chemes HE, Alvarez Sedo C. Tales of the tail and sperm head aches: changing concepts on the prognostic significance of sperm pathologies affecting the head, neck and tail. *Asian J Androl* (2012) 14(1):14–23. doi: 10.1038/aja.2011.168

27. Sapiro R, Kostetskii I, Olds-Clarke P, Gerton GL, Radice GL, Strauss IJ. Male Infertility, impaired sperm motility, and hydrocephalus in mice deficient in sperm-associated antigen 6. *Mol Cell Biol* (2002) 22(17):6298–305. doi: 10.1128/MCB.22.17.6298-6305.2002

28. Chemes HE, Olmedo SB, Carrere C, Oses R, Carizza C, Leisner M, et al. Ultrastructural pathology of the sperm flagellum: association between flagellar pathology and fertility prognosis in severely asthenozoospermic men. *Hum Reprod (Oxford England)* (1998) 13(9):2521–6. doi: 10.1093/humrep/13.9.2521

29. Vanaken GJ, Bassinet L, Boon M, Mani R, Honore I, Papon JF, et al. Infertility in an adult cohort with primary ciliary dyskinesia: phenotype-gene association. *Eur Respir J* (2017) 50(5). doi: 10.1183/13993003.00314-2017

30. Chemes HE. Phenotypic varieties of sperm pathology: Genetic abnormalities or environmental influences can result in different patterns of abnormal spermatozoa. *Anim Reprod Sci* (2018) 194:41–56. doi: 10.1016/j.anireprosci.2018.04.074

31. Song Y, Brady ST. Post-translational modifications of tubulin: pathways to functional diversity of microtubules. *Trends Cell Biol* (2015) 25(3):125–36. doi: 10.1016/j.tcb.2014.10.004

32. LeDizet M, Piperno G. Identification of an acetylation site of chlamydomonas alpha-tubulin. *Proc Natl Acad Sci USA* (1987) 84(16):5720–4. doi: 10.1073/pnas.84.16.5720

33. Li L, Yang XJ. Tubulin acetylation: responsible enzymes, biological functions and human diseases. *Cell Mol Life Sci CMLS* (2015) 72(22):4237–55. doi: 10.1007/s00018-015-2000-5

34. Janke C, Montagnac G. Causes and consequences of microtubule acetylation. *Curr Biol* (2017) 27(23):R1287–r92. doi: 10.1016/j.cub.2017.10.044

35. Bhagwat S, Dalvi V, Chandrasekhar D, Matthew T, Acharya K, Gajbhiye R, et al. Acetylated alpha-tubulin is reduced in individuals with poor sperm motility. *Fertil Steril* (2014) 101(1):95–104.e3. doi: 10.1016/j.fertnstert.2013.09.016

36. Dobrokhotov O, Samsonov M, Sokabe M, Hirata H. Mechanoregulation and pathology of YAP/TAZ via hippo and non-hippo mechanisms. *Clin Trans Med* (2018) 7(1):23. doi: 10.1186/s40169-018-0202-9

37. Xu Q, Liu X, Liu W, Hayashi T, Yamato M, Fujisaki H, et al. Type I collagen-induced YAP nuclear expression promotes primary cilia growth and contributes to cell migration in confluent mouse embryo fibroblast 3T3-L1 cells. *Mol Cell Biochem* (2018) 450(1–2):87–96. doi: 10.1007/s11010-018-3375-z

38. Grampa V, Delous M, Zaidan M, Odye G, Thomas S, Elkhartoufi N, et al. Novel NEK8 mutations cause severe syndromic renal cystic dysplasia through YAP dysregulation. *PloS Genet* (2016) 12(3):e1005894. doi: 10.1371/journal.pgen.1005894

39. Habbig S, Bartram MP, Sagmuller JG, Griessmann A, Franke M, Muller RU, et al. The ciliopathy disease protein NPHP9 promotes nuclear delivery and activation of the oncogenic transcriptional regulator TAZ. *Hum Mol Genet* (2012) 21(26):5528–38. doi: 10.1093/hmg/dds408

40. Habbig S, Bartram MP, Muller RU, Schwarz R, Andriopoulos N, Chen S, et al. NPHP4, a cilia-associated protein, negatively regulates the hippo pathway. *J Cell Biol* (2011) 193(4):633–42. doi: 10.1083/jcb.201009069

41. Kim M, Kim M, Lee MS, Kim CH, Lim DS. The MST1/2-SAV1 complex of the hippo pathway promotes ciliogenesis. *Nat Commun* (2014) 5:5370. doi: 10.1038/ncomms6370

42. Pugacheva EN, Jablonski SA, Hartman TR, Henske EP, Golemis EA. HEF1-dependent aurora a activation induces disassembly of the primary cilium. *Cell* (2007) 129(7):1351–63. doi: 10.1016/j.cell.2007.04.035

43. Ke B, Chen Y, Tu W, Ye T, Fang X, Yang L. Inhibition of HDAC6 activity in kidney diseases: a new perspective. *Mol Med (Cambridge Mass)* (2018) 24(1):33. doi: 10.1186/s10020-018-0027-4

44. Belet U, Danaci M, Sarikaya S, Odabas F, Utas C, Tokgoz B, et al. Prevalence of epididymal, seminal vesicle, prostate, and testicular cysts in autosomal dominant polycystic kidney disease. *Urology* (2002) 60(1):138–41. doi: 10.1016/S0090-4295(02)01612-6

frontiers | Frontiers in Endocrinology

TYPE Original Research
PUBLISHED 23 June 2023
DOI 10.3389/fendo.2023.1155639

OPEN ACCESS

EDITED BY
Tao Luo,
Nanchang University, China

REVIEWED BY
Xiaojin He,
First Affiliated Hospital of Anhui Medical University, China
Susana Seixas,
Universidade do Porto, Portugal

*CORRESPONDENCE
Erpo Tian
tianep@jxr-fertility.com

†These authors have contributed equally to this work

RECEIVED 31 January 2023
ACCEPTED 29 May 2023
PUBLISHED 23 June 2023

CITATION
Liu M, Dai S, Zhang J, Yang Y, Shen Y, Liu H, Yang Y, Jiang C and Tian E (2023) A novel mutation in *CFAP47* causes male infertility due to multiple morphological abnormalities of the sperm flagella. *Front. Endocrinol.* 14:1155639. doi: 10.3389/fendo.2023.1155639

A novel mutation in *CFAP47* causes male infertility due to multiple morphological abnormalities of the sperm flagella

Mohan Liu[1†], Siyu Dai[2,3†], Jiying Zhang[1†], Yihong Yang[4], Ying Shen[5], Hongqian Liu[2,3], Yanting Yang[2,3], Chuan Jiang[5] and Erpo Tian[6*]

[1]State Key Laboratory of Biotherapy and Cancer Center, West China Hospital, Sichuan University and Collaborative Innovation Center, Chengdu, China, [2]Department of Obstetrics and Gynecology, West China Second University Hospital, Sichuan University, Chengdu, China, [3]Medical Genetics Department/Prenatal Diagnostic Center, West China Second University Hospital, Sichuan University, Chengdu, China, [4]Key Laboratory of Obstetric, Gynecologic and Pediatric Diseases and Birth Defects of Ministry of Education, Reproduction Medical Center of West China Second University Hospital, Sichuan University, Chengdu, China, [5]Department of Obstetrics/Gynecology, Key Laboratory of Obstetric, Gynecologic and Pediatric Diseases and Birth Defects of Ministry of Education, West China Second University Hospital, Sichuan University, Chengdu, China, [6]Department of Andrology, Xi'nan Gynecology Hospital, Chengdu, China

Introduction: A previous study suggested that loss of CFAP47 function is involved in multiple morphological abnormalities of the sperm flagella (MMAF) in humans and mice. However, the comprehensive role of *CFAP47* in spermatogenesis is largely unknown.

Methods: Whole-exome sequencing (WES) was conducted to identify pathogenic variant in two patients with MMAF. The functional effect of the identified mutations was investigated by immunofluorescence staining and western blotting. Intracytoplasmic sperm injection (ICSI) was used to assist fertilization for the patient with MMAF.

Results: In this study, we identified a novel missense mutation (c.1414G>A; p.V472M) in *CFAP47* in two unrelated patients with oligoasthenoteratozoospermia. Intriguingly, in addition to the MMAF phenotype very analogous to the previous report, the two patients notably presented abnormal morphology of sperm heads, the sperm mitochondrial sheath was obviously disorganized, and the sperm annulus were almost defective. Further functional experiments confirmed that the expression of CFAP47 was markedly reduced in the spermatozoa of the patients. Mechanism analysis suggested that CFAP47 might regulate the expression of CFAP65, CFAP69 and SEPTIN4 through their physical interactions and thus modulating sperm morphogenesis.

Conclusion: we revealed a novel mutation in *CFAP47* and further expanded the phenotype and mutation spectrum of *CFAP47*, as well as the potential mechanism of *CFAP47* manipulating spermatogenesis, finally providing important guidance for genetic counseling and targeted treatment for *CFAP47* mutation-related male infertility.

KEYWORDS

asthenoteratozoospermia, MMAF, CFAP47, hemizygous mutation, WES

Introduction

Infertility refers to a couple failing to conceive after 12 months of unprotected regular sexual intercourse (1, 2). It affects approximately 15% of couples worldwide, and male factors contribute to more than half of the cases (3). Spermatogenesis disorders include sperm defects in quality or quantity, which is manifested as the decreased sperm number, reduced sperm motility or abnormal sperm morphology (4). According to the criteria published in 2010 by the World Health Organization (WHO), teratozoospermia is defined as the presence of spermatozoa with abnormal morphology over 96% in one-time ejaculation (5). The phenotype and etiology of teratozoospermia are highly heterogeneous, and recent research based on animal models and genetic analysis has uncovered certain disease-causing or disease-promoting genes (6). Sperm head abnormalities are observed in teratozoospermia patients, mainly including macrozoospermia and globozoospermia. *Aurora kinase C* (*AURKC*) is the only definite cause of macrozoospermia (7); dysfunction of *dpy-19 like 2* (*DPY19L2*) (8), *chromosome 7 open reading frame 61* (*C7orf61*) (9), *c2 calcium-dependent domain containing 6* (*C2CD6*) (9), *gametogenetin* (*GGN*) (9), *coiled-coil domain containing 62* (*CCDC62*) (10), *calicin* (*CCIN*) (11), *protein interacting with PRKCA 1* (*PICK1*) (12), *spermatogenesis associated 16* (*SPATA16*) (13) and *zona pellucida binding protein 1* (*ZPBP1*) (14) are associated with globozoospermia. Multiple morphological abnormalities of the sperm flagella (MMAF) is a kind of asthenoteratozoospermia with defects in the sperm tail and reduced sperm motility (progressive motility of spermatozoa less than 32%) (5). Thus far, 42 MMAF-associated genes have been identified (6, 15, 16). However, a large number of asthenoteratozoospermia cases could not be explained. Therefore, a more comprehensive investigation of the pathology and molecular mechanisms of asthenoteratozoospermia is needed to further boost diagnosis efficacy.

Recently, Liu et al. suggested that *Cilia and flagella-associated protein 47* (*CFAP47*) is an MMAF-associated gene (17). They showed that patients with hemizygous *CFAP47* variants exhibit a typical MMAF phenotype, and the sperm ultrastructure shows an abnormal axoneme, including disorganized outer dense fibers (ODF), peripheral microtubule doublets (DMTs), and central pair of microtubules (CPs) (17). *CFAP47*-mutated male mice are sterile, with decreased sperm motility and abnormal flagella morphology (17). Therefore, the involvement of *CFAP47* in spermatogenesis is proved, and future studies should evaluate *CFAP47* mutations in larger cohorts to explore the comprehensive function of *CFAP47* in sperm morphology development.

Herein, we reported two infertile patients who carried a novel hemizygous mutation c.1414G>A [p.V472M] in *CFAP47*. Bioinformatics analysis and functional studies *in vitro* supported the pathogenicity of this mutation. Intriguingly, aside from the typical MMAF phenotype, numerous malformed sperm heads, defective sperm annulus, and aplasia sperm mitochondrial sheaths were evidently observed in the patients by exhaustive morphology analysis. Functional experiments indicated that CFAP47 might regulate the expression of CFAP65, CFAP69 and SEPTIN4 to mediate sperm morphogenesis. Our work highlighted a potential role of *CFAP47* in sperm head and tail formation in humans, broadening the gene variant and phenotype spectrum of *CFAP47* in male infertility.

Materials and methods

Study subjects and sample collection

The two infertile patients and their parents were recruited from the West China Second University Hospital of Sichuan University, and the chromosomal karyotypes of the patients were normal. This study was conducted following the tenets of the Declaration of Helsinki, and ethical approval was obtained from the Ethical Review Board of West China Second University Hospital, Sichuan University. We obtained written informed consent from each study participant.

Genetic analysis

Peripheral whole blood samples were collected from patients and their parents for genetic analyses. Using a whole blood DNA-purification kit (51104, QIAGEN), genomic DNA was extracted from peripheral blood samples of patients and their parents. Whole-exome sequencing (WES) and bioinformatics analyses were performed on the patients' samples. One microgram of genomic DNA was used for exon capture utilizing the Agilent

Sure Select Human All Exon V6 Kit (Agilent Technologies) and then sequenced on the Illumina HiSeq X system (Illumina). PCR amplification was accomplished with Dyad Polymerase (Bio-Rad Laboratories), and an ABI377A DNA sequencer (Applied Biosystems) was utilized to sequence the PCR products. Functional annotation was performed using ANNOVAR through a series of databases, including the 1000 Genomes Project, dbSNP, HGMD, and ExAC. Next, PolyPhen-2, SIFT, and M-CAP were used for functional prediction. Subsequently, variants were ignored if (1) the minor allele frequency was ≥1% in the public database including the gnomAD, ExAC Browser, and 1000 Genomes Project because the pathogenic variants account for male infertility are rare in human populations; (2) the variant located in 3′ or 5′ untranslated regions, noncoding exons, or intronic sequences except splice sites; and (3) the variant was not predicted damaging by PolyPhen-2, SIFT, and M-CAP. The primers used in PCR analysis were as follows: F, 5'-ACCATTATGAGCTAGCTTTCCTT-3'; and R, 5'-ACAGTAACAACAAAGCCAGGT-3'.

Immunofluorescence staining

The sperm from patients and the normal controls and mouse sperm cells were fixed in 4% paraformaldehyde, permeabilized with 0.3% Triton X-100 for 10 min, and blocked with 5% BSA or 30% donkey serum for 60 min at room temperature. The slides were then sequentially incubated with primary antibodies at 4°C overnight. The primary antibodies used were anti-CFAP47 (1:50, sc-514714, Santa Cruz Biotechnology) and α-tubulin (1:100, A11126, Thermo Fisher Scientific), CFAP65 (1:50, HPA055156, Sigma–Aldrich), CFAP69 (1:50, bs-15278R-A647, Bioss), COXIV (1:50, 11242-1-AP, Proteintech) and SEPTIN4 (1:50, 12476-1-AP, Proteintech). The next day, 1 × PBS was used to wash the samples three times. Then, the samples were incubated with AlexaFluor 594 anti-rabbit secondary antibodies (1:1000, 1927937, Thermo Fisher) and AlexaFluor 488 anti-mouse secondary antibodies (1:1000; A32723, Thermo Fisher) for 2 h in room temperature or coincubated with peanut agglutinin (PNA, 1:50, RL-1072-5, Vector). Subsequently, we used 1 × PBS to wash the slides three times. Then, the slides were counterstained with 4,6-diamidino-2-phenylindole (DAPI, D9542-1MG, Sigma-Aldrich) to label the nuclei. Finally, the slides were sealed in coverslips. Images were obtained by a laser scanning confocal microscope (Olympus). For immunofluorescence staining of mouse testis, after careful xylene dewaxing and gradient ethanol rehydration, the tissue sections were submerged in boiling 10 mM citrate buffer (pH 6.0) for 10 min. Then, the sections were cooled to room temperature and washed with 1 × PBS for 5 min. Subsequently, the sections were treated with 3% hydrogen peroxide solution for 10 min. After washing with 1× PBS, the slides were blocked with 10% normal donkey serum for 30 min and incubated with primary antibodies at 4°C overnight and with Alexa Fluor 488 or Alexa Fluor 594 antibodies for an additional 2 h at room temperature. The primary antibodies used were anti-CFAP47 (1:50), anti-CFAP65 (1:50) and anti-CFAP69 (1:50). Slides of testicular tissues were observed using an LSM800 confocal microscope (Carl Zeiss AG).

Western blotting

Proteins were isolated from sperm cells. Protein quantitation was performed by a BCA Protein Assay (23227, Thermo Fisher) according to the manufacturer's instructions. Next, protein denaturation was performed at 100°C for 10 min. The denatured proteins were separated on 10% SDS-polyacrylamide gels. Then, these proteins were transferred into a 0.45 μm pore size polyvinylidene difluoride (PVDF) membrane (ISEQ, 00010, Millipore) by wet transfer. Subsequently, 5% skimmed milk was used to block the transferred membrane. Next, the transferred membrane was incubated in primary antibody: anti-CFAP47 (1:500), anti-CFAP65 (1:1000) and anti-CFAP69 (1:500), anti-GAPDH (1:1000, ab8245, Abcam) solution at 4°C overnight. Subsequently, the membrane was washed with 1 × TBST three times. Then, the membrane was incubated with goat anti-mouse IgG secondary antibody-HRP (1:5000, 32230, Thermo Fisher Scientific) in 5% skimmed milk at room temperature for 1 h and then wash the membrane with 1 × TBST three times. Finally, immunoblots were developed using Thermo Scientific™ Pierce™ ECL Western Blotting Substrate (TWBKLS0500, Millipore).

Electron microscopy and concentrated Papanicolaou staining

For scanning electron microscopy (SEM), the sperm samples were centrifuged at 400×g for 10 min at room temperature. The supernatants were carefully aspirated, and the pellets were suspended and fixed in 2.5% glutaraldehyde for 30 min at 4°C. Next, the samples were evenly spread onto slides and fixed in 2.5% glutaraldehyde overnight at 4°C. Following primary fixation, the slides were washed three times in 1×PBS and gradient dehydration was performed sequentially with 30%, 50%, 75%, 95%, and 100% ethanol for 10 min. Subsequently, the slides were dried to temperature with a CO2 critical-point dryer (Eiko HCP-2, Hitachi). Finally, all of the dried specimens were mounted on aluminum stubs, sputter-coated by an ionic sprayer meter (Eiko E-1020, Hitachi), and analyzed by SEM (Hitachi S3400).

For transmission electron microscopy (TEM), sperm samples were washed routinely and centrifuged at 400 × g for 15 min. Then, the seminal plasma was removed, and the sperm pellets were fixed in 3% glutaraldehyde. Next, the samples were postfixed in 1% buffered OsO4, dehydrated through gradient acetone solutions, and embedded in Epon 812. Finally, the ultrathin sections (80 nm) were double-stained with lead citrate and uranyl acetate before being observed and photographed via TEM (TECNAI G2 F20, Philips).

Isolation of mouse spermatogenic cells

Spermatogenic cells were obtained through cell diameter/density at unit gravity. In brief, mouse germ cells were isolated from the testicular biopsy tissues of obstructive azoospermia patients with informed consents and 8-week C57BL/6 male mice, respectively. In order to remove cell aggregates, spermatogenic cells were resuspended in 25 ml of 0.5% BSA solution and filtered through an 80 mm mesh. The cells were resuspended in buffer containing 0.5% BSA and loaded in an STA-PUT velocity sedimentation cell separator (ProScience) for gradient separation after passage through a mesh filter. Germ cell populations were collected for subsequent analysis.

Protein–protein interaction network

Standardize gene names from Uniprot Knowledgebase (UniprotKB, http://www.uniprot.org), selecting "Homo sapiens". Built on the co-targets result, the PPI network was conducted by Search Tool for the Retrieval of Interacting Genes (STRING, http://cn.string-db.org/). We put the known MMAF causative genes and *CFAP47* into the STRING analysis. The relevant parameter settings are as follows: 1) Network Type: full STRING network; 2) Required score: highest confidence (0.900); 3) Size cutoff: no more than 10 interactors.

Co-immunoprecipitation

The protein collected from human testes from obstructive azoospermia patients with informed consents was incubated with 7 µl of target antibodies overnight at 4°C. Subsequently, we added the mixture of each sample to a microcentrifuge tube containing 40 µL of prewashed Protein A/G magnetic beads (88803, Invitrogen), and the samples were incubated for 2 h at room temperature with constant rotation. After washing with 1 × PBS three times, the coimmunoprecipitated proteins were eluted with standard 5 × SDS sample loading buffer and heated for 10 min at 100°C. Finally, the co-immunoprecipitants were separated on 10% SDS-polyacrylamide gels and PVDF membranes for immunoblot analysis, as described above.

Results

Identification of a *CFAP47* missense variant in two unrelated infertile men

Two oligoasthenoteratozoospermia patients were recruited for our study. Whole-exome sequencing was next performed on the two patients (Figure 1A). Intriguingly, a novel missense mutation of c.1414G>A [p.V472M] in *CFAP47* was identified in both patients (Figure 1A). This *CFAP47* mutation has a low allele frequency in East Asian populations in public databases (Table 1) and was predicted to be harmful through the prediction of SIFT, PolyPhen-2, and M-CAP tools (Table 1). Subsequent sequence alignment analysis found that this amino acid was conserved in multiple species (Figure 1B). These findings indicated that this hemizygous mutation in *CFAP47* might be a potential pathogenic factor for the sterile phenotype of patients.

Presentation of MMAF in two infertile patients

To explore the detailed infertile phenotypes in the two patients, we performed semen analysis according to WHO guidelines. The results indicated dramatic decreases in sperm count, sperm motility accompanied by aberrant sperm morphology (Table 1). Papanicolaou staining and SEM were further used to analyze sperm morphology in detail. Unlike the normal control, the spermatozoa from the patients exhibited a typical MMAF phenotype, including absent, short, and coiled flagella (Figure 2A, B). Strikingly, the patients' sperm also exhibited anomalous morphology in the sperm head, such as pyriform head, small head, or round head (Figure 2A, B). Noticeably, the impaired conjunction between the midpiece and principal piece was apparent, suggesting that the patients might have defective sperm annulus (Figure 2B).

TEM was performed to investigate the ultrastructure of spermatozoa. In contrast with the well-organized peri-axonemal and axonemal structures in the normal sperm flagella, the sperm flagella of the patients showed severe disorganization or absence of the peri-axonemal and '9 + 2' axonemal components and the disarrangement of mitochondrial sheaths and dense fibers (Figure 2C). Strikingly, typically swollen mitochondria were present in the middle piece (Figure 2C). Based on this phenomenon, COXIV, a marker of mitochondrial sheath integrity, was used to analyze defects in the mitochondrial sheath. In control sperm, COXIV localized to the midpiece of sperm flagella, but it disappeared completely in the sperm of patients (Figure 3A). Intriguingly, most patients' spermatozoa exhibited irregular and unconsolidated nuclei (Figure 2C). Additionally, the majority of the acrosomes were small or even absent in the sperm heads of the patients (Figure 2C). Immunofluorescence staining of PNA also demonstrated disrupted or absent acrosomes in the sperm of patients (Figure 3B). All evidence indicates that *CFAP47* mutation contributes not only to the MMAF phenotype but also to abnormalities in the sperm head and annulus.

The deleterious effect of this missense variant on CFAP47 expression and function

To investigate the impact of this variant on CFAP47 protein structure, PyMOL Viewer software was used to visualize the effects of altered residues on protein-structure models (Figure 4A). The amino acid sequence of predicted structure of CFAP47 included the residues from 1 aa to 754 aa. Mutant V472M showed it may affect the stability of the original β-sheet region for methionine occupied more space than valine, indicating that the structure of CFAP47 was

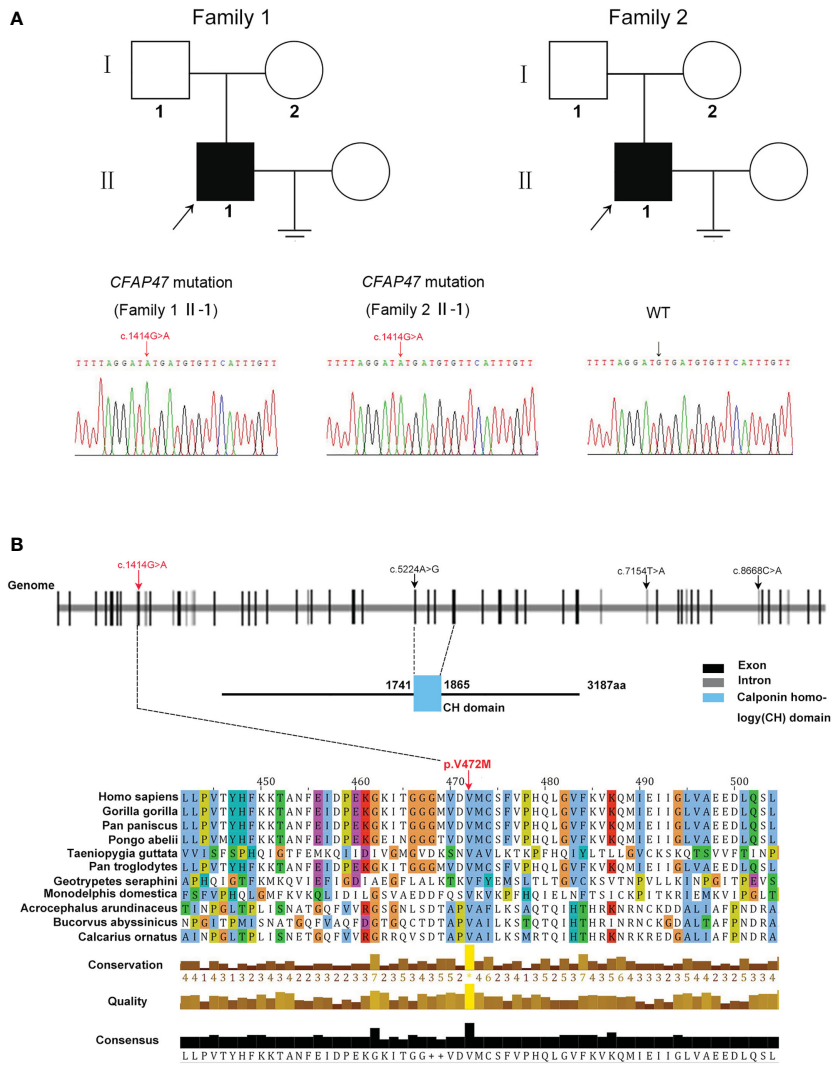

FIGURE 1
Identification of a novel variant of X-linked *CFAP47* in oligoasthenoteratozoospermia patients. **(A)** Pedigree structure of two families affected oligoasthenoteratozoospermia. The probands are indicated by black arrows. Sanger sequencing confirmed a hemizygous *CFAP47* missense variant in the two families. The detailed position of the variant (c.1414G>A) is indicated by red arrows. **(B)** CFAP47 protein structure, localization of variants in the genome, and conservation of mutant amino acids in various species. The red arrow indicates the position of the mutation in our study. The black arrow indicates the mutations that have been reported. Residue V472 is conserved across species.

disordered. To further determine the impact of c.1414G>A on CFAP47 expression, we detected CFAP47 expression in the patients' spermatozoa via immunofluorescence staining. CFAP47 expression was mainly distributed in flagella in control spermatozoa, while CFAP47 staining was barely detected in the spermatozoa of patients (Figure 4B). Meanwhile, western blotting showed similar results of significantly decreased protein expression of CFAP47 in the patients' sperm lysates compared to the fertile control (Figure 4C).

STRING analysis (https://cn.string-db.org/) revealed that CFAP47 may be connected with CFAP69, a key molecule involved in sperm flagellar formation (Figure 5A) (18). Co-immunoprecipitation further verified the binding between CFAP47 and CFAP69 in human testis lysates (Figure 5B). In addition, a previous study demonstrated that CFAP47 regulated and interacted with CFAP65 (17), which has been suggested to regulate sperm head development (19). Strikingly, the expression levels of CFAP69 and CFAP65 were validated to be sharply reduced in the sperm of the two patients compared to the normal control via immunofluorescence staining and western blotting (Figure 5C-E). In addition, the immunofluorescence assay confirmed the colocalization of CFAP47 with CFAP65 and CFAP69 in mouse spermatogenic cells at different stages (Supplemental Figure 1, 2) (20), as well as mouse testis sections (Supplemental Figure 3). We further detected the expression and localization of SEPTIN4, an essential protein for sperm annulus formation (21), by immunofluorescence staining in the patients' sperm. As expected, the SEPTIN4 signal was located in the annulus in normal control

TABLE 1 Semen and variant analysis in the two patients harboring hemizygous a *CFAP47* mutation.

		P1	P2	References
	Sperm volume (mL)	1.9	3.8	>=1.5
	Sperm concentration(10^6/mL)	6.0	0.9	>=15
	Motility (A+B, %)	21	11.0	>=40
Semen	Vitality (%)	1.0	5.8	>=58
parameters	Normal spermatozoa (%)	1	2.7	>=4
	Defective spermatozoa (%)	99	97.3	
	pyriform head (%)	18	37	
	Round head (%)	32	29	
	Coiled flagella (%)	39	47	
	Absent flagella (%)	5	9.4	
	Bent flagella (%)	52	34.9	
	cDNA mutation	c.1414G>A	c.1414G>A	
	Protein changes	p.V472M	p.V472M	
	Mutation type	Missense	Missense	
	Genotype	Hemizygous	Hemizygous	
Variants	Allele frequency			
analysis	in ExAC Browser (ExAC_EAS)	0.0091	0.0091	
	GnomAD (gnomAD_exome_EAS)	0.0094	0.0094	
	1000 Genomes Project (1000g2015aug_eas)	0.0092	0.0092	
	Function Prediction			
	SIFT	Deleterious	Deleterious	
	Polyphen-2	Probably damaging	Probably damaging	
	M-CAP	Deleterious	Deleterious	

RefSeq accession number of CFAP47: NM_001304548.

10.3389/fendo.2023.1155639

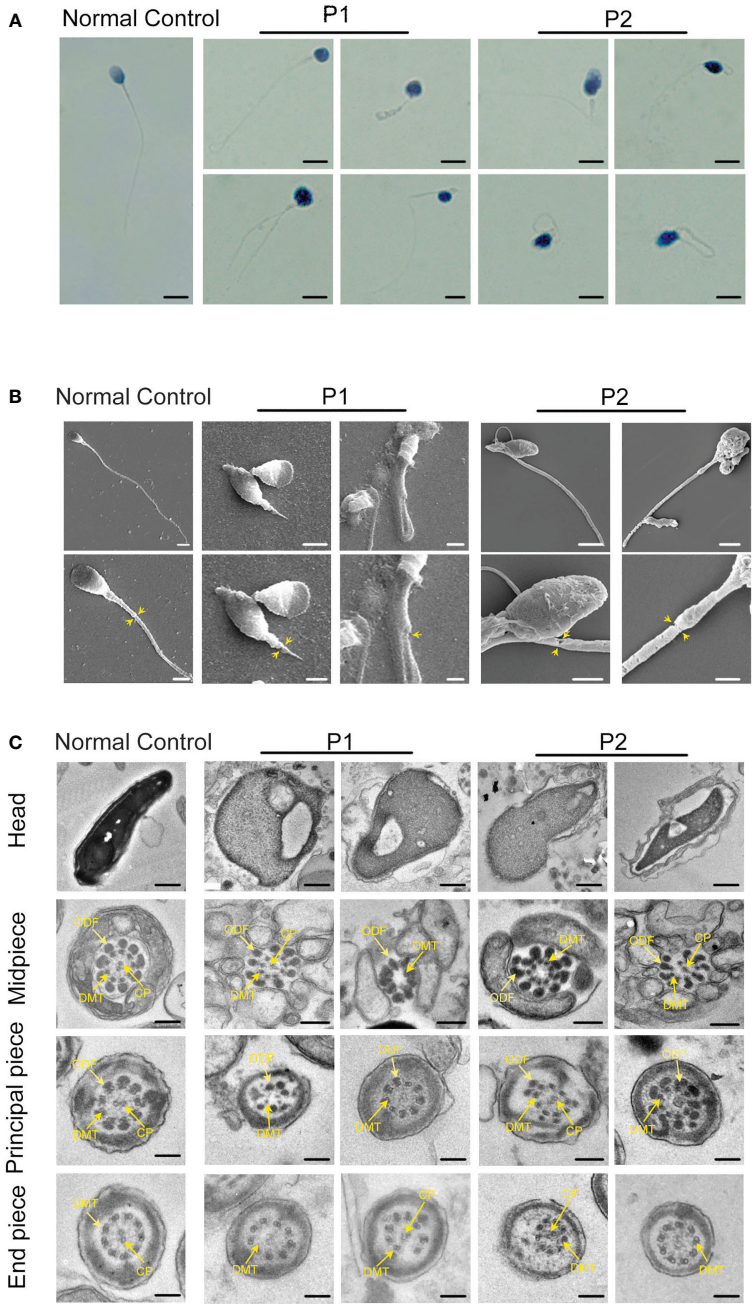

FIGURE 2
Sperm morphology and ultrastructure analysis for patients harboring hemizygous *CFAP47* variant. **(A)** Papanicolaou staining of spermatozoa obtained from normal control and patients. The patients' sperm showed irregular morphology (Scale bars, 5 μm). **(B)** Morphological defects in sperm were observed in the patient by SEM. The abnormal annulus of patients is indicated by yellow arrows (Scale bars, 5 μm). **(C)** TEM showed abnormal ultrastructure of the head and flagellum from the patients' spermatozoa compared to normal control (ODF, outer dense fibers; DMT, peripheral microtubule doublet; CP, central pair of microtubules; Scale bars, 200 nm).

but was almost disappeared in patients (Figure 5F). Co-immunoprecipitation further confirmed the physical interactions between CFAP47 and SEPTIN4 (Figure 5B), suggesting that CFAP47 might also be related to sperm annulus formation by regulating SEPTIN4. These results demonstrated that CFAP47 might regulate sperm morphology development by modulating the expression of CFAP65, CFAP69 and SEPTIN4.

Outcomes of intracytoplasmic sperm injection in patients carrying *CFAP47* mutation

ICSI is a commonly used assisted reproductive technology (ART) to help sterile patients (22). ICSI cycles were attempted for our patients, and written informed consent was obtained for the

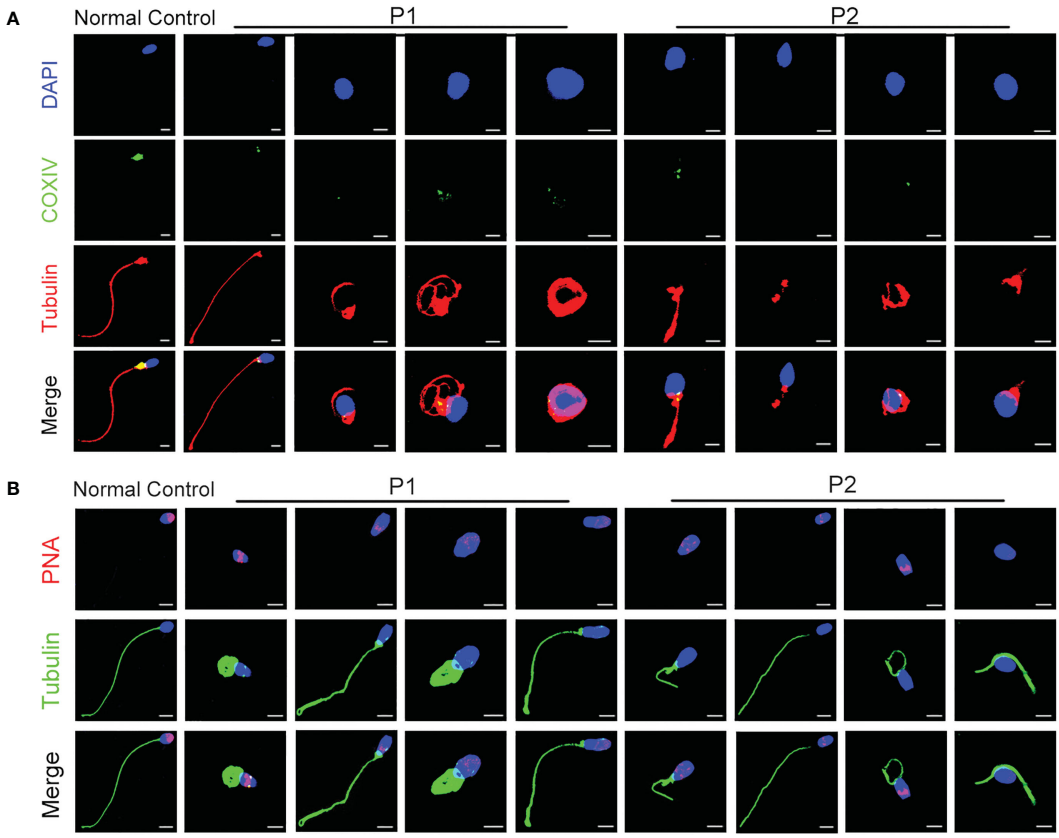

FIGURE 3
The characterization of spermatozoa in patients. **(A)** COXIV immunostaining disappeared in the sperm of patients compared to the normal control (Blue, DAPI; green, COXIV; red, α-tubulin; scale bars, 5 μm). **(B)** The immunostaining of PNA exhibited imperfect acrosomes in sperm cells of patients compared to the control subject (Blue, DAPI; green, α-tubulin; red, PNA; scale bars, 5 μm).

procedure (Table 2). For patient A, his wife was followed up for one ICSI cycle—with eight oocytes retrieved after gonadotrophin-releasing hormone (GnRH) treatment. Five mature oocytes (metaphase II, MII) were collected, and one 8 II (the embryo has eight cells, the blastomere is uniform, and the fragment is 10% to 20%) was transferred. Regrettably, his wife has not succeeded in pregnancy. For patient B, his wife experienced a long GnRH agonist protocol in the first cycle. Six oocytes were retrieved, four mature oocytes were microinjected successfully, and only one oocyte was normally fertilized (1PN/injected oocytes = 25%). Following extended culture, we obtained one available D3 embryo that failed to develop after being transferred. After this progress, this couple continues the second cycle and chooses the antagonist protocol. We retrieved three metaphase II oocytes and injected them; however, they failed to develop after reaching the available D3 stage. However, a previous study reported satisfactory ICSI outcomes of a loss-of-function mutation in *CFAP47* in humans and male mice (17). We speculated that additional female risk factors for infertility should not be excluded, and more cases need to be investigated to clarify the role of this mutation in ICSI outcomes.

Discussion

In our study, we highlighted that in addition to MMAF, *CFAP47* mutation is associated with severe defects in other spermatozoa morphology, including sperm head, annulus and mitochondria. Furthermore, CFAP47 was first demonstrated to interact with CFAP69 and SEPTIN4, and further mediate their expression. With our experimental data, we suggest that *CFAP47* may be involved in sperm morphogenesis both in head development and flagellum assembly.

A previous study on an animal model reported a necessary role of *Cfap47* in spermatogenesis in mice, and their patients with *CFAP47* mutations were infertile, characterized by abnormal sperm motility and sperm flagellum morphology (17). However, the phenotype and mutation spectrum of *CFAP47* in humans have not been comprehensively studied. The underlying mechanism by which *CFAP47* regulates reproductive biology is also largely unknown. In the present study, we detected a novel missense mutation of *CFAP47* in two sterile patients from two unrelated families. By a comprehensive morphology analysis, we first suggested that *CFAP47* mutation is also linked to the abnormal

10.3389/fendo.2023.1155639

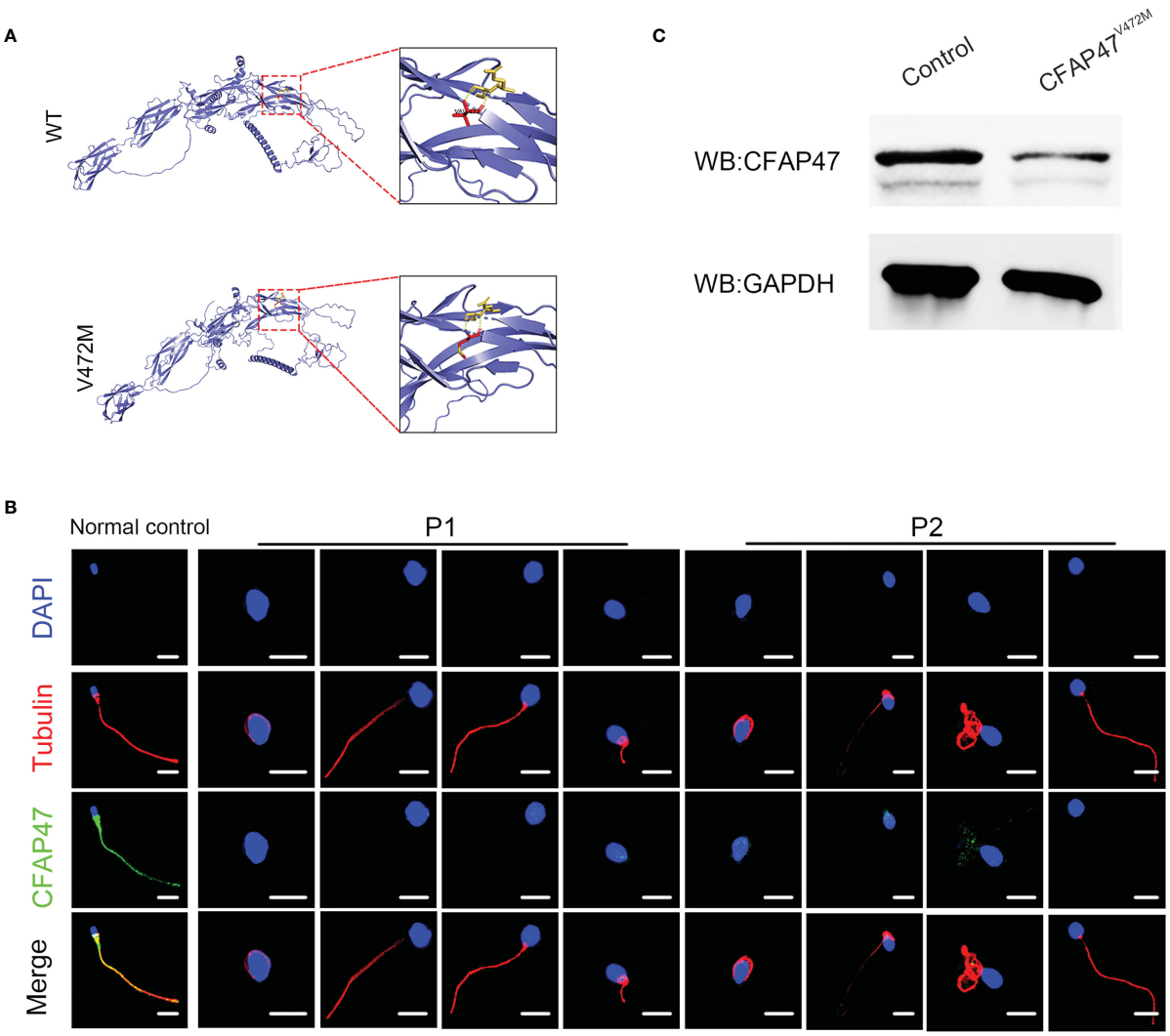

FIGURE 4
Expression analysis of *CFAP47* in the spermatozoa from a male control individual and men harboring hemizygous *CFAP47* variants. **(A)** Structural illustration of the missense mutation in CFAP47. **(B)** Immunoblotting assays revealed that CFAP47 was dramatically reduced in the spermatozoa of patients harboring *CFAP47* mutation. **(C)** Immunofluorescence staining reflected a marked decline in CFAP47 expression in the patients' sperm compared with that in the normal control (Blue, DAPI; red, α-tubulin; green, CFAP47; scale bars, 5 μm).

sperm annulus and head morphology. Moreover, our mechanistic study found that CFAP47 could interact with CFAP65, CFAP69 and SEPTIN4 to further regulate their expression. In particular, CFAP69 and CFAP65, as known MMAF pathogenic genes, are required for sperm morphogenesis. Wang et al. reported that CFAP65 is expressed in the acrosome area and flagellar midpiece in normal human spermatozoa (19), and CFAP69 is localized to the sperm flagellum (18). SEPTIN 4 is essential for the structural and mechanical integrity of the spermatozoa annulus (21). Therefore, our findings demonstrated a potential mechanism by which CFAP47 might regulate spermatogenesis by mediating the expression of CFAP65, CFAP69 and SEPTIN4. In fact, there are a few genes that show phenotype heterogeneity to a certain extent. For example, *FSIP2* was initially reported as a pathogenic gene of MMAF (23), while Zheng et al. confirmed that deleterious mutations in *FSIP2* are responsible for abnormal acrosome biogenesis (24); loss-of-function mutations in *DNAH6* (25) were first detected in three MMAF patients by Tu et al. but also screened compound heterozygous variants in *DNAH6* in a patient who presented sperm head anomaly (26). These studies strongly suggested that some pivotal proteins may not perform a single function but also play a various role during spermatogenesis.

Sex chromosomes play a key role in sex determination and reproductive function (27). Other than genes located in the autosomal chromosome, sex chromosome genes lack corresponding alleles in males. Therefore, harmful mutations in sex chromosome genes have a direct impact on male infertility occurrence. To date, limited causative genes in sex chromosomes have been acknowledged. Partial deletion of *testis expressed 11 (TEX11)* leads to azoospermia due to meiotic arrest (28); mutations in *androgen receptor (AR)* attenuate AR regulation of target gene expression and cause oligozoospermia and azoospermia

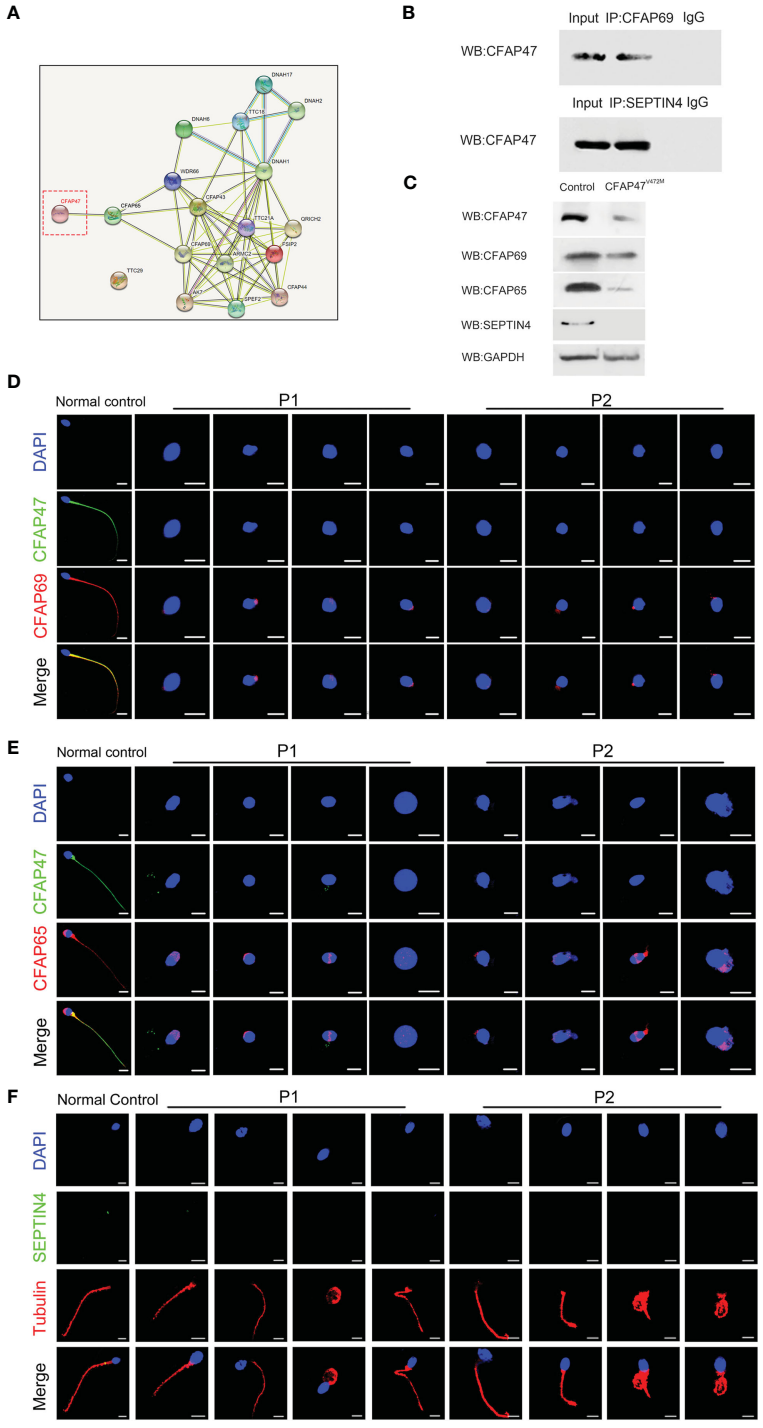

FIGURE 5
The altered expression of key molecules involved in spermatogenesis is mediated by CFAP47. **(A)** The protein interaction network was predicted by in silico software STRING for the human CFAP47 protein. Known interactions: the light blue lines symbolize that the two connected proteins are from curated databases, and the red lines represent that the proteins are experimentally determined; Predicted interactions: the green lines symbolize that the two connected proteins are gene neighborhood, the orange lines represent that the proteins are gene fusions, and the dark blue lines represent that the proteins are gene co-occurrence; Others: the yellow lines symbolize that the two connected proteins are textmining, the black lines represent the co-expression proteins, and the gray lines represent the protein homology. **(B)** Co-immunoprecipitation analysis showing the binding of CFAP47 with CFAP69 and SEPTIN4 using human testis lysates. **(C)** Immunoblotting assays revealed that CFAP65 and CFAP69 were dramatically reduced in the spermatozoa of patients harboring *CFAP47* mutations. **(D, E)** The signals of CFAP69 **(D)** and CFAP65 **(E)** were clearly reduced in the sterile patients by fluorescence detection (Blue, DAPI; green, CFAP47; red, CFAP65 and CFAP69; scale bars: 5 μm). **(F)** Expression of SEPTIN4 was not visible in the sperm annulus of patients compared to normal control (Blue, DAPI; green, SEPTIN4; red, α -tubulin; scale bars, 5 μm).

10.3389/fendo.2023.1155639

TABLE 2 Clinical features of the patients' spouses with ICSI treatment.

		Spouse of P1	Spouse of P2
Age(y)		25	28
Length of primary infertility history (y)		3	4
BMI		18.4	19.1
Basal hormones	FSH (IU/L)	7.6	11.1
	LH (IU/L)	3.3	6.9
	E2 (pg/mL)	15.7	38.9
	PRL (ng/ml)	9.2	13.3
	Prog (ng/ml)	0.42	0.7
	Testo (ng/ml)	0.36	0.41
Cycle 1	Protocol	Long	Long
	E2 level on the trigger day (pg/mL)	2585	602
	No. of follicles ≥ 14 mm on the trigger day	5	2
	No. of follicles ≥18 mm on the trigger day	3	1
	No. of oocytes retrieved	8	6
ICSI progress	Oocytes injected	5	4
	Fertilization rate (%)	60% (3/5)	25% (1/4)
	Cleavage Rate (%)	100% (3/3)	100% (1/1)
	Available D3 embryos	1	1
Cycle 2	Protocol		Antagonist
	E2 level on the trigger day (pg/mL)		13.3
	No. of follicles ≥ 14 mm on the trigger day		5
	No. of follicles ≥18 mm on the trigger day		1
	No. of oocytes retrieved		3
ICSI progress	Oocytes injected		3
	Fertilization rate (%)		66.7% (2/3)
	Cleavage Rate (%)		100% (2/2)
	Available D3 embryos		1

(29); dysfunction of *adhesion G protein-coupled receptor G2* (ADGRG2) results in a buildup of fluid within the testis and an accumulation of spermatozoa within the efferent ducts (30); *PIH1 domain containing 3* (*PIH1D3*) is involved in the assembly of the dynein arm of the ciliary axoneme, and defects in this gene lead to primary ciliary dyskinesia (PCD) (31); *Ubiquitin specific peptidase 9 Y-linked* (*USP9Y*) is expressed specifically in testis in a germ cell-dependent fashion and the absence of USP9Y has been suggested to cause spermatogenic failure (32). Hence, more sex chromosome gene pathogenicity and biological functions in male reproduction need to be explored. In the current study, we identified a novel homozygous mutation in *CFAP47*, which is located on the X chromosome, in two infertile patients. Our findings expanded the causative mutation of male infertility on the X chromosome, providing more valuable information for the diagnosis and treatment of male infertility.

In conclusion, our study identified a novel missense mutation in *CFAP47* in two infertile male patients with various sperm morphology abnormalities, first revealing *CFAP47* as a candidate causative gene of sperm multiple morphological abnormalities. Functional analysis demonstrated the underlying molecular mechanism by which CFAP47 regulates sperm morphogenesis. Our work presented more detailed information on the pathogenesis of *CFAP47* mutation and provided direct evidence that suggests the involvement of *CFAP47* in spermatogenesis.

Data availability statement

The datasets presented in this article are not readily available because the datasets generated during and analyzed during the current study are available from the corresponding author on

reasonable request. Requests to access the datasets should be directed to ET, tianep@jxr-fertility.com.

Ethics statement

The studies involving human participants were reviewed and approved by Ethics Committee of the Second West China Hospital of Sichuan University. This study was performed in line with the principles of the Declaration of Helsinki. The patients/participants provided their written informed consent to participate in this study.

Author contributions

ET supervised the study experiments. YiY conducted the clinical evaluations. YS analyzed the WES data. SD and JZ performed immunofluorescence staining. ML, YaY, HL, and CJ performed TEM and SEM. ML and SD provided figures and writing guidance. ML wrote the first article draft. ET revised the manuscript. All authors contributed to the article and approved the submitted version.

Conflict of interest

The authors declare that the research was conducted in the absence of any commercial or financial relationships that could be construed as a potential conflict of interest.

Publisher's note

All claims expressed in this article are solely those of the authors and do not necessarily represent those of their affiliated organizations, or those of the publisher, the editors and the reviewers. Any product that may be evaluated in this article, or claim that may be made by its manufacturer, is not guaranteed or endorsed by the publisher.

Supplementary material

The Supplementary Material for this article can be found online at: https://www.frontiersin.org/articles/10.3389/fendo.2023.1155639/full#supplementary-material

References

1. Mascarenhas MN, Flaxman SR, Boerma T, Vanderpoel S, Stevens GA. National, regional, and global trends in infertility prevalence since 1990: a systematic analysis of 277 health surveys. *PloS Med* (2012) 9(12):e1001356. doi: 10.1371/journal.pmed.1001356

2. Datta J, Palmer MJ, Tanton C, Gibson LJ, Jones KG, Macdowall W, et al. Prevalence of infertility and help seeking among 15 000 women and men. *Hum Reprod* (2016) 31(9):2108–18. doi: 10.1093/humrep/dew123

3. de Ligny W, Smits RM, Mackenzie-Proctor R, Jordan V, Fleischer K, de Bruin JP, et al. Antioxidants for male subfertility. *Cochrane Database Syst Rev* (2022) 5(5): CD007411. doi: 10.1002/14651858.CD007411.pub5

4. Dai S, Liu M, Liu M, Jiang C, Yang Y, Han H, et al. Population-based genetic analysis in infertile men reveals novel mutations of ADAD family members in patients with impaired spermatogenesis. *Hum Mol Genet* (2023) 27:ddad012. doi: 10.1093/hmg/ddad012

5. World Health Organization. *WHO laboratory manual for the examination and processing of human semen. 5th edn*. Cambridge: Cambridge University Press (2010). p. 272.

6. Jiao SY, Yang YH, Chen SR. Molecular genetics of infertility: loss-of-function mutations in humans and corresponding knockout/mutated mice. *Hum Reprod Update* (2021) 27(1):154–89. doi: 10.1093/humupd/dmaa034

7. Fellmeth JE, Ghanaim EM, Schindler K. Characterization of macrozoospermia-associated AURKC mutations in a mammalian meiotic system. *Hum Mol Genet* (2016) 25(13):2698–711. doi: 10.1093/hmg/ddw128

8. Koscinski I, Elinati E, Fossard C, Redin C, Muller J, Velez de la Calle J, et al. DPY19L2 deletion as a major cause of globozoospermia. *Am J Hum Genet* (2011) 88 (3):344–50. doi: 10.1016/j.ajhg.2011.01.018

9. Oud MS, Okutman Ö, Hendricks LAJ, de Vries PF, Houston BJ, Vissers LELM, et al. Exome sequencing reveals novel causes as well as new candidate genes for human globozoospermia. *Hum Reprod* (2020) 35(1):240–52. doi: 10.1093/humrep/dez246

10. Li Y, Li C, Lin S, Yang B, Huang W, Wu H, et al. A nonsense mutation in Ccdc62 gene is responsible for spermiogenesis defects and male infertility in repro29/repro29 mice. *Biol Reprod* (2017) 96(3):587–97. doi: 10.1095/biolreprod.116.141408

11. Zhang XZ, Wei LL, Jin HJ, Zhang XH, Chen SR. The perinuclear theca protein calicin helps shape the sperm head and maintain the nuclear structure in mice. *Cell Rep* (2022) 40(1):111049. doi: 10.1016/j.celrep.2022.111049

12. Xiao N, Kam C, Shen C, Jin W, Wang J, Lee KM, et al. PICK1 deficiency causes male infertility in mice by disrupting acrosome formation. *J Clin Invest* (2009) 119 (4):802–12. doi: 10.1172/JCI36230

13. Dam AH, Koscinski I, Kremer JA, Moutou C, Jaeger AS, Oudakker AR, et al. Homozygous mutation in SPATA16 is associated with male infertility in human globozoospermia. *Am J Hum Genet* (2007) 81(4):813–20. doi: 10.1086/521314

14. Yatsenko AN, O'Neil DS, Roy A, Arias-Mendoza PA, Chen R, Murthy LJ, et al. Association of mutations in the zona pellucida binding protein 1 (ZPBP1) gene with abnormal sperm head morphology in infertile men. *Mol Hum Reprod* (2012) 18(1):14–21. doi: 10.1093/molehr/gar057

15. Touré A, Martinez G, Kherraf ZE, Cazin C, Beurois J, Arnoult C, et al. The genetic architecture of morphological abnormalities of the sperm tail. *Hum Genet* (2021) 140(1):21–42. doi: 10.1007/s00439-020-02113-x

16. Dai S, Liang Y, Liu M, Yang Y, Liu H, Shen Y. Novel biallelic mutations in TTC29 cause asthenoteratospermia and male infertility. *Mol Genet Genomic Med* (2022) 10(12):e2078. doi: 10.1002/mgg3.2078

17. Liu C, Tu C, Wang L, Wu H, Houston BJ, Mastrorosa FK, et al. Deleterious variants in X-linked CFAP47 induce asthenoteratozoospermia and primary male infertility. *Am J Hum Genet* (2021) 108(2):309–23. doi: 10.1016/j.ajhg.2021.01.002

18. He X, Li W, Wu H, Lv M, Liu W, Liu C, et al. Novel homozygous CFAP69 mutations in humans and mice cause severe asthenoteratospermia with multiple morphological abnormalities of the sperm flagella. *J Med Genet* (2019) 56(2):96–103. doi: 10.1136/jmedgenet-2018-105486

19. Wang W, Tian S, Nie H, Tu C, Liu C, Li Y, et al. CFAP65 is required in the acrosome biogenesis and mitochondrial sheath assembly during spermiogenesis. *Hum Mol Genet* (2021) 30(23):2240–54. doi: 10.1093/hmg/ddab185

20. Russell L, Ettlin R, Sinha Hikim A, Clegg E. *Histological and histopathological evaluation of the testis*. Clearwater, FL, USA: Cache River Press (1990).

21. Kissel H, Georgescu MM, Larisch S, Manova K, Hunnicutt GR, Steller H. The Sept4 septin locus is required for sperm terminal differentiation in mice. *Dev Cell* (2005) 8(3):353–64. doi: 10.1016/j.devcel.2005.01.021

22. Gameiro S, Finnigan A. Long-term adjustment to unmet parenthood goals following ART: a systematic review and meta-analysis. *Hum Reprod Update* (2017) 23 (3):322–37. doi: 10.1093/humupd/dmx001

23. Martinez G, Kherraf ZE, Zouari R, Fourati Ben Mustapha S, Saut A, et al. Whole-exome sequencing identifies mutations in FSIP2 as a recurrent cause of multiple morphological abnormalities of the sperm flagella. *Hum Reprod* (2018) 33(10):1973–84. doi: 10.1093/humrep/dey264

24. Zheng R, Wang Y, Li Y, Guo J, Wen Y, Jiang C, et al. FSIP2 plays a role in the acrosome development during spermiogenesis. *J Med Genet* (2022) 60(3):254–264. doi: 10.1136/jmedgenet-2021-108406

25. Tu C, Nie H, Meng L, Yuan S, He W, Luo A, et al. Identification of DNAH6 mutations in infertile men with multiple morphological abnormalities of the sperm flagella. *Sci Rep* (2019) 9(1):15864. doi: 10.1038/s41598-019-52436-7

26. Li L, Sha YW, Xu X, Mei LB, Qiu PP, Ji ZY, et al. DNAH6 is a novel candidate gene associated with sperm head anomaly. *Andrologia* (2018). doi: 10.1111/and.12953.

27. Skaletsky H, Kuroda-Kawaguchi T, Minx PJ, Cordum HS, Hillier L, Brown LG, et al. The male-specific region of the human y chromosome is a mosaic of discrete sequence classes. *Nature* (2003) 423(6942):825–37. doi: 10.1038/nature01722

28. Yatsenko AN, Georgiadis AP, Röpke A, Berman AJ, Jaffe T, Olszewska M, et al. X-Linked TEX11 mutations, meiotic arrest, and azoospermia in infertile men. *N Engl J Med* (2015) 372(22):2097–107. doi: 10.1056/NEJMoa1406192

29. Hasani N, Mohseni Meybodi A, Rafaee A, Sadighi Gilani MA, Mohammadzadeh R, Sabbaghian M. Spermatogenesis disorder is associated with mutations in the ligand-binding domain of an androgen receptor. *Andrologia* (2019) 51(10):e13376. doi: 10.1111/and.13376

30. Patat O, Pagin A, Siegfried A, Mitchell V, Chassaing N, Faguer S, et al. Truncating mutations in the adhesion G protein-coupled receptor G2 gene ADGRG2 cause an X-linked congenital bilateral absence of vas deferens. *Am J Hum Genet* (2016) 99(2):437–42. doi: 10.1016/j.ajhg.2016.06.012

31. Olcese C, Patel MP, Shoemark A, Kiviluoto S, Legendre M, Williams HJ, et al. X-Linked primary ciliary dyskinesia due to mutations in the cytoplasmic axonemal dynein assembly factor PIH1D3. *Nat Commun* (2017) 8:14279. doi: 10.1038/ncomms14279

32. Luddi A, Margollicci M, Gambera L, Serafini F, Cioni M, De Leo V, et al. Spermatogenesis in a man with complete deletion of USP9Y. *N Engl J Med* (2009) 360(9):881–5. doi: 10.1056/NEJMoa0806218

Frontiers in Endocrinology

Explores the endocrine system to find new therapies for key health issues

The second most-cited endocrinology and metabolism journal, which advances our understanding of the endocrine system. It uncovers new therapies for prevalent health issues such as obesity, diabetes, reproduction, and aging.

Discover the latest Research Topics

See more →

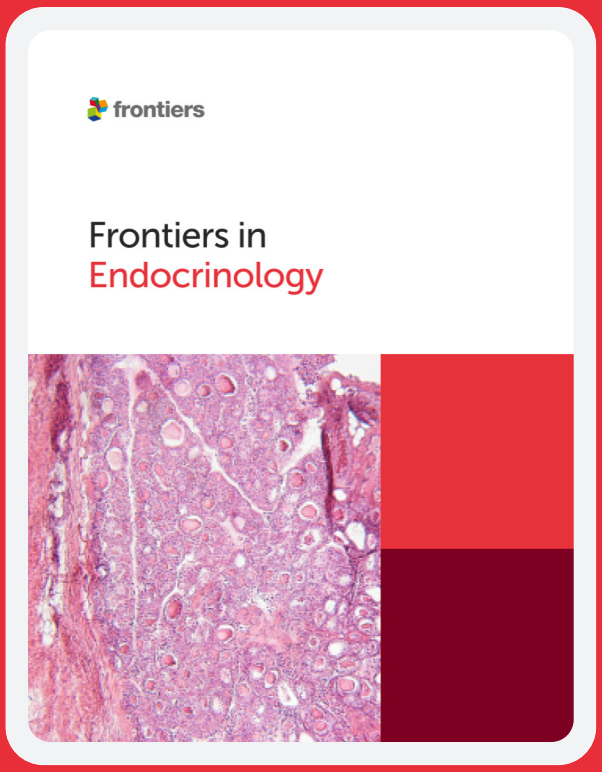

Frontiers

Avenue du Tribunal-Fédéral 34
1005 Lausanne, Switzerland
frontiersin.org

Contact us

+41 (0)21 510 17 00
frontiersin.org/about/contact